

NASA-CR-173,412

NASA-CR-173412 P-120

1984 0013809

A Reproduced Copy

N

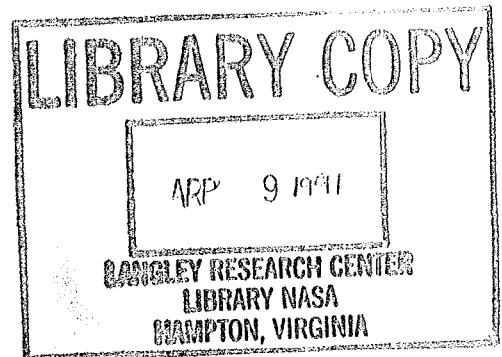
Reproduced for NASA

by the

NASA Scientific and Technical Information Facility



NF01466



BEST

AVAILABLE

COPY

**All Missing Pages
Missing in Original
Document**

AVAILABILITY NOTICE

A major purpose of the Technical Information Center is to provide the broadest dissemination possible of information contained in DOE's Research and Development Reports to business, industry, the academic community, and federal, state and local governments.

Although a small portion of this report is not reproducible, it is being made available to expedite the availability of information on the research discussed herein.

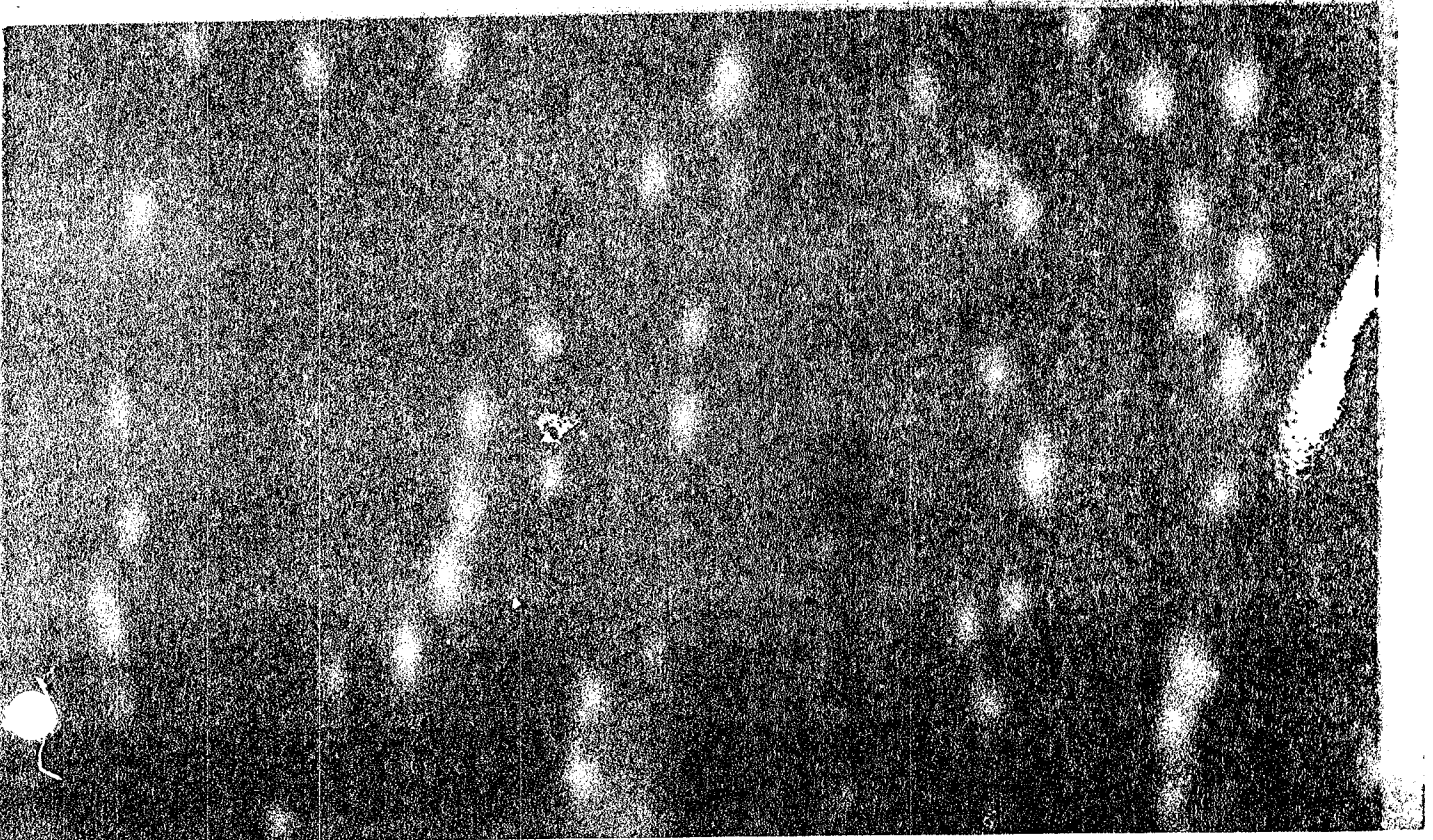
1

SAE The Engineering
Resource For
SAE Advancing Mobility



**PROCEEDINGS OF THE
TWENTIETH
AUTOMOTIVE TECHNOLOGY
DEVELOPMENT CONTRACTORS'
COORDINATION MEETING**

P-120



CONF-821055--

DE83 016840

**PROCEEDINGS OF THE
TWENTIETH
AUTOMOTIVE TECHNOLOGY
DEVELOPMENT CONTRACTORS'
COORDINATION MEETING**

P-120

**Sponsored by:
U.S. Department of Energy
Office of Vehicle and Engine R&D
Conservation and Renewable Energy**

**Published by:
Society of Automotive Engineers, Inc.
400 Commonwealth Drive
Warrendale, PA 15086
April 1983**

NOTICE

This report was prepared as an account of work sponsored by the United States Government. Neither the United States nor the United States Department of Energy, nor any of their employees, makes any warranty, express or implied, or assumes any legal liability or responsibility for the accuracy, completeness, or usefulness of any information, apparatus, product, or process disclosed, or represents that its use would not infringe privately owned rights. Reference herein to any specific commercial product, process, or service by trade name, mark, manufacturer, or otherwise, does not necessarily constitute or imply its endorsement, recommendation, or favoring by the United States Government or any agency thereof. The views and opinions of authors expressed herein do not necessarily state or reflect those of the United States Government or any agency thereof.

ISBN 0-29583-021-8

Printed and Bound by Publishers Choice Book Mfg. Co.
Harris, Pennsylvania 15006

TABLE OF CONTENTS

Program Overview, Albert A. Chesnes	1
---	---

STIRLING TECHNOLOGY SESSION

An Overview of the U.S. Department of Energy's Automotive Stirling Engine Technology Development Program, Patrick L. Sutton	3 ✓
The 4-26 Solar Stirling Engine—A Progress Report, Stan Holgersson and Worth H. Percival	7
Heat-Activated Heat Pump Development and Potential Application of Stirling Engine Technology, P. D. Fairchild and C. D. West	17 <i>Diff?</i>
Stirling Engine Applications Study, W. Peter Teegen and David R. Cunningham	33 ✓
Automotive Stirling Engine Development Program—Overview and Status Report, Noel P. Nightingale	53 ✓
Automotive Stirling Engine Development Program—Mod I Stirling Engine System Performance, Albert Richey	63 ✓
Upgraded Mod I Stirling Engine Design (Mod I-A), Bengt-Ove Moodysson	69 ✓
Automotive Stirling Engine Development Program—Mod I Stirling Engine Emissions with Exhaust Gas Recirculation, Roger A. Farrell	87 ✓
Automotive Stirling Engine Development Program—Stirling Engine Alternative Fuels Test Results, Robert A. Battista	93 ✓
Stirling Engine Materials Research at NASA Lewis, MIT, and USAB, Joseph R. Stephens, Michael T. Cronin, and Erik Skog	103 ✓
Free-Piston Stirling Hydraulic Drive for Automobiles, Donald G. Beremand, Jack G. Slatby, and David Mico	115 ✓
A Look at a Cooled, Insulated Stirling Engine, William A. Tomazic	131 ✓

GAS TURBINE TECHNOLOGY SESSION

Advanced Gas Turbine Technology Development (Systems and Components), R. A. Rackley and D. M. Kreiner	145 ✓
Advanced Gas Turbine Technology Development: AGT 100 Systems and Components, H. E. Helms and R. A. Johnson	155 ✓
Ceramic Applications in Turbine Engines (CATE), S. R. Thrasher	167 ✓

CERAMIC TECHNOLOGY SESSION

Development of Ceramic Components for Gas Turbine Engines, Lance E. Groseclose, Peter W. Haitman, and Jenn Chang	181 ✓
Advanced Gas Turbine Ceramic Component Development, G. L. Boyd, D. W. Carruthers, J. R. Kidwell, and D. W. Richardson	189 ✓
Ceramic Technology Progress Report—DOE/AMMRC Ceramic Materials Program, R. Nathan Katz and Edward M. Lence	199 ✓
Streamed Sighting for High Performance Thermomechanical Applications, Wayne D. Pizzo and Charles D. Greshovich	205 ✓
Highlights in the Development of the KTT Automotive Gas Turbine, Sven-Olof Kronqvist	211 ✓

HEAVY DUTY TRANSPORT TECHNOLOGY SESSION

DOE/NASA Heavy-Duty Transport Technology Program, Harry W. Davison	228	✓
The Cummins Advanced Turbocompound Diesel Engine Evaluation, John L. Hoshne and John R. Warner	231	✓
Status Report on Diesel Organic Rankine Compound Engine for Long-Haul Trucks, Michael D. Koplow, Lucco R. DiNanno, and Francis A. DiBella	243	✓
Light Duty Vehicle Diesel Engine Assessment Program—Passenger Car Diesel Engine of the Future, Roy Kemo, Luigi Tuzzi, and Raj Sekar	261	✓
TACOM/Commins Adiabatic Engine Program, Walter Bryzik	273	
Fabrication, Testing and Brining of Dispersed-Silica Toughened Alumina, A. J. Moorhead, P. F. Bucher, R. J. Lauf, and C. S. Morgan	281	✓

INDUSTRY PERSPECTIVES—PANEL DISCUSSION

Industry Perspectives—Panel Discussion Summary	303	No
--	-----	----

ALTERNATIVE FUELS I SESSION

Utilization of Alternative Fuels in a Diesel Engine, S. S. Lutz, S. M. Geyer, and M. J. Jacobus	307	✓
The Ability for Conventional IC Engines to Run on Fuels Derived from Coal and Oil Shale, J. R. Needham, S. R. Norris-Jones, and B. M. Cooper	317	✓
Effective Value of Evaporation Constant for Hydrocarbon Fuel Droplets, J. S. Chin and A. H. Lefebvre	328	✓
Identification and Evaluation of Optimized Alternative Fuels, Norman R. Sofar, John A. Russell, Thomas W. Ryan, III, and Timothy J. Callahan	333	✓

ALTERNATIVE FUELS II SESSION

Summary: Report of Hydrogen SI Engine Research, Robert R. Adt, Jr., Michael R. Swain, and John M. Pappas	349	✓
Gasoline Fuel Safety Assessment—Status Report, M. C. Krupka, F. J. Edelkuty, J. R. Bartlett, and K. D. Williamson, Jr.	359	✓
Research Investigation of Alcohol Usage in Spark Ignition Engines, L. H. Browning, J. F. Nebolon, and R. K. Peffer	367	✓
Evaluation of Fuel Additives to Reduce Engine and Fuel System Material Problems with Methanol-Gasoline Blends, C. F. Rodriguez and J. P. Cuellar, Jr.	377	✓

PROGRAM OVERVIEW

Good morning ladies and gentlemen--and welcome to the Twentieth Automotive Technology Development Contractors' Coordination Meeting.

As indicated in your programs, the Conference this year will contain some new features. First of all, there will be no concurrent sessions. Concurrent sessions were the major complaint received from former conference attendees, and every effort has been made to streamline program activities so concurrent sessions were not required. We have also added an innovation called the Industry Perspectives Session on Wednesday afternoon. Scheduled at the conclusion of the engine technology presentations, this open forum has been included to encourage constructive feedback from industry aimed at improving program content, technology transfer, and government-industry cooperation.

At this time last year, at our last conference, the program and funding for vehicle propulsion R&D had not been finalized for FY 1982. On December 23 the Appropriation Bill, which includes our budget, was signed. Total funding authority was \$37.7 million, with \$33.5 million programmed for vehicle propulsion technology and \$4.2 million for alternative fuels. In addition to an overall reduction in budget, the program was also refocused in FY 1982. As part of the National Energy Policy Plan of 1981, all government agencies began withdrawing or reducing federal support from programs where sufficient market incentives exist to accomplish their objectives. Our programs initiated a re-orientation away from commercialization, demonstration, or specific product related activities, and concentrated on proof-of-concept type development rather than final product designs, on high-risk high-payoff long-term technology barriers where the high risks involved prohibit industry "going it alone", and on generic research which had the potential for widespread applications.

The refocusing had several impacts on our FY 1982 activities. All near-term development or demonstration projects were phased out, and no new projects with short-term objectives were initiated. The gas turbine and Stirling engine programs were transitioned from full engine system type projects to a proof-of-concept structure where fewer engine builds are required and achievement of objectives is measured by dynamometer evaluations of test-bed engines. This structure allows for a shift of responsibility in areas such as powertrain development, vehicle integration, and final engine design to industry, with government's principal function limited to proof of the basic concept. This shift is in line with the overall emphasis on supporting critical technology needs, and the general concentration on fundamental technological barriers. During FY 1982 significant effort was expended, particularly in the area of heavy duty transport technology development, to promote widespread industry involvement not only in the solution of technical problems, but in their identification and characterization.

Major FY 1982 activities were centered in four areas. In the automotive gas turbine area, the first build and preliminary evaluations of proof-of-concept test bed engines were completed by both industry teams involved in the program. In parallel, a continuing effort on development of ceramics processing and materials technology was carried out. In the Stirling automotive engine program, the first build of a U.S. manufactured test bed engine was completed, and dynamometer evaluations of the MOD I design, including transient performance were accomplished. Transfer of the Swedish technology base to the U.S. contractor, including comprehensive test cells and facilities, was also completed. In the heavy duty transport area, a wide range of research and development projects were initiated with emphasis on advanced uncooled diesel engines and waste-heat utilization. And finally, in the alternative fuels areas, efforts were continued to expand the technical data base for alcohol, gaseous, and synthetic fuels utilization. All of these activities will be covered in some detail in the sessions today and during the next three days, along with specific results and accomplishments.

What is the outlook for FY 1983? As far as the budget is concerned, again this year the program and funding are not finalized. The administration request to Congress for funding in our area is \$2.28 million. This request reflects the administration's thrust to redirect energy conservation research away from end use products toward more general research with a wide application. Under this approach, all end-use oriented technology development programs will be phased out, and specific projects in basic ceramics materials research continued. In contrast, the House Subcommittee on Transportation, Aviation, and Materials made a recommendation to the Appropriations Committee, considered a majority opinion, of \$41.4 million for our programs in FY 1983 covering basically the same project areas as FY 1982. The House Subcommittee on Energy Development and Applications made a recommendation to the Appropriations Committee, considered a minority opinion, of \$30.6 million, reflecting some reduction over FY 1982, mainly in the alternative fuels area. However, to date there have been no official appropriation actions on which to base a meaningful forecast of final budget authority.

Again this year, we are operating under a continuing resolution. The main impacts of the resolution are in three areas until FY 1983 appropriations are finalized. First, all FY 1982 programs and activities are to be continued at FY 1982 funding and planning levels. Secondly, there are to be no new program starts or program terminations unless specifically spelled out in the resolution. There were no such actions in our area. And lastly, there are to be no significant reductions in employment levels below those in effect on 9/30/82. The resolution actually runs until December 17, 1982 under the assumption that an actual appropriation bill will be enacted by that date.

What can we expect during FY 1983? It is clear that there will be a continuing focus on long-term, high-risk, potentially high-payoff basic research as the government's role—with an expanded reliance on the private sector to bring new technologies to the marketplace. It is also clear that there will be continuing budgetary pressures to restrain spending and carefully evaluate program priorities to maximize utilization of limited available funding. A key resource, the project management services provided by the NASA Lewis Research Center, will be continued in FY 1983. And finally, it is certain that ceramics technology development will be the dominant R&D activity throughout our program agenda.

Albert A. Cheneas, Director
Technology Development & Analysis Division
Office of Vehicle and Engine R&D

STIRLING TECHNOLOGY SESSION

An Overview of the U.S. Department of Energy's Automotive Stirling Engine Technology Development Program

Patrick L. Sutton
U.S. Department of Energy
Washington, DC

ABSTRACT

Presented from the point of view of the U.S. Department of Energy's Program Office, the overview is a synopsis of the Automotive Stirling Engine Technology Development Program's accomplishments of the 1981-82 program year and the program's current status. The MOD I Stirling engine is the focal point of the program. Four MOD I engines have been and continue to be tested and evaluated. Areas of study include: power and efficiency; materials and component development, including use of ceramics; engine downsizing and packaging; hydrogen containment; durability/reliability; multifuel capability; and others. Upcoming program-sponsored projects are briefly described.

THE AUTOMOTIVE STIRLING ENGINE TECHNOLOGY DEVELOPMENT PROGRAM, sponsored by the U.S. Department of Energy (DOE), has made excellent progress in the 1981-82 program year, particularly in light of the very difficult task it has undertaken - building a better automobile engine. Important steps forward have been made in all areas critical to engine acceptance.

This overview of the program, presented from the point of view of the DOE Program Office, focuses on the accomplishments of the past year and provides a summary of the current status of the automotive Stirling engine and the research and development program.* Progress in the areas critical to engine acceptance is briefly described. These areas include:

*This overview is based on the opening remarks of the author as leader of the Stirling engine session of the 1982 Automotive Technology Development/Contractors' Coordination Meeting, October 25-28, 1982, in Dearborn, Michigan.

the MOD I engine; power and efficiency; materials and component development, including the use of ceramics; engine downsizing and packaging; hydrogen containment and its effects on durability/reliability; and multifuel capability.

THE MOD I ENGINE

The MOD I engine is the backbone of DOE's program. It is an engine which has been designed, built, and is now being tested within the DOE-funded program. The DOE now has four of these engines under testing. Two are at United Stirling of Sweden (USAB) - one is used for component development and another for durability testing. A third engine has been installed in a test vehicle and is used for transient performance and control testing at American Motors General. The fourth engine was built at Mechanical Technology, Inc. (MTI) with many components that were manufactured in the United States. MTI is using this engine for component development.

To date, under DOE program-sponsored testing, the total accumulated engine hot running time is over 1,300 hours. Based on the results of testing an earlier design, the P-40, the MOD I engine is an improved design which has resulted in increased reliability.

POWER AND EFFICIENCY

The power and efficiency measured in the testing are very repeatable and agree well with the predictions from analytical computer models. All major program milestones including steady state and transient engine characterization have been met on schedule. The transient testing, which includes the U.S. Environmental Protection Agency's (EPA's) CVS emissions and fuel economy testing, has yielded predictable and repeatable results.

MATERIALS AND COMPONENT DEVELOPMENT

Both the P-40 and MOD I engines have heater heads made from the same materials. The cylinder and regenerator housings are investment cast from Haynes Stellite 31, a cobalt-base alloy, and the tubes are made of Multimet N155 which has a high cobalt content. Both engines are intended to operate at a heater head temperature of 720°C.

The current component development is directed at uprating the MOD I engine by incorporating components with improved technology. This effort is called MOD IA and is scheduled to be tested on an engine in April 1983. An important feature of the MOD IA is the incorporation of low-cost, nonstrategic heater head materials.

For example, the MOD I engine contains approximately 22 pounds of cobalt. The MOD IA will contain no cobalt, and its heater head temperature is designed for a 100°C increase to 820°C. The selected casting material is XF818 and the tube material is CG-27. These materials were qualified by testing in a P-40 engine for 1,500 hours at 820°C.

CERAMIC MATERIALS - The topic of ceramic materials is very popular today in the circle of advanced heat engines researchers/engineers. The use of ceramics has been encouraged primarily by the gas turbine industry. The adiabatic diesel is also very attractive. The Stirling engine development program is in a position to take advantage of this exploding technology and is actively seeking new research projects in ceramic concepts for application to the automotive Stirling. Three such projects are described below:

- The National Aeronautics and Space Administration (NASA) issued a Request for Proposals (RFP) in July for a Ceramic Automotive Stirling Engine Study. Proposals have been received and are in the final stage of the evaluation process - two proposals are being given strong consideration at this time. The selection decision is expected in the very near future.

- An open cell silicon carbide (SiC) foam material is being evaluated for a regenerator matrix material. Rig testing to date indicates that this material will perform better than the fine screen material currently in use. The cost of this SiC materials is predicted to be one-tenth the cost of the screen.

- This item is a direct result of a gas turbine development. Coors developed a ceramic gas turbine air preheater for a General Motors (GM) turbine which looks very promising for a Stirling air preheater. MTI is preparing to rig test sample test sections of this technology, and if their rig tests are positive, MTI is planning for Coors to develop ceramic air preheaters for the Stirling engine.

DOWNSIZING AND PACKAGING

During the past year, MTI has been studying the downsizing of the automotive Stirling engine. Their study focused on a 45-horsepower engine for a 2,500-pound test-weight car. The results of this conceptual design study confirmed that there are no major problems in downsizing. The engine configuration selected packaged very well into a front-wheel drive Chrysler K car. The engine's specific weight was estimated to be 4.3 pounds per horsepower. Emphasis was placed on mechanical design to reduce cost, and it is apparent that the cost of the existing reference engine could be reduced considerably. The results of this downsized engine study are being incorporated into an updated reference engine design which will be completed in March 1983.

HYDROGEN CONTAINMENT

The goal for hydrogen (H₂) containment is a 6-month period between recharges. Toward this end, the program continues to address three major areas concerning the control of H₂ leakage: reduction of diffusion of H₂ through the heater head tubes; reduction of piston ring friction and wear; and improvement of piston rod seal durability.

By doping the H₂ charge with 1% carbon dioxide (CO₂), program researchers have reduced H₂ diffusion through the heater head tubes by a factor of 30. Sound progress has also been made in the area of piston ring development. Friction and wear have been reduced by a factor of 2 in rig tests and engine tests are expected to confirm this.

The third area concerning H₂ containment, piston rod seal durability, has received a lot of attention. The current engines are using a pumping-ring-type sliding seal developed by USAB. This seal has shown good results in steady state durability testing, but its durability has been somewhat erratic in automotive driving cycle loading. For the last few years, the program has been supporting fundamental studies on sliding pumping seals. It appears that these studies are now beginning to produce fruitful results. Analytical models of pumping ring seals are being used by researchers to understand how these seals work and how to design new seals. MTI's rig testing of a new seal has yielded some very promising results, and MTI is optimistic that it is near a major advance in the connecting rod seal.

MULTIFUEL CAPABILITY

About a year ago, a P-40 was tested at MTI using five different fuels: commercial low-lead gasoline, shale-oil-derived marine diesel, 10%/90% alcohol/gasoline, experimental referee-broadcut specification aviation turbine fuel, and commercial automotive diesel. No hardware changes were made to accommodate the different fuels. All data were collected under steady

state conditions with a total accumulation of 80 hours of engine running time. The tests concluded that the engine runs well on each of the five listed fuels, and the performance using each fuel is similar.

INDUSTRY EVALUATION

In addition to the projects in ceramics research previously described, a comprehensive industry testing project is currently going through the DOE procurement approval process. The project, entitled "Industry Test and Evaluation of MOD I Stirling Engines," has been established to provide independent testing and evaluation, by the automotive industry, of the developing Stirling technologies.

This project is expected to: (1) enhance the transfer of these technologies to U.S. industry; and (2) to provide a mechanism for the feedback of industry suggestions and recommendations into the mainline technology development efforts.

To carry out this project, two additional MOD I engines and appropriate spare hardware will be fabricated and delivered to the Government. These engines will then be loaned to qualified automotive companies for their independent testing and evaluation.

For purposes of this task, qualified automotive companies are defined as: (1) a major U.S. domestic automobile and/or light-duty vehicle manufacturer or an automotive and/or light-duty engine manufacturer, (2) owning or having access to appropriate engine test facilities in the continental United States, and (3) having the engineering and technical staffs required for engine development testing.

The test and evaluation efforts will be carried out by automotive company personnel at automotive company expense. The Government, through amendment to the MTI contract, will furnish the engines and provide the necessary training of company personnel in MOD I engine safety and operating procedures. The automotive companies will be asked to provide a written report of their evaluations and recommendations to the Stirling Engine Project Office so that any appropriate modifications can be made in project activities.

BUDGET STATUS

The DOE's Automotive Stirling Engine Technology Development Program has been administratively as well as technically successful. The program has proceeded on schedule and within its financial means during a time of uncertain and shrinking budgets in both public and private sectors. Currently, the Stirling program is operating under a continuing resolution; the DOE does not, at this time, have official Congressional marks or appropriations. However, recommendations by the appropriate Congressional committees for continuing the program vary between \$12 million and \$15 million for Fiscal Year 1983.

ACKNOWLEDGEMENTS

The high degree of success effected by the DOE's Stirling engine program is a direct result of many highly qualified people "doing their jobs" exceptionally well. The Program Office is deeply impressed with the progress that has been made and extends its highest praise to all of the people working under this program at Mechanical Technology, Inc. (MTI), United Stirling of Sweden (USAB), American Motors General, and the National Aeronautics and Space Administration (NASA).

The 4-95 Solar Stirling Engine - A Progress Report

Stan Holmanson
United Stirling-Sweden

Worth H. Percival
United Stirling-U.S.A.

ABSTRACT

The Stirling engine is shown to be an ideal choice for a solar plant. Solar dish systems are described and the elements of module efficiency are given. The United Stirling 4-95 engine background and the four required solar modifications are described, including lubrication system, induction alternator, control system and receiver. Past and present solar dish programs are outlined and recent solar engine test results from Georgia Tech and Edwards, CA. are given. An overall module efficiency of 27.8% was achieved. Finally, manufacture cost estimates are presented.

THE STIRLING ENGINE is an ideal choice for a solar power plant because it operates at high efficiency and from an external heat source. John Ericsson designed the first solar powered Stirling engine over 100 years ago. He used a concentrating mirror, which was kept pointed at the sun, with the engine's cylinder at the focal plane. Engine thermal efficiency estimated from catalog data was about one percent.

Today we combine the engine and the concentrating mirror in essentially the same way Ericsson did. The difference is that the power density of the engine has increased three orders of magnitude and its thermal efficiency now exceeds 38 percent. An obvious rule is, the higher the engine efficiency, the smaller the mirror. Since the mirror system--termed the parabolic dish--is several times more expensive than the engine, thermal efficiency has a leverage effect on overall cost.

SOLAR DISH SYSTEMS

Presently, the point focusing solar dish systems utilize parabolic concentrators ranging from about 6 to 15 meters in diameter. The concentrator is mounted on a two-axis tracking mechanism that allows it to accurately follow the sun throughout the day. Each dish furnishes concentrated solar energy to its own individual receiver and power conversion unit (PCU), in contrast to central receiver systems which employ a field of reflectors (heliostats) to concentrate solar energy into a single receiver located on top of a tower. The dish system is a modular or distributed system. Whereas for the central receiver system the entire field and tower must be completed before generating power, the modular dish system has the potential to furnish power as soon as the first dish is installed. For the near term applications, the PCU will drive an induction generator and the modules will supply electric power to a utility grid for oil and gas displacement and peak shaving. In the future, stand-alone applications will be considered, such as for small villages, islands, industrial and military installations.

Solar dish system efficiency, from solar input to electrical power output, is the product of concentrator efficiency, receiver efficiency, net PCU efficiency (auxiliaries included), and generator efficiency. If the PCU is the Stirling engine, the resultant overall efficiency ranges from 26 to 28 percent, based on state-of-the-art technology. With improvements in receiver, engine and generator designs, overall efficiency is expected to ex-

ceed 30 percent in the near future.

Additional benefits of the Stirling engine in a solar dish power system include: thermal efficiency insensitive to engine size and rated power; excellent part load performance; the hybrid option--the potential to operate under cloud cover and at night by means of fossil fuel combustion with a special receiver; all components mass producible--a vital consideration for systems cost reduction.

THE 4-95 SOLAR STIRLING ENGINE

BACKGROUND - The solar Stirling engine has its roots in the United Stirling development program going back to 1972 when the decision was made to concentrate on four cylinder double-acting designs, rather than the classical displacer type. Double-acting engines have proven to be lighter, more compact and less costly compared to multi-cylinder displacer engines.

In 1975 a new four cylinder double-acting 40 kW engine was designed and first tested in 1976. Originally termed the P40, it is now designated the 4-95, having a displacement of 95 cc/cylinder. The design objective was to achieve a reliable experimental engine for the development of specific components.

A cross section of the 4-95 engine, equipped with its external combustion system, is seen in figure 1.

Twenty-five 4-95 engines have been built for in-house use, as well as for testing by government and private organizations in this country, Britain, France, and West Germany. An earlier version of the engine also played a key role as the baseline engine in the DOE/NASA ASE program. As of September, total test time for all 4-95 engines on dynamometers and in demonstration programs exceeds 29,500 hours. The longest time on one engine is 11,500 hours.

The 4-95 has been tested in such varied applications as in generating sets, passenger cars, a van, heat pump drive and a submersible. Its heat sources have included gasoline, diesel fuel, methanol, natural gas, wood chips, biomass gas and solar energy.

CONVERSION FOR SOLAR APPLICATIONS - Modifications to the 4-95 engine for solar applications during 1980-81 consisted mainly of the removal of combustion system components, rather than developing new components. Figure 2 shows a cross section of the solar Stirling engine. As can be seen in com-

parison with figure 1, the solar version is virtually a "naked" engine. It is simple even in comparison to a IC engine, not requiring a valve mechanism, injection system or ignition system. This simplicity results in far greater reliability. The solar engine does not need any of the following major components, essential to the combustion system, which are the main source of maintenance problems:

Blower drive gear	Igniter
Air preheater	Fuel pump
Combustion chamber	Air atomizing pump
Fuel nozzle	Fuel/air controls
Turbulator	Emission controls
Combustion blower	Air, fuel, exhaust ducts

Each of the above 12 items are assemblies, comprised of many parts. In addition, the solar engine driven accessories include only a water pump. The efficiency of the solar engine is higher than the fossil fueled engine because of the absence of parasitic losses associated with the combustion air blower and variable speed drive gear. The combined advantages of fewer parts, higher efficiency and greater reliability increases the cost effectiveness of the solar Stirling engine.

Specific modifications to the 4-95 engine for solar power have included: 1) the design of a "dry sump" lubrication system suitable for inverted operation, 2) integration of an induction generator with the engine, 3) a simplified control system, and 4) the design of a "solar-only" receiver and engine heater (solar absorber) to match the solar flux pattern from the concentrator. Items 1 and 2 were done under contract from JPL in late 1980. Items 3 and 4 were initiated and funded by United Stirling, beginning in 1981.

The lubrication system changes for inverted operation included machining numerous holes and slots to form oil drain passages in the crankcase bulkheads. To further assure dry sump operation under dynamic conditions, an external scavenging pump was installed, driven from one of the crankshafts. The external pressure lubrication pump was fitted adjacent to the scavenge pump. An external oil drain tank was installed below the lowest drainage point and connected to crankcase outlets by short pipes.

The generator was based on a commercial 3 phase, 25 kW induction motor of recent design. An induction motor operates as a generator without any modifications, if connected to a grid.

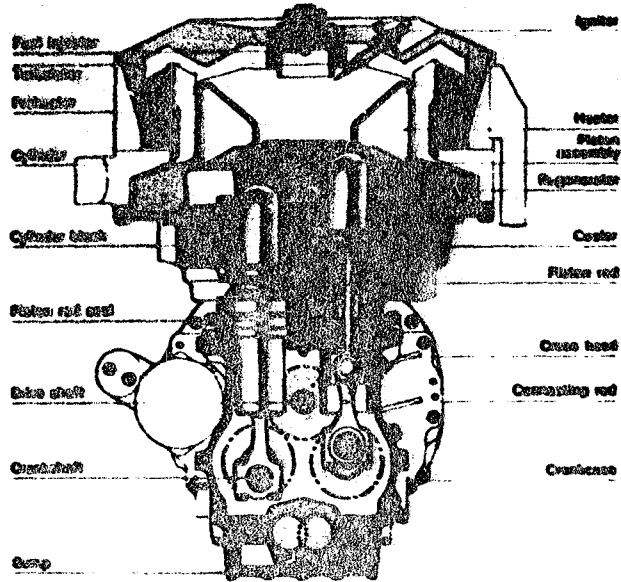


FIG. 1 - CROSS SECTION OF 4-95 STIRLING ENGINE

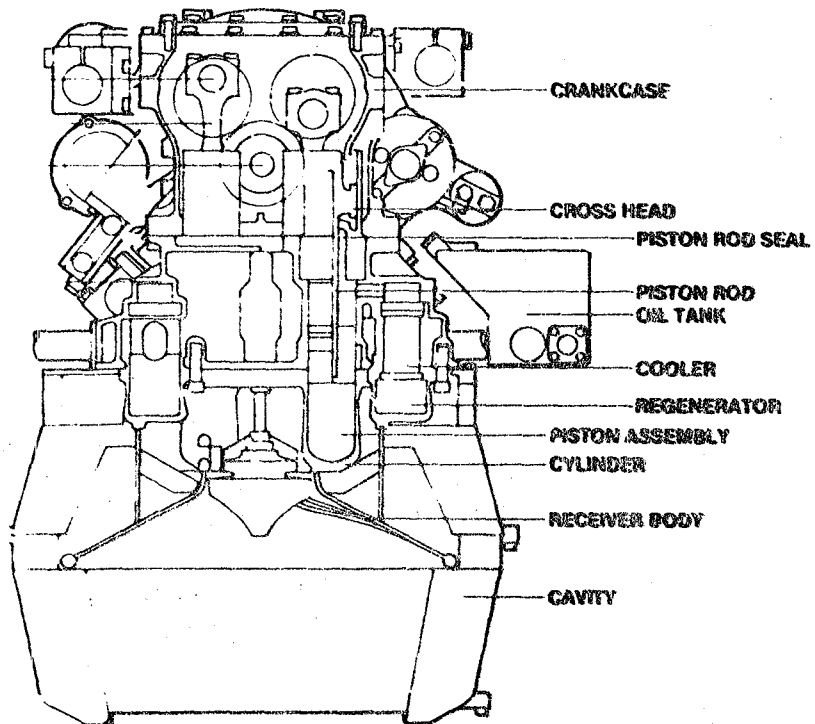


FIG. 2 - SOLAR STIRLING ENGINE

when its speed slightly exceeds synchronous speed (1800 rpm). The grid establishes the voltage and frequency and also provides the excitation. Peak efficiency is about 93 percent. It is driven directly from the engine through a flexible coupling, and was integrated with the engine crankcase by an aluminum inter casing. The engine is started from the grid by the induction machine, when the heater temperature reaches about 500°C. Power factor is corrected to about 0.95 by capacitors.

Control system changes were mainly directed at simplifying the automotive controls. The principle of controlling engine torque by varying mean gas pressure was again continued. Whereas in a combustion engine the heat input is controlled so as to follow the load changes, in a solar engine the heat input (insolation) cannot be controlled. Therefore, engine power must be adjusted to match the solar input at all times. This is done in two ways. First, engine speed of 1800 rpm is kept constant by the induction alternator when connected to a 60 Hz grid, and the alternator matches output current to engine torque from idle to full load. Second, the output from thermocouples on the heater tubes, in conjunction with an electronic digital control unit, actuates solenoid gas valves to maintain constant temperature by increasing or decreasing torque. If the heater temperature exceeds a set point (about 720°C), a valve admits additional gas (hydrogen or helium) which increases torque (and hence power) to reduce the temperature. Conversely, with a decrease in temperature, a second valve allows gas to be pumped back to a storage bottle. Should the engine overspeed, due to a loss of grid for example, a third solenoid valve acts to short circuit the engine working spaces which drops torque in a fraction of a second. The electric valve system does not have the very fast response of the automotive hydraulic-servo control, but it is a lower cost system and quite adequate for the slower input variations from a solar concentrator. Figure 3 shows a layout of the control system.

The solar receiver is considered by United Stirling to be an integral part of the engine. In the case of Brayton or Rankine cycle machines the receiver is usually considered as a separate component. This is also possible for the Stirling if an intermediate heat transfer loop were used--a sodium heat pipe for example. The present solar-only Stirling receiver consists of the following three major components:

- 1) The engine heater assembly, shown in figure 4 and sometimes called the receiver body, which is a tubular heat exchanger in the form of a cone designed to match the solar flux pattern. The solar rays impinge directly on the conical surface of tubes--there is no intermediate heat transfer medium. The engine working gas, hydrogen or helium, is contained within the tubes. The principal changes in the heater as compared to the standard automotive type heater are an increase in diameter from about 240mm to 400mm, and removal of all finned surfaces.

- 2) The receiver cavity surrounding the engine heater, which consists of a sheet metal housing with internal "white" insulation shaped to prevent radiation and conduction losses.

- 3) An aperture plate or cone which is located at the mouth of the receiver cavity. It has a round aperture of about 200mm diameter at the focal plane, which is about 300mm from the apex of the heater cone. The aperture is sized to capture approximately 99% of the focused solar beam and hence minimize radiation and convection losses. The solar rays, after passing through the aperture, diverge to produce a uniform flux distribution over the heater tube surfaces, in the ideal case. Solar intensity on the heater surface is about 60 watts/cm² (about 600 suns) when insolation is 1 kW/m².

Also shown in figure 3 is an artist's rendition, of the complete solar Stirling powerplant including the 4-95 engine, induction generator and receiver, in its orientation at the solar zenith.

SOLAR DISH PROGRAMS

Interest by United Stirling in solar thermal power began in 1976 as a result of internal studies of future markets for Stirling engines. This marketing strategy was reviewed at the Fourth International Symposium on Automotive Propulsion Systems, in April 1977. It was concluded that solar energy was high on the list of attractive applications.

In August, 1977, DOE named JPL as manager of a program to develop solar point focusing parabolic dish technology. The assignment also included investigation of various power conversion units. NASA-Lewis was named to support the power conversion area.

DOE sponsored solar activities with United Stirling have included:

- 1) A NASA study in 1979 of a 15 kW

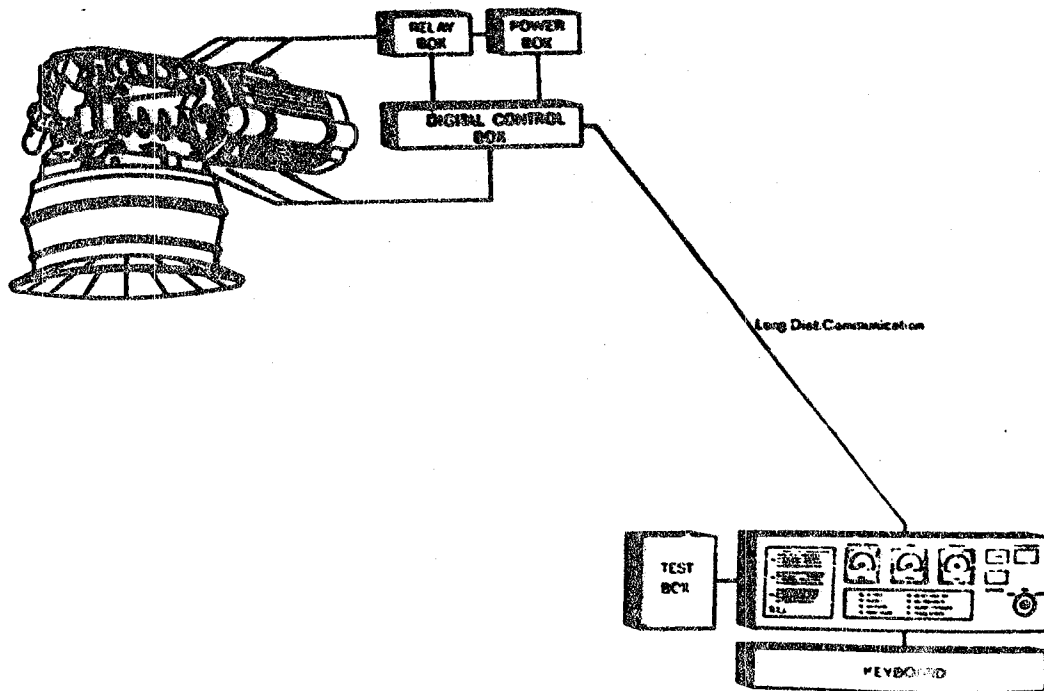


FIG. 3 - USAB DIGITAL CONTROL SYSTEM LAYOUT

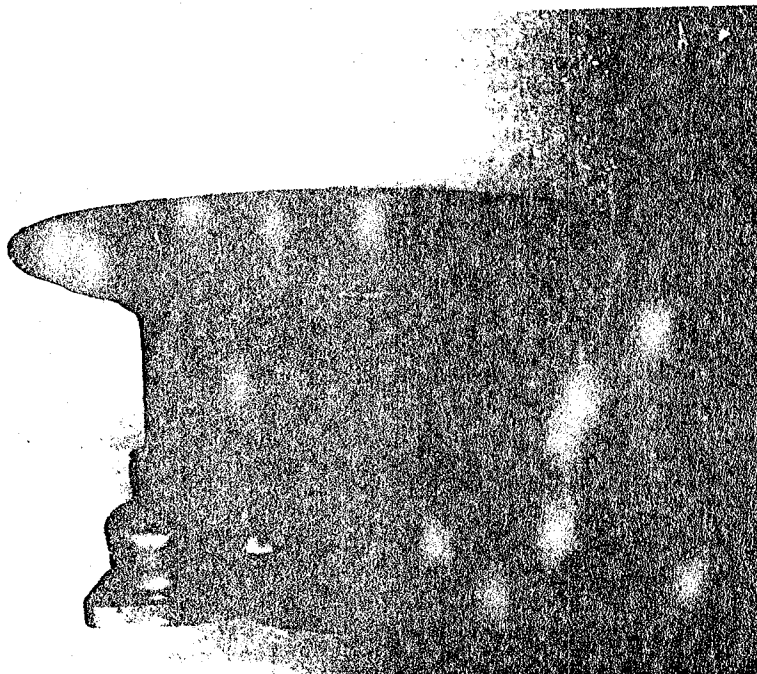


FIG. 4 - THE 4-95 SOLAR HEATER

kinematic solar Stirling engine optimized for design, performance and cost.

2) A JPL contract in 1980 to modify a 4-95 engine for inverted operation and integration of the engine with an induction alternator and a hybrid (solar plus gas fuel heated) receiver designed and constructed by Fairchild-Stratos. The complete PCU was tested on the JPL Test Bed Concentrator (TBC) at Edwards, California in 1981.

United Stirling in-house funded solar activities have included:

1) Modification of another 4-95 engine for inverted operation and integration with a solar-only receiver and induction alternator. The PCU was tested at the Georgia Tech solar facility in 1981, to be described later.

2) Further modification of the above 4-95 engine to include a digital power control system and an improved engine heat exchanger (solar absorber). Testing of the PCU at Edwards during 1982 will be described later.

The most recent solar program, now in progress, involves a cost sharing contract between DOE and a team of 8 contractors, including United Stirling. It is termed the Vanguard project and is aimed at the development of a commercial prototype dish-Stirling module to be installed at Palm Springs in 1983. The contract also calls for marketing and engineering studies of multi-module farms.

In the 1977-79 time frame, DOE apparently believed the preferred ranking for solar heat engine cycles was Rankine first, Brayton second and Stirling third, based on what they perceived was the state of development for small powerplants in the 15-25 kW range. Today the order has been practically reversed. Total running time on solar dish powerplants is, for Stirling 360 hours, for Rankine 33 hours, while the Brayton is scheduled to start running in January, 1983.

What has happened to change the picture? First, the state of Stirling development overseas at United Stirling was not well known, and the state of development of small Brayton and Rankine cycle turbines was somewhat overestimated; and second, in 1980, United Stirling made a strong commitment to solar power as the primary target for commercial development of their engines. Production of the model 4-95 solar engine is expected to begin in 1984.

UNITED STIRLING SOLAR TESTS

GEORGIA TECH - The Georgia Tech solar site is a small central receiver system comprising a field of 550 glass mirrors,

each 3 feet in diameter. The mirrors track the sun and focus onto a 70 foot high tower platform. In 1981 United Stirling contracted to test a 4-95 engine inverted on the platform with the induction generator connected to the Atlanta grid. The program was intended to parallel the JPL program and provide experience with several solar-only receivers recently designed at United Stirling. In spite of weather problems, this pioneering effort in modern solar electric power accomplished its goals. After adjustment of the system, over 18 kW was fed to the grid on November 18. Achievements of the program included: Three solar-only engine heat exchangers were successfully tested for the first time under sunlight intensity roughly equal to that from a parabolic dish concentrator; the 4-95 solarized engine proved itself in the solar environment, performing as designed with automatic temperature control and without requiring maintenance during the 35 hours of test running. A total of 175 kW hrs were fed to the grid. The 4-95 engine on the tower platform is shown in figure 5.

EDWARDS, CALIFORNIA - In 1982 United Stirling and JPL agreed to cost share a test program, with JPL supplying the TBC and United Stirling a 4-95 engine similar to the one tested at Georgia Tech. Testing was to be done at JPL's Parabolic Dish Test Site located at Edwards Air Force Base in the Mojave Desert, California. The TBC is an 11 meter diameter dish, constructed of 224 individual mirrors (facets) which are mounted on a steel truss framework. It is shown in figure 6. Each mirror has a spherical curvature and can be adjusted to optimize the solar flux pattern for a particular PCU. In the case of the 4-95 engine this was done so as to match the heat exchanger surface and avoid spillover beyond the 400mm outer circle as well as on the center conical plug (see figure 2). With all facets uncovered, the TBC can deliver as high as 80 kW through a 200 mm aperture.

Engine testing has been going on since January, except for interruptions resulting from other JPL scheduled activities with the TBC, including flux mapping, realignment of facets, and testing of heat resistant materials in the focal zone.

The engine test program has involved comparing and measuring engine performance:

- o for two solar heat exchangers
- o for two electronic control sys-

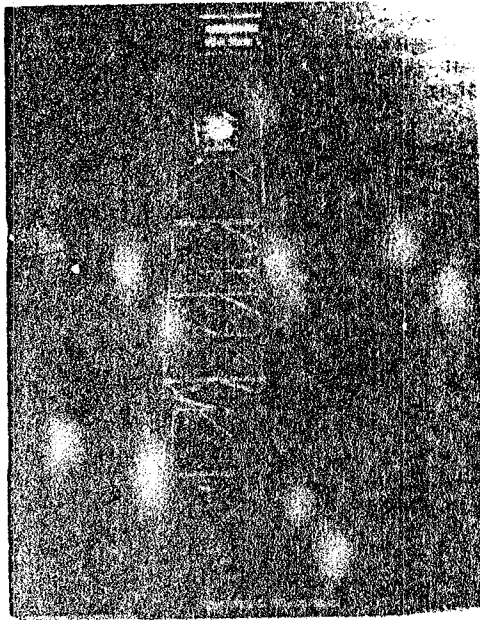


FIG. 5 - SOLAR TOWER AND 4-95 ENGINE AT GEORGIA TECH

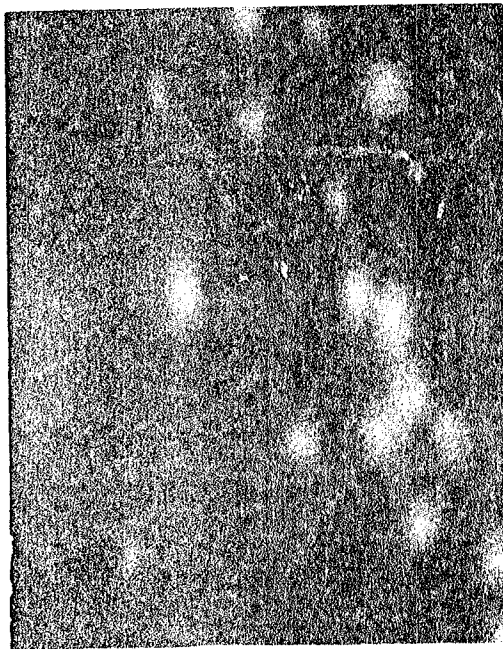


FIG. 6 - JPL TEST BED CONCENTRATOR

- tems
- o for two gases
- o for several facet alignments
- o for several receiver positions
- o for a range of heater temperatures

Figure 7 is a view of the solar 4-95 with receiver and generator ready for installation in the TBC.

The only engine related forced outages in 360 hours of running have been a fatigue failure of a piston rod at a misaligned hole, and a leak in a heater tube at a welded seam--current practice is to use only seamless tubes. Basic engine availability, defined as the ability to start running when scheduled, weather permitting, has been very high--exceeding 98 percent. No leakage problems with the PL piston rod seals have occurred and the cylinders have remained dry and free of oil. This is particularly significant since the seals are operating from nearly horizontal to nearly inverted, in contrast to the vertical orientation of the combustion type engines.

The engine has been tested on both hydrogen and helium on the TBC, although hydrogen is preferred because of slightly better performance. Performance highlights on hydrogen include:

- o 25 kW electrical output at normalized insolation of 1 kW/M^2
- o 27.8 percent overall conversion efficiency
- o 250 kW hours generated in one day
- o 13.5 hours operation during July day
- o 35.9 percent PCU efficiency = $\frac{\text{electric output to grid}}{\text{thermal input to heater}}$

Figure 8 includes 3 sample plots of data from a July test showing insolation, power output and heater tube temperature, over one day. The horizontal marks are two hour increments. The oscillations in power in the morning are believed to be due to wind blowing into the open aperture which increases convection losses. Studies and tests are being made of special fused silica windows to reduce convection and radiation losses from the receiver.

Figure 9 is a bar graph illustrating power levels and efficiency breakdown for the complete module. The engine being tested at Edwards has been designated by United Stirling as the Solar I design. Planned continued development aims to upgrade the Solar I engine in terms of durability and reduced manufacturing cost. The upgraded engine, which is intended for high volume pro-

duction is called the 4-95 Solar II engine. Current development plans will result in production prototype drawings of the Solar II engines by November 1982 and start of testing of production prototypes by June 1983.

Current testing at Edward's test station of a 4-95 baseline solar engine will continue through the end of 1982 to support the design of the Solar II engine.

COST OF DISH/STIRLING SYSTEM

Production cost studies of the 4-95 engine have been made on a nearly continuous basis at United Stirling over the past 4 years. Additional 4-95 engine cost studies have been made by JPL and Pioneer Engineering of Detroit. Complete manufacturing documentation has been prepared for the solar engine.

During the past year, manufacturing cost studies of several proprietary solar dish designs have been made by Pioneer Engineering for a production rate from 100 to 100,000 annual volume.

Conclusions from the various studies indicate that a complete solar Stirling/dish system can be sold to a utility customer for under \$1800/kW, installed, in 1982 dollars. Levelized busbar energy costs are estimated at about 12 cents/kW hour. In the initial stages of manufacturing and marketing it is expected that third party financing will be used, and that both new equipment tax credits, as well as, federal and state solar tax credits will benefit the financing of solar programs.

Engine production is expected to take place in both USA and in Sweden. Final manufacturing plans will depend on economic conditions at the time. This year United Stirling has been cooperating with E.F. Hutton & Co. to locate a U.S. joint venture partner for the commercialization and marketing of the system known as the Parabolic Dish Stirling Module.

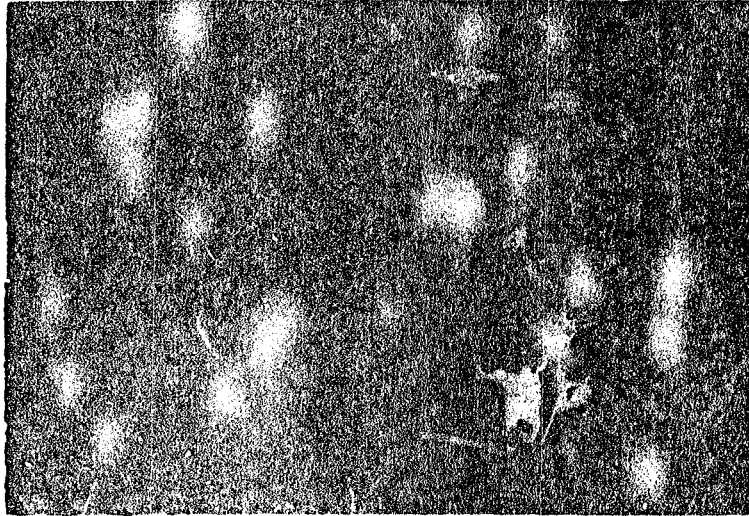


FIG. 7 - SOLAR RECEIVER AND 4-95 ENGINE

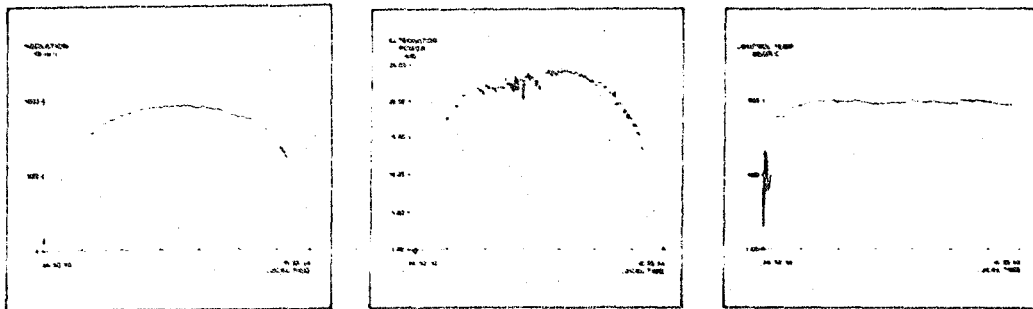


FIG. 8 - INSOLATION, POWER AND TEMPERATURE FROM JULY TEST

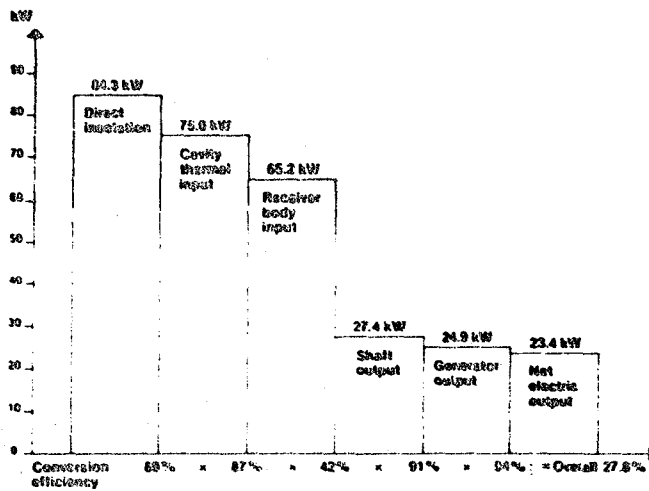


FIG. 9 - SYSTEM POWER LEVELS AND EFFICIENCY BREAKDOWN

Duf

Heat - Activated Heat Pump Development and Potential Application of Stirling Engine Technology

P. D. Fairchild
Energy Division
Oak Ridge National Laboratory
Oak Ridge, TN
C. D. West
Engineering Technology Division
Oak Ridge National Laboratory
Oak Ridge, TN

ABSTRACT

This paper presents a brief overview of the heat-activated heat pump technology development program being carried out by Oak Ridge National Laboratory (ORNL), for the Department of Energy's Building Equipment Research Division with emphasis on the Stirling engine technology projects. This paper 1) reviews the major projects as they were formulated and carried out under the previous "product development" guidelines, 2) discusses the revised technology development focus and current status of those major hardware projects, 3) presents our assessment of the key issues involved in applying Stirling engine technology to heat pump equipment, and 4) describes the approach and planned future activities to address those issues. For completeness, the paper also includes brief descriptions of two projects in this area supported by the Gas Research Institute (GRI).

HEAT-ACTIVATED HEAT PUMP DEVELOPMENTS

At ORNL we have been conducting inhouse research on heat pumps since 1976 and since 1978 we have been assisting DOE in managing a contracted R&D program involving advanced residential and commercial heat pump technologies. A major portion of the DOE/ORNL contracted R&D resources has been allocated toward development of heat-activated heat pumps. The rationale for this is based on the potential fuel efficiency improvement such a product could offer in combination with a large market potential.

PROGRAM RATIONALE AND PROJECT MAKEUP - Conventional combustion heating equipment (gas or oil furnace, for example) currently achieves about 75% efficiency and, when developed to its ultimate potential, can approach but not exceed 100% efficiency. Heat-activated heat pumps, of

which the gas-fired heat pump is the predominant example, offer a potential heating coefficient of performance (COP) exceeding 1.0, that is, delivering a heating effect greater than the heating value of the input fuel. A gas heat pump currently envisioned as a typical 1990's residential product should use 30 to 50% less gas than the advanced gas furnace, as illustrated in Fig. 1.

With regard to market potential, about 54% of the nation's 75 million homes are heated using natural gas, as shown in Fig. 2. Furnaces and other gas heating appliances generally have a 15-20 year life expectancy, which creates a continuing replacement/retrofit market of about a million units per year. With addition of new homes, the potential market in residential heating alone is estimated at approximately 1.5 million units annually. With the cooperative support of the gas utility industry, the gas heat pump is emerging as an important option for improved fuel efficiency in residential and commercial buildings in the 1990's if its viability in the marketplace can be established.

There are two basic types of heat-activated heat pumps. The first uses an absorption cycle and the second replaces the electric motor of the conventional electric heat pump with a fueled prime mover (engine-driven). Of course, one of the key advantages of the heat-activated system is that in the heating mode, waste heat can be recovered to augment the heating effect produced by the heat pump cycle, as shown in Fig. 3, thus increasing the heating capacity and COP significantly. In most cases, systems developed for use with natural gas can also be oil-fired with appropriate modifications to the combustion system.

Development projects to date have included two absorption and four heat engine-driven heat pump concepts. The general strategy when these major projects were selected involved supporting

* Research sponsored by the Office of Building Energy Research and Development, U.S. Department of Energy, under contract W-7405-eng-26 with the Union Carbide Corporation.

FUEL UTILIZATION OF ALTERNATIVE HEATING SYSTEMS

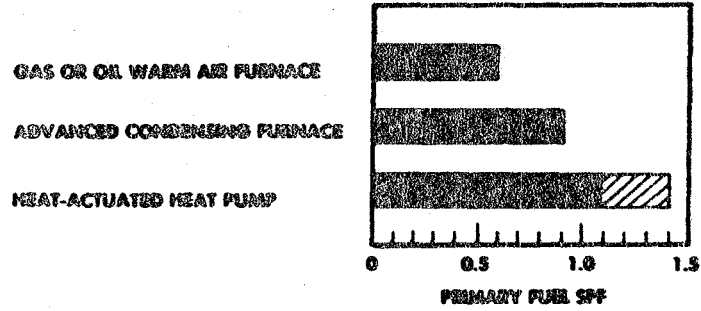
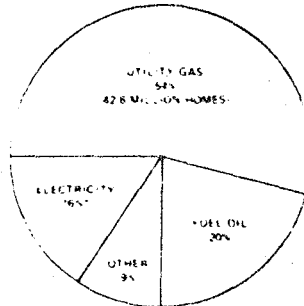


Fig. 1

DISTRIBUTION OF HOME HEATING ENERGY SOURCES
78.6 MILLION HOMES*



*ELECTRIC HEAT PUMPS INSTALLED IN APPROXIMATELY 2 MILLION HOMES
3% OF TOTAL HOMES!

SOURCE: AIR CONDITIONING, HEATING, AND REFRIGERATION NEWS,
JULY 23, 1979; APRIL 7, 1980; JANUARY 5, 1981 ISSUES

Fig. 2

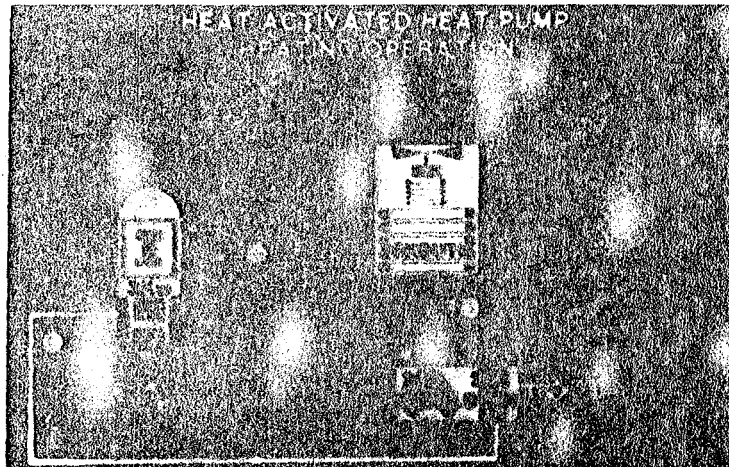


Fig. 3

different concepts with differing levels of risk and ultimate performance potential. Absorption heat pump technology was viewed as being more well-established and, thus lower risk, because of similar commercially available equipment (i.e., absorption chillers and gas air conditioners). However, it offered only moderate fuel efficiency improvement. Heat-engine-driven technology, on the other hand, seemed to entail higher technical and business risk, but offered more dramatic performance gains. Table 1 compares the assessed risk and efficiency objectives for the concepts selected for major prototype development efforts.

REVIEW OF PROTOTYPE SYSTEM DEVELOPMENT

PROJECTS - The absorption heat pump prototype development projects are summarized in Table 2. One of these systems, developed by Allied Corporation and Phillips Engineering Company, uses an unconventional organic-fluid working pair: ETFE (ethyl-tetrahydrofurfuryl ether) as the absorbent and R-133a as the refrigerant. The second absorption project, a heating-only system developed by Arkla Industries, Inc., utilizes ammonia and water as working fluids and employs technology used by Arkla in an existing line of residential gas-fired absorption air-conditioners. As indi-

cated, both of these development projects have been carried out successfully through laboratory prototype testing. Both projects yielded prototype hardware which achieved the target heating COP of 1.25 in laboratory testing. In contrast, the two heat-engine-driven projects selected early for prototype heat pump system development, i.e., the Stirling/Rankine and Brayton/Rankine projects, have experienced serious technical problems and have thus far failed to achieve their prototype performance targets. The two projects are summarized in Table 3

The free-piston Stirling engine (FPSE) system developed by General Electric Company (Advanced Energy Programs Department, Valley Forge, PA), uses an inertia compressor integrally coupled to the FPSE such that the engine/compressor assembly acts as a single spring/mass resonating system. As indicated, two iterations of prototype hardware failed to meet performance targets and current efforts are more limited, concentrating on technology development aspects of engine/compressor coupling dynamics and engine performance diagnostics.

The second heat-engine projects, scaled for application in commercial buildings, is being developed by AiResearch Manufacturing Company of

Table 1. Comparison of performance potential and risks for EAHP concepts

Concept/Technology	Assessed Risks (technical and business)	Target COP ² for Prototype Hardware (heating/cooling)
Absorption cycle (single stage)	Moderate	1.25/0.50
Gas-turbine-driven (Brayton/Rankine)	Moderate to High	1.30/1.00
Free-piston-Stirling engine driven (Stirling/Rankine)	High	1.60/0.85

²Target fuel COP at rating point of 8.3°C (47°F) ambient for heating and 35°C (95°F) for cooling, where fuel COP is defined as the heating or cooling effect divided by the energy value of the fuel used. Target values are steady-state, excluding parasitics.

Table 2. Absorption heat pump projects

Description	Developer	Status/Accomplishments
• Organic-Working Fluids (R-133a/ETFE)	Allied Corporation ^a	• Lab prototype complete
• Single-Stage Cycle	(Phillips Engineering Major Subcontractor)	• Achieved 1.25 heating COP ^b
• Heat-Cool		
• Residential		
• Ammonia-water	Arkla Industries	• Lab prototype complete
• Single-Stage		• Achieved 1.25 heating COP ^b
• Heating Only		
• Residential		

^aAllied project cosponsored by the Gas Research Institute.

^bFuel COP at 8.3°C (47°F). Values are steady-state test results (excluding parasitics) for prototype hardware.

Table 3. Heat engine-driven systems heat pump prototype projects

Description	Developer	Status/Accomplishments
<ul style="list-style-type: none"> • Stirling/Rankine FPSE-driven spring/mass resonating engine compressor) • Heat/Cool • Residential 	General Electric ^a	<p>Two Prototype Iterations</p> <ul style="list-style-type: none"> • Proto 1 system tested at 1.2 COP_H vs 1.6 goal • Proto 2 engine 7 percentage points below η_{cycle} goal of 32% • Current UCC/ORNL project has technology focus
<ul style="list-style-type: none"> • Brayton/Rankine gas-turbine driven <p>(high speed rotating engine/compressor assembly)</p> <ul style="list-style-type: none"> • Heat/Cool • Commercial (rooftop) 	Garrett/AiResearch ^b (Dunham/Busch & Lennox Subcontractors)	<ul style="list-style-type: none"> • Brayton engine for proto heat pump 8 percentage points below η_{cycle} goal of 27% • Proto system assembly for functional test • GRI project near-term focus on engine η_{cycle} improvement

^aGE project cosponsored by the Gas Research Institute through 7/82.

^bGarrett/AiResearch project cosponsored by DOE and GRI through 9/82 under a subcontract with Union Carbide Corporation through Oak Ridge National Laboratory (UCC/ORNL).

California, a Division of Garrett Corporation. The system uses a gas turbine (Brayton cycle) engine driving a high-speed centrifugal compressor through a magnetic coupling. Figure 4 shows both the compressor and the Brayton engine side of that rotating assembly. Figure 5 shows a mock-up of the complete engine assembly, including the combustor, recuperator, and sink heat exchanger. Prototypes of this combustor/engine/compressor assembly have been fabricated and shipped to Dunham-Bush and Lennox for incorporation into heat pump system prototypes. However, to date the prototype Brayton engine assembly has only attained a cycle efficiency of 19% versus a 27% goal, despite extended testing and modification efforts. Therefore, assembly and testing of the prototype heat pump systems is being conducted more for operational checkout and to confirm hardware integration than for any

meaningful system performance results. The UCC/ORNL subcontract with AiResearch expired at the end of September 1982, but the project is being continued under the GRI contract. It is our understanding that GRI and AiResearch plan to defer the planned "Field Test" phase until another generation of prototype engine hardware is developed and tested at a cycle efficiency approximately five (5) percentage points above the current level (i.e., the prototype engine efficiency target revised to an approximate level of 24%).

PROOF-OF-CONCEPT ENGINE/COMPRESSOR PROJECTS — In addition, there are two heat-engine-driven projects aimed at laboratory proof-of-concept engine/compressor testing or so-called "bread-board" systems rather than prototype heat pump hardware. The concepts involved were considered to be in an earlier state of development, without

ORNL PHOTO 3759-80



Fig. 4

ENGINE ASSEMBLY MOCKUP

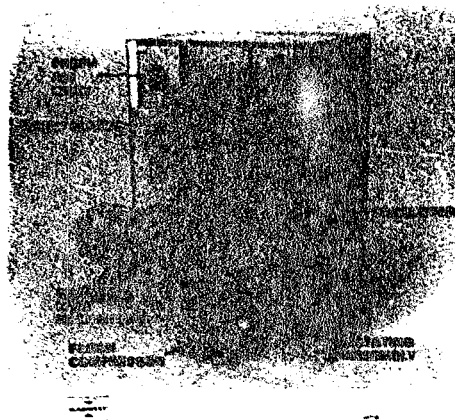


Fig. 5

sufficient "technology readiness" established to warrant prototype development. These projects are summarized in Table 4.

The breadboard engine/compressor development by Consolidated Natural Gas Research Company with Mechanical Technology Incorporated (CNG/MTI) together with the GE Stirling/Rankine project, will be covered in some detail in following sections of this paper.

The free-piston internal combustion engine/compressor development by Honeywell, Inc. (Technology Strategy Center) with Tectonics Research, Inc. uses a two-stroke, loop-scavenged, linear free-piston engine, designated the Braun Linear Engine, direct-coupled to drive the refrigerant compressor piston. Figure 6 shows a sectioned Braun Linear Engine/air compressor (the center section between the power cylinder and the work output/compressor cylinder houses a rack-and-pinion type balancing mechanism, which provides smooth, vibration-free operation). Figure 7 shows the refrigerant compressor being tested as a component (electric motor-driven).

Perhaps the most significant accomplishment under this project has been in the area of seal development. A proprietary hermetic bellows seal of infinite-life design has been demonstrated in

dynamic testing on the engine and in the separate compressor component tests. The final proof of this concept involves testing of the integral engine/seal/compressor assembly under refrigerant conditions representative of heat pump service. The breadboard system for this testing is shown in Fig. 8.

In addition to the heat-engine-projects being cosponsored by GRI and DOE, GRI is supporting two other HAHP projects, both Stirling engine-driven. Sumpower, Inc. is conducting a development project which involves a free-piston Stirling engine coupled to a Stirling cycle heat pump, the so-called duplex Stirling HAHP concept. The major advantage of such a machine is that it can be hermetically sealed in a single pressure enclosure and uses a single common working fluid in both heat pump and heat engine. A breadboard system test of the heat engine/heat pump assembly is scheduled for the near future. The other project involves the use of a kinematic Stirling engine to drive a conventional refrigerant compressor. That project is being conducted by Stirling Power Systems of Ann Arbor, Michigan.

APPRAISAL OF PRIOR HAHP DEVELOPMENT APPROACH - To summarize the heat-activated heat pump projects, our development experience has

Table 4. Heat-engine-driven proof-of-concept projects

Description	Developer	Status/Accomplishments
• Braun Linear Engine Compressor (free-piston, internal combustion, engine-driving integral compressor)	Honeywell (Tectonics Research, Major Subcontractor)	• Component development complete/novel seal • Lab "breadboard" system: proof-of-concept
• Stirling/Rankine FPSE-Driven (Diaphragm-actuated, hydraulic transmission for coupling to refrig. compressor)	CNS Research (MTI Major Subcontractor)	• Compressor/transmission development complete • FPSE verification • Lab "breadboard" system planned

ORNL PHOTO 4844-81

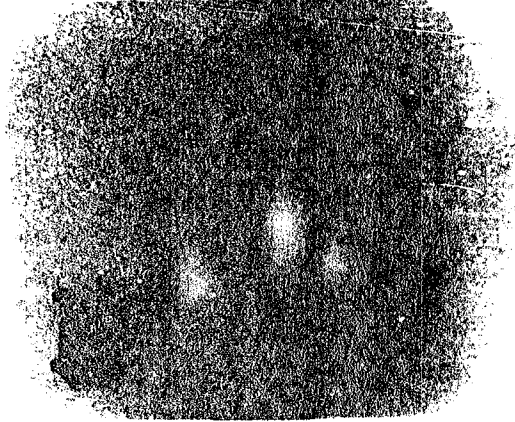


Fig. 6

ORNL PHOTO 8739-82



Fig. 7

ORNL PHOTO 8742-82

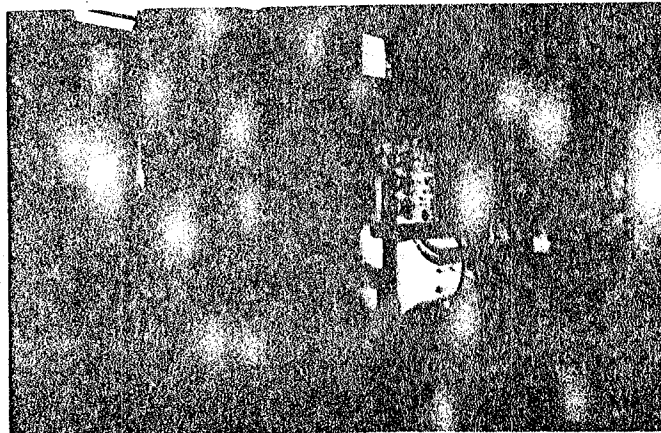


Fig. 8

confirmed the early assessment of the technical risks associated with some of the heat-engine-driven concepts in comparison to the absorption cycle concepts. But more importantly, it has illustrated the pitfalls associated with a "fast track" product development approach when there are still major technical uncertainties. In retrospect, a more measured, sequential approach involving verification of prime mover performance and engine/compressor integration before starting any work on the packaged heat pump system or attempting to analyze consumer acceptance seems to be a more prudent and cost effective approach than the one taken with the GE and AiResearch projects. Of course, there was considerable pressure in the late 1970's when those projects were started to accelerate development and commercialization of energy efficient, potentially viable products on the basis that the R&D investment would be quickly returned to the nation in reduced energy consumption. With that pressure reduced due to the present administration's different philosophy, the other two heat engine projects (which were in an early stage in 1981) were restructured to the present proof-of-concept engine/compressor developments. Decisions were also reached at that time to initiate phasedown of the absorption projects and the AiResearch project. Therefore, the General Electric (GE) project is the only one originally formulated and carried out under the previous "product development" philosophy that has been restructured to continue as a technology development activity.

STIRLING ENGINE-DRIVEN HAHP PROJECTS

Attention will now be focused on the free-piston Stirling engine technology area. The reasons for our interest in this particular heat engine involve several aspects, besides its potential for high efficiency, which would make it particularly well suited for HAHP application. First, the Stirling offers very low noise characteristics compared to a conventional internal combustion (IC) engine, since there are no

periodic explosions that have to be muffled and no valve noises. Since it uses external combustion and is thus more readily susceptible to exhaust cleanup, it offers low emissions. The free-piston configuration also offers the apparent advantage of pure linear motion with reduced side loads for low wear and long life potential.

The following two sections describe our experiences to date with the free-piston Stirling engine-driven development projects.

GE PROTOTYPE DEVELOPMENT PROGRESS AND REVISED FOCUS - A chronology of the major events during the course of the GE development work is presented in Wordslide 1. The GE engine/compressor configuration is illustrated schematically in Fig. 9, which includes a summary of the principal characteristics and design features. Heat input provided by the gas combustor provides thermal energy to the Stirling engine working fluid, helium, through the so-called "heater head." The displacer shuttles the helium between the hot and cold spaces thus generating the driving pressure wave for the power piston. The cold space temperature is determined by the cooler, which is water cooled. The regenerator provides thermal energy storage and (due to the large role of stored energy in this cycle) must have high effectiveness. The power piston is directly connected to the compressor housing with the refrigerant being compressed by another free piston (compressor piston) reciprocating within the housing. This is called a linear inertia compressor. The engine displacer and the engine power piston operate with a phase and displacement relationship that creates the Stirling thermodynamic cycle, as shown in Fig. 10. The figure also illustrates the phase and displacement relationship of the compressor piston reciprocating within the housing. Another variable, the refrigerant condition, is controlled by the external conditions imposed on the refrigerant by the building load and outdoor ambient conditions. Figures 11 and 12 are photographs of the first prototype (Proto 1) engine and compressor

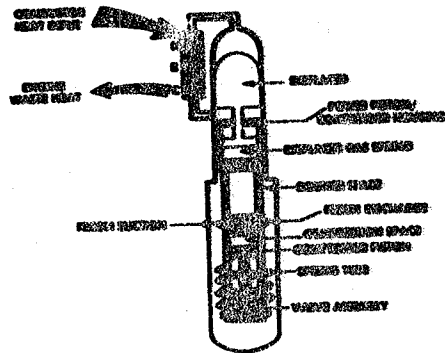
DNV/MS-23342

CHRONOLOGY OF GE DEVELOPMENT PROJECTS

- American Gas Association (AGA) and GE initiated Phase I program to evaluate HAHP's in 1975
 - result was selection of Stirling/Rankine concept for further development
- DOE joined with AGA and GE in 1976 for Phase II contract to accelerate development and demonstration of residential HAHP product
 - Gas Research Institute (GRI) replaces AGA in 1977
- Phase II Program involved two iterations of prototype hardware designated Proto 1 (completed early 1979) and Proto 2 (concluded in 1981)
 - performance/efficiency goals not attained
- Technology Development activities have continued under UCC/DOE subcontract (Phase III)

Wordslide 1

**FERTILIZER ENGINE/COMPRESSOR CHARACTERISTICS
AS COMPRESSOR**



- Free Water 4.0 Gp (4.0 lbs) before starting 4.0 Gp
• design pressure 60 bar
• Capacity 100 lbs
• $T_c = 60^\circ\text{C} (140^\circ\text{F})$
• design stroke 3.3 cm (1.3 in.)
- In-line In-line Compression (stroke-rolling)
- Ultrasonic Seal Features
- Method One Chamber (through-out sealed)

Fig. 9

**OPERATION OF FERT-FERTON STRIPPER ENGINE/
FERT-FERTON LINEAR COVERIDGE**

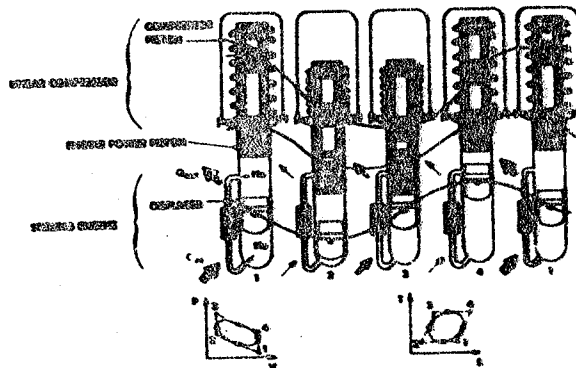


Fig. 10

ORNL PHOTO 4006-02

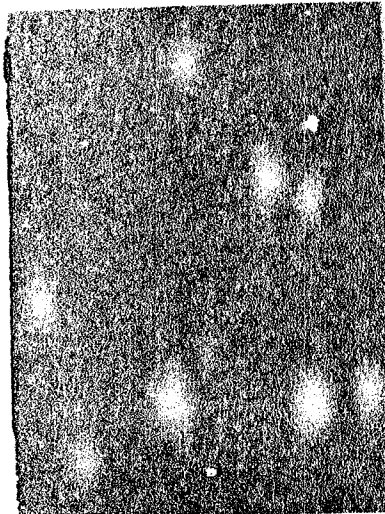


Fig. 11

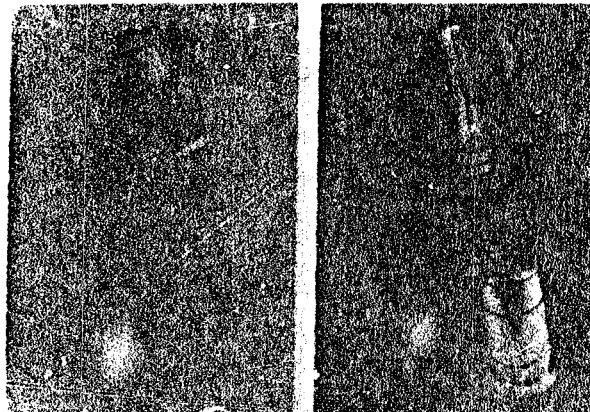


Fig. 12

hardware and Fig. 13 shows the fully-assembled prototype outdoor unit. Proto 1 test results are summarized in Wordslide 2, together with early results from the second prototype (Proto 2) hardware. Because of the Proto 2 engine/compressor performance results and the development priority assigned to the performance improvement efforts, Proto 2 system tests were never conducted. Lack of component testing capability for the engine proved to be a disadvantage in diagnosing the performance problems. Both the combustor and compressor were tested as components prior to integrated testing. However, the engine performance could only be determined from integrated test results. The Proto 2 integrated combustor/engine/compressor assembly in test is shown in Fig. 14.

Wordslide 3 summarizes the final Proto 2 results and the conclusions reached subsequently regarding further work on the GE configuration. The Phase III "Technology Development" subcontract with UCC/ORNL focused on obtaining com-

ponent level performance data on the existing engine/compressor assembly. We still do not have sufficient data on hand, for example, to reach an informed decision on the overall viability of the GE engine/compressor configuration and particularly its dynamic sensitivity.

ENGINE/COMPRESSOR DEVELOPMENT WITH CNG/MTI - A chronology of the development project with Consolidated Natural Gas Research Co. and Mechanical Technology, Inc. (CNG/MTI) is presented in Wordslide 4. The objective of the current program is the development of a diaphragm-coupled refrigerant compressor for eventual application to an advanced hermetic FPSE-driven HAHP. The project scope specifically excludes engine development and requires verification testing of the Engineering Model (EM) FPSE performance as a component prior to coupling the engine and compressor.

The CNG/MTI engine/compressor configuration is illustrated schematically in Fig. 15, which includes a summary of the principal character-

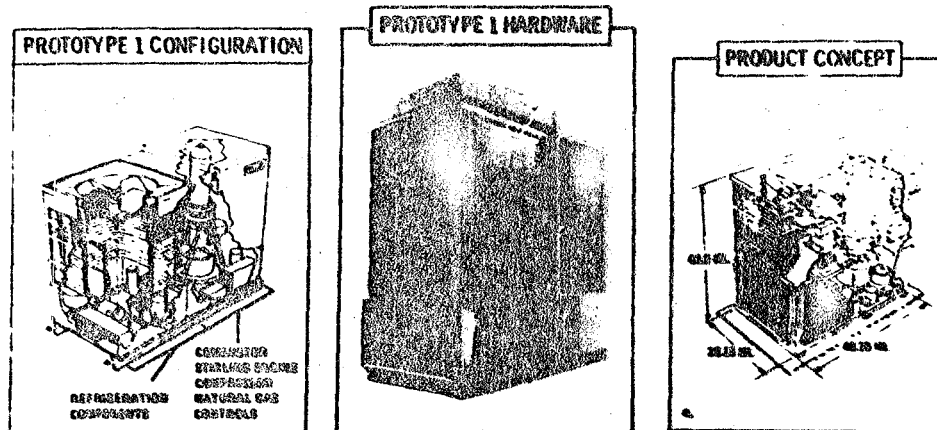


Fig. 13

GE PROTOTYPE DEVELOPMENT

Phase II Program - DOE/ERE Contract

- Development and testing of Proto 1 completed in early 1979
- Proto 1 demonstrated technical feasibility of FPSE-driven compressor in MAMP lab prototype, but fell short of performance targets
 - System heating COP (fuel based) @ 0.5°C - 1.2 vs 1.6 goal
 - System cooling COP @ 35°C - 0.5 vs 0.85 goal
 - Engine power output 2.1 MW vs 3 MW goal
 - Engine cycle efficiency 26% vs 30% goal
- Design modifications in Proto 2 to increase engine operating frequency and reduce losses yielded disappointing performance results
 - 25% indicated engine efficiency at 2.75 MW output power vs Proto 2 goal of 32% at 3 MW
 - Second gas spring absorbed over 20% of output power, reducing power delivered to compressor

Wordslide 2

ORNL PHOTO 4027-82

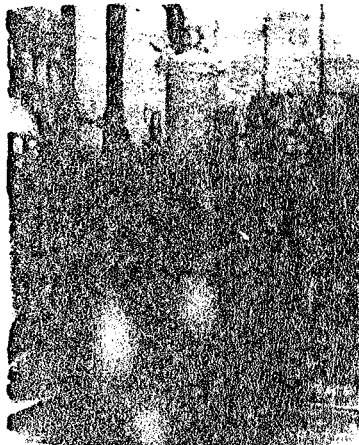


Fig. 14

ORNL/MS-23344/R1

GE PROTOTYPE DEVELOPMENT

(Continued)

- Subsequent modified FPSE yielded higher efficiency (27-28% indicated), but delivered less power (~ 2 MW)
 - Analytical models found to be inadequate for use as design tool for engine modification
- Development and testing of Proto 2 concluded in 1981 (combustor/engine/compressor assembly only, no system level tests)
 - Concluded that technology readiness had not been properly established at outset of Phase II "product development" program
 - Independent review of program by NASA-LERC in January 1982 provided guidance for structuring Phase III Technology Development project

Wordslide 3

CHRONOLOGY OF CNG/MTI DEVELOPMENT

- Engineering Model (EM) FPSE is product of Joint CNG/MTI privately-funded engine development program underway at MTI for several years
- MCC/ORNL subcontract with CNG/MTI started June 1980, when NAMP projects still strongly oriented toward product development and commercialization
- In March 1981, MCC/ORNL redirected program and revised scope to focus on diaphragm-coupled refrigerant compressor development and test/evaluation of FPSE-driven (engine/compressor) assembly
- Current scope of technical effort emphasizes:
 - development of diaphragm-actuated hydraulic transmission for engine-to-compressor coupling
 - compressor development
 - matching EM engine and compressor operating characteristics for operating in breadboard assembly

Wordslide 4

PRINCIPAL ENGINE/COMPRESSOR CHARACTERISTICS
CNG/MTI CONFIGURATION

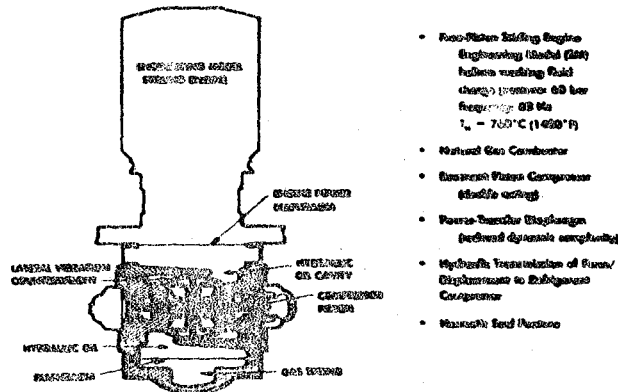


Fig. 15

istics and design features. FPSE operation is similar to that described for the GE engine, although there are certain design features considered proprietary by MTI. The compressor and coupling concept, however, is completely different. In this concept, power is transferred from the engine through a flexible metal diaphragm and hydraulic transmission and delivered to the refrigerant compressor (through the volumetric displacement of the diaphragm, and corresponding displacement of the oil in hydraulic transmission, to the compressor piston). The hydraulic transmission is considered as one subassembly, consisting of the engine power diaphragm, gas spring diaphragm (restoring force function), transverse vibration balancer (counterweights), and the hydraulic oil. The compressor subassembly includes the cylinder heads, valves, pistons, and the refrigerant gas. The three subassemblies - engine, transmission, and

compressor - form a coupled resonant system. One of the potential advantages of this configuration over the GE configuration is reduced dynamic complexity. The use of the power-transfer diaphragm has eliminated one degree of freedom in the resonant system, which should improve its operating stability and control. Of course, lifetime of the diaphragm, which must undergo some 10^9 stress reversal per year, becomes a crucial question: present evidence, including operating experience in England with diaphragm-sealed Stirling engines, strongly indicates that diaphragm material and designs can be selected to give infinite fatigue life. Figures 16 and 17 are photographs of the EM engine hardware which show that there are also some differences from the GE machine in FPSE design features, notably the monolithic heater head configuration.

Wordslide 5 summarizes the current status of the CNG/MTI project. The next year is critical

ORNL PHOTO 4010-82

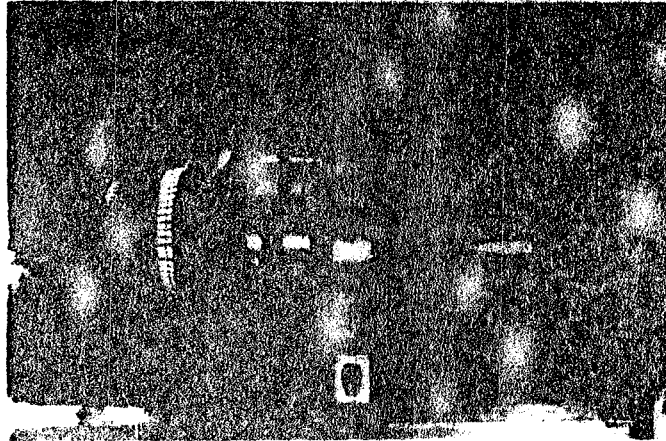


Fig. 16

ORNL PHOTO 4009-82

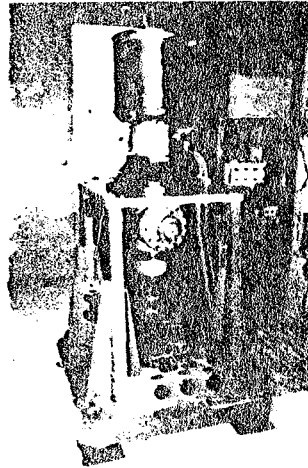


Fig. 17

ORNL/NS-23346

FPSE-DRIVEN COMPRESSOR DEVELOPMENT
(CNS/MTI Subcontract)

- o UCC/ORNL scope with CNS/MTI specifies:
 - use of EM engine (when available) in breadboard assembly
 - prerequisite tests to verify that it will operate over MAP operating range
- o EM Engine Verification Testing now underway
- o All design work and matching analyses on compressor, hydraulic transmission, and breadboard engine/compressor assembly completed June 1982 and all component hardware ordered
- o Compressor Component testing and Breadboard System Testing should commence by end of 1982

Wordslide 5

in establishing the technical viability of this new configuration with regard to thermal performance and operating stability and control. However, even if test results are positive, key technology issues will remain to be solved on durability, reliability, and attaining all of these desired characteristics at reasonable manufacturing cost.

TECHNOLOGY ISSUES AND DEVELOPMENT APPROACH -

Throughout the earlier sections of this paper, several issues were identified with regard to applying free-piston Stirling technology to HAHP development. What we perceive to be the key issues seem to fall into three general categories, as summarized in Table 5. The two hardware development projects just described are not our only efforts at resolving these issues. In 1981 we formulated a more generic plan of work in this area, a plan which we began to implement this year. The plan is diagrammed in Fig. 18. The three main elements of the technology development program are: 1) determining the state-of-development of the free-piston Stirling engine itself (prime mover development; 2) engine/compressor coupling and related dynamic design issues (possibly including compressor development or dynamic seals); and 3) development and validation of analytical design tools. The program will take maximum advantage of technology being developed at NASA-LeRC, MITI, Argonne, and JPL under other DOE programs (Automotive Stirling, ECUT/previously Fossil Energy, Solar, etc.).

We have started a survey and assessment of available FPSE performance measurements (both published and unpublished). The assessment should determine whether there is sufficient experimental data available to permit establishing a state-of-the-art (SOA) "benchmark" on FPSE thermal and mechanical efficiency. The survey will provide the beginnings of an experimental data base on FPSE system and component performance which can be used for validation of analytical codes. The survey may also provide some preliminary comparisons of engines operated with different types of loads (simple dashpot, alternator, inertia compressor). Analysis of the measured data may yield some useful information

about the effect that the load characteristics have on FPSE performance. If there are sufficient data to establish SOA engine performance, then this will be compared with the performance "target" required for economic viability (in the engine-compressor application). A separate program analysis task would be required to reexamine the nominal 30% engine efficiency target set for the development program several years ago and to confirm or modify it as appropriate.

A survey and assessment of FPSE dynamic and thermodynamic analytical codes is also underway. It is known that the most complex codes (so-called third-order codes) do not always give the best results; therefore, we will attempt to define what level of sophistication is necessary for design purposes and thereby to select one or two candidate FPSE codes for validation against the experimental data available. Emphasis is being placed on FPSE dynamic codes and methods for handling interaction between the mechanical/gas dynamics and the Stirling cycle thermodynamics. Much effort has gone into development of thermodynamic cycle codes for kinematic Stirling engines and some comparative analyses of those computer codes have already been reported.

We also propose design and development of a versatile test load device to aid in understanding the complex gas/mechanical dynamics of the FPSE-load system (including interaction with Stirling cycle thermodynamics) and to simulate FPSE/compressor coupling. Testing would provide the required experimental data on dynamic sensitivity and "matching" of the driven load (i.e., refrigerant compressor) to the FPSE output characteristics.

New project activities started this year under this generic technology effort are summarized in Wordslide 6. We plan to effect close coordination between these activities and the hardware development work during the coming year. The plan focuses on issues in the performance/efficiency category. However, the plan recognizes that other issues related to life requirements and cost must be a continuing concern in the development process because of their critical importance in the eventual application in HAHP's.

Table 5. Current appraisal of key issues FPSE/compressor technology

Performance Efficiency	Cost	Durability & Reliability
<ul style="list-style-type: none"> • FPSE efficiency (SOA and potential with mature technology) 	<ul style="list-style-type: none"> • Equipment cost premium vs operating cost savings 	<ul style="list-style-type: none"> • Design life vs heat pump requirements
<ul style="list-style-type: none"> • Engine/compressor integrated performance <ul style="list-style-type: none"> - dynamic sensitivity, stability, controls - best configuration 		<ul style="list-style-type: none"> • Service calls/maintenance requirements
<ul style="list-style-type: none"> • Analytical tools (dynamic and thermal) 		

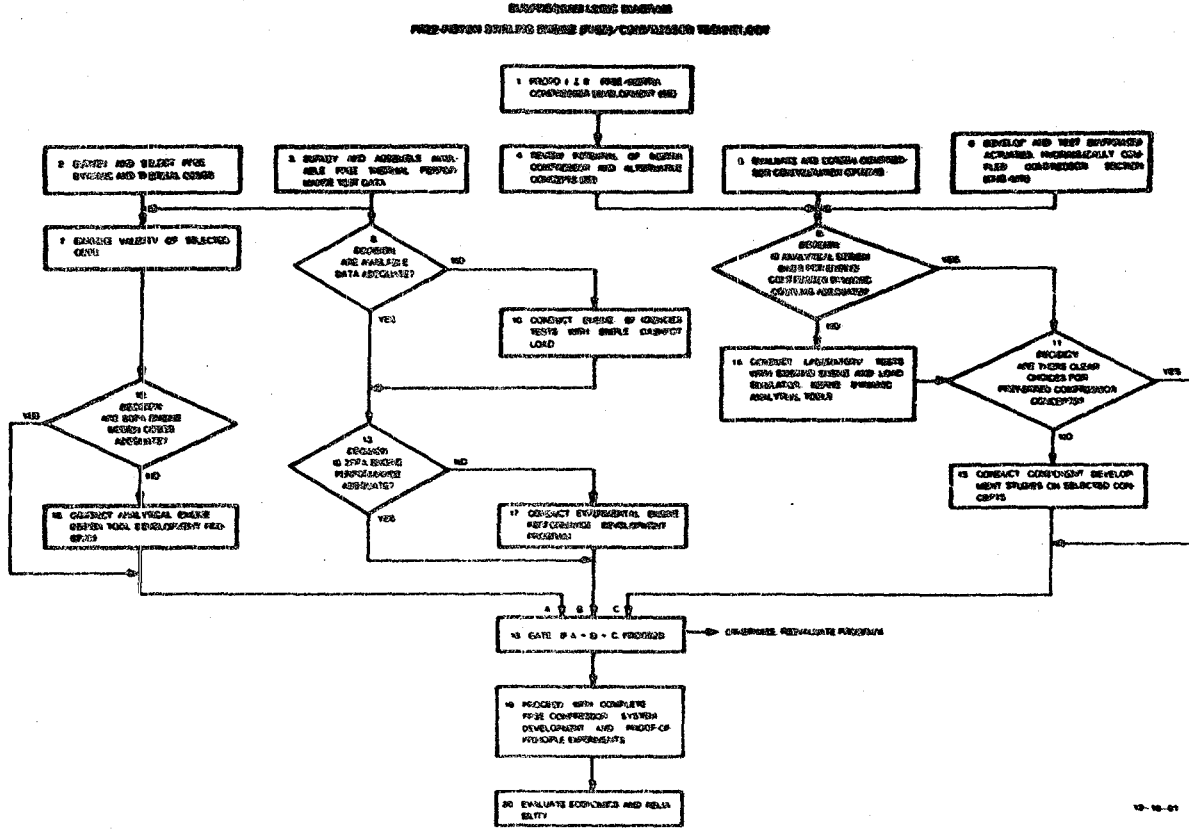


Fig. 18

STIRLING/RANKINE TECHNOLOGY
NEW DEVELOPMENT ACTIVITIES

ORNL Inhouse - FPSE Hardware and Analytical Tools Assessment

- Survey/evaluate dynamic and thermal codes
- Document available FPSE experimental results

NASA-LeRC Interagency Agreement

- Experimental tests to provide data for model validation (FPSE/component performance)
- Assess variable load-absorption devices for FPSE
- Endurance testing

Argonne National Lab - Cosponsored with DOE/ECU Program

- Oscillating flow tests to provide heat transfer, pressure drop correlations for analytical models

CONCLUSIONS

This paper represents an attempt to describe where we have been, what we have learned, and where we are going in development of technology for application in future heat-activated heat pumps. Emphasis has been placed on Stirling engine-driven HAHP technology, with its many challenging development problems, because it was early identified as having high potential for this application and that positive assessment (of its high efficiency potential and other needed attributes) continues. Based on the review presented in the preceding sections, we offer the following summary observations and conclusion.

- In retrospect, the previous "Product Development" efforts on engine-driven HAHP's were premature; i.e., they were undertaken before the technology was sufficiently advanced to warrant such an approach.
- The technical problems are now better understood and can therefore be broken down into more manageable technology development tasks or projects.
- It is still not clear how best to actuate a heat pump cycle with a free-piston Stirling

engine. Until this load-engine coupling and control issue is better understood and preferred engine/transmission/compressor configurations identified, it will be difficult to undertake or properly focus R&D on such critical issues as durability, reliability, or cost.

- To the extent feasible, we plan to use available engine technology rather than to develop it ourselves, so that this program can concentrate its resources on the issues related to application in HAHP's.
- The free-piston Stirling engine-driven HAHP is still an attractive and interesting equipment option for the future, but it continues to involve high risks (technical and business), even after several years of development work.

We view this conference as an excellent forum in which to present this information, so that we might obtain constructive feedback from you. Therefore, having presented our assessment and current views on the issues and our planned development approach, we ask for your guidance and input.

QUESTION AND ANSWER PERIOD

Q: What were your cost goals originally when you set out on this product development work?

A: Our cost goal was a five-year payback as opposed to the nearest equivalent product. GE did extensive market evaluations throughout the course of that development work, so that value floated some, and as a matter of fact, the nearest equivalent product changed from a high efficiency furnace/air conditioner combination in the beginning to an advanced electric heat pump

at the end. But as I said, the cost premium was geared to a five-year payback, and so it depended on the area of the country as to what you could afford to sell this for versus the competition. The northern states look better for any type of heat actuated heat pump because the primary benefit is in the heating operation. So you are looking for a location that has a high heating load as compared to cooling load. In general, that probably translated into something like a 25-30% cost premium if I remember correctly.

Stirling Engine Applications Study

W. Peter Tsagan and David R. Cunningham
Arthur D. Little, Inc.

ABSTRACT

see surveyed
This paper surveys potential applications for Stirling engines in the power range from 0.5 to 5000 hp. Applications are grouped into a small number of classes (10), with the applications in each class having a high degree of commonality in performance and cost requirements. A review of conventional engines was then undertaken to determine the nature of the competition faced by a new engine system. In each application class the Stirling engine was compared to conventional engine systems, assuming that objectives of ongoing Stirling engine development programs are met. This ranking process indicated that Stirling engines showed potential for use in all application classes except very light duty applications (lawn mowers, etc.). However, this potential is contingent on demonstrating much greater operating life and reliability than has been demonstrated to date by developmental Stirling engine systems.

STIRLING ENGINES have been under development for over 40 years by organizations in Sweden, The Netherlands, and the United States. However, the interest level in the Stirling engine as a clean, efficient power converter has increased dramatically in the last 8-10 years as a result of rising work oil prices and concern for the environment.

Stirling engines have a number of potential advantages which have provided the incentive for these programs, including:

Multi-Fuel Capability which allows operation with a wide range of fossil fuels, as well as non-conventional heat inputs, such as solar energy, biomass, nuclear, and thermal storage.

High Thermal Efficiency which results in more economic operation in those applications where fuel costs are important.

Low Emission Levels in fuel fired applications as a result of being external com-

bustion engines. This advantage is particularly important in vehicular and closed environment applications (mines, etc.).

Low Noise and Vibration resulting from the use of mechanically balanced mechanisms, the lack of valves, and relatively low operating speeds.

High Power Density Potential when operating with high pressure gases. This advantage is often important in vehicular applications.

High Reliability and Long Life resulting from outwardly simple mechanical configurations and relatively few moving parts (no valves, etc.).

Good Part Load and Variable Speed characteristics which are important for vehicular and some generator applications.

Many of the above advantages have been demonstrated in operating hardware. For example, efficiency levels in excess of 35% have been achieved as part of the automotive program and engines have been operated using solar, isotope and thermal storage heat inputs. However, other attributes, such as high reliability, have not yet been demonstrated with the consistency required for commercial systems.

Despite its demonstrated and projected attributes, the Stirling engine has still not found commercial acceptance. The reasons for this are complex and several of them are discussed briefly below.

The primary funding for Stirling engine developments, particularly in the United States, has been for automotive applications. The low emission levels and high thermal efficiency (i.e., good gas mileage) potential of the Stirling engines make them well-suited for this application. However, the highly developed Internal Combustion (I.C.) engines now used, have themselves been the subject of continuing development effort over the last decade and are now, when combined with smaller cars, providing improved mileage and emission characteristics. These characteristics are

achieved with engines having a cost (\$25-30/kW) which probably cannot be achieved with a Stirling engine - even in mass production quantities. The projected performance characteristics of advanced automotive Stirling engines (1,2) indicate, however, that Stirling engines may have efficiency, fuel flexibility, and emission advantages over conventional I.C. engines. These advantages could become increasingly important in the future depending on cost and availability of clean automotive fuels.

As a practical matter, conventional I.C. engines can address many of the applications considered for Stirling engines. I.C. engines have the benefit of over 50 years of extensive development and a firmly established sales/maintenance infrastructures throughout the world. As such, Stirling engines will require significant advantages over conventional engine options in order to result in a significant market penetration.

Current technology Stirling engines still have not demonstrated the life and reliability required to address the applications for which they are being considered. It is not certain that the technical reasons for the lack of demonstrated reliability can be successfully addressed for the mass market applications, while still maintaining the other required attributes (for example, high efficiency implies high operating temperatures which complicates the task of achieving reliability and cost goals).

Many engine systems indirectly utilize the production economies of the automotive and truck markets to maintain relatively low engine costs in a wide variety of applications. Examples of this include engine driven pumps, inboard marine engines, and standby engine/generators, which often use automotive or truck engine blocks as the basic building component. Stirling engine technology will be at a disadvantage in such applications if the automotive Stirling engine program is not pursued.

Applications requiring unconventional heat inputs such as solar energy, can often be addressed by other external heat input engines. For example, several studies indicate that Stirling engines combined with high concentration ratio parabolic dish concentrators are an attractive solar power option. However, there are several options being actively pursued for solar power including photovoltaics, solar driven Rankine engines, and solar driven Brayton engines. The early stage of development of these solar power technologies complicates the task of selecting the system with the best commercial potential and, therefore, the potential role of Stirling engines.

The above factors must be addressed when considering the prospects for Stirling engine

Numbers in parentheses designate references at end of paper.

commercialization efforts. In particular, the issues are:

For what combination of applications do Stirling engines show significant advantages over probable competitive systems?

What operating characteristics and cost goals must be achieved for Stirling engines to result in large penetrations into such markets?

What is the estimated size of potential markets for Stirling engines.

What are the operational characteristics that Stirling engines would need to have to penetrate these markets?

This paper summarizes the results of a program sponsored by the Department of Energy and NASA Lewis Research Center to address the above issues in order to determine which Stirling engine applications are most likely to be successful and what emphasis new R&D initiatives should have to accelerate the introduction of Stirling engines in attractive application areas.

CLASSIFICATION OF APPLICATIONS

A review of the literature supplemented with conversations with industry participants identified over 100 applications for engines.

Most (at least 90%) of these applications are now served, or could be served, by internal combustion engines. Almost all these applications have at one time or another also been considered as potential markets for Stirling engines. It is not practical to consider the potential benefits of Stirling engine use in over 100 individual application classes. However, many of these applications have similar cost, performance, and capacity requirements. For example, the engine requirements for a residential heat pump and a military generator are similar in almost all respects even though the end use functions differ greatly.

The grouping of such a large number of overlapping and divergent applications into a small number of classes is a highly judgemental process. A computer based "Cluster Analysis" technique was utilized in order to assist in the grouping process. This technique required assigning numerical weighting to the various application requirements and then logically grouping applications so as to maximize common desired characteristics.

As a result of both the Cluster Analysis and informed judgements, engine applications were reorganized into ten categories having common requirements. Information provided for each class of applications includes the following:

- The power requirements of engines commonly utilized for applications which are now served by conventional engines or which are likely to be needed for applications not now served by any engine type.

- Estimated aggregate market size. For applications now served by conventional I.C.

engines, the market indicated is the actual sales of engines usually used in the application class under consideration. The term NCP (no commercial practice) is used where there is no significant commercial use of any conventional engine on which to base market size.

-The important operational characteristics required of each application class. Several of the important characteristics of each application class identified in Table 1 are outlined briefly below.

Table 1
Summary Of Application Class Grouping

Application Class	Power Range	1980 Market Size (Annual)	Qualitative Requirements
A. Heat Pump & Total Energy			
Residential Heat Pump	2-10 kW	- Limited practice to date - Large potential if technical and cost goals achieved	- Long life - High efficiency - Low noise & vibration - Low emission; - Heat recovery - Very high reliability - Low maintenance
Commercial Heat Pump	30-60 kW		
Industrial Heat Pump	100-200 kW		
B. Industrial Equipment			
Industrial Indoor Eq. (Forklifts-Gas)	15-175 kW	55,600	- High efficiency - Long life - Low emissions - Average cost - Good load following - High reliability
Industrial Outdoor Eq.	5-525 kW	61,400	
Compressors for Construction	20-500 kW	26,100	
Isolated Power Generation	6-475 kW	381,600	
Misc. Generation	1-560 kW		
Agricultural Irrigation	3-300 kW	27,900	
Fire Pumps	60-450 kW	7,400	
C. Isotope or Reactor Powered			
Ground Power Units	20-100 kW	- NCP** - Significant potential for space applications as space power needs increase	- Very high reliability - Long life - High efficiency - Low weight (space applications) - Low noise and vibration - Good load following
Spaceborne Power Units	1-1000+ kW		
D. Long-Run, Remote, Potentially Multi-Fuel Applications			
Ventilating Fans			- Low maintenance - Long life - High efficiency - Multi-fuel use - Simple construction & maintenance - High reliability
Portable Refrigeration		21,500	
Mobile Refrigeration	8-50 kW	Small	
Gas Gathering	25-450 kW	Small	
Third World or Remote Power Generation	8-150 kW	- Large potential for biomass fired systems	
Oil Pumping	8-200 kW	Small	
E. Low Usage Equipment			
E.1. Low Power			
Compressors (Consumer) (Gas)	3-12 kW	10,300	- Low cost - Compact - Simple operation - Lightweight - High reliability
Generators (Portable) (Gas)	1-10 kW	205,200	
Generators (Rec. Veh)	1-10 kW		
Consumer Goods (Lawn & Garden)	2-20 kW	9,926,000	
Pumps (General Purpose)	1-12 kW	77,400	
Log Splitters	2-8 kW	144,600	
Chain Saws		2,473,600	
Snowmobiles		101,500	
E.2. High Power			
Welders	8-175 kW	96,000	
Pumps-Contractor	12-425 kW	33,800	
Generators (Emergency)	11-560 kW	169,700	
E.3. Back Pack Power Supply			
	1-4 kW		

Table 1 (Continued)

Application Class	Power Range	1980 Market Size (Annual)	Qualitative Requirements
F. Military			
Portable Electric Generators	< 15 kW > 15 kW	No longer produced 400-600*	- Fuel switching - Low noise & vibration - High efficiency - Good load following - High reliability - Low weight - Small size
G. Mobile Light Duty			
Passenger Car	20-110 kW	6,527,800	- Low cost - Small size - Low weight - Low emissions - Good load following - High reliability - High efficiency
Agricultural Eq. Self-Powered	9-425 kW	36,600	
H. Mobile Heavy Duty			
H.1. Small (1-110)			
Agricultural Tractors	16-110 kW	144,700	- Low emissions - High efficiency
Trucks	60-110 kW	1,745,900	- Fuel switching - Long life
Construction Equipment	1-110 kW	213,400	- Good load following
Marine: Pleasure & Light Commercial	2-110 kW		
Mining: Surface	20-110 kW	1,500	
Mining: Underground Forestry Equip.	22-110 kW	400	
Railroad Maintenance	22-110 kW	300*	
H.2. Large (110+)			
Agricultural Tractors	110-350 kW	43,300	
Trucks & Buses	110-400 kW	1,152,100	
Construction Equipment	110-560 kW	41,700	
Marine: Pleasure & Light Commercial	110-350 kW	58,300	
Locomotives	75-2250 kW	Small	
Tactical Vehicles	60-300 kW	8,700	
Military Tanks	1,120 kW	720	
I. Solar Thermal and Thermal Storage Power Applications			
I.1. Solar Power Pumps			
Solar Powered Pumps	} ~ 10-100 kW	- Several dozen demonstrations in operations - Large potential contingent on technology developments	- Reliable - Long life - High efficiency - External heat source - Low maintenance - Low cost - Low noise and vibration
Solar Powered Compressors			
Solar Powered Alternators			
Dish Mounted Generators			
I.2. Thermal Storage Applications (Underwater)			
Mining Submarine	~ 10-200 kW	NCP**	
Military Submarine			
Pleasure Boat Total Energy Sys.			
General Purpose Submarine			
Research Submarine			
Off Shore Exploratory Submarine			
Unmanned Surveillance Submarine			
Short Term Underwater Plant			
I.3. Thermal Storage Applications (Land Based)			
Shopping Car	~ 1-50 kW		
Regenerative Braking System for MD vehicles			
Hybrid Vehicle			
Wheelchair			

Table 1 (Continued)

Application Class	Power Range	1980 Market Size (Annual)	Qualitative Requirements
L. Large Multifuel			
Municipal Power Generation		< 1000	- Multi-fuel use
Industrial Cogeneration	1000-5000 kW	< 1000	- Long life
Gas Pipeline	1000-5000 kW		- Low maintenance
			- High efficiency

*Estimates.

**NCP - No commercial practice.

HEAT PUMP AND TOTAL ENERGY - In a heat pump/total energy application, an engine would need low emissions, good fuel efficiency, very low noise and vibration, heat recovery, infrequent maintenance, long life, and good startability. Not so critical to engine success in this application are low engine cost and weight, small engine size and good load following.

INDUSTRIAL EQUIPMENT - Fuel switching capability, low noise and vibration, heat recovery, low weight and small engine size are not critical in industrial equipment. However, low emissions, good fuel efficiency, long life, good startability, low cost and good load following are important in these applications.

SPACE POWER - In a nuclear (isotope or reactor) space power system, fuel efficiency, low noise and vibration, life, startability and load following are critical parameters. Fuel switching, low emissions, heat recovery and low engine cost are not important in these applications.

LONG-RUN, REMOTE, MULTI-FUEL APPLICATIONS - In a rural power system, fuel switching, fuel efficiency, low maintenance, long life and startability are important characteristics. Low emissions, low noise and vibration, heat recovery and engine size and weight are not critical.

LOW USAGE EQUIPMENT - In low usage equipment the main factor for success are very low cost, startability, low engine weight and small size. Other factors are not critical such as efficiency or heat recovery.

MILITARY - Fuel switching, fuel efficiency, low noise and vibration, load following, and startability are important, as are small size, low weight, low maintenance and long life. Low emissions, heat recovery and low cost are not as critical.

MOBILE LIGHT DUTY - Nearly all factors mentioned previously are important in light mobile power applications, particularly emissions, cost, and load following.

MOBILE HEAVY DUTY - In medium duty mobile power applications, fuel switching and efficiency, low emissions, long life and good load

following are important, but heat recovery, low engine cost and weight are not as important as for the light duty mobile power.

SOLAR THERMAL AND THERMAL STORAGE POWER - Most solar thermal power units employing Stirling engines assume that thermal energy storage is incorporated with the solar receiver in order to reduce problems associated with transient operation. The Stirling engine would, in fact, be operating from thermal storage. These seemingly diverse applications are, therefore, grouped together since they could be served by a common class of engine designed to operate from a high temperature thermal storage media. In these applications, efficiency, low maintenance, long life, low cost, and reliable startability are important. Low emissions do not apply and fuel switching as well as heat recovery are not critical.

LARGE MULTI-FUEL - Large stationary power systems generally operate with a high duty cycle. The critical characteristics of these systems will be high thermal efficiency and a multi-fuel capability. Both these characteristics lead to lower fuel operating costs which are a dominant cost factor with high duty cycle equipment. Other characteristics such as low size and weight and good startability are not particularly important.

CONVENTIONAL ENGINE MARKETS AND PERFORMANCE CHARACTERISTICS

Most applications being considered for Stirling engines are presently being served or could be served by one or more conventional engine systems. As a practical matter, Stirling engines will have to show some combination of technical and economic advantages to displace the conventional engines now utilized. It is, therefore, important to have an understanding of the market for conventional engines and the characteristics of engines now used in major market segments in order to evaluate the prospects for Stirling engines in each application class.

CURRENT ENGINE SALES - Table 2 summarizes the United States sales of engines in the power range from 0.5 to 5000 hp in 1978. The

Table 2

U.S. Engine Production; 1/2 To 5000 HP, 1978

	Spark Ignition		Diesel		Gaseous Fuel Only	Gas Turbine
	Non-Automotive	Automotive*	Non-Automotive	Automotive		
TOTAL	13,740,777	11,864,643	388,438	227,543	<1500 est.	<1500 est.
RATED RPM						
<1500	178,846	11,864,643	388,438	227,543	<1500 est.	<1500 est.
1501 - 2999						
3000 - 3999						
>4000	13,561,931					
METHOD OF COOLING						
Air	13,504,068		19,423			<1500 est.
Liquid	236,709	11,864,647	369,016	227,543	<1500 est.	
NUMBER OF CYLINDERS						
1	13,245,778		15,886		<1500 est.	Not applicable
2 & 3	231,714		17,373			
4	110,690	759,205	106,068	415*		
6	38,384	3,405,456	205,100	133,074*		
8 and up	114,211	7,699,982	44,011	94,054*		
DISPLACEMENT						
in ³	cc					
<20	328	12,348,283			20,815	Not applicable
20 - 75	328 - 1230	1,051,832				
76 - 150	1230 - 2460	36,990	298,981			
>150	>2460	293,672	11,565,662	367,622		

* Estimated from sales data

Source: U.S. Department of Commerce, Power Systems Research, Forecast Associates Inc., Arthur D. Little, Inc. Estimates

total number of engines sold annually is about 26 million. Of these about 25.6 million (98%) are spark ignition engines and about 0.62 million (2%) are Diesel engines. In addition, a small number of gas fired reciprocating engines (about 1500) and gas turbines (about 1500) are also sold in this power range.

Approximately 92% of all spark ignition engines have rated outputs below 150 hp. Within this engine class there are two types of engines which account for nearly 87% of all engines sold.

Over 12 million engines with capacities of under 10 hp are sold annually. These are typically low usage engines used in such widespread applications as lawn mowers, chain saws, and snow blowers. The major portion of these engines are provided by either Briggs and Stratton or by Tecumseh.

Over 7 million engines are produced annually with rated power outputs of between 60 and 150 hp for vehicular applications. Most of these are for automotive use. However, a significant number are also used in such applications as light trucks, and tractors. Over 1/2 dozen manufacturers (primarily automotive companies) participate in this market area.

The sales distribution of Diesel engines is more evenly distributed than for spark ignition engines. Widespread applications for Diesels include compressor drives, farm equipment, and generator sets. However, approximately 60% of Diesel sales are for automotive and truck propulsion applications.

Within the power range considered the reciprocating internal combustion engines are similar in design and concept. Many are versions of automotive engines which achieve their rated power at relatively high crankshaft speeds (over 1,200 rpm) and are commonly referred to as "high speed engines". High speed engines in the 400-1000 hp range are not a large share of the market.

Engines with power outputs in excess of 1000 hp generally are operated at lower speeds. The lower speeds are usually dictated by large cylinder bores and longer operating life requirements. The industry classifies these as low speed (up to 400 rpm) and medium speed (400-1200 rpm) engines.

The total volume of low speed engines is less than 2000 units per year. Major uses for these larger engines are for marine propulsion, locomotives, municipal generating

stations, and gas pipeline compressor stations.

ENGINE COST AND PERFORMANCE CHARACTERISTICS - There is a wide range of engines now in use with over 50 manufacturers producing, at least 670 engine models. However, within broad engine categories (small low usage, automotive, low speed Diesel, etc.) the technical characteristics of engine types fall within a relatively narrow band. This fact is reflected in the highly competitive nature of the engine business where relatively modest differences in performance or cost can influence sales.

LOW USAGE ENGINES - The most important characteristic of these small, mass produced, spark ignition engines are their very low cost (\$15-25/kW), small size, and low weight. These are all critical for the types of applications in which these engines are normally used.

The relatively short life (typically 500-1000 hours) and poor fuel efficiency (10-15%) of these engines does not strongly detract from their capability to function adequately in their most common applications. For example, a useful life of 500 hours represents over 10 lawn cutting seasons in a typical lawn mower application.

AUTOMOTIVE ENGINES (SPARK IGNITION) - As with low usage engines, spark ignition automotive engines have a cost of \$20-30/kW. This low cost reflects both the economics of mass production and the relatively modest operational life (3000-4000 hours) required of such engines. The modest life goals, in turn, allow for higher operational speeds (higher rated outputs) and lighter weight construction.

The efficiency indicated is in the 25-30% range. This efficiency range is at the lower end of that expected from Stirling engines, which would provide the Stirling engine with a fuel economy advantage.

The emission levels indicated for the automotive engines satisfy present Federal regulations and will continue to do so under proposed law.

HIGH SPEED DIESELS - This class of engine includes those now used in automotive applications, which are estimated to cost \$25-40/kW. Non-automotive engines have a significantly higher cost (\$150-300/kW) than their automotive or spark ignition counterparts. Benefits derived from this significantly higher cost include higher efficiency, in the 30-35% range, and longer life (up to 20,000-30,000 hours). The higher cost of these engines facilitates establishing a competitive position for Stirling engines in applications which they serve. Recent systems studied at NASA indicate that the efficiency of a well-developed Stirling engine may be better than Diesels in the high speed range.

MEDIUM AND LOW SPEED DIESELS - These engines are typically used in applications where long life and high reliability is

required. The resultant robust construction and the low production quantities lead to engines with relatively high costs in the \$200-500/kW range.

The fuel efficiency of these engines is generally very high (35-40%) and, in addition, some engines in this class have a limited multi-fuel capability. Diesels are run on anything from No. 2 Diesel down to the heavy distillates such as bunker "C". The more common gaseous fuel is natural gas, although all sorts of other combustible gaseous fuels such as sewer gas have been used.

These engines are usually relatively heavy and bulky as compared to the "high speed" engine classes. For example, their specific weight is typically in the 10-30 kg/kW range as compared to spark ignition automotive type engines with specific weights of 2-4 kg/kW. Consequently, there will be considerable flexibility in the physical design of Stirling engines (size, weight, layout) when used in applications now served by low speed internal combustion engines.

A very important feature of engines in this class is their high reliability as measured by maintenance intervals and useful life. Many engines in this class have lives in excess of 20,000 hours (time to major overhaul) and will operate with maintenance intervals of 1,000-2,000 hours. The exceptional reliability is in a totally different class than that achieved or needed by automotive engines and could be one of the more difficult goals to be met by a new engine development.

GAS TURBINES - The market for gas turbines under 3730 kW (5000 hp) is extremely limited. The primary reason for this is their relatively high initial cost (\$150-300/kW) and poor efficiency (20-25%), when purchased in physically small sizes and moderate turbine inlet temperatures (i.e., about 1700°F).

RANKINE ENGINES - Rankine cycle engines are similar to Stirling engines in their capability to utilize solid fuels and non-conventional heat inputs (solar, nuclear, thermal storage). In the size range of interest, however, the efficiencies of Rankine systems are generally considerably lower (at 15-25%) than those projected (30-40%) for similar size, well-developed Stirling systems.

Rankine cycle engines require large amounts of heat transfer area and relatively complex series of expanders, pumps, and controls for their operation. As such, the limited practice to date has resulted in costs in the \$1,000-3,000 per kW range. Projections for larger production quantities are in the \$500-1500 range, depending on capacity and operating temperature.

SELECTION OF REPRESENTATIVE ENGINES - Table 1 specifies a conventional engine which would be typical of that either used or which could be used in each application class previously identified. Performance and cost

Table 3
Characteristics Of Representative Conventional Engines

Application Class	Manufacturer/Model	Fuel	Rated Power kW @ RPM	Efficiency %	Cooling	Mean. Interval hrs.	Life hrs.	Production Volume Units/Yr	Cost \$/kW
- Low usage equipment - Reserve Power	Briggs & Stratton/ 62,500	Gasoline	2.2 @ 3600	19-15	Air	25	400	1.1 x 10 ⁶	50
	Lister Diesel L1 1 (A)	Diesel	3.4 @ 1500	30	Air	1000	25,000- 30,000	Low Thousands	~ 400
- Mobile Light Duty - Mobile Medium Duty - Industrial Equipment - Heat Pump & Total Energy - Military	GM 173 CID	Gasoline	62 @ 4800	22-25	Water	208	2,000- 3,000	640,000	25
	CATERPILLAR 3304	Diesel	70 @ 1800	34	Water	1000	30,000	13,600	110-125
- Large Stationary Power	Diesel Colt-Fairbanks Horse 38 TD	Diesel, Gas, Heavy Distillate, etc.	3000 @ 900	37	Water	10-20,000	100,000+	< 100	250
	Gas Turbine Detroit Diesel Allison Division of GM 50 1A8	Kerosene, Jet-A	3120 @	24	Air	10-20,000	60,000	< 1,500*	125
	Diesel Engine Thermo Electron/Peter- Brotherhood	Multifuel Coal, Oil, Gas	1000-15,000	15-25	Air/Water	10-20,000	100,000+	< 200	650
- Solar Thermal - Space Power	None								

*Total production of large gas turbines.

information is presented for each representative engine to provide a benchmark by which to judge Stirling engines in those applications. Also noted is the production volume of the representative engine.

There is no single set of technical or cost goals which must be achieved by Stirling engine systems. For example, automotive applications set particularly stringent cost requirements on the Stirling engine (about \$25/kW) but only requires 2,000-3,000 hours of operation life, which allows additional flexibility in the choice of hot section materials and system design. In contrast, a heat pump application might allow costs 4 to 5 times those of an automobile engine but would require a useful life of over 20,000 hours.

As noted on Table 3, there are some applications where there is no present commercial practice, with conventional engines. These applications include nuclear/space power and solar power. For these application classes the possible competitive engines are thermo-electrics, Brayton cycle, and Rankine cycle engines.

STATUS OF STIRLING ENGINE SYSTEMS

Even though Stirling engines have been under development for over 40 years, fewer than 500 kinematic engines and 50 free piston engines have been built. The actual operating experience with Stirling engines is, therefore, quite limited. This complicates analysis of their potential technical performance

and cost characteristics. A brief overview of the development status is provided below.

KINEMATIC ENGINES - The most extensive recent experience that is well-documented with kinematic Stirling engines has been achieved with those based on the 4-95 (P-40) engine designed by United Stirling of Sweden. Various modifications of this engine have evolved over a period of seven years and it is the basis of the MOD-I engine, being developed as part of the DOE/NASA Advanced Automotive Stirling Engine (ASE) Program, and a solar operated engine, which recently initiated testing as part of the JPL solar thermal/parabolic dish program.^(3,6) This engine is a four-cylinder, double-acting configuration which can produce 40 kW (55 hp) under design conditions. As of January 1981, 21 engines of this basic design had been built and over 13,000 hours of operation had been accumulated.⁽⁸⁾ However, the accumulated hours of operation have usually entailed numerous unplanned shutdowns and the reliability of critical subsystems (primarily seals and heater head) are still in question.

Most of the following commentary on the performance characteristics of kinematic Stirling engines is based on the 4-95 engine and its more recent derivatives.

EFFICIENCY - Stirling engine efficiencies of 30% have been consistently demonstrated on test and demonstration engines for over 15 years.^(3,6) More recent tests with the MOD-I engine and solar version of the 4-95 have demonstrated efficiency levels in excess of

35% (including burner and parasitic power losses), (1,7) and projections by NASA indicate potential for automotive engine efficiencies in the low 40% and in the high 40% for certain stationary applications of automotive derived engine applications that do not use a combustor, i.e., solar. The efficiency capabilities of Stirling engines are, therefore, well-demonstrated, and further improvements might be expected, as higher temperature heater head materials are developed.

MULTI-FUEL CAPABILITY - The MOD-I engine has been operated on most liquid fuels (gasoline, Diesel, etc.) of near-term interest as a motor fuel. (8) Philips operated a biomass fired engine using a heat pipe heat transfer system (9) and more recently, Sunpower, Inc. has operated a simple hot air Stirling engine directly fired by charcoal and rice husks. (10,11)

The basic multi-fuel capability of a Stirling engine has, therefore, been extensively demonstrated, particularly when using liquid and gaseous commercial fuels.

LOW EMISSIONS - One of the major incentives to the development of Stirling engines has been their potential for low exhaust gas emission operation as the result of being an external combustion engine. The MOD-I engine has been extensively tested over the range of power output and has resulted in emission levels well below those required of present and projected regulations, (1) and below those of competitive I.C. engines.

NOISE AND VIBRATION - Stirling engines have no valves, can be fully balanced, and use a continuous combustion process in their operation. As a result, they have low operational noise levels and minimum vibration. These attributes have been demonstrated on several engines including the MOD-I and the V160 engine of SPS. Both these engines demonstrated noise levels of less than 70 DB (a comparable Diesel can be over 90 DB) (12) and very low mechanical vibration levels. This characteristic makes the use of such engines in applications requiring low noise levels (heat pumps, indoor vehicles, etc.) particularly attractive.

HEAT RECOVERY - In the Stirling engine, the major source of heat is from the cooler. A small amount of heat is also available from the combustor, after passing through the air preheater. Thus, it is relatively simple to collect reject energy from a Stirling engine. The disadvantage with heat recovery in the Stirling engine is that since engine efficiency is inversely proportional to the cooling temperature it is desirable to extract heat from the engine at as low a temperature as possible. This, in some cases, reduces the usefulness of the collected heat.

STARTABILITY - The high energy flux of the combustion chamber/heater head subassembly of the MOD-I engine results in allowing the engine to become operational very quickly from a cold start. As a result, the Stirling engine startability is comparable to that of

I.C. engines (and probably better than that of Rankine cycle or gas turbine engines) and is sufficient for all applications of interest.

PART LOAD OPERATION - In the Stirling engine, power output is proportional to the working gas pressure and the swept volume and, therefore, there are two common methods of controlling the power output. One is to adjust the volume that is swept and the other is to adjust the mean pressure of the engine, usually in conjunction with a change in the rpm. Most Stirling engines to date, including the MOD-I are controlled by adjusting the working gas pressure and rpm of the engine. Experience on the MOD-I engines show excellent part load operating characteristics, (1) which is critical in vehicular applications.

SYSTEM SIZE AND WEIGHT - Stirling engines developed to date have usually been somewhat heavier and larger than conventional engines, particularly in applications utilizing light duty Internal Combustion engines. The primary reason for this is that Stirling engines require a relatively large and complex external combustion system.

This combustion system includes the blower, heater head heat exchanger, air preheater system, insulation and associated controls.

In addition, almost all the waste heat (85%) in a Stirling engine must be rejected through a radiator (in air cooled systems) as compared to only about 60% in an I.C. engine. (1)

One of the major focusses of the automotive program has been to adapt the 4-95 designs to result in engines of acceptable size and weight for automotive applications. This program has been successful in that the MOD-I style engine has been installed in the engine compartment of an American Motors automobile. It should be noted, however, that this engine is still larger and heavier than an I.C. engine of similar capability. Including ancillaries (such as battery, radiator, exhaust, etc.) it appears that a 3000 pound vehicle powered by the MOD-I Stirling engine will be 200-300 pounds heavier than the same vehicle powered by a conventional engine. (13) Later modifications will reduce the weight of the basic engine, but it is difficult to project a total engine system weight of less than that of a conventional I.C. engine.

It should be noted that the incremental size and weight differences of Stirling engines relative to conventional engines appear to be modest and will not, in itself, be a major barrier for Stirling engine use in most of the applications under consideration.

SYSTEM COST - A number of general studies have been performed in an attempt to quantify the cost of Stirling engine systems when produced in quantities sufficient for automotive use. They were conducted by both automobile manufacturer and independent companies that conventionally do costing analysis for the automobile industry. All studies seem to

agree that the automotive Stirling engine would be 50-100% more expensive than the same size internal combustion engine currently considered for automotive use, assuming the same production rates and power outputs.

Therefore, most developers of Stirling engines have assumed that they would be premium cost engines and that this premium would be justified by their superior efficiency, emission, multi-fuel, and noise characteristics.

However, a major goal of the NASA automotive Stirling engine program is engine cost reduction. Therefore, there is a continuing effort toward cost reduction of the automotive Stirling engine.

In many high duty cycle stationary applications (total energy, generator sets, etc.) the I.C. engines often cost well in excess of \$100-200 per kW (4-8 times that of automotive engines). In these premium cost applications, Stirling engines may not carry a significant cost premium as compared to the most likely competition.

LIFE AND MAINTENANCE - The Stirling engine has good potential for low maintenance and long life. The lubricating oil is not in contact at any time with combustion products and there are no valves or complex, precise injection, or ignition systems to need maintenance. Potential reliability problems unusual to the Stirling engine include unlubricated piston seals, rod seals, heater heads, and gas compressor systems, in engines that use that method of power control.

Most engines built to date have been experimental in nature and, therefore, life and maintenance data is still quite limited. Although individual engines have been operated in excess of 5000 hours, this operation has generally been accompanied by numerous shutdowns where various components (seals, heaters, etc.) were changed. Table 4 provides information on the testing experience with size ASE engines leading to the MOD-I designs. As indicated, testing times on any given unit are typically in the tens of hours range.

There are several reasons why more reliable operation has not been achieved and none, in themselves, appear to be unsolvable using identifiable technology. A study of automotive derived Stirling engines for stationary applications identified design modifications that would allow a 50,000 hour life at reduced power, while still maintaining good engine efficiency. Nevertheless, long-term, reliable operation is one of the few potential attributes of a Stirling engine which has not yet been satisfactorily demonstrated.

FREE PISTON ENGINES - Free piston Stirling engines have only been investigated, as a practical matter, for commercial applications over the last 10 years and total expenditures have been on the order of \$10 million, a very modest amount for a new engine development program. The status of this technology

should be viewed taking into consideration the limited resources devoted to its development.

Most of the favorable attributes (low emissions, low sound, etc.) have been reasonably well-demonstrated on free piston equipment tested at Sunpower, General Electric, and MIT. However, the cumulative operating time of free piston engines in the size range of interest is still less than 5000 hours with the longest operation of a single engine being about 500 hours. Despite the superficial simplicity, of a free piston Stirling engine, there are still difficulties in transforming this simplicity into mechanically reliable hardware.

Free piston engines do not require shaft seals as do kinematic engines. However, they still require piston seals, high temperature heater heads, and relatively complex control systems. As a result, reasons for shutdown in free piston equipment has, to a great extent, paralleled that of kinematic equipment. Due to the limited amount of operational experience, there is not a statistical breakdown of the shutdown modes.

RANKING OF STIRLING ENGINE APPLICATIONS

Stirling engine application classes were ranked for two different stages in the development of Stirling engines; current technology and developed technology.

For current Stirling engine technology, none of the terrestrial applications were shown as being promising for Stirling engines, due to their lack of demonstrated life and reliability. A more meaningful exercise is the assessment of the potential of future, more developed Stirling engines that meet reliability and life goals of the various development programs. No changes are assumed for conventional engine technology since the time period for developments in this area are long, relative to those in the comparatively undeveloped Stirling engine field. In the ranking it is still assumed that Stirling engines do not compare favorably with internal combustion engines relative to cost, weight, and size due to previously discussed factors. Figure 1 summarizes the ranking of the applications for developed Stirling engine technologies.

The top row in each category is the weight. This is the importance of that particular attribute (such as low emissions or low cost) to the application. The second row is the assessment of conventional engine technology to that application. The upper left hand number is the raw score given that engine and the lower right hand number is the weighted score. The third row is the assessment of Stirling engine technology in that application. The upper left hand number is the raw score given that engine and the lower right hand number is the weighted score.

For both the conventional and Stirling engine technologies the score is based on the

Table 4

**Summary Of Accumulated Operation Time For ASE Engines
And Mean Operating Time To Failure**

<u>ENGINE</u>	<u>OPERATION TIME</u>	<u>MEAN OPERATING TIME TO FAILURE (hrs)*</u>
ASE 40-1 (NASA)	238.0	6.43
ASE 40-7 (MTI)	206.0	7.95
ASE 40-8 (Spirit)	292.44	3.75
ASE 40-12 (Concord)	140.4	14.04
ASE 40-4 (USSw)	6134.46	91.56
ASE 58-1 (USSw)	172.06	15.64

* All classes of failures, since initial start of the engine, are included in the calculation of mean time to failure. This includes, for example, replacement of components due to residual core particles in engine due to improper cleaning, burner blower belt failure, cracked spark plug, etc.

SOURCE: NASA/Lewis ASE Program, Reference

engine that is best-suited or is currently being used in that application. The performance of these engines assumes the "high quality" end of currently available technology for conventional engines and the successful completion of ongoing development programs for the Stirling engine.

The column labeled "totals" includes the sum of the weights (row 1) and the sum of the weighted scores, in rows 2 and 3, for conventional engines and Stirling engines, respectively. The column labeled "engine score" is the sum of the weighted scores divided by the sum of the weights for conventional engines and Stirling engines in rows 2 and 3, respectively. The column labeled "classification spread" is the difference between the Stirling engine score and the conventional engine score. The greater this number, the better the Stirling engine looks relative to a conventional engine.

The ranking process requires making numerous judgements as to the relative performance characteristics of both internal combustion and Stirling engines. Making these judgements is complicated by the limited operational experience with Stirling engines. The judgements made relative to conventional engine technologies are consistent with the characteristics listed in Table 3 for representative engines in each category. This ranking process is useful in highlighting

major issues affecting the potential use of Stirling engines. However, due to the highly judgemental nature of individual entries to the ranking process, undue importance should not be attached to modest numerical differences in total scores.

Figure 2 summarizes the results of ranking process. There is a rather wide range in the potential for Stirling engines in the different application classes. For purposes of this discussion the applications were divided into three categories.

NOT PROMISING

Low Usage Equipment - Application is not dependant on the attributes of the Stirling engine for success. Depends heavily on factors such as cost, size, and weight in which the Stirling engine does not fair well, and has very stiff competition from conventional engine alternatives.

INTERMEDIATE - In these applications the potential advantages of Stirling engines, even in their developed state, appear to be modest as compared to more conventional alternatives. However, in applications with very large market potentials, these modest advantages could still have significant total impacts on a national scale.

Light Duty Mobile - Competition from conventional engine technology (Diesel and Otto cycle engines) is extremely keen, with both types receiving intensive development

		Fuel Switching	Emissions	Fuel Efficiency	Noise & Vibration	Heat Recovery	Maintenance	Long Life	Stability	Low Engine Cost	Low Engine Weight	Small Engine Size	Load Following	Totals	Engine Score	Ratio Rating	Classification Spread
Total Energy/ Heat Pump	C	7	8	9	9	10	8	9	8	6	2	5	4	85		1.508	
	S	2	7	8	4	6	6	7	7	8	8	8	8	487	5.847		
Industrial Equipment	C	14	98	54	36	80	49	63	53	38	12	30	32	625	7.253		
	S	9	8	8	6	8	8	7	7	4	5	5	8	84		.750	
Space Power	C	5	8	6	5	0	5	7	7	6	2	5	8	422	6.594		
	S	2	7	6	7	0	30	40	40	30	14	35	72	470	7.244		
Remote, Multi- fuel Power	C	10	56	36	36	0	30	40	40	30	14	35	72	98		1.346	
	S	8	6	8	8	0	40	50	49	30	12	30	58	350	6.362		
Low Usage Equipment	C	0	0	9	9	0	10	10	0	6	6	8	447	7.707			
	S	-	-	3	10	-	10	10	-	2	4	2	68		1.710		
Military/Quiet Power	C	-	-	27	50	-	100	100	0	12	24	16	385	5.290			
	S	-	-	9	6	-	9	10	-	4	4	7	480	7.000			
Mobile Power (Light Duty)	C	9	2	0	5	4	6	7	8	6	5	5	6	60		.894	
	S	2	2	3	4	2	6	6	7	8	8	8	7	400	6.687		
Solar Thermal	C	18	4	18	20	8	38	38	58	48	40	40	42	347	5.783		
	S	9	6	6	8	6	8	8	7	6	5	5	6	77		.864	
Large Stationary Power	C	4	3	3	5	0	5	2	8	10	8	7	5	494	6.286		
	S	1	3	3	4	-	7	7	7	9	9	8	7	548	7.130		
Mobile Power (Medium Duty)	C	4	3	3	5	0	5	2	8	10	8	7	5	85		.853	
	S	1	3	3	4	-	7	7	7	9	9	8	7	594	6.507		
Solar Thermal	C	4	3	3	5	0	5	2	8	10	8	7	5	651	7.570		
	S	9	6	6	8	6	8	8	7	6	5	5	6	77		1.000	
Large Stationary Power	C	4	4	7	4	7	8	8	8	7	7	9	511	6.636			
	S	26	32	58	28	23	68	64	55	25	28	35	72	583	7.836		
Solar Thermal	C	5	0	9	7	5	8	9	8	8	7	7	7	89		1.212	
	S	7	6	6	8	0	6	6	7	4	5	5	7	603	6.288		
Large Stationary Power	C	6	6	6	6	6	6	6	6	6	7	7	8	880	7.500		
	S	30	0	72	50	40	64	72	64	48	48	60	56	72		1.041	
Large Stationary Power	C	8	8	9	7	3	7	9	5	4	2	2	8	401	6.661		
	S	4	6	8	6	7	7	8	7	6	5	5	8	585	7.722		

Figure 1 Stirling And Conventional Engine/Application Assessment -- Developed Technology

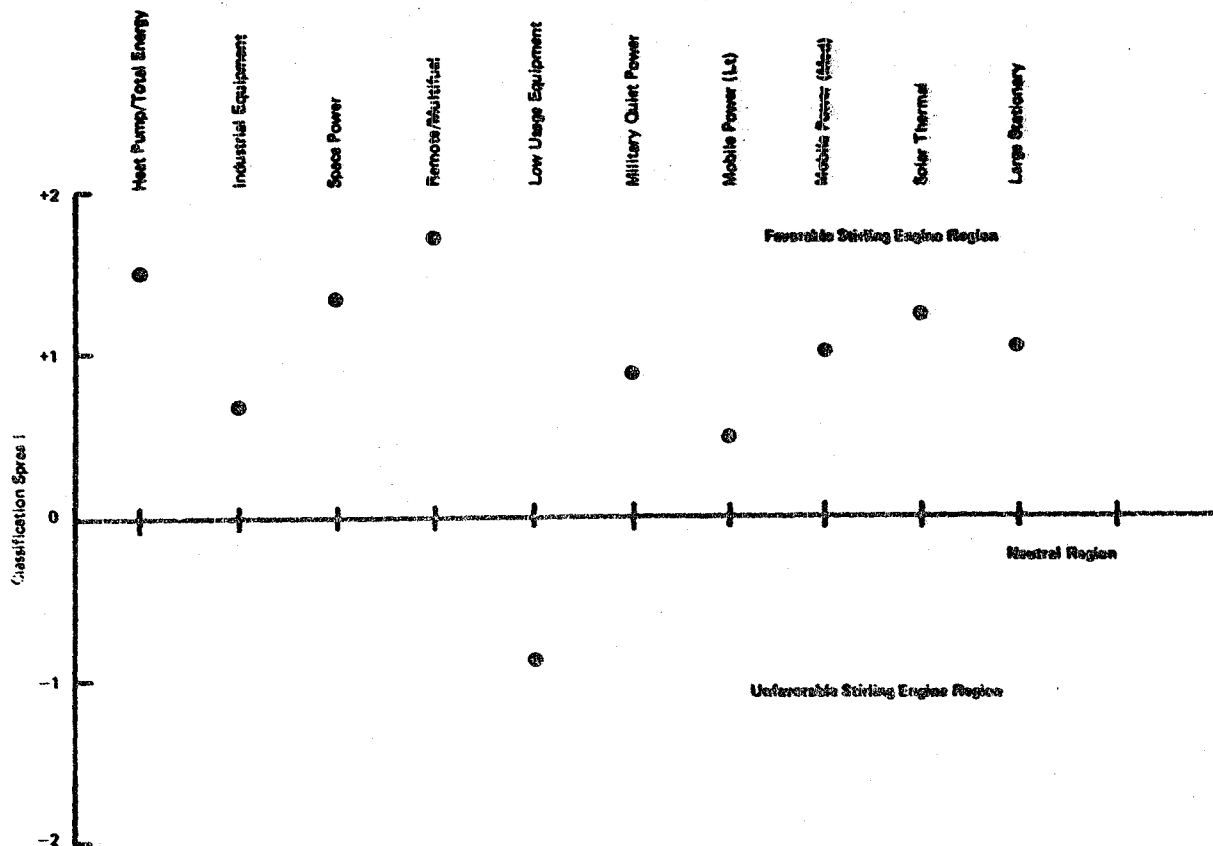


Figure 2 Relative Ranking Of Stirling Engine Applications

effort from public and private sources. Cost, size, and weight restrictions are severe, and there is significant infrastructure for conventional engine technology already in place. However, the potentially large market and impact of these engines may warrant continued parallel development of the technology.

Industrial Equipment - There is a relatively small market which is reasonably well-served by conventional alternatives, although positive attributes of Stirling engines are potentially important in these applications.

Military Quiet Power - Also a relatively small market with difficult (expensive and time consuming) certification procedures (military specs) and control requirements. However, cost not as critical and advantages of Stirling engines are important in this application.

PROMISING

Heat Pump/Total Energy - Has a large potential market, and few competitive engines. Attributes of Stirling engine technology (low noise, low emissions, high efficiency) are

critical in this application and cost, weight, and size requirements are not as critical.

Space Power - Although a small market, in terms of number of units sold, potential attributes of free piston Stirling engines very important, and cost not an important factor.

Remote Multi-Fuel - Competition is not currently serving this market adequately (primarily using inexpensive gasoline engines and small Diesels), since none are multi-fuel. Cost, size, and weight constraints are not critical. Market is large particularly in remote areas of developing countries. There is also potential for significant domestic market, in remote areas or in second or vacation homes away from the power lines.

Medium Duty Mobile Power - Although competition is tough, cost, size, and weight constraints are less than with light duty mobile power and Stirling engine attributes are as important in this operation.

Solar - Large potential market competition is from Rankine cycle and Brayton engines, as well as photovoltaics. Stirling engine attributes such as efficiency are

important in this application although cost and low maintenance are important constraints.

Large Stationary Power - Cost, weight, and size constraints not critical. Multifuel capability desirable as are other Stirling attributes. Market relatively small, and will not likely justify development of engines specifically for this market.

These nine applications represent more than 90% of unit sales, excluding small, light duty applications, such as lawn mowers, chain saws, garden tractors, etc.

SELECTION OF BASELINE STIRLING ENGINE SYSTEMS

There are a number of applications with diverse markets which show good potential of being served by Stirling engines, assuming engines are developed which meet the primary goals of present development programs.

Common engine designs can be developed which, with minor modifications, can be used to serve a multiplicity of applications. Developing a small number of baseline engine systems has the following advantages:

- Results in engines which can serve a variety of potential markets, thereby reducing development risks.

- Allows for reduced development and manufacturing costs, since a small number of common engine designs can be produced in larger quantities.

- Addresses specialized markets with particularly favorable near-term potential with engines which can be eventually used in larger market segments.

It should be noted that the above approach for Stirling engines is not fundamentally different from that followed with conventional engines. Basically, similar engines are often used to satisfy widely divergent applications. For example, automotive engines are used for irrigation pumping, and on a limited basis, for commercial scale gas fired heat pumps (in Europe only, at this time).

Four engine classes were identified which could address all the favorable applications listed above; simple rural power; silent power generators; automotive and automotive derived engines; and large, high duty cycle, stationary power.

A small number of engines in each class could be used to serve a multiplicity of applications. This concept is illustrated in Figures 3 and 4 for silent power generators and automotive or automotive derived engines. For example, engines in the latter category could be used for commercial heat pumps, marine drives, and water pumping functions as well as for the larger markets represented by mobile power. These smaller market segments may represent near-term opportunities for Stirling engines since the Stirling engine attributes were often of paramount importance in several of those functions.

Conceptual engine designs were prepared for each of the four engine classes. In these conceptual designs, the engine system is defined as all those components needed to perform in a given application including cooling systems and pumps, combustors, batteries, control systems, and, in some cases, fuel tanks, not just the prime mover or mechanical part of the system.

For each application class there are a number of Stirling engine configurations which could be selected as the baseline design. For example, either free piston or kinematic Stirling engines could, in principle be used in all application classes. In this section, the baseline engine design selections are consistent with the emphasis of current programs.

The conceptual designs selected were: Rural Power Unit - 1 kW hot air kinematic engine using biomass fuel; Silent Power Unit - 3 kW free piston engine with linear alternator; Automotive Derived Power - 55 kW kinematic engine based on MOD-I design (propulsion), and - 30 kW automotive engine derated for longer life; Stationary Power - Scaled-up automotive engine system.

Figure 5 illustrates the design of a commercial heat pump system using an automotive derived engine. Table 5 provides a comparison of this design with a "conventional option" using a Diesel engine. As indicated, the Stirling engine would have significant performance advantages relative to such important parameters as efficiency, noise levels, and emissions as compared to the alternative arrangement based on already demonstrated Stirling engine characteristics. However, the potentially favorable application places severe constraints on engine life (20,000+ hours) and time-between-maintenance requirements (2,000+ hours) both to satisfy application needs and to meet the competition presented by an I.C. engine. As indicated in Table 5 these requirements are still "To Be Demonstrated" for Stirling engine systems, although, as indicated previously, some studies have indicated that these goals may be achievable through operational and design modification and/or derating. The other conceptual designs indicate equally favorable potential for Stirling engines if life and reliability issues can be successfully resolved.

SUMMARY AND CONCLUSIONS

Stirling engines have already demonstrated many of the requirements needed to be attractive for use in application classes of potential interest. In particular, high efficiency, multi-fuel capabilities, low noise and vibration, as well as low emission levels, are characteristics which have been demonstrated on test systems. Even those characteristics which put Stirling engines at a disadvantage relative to more conventional

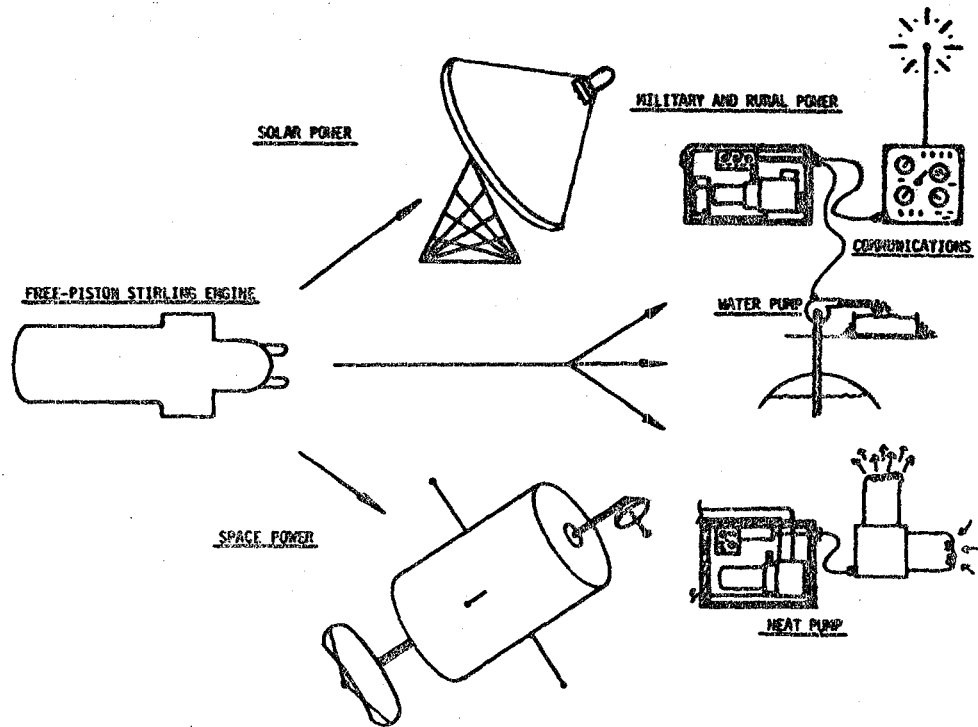


Figure 3 Applications Potentially Served By Silent Power Generator

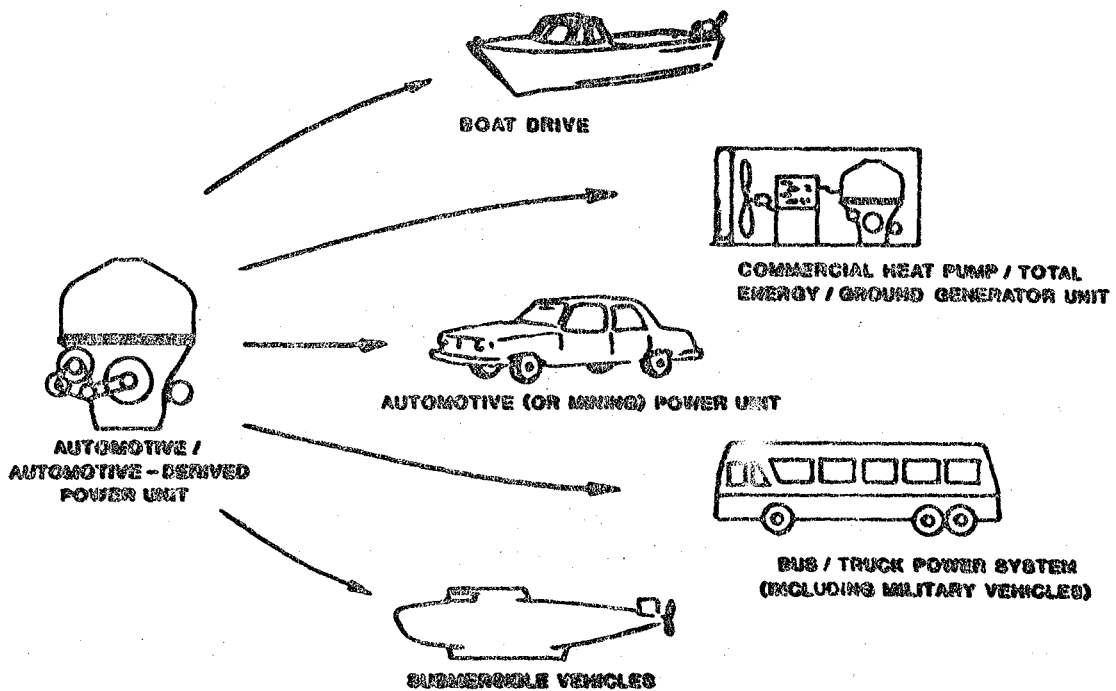


Figure 4 Applications Potentially Served By An Automotive Or Automotive Derived Stirling Engine

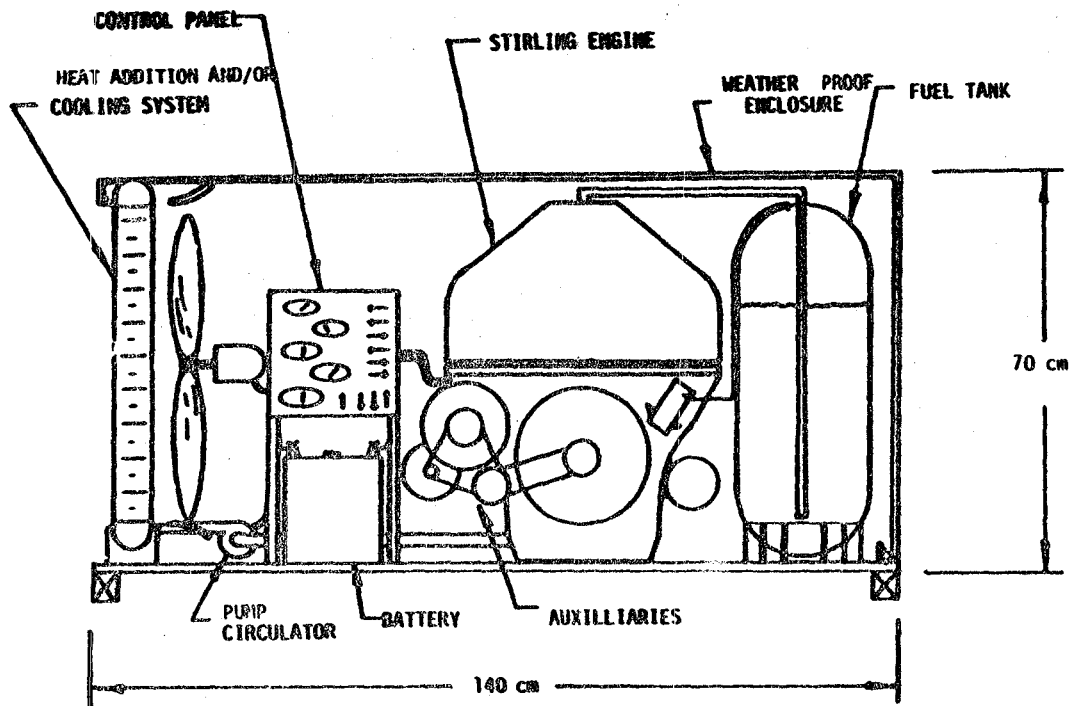


Figure 5 Conceptual Design Of An Automotive Derived Engine In A Commercial Heat Pump Application

Table 5

Comparison Of Conceptual Design Parameters With Application Requirements —
Automotive Derived Total Energy/Heat Pump Drive

	Application Class Requirements	Representative ¹ Engine Capability	Stirling Engine Capability
Power Level	30-100 kW	70 kW	Can Cover Range
Efficiency	30-40%	34%	35-40%
Emissions	Site Specific	Questionable for Many Applications	Inherently Low and Within Requirements
Noise Level	Site Specific (Only Local Regulation at Present)		
Heat Recovery	Primary Importance	From Exhaust Gases, Oil Sump and Coolant; at Some Additional Cost	From Coolant; Minimal Additional Cost
Maintenance Interval	1-2 Times/Yr (2,000-5,000 Hours)	1,000 Hours	TBD ²
Life Before Major Overhaul	7-15 Yrs — 15,000-25,000 Hours	~30,000 Hours	TBD ²
Multi Fuel Capability	Highly Desirable, but Not Critical	Very Limited	Excellent
Cost	\$200-\$500/kW	\$150-\$300/kW ³	Higher End of Cost Range Probably Achievable
Weight	7-20 kg/kW	10 kg/kW	Within Range
Size	.005-.015 m ³ /kW	0.015 m ³ /kW	Within Range

1. Assumed to be a Caterpillar 3306.
2. Need "to be demonstrated" by future program initiatives.
3. Depending on System Configuration.

options, such as size, weight, and cost may not be serious drawbacks in most of the applications of primary interest. Many of the more favorable applications are now served or could be served by relatively high cost (\$100+ per kW), heavy duty engines. This provides additional incentive and flexibility in the design of suitable Stirling engine systems with regard to engine cost requirements.

Table 6 qualitatively summarizes the overall results of the study and identifies those critical improvements in performance which Stirling engine systems must achieve to be consistent with the broad requirements in each application class. The identification of key development issues assumes that ongoing activities are reasonably successful in achieving programmatic objectives. For example, it was assumed that the off design performance goals of the free piston heat pump programs can, in fact, be demonstrated, that efficiency projections for automotive systems will be achieved, and that automotive technology could be scaled up to result in large stationary power units. With these assumptions, there remain several critical development needs which are not adequately addressed by ongoing programs. A common theme for all application classes is the need to emphasize designs which are consistent with long life, low maintenance operation. The quantitative disparity between the life requirements of almost all applications of interest and the engine durability demonstrated to date is very large. All applications, except automotive and other light duty vehicular, require engine lives in excess of 20,000 hours. On this important issue, the requirements of the automotive application are relatively modest, being only about 3500 hours.

If these life and reliability goals can be demonstrated without large compromises in other required features (such as high efficiency) or large increases in cost, the Stirling engine would be a highly competitive option in all but very light duty applications. On the other hand, without achieving (or at least approaching) these life and reliability objectives, the other desirable attributes of the Stirling engine will not be sufficient to result in commercially viable systems.

Also indicated is the need to consistently demonstrate high efficiency levels in order to satisfy application class requirements.

This is due to the fact that Stirling engines must often compete with I.C. engines which can have efficiencies ranging from 25% for smaller gasoline engines to 40% for larger low speed, Diesel engines. It will be important for Stirling engines to show a distinct efficiency advantage to provide an incentive to pursue their development. This is especially true for automotive applications where lower fuel consumption would be a major incentive to off-set higher first costs (by as much as 50%), and larger size and weight. These high efficiency goals are, in fact, state goals of ongoing programs. The need to actually demonstrate a consistent capability to meet these goals is shown to emphasize their importance.

The important development needs for Stirling engines, i.e., most critically to demonstrate longer life and higher reliability, are common to all the application classes. The overwhelming need in this area should guide future program initiatives so that resources can be focussed on addressing this critical issue. Present programs have, for the most part, emphasized achieving other important operational goals (low emissions, lower cost, etc.) and system issues with relatively modest resources directed toward technology developments to specifically address life and reliability questions.

All the application classes share some common technical issues impacting of life and reliability, namely piston seals, shaft seals, and high temperature combustor/heater head subsystems. The details of the technical requirements for those subsystems can differ significantly between applications and system configurations. For example, low power level free piston systems can have a gas gap or hydrodynamic seals where high power density, double acting, automotive kinematic engines require sliding seals. Despite these differences, it appears that there is a high degree of commonality between the essential issues of life and reliability which face the different Stirling engine application class. As a result, Stirling engine development programs for ostensibly different applications might have a high degree of overlap in their development needs. This could provide additional opportunities to more effectively use limited resources to address basic technical issues common to a range of Stirling engine systems.

Table 6

Summary -- Stirling Engine Status And Development Needs

<u>APPLICATION CLASS</u>	<u>TECHNOLOGY STATUS</u>	<u>IMPORTANT DEVELOPMENT NEEDS</u>
Simple Rural Power	Recent testing indicates good promise for simple fired hot air engine	<ul style="list-style-type: none"> - Demonstrate life in excess of 10,000 hours with low maintenance requirements - Improve efficiency to 15-25% range
Silent Power	Testing of both free piston and kinematic engines have demonstrated most of technical requirements	<ul style="list-style-type: none"> - Demonstrate life in excess of 20,000 hours - Demonstrate capability of 2,000 hours operation without maintenance - Consistently achieve efficiencies in excess of 30%
Automotive and Automotive Derived Engines		
(a) Automotive	Testing has demonstrated most important operating requirements and projections indicate further improvements in efficiency	<ul style="list-style-type: none"> - Demonstrate life of 3,500 hours with low maintenance requirements - Demonstrate that efficiency projects can be achieved
(b) Automotive Derived	Same as automotive	<ul style="list-style-type: none"> - Demonstrate life in excess of 20,000 hours with low maintenance requirements
(c) Stationary Power	Design studies and automotive testing both show promise of achieving most of required operational characteristics	<ul style="list-style-type: none"> - Demonstrate life in excess of 50,000 hours - Demonstrate overhaul intervals in excess of 5,000 hours. - Demonstrate capability of 40% efficiency on range of liquid and gaseous fuels

REFERENCES

1. "Automotive Stirling Engine Development Program - MOD-I Stirling Engine System Performance," M. Dowdy, presented at Automotive Technology Development Contractor Coordination Meeting, MTI Report No. 81 ASE 224 PR 17, October 1981.
2. Automotive Stirling Engine Development Program: Quarterly Technical Progress Report for Period: January-March 31, 1981, MTI Report No. 81 ASE 213 QT 12; NASA CR-165393, August 1981.
3. Design Study of a Kinematic Stirling Engine for Dispersed Solar Electric Power Systems: United Stirling of Sweden - Final Report; NASA CR-159588; 1980.
4. "First Phase Testing of Solar Thermal Engine at United Stirling," W. Percival, H. Nelwing; presented at Annual Parabolic Dish Solar Thermal Program Review 1981, sponsored by Jet Propulsion Labs.
5. "Test Results and Facility Description for a 40 Kilowatt Stirling Engine," G. Keha, J. Cairrelli, R. Walter, NASA Lewis Research Center, NASA TM-82620, June 1981.
6. Stirling Engines; G. Walker, Clarendon Press, Oxford, 1980.
7. "Stirling Power Conversion Unit Continues to Meet Goals," PDTS Highlights Vol. 2 No. 2 by Jet Propulsion Labs for DOE, April 1982.
8. Communiqué from NASA Lewis Research Center in presentation to DOE.
9. "The Potential of the Philips Stirling Engine for Pollution Reduction and Energy Conservation," R. Maijer, C. Spigt, presented at Second Symposium on Low Pollution Power Systems Development, organized by Committee on the Challenges of Modern Society of the NATO; November 1974.
10. "Design of a Low pressure Air Engine for Third World Use," J. Wood, B. Chagnot, L. Penwick, Sunpower, Inc., 17th IECEC Proceedings, August 1982.
11. Personal Communications with Sunpower, Inc.
12. "VI60 Stirling Engine...For a Total Energy System," Stirling Power Systems, presented at 5th International Symposium on Automotive Propulsion Systems, April 1980.
13. Automotive Stirling Engine Development Program: Quarterly Technical Progress Report for Period October 1, 1979 - December 31, 1979, MTI Report No. 80 ASE 116 QT 7, NASA CR-159827, May 1980.
14. A Conceptual Study of the Potential for Automotive-Derived and Free-Piston Stirling Engines in 30-500 Kilowatt Stationary Power Applications, A. Vatsky, H. Chen, J. Dineen, Mechanical Technology, Inc. MTI Report No. 81TR38, NASA Report No. NASA CR-165274, May 1981.

Automotive Stirling Engine Development Program Overview and Status Report

Noel P. Nightingale
Mechanical Technology Inc.

ABSTRACT

The Automotive Stirling Engine (ASE) Development Program has been under contract from DOE/NASA since March 1978. Four Mod I engines have accumulated more than 1338 total test hours. One of these engines was installed in a transient test bed (TTB) where its transient characteristics were evaluated. This accomplishment marked the completion of a major program milestone, established at the program's inception and scheduled for completion by September 30, 1982. The ASE program has continued to meet its contractual requirements despite the uncertainty surrounding Government appropriations.

Major design changes were made in the Reference Engine System Design (RESD) to reduce manufacturing cost. Advances were achieved in the areas of combustion, low-cost material, seals, drive system, regenerator, and control system development. A design effort to upgrade the Mod I is proceeding on schedule for system test in April 1983.

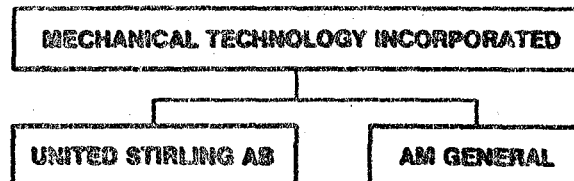
THE AUTOMOTIVE STIRLING Engine Development Program was awarded to Mechanical Technology Incorporated (MTI) in March 1978 to develop automotive Stirling engines and to transfer Stirling engine technology to the United States. United Stirling AB (USAB) of Sweden is a major subcontractor to MTI due to its extensive and qualified background in Stirling engine development. American Motors (AM) General, a second subcontractor, provides the critical link between the engine system and vehicle (see Figure 1). The performance objectives of the ASE program are:

- 30% improvement in fuel economy over equivalent production spark-ignition engine
- Low exhaust emissions (grams per mile)
 - HC \leq 0.41
 - CO \leq 3.40
 - NO_x \leq 0.40
 - Total Particulate Level \leq 0.20

REFERENCE ENGINE SYSTEM DESIGN

The Reference Engine System Design (RESD) is defined as that engine providing the best fuel economy while also meeting or exceeding the ASE program objectives. The initial RESD was completed and reviewed in January 1980. In March 1981, the RESD was updated. This update resulted in a combined mileage projection of 41.1 mpg (unleaded fuel), with the engine installed in a 1984 X-body 2870-lb curb-weight vehicle. A cross section of the updated RESD is shown in Figure 2. Immediately following this design update, the RESD was submitted to Pioneer Engineering and Manufacturing Company for an estimate of its manufacturing cost. The results showed the transfer cost to be above but competitive with internal combustion and diesel engines.

Further, it was apparent that the trend in vehicle systems was headed towards a considerable downscale in curb weights, to weights well below that of an X-body vehicle. As a result, concern arose as to whether Stirling engines could be packaged in small-size vehicles. Therefore, during the past year, the RESD task has concentrated on reducing manufacturing cost and evaluating downscaling effects on the engine design.



013431

Fig. 1 Automotive Stirling Engine
Program Contractors

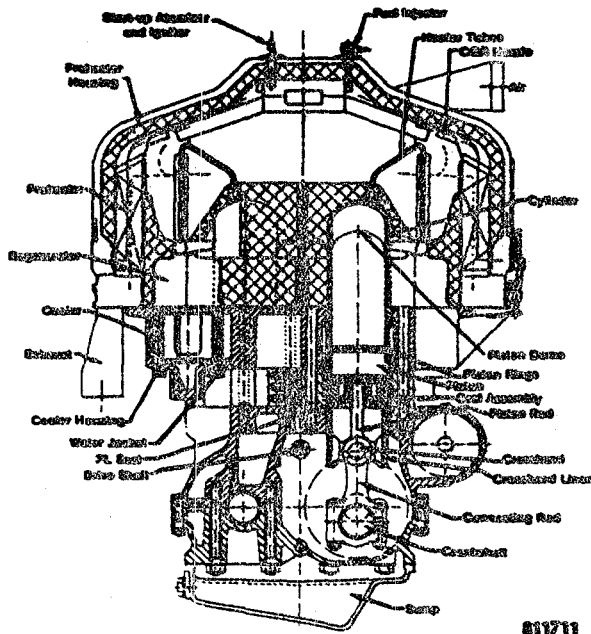


Fig. 2 Reference Engine System Design

RESD COST REDUCTION - A value-engineering design effort was initiated on the RESD that emphasized the need for manufacturing cost reduction. All proposed design changes were evaluated against the baseline cost established from the Pioneer study. The following material substitutions reduced the cost of specific components:

- Heater head tube material changed from Inconel 625 to iron-base CG-27.
- Gas cooler tubes material changed from stainless steel to phosphate-coated carbon steel.
- Preheater matrix material changed from Sandvik 253MA to Armco 12SR or 18SR.

Further, several design concepts were incorporated to reduce the RESD manufacturing cost:

- One-piece equal-angle cast-iron V-block
- Perforated plate gas cooler
- One-piece piston dome and rod assembly
- Balance shaft elimination.

Table 1 summarizes the manufacturing cost reductions associated with each of these concepts.

DOWNSIZED RESD STUDY - In reviewing the requirements for the downsized RESD, it was concluded that a 2250-lb curb-weight vehicle with an engine compartment equal to a K-body vehicle would be used. The study results showed that a V-drive or U-drive four-cycle Stirling engine could be designed and packaged to perform in a small-size vehicle while meeting and exceeding

program objectives. A preliminary cross section of a downsized RESD is shown in Figure 3. A major design concept utilized in the downsized RESD was the use of an annular heater head as opposed to the canister heater head used in the Mod I engine and full-size RESD. Figure 4 shows the profile of an annular heater head with one quadrant removed. Note the compact, simple construction as compared to the canister heater head (Figure 5) with canister regenerators placed on an outside radius from the cylinders.

PROOF-OF-CONCEPT PROGRAM

Within the ASE program, the Mod I is the experimental engine. As the first of two experimental designs originally planned, the Mod I was designed early in the program and tested during the past year. The second experimental design was designated the Mod II. Due to funding cutbacks, the Mod II design and its associated development efforts were never initiated. Since the funding cutbacks were so extensive, the only alternative was to make the Mod I engine the program's only experimental engine. Because the Mod II engine design was postponed and the RESD embodied the technologies and design concepts that would have culminated in a Mod II engine, it was reasoned that the existing Mod I engine could be used to develop and demonstrate RESD technologies. Hence, the proof-of-concept program emerged. The Mod I engine hardware program would demonstrate and develop those technologies that were not initially in the Mod I but were embodied in RESD technologies. This technology demonstration would be accomplished through a series of two upgraded Mod I designs, identified as the Mod I-A and Mod I-B engines. Figure 6 compares the design and test schedules of the Mod I-A and Mod I-B engine systems to the original Mod II program plan. Further, the approach of upgrading the Mod I design, as opposed to starting a new Mod II design, was economical. The upgraded Mod I would use basic Mod I hardware, thus eliminating the high cost of new tooling.

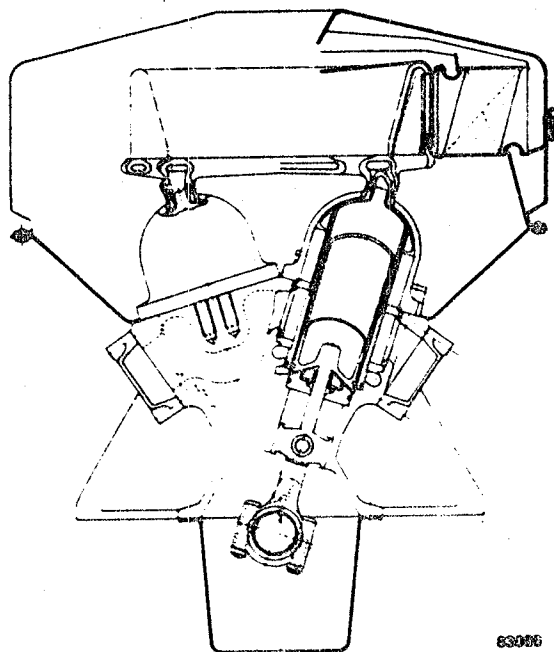
MOD I-A ENGINE

DESIGN GOALS - Design goals were established for the Mod I-A engine consistent with the proof-of-concept program and its milestones. Since existing Mod I engine hardware would be used, there were limitations to the improvement that could be demonstrated. Figures 7, 8 and 9 show the goals established for the Mod I-A, their time frame, and how these goals compared to the

Table 1. RESD Manufacturing Cost Reductions

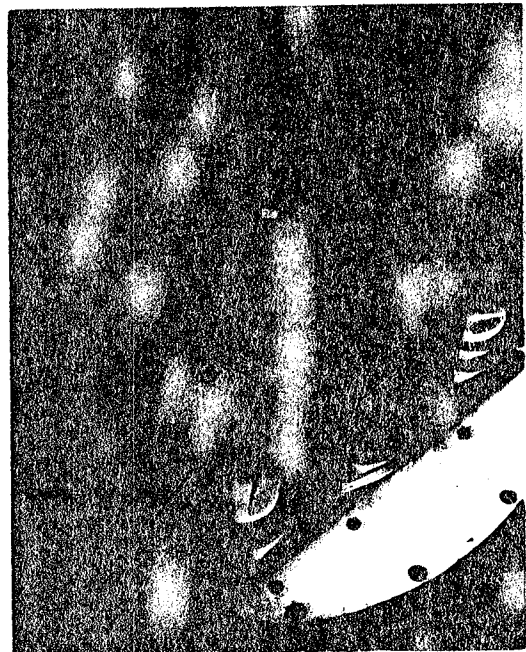
Material Substitution	Baseline Cost	Design Change	Cost	Total Cost Reduction
Heater Head Tube	\$24	One-Piece V-Block	\$25	\$220
Gas Cooler	202	Gas Cooler Configuration	21	
Preheater Matrix	24	Piston Dome & Rod Assembly	21	
		Balance Shaft Elimination	14	
			\$220	\$221/Engine

63040



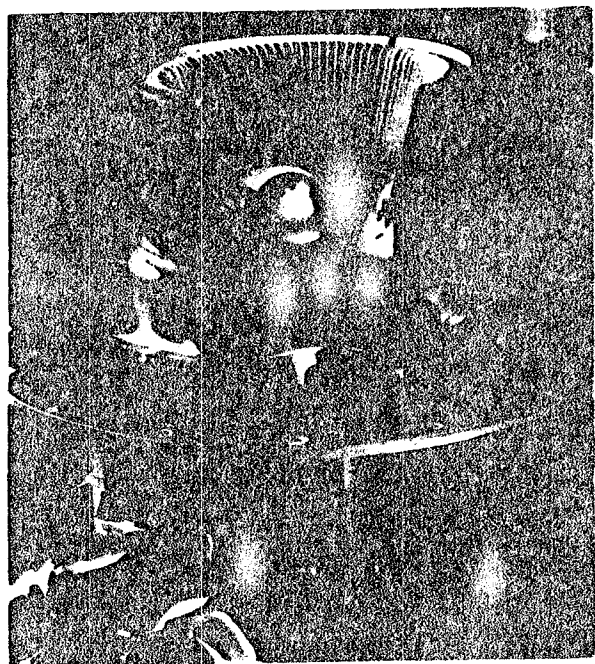
83006

Fig. 3 Downsized RESD



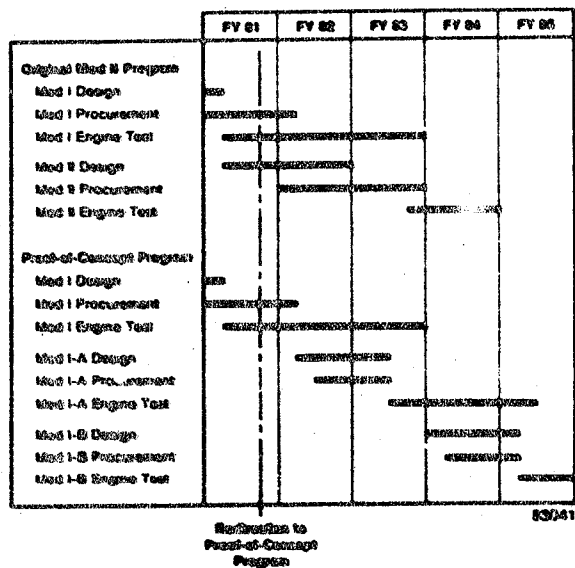
CT70611-8

Fig. 5 Canister Heater Head



MX-18420

Fig. 4 Annular Heater Head



Workflows to Proof-of-Concept Program

83041

Fig. 6 ASE Proof-of-Concept Program Plan

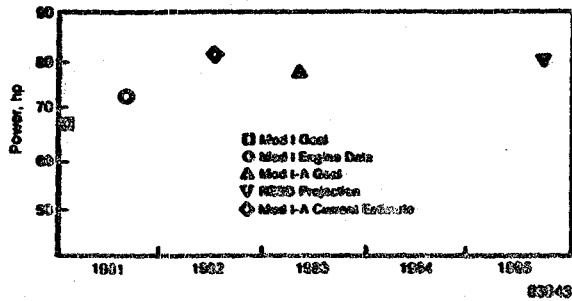


Fig. 7 Engine Power Design Goals (Mod I, Mod I-A, RESD)

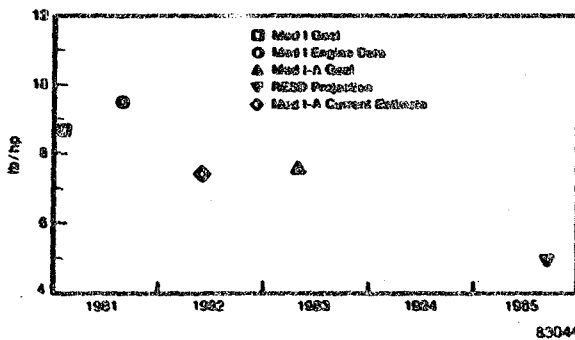


Fig. 8 Engine Specific Weight Design Goals (Mod I, Mod I-A, RESD)

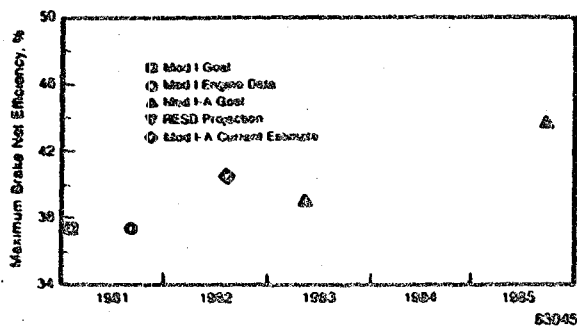


Fig. 9 Maximum Brake Net Efficiency (Mod I, Mod I-A, RESD)

Mod I (both projected and actual data) and the RESD. The figures show comparisons for power, specific weight, and maximum brake net efficiency goals and include estimates for the current configuration of the Mod I-A design. Table 2 summarizes the Mod I-A design goals.

DESIGN CHANGES - In upgrading the current Mod I engine to the Mod I-A engine, design changes were made that followed the proof-of-concept program by drawing on RESD technology.

Part-Power Optimization - Since engines operate at low speeds during most of an automotive driving cycle, the RESD had been optimized at part power to provide peak efficiencies at low engine

speeds. To upgrade the Mod I, additional part-power optimization was made. This resulted in a Mod I-A design with smaller regenerator and cooler diameters than those in the current Mod I engine. This design approach provided the Mod I-A with a major weight and cost benefit.

Operating Temperature - The current Mod I engine operated at 720°C. In upgrading the design, the operating temperature was raised to 820°C, a temperature consistent with the RESD. This higher operating temperature provided the Mod I-A with the higher Carnot-cycle efficiency potential of the RESD.

Weight - Since the weight of the current Mod I engine was above its 587-lb goal, one of the major design goals for the Mod I-A was a 100-lb weight reduction. Weight reduction was accomplished by designing a smaller diameter preheater, reduced-size heater head housings and lighter control system components.

Improved Efficiency - To improve engine efficiency, losses were reduced in the seal and drive systems as well as in the external auxiliaries.

Nonstrategic Materials - One goal of the RESD, and therefore of the Mod I-A, was the use of low-cost materials void of strategic elements. Design of the Mod I-A using nonstrategic materials in the heater head was a major step toward achieving this goal. The Mod I-A cylinder and regenerator housings would be cast from XF-818, an iron-based material, rather than from the cobalt-based alloy HS-31 used in the current Mod I. Tube material was changed from the cobalt-based alloy N155 multimet to CG-27. Table 3 compares the dramatic reduction in the use of strategic materials in the Mod I-A design to that of the current Mod I. When compared to the materials estimates for the RESD, the design of the Mod I-A was consistent with the proof-of-concept program. Figure 10 compares the current Mod I with the lighter, smaller and more powerful Mod I-A engine. The major design improvements discussed in the above subsections are identified for reference.

Table 2. Mod I-A Design Goals

	Unit	Mod I		Mod I-A		RESD
		Goal	Data	Goal	Current Estimate	
Power	hp	67.5	72.3	76.0	80.0	69.0
Specific Weight	lb/hp	8.8	9.5	7.5	7.3	4.9
Maximum Brake Net Efficiency	(%)	37.7	37.4	38.0	40.6	43.5

83046

Table 3. Reduction in Strategic Elements in Mod I-A Design

Element	Mod I	Mod I-A	RESD
Strategic Cobalt	22.4 lb	0.0 lb	0.0 lb
Strategic Chromium	36.2 lb	23.2 lb	15.7 lb
Iron	218.3 lb	228.6 lb	212.4 lb

83047

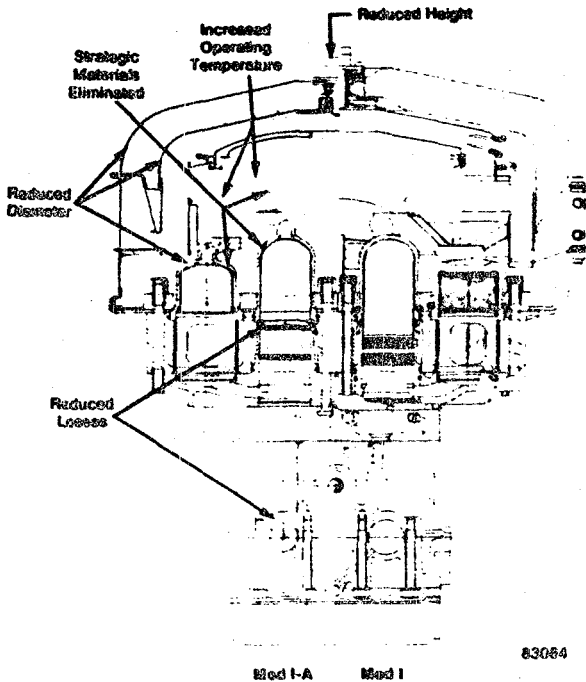


Fig. 10 Mod I-A Compared to Mod I

COMPONENT DEVELOPMENT

In support of the design concepts and technologies being incorporated into the Mod I-A engine design, an extensive component development is underway. Although many components are currently under development, two key components, fuel nozzles and low-cost materials, are discussed in the following subsections.

FUEL NOZZLES - The current Mod I single-orifice fuel nozzle was designed for air atomization. This design required a separate air compressor, an extra auxiliary that demanded as much as 3% of the engine power. Fuel nozzle development for the Mod I-A was directed toward a nonair-atomized design and a lower idle fuel flow. Current Mod I idle fuel flow was approximately 0.45 gm/sec. Since a major percent of the automotive driving cycle is spent at idle, it was determined that reduced losses in the Mod I-A would lower the idle fuel flow to 0.25 gm/sec. This would provide the Mod I-A with a significant gain in fuel economy.

Several types of fuel nozzles were evaluated for spray quality. Based on this evaluation, two fuel nozzles, a piloted air blast nozzle and a Delavan dual-orifice nozzle were selected for further evaluation in a free burning rig and a combustion performance rig. The free burning rig test compared the ignition and blowout limits of these two nozzles to the limits of the current Mod I fuel nozzle. Both experimental nozzles demonstrated an ignition delay time less than 0.2 seconds, a 33% improvement over the current Mod I

single-orifice air-atomized fuel nozzle. Blowout performance of these two nozzles was also satisfactory, and occurred in a fuel flow range of 0.1 to 0.25 gm/sec. As a result of these tests, the Delavan dual-orifice fuel nozzle was selected for the Mod I-A engine. Figure 11 compares the smaller Delavan fuel nozzle to the larger single-orifice fuel nozzle on the current Mod I engine.

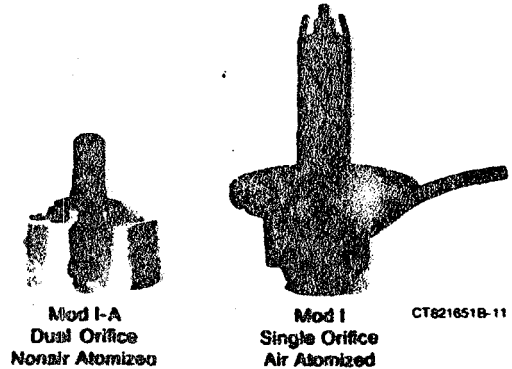


Fig. 11 Fuel Nozzle Comparison

MATERIAL/HIGH TEMPERATURE DEVELOPMENT - For the RESD to meet its design goals, the hot engine components must be capable of reliable and durable operation at a heater head temperature of 820°C. Further, the low-cost casting alloys used as heater head materials must be capable of operating at this high temperature. Since the inception of the ASE Program, the development of low-cost casting alloys has concentrated on eliminating cobalt-base materials (HS-31 and N155 multimet) in the cylinder and regenerator housing castings and tubes, respectively. After considerable screening, the alternative casting materials to HS-31 were reduced to CRM-6D, XF-818 and SA-F11. The alternative tube materials to N155 multimet were reduced to: Inconel 625, SANICRO-32, 12RN72 and CG-27. Although the development effort continues to obtain fundamental design data on these materials, actual engine tests were also considered essential to determine oxidation effects. Therefore, a P-40 heater head was configured with different casting and tube materials in each quadrant. The heater head was placed in a P-40 engine (HTP-40) and tested under cyclic load at 820°C. The material combinations for each of the four quadrants in the heater are shown in Table 4. Spare heater quadrants were available in case of failure. After 1454 test hours, the engine was stopped due to repeated failures in the 12RN72 tubes. Tubes in the quadrant containing 12RN72 are being replaced with cobalt-base N155 multimet tubing and tests will resume toward the goal of 2000 hours. The test cycle was set up to subject the heater head to increasing pressure and cyclic load in order to accelerate fatigue and creep damage. Pressures were increased to higher levels every 500 hours, until failure was expected near the 2000-hour test point.

Table 4. HTP-40 Heater Head Quadrant Material Combinations

Quadrant No.	Coating Material	Tube Material
1	HS-31	Inconel 625
2	CFM-6D	Sanicro-32
3	XF-818	12RN72
4	SA-F11	CG-27

83050

MOD I ENGINE TEST PROGRAM

Four Mod I engines are currently testing in the ASE program. As shown in Figure 12, a total of 1338 test hours have been accumulated. Engines Nos. 1, 2, and 3 were procured and assembled at USAB, whereas Engine No. 10 was of U.S. manufacture and assembled at MTI. The number "10" was assigned to the MTI-assembled engine to identify it from the three European-manufacture/USAB-assembled engines. The manufacture, assembly and test of Engine No. 10 marked a distinct demonstration of the level of Stirling engine technology transfer to the U.S. During the procurement phase for Engine No. 10, more than 30 U.S. vendors participated.

Engine No. 1 has accumulated a total of 613 test hours. After an acceptance test with a new digital control, this engine was shipped in early February to AM General for installation in a Lerma vehicle, designed to serve as a transient test bed (TTB). This installation was completed by the end of May and the initial testing began. Figure 13 shows the TTB installation. This installation helped to achieve a major program milestone by allowing the transient characteristics of the Mod I engine to be evaluated and accomplished on schedule at the end of September 1982. Currently, Engine No. 1 has logged 92 test hours in the TTB, 369 starts (124 in the TTB) and 619 miles.

Three separate Constant Volume Sampling (CVS) tests were conducted on the TTB. Results showed repeatability and fuel economy consistent with predictions. HC and CO emissions levels met program goals and NO_x emission levels also compared favorably with predicted levels. The exhaust gas recirculation (EGR) system used in the current Mod I gives NO_x levels above the program goal of 0.4 grams per mile. With further combustion system development in the Mod I-A engine, this goal will be met by virtue of the higher mileage predicted for the RESD as compared to the Mod I mileage.

Engine No. 2 has remained at USAB, where it has completed a series of development tests and accumulated a total of 425 test hours. This engine was assembled initially as a basic Stirling engine (BSE). A BSE, shown in Figure 14, does not have a control system and auxiliaries mounted on it. This configuration provided the capability of measuring engine power and efficiency without the interference of these system losses. Engine No. 2 was tested to evaluate an EGR combustor system.

This engine was then reconfigured as a Stirling Engine System (SES) to include all control system components and auxiliaries. Figure 15 shows the Mod I engine configured as an SES. The data obtained from the tests performed on Engine No. 2 provide back-to-back comparisons of BSE and SES power and efficiency losses.

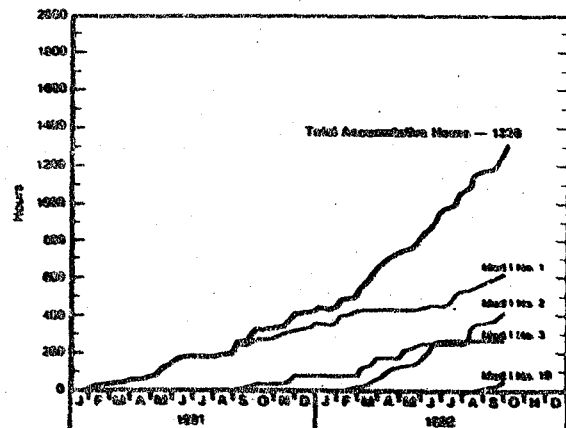
After an initial functional checkout at USAB, Engine No. 3 was shipped to MTI where a complete functional test and an acceptance test were conducted. This engine is currently being reassembled at USAB to begin a 2000-hour endurance test program. Engine No. 3 has accumulated a total of 261 test hours.

Engine No. 10 completed assembly at MTI in August and has accumulated a total of 39 test hours. It is currently undergoing an acceptance test. Figure 16 summarizes the major program milestones accomplished during the past year on each of the four Mod I engines.

MOD I ENGINE HARDWARE DEVELOPMENT

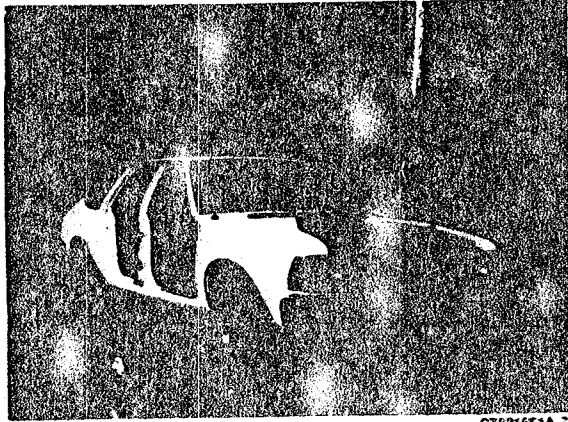
The Mod I engine program did encounter various development problems. Although many of these problems were minor ones and were solved during the normal course of development, the following subsections discuss four areas where major problems occurred.

CASTINGS - The Mod I engine assembly schedule had been paced by the delivery of cylinder and regenerator housing castings. The castings (Figure 17) are finished machined and brazed with tubes to form a heater head assembly. Two casting vendors were established to supply these castings: Bulten-Kantheil in Sweden and Precision Castparts (PCC) Corp. in Oregon. Both foundries experienced porosity problems with the cylinder castings. During the casting process, the regenerator housing experienced core failures during the waxing process. This was due to high loads on the cantilevered core "wings". Initially, a high scrapage rate was experienced, which caused delayed delivery dates. This experience served as input to the Mod I-A design.



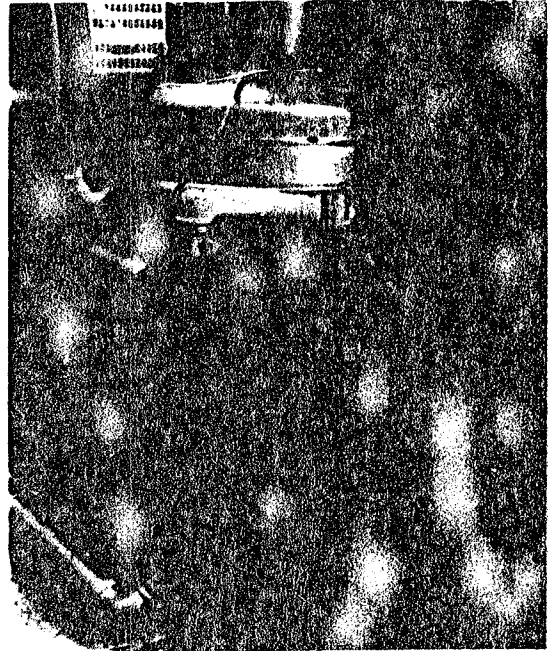
83049

Fig. 12 Mod I Engine Test Hours



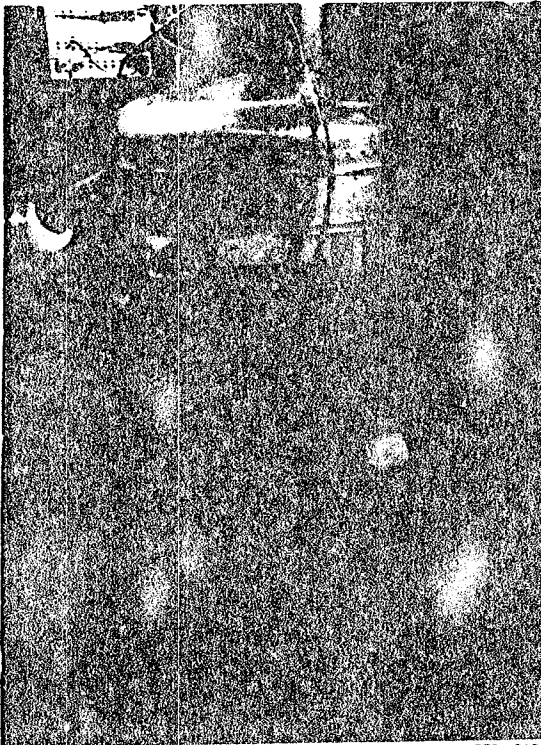
CT821651A-7

Fig. 13 Mod I Engine Installation in Transient Test Bed



CT81752

Fig. 15 Mod I Stirling Engine System



CT811812

Fig. 14 Mod I Basic Stirling Engine

	1981				1982													
	A	S	O	N	D	J	F	M	A	M	J	J	A	S	O	N	D	
Engine No. 1							▼ Completed Acceptance Test											
								▼ Digital Control Installed										
								▼ Shipped to AMG										
								▼ Completed Installation in Lerma										
								▼ Initial CVS Tests										
								▼ Completed Mod I Transient Characterization										
Engine No. 2								▼ Start Functional Test										
Engine No. 3																		
Engine No. 10 (USA Mill)																		

83085

*Basic Stirling Engine
**Stirling Engine System

Fig. 16 Mod I Engine Test Milestones

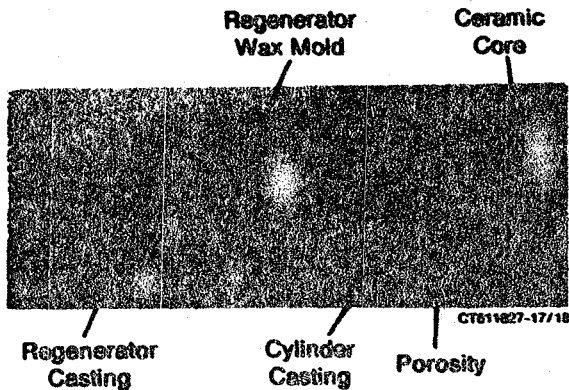


Fig. 17 Mod I Cylinder and Regenerator Rousing Castings

A second development problem with the Mod I arose during the crucial transient test bed program conducted on Engine No. 1. Engine No. 1 was configured with an electronic digital control. Use of this control greatly increased the engine's cold start transient start-up time from the slower start-up time experienced earlier with an analogue control. As a result, the rear row tubes and fins in the heater head expanded thermally at a more rapid rate than the inherently cooler manifold. This increase caused areas of high stress in the braze between the tubes and manifold. To relieve this stress and provide flexibility in the tube arrangement, the fins were cut between each tube row from halfway above the manifold base as shown in Figure 18.

The Mod I engine was initially designed and built with a combustion gas recirculation (CGR) system. As shown in Figure 19, the CGR system recirculates a small percentage of the exhaust gases back into the combustor before these gases exit through the preheater. The CGR system controls NO_x emission levels by reducing flame temperature. Figure 20 shows both top and bottom views of the CGR combustor liner.

Ejector nozzles in the combustor liner are used to pump exhaust gases back into the combustion chamber before these gases exit through the preheater. Early engine testing showed large variations in the circumferential temperature profile on the heater tube walls, thus indicating poor mixing of fuel and air resulting in unstable combustion. Further, during cold start transients, thermal stress failures were experienced in the support structures between the liner and preheater. Analysis showed that the lighter combustor liner expanded more rapidly than the colder, more massive preheater. This growth differential overstressed the support structures, leading to their failure. As a result, Engines Nos. 1 and 3 were retrofit with an EGR system that recirculates exhaust gases back into the combustor after these gases exit through the preheater. This modification allowed for a lighter, more flexible combustor liner design, thereby avoiding thermal fatigue failure of support structures.

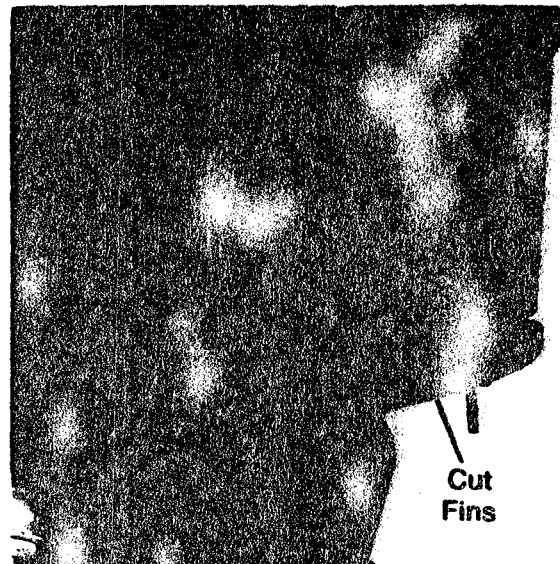


Fig. 18 Mod I Heater Head with Cut Fins

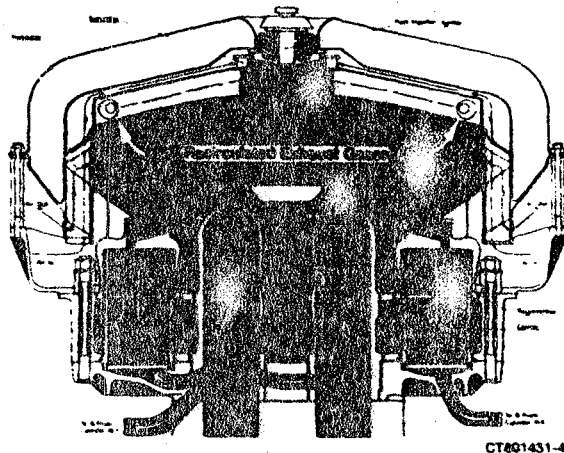


Fig. 19 Mod I Combustion Gas Recirculation System (CGR)



Fig. 20 Mod I Combustion Gas Recirculation (CGR) Liner

Although the CGR system experienced the above development problems, it is the more efficient system and therefore is incorporated into the RESD. The EGR system has several disadvantages. First, it reduces blower efficiency since inlet air temperature is higher than on a CGR system. Further, since inlet air contains exhaust gases, preheater clogging is more likely to occur in an EGR system. However, the CGR system was determined to require further development before being configured into the Mod I-A and Mod I-B engine hardware.

MOD I PERFORMANCE

The Mod I engine characteristics for both power and efficiency, as measured on Engine No. 1 with a CGR combustor, are shown in Figures 21 and 22, respectively. These data are compared to the Mod I performance predictions. When data from Engines Nos. 2 and 3 are compared to data from Engine No. 1, consistency in power levels but not in efficiency levels is evident. Figure 23 shows power levels at the maximum working gas pressure of 15 MPa for all three engines. Engine No. 2, when tested as a BSE, had an understandably higher power level since auxiliary losses were not included. When configured with an EGR system, Engines Nos. 1 and 3 showed approximately the same power levels as Engines Nos. 1 and 2 with a CGR system. Although analyses are not complete, the improved circumferential temperature profile experienced with an EGR combustor could be cancelled by increased blower power.

The earlier efficiency levels measured on Engine No. 1 have not been duplicated in subsequent testing on this engine or on Engines Nos. 2 and 3. Generally, the efficiency levels remain below 35% as shown on Figure 24.

When configured with an EGR system, Engines Nos. 1 and 3 showed lower efficiencies than Engines Nos. 1 and 2 configured with a CGR system. Further analysis showed that blower efficiency did decrease with the higher inlet air temperature associated with an EGR system. Analyses are being performed on engine-to-engine hardware differences to account for any causes for efficiency level variations.

MOD I TRANSIENT PERFORMANCE

As stated, Engine No. 1 was installed in a transient test bed to evaluate control, emissions and fuel economy performance. The transient test bed is an American Motors Corp. Lerma vehicle chassis with a Chrysler wide-ratio 3-speed automatic transmission with lockup, a 2.73-rear axle ratio, air conditioning, power steering and power brakes. Inertia weight of the TTB is 3750 lb. Fuel economy predictions were made for Engine No. 1 with an EGR combustor system using unleaded fuel at 11.1 hp road load:

- Urban Mileage: 19.1 mpg
- Highway Mileage: 30.0 mpg
- Combined Mileage: 22.8 mpg.

NO_x emission levels were predicted to be 0.84 grams per mile. HC and CO emission goals for the program were 0.41 and 3.4, respectively. Table 5 summarizes the transient test data.

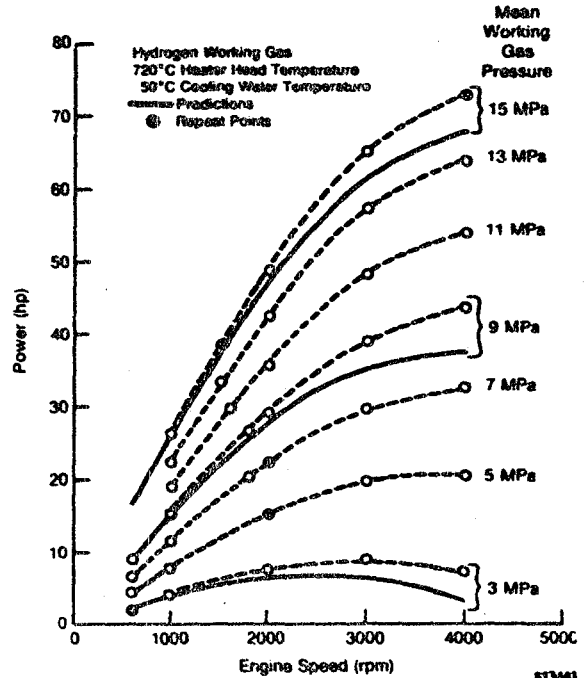


Fig. 21 Mod I Stirling Engine System Data Power Characteristics

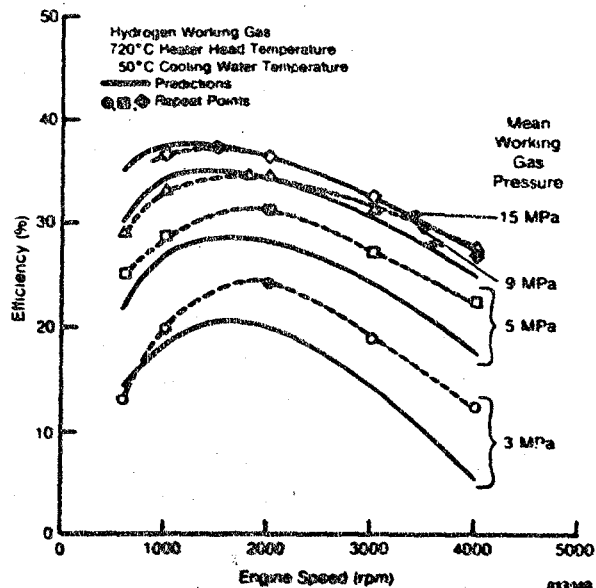


Fig. 22 Mod I Stirling Engine System Data Efficiency Characteristics

Table 5. Mod I Transient Test Data (CVS Testing)

Run No.	Urban Cycle (Particulates = 0.667 g/m ³)				Highway (Particulates = 0.666 g/m ³)				Combined Fuel Economy (mpg)
	HC*	CO*	NO _x *	mpg	HC*	CO*	NO _x *	mpg	
1	0.225	3.43	0.96	19.9	0.004	0.28	0.75	31.7	23.9
2	0.286	3.27	0.90	18.8	0.005	0.25	0.62	32.1	23.2
3	0.247	3.21	0.84	19.2	0.004	0.40	0.61	32.4	23.5

*Gram per mile

83040

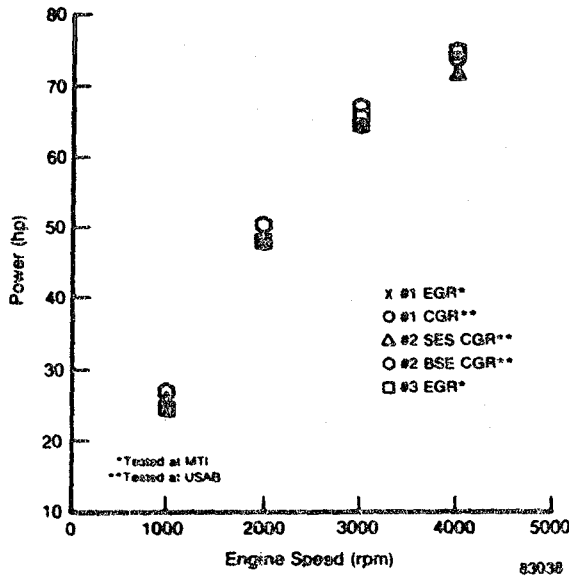


Fig. 23 Mod I Stirling Engine System Data Power Comparisons (at 15 MPa Working Gas Pressure)

SUMMARY

This paper has described the major ASE program accomplishments made during the past year. Time and space do not allow for reporting on all activities. The advances made in Stirling engine technology is moving ahead very rapidly. Improvements are being made in the use of ceramics for not only the preheater but also for the regenerator matrix. Such breakthroughs will have a profound effect on reducing manufacturing cost. Combustion system development is directed toward effective fuel nozzle designs with large turndown ratios. The successful development of a CGR combustor system is imminent. Piston rings and main seals are continually under development to improve reliability, durability and installation simplicity. If the Stirling engine is to be adapted successfully to the automotive mission, the control system must be capable of reliable and repeatable transient performance. Development is also focused on the use of an air flow meter and fuel flow meter to better mate with an automotive electronic digital control to allow precise and rapid control of fuel and air ratios. A major program goal next year will be the assembly and test of the Mod I-A engines to demonstrate higher efficiency and lower specific weights.

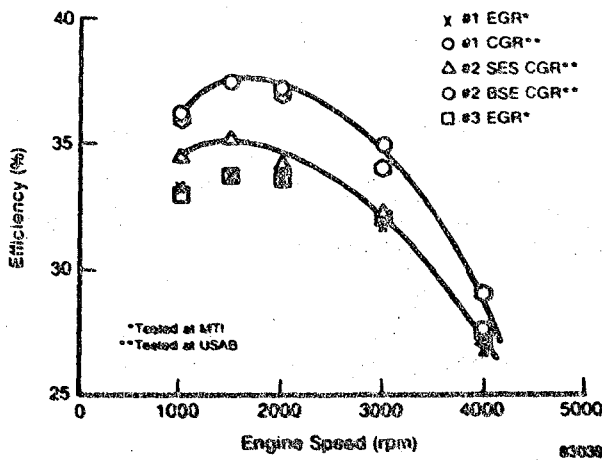


Fig. 24 Mod I Stirling Engine System Data Efficiency Comparisons (at 15 MPa Working Gas Pressure)

Automotive Stirling Engine Development Program Mod I Stirling Engine System Performance

Albert Richey
Mechanical Technology Inc.

ABSTRACT

The Mod I Stirling Engine, the first Stirling Engine designed specifically for automotive application, is under development at Mechanical Technology Incorporated (MTI) as part of the Department of Energy-sponsored Automotive Stirling Engine (ASE) Program. The initial characterization of the first Mod I engine was completed in August 1981. Since that time, development efforts have added significant steady-state data to the design base, as well as accomplished initial engine transient evaluation through fuel economy testing. Relative to earlier P-40 Stirling engine-powered vehicles within the ASE program, fuel economy improvements of up to 50% have been achieved with the Mod I engine. An advanced version of this engine, the Mod I-A, is currently in the design stage; analytical projections indicate substantial improvements in engine specific weight and fuel economy.

MOD I STIRLING ENGINE SYSTEM DEVELOPMENT during the past year has concentrated on the building and testing of two additional engines, and the continued testing of the initial Mod I engine. Improvements identified during the early stages of the Mod I testing are being pursued in the Mod I development program, as well as in the design of an advanced Mod I engine, the Mod I-A.

Testing of the Mod I engine has established performance levels during steady-state operation and has documented auxiliary power consumption. Base-line transient test bed assessments have demonstrated significant improvements in fuel economy relative to previous Stirling-powered vehicles. *re-estimated* This paper presents the results of these test programs and projects performance improvements achievable in the Mod I-A engine.

ENGINE CHARACTERIZATION DATA

Figure 1 presents power characteristics for the engines tested in the Mod I development program; for the sake of clarity, only the 15 MPa and 5 MPa mean charge pressure levels are

included. The 15 MPa performance curve represents the maximum available power level, and the 5 MPa data provide performance indications at average operating conditions in a vehicle system. The total engine-to-engine power variation was less than 2 kW at all power levels, while the maximum power level demonstrated by all engines also exceeded the minimum level established as the final acceptance criteria.

Figure 2 shows efficiency levels attained during engine testing. In comparison to power variations, the variation in efficiency level from engine to engine was greater. Engine #1, during final acceptance testing at United Stirling of Sweden (USAB), showed the most significant deviation in efficiency level performance. Although

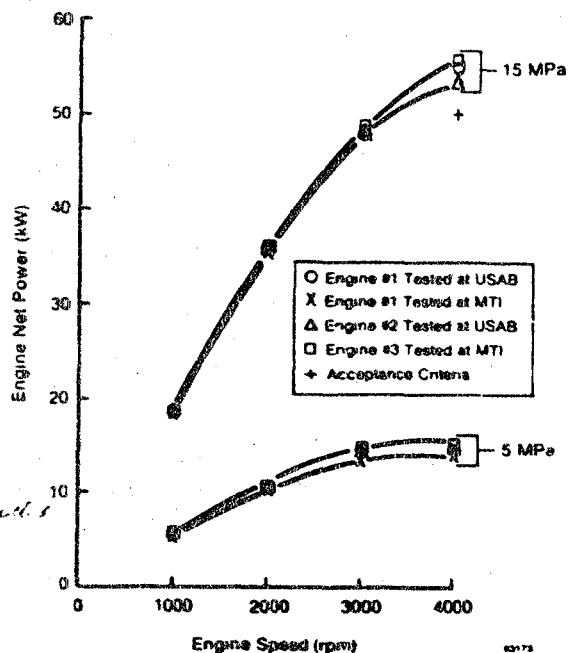


Fig. 1 Mod I Stirling Engine Net Power

the reason for this variation is not completely understood at this time, three contributing factors serve to qualitatively explain the higher efficiency level of Engine #1:

1. This engine ran with the initial version of the combustion gas recirculation (CGR) combustor, for which high-temperature spreads were measured on the heater head tubes and working gas temperature. Although the measured average heater head temperature level was maintained equal to that used during other engine testing, the actual effective working gas temperature could be higher than indicated due to the incomplete temperature coverage on the heater head.
2. Following steady-state acceptance testing, transient tests indicated the desirability of modifications to achieve more rapid changes in engine power during deceleration. This effect was achieved by enlarging the internal lines leading to the working gas removal system, thus increasing dead volume in the engine cold space and resulting in a lower steady-state efficiency level. (All other engines have since incorporated the enlarged internal lines, as did Engine #1 for its testing at MTI and for the Lerma transient test bed installation.)
3. During the final acceptance testing, engine performance may have been affected because spacer rings above the regenerators became

warped, causing changes in hot space dead volume and altering flow distribution through the regenerator.

Engine #1, as tested at MTI, utilized an exhaust gas recirculation (EGR) combustor, enlarged internal lines, and non-warped spacer rings. It should be noted that the performance of the engine in this configuration agrees very well with that demonstrated by Engine #2 and #3. Furthermore, the efficiency levels of all engines met or exceeded those established as acceptance criteria.

As mentioned earlier, high heater head temperature spreads were encountered during the initial testing of Engine #1 with a CGR combustor (Figure 3). Due to the rigid construction of the CGR combustor, warping of combustor mountin and sealing hardware was also encountered during the rapid thermal transients of engine starts. Therefore, it was concluded that further CGR development was required and that EGR combustors would serve as interim combustors for the Mod I engine. As shown on Figure 3, the heater head temperature spread is drastically reduced with the EGR combustor.

Testing of an EGR system for the Mod I engine was accomplished using two engines to establish and verify an optimum EGR schedule for providing acceptable emission control and engine performance

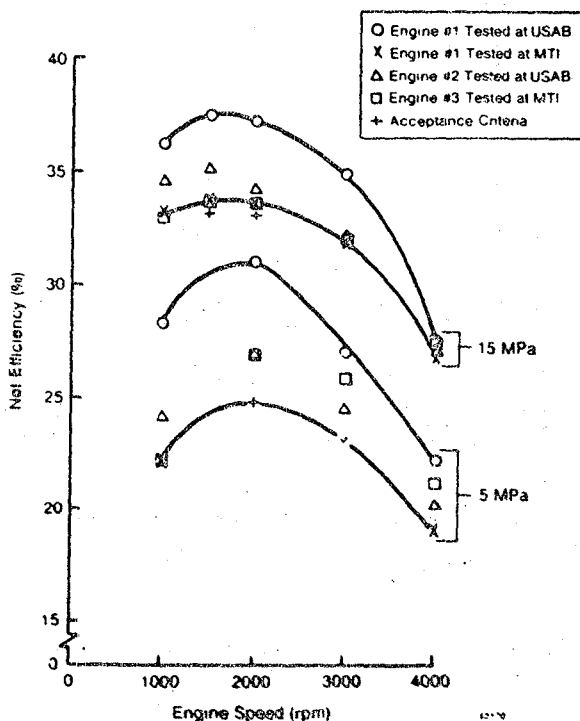


Fig. 2 Mod I Stirling Engine Net Efficiency

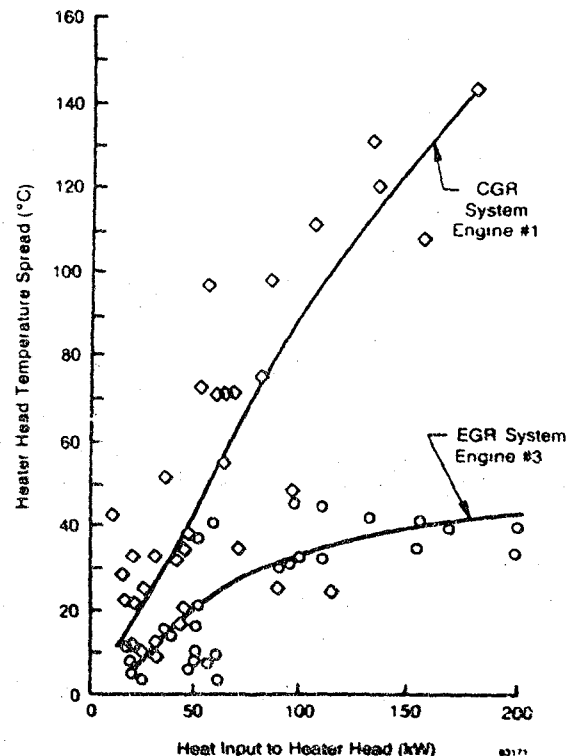


Fig. 3 EGR/CGR Heater Head Temperature Spread

(1).* The performance impact of the selected EGR schedule is shown on Figures 4 and 5. Figure 4 illustrates the degradation of engine power with increasing amounts of EGR; the selected EGR schedule is superimposed on this curve and shows a negligible effect on power level. Similarly, Figure 5 shows engine net efficiency degradation with increasing EGR and also includes the selected EGR schedule. The EGR impact at the maximum efficiency point is small (0.3 percentage points) and, at the average operating point, shows an efficiency degradation of 0.5 percentage points.

A comparison of emissions characteristics of the EGR and CGR combustors showed a decrease in CO emissions, with an increase in NO_x emissions level; hydrocarbon (HC) emissions were negligible with either combustor. As illustrated on Figure 6, the EGR system provides improved CO emissions characteristics at the higher fuel flow rates. The NO_x comparison (Figure 7) shows that emissions are higher with the EGR combustor than with the CGR combustor; nevertheless, based on current Mod I fuel economy levels, maximum NO_x emissions levels of 1.0 g/mi will be met with the EGR system.

AUXILIARY POWER CONSUMPTION

Testing included documentation of Basic Stirling Engine (BSE) and Stirling Engine System (SES)

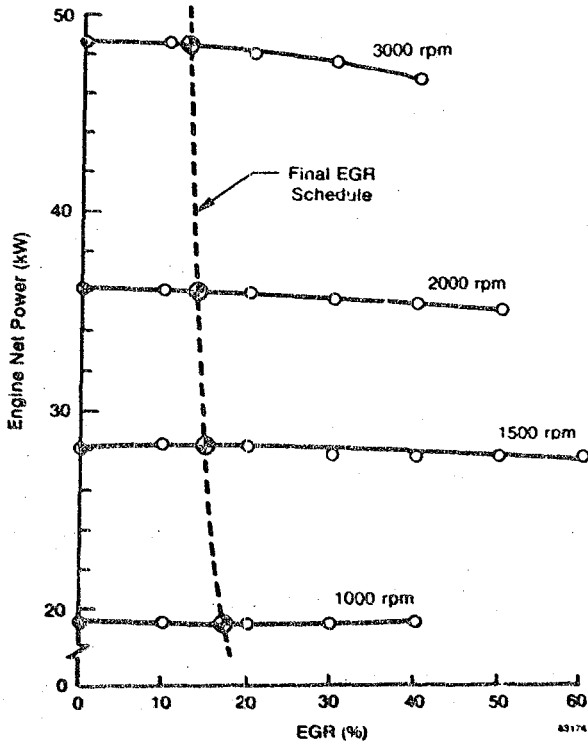


Fig. 4 Effect of EGR on Power (15 MPa)

*Numbers in parentheses indicate references at end of paper.

performance on the same engine. The difference in performance level between these two configurations represents the power consumed by various auxiliaries. Figure 8 presents the measured power difference obtained via tests on Mod I Engine #2, compared to the summation of measured power consumption obtained via rig testing of the individual auxiliaries. The total auxiliary power is the measured difference in power output between BSE and SES tests.

The auxiliary rig tests measured power required for SES steady-state operation; the following operating conditions applied:

1. Hydrogen Compressor: operating in the short-circuit mode

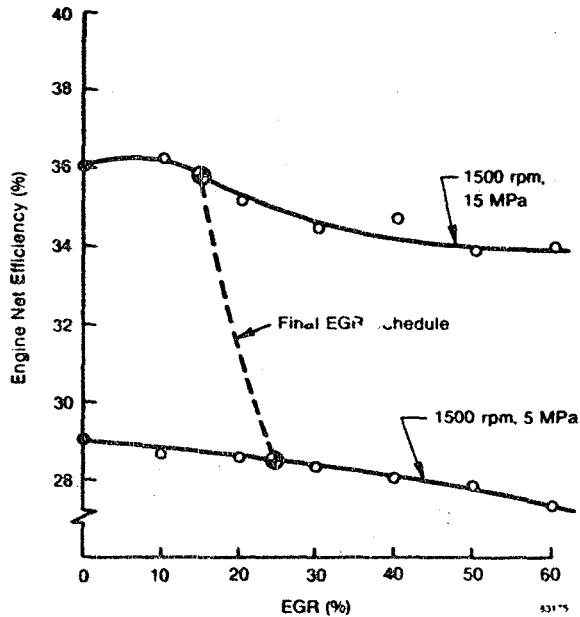


Fig. 5 Effect of EGR on Efficiency

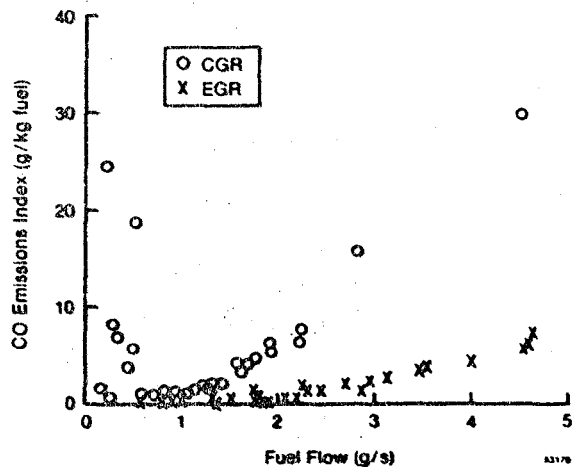


Fig. 6 CO Emissions - Mod I Stirling Engine

2. Combustion Air Blower: nominal operating line controlled by air throttle setting
3. Atomizer Air Compressor and Servo Oil Pump: atomizer air compressor discharge controlled via pressure relief valve as in engine operation.

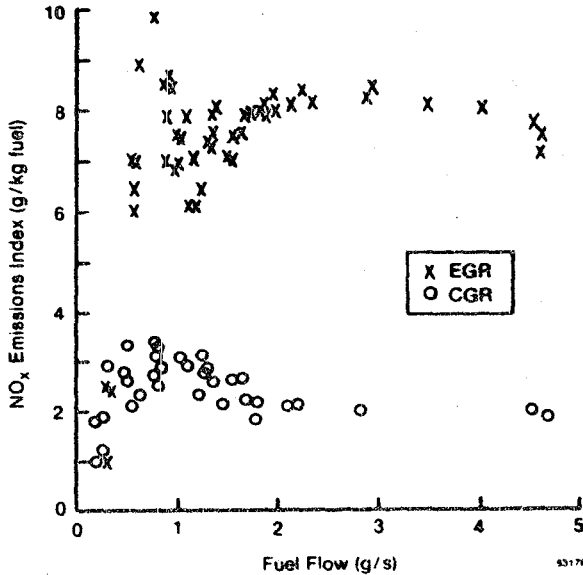


Fig. 7 NO_x Emissions - Mod I Stirling Engine

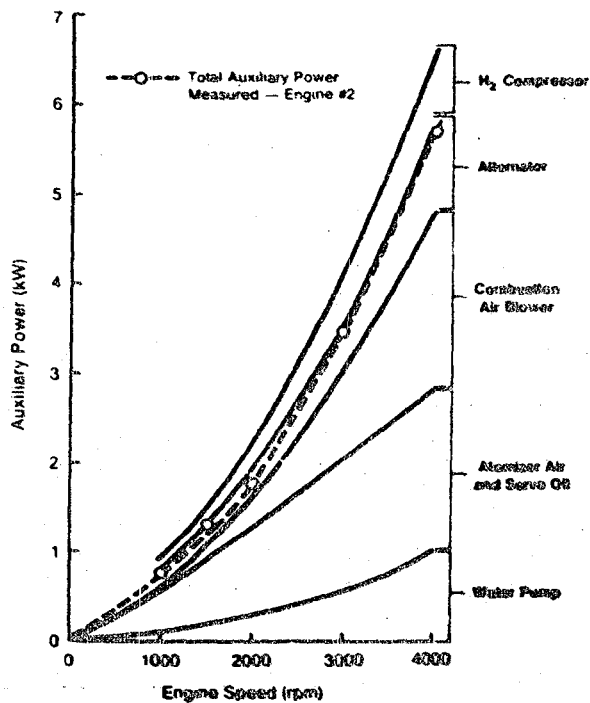


Fig. 8 Mod I Stirling Engine Auxiliary Power (15 MPa)

tion. Servo oil pump providing flow to compensate for system bypass leakage

4. Alternator: providing power for electronic control system.

The comparison of total measured auxiliary power to the summation of individual component power requirements reveals excellent agreement (see Figure 8), with a difference of approximately 0.7 kW at maximum power.

ENGINE UTILIZATION RATES

Since the start of the Mod I development program in January 1981 through September 1982, 1338 hours of testing have been accumulated on four engines. Figure 9 presents this test experience as an average monthly utilization rate, and compares it to the utilization rate achieved with the P-40-7 Stirling engine at MTI's facility during calendar year 1981. It is noteworthy that the average utilization rate for the Mod I engines, even during the initial familiarization testing, is 50% higher than that achieved with the P-40, a more mature engine. The Mod I engine design changes, directed at improved reliability/operability, have resulted in a decrease in engine downtime.

TRANSIENT TEST BED (TTB) FUEL ECONOMY

Mod I Engine #1 is dedicated to the development of transient systems within the ASE program. To provide this capability, it has been installed in an AMG Lerma Transient Test Bed (TTB) for optimization of engine/vehicle system characteristics and development of the various engine control systems. Performance improvements realized through this development process can be measured

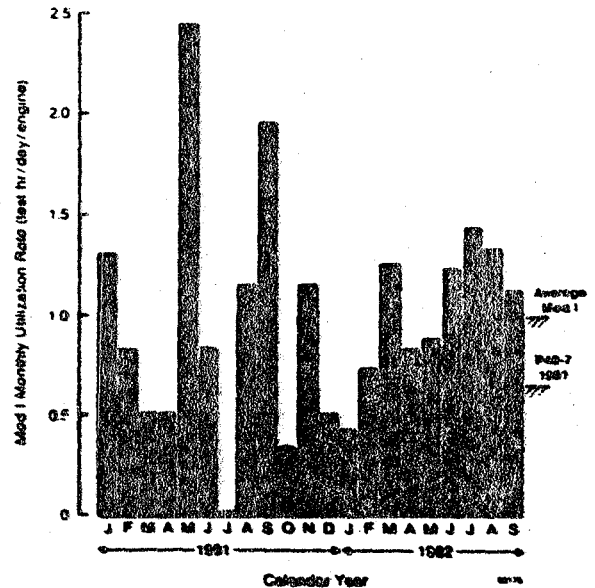


Fig. 9 Mod I Test Experience

by improvements in vehicle fuel economy; hence, an initial TTB mileage evaluation was established to provide the base line for this testing, and extensive documentation was acquired to enable assessment of any system changes. First, Engine #1 was fully characterized in MTI's test facility prior to installation in the Lerma TTB. Emissions data and standard engine performance data were recorded and utilized to provide base-line engine maps for computer code assessment of vehicle mileage and comparison to any engine modifications accomplished during development. (Engine characterization will be repeated in the event significant modifications are incorporated.) Following characterization and installation, base-line Constant Volume Sampling (CVS) tests were accomplished and analytical mileage projections were established utilizing MTI's vehicle simulation code. Three separate tests, each consisting of a cold start urban cycle and a highway cycle, were conducted. Test results to date, along with projections, are shown on Table 1. Excellent agreement with projections, including both mileage and NO_x emissions levels, has been achieved. The data repeatability for the three runs was excellent, with a standard deviation in mileage of 1-2%. The progress of the ASE program, as measured by this base-line testing, is shown in Figure 10. A direct comparison of as-recorded fuel economy between Mod I data and previous P-40 vehicle data is invalid due to the differences in test weights and power-to-weight ratios for the three vehicles; accordingly, the P-40-powered vehicles have been analytically adjusted on Figure 10 to show performance that would result at the same power-to-weight ratios and test weights. As adjusted, the Mod I base-line testing represents a 50% and 26% mileage improvement over the P-40 Opel and Spirit vehicles, respectively. Figure 11 presents a breakdown of the energy consumed during the urban and highway cycles for the Mod I Lerma system. As is illustrated, significant amounts of the total engine energy use (27% of urban cycle and 38% of highway cycle) are consumed by lower-end engine friction drive unit, seals, rings), auxiliaries and cold-start penalty.

MOD I-A PERFORMANCE

The Mod I-A engine design (2) is aimed at providing improved performance levels relative to the Mod I, and also at continued proof-of-concept demonstration of a projected advanced ASE design, known as the Reference Engine System Design. In addition to the normal design goal of improved cycle efficiency, the Mod I-A design effort is addressing the energy consumption losses determined by the Mod I Lerma system testing. Table 2 summarizes analytically projected improvements in the Mod I-A engine and compares them to current analytical modelling of the Mod I engine. Several design changes (see Table 3) contribute to these maximum power and efficiency level improvements; these include:

- Increased set temperature to provide improvement in cycle efficiency
- Redesign of heater head and regenerator to achieve improved castability and more optimum part power performance with minimal effect on maximum engine power output
- Incorporation of rolling element bearing drive unit and improved seal designs to decrease friction losses
- Incorporation of new fuel nozzle system to eliminate air atomizer compressor and associated power loss.

Table 1 Lerma Vehicle Test Data

Description	Urban			Highway	Combined	
	HC g/mi	CO g/mi	NO _x g/mi	Mileage mpg	mpg	
9/21 Test	0.23	3.4	0.96	19.9	31.7	23.9
9/24 Test	0.29	3.3	0.90	18.6	32.1	23.2
9/25 Test	0.25	3.2	0.84	19.2	32.4	23.5
Standard Deviation	0.025	0.092	0.069	0.45	0.29	0.29
Mean	0.26	3.3	0.90	19.3	32.1	23.5
Projections	-	-	0.84	19.1	30.0	22.8

11.1 hp @ 30 mph Dynamometer Power Setting
 3290 lb Inertia Weight Setting
 2.73 Air Flow

P-40 Opel	P-40 Spirit	
△	◇	Measured
△	◇	Adjusted to TTB Power/Weight

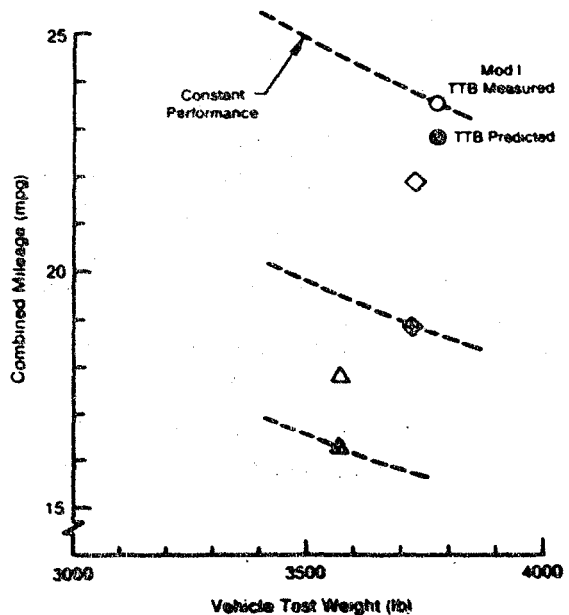
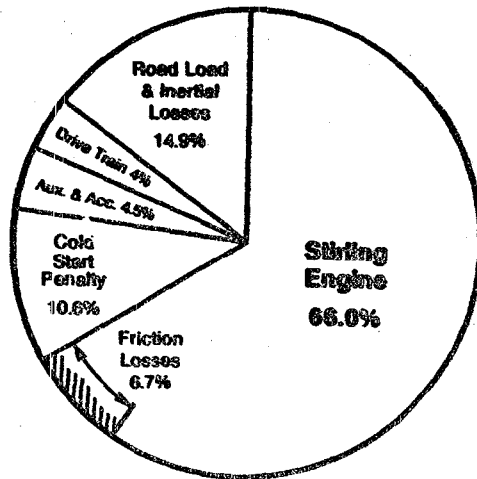
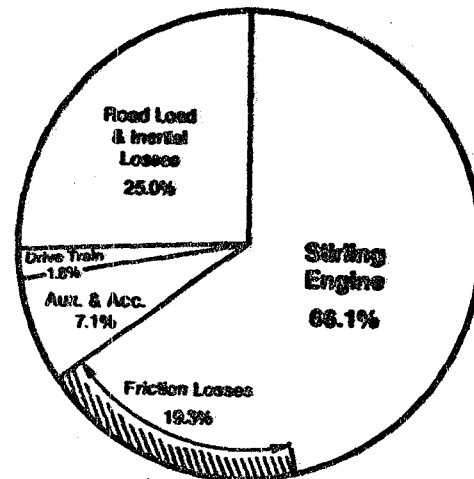


Fig. 10 Vehicle Fuel Economy Comparison



URBAN CYCLE



HIGHWAY CYCLE

Fig. 11 Lerma Vehicle Energy Consumption

63169

Table 2 Mod I-A Performance Projection

Operating Condition	Parameter	Mod I-A	Δ from Mod I
15 MPa 4000 rpm (Maximum Power)	Net Power	80.26 kW	+10.2 kW
	Net Efficiency	28.9%	+2.7 pt
15 MPa 1500 rpm (Maximum Efficiency)	Net Efficiency	40.76%	+3.07 pt
	Net Power	12.57 kW	+2.43 kW
5 MPa 2000 rpm (Average Operating Point)	Net Efficiency	33.04%	+4.95 pt
	Specific Weight		
	kg/kW	4.4	-24%
	lb/hp	7.3	

Table 3 Major Improvement Areas for the Mod I-A Stirling Engine System

Change	Δ Maximum Net Power	Δ Maximum Net η
Increased Set Temperature (720 \rightarrow 820°C)	+7	+1.0% pt
Part Power Optimization	-2	+1.0% pt
Decreased Friction Losses	+1.2	+0.7% pt
Elimination of Atomizer Air Compressor	+0.5	+0.3% pt

In addition to these steady-state performance improvements, a reduction in cold-start penalty is projected as a result of the lighter-weight, redesigned heater head and external heat system. It is anticipated that a 17% reduction in stored heat (which translates to a 0.5 mpg urban mileage improvement) will be achieved with the Mod I-A design. The overall projection for the Mod I-A engine is that combined fuel economy will improve approximately 3 mpg or 13% relative to the current Mod I system.

REFERENCES

- Farrell, R., "Mod I Stirling Engine Emissions with Exhaust Gas Recirculation," Mechanical Technology Incorporated, Automotive Technology Development Contractor Coordination Meeting, October 1982.
- Moodysson, E., "Upgraded Mod I Stirling Engine System Design," United Stirling of Sweden, Automotive Technology Development Contractor Coordination Meeting, October 1982.

Upgraded Mod I Stirling Engine Design (Mod I - A)

Bengt-Ove Moodysson
ASE Program (MSc)
United Stirling AB

INTRODUCTION

The work reported in this paper is part of the engine development tasks within the Automotive Stirling Engine Program. A first generation engine, called Mod I has been developed within the program and has been under test since the beginning of 1981. To date four engines have been built and tested for over 1300 hours.

These engines now serve as baseline experimental engines in the program. The upgrading of Mod I will prove technologies embodied in the Reference Engine System Design (RESO).

The paper highlights design improvements in the first phase of this "Proof-of-Concept." Main objectives for the present design, called Mod I-A, have been:

- improved power and power density (specific weight)
- improved fuel economy, efficiency ^{20% down}
- cold start penalty

Table 1 shows Mod I-A goals relative to Mod I data. In addition the design has focused on:

- reduced manufacturing cost,
- void of strategic materials,
- better packageability (reduced size).

Mod I-A is due to be tested in April 1983, and to demonstrate also improved durability and reliability and transient capability.

ENGINE DESIGN DESCRIPTION - BASIC CONFIGURATION

The general Mod I-A configuration is the same as for Mod I, which in turn was based on United Stirling's P40 engine. The configuration is characterized by a combustor on top facing downwards, a plate-type counter-flow air-preheater surrounding a heater head, which consists of a circular array of involute shaped tubes connected to parallel cylinders and regenerator housings. The four cylinders are arranged in a square, placed on

an engine block which in turn is placed on the crank-case. The displacement is 123 cc per cylinder. The crank-case contains two crank-shafts which are synchronized and coupled to an output shaft by gears. The reciprocating parts are of a cross-head type design in order to achieve a linear piston-rod movement which makes it possible to efficiently seal off the volumes containing the working fluid.

(Refer to Fig. 1.)

In designing for automotive application, high power to weight ratio is an important objective. This has been achieved mainly by use of aluminium in most of the cold parts of the engine and by having only one regenerator/gas cooler unit per cylinder. The mechanical integration of the engine is achieved by the use of tie-bolts between the heater head and the crank-case.

ENGINE DESIGN DESCRIPTION - DESIGN GOALS

With the overall design goals in mind, representing a step forward to meet the characteristics projected for RESO, the Mod I-A design has become specified gradually based on

- Mod I experiences, strengths/weaknesses
- results from component development
- design studies and analysis of alternative component configurations.

(Refer to Fig. 2.)

The major design changes from Mod I to Mod I-A, which are intended to prove concepts in the RESO, relate to:

- part power performance optimization, reduced losses
- increased operating temperature in a lower cost non-strategic materials heater head (specified design temperature is 820°C)
- lower specific weight and less complexity.

Table 1

	Mod I DATA	Mod I-A*) GOALS
POWER (Kw)	53.9	58
(hp)	72.3	78
WEIGHT (Kg)	312	263
(lb)	688	580
SPECIFIC WEIGHT (Kg/Kw)	5.8	4.5
(lb/hp)	9.5	7.5
BRAKE THERMAL EFFICIENCY (%)		
MAXIMUM	37.4	39
PART POWER	31.0	33
SPECIFIC FUEL CONSUMPTION (lb/hp-hr)		
MINIMUM	0.368	0.353
PART POWER	0.445	0.418
*) Power and efficiency goals assume increased operating temperature to 820°C.		

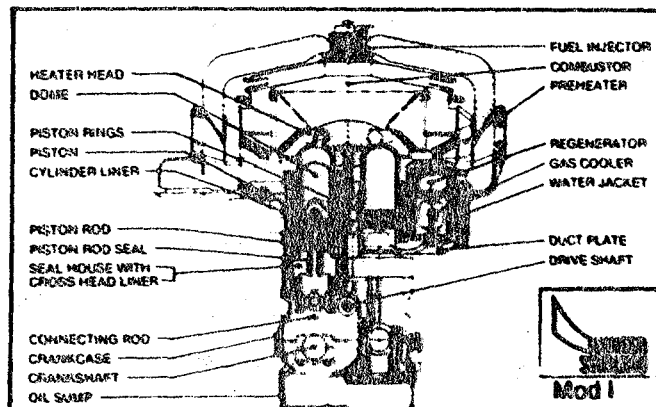


Fig. 1

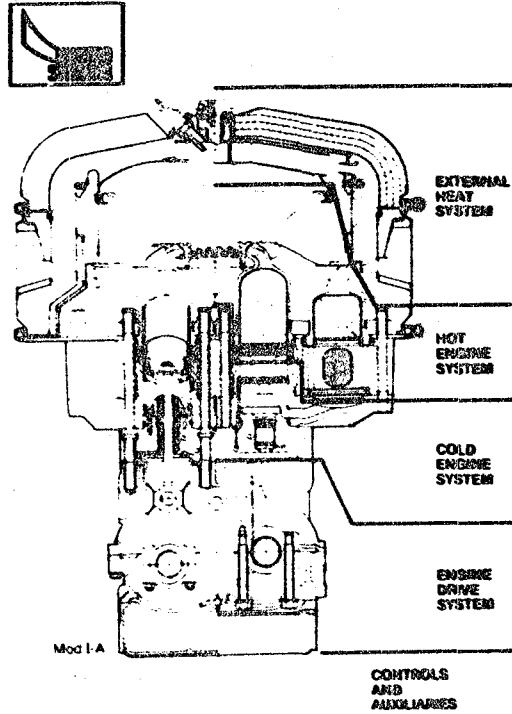


Fig. 2

Therefore, and also for improving reliability and demonstrating endurance and cost reduction potentials, all engine subsystems have been upgraded in various ways. Table 2 summarizes salient Mod I-A advances.

To reduce hardware risks, Mod I and Mod I-A subsystems are also designed for interchangeability.

ENGINE DESIGN DESCRIPTION - EXTERNAL HEAT SYSTEM

The Mod I-A external heat system is the same type as the present for Mod I. It has a counter-flow recuperative air preheater. The heat exchanger matrix consists of a large number of thin plates, seam welded together.

(Refer to Fig. 3.)

The new design is less bulky since the preheater is located closer to the heater tube array.

More efficient insulation is used to further reduce overall size. Air and exhaust gas manifolds, optimized for flow distribution, are more integrated to the preheater.

The entire unit has also been made more tolerant to thermal transients.

Internal seals and those at the bottom plate and upper cover should be more reliable. System assembly is simplified by using clamping rings instead of numerous bolts around the periphery.

The cover is shaped to allow combustion gas recirculation (CGR) or exhaust gas recirculation (EGR) type combustor. Both types are under experimental evaluation. However the current design calls for an EGR system.

ENGINE DESIGN DESCRIPTION - PREHEATER

The preheater plates consist of a corrugated part in which the true counter flow occurs.

Both ends are extended to form headers for the air and combustion gases.

(Refer to Fig. 4.)

The distance between two plates is defined by the corrugation and the plates are welded together in a cylindrical structure. The gap between all plates is kept constant by bending the plates in an involute shape.

The exhaust gas is collected in a manifold just outside the matrix and from there it is diverted through exhaust pipes. The fresh air from the blower is directed into a manifold before it enters the preheater matrix. In this way the air will be evenly distributed over the entire preheater matrix.

(Refer to Fig. 5.)

Based on optimization for part power, the number of plates has been decreased. In order

to reduce heat conduction losses and cold start penalty, the plate thickness has also been decreased from 0.15 to 0.1 mm which contributes to lower weight and cost as well.

Cost-competitive material alternatives have been tested for formability and weldability. The selected material, 253 MA has the following composition, (%):

	Fe	C	Si	Mn	P	S	Cr	Ni	N
bal.	0.08	1.7	0.8	0.04	0.03	21	11	0.17	

ENGINE DESIGN DESCRIPTION - COMBUSTOR

A reliable combustor system and combustion control is required to meet emission objectives.

- NO_x = 0.4 g/mile
- CO = 3.4 g/mile
- HC = 0.41 g/mile
- Particulates = 0.2 g/mile

In order to keep the low NO_x level, the combustion temperature must be limited. With a CGR combustor this is achieved by means of ejectors in the preheated air path. Part of the combustion gases are withdrawn before entering the preheater and recirculated into the combustion area where it decreases the temperature. In an EGR combustor, exhaust gases are instead recirculated after passing the preheater. The blower has to feed gas back through the preheater into the combustion area. This adds complexity to the air/fuel system and, indicated by comparative tests, reduces overall efficiency.

(Refer to Figs. 6a and b.)

The Mod I CGR combustor has the space between an upper and a lower liner divided into 10 channels separated from each other by straight partition walls. This honeycomb structure has suffered from stiffness.

Thermal transients have caused geometrical deformations resulting in widely varying heater temperature profiles. Back-up EGR combustors have not shown such tendencies. (Refer to Fig. 7.) A Mod I-A design has been performed (EGR). Matching this type combustor with a non-air atomized fuel nozzle is in progress but disadvantages for the air blower and throttle remain.

(Refer to Fig. 8.)

In parallel, a lighter and more flexible CGR combustor is being developed. Its air and combustion gas mixing channels are separate tubes. They are free to expand independent of a single upper liner which carries the ejectors and attaches to the preheater. Its cold start penalty (weight) and cost are significantly lower than for the present Mod I CGR version.

Table 2

Improvement Sub-system	Fuel Economy	Specific Weight	Reliability Durability	Manufacturing Cost	Feasibility Maintainability
External heat exchanger	<ul style="list-style-type: none"> Reduced cold start penalty Reoptimized air preheater Improved insulation & seals 	<ul style="list-style-type: none"> Thinner sheet metal parts Lighter design combustor Integrated manifolds 	<ul style="list-style-type: none"> More flexible combustor designs Improved preheater joints 	<ul style="list-style-type: none"> Reduced number of preheater plates & welds Fewer and less machined parts 	<ul style="list-style-type: none"> Smaller outside diameter Less air casing replaced
Hot engine system	<ul style="list-style-type: none"> Reoptimized for 800° C. part power Reduced cold start penalty Better internal gas flow distribution 	<ul style="list-style-type: none"> Lighter cylinders, reg. housings, fins Smaller regenerator coolers Lighter flame shields & insulation 	<ul style="list-style-type: none"> Endurance analysis in more depth Redesign for better castability More flexible fins Simpler insul. covers 	<ul style="list-style-type: none"> Non-strategic materials, lighter Smaller regenerators for alt. firing Reduced number of power tubes 	<ul style="list-style-type: none"> Smaller regenerators allow for reduced preheater diameter Better access to main cooling/Ranges
Cold engine system	<ul style="list-style-type: none"> Improved piston ring configuration Dead volume reduction 	<ul style="list-style-type: none"> Most structural parts modified Redesigned reciprocating parts Less sheet tube plumbing 	<ul style="list-style-type: none"> Parts integration Lower line tolerances Reduced number of o-rings Improved main seal & piston ring functions 	<ul style="list-style-type: none"> Parts integration, less machining Reduced number of o-rings Simplified (& less) plumbing 	<ul style="list-style-type: none"> Better interfaces to the external gas systems
Engine drive system	<ul style="list-style-type: none"> Reduced bearing friction (spin) Reduced lub. oil pump capacity Alternatively roller element bearings 	<ul style="list-style-type: none"> Chain link option removed Reduced counter weights General weight savings 	<ul style="list-style-type: none"> Con-rods up-dated 		<ul style="list-style-type: none"> Reduced size bottom and top-out has been performed but not detailed
Controls and auxiliaries	<ul style="list-style-type: none"> Removed preheater air compressor Reduced burner driver power 	<ul style="list-style-type: none"> Redesigned power control blocks Aluminum pulleys and brackets 	<ul style="list-style-type: none"> Redesigned burner driver drive Modified servo or system 	<ul style="list-style-type: none"> Removed components Simplified control schemes Less plumbing and wiring Reduced number of o-rings 	<ul style="list-style-type: none"> General up-dates of the entire arrangement

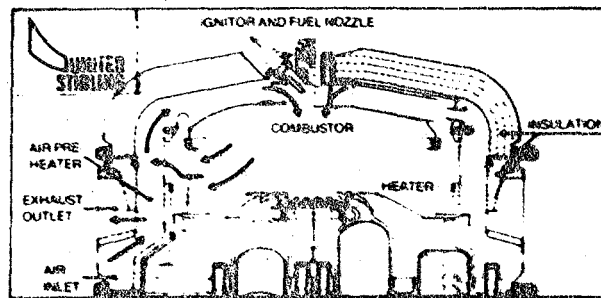


Fig. 3

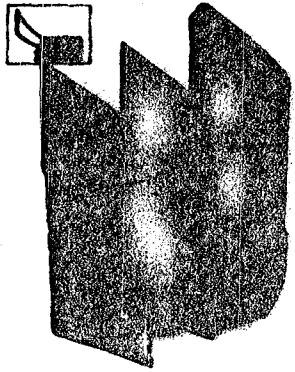


Fig. 4

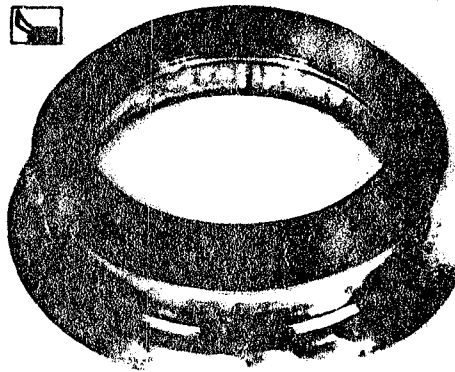


Fig. 5

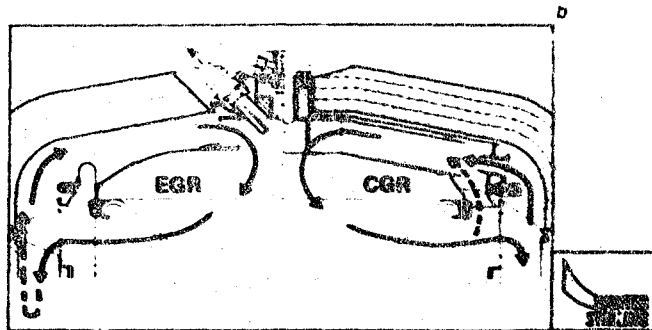
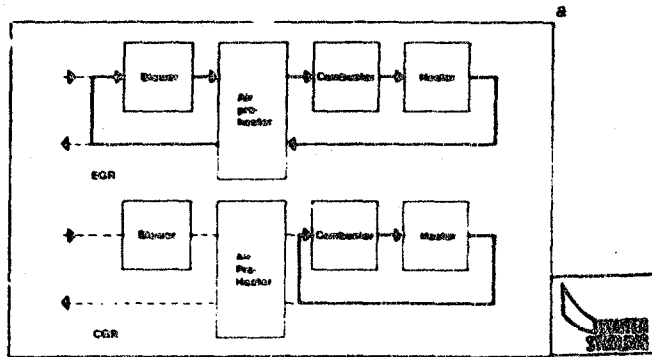


Fig. 6 (a and b)

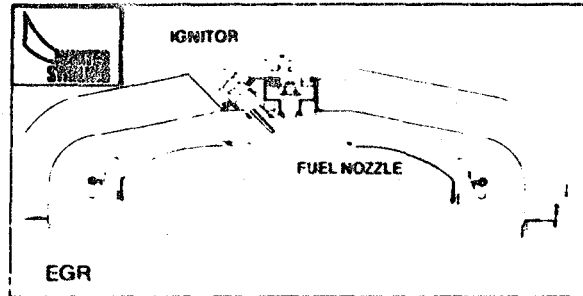


Fig. 7

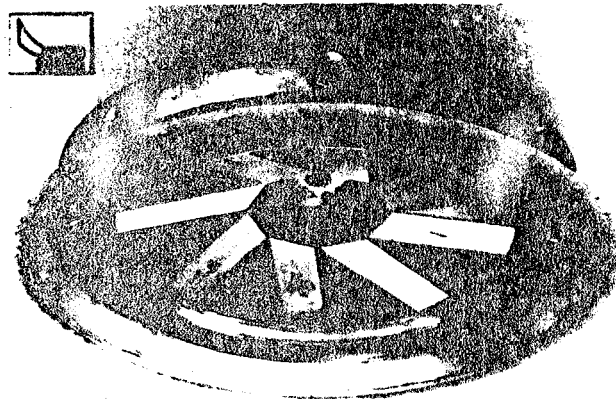


Fig. 8

ENGINE DESIGN DESCRIPTION - HOT ENGINE SYSTEM

The Stirling cycle heat exchangers (heater, regenerators, and coolers), have been reoptimized for automotive part power conditions with increased operating temperature, 820°C instead of 720°C. This has resulted in reduced dimensions, especially for the regenerator/cooler unit. The temperature increase gives significant efficiency improvements. In addition, reduced size hot parts give less cold start penalty. The resizing also gives other benefits like lower weight and thereby reduced manufacturing costs.

In order to further reduce manufacturing costs, the heater head has been designed for low-cost non-strategic materials. Therefore the cycle optimization has been iterated with a thorough stress analysis. Relative material costs, alloy composition, and the stress analysis logics are shown in Figs. 9 and 10. Selected materials are

- tubes: CG-27 for low chromium content
- castings: XF-818 for weldability (repair)

Of course the selection is based on a wide range of criteria and the properties mentioned are only special advantages for each material.

In redesigning the cylinder and regenerator housing, special attention has been paid to improve (investment) castability and it is believed from vendor consultations, that the present design is much better than the original for Mod I.

Heater Head - The Mod I-A heater head has retained the conically involute shaped tubes and one canister regenerator per cylinder. Involute shaped heater tubes with a 90 degree span means that the manifolds can be located close to the center of the cylinders and regenerator housings for a good working gas flow distribution. This heater tube geometry also gives a constant gap along the tubes, which results in a good outside flow distribution and heat transfer from the combustion gases.

(Refer to Fig. 11.)

The Mod I heater heads were made with Haynes Stellite in the housings and with Multimet in the tubes.

The redesign for less costly iron base alloys and elevated operating temperature (820°C) has also allowed for other improvements: a lighter flame shield, simpler insulation cover plates, cheaper surface extension fins, and T/C instrumentation on the outer straight part of the tubes.

(Refer to Fig. 12.)

Regenerator - The regenerator dimensions and porosity have been optimized with regard to the combined effect of cycle efficiency parameters and the cold start penalty for both

the matrix and its housing. The flow distribution gap above the regenerator has been carefully tuned to the dome-shaped top of the housing. This shape has contributed much to reduced stresses and thereby smaller wall thickness and lower weight, which results in less heat conduction and cold start penalty. The reduced diameter also made it possible to simplify the tie-bolted flanges for the whole heater head: two split flanges per quadrant without retainer rings: 8 instead of 24 pieces.

Gas Cooler - The part power optimization takes into account the number of cooler tubes, which has been reduced by almost 25%.

Weight and cost decreases correspondingly.

ENGINE DESIGN DESCRIPTION - COLD ENGINE SYSTEM

Static Parts - For experimental purposes, the Mod I structural cold engine system was made up from several mating parts separated by numerous high pressure static seals. This gives component testing flexibility but also requires many extra machining tolerances and rigid quality controls since the functions of piston rings and main rod seals are so sensitive to misalignment and dome gap variations.

(Refer to Fig. 13.)

The Mod I-A design integrates a number of these mating parts. This reduces weight and manufacturing costs and simplifies the assembly. Engine reliability also becomes improved via relaxed tolerance stack up and reduced number of seals. For example, the cylinder-liner/duct-plate integration eliminates 8 large diameter o-rings and the seal-housing/plumbing integration eliminates 12 smaller o-rings. These integrated parts are made in nodular cast iron and aluminium respectively.

The smaller cooler diameter results in reduced loading on the duct plate. Its wall thickness and support ribs have therefore been decreased to give lower weight. With the new preheater bottom plate, the cast-on flange of the water jacket can be eliminated.

Reciprocating Parts and Their Seals - The piston rings have to efficiently separate the expansion side and the compression side cyclic pressures from each other. Differences in seal capacity will result in deviating cycle pressures unless a well defined "reference pressure", equal for the four cycles, is maintained between the rings. Mod I has this space connected to the common minimum pressure line. (Refer to Fig. 14.) By arranging this venting through the cylinder liner, the whole dome volume can be closed off from participating in rapid power changes. Cap-seal removal also requires the same arrangement. In order not to pass over the venting connection, the piston rings must be more than one stroke apart. This means that the upper ring is now

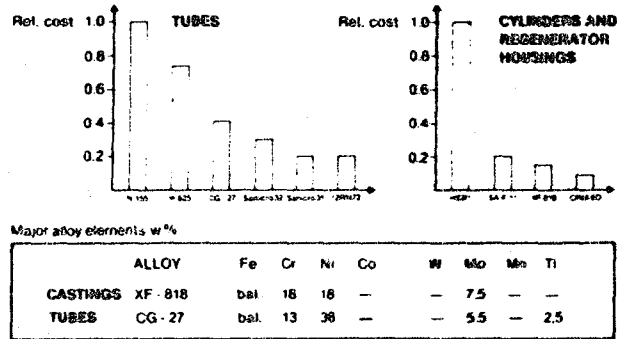


Fig. 9

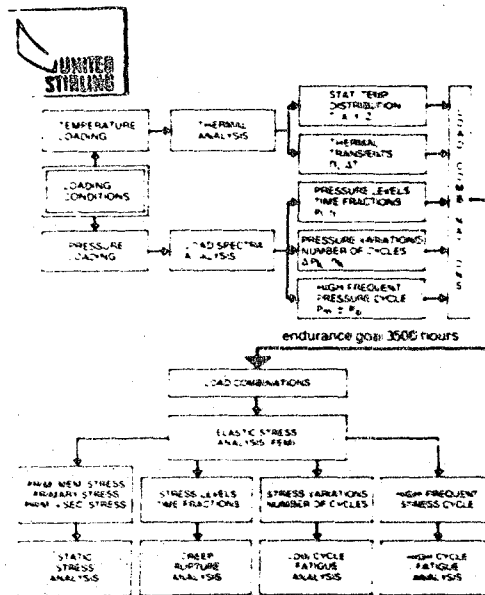


Fig. 10

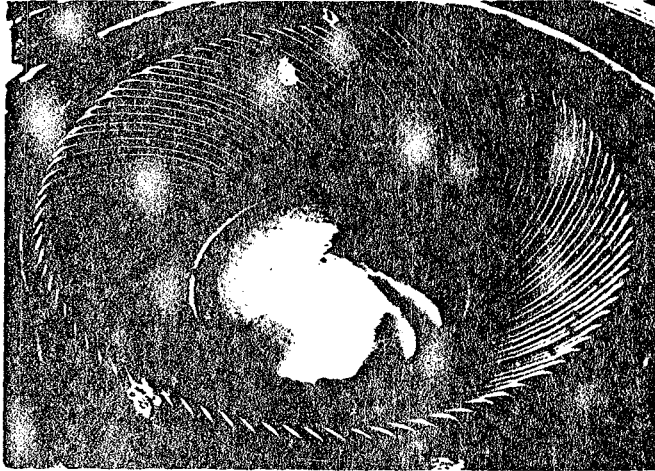


Fig. 11

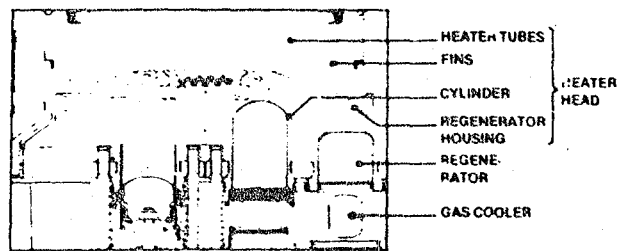


Fig. 12

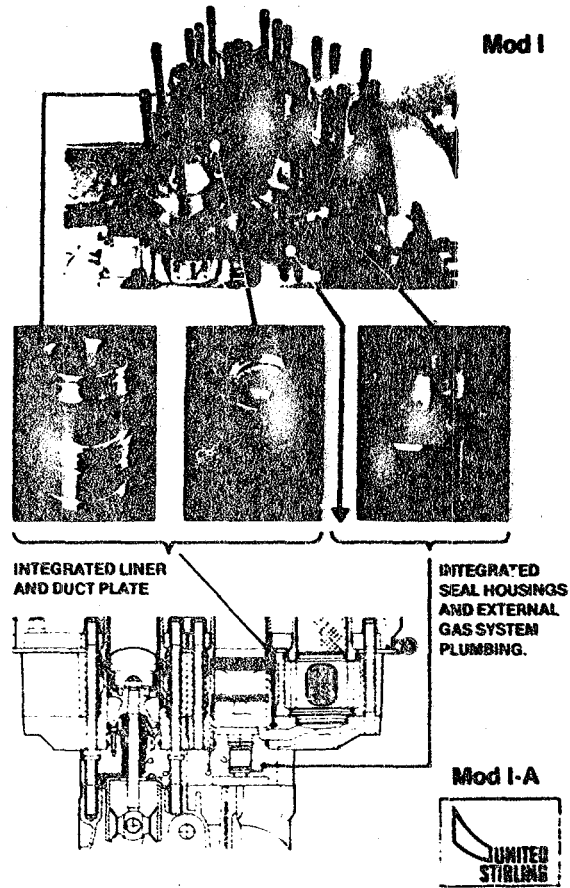


Fig. 13

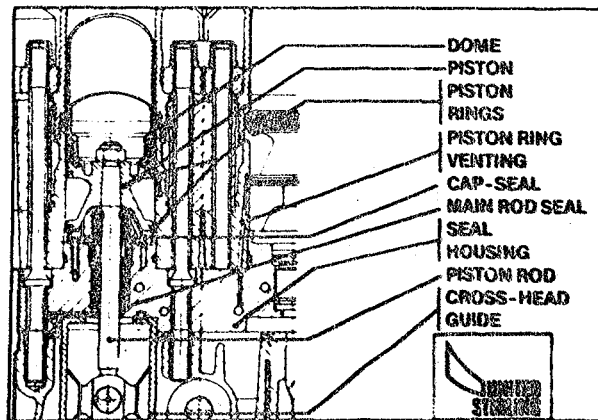


Fig. 14

sliding closer to the hot side of the engine. On the other hand, the dome to piston attachment area is redesigned to reduce heat flow to the ring groove. It also still reverses below the highest cooling water level. The piston is even designed to accept an alternative pressure-balanced type of piston ring, which is now being rig tested.

The sliding piston rod main seal system is basically the same as for the present Mod I. The seal cartridge parts are only slightly modified to give favourable operating conditions. The general principle is to guarantee good alignment and linear movement back and forth. The rod centers all mating surfaces. The rod in turn is centered by the crosshead and the piston guiding ring. Therefore the cross head guides are mounted into the seal housing plate before final machining, giving a more accurate concentricity to the diameter that is piloting the cylinder liner. The seal cavity dimensions can allow altered PL-seal geometries to be tested.

The Mod I-A pistons and domes are significantly lighter than their predecessors and lend themselves better to low cost production. The weight reduction also results in smaller crankshaft balance weights.

ENGINE DESIGN DESCRIPTION - ENGINE DRIVE SYSTEM

The Mod I engine drive system is a dual crankshaft design chosen for structural symmetry and ease of assembly in the heater head area. Two of the four cylinders in a square formation are connected to each crankshaft. Synchronizing the four working cycles with a 90 degree phase-angle apart can be made in different ways.

(Refer to Fig. 15.)

Mod I has the two crankshafts coupled to an output shaft by gears but also has built-in possibilities to use a chain or links for the synchronization. Maintaining these options means a weight penalty.

(Refer to Fig. 16.)

Mod I-A retains the gears. Omitting the alternative synchronizations makes it possible to reduce not only weight but also crankshaft bearing dimensions and mechanical friction losses. One motoring unit with reduced bearings has been tested without any functional problems. It was also tested with a reduced capacity oil pump and alternative synthetic lubricating oil. Although the expected performance gain remains to be validated, the mentioned modifications will be introduced on Mod I-A.

In parallel, a more advanced design, using rolling element bearings instead of plain bearings will be evaluated through functional rig testing. It has lower projected frictional

losses and a better low-speed/high-pressure capability. After successful testing, this drive will be a stronger candidate for the Mod I-A engine drive system.

ENGINE DESIGN DESCRIPTION - CONTROLS AND AUXILIARIES

Power Control - The Mod I power control system has been built into modular blocks according to the scheme. Major parts of this system are the hydrogen storage tank, hydrogen compressor, supply, dump and short circuiting spool valve and servo actuator.

(Refer to Fig. 17.)

To increase power, the spool valve is moved upward by the actuator. Thereby, hydrogen flows from the high pressure storage tank via the spool valve through the supply line to the engine.

To decrease power, the spool valve is reversed. During the initial part of the movement, dumping of hydrogen from the engine via the compressor to the storage tank decreases the power output. During the second part, short circuiting of hydrogen between the cycles is added, thus giving a quick decrease of power.

Mod I-A Modifications - For Mod I-A, the power control system, in a variety of ways, has become less complicated and heavy. The general re-arrangement is shown schematically in Fig. 18. It has less plumbing and a reduced number of fittings and high pressure seals. This is partly due to the introduction of an integrated seal housing design. The new arrangement also improves the serviceability of the entire engine system.

(Refer to Fig. 18.)

Air/Fuel Control - Mod I uses the Bosch K-jetronic mechanical fuel injection system as the air-fuel control device. Disadvantages with this system are: high pressure drop, especially at low air flows, difficulties in changing the air-fuel ratio and difficulties with altitude and pressure corrections. An alternative is a system with a separate air flow transducer with temperature and pressure corrections, and a fuel metering pump with an equalizer valve as the fuel distributor. Such a system gives a lower air pressure drop with lower blower power consumption as a result, and a simple way of changing the air-fuel ratio.

(Refer to Fig. 19.)

Mod I-A Modifications - Mod I-A will demonstrate better automotive adaptability. A new air/fuel system and combustion control has been developed for the Mod I-A. The system shown schematically in Fig. 20 utilizes a piloted air blast fuel nozzle and will be

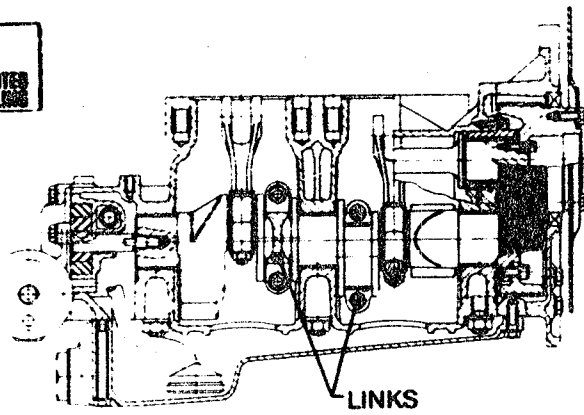


Fig. 15

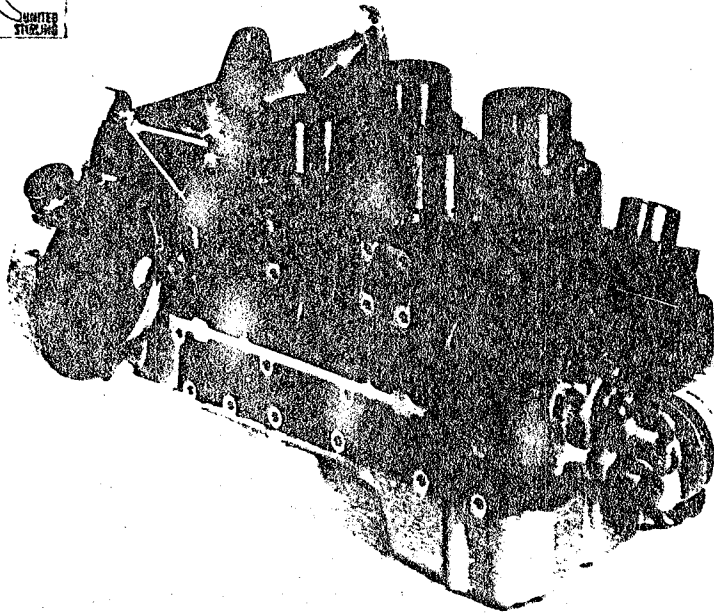
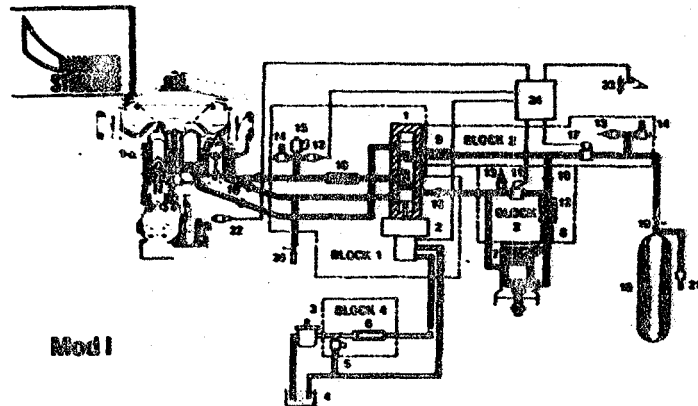


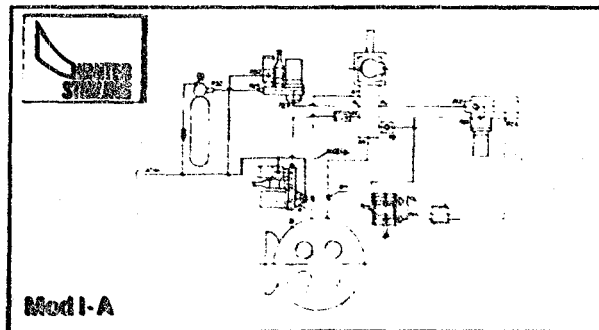
Fig. 16



Mod I

- | | | |
|---|--|-------------------------------|
| 1. SUPPLY, DUMP AND SHORT-CIRCUIT SPOOL VALVE | 8. HYDROGEN FILTER | 18. HYDROGEN FILTER |
| 2. ELECTRO-HYDRAULIC SERVO ACTUATOR | 9. HYDROGEN FILTER | 17. SHUT-OFF VALVE |
| 3. OIL PUMP | 10. CHECK VALVE | 16. HYDROGEN STORAGE TANK |
| 4. OIL TANK | 11. COMPRESSOR SHORT-CIRCUITING SOLENOID VALVE | 19. SHUT-OFF VALVE |
| 5. CONSTANT PRESSURE VALVE | 12. HYDROGEN COOLER | 20. HYDROGEN REFILLING VALVE |
| 6. OIL FILTER | 13. PRESSURE TRANSDUCER | 21. TEMPERATURE MELTING DISC |
| 7. HYDROGEN COMPRESSOR | 14. SAFETY VALVE | 22. SPEED TRANSDUCER |
| | 15. EXTERNAL BUMP VALVE | 23. ACCELERATOR POTENTIOMETER |
| | | 24. ELECTRONICS |

Fig. 17



Mod I-A

Fig. 18

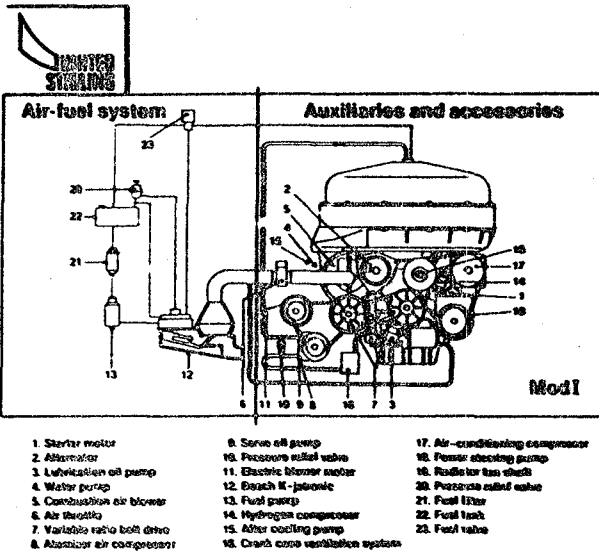


Fig. 19

governed by a digital control unit integrated with the high response digital power control of the engine. This will eliminate the need for the present hydraulically controlled speed variator between the engine and the air blower drive. The blower drive, now a high speed flat belt version, has been changed to a gear drive design.

(Refer to Fig. 20.)

Otherwise, the Mod I-A auxiliaries basically remain the same but with the arrangement revised using low-weight aluminium brackets and pulleys.

SUMMARY

The automotive Mod I-A Stirling Engine design described in this paper represents the first phase of the Proof-of-Concept program. The design, based on Mod I evaluations and supported by separate component developments performed at NASA, MTI and United Stirling AB, is anticipated to include a sound balance between development risks and technology advancement.

Procurement of long lead components has been in progress since last May and remaining detail design will be completed in January

1983. The first Mod I-A assembly test is scheduled for April 1983.

The preliminary Mod I-A performance predictions presented in a separate paper, indicate that those design goals can be met.

Approaching the design completion it also seems most probable that the specific weight improvements will be achieved. Table 3 predicts this important improvement.

Several functional refinements as well as manufacturing simplifications and especially the void of expensive strategic materials will add up to make the Mod I-A a promising platform for further upgrading towards the final program objectives.

ACKNOWLEDGEMENT

The work reported in this presentation was performed by United Stirling AB as subcontractor to Mechanical Technology Incorporated, 968 Albany-Shaker Road, Latham, New York 12111. Mechanical Technology Incorporated is the Automotive Stirling Engine Development Program prime contractor to the National Aeronautics and Space Administration's Lewis Research Center, Cleveland, Ohio 44135, under prime contract No. DEN 3-32. The program is part of the U.S. Department of Energy, Office of Vehicle and Energy R & D.

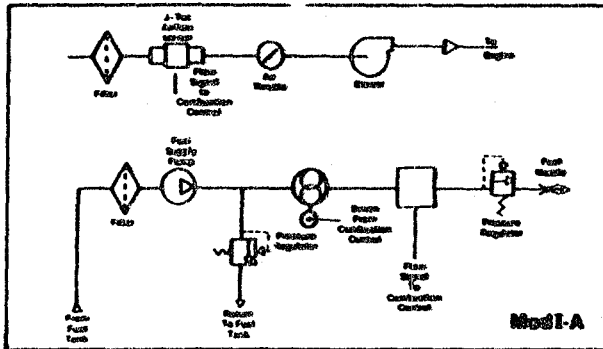


Fig. 20

Table 3

WEIGHT AND POWER COMPARISON

		P 40*)	Mod I	Mod I-A**)
Weight of subsystems				
External heat systems	Kg		45	36
Hot engine system	"		48	36
Cold engine system	"		52	46
Engine drive system	"		68	58
Engine controls and auxiliaries	"		100	86
Total weight (Dry weight)	"	328	312	269
" "	lb	724	688	590
Peak power				
	kW	40	53.8	58
	hp	54	72.3	78
Specific weight				
	Kg/kW	8.2	5.8	4.5
	lb/hp	13.4	9.5	7.5

*) the initial baseline engine

**) design goals

Automotive Stirling Engine Development Program Mod I Stirling Engine Emissions with Exhaust Gas Recirculation

Roger A. Farrell
Mechanical Technology Inc.

ABSTRACT

Steady-state emissions testing of three Mod I Stirling engines burning unleaded gasoline was performed with exhaust gas recirculation (EGR) at United Stirling of Sweden (USAB) and Mechanical Technology Incorporated (MTI). Both constant and variable EGR were evaluated for their impact on gaseous emissions. EGR was found to have an exponential effect on NO_x , but none on CO and HC if $\lambda > 1.2$. The testing, in addition to demonstrating good engine-to-engine repeatability, showed that Automotive Stirling Engine (ASE) Development Program requirements for NO_x , CO and HC can be met with EGR.

ONE OF THE REQUIREMENTS of the Department of Energy-sponsored ASE Program (NASA Contract DEN3-32) is to demonstrate vehicle emissions over the urban CVS cycle that comply with the following:

Emission	g/mi	Equivalent Index* g/kg of Fuel
NO_x	0.4	2.72
CO	3.4	23.1
HC	0.41	2.78

EGR, defined as the dry volume of recirculated products divided by the dry volume of incoming air, was selected as the prime method of emissions control for the Mod I engine (a first-generation automotive Stirling engine). EGR is directed specifically at NO_x , where the increased heat capacity of the combustion products lowers flame temperature and, hence, NO_x . EGR is also expected to reduce CO by providing increased water for CO oxidation. CO and HC are mainly influenced by combustor turbulent mixing, stoichiometry, and ignition delay, which are in turn influenced by combustor pressure drop, swirl

*Equivalent emissions index assuming 19.3 mpg and unleaded gasoline.

intensity, λ (air/fuel divided by stoichiometric air/fuel), fuel nozzle design, and igniter location.

The Mod I engine (Figure 1) utilizes a combustor equipped with a swirler to provide turbulent mixing and aerodynamically stabilized combustion. Most of the combustion reaction occurs in the volume between the flame shield and the heater tubes. The completion of CO oxidation and NO_x formation occurs in the area surrounding the heater tubes and between the tube rows.

The EGR system (Figure 2) recirculates engine exhaust products to the suction side of the blower. The amount of EGR is a function of throttle opening, blower speed, and EGR valve area. Steady-state testing burning unleaded gasoline was conducted to determine the effect of EGR on gaseous emissions. Variables included engine power, EGR, and λ . Measurements of NO_x , CO, HC and O_2 were recorded at both USAB and MTI, while those of NO and CO_2 were taken only at MTI. In the case of

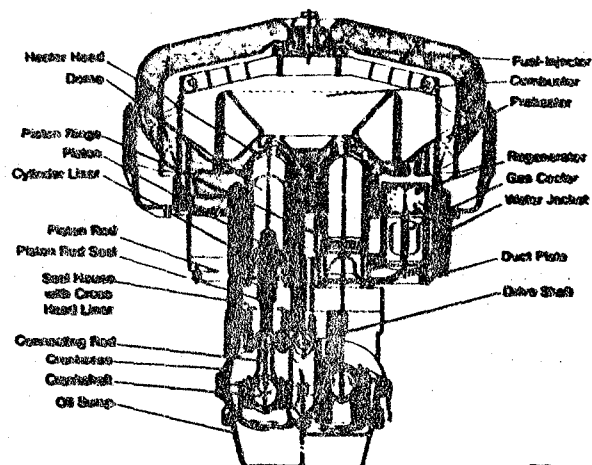


Fig. 1 Mod I Stirling Engine

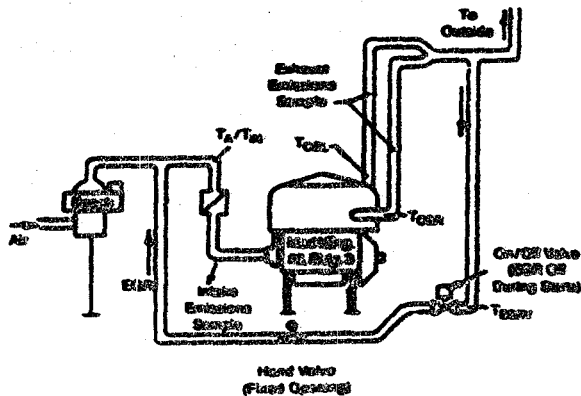


FIG. 2 Mod I Engine EGR Configuration

O₂ and CO₂ measurements were taken to determine λ and λEGR. Three engines were tested:

Engine	Date	Location	No. of Test Points	EGR	Power
2	5/62	USAB	60	Constant %	1500 - 2 g/h Fuel Flow
3	6/62	MTI	60	Constant Area	1500 - 1500
1	7/62	MTI	11	Constant Area	1500 - 1500
			123		

TEST PROCEDURE AND MEASUREMENTS

Initial EGR testing, conducted in Sweden at USAB, concentrated on the region from idle to 2 g/s fuel flow* since most of the CVS cycle is run at part power. In fact, 96% of the urban CVS cycle occurs within the region tested. At each test point, EGR metering area was adjusted to maintain constant EGR as engine power (fuel flow) varied. Emissions were measured at 0, 10, 20, 30, 40, 50, and 60% EGR. Based on these results, a tentative EGR requirement for the vehicle was determined, and design of an EGR control system was initiated.

Since it is much easier to design an on/off, as opposed to a modulated, EGR control system, the ensuing tests at MTI evaluated the effect of constant-area restriction on the EGR line with a simple on/off solenoid control (similar to the method used on the earlier P-40 engine). With a constant-area EGR restriction, the amount of EGR varies with fuel flow because of the air blower and throttle characteristics. As a result, EGR increases as power decreases.

Both USAB and MTI used measurements of O₂ or CO₂ in the exhaust (E) and combustor inlet (I) to determine EGR:

$$\lambda \text{EGR} = \frac{100(X_{\text{CO}_2})_I}{(X_{\text{CO}_2})_E - (X_{\text{CO}_2})_I} \quad (1)$$

$$\lambda \text{EGR} = \frac{100 [0.2095 - (X_{\text{O}_2})_I]}{(X_{\text{O}_2})_I - (X_{\text{O}_2})_E}$$

*Maximum power fuel flow ~4.5 g/s

where, X_{CO₂} and X_{O₂} represent the mole fractions of CO₂ and O₂, respectively. Because both CO₂ and O₂ are measured dry, the λEGR calculated does not include water vapor in the air or exhaust products. All USAB calculations were based on O₂, while those of MTI were derived from CO₂, or the average of CO₂ and O₂.

Similarly, λ was determined from exhaust O₂ and CO₂, and a fuel hydrogen/carbon ratio (R):

$$\lambda = \frac{1 + \frac{R}{4} X_{\text{CO}_2}}{4.77 X_{\text{CO}_2} \left(1 + \frac{R}{4}\right)} \quad (2)$$

$$\lambda = \frac{1 + \frac{R}{4} (1 - X_{\text{O}_2})}{(1 - 4.77 X_{\text{O}_2}) \left(1 + \frac{R}{4}\right)}$$

The engine test cell facilities and nonemissions measurements are described in detail in (2) and (3), and the emissions equipment is defined in Table 1.

Table 1. Emissions Equipment

Analyte	Manufacturer		Type
	USAB	MTI	
O ₂	Sorenson	Beckman 755	Paramagnetic
CO ₂	-	North AEA	Non-dispersive infrared
CO	Beckman 894	North AEA	Non-dispersive infrared
NO _x	Beckman 625	Beckman 695	Chemiluminescent
HC	Beckman 602	Valco 1400	Flame Ionization

GASEOUS EMISSIONS TEST RESULTS

USAB NO_x emissions at constant λEGR are illustrated in Figure 3. The value of λ varied between 1.5 at idle to 1.2 at higher fuel flows (Figure 4). The influence of EGR on NO_x is clearly indicated. As EGR increases, the proportion of CO₂ and H₂O (e.g., the normal products of complete combustion) in the combustion zone increases, raising the heat capacity and lowering the flame temperature a proportionate amount. Due to the exponential effect of flame temperature on NO_x, NO_x is reduced. In fact, since flame temperature varies proportionately with EGR, NO_x is an exponential function of EGR; i.e., as EGR increases, its effectiveness in reducing NO_x diminishes.

NO_x emissions in Figure 3 are presented as emissions index (EI NO_x) defined as the grams of NO_x per kilogram of fuel. Emissions index is directly related to ASE Program emissions goals expressed in g/mi and the urban CVS cycle mileage (mpg):

$$\text{EI} = \frac{(\text{g/mi})(\text{mpg})(1000 \text{ g/kg})}{\rho_f} \quad (3)$$

where ρ_f = density of unleaded gasoline = 2841 g/gal. Thus, to achieve 0.4 g/mi, 60-70% EGR is required, while ~25% EGR would suffice if 1.0 g/mi is required.

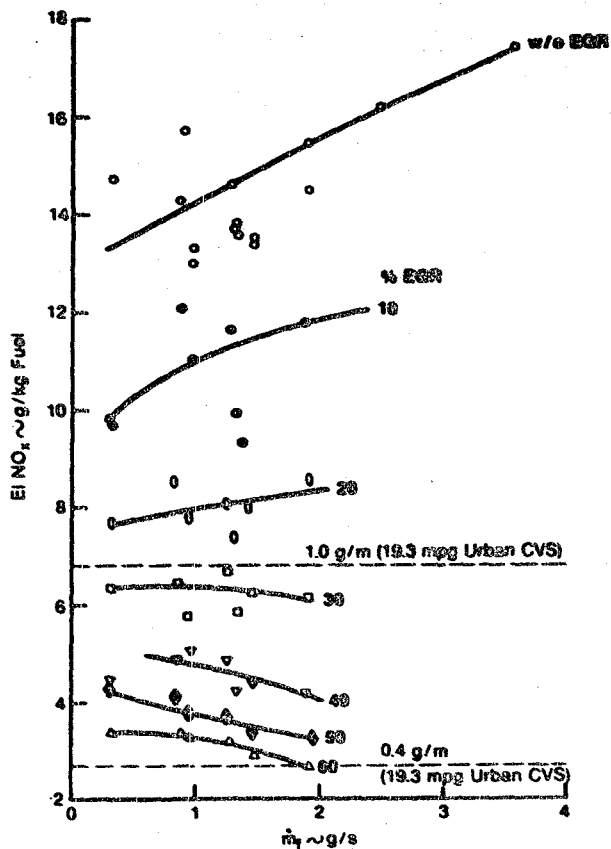


Fig. 3 Mod I Engine #2 NO_x Emissions with % EGR

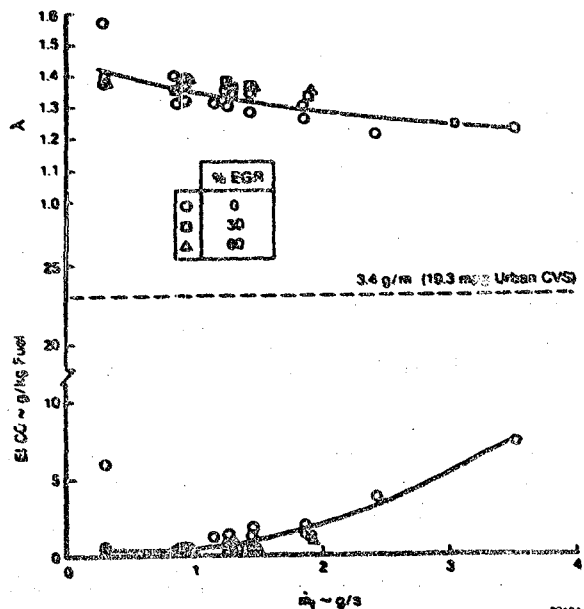


Fig. 4 Mod I Engine #2 λ and CO Emissions

CO and HC emissions data from USAB were both extremely low; CO emissions (Figure 4) are well below the ASE Program requirement of 3.4 g/mi. There may be a positive influence of EGR on CO, but the effect, if any, is slight. HC emissions (not shown) were less than 0.1 g/kg or an order of magnitude lower than required.

MTI testing in two Mod I engines utilized a constant-area restriction in the EGR line, as previously described. Three EGR schedules were used: "no EGR," "intermediate EGR" and "maximum EGR." In the first case, the solenoid control valve was shut, preventing any recirculation. Maximum EGR was obtained by removing all restrictions from the line; intermediate EGR was obtained by adjusting a hand valve to obtain an NO_x level of ~ 1.0 g/mi.

The intermediate- and maximum-case EGR characteristics are illustrated in Figure 5. The non-EGR case (not shown) is 0%. As power is reduced (lower fuel flow), air flow is restricted, increasing the AP across the EGR circuit (see Figure 2), and causing EGR to increase. Also shown in Figure 5 are the three λ schedules (A, B, and C) that were used during testing. The USAB schedule (D) (Figure 4) is very close to (C).

The effects of EGR and λ on NO_x are given in Figure 6. As was the case with USAB data, the influence of EGR on NO_x from engines No. 3 and 1 is pronounced and exponential in nature (Figure 7). The repeatability of NO_x is good, especially at intermediate-EGR levels and the change in λ does not appear to affect NO_x . The maximum EGR schedule would suffice to meet a 0.4-g/mi NO_x .

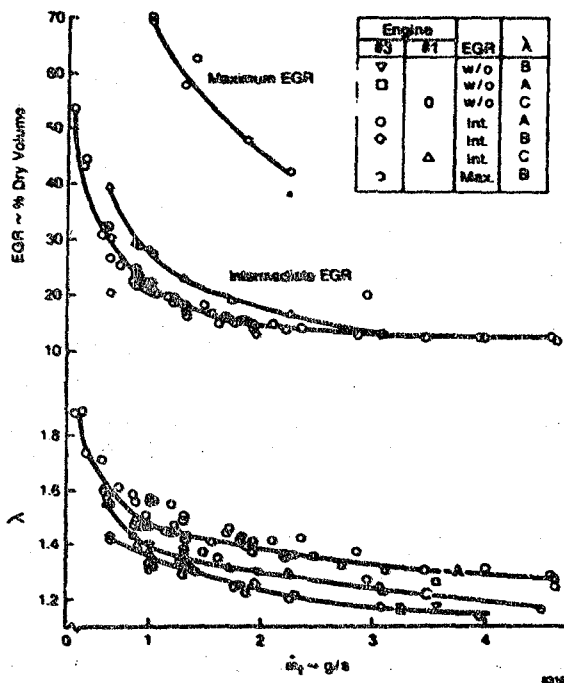


Fig. 5 Mod I Engine Variation in λ and EGR with Fuel Flow

requirement. The intermediate EGR schedule is seen to be very close to 1.0 g/mi; in fact, if the intermediate NO_x results are estimated for the CVS cycle using 12-time weighted fuel flows (4), predicted CVS cycle NO_x would be 0.88 g/mi, corresponding to a 0.4% decrease in engine efficiency relative to the non-EGR case.

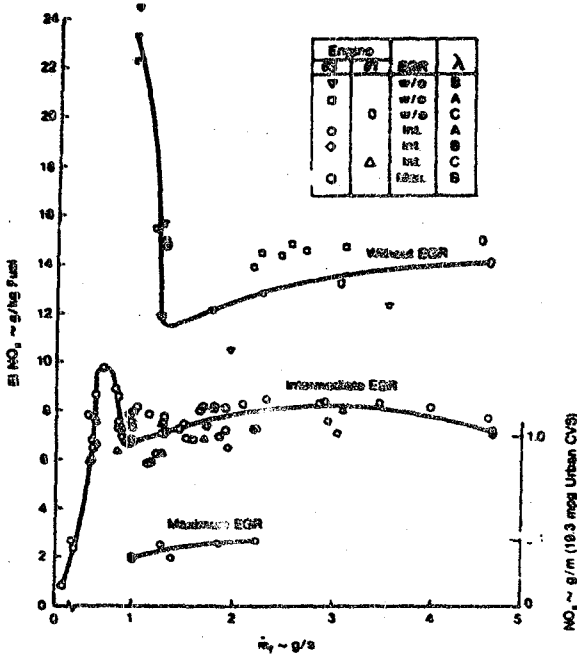


Fig. 6 Mod I Engine NO_x Emissions With/Without EGR

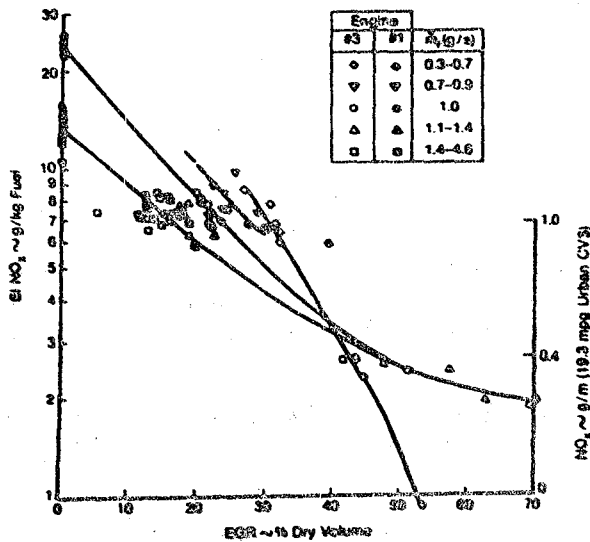


Fig. 7 Effect of EGR on Mod I Engine NO_x Emissions

A comparison of the NO_x emissions of all three Mod I engines is given in Figure 8. Once again, the agreement is good, especially with EGR. The tendency of NO_x to peak at fuel flows of 1.0 g/s or less is not completely understood, but appears to be characteristic of the turbulator combustor. For example, the same curve shape was seen during alternative fuels testing of the P-40 engine with EGR; see Figure 9 and (5). A possible explanation is that offsetting effects occur as fuel flow decreases:

- EGR increases, leading to lower NO_x
- λ increases, causing flame temperature, residence time, and hence, NO_x to decrease (this statement is true if mixing of fuel and air is perfect prior to combustion; e.g., λ is uniform in the reaction zone)
- Efficiency of combustion mixing decreases because air flow is decreasing which, in turn, leads to lower combustor ΔP and turbulent mixing. With large variations in λ inside the combustor, the burning reaction is characterized as a turbulent diffusion flame; e.g., combustion occurs at near-stoichiometric conditions where NO_x formation is highest; thus, NO_x increases.

At very low fuel flows, the first and second effects dominate; as fuel flow increases, the third effect dominates. Further increases in fuel flow improve mixing so that NO_x again decreases.

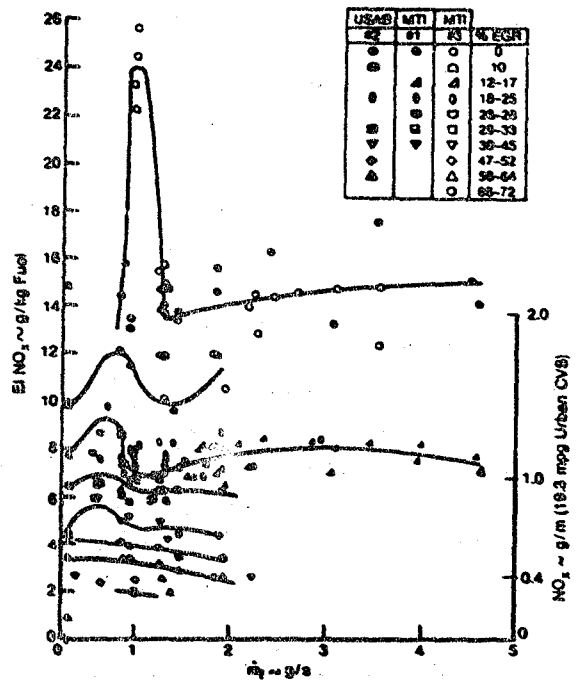
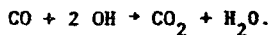


Fig. 8 Mod I Engine NO_x Emissions With/Without EGR

CO emissions results from MTI testing of Mod I engines No. 3 and 1 (Figure 10) indicate an effect of both EGR and λ on emissions. At first glance, the effect of EGR on CO seems to contradict USAB test results (Figure 4). However, careful analysis shows that this is not the case. In fact, CO emissions are very repeatable among the three engines.

Comparing Figures 4 and 10, CO increases with fuel flow due to the concurrent increase (with fuel flow) in combustor air flow, thus reducing the amount of residence time in which CO oxidation can occur. For the lowest λ (least excess air), schedule (B), increased EGR is beneficial to CO, probably due to the increased presence of OH radicals promoting the oxidation of CO (6):



As λ becomes leaner ((B) \rightarrow (D) \rightarrow (C) \rightarrow (A)), the impact of EGR on CO emissions is slight or nonexistent, leading to the conclusion that as long as enough excess air is present; e.g., $\lambda > 1.2$, EGR does not influence CO. A study of Figure 10 indicates the importance of accurately controlling λ . If λ decreases below 1.2 (schedule (B), the CVS requirement of 3.4 g/mi could be exceeded).

The repeatability of data and the extreme sensitivity of CO to λ are clearly indicated in Figure 11. It may be concluded that:

- Neither EGR nor fuel flow are important in determining CO emissions
- CVS cycle compliance can be assured by maintaining $\lambda > 1.2$
- CO emissions for all three engines are consistent.

HC emissions (expressed as methane) obtained during MTI testing (Figure 12) are well below the CVS cycle requirement of 0.41 g/mi; in fact, most of the HC emissions are an order of magnitude less than the requirement. USAB data, as previously mentioned, were less than 0.1 g/kg; however, the HC emissions do not reflect those that would be obtained during an engine start-up sequence. Vehicle experience indicates that HC generated due to ignition delay and cold start may be 90% or greater of the total measured.

CONCLUSIONS

EGR, in combination with the turbulator combustor, is a viable method of controlling Mod I Stirling engine exhaust emissions. The effect of EGR on NO_x was exponential, as expected (1). If steady-state engine data are projected over the vehicle CVS urban cycle, an NO_x goal of 1.0 g/mi could be met with 25-30% EGR, while a goal of 0.4 g/mi would require 40-70% EGR.

DATA CORRECTED TO 15°C AMBIENT, 60% RELATIVE HUMIDITY

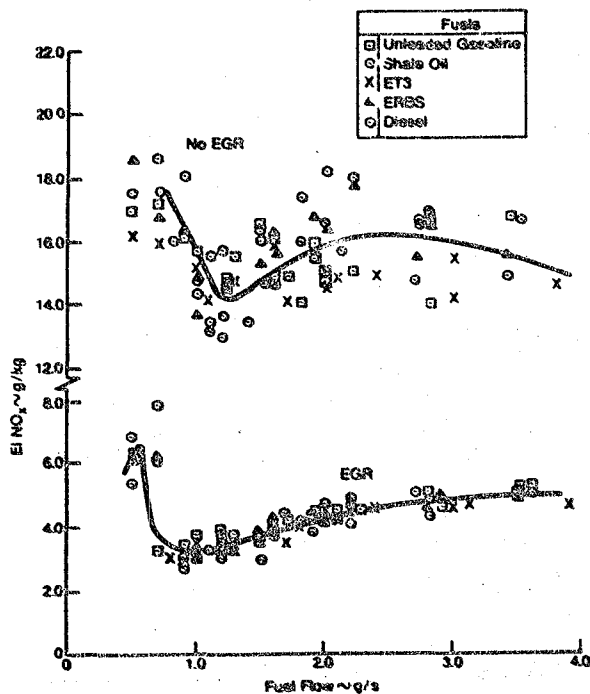


Fig. 9 NO_x Emissions - P-40-7-15 - All Fuels

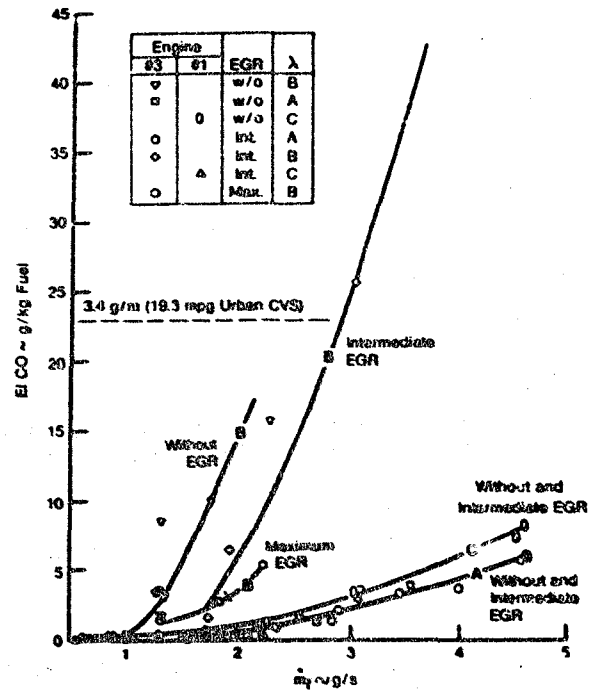


Fig. 10 Mod I Engine CO Emissions With/Without EGR

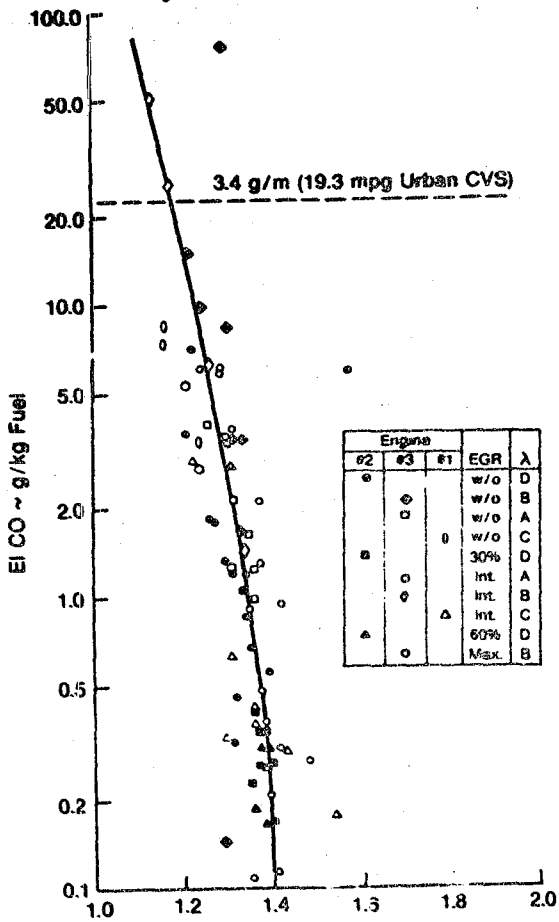


Fig. 11 Effect of λ on Mod I Engine CO Emissions

Both CO and HC emissions were low as long as λ was greater than 1.2; a slight positive effect of EGR on CO may exist. Projecting steady-state CO and HC emissions over the CVS cycle indicates levels well below program requirements; however, it must be emphasized that the steady-state projections do not account for start-up and transients encountered during the CVS cycle. Since HC and CO are adversely affected by start-up and transients, actual vehicle measurements are anticipated to be higher than indicated in this paper.

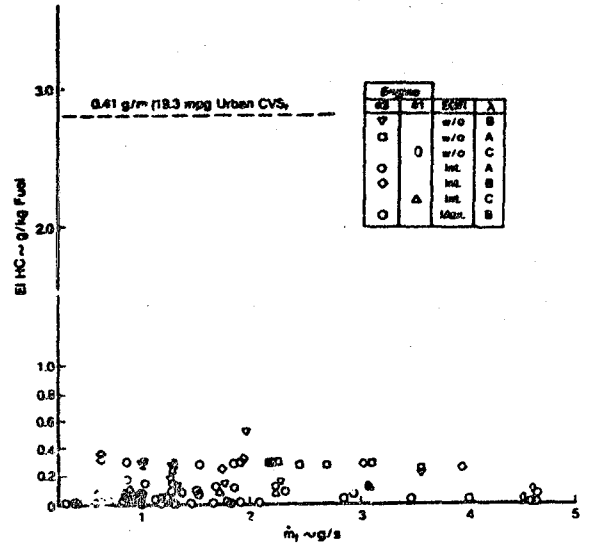


Fig. 12 Mod I Engine HC Emissions With/Without EGR

REFERENCES

1. Battista, R. A., and Thomas, M. E., "Effects of Inlet Conditions and Water Injection on Emissions from Dual-Fuel Industrial Gas Turbine," ASME Paper 81-GT-47, March 1981.
2. Nightingale, N. P., "USSw Acceptance Test Report Mod I BSE S/N 2," MTI Report No. 82ASE270ER40, July 1982.
3. Daly, J. W., "Combined Alternate Fuels and General Development Test Results of ASE P-40-7," MTI Report No. 82ASE264ER38, August 1982.
4. Nightingale, N. P., "USSw Acceptance Test Report for Mod I SES No. 1," MTI Report No. 81ASE237ER32, September 1981.
5. Battista, R. A., "Stirling Engine Alternative Fuels Test Results," MTI Report No. 82ASEPR21, CCM Paper, October 1982.
6. Battista, R. A., and Farrell, R. A., "Development of an Industrial Gas Turbine Combustor Burning a Variety of Coal-Derived, Low-Btu Fuels and Distillate," ASME Paper 79-GT-172, March 1979.

Automotive Stirling Engine Development Program

Stirling Engine Alternative Fuels Test Results

Robert A. Battista
Mechanical Technology Inc.

ABSTRACT

Emissions measurements were made on a 40-kW (54-hp) Stirling engine burning five liquid fuels - unleaded gasoline, shale-derived marine diesel, gasohol (ET-3), ERBS, and commercial diesel. Emissions were measured with and without exhaust gas recirculation (ERG), and the results showed little difference in the levels of NO_x , CO, and HC emissions for all the fuels tested, particularly with EGR.

~~This paper reviews~~ ^{see attached} the results of the test and correlations of the emissions data with external heat system (EHS) parameters. The effects of the fuel type on the performance of the EHS is also discussed.

THE DEVELOPMENT of a high-efficiency, low-emissions combustion system is a major requirement of the ongoing Automotive Stirling Engine (ASE) Development Program at Mechanical Technology Incorporated (MTI). Among the major program goals are to demonstrate that the use of alternative fuels is not detrimental to engine operation, performance, emissions, or fuel economy, and to determine the degree of minor modifications or necessary adjustments when switching fuels. This paper covers the results of the first comprehensive tests of combustion/emissions where a Stirling engine was run with no hardware changes.

In December 1981, emissions measurements were made on a 40-kW (54-hp) U-4 Stirling engine (P-40-7, Build 15) burning a variety of liquid fuels. The engine was configured in such a way that measurements could be made with or without exhaust gas recirculation (EGR), enabling not only the determination of the differences in emission levels of the various fuels, but also the evaluation of the effect of EGR on NO_x , CO, and HC for each fuel.

For the External Heat System (EHS), consisting of the combustor, preheater, fuel nozzle, and air/fuel control, including inlet and exhaust systems, pressure and temperature measurements were taken to determine the effect (if any) of the various fuels on overall EHS performance. Any

deterioration in the system over the course of the test program was monitored; other engine parameters were also measured during testing. This paper concentrates on the results of the emissions measurements; EHS performance results are also discussed. Results of overall engine performance can be found in (1)* and further details of the emissions results in (2) and (3).

TEST DESCRIPTION

TEST CONDITIONS - The five fuels listed below were tested over a load range from idle to maximum power:

1. Unleaded Gasoline
2. Shale-Oil-Derived Marine-Diesel
3. Research-Grade Gasohol (ET-3)
4. Experimental Referee-Broadened-Specification (ERBS) Turbine Fuel
5. Commercial Diesel

Table 1 summarizes the fuel properties, and Table 2 describes the test matrix run on each fuel. After the last fuel was tested, several load points (burning unleaded gasoline) were repeated. Emissions measurements were made with and without EGR at each test point of the matrix.

The EGR levels achieved during each test series are shown in Figure 1. For each fuel tested, the variation of EGR with fuel flow was similar. The largest differences in EGR levels occurred at fuel flows less than 2.0 g/s. The figure also indicates that the EGR valve closed at fuel flows of 0.7 g/s and lower; however, this is the normal method of operation for the valve.

Overall EGR levels appear to be somewhat lower than those measured during the acceptance test of this P-40 engine, as well as for those measured during the P-40-1 acceptance test. This may have been due to differences in pressure losses across the EGR circuit during each test. The

*Numbers in parentheses designate references at end of paper.

Table 1. Fuel Properties

(Analysis made at Phoenix Chemical Laboratory, Inc., Chicago, Illinois, May 1982)

		Unleaded Gasoline ^a	State-Derived Marine Diesel ¹	Gasohol (ET-3) ²	ERBS ³	Commercial Diesel ¹
Carbon	wt %	86.00	86.52	82.30	86.94	86.85
Hydrogen	wt %	13.84	13.28	14.05	12.73	12.78
Sulfur	wt %	0.02	<20 ppm	0.02	0.045	0.095
Nitrogen	wt %	0.003	0.002	0.003	0.011	0.008
Oxygen	wt %	0.13	0.10	3.63	0.17	0.16
Lead	ppm	22.9	<0.1	9.9	<0.1	<0.1
Specific Gravity		0.752	0.834	0.767	0.838	0.843
API Gravity		56.7	38.2	53.0	37.4	36.4
Viscosity @ 40°C	C.S.	0.55	2.54	0.59	1.62	2.10
Heating Value	Btu/lbm					
Gross		19.610	19.720	18.844	19.525	19.507
Net		18.347	19.508	17.562	18.363	18.340

¹Average of two samples taken at different times during testing
²One sample, second sample indicated something other than gasohol
³One sample only, second sample can almost empty 823290

Table 2. Engine Test Point Matrix

P _{mean} (MPa)	Idle	Engine Speed (rpm)			
		1000	2000	3000	4000
15	—	4	3	2	1
10	—	5	6	7	8
7	—	12	11	10	9
5	—	16*	15	14	13
Idle	17	—	—	—	—

*Because of test difficulties, test point 16 was not run

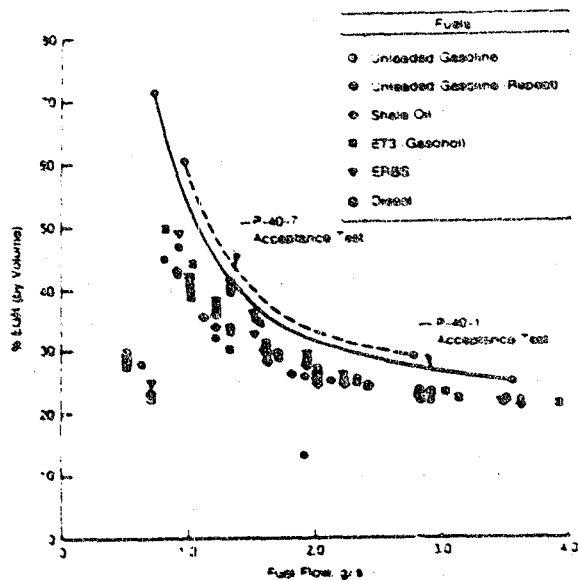


Fig. 1 EGR Variation During Alternative Fuel Tests

blower speed was also lower than usual because of variator belt slippage. It should be noted that the EGR values reported for this alternative fuels test are volumetric ratios of dry exhaust products to dry air, as determined from measurements of CO₂ in the combustor inlet and exhaust. The CO₂ measurement was also used to calculate and set λ values. At the start of each day's testing, or when a new fuel was tested, the λ value at cruise (2700 rpm, P_{max} = 120 bar) was checked and set at -1.25. The variation of λ with fuel flow for all fuels is shown in Figure 2.

EMISSIONS MEASUREMENTS - Details of the Gas Analyzer System used to measure CO, CO₂, NO_x, and HC may be found in (2) and (3). Smoke samples, using a Von Brand Smoke System, were also taken during testing by passing a sample through a moving filter paper (~100 mm/min); the smoke number (100 indicates a totally clear exhaust) can then be determined by measuring the reflectance of the sample relative to the clean paper. In order to eliminate interference of water vapor on NO_x measurement, moisture in the sample was removed by drawing it through a refrigeration bath prior to it entering the NO detector. It is important to note that the water knockdown is done after the NO_x + NO converter, since NO is much less soluble than NO₂, minimizing the amount of NO_x lost during H₂O removal. CO₂ scrubbers were used in the CO sample line to prevent interference of CO₂ with CO detection.

All of the gas analyzers were calibrated prior to each day's testing, and several calibration checks were made during testing and at the end of each day. The raw emissions data were then corrected for any instrumentation drift.

OTHER INSTRUMENTATION - Locations of EHS temperature and pressure measurements are shown schematically in Figure 3 at each radial position

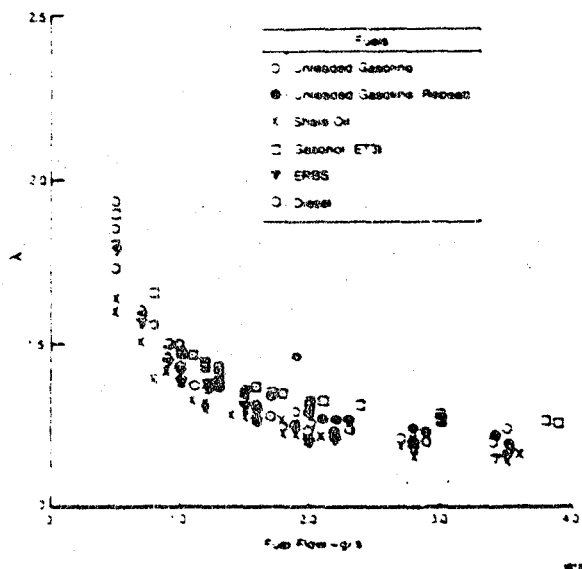


Fig. 2 Lambda Variation During Alternative Fuel Test (All Fuels)

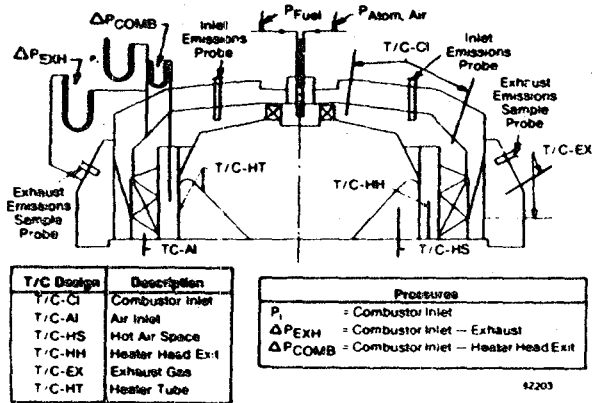


Fig. 3 Instrumentation Schematic

shown, at least four thermocouples were located circumferentially around the EHS. Most of the thermocouples indicated are standard engine test instrumentation; additional thermocouples were used to determine combustor inlet, exhaust temperature distributions and, along with the pressure measurements, to detect any deterioration or abnormalities in performance. There was concern that operation with heavy fuels could cause plugging of the preheater.

TEST RESULTS

A complete summary of the raw emissions data (corrected for instrumentation drift) recorded for all five fuels, and including average temperature data throughout the EHS may be found in (3). Pressure data are discussed in the next section.

The NO_x Emissions Index for each fuel is compared in Figure 4. Data are shown both with and without EGR. As noted previously, EGR percentage was determined by measuring CO₂ in the exhaust and inlet to the combustor (preheater discharge); thus,

$$\%EGR = \frac{X_{CO_2, Inlet}}{X_{CO_2, Exhaust} - X_{CO_2, Inlet}} \times 100$$

or (1)

$$\%EGR = \frac{\text{Volume of Dry Exhaust Recirculated}}{\text{Volume of Dry Air}} \times 100$$

where:

$$X_{CO_2} = \text{Mole Fraction of } CO_2 \text{ (Measured Dry)}$$

The data, plotted as a function of fuel flow, were corrected for inlet humidity following the gas turbine practices (4,5,6) of correcting to an absolute humidity of 0.063 g H₂O/g dry air. This corresponds to a 15°C day with 60% relative humidity. A correlation of the form

$$NO_{x, iso} = NO_{x, meas} \times e^{k(H-0.063)} \quad (2)$$

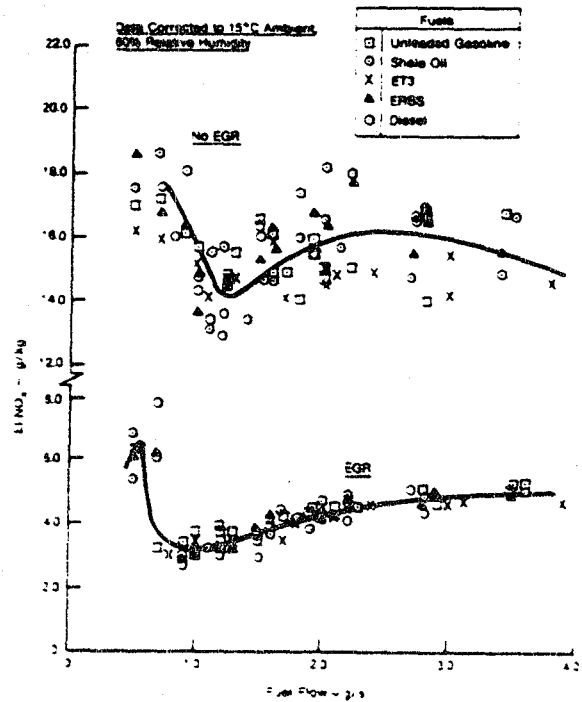


Fig. 4 NO_x Emissions P-40-7-15 (All Fuels)

was used, where H = measured absolute humidity. A value of k = 23 (previously used by the author to correct gas turbine emissions) was chosen. In view of the lack of similar relationships for the Stirling engine, the application of gas turbine practices seemed justified, since both are continuous combustion systems, and the excess air factor in the primary zone of gas turbine combustors is very close to that of a Stirling engine combustor.

The correction reduced the scatter in unleaded gasoline data between the initial and final tests (3). The effect of humidity was more pronounced without EGR; with EGR, the ambient moisture effect was overshadowed by H₂O and other diluents in the recirculated exhaust.

The important result is that NO_x levels for all five fuels are similar, particularly with EGR; thus, a single combustor can be designed, using a fixed EGR or CGR (combustion gas recirculation) schedule, that will satisfy the CVS cycle emissions burning a variety of fuels. Admittedly, the properties of the fuels tested do not differ greatly (Table 1), but the results nonetheless represent a significant milestone.*

In general, the steady-state NO_x levels of the P-40 Stirling engine at the levels of EGR achieved were above the CVS limit of 1.5 g/mi when based on a mileage figure of 22.4 mpg (corresponding to an EI of 3.2 g/kg), especially near idle where the EGR level drops off. The air-fuel

*Fuels with higher nitrogen content or different flame temperatures may require altered levels of EGR/CGR for NO_x compliance.

system is rather cyclic at low fuel flows, as indicated in the idle emissions traces of Figure 5. The air/fuel variation is reflected in the oscillation in the CO₂ level. Under these conditions, actual CVS cycle emissions will differ significantly from calculated emissions, based on values taken from Figure 4, which represents values midway between maximum and minimum peaks, not time-average values.

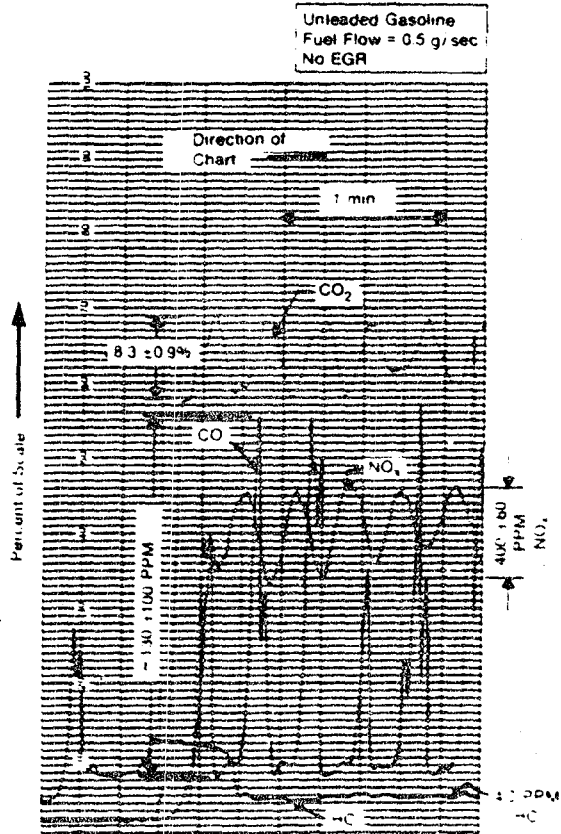


Fig. 4. Idle Emissions at Idle

Also, at these low fuel flows, the residence times are long and the temperatures are high to produce significant concentrations of NO_x and which are approximately the size of those at higher fuel flows. NO_x will therefore appear higher at the fuel flows shown compared to fuel flows in terms of the emissions index.

In order to evaluate the data in terms of its usefulness in the design of the ignited Mod 1 engine and combustor, it was checked in terms of parameters that more generally influence NO_x such as T_{in} , combustor inlet temperature, and EGR.

The ratio of NO_x emissions index measured with EGR to that measured without EGR is a function of EGR as shown in Figure 6. Since the combustor inlet temperature differed for non-EGR conditions, the data were adjusted to correspond to the non-EGR condition inlet temperature, taking

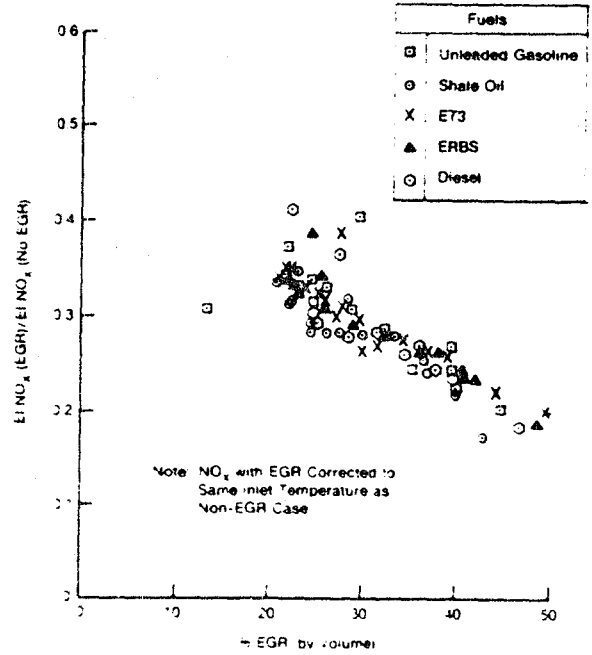


Fig. 5. Effect of EGR on NO_x Reduction

into account the effect of inlet temperature on flame temperature and, thus, NO_x formation. Again, the correction used was typical of gas turbine practice, and was of the form:

$$NO_{x, CORR} = NO_{x, Meas} \left(\frac{T_{ref}}{T_{meas}} \right)^{1.8} \quad (1)$$

where:

- $NO_{x, CORR}$ = Measured NO_x with EGR
- $NO_{x, Meas}$ = Measured NO_x without EGR
- T_{ref} = reference inlet temperature
- T_{meas} = measured inlet temperature with EGR valve closed
- T_{meas} = Measured inlet temperature with EGR valve open
- n = constant = 1.8 (ref. 1)

It can be seen from Figure 6 that NO_x reduction is relatively insensitive to fuel type.

Although the degree of NO_x reduction for the Mod 1 engine should be similar to that of the base engine for a given amount of burnt diluted exhaust, the absolute value will differ because of the differences in reacting conditions and combustion designs. These parameters determine the reaction temperatures, residence time, surface conditions, and rates of heat rejection, all of which influence NO_x emissions levels. Obviously, the P-40 data taken here cannot begin to account for all of these effects, however, knowledge of the effect of T_{in} and inlet temperature on NO_x without EGR, coupled with the NO_x reduction ratios of Figure 6,

can be used in preliminary combustor evaluation. Emissions Index was adjusted to an arbitrary reference inlet temperature of 800°C using Eq. (3) and plotted as a function of λ . Although the correlation cannot totally describe the NO_x data, it does afford a somewhat better representation than the uncorrected data (Figures 7 and 8). Figure 9 compares the non-EGR NO_x levels as a function of λ for all the fuels tested.

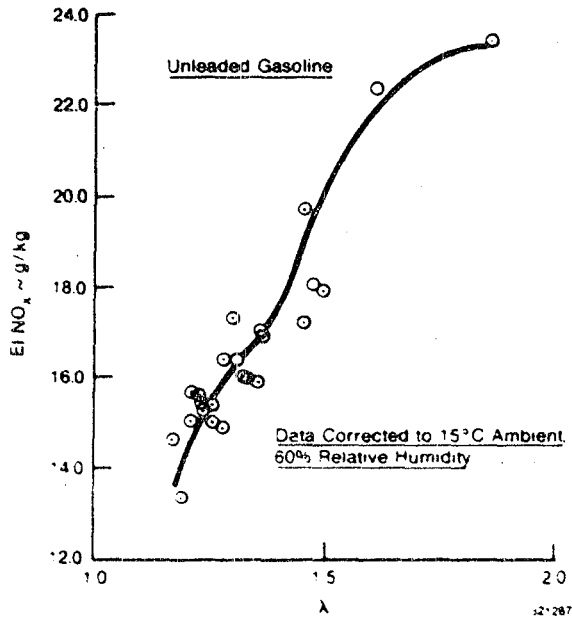


Fig. 7 Effect of λ on NO_x Emissions Corrected to 800°C Inlet 2-20-7-15 - No EGR

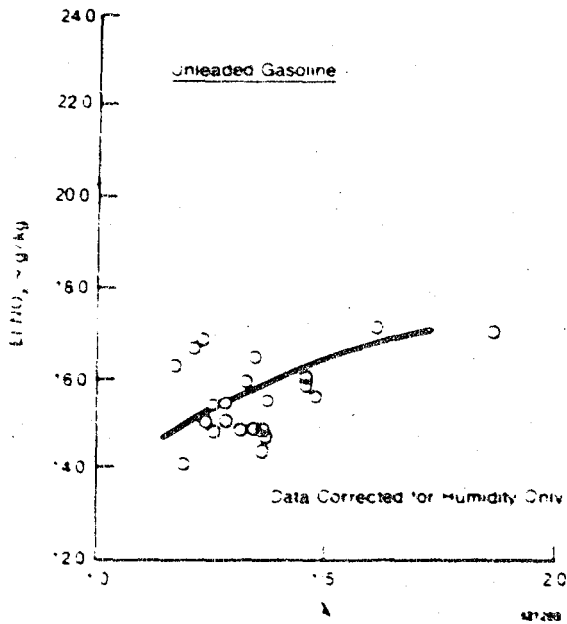


Fig. 8 Effect of λ on uncorrected NO_x Emissions 2-20-7-15 - No EGR

The increase in Emissions Index with increasing λ is consistent with the fact that residence time also increases while fuel flow decreases; thus, even though the flame temperature is decreasing, Emissions Index can increase. An explanation for the inflection point (most distinguishable for the diesel fuel data) has not yet been found, although the classical NO_x versus λ curve peaks at a slightly lean condition ($\lambda > 1.0$). The value of λ , at maximum NO_x depends, among other things, on residence time.

CO and HC emissions for each fuel are shown in Figures 10 and 11. Again, the emissions were similar for all fuels tested. The slight difference in CO emissions among fuels appears to be due to the deviation in λ , as indicated in Figures 12 and 13, and not fuel properties as one might expect.

The gasoline data compare favorably with previous engine data (2,3). Both CO and HC are below the CVS limits of 27.4 g/kg fuel (3.4 g/mi at 22.4 mpg) and 3.9 g/kg fuel (1.1 g/mi at 22.4 mpg), respectively. It is interesting to note that the CO emissions with EGR were lower than those without EGR, except at very low fuel flows. This may be due to several reasons: 1) the additional mass flow may produce better mixing, resulting in more complete combustion; 2) a stronger influence is perhaps the H₂O content in the exhaust gas which can result in an increase in H₂ partial pressure in the reaction zone, thus increasing the $\text{CO} \rightarrow \text{CO}_2$ reaction.

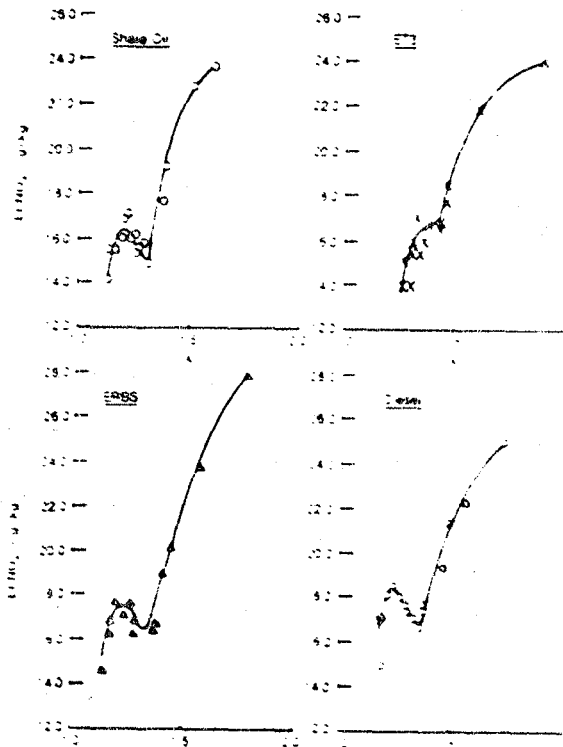


Fig. 9 Effect of λ on NO_x Emissions Corrected to 800°C Inlet Temperature 2-20-7-15 - No EGR

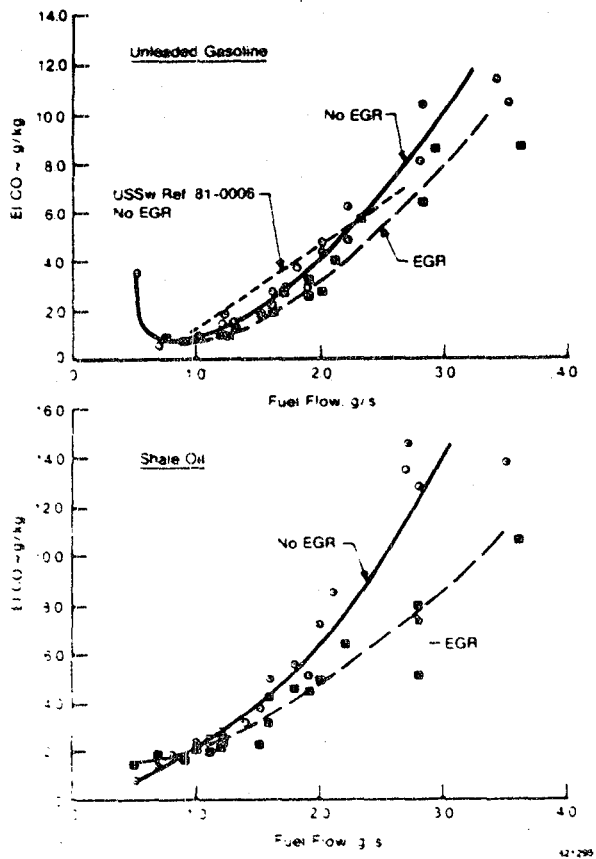


Fig. 10 CO Emissions P-40-7-15

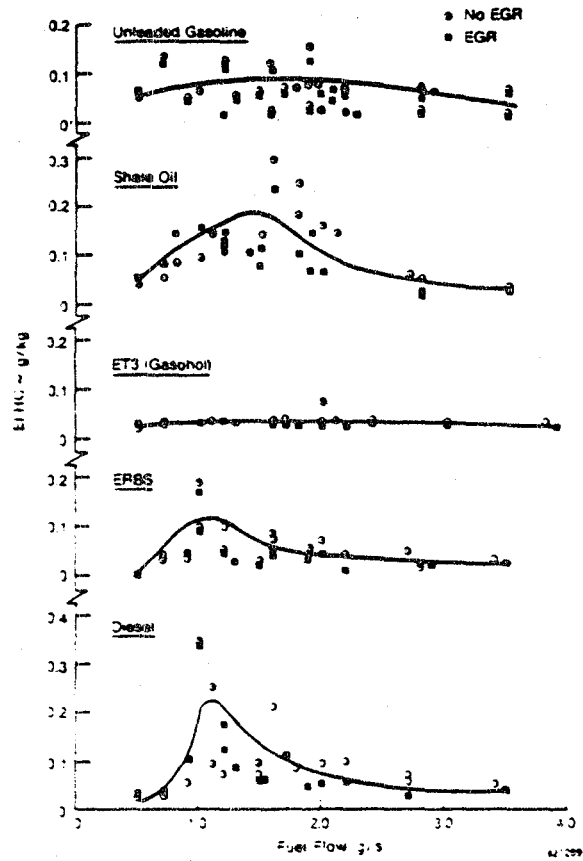


Fig. 11 HC Emissions P-40-7-15

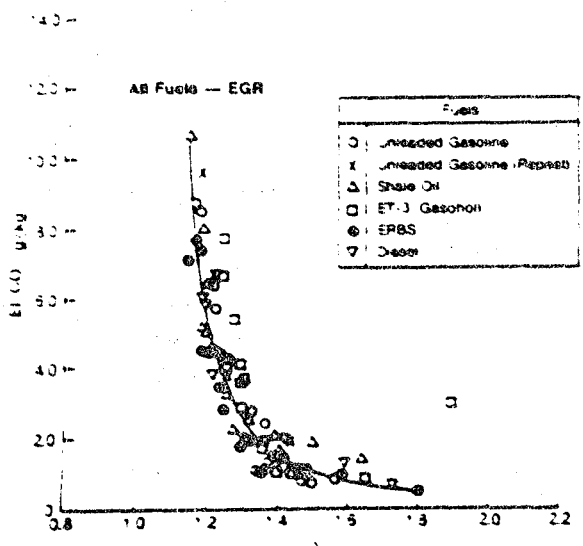


Fig. 12 CO Emissions versus λ (P-40-7-15)

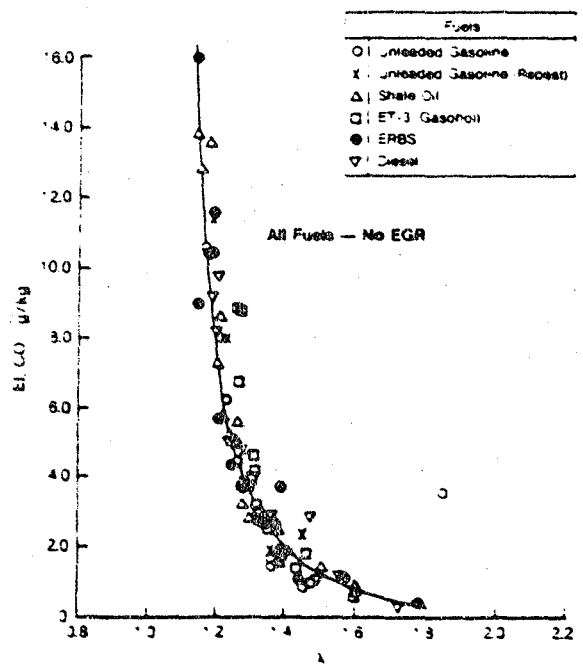


Fig. 13 CO Emissions versus λ (P-40-7-15)

rate; and 3) for values of λ near 1.0, the longer residence time associated with the non-EGR condition (lower mass flows than comparable operating points with EGR) as well as the higher temperatures, may inherently result in high CO concentrations as CO approaches equilibrium values. At low fuel flows and large values of λ , the quenching effect of the exhaust gas predominates and CO with EGR becomes greater than that without. Although very similar, Figures 12 and 13 also support this trend.

Steady-state HC emissions were extremely low for all the fuels tested. Ambient HC levels in the test cell were, in fact, an order of magnitude higher than the exhaust emissions. One might expect HC emissions to be low, considering the high reaction temperatures and large numbers of hot surfaces where reactions occur. It is important to emphasize that these are steady-state data. As Figure 5 clearly illustrates, the emissions levels can vary considerably during cyclic or unsteady conditions. During transients, considerable variation in emissions levels can be expected, and steady-state relationships between emissions and combustion parameters are not necessarily valid. This is especially true during start-up. Thus, integration of steady-state results over the CVS cycle (to determine compliance) is, at best, a crude approximation, particularly if a combustor is known to perform poorly during transients. Even in the cases where transient times are long relative to combustion reaction times, and the combustor is stable and well designed, it is difficult to account for the effects of thermal time lags on the rest of the EHS; however, in this case, the predictive accuracy is certainly improved.

The smoke data have not formally been reduced; however, the filter paper was clean at all steady-state points, and smoke numbers greater than 95 (i.e., nonvisible range) were expected.

ENGINE AND EHS PERFORMANCE

Overall, the P-40 engine performed favorably with the five fuels tested. Even though engine performance was low due to general engine component deterioration (1), nothing detrimental to the engine or the EHS was detected during testing that could be attributed to the use of alternate fuels. The entire test program was run without any modification to either the combustor or control system.

Although not part of the test plan, cold starts were made (using gasohol (ET-3), ERBS, and unleaded gasoline) with little problem. Ignition with diesel fuel and shale marine-diesel was possible with a warm engine; i.e., within ~10 minutes after shutting off the engine and with tube temperatures between 300 and 250°C. The latter ignitions, however, were very sooty; smoke was visible for several minutes until the engine warmed up.

Pressure and temperature data did not indicate any deterioration in combustor or preheater performance. Pressure drop ratio across the combustor and heater head is shown in Figure 14;

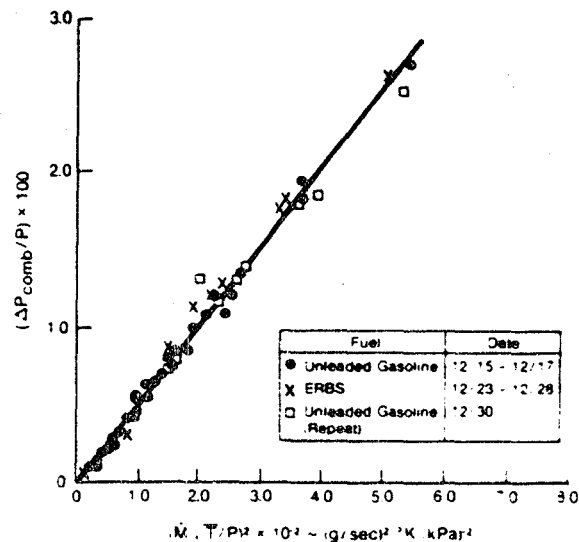


Fig. 14 Combustor Pressure Drop Ratio P-40-7-15 Alternative Fuels Test

data are plotted as a function of the mass flow parameter; i.e.:

$$\frac{P_{ci} - P_{PHi}}{P_{ci}} = \frac{M^2 R_u T_{ci}}{P_{ci}^2 A_{ce}^2} \left(\frac{M}{P_{ci}} \right)^{-2} \quad (4)$$

where:

- P_{ci} = Combustor inlet pressure
- P_{PHi} = Preheater inlet pressure
- M = Total mass flow into combustor
- R_u = Universal gas constant
- T_{ci} = Combustor inlet temperature
- M_w = Molecular weight
- A_{ce} = Effective open area of combustor

It should be pointed out that the value of M actually calculated was not the total mass flow since it was calculated using the volumetric EGR values; i.e.:

$$M = M_{fuel} A/F \left(1 + \frac{\%EGR}{100} \right) \quad (5)$$

where M_{fuel} is the measured fuel flow.

Data are shown for the initial and final gasoline tests, as well as the test with ERBS fuel (run toward the middle of the test sequence). The data show no change in combustor/heater head effective area, indicating no plugging or damage to the components. Inspection of the hardware after the final gasoline test did indicate some plugging and thermal damage of the heater tube fins; however, the open fin area is large compared to the combustor area, and any change in overall

pressure drop resulting from this damage will be within the data scatter.

Figure 15 shows the pressure drop (in mm H₂O) across the combustion side of the preheater. (The drop across the air side was not measured.) The mass flow function in Figure 15 now includes fuel flow as well as air flow, and approximate EGR mass flow. Again, there is no evidence of any change in pressure drop characteristics between the initial and final test sequences. The post-test inspection did not reveal any plugging of the preheater, as had originally been feared.

Figure 16 is a further example of the consistency of the preheater performance and the insensitivity to fuel type. Figure 16 also shows the temperature difference across the combustion side of the preheater for the initial and final gasoline tests, and the tests with gasoline (ET-3) and commercial diesel fuel. Similar results were evident with the other fuels. The results also show no difference in temperature rise for the EGR or non-EGR cases in the combustion side of the preheater for a given mass flow. The temperature differences across the air side of the preheater exhibited the same insensitivity to fuel type although about a 40°C difference in the temperature rise between the EGR and non-EGR conditions was observed. For further discussion of the results, the reader is referred to the report.

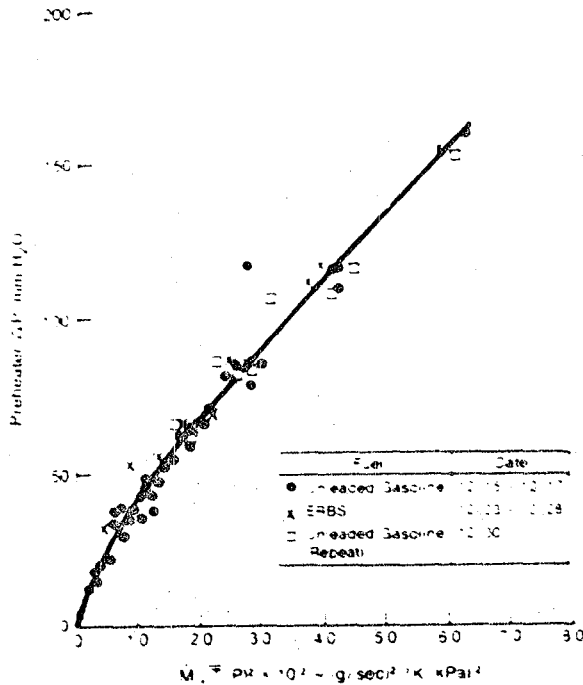


Fig. 15 Preheater Pressure Drop Combustion Gas Side P-40-7-15 Alternative Fuels Test

SUMMARY AND CONCLUSIONS

The multifuel capability of the P-40 Stirling engine has been clearly demonstrated, and the emissions results have shown that a single combustor and EGR schedule can be designed to meet the CVS cycle emissions requirements while burning a variety of liquid fuels. There was essentially no difference in NO_x levels with EGR for the five fuels tested.

Although parametric studies of the magnitude necessary to establish NO_x correlations as a function of various EHS and combustor parameters were well beyond the scope of this test, rough correlations were made with some success; these can be used to establish preliminary EGR combustor requirements for the Upgraded Mod 1 engine.

Steady-state CO and HC emissions data indicate that this should not present a problem if the NO_x emissions requirements can be achieved; however, unstable operation at low fuel flows and poor combustion efficiencies during transients can easily result in CO and HC emissions that exceed allowable limits, particularly if combined with long ignition delay times. Combustion and control stability at low power is, in fact, a current concern, and is being addressed in MTI's current development program for the Upgraded Mod 1. There is evidence that firing transients in the present Upgraded Mod 1 design can result in a dramatic increase in HC emissions. A current goal of the Upgraded Mod 1 combustor design is reduced idle fuel flow and transient combustor instability.

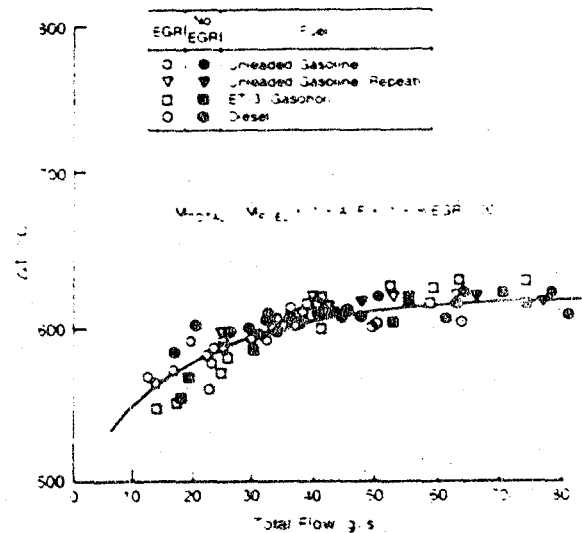


Fig. 16 Temperature Difference Across the Combustion Side of the Preheater (P-40-7-15)

REFERENCES

1. Daly, J., "Combined Alternate Fuels and General Development Test Results of ASE P-40-7," MTI Report No. 82ASE26-ER38, August 1982.
2. Battista, R., "Alternate Fuels' Emission Performance of a Stirling Engine," MTI Report No. 82ASE259PR20, Presented at the Automotive Technology Development CCM - Alternate Fuels Utilization, April 14, 1982.
3. Battista, R., "P-40 Engine Emissions Test Results," MTI Report No. 82ASE260ER37, June 1982.
4. Donovan, P., and Cackette, T., "The Effect of Ambient Conditions on Gas Turbine Emissions - Generalized Correction Factors," ASME Paper 78-GT-87, April 1978.
5. Rubins, P. M., and Marchionna, N. R., "Evaluation of NO_x Prediction-Correlation Equations for Small Gas Turbines," AIAA Paper No. 76-612, July 1976.
6. Sullivan, D. A., "A Simple Gas Turbine Combustor NO_x Correlation, Including the Effect of Vitiated Air," ASME Paper 76-GT-5, March 1976.

Stirling Engine Materials Research at NASA Lewis, MTI, and USAB

Joseph R. Stephens
National Aeronautics and Space Administration
Lewis Research Center
Cleveland, OH

Michael T. Cronin
Mechanical Technology Inc.
Latham, NY

Erik Skog
United Stirling Sweden
Malmo, Sweden

ABSTRACT

A coordinated materials research program for the automotive Stirling engine is under way at NASA Lewis Research Center, Mechanical Technology Incorporated, and United Stirling Sweden. The programs at the three organizations have emphasized the high-temperature materials associated with the heater head. NASA Lewis has focused on creep-rupture properties, hydrogen permeation and embrittlement, oxidation resistance, and simulated engine condition effects on heater-head tubes. MTI has been responsible for fatigue evaluation and failure analysis. USAB has been evaluating materials in engine operation and creep-rupture tests of internally pressurized heater-head tube alloys. ~~This paper provides an~~ update of research conducted at the three organizations over the past year.

THE STIRLING ENGINE is under investigation in the DOE/NASA Stirling Engine project as an alternative to the internal combustion engine for automotive applications. Development of the Stirling engine is under way through a contract with Mechanical Technology Incorporated (MTI) and a sub-contract with United Stirling Sweden (USAB). NASA Lewis Research Center has management responsibility for these contracts. In addition to this role, Lewis has also conducted supporting research and technology development in areas such as materials, seals, controls, combustors, and engine system analysis. On the basis of a materials technology assessment of the Stirling engine by Lewis, the heater head was concluded to be the most critical component. Primary gaps that were found to require research and development included mechanical property data on candidate alloys under Stirling engine operating conditions; compatibility, permeation, the effects of the high-pressure hydrogen working

fluid on the mechanical properties of tube and cast alloys; and the effects of substituting less costly, lower-strategic-element-content alloys for alloys containing the strategic metal cobalt that are now used in prototype engines.

A coordinated approach by Lewis, MTI, and USAB has been undertaken to overcome the materials problems associated with the Stirling engine for automotive applications. Lewis has focused on base-line creep-rupture properties of candidate alloys for the cylinders, regenerator housings, and heater-head tubes, oxidation resistance and hydrogen permeation of the heater-head tubes under simulated engine operating conditions, and the effects of high-pressure hydrogen on creep rupture. MTI has been responsible for determining the fatigue properties of candidate cast alloys for the cylinders and regenerator housings. Fatigue testing in air has been completed and tests in high-pressure hydrogen are under way. USAB has been operating a P-40 engine (prototype automotive Stirling engine) under conditions that are anticipated to exist in the upgraded Mod 1 versions of the automotive Stirling engine. Candidate heater-head tube alloys are also being creep-rupture tested by USAB using internal helium gas pressures at temperatures to 850° C.

This paper summarizes the materials research conducted by Lewis, MTI, and USAB during the past year.

RESULTS

HEATER-HEAD TUBE ALLOYS - Candidate heater-head tube alloys were evaluated in the Stirling engine materials simulator rigs at Lewis.

Tube Degradation - NASA Lewis has operated Stirling engine materials simulator rigs for 4 yr to evaluate candidate tube alloys. Engine conditions of temperature, pressure, environment (combustion gases and internal hydrogen), operating time, and cyclic operation are simulated in these rigs. The endurance tests in the Stirling engine materials simulator rigs provide a means of ranking candidate alloys. Time to failure (tube wall

rupture) is the primary criterion for such a ranking. Since helium does not permeate the tube walls (nominally 0.9 mm thick) at a measurable rate under conditions used in the rigs, helium gas pressure, and hence stress in the tubes, remains essentially constant during testing at 820° C. In contrast, hydrogen permeates the tube walls during each 5-hr cycle, thus lowering the gas pressure and the resulting stress in the tubes (although pressure losses are substantially reduced by hydrogen mixtures containing 1 percent CO₂. Failure time with helium (i.e., the higher stressed tubes) has thus been selected as the failure criterion. In table I, the performance of 17 alloys (compositions in table II) is arranged into five groups based on the alloy lives in a 3500-hr endurance test (the design goal for automotive Stirling engines). Two of the alloys, CG-27 and Incoloy 901, had no failures during the 3500 hr at 820° C and 15-MPa pressure. Two alloys, Inconel 625 and W545, had average failure lives (based on four tube failures) of 2851 and 2776 hr, respectively. Two hydrogen-filled W545 tubes failed at an average time of 2772 hr, indicating a possible hydrogen embrittlement of this alloy. One alloy, 12RN72, failed between 1500 and 2500 hr, while all remaining alloys failed prior to 1500 hr of testing.

On the bases of the initial 3500-hr endurance test, oxidation resistance, tube formability, and resistance to hydrogen permeation, CG-27 was selected as the leading candidate alloy for automotive Stirling engine applications. A second 3500-hr endurance test was conducted at Lewis using only CG-27. Sixteen tubes were tested at 820° C and a gas pressure of 20.7 MPa (the estimated peak pressure experienced in automotive Stirling engines). CG-27 tubes sustained this extreme test pressure for 3500 hr without any failures.

Hydrogen degradation of candidate tube alloys in the Lewis rigs can be estimated from the ratio of time-to-failure with the H₂ + 1 percent CO₂ gas as compared with time-to-failure for helium-filled tubes. As described previously, failure of the helium-filled tubes was expected to occur earlier since a higher internal pressure was maintained throughout the test. If, however, in spite of lower internal pressures due to diffusional losses, hydrogen degraded the high-temperature strength of any of the alloys, failure could occur earlier in the tubes containing H₂ + 1 percent CO₂. Table III indicates that four alloys exhibited evidence of such possible hydrogen degradation. These alloys are Inconel 750, 12RN72 cold worked, W545, and 19-9DL. The ratio R of endurance life for H₂ + 1 percent CO₂ tubes to that for helium-filled tubes ranged from a low of 0.64 for Inconel 750, a nickel-base alloy, to 0.88 for 19-9DL. The two alloys that had no failures in 3500 hr, CG-27 and Incoloy 901, have unknown R values. In both cases, however, hydrogen degradation does not appear to be a problem.

Hydrogen Permeation - The Lewis Stirling engine materials simulator rigs also provide a measure of hydrogen permeation through the candidate tube alloys. The alloys are presented in three groups in table IV for the H₂ + 1 percent CO₂ gas mixture. It has been postulated that a permeability constant ϕ lower than 1×10^{-6} cm²/sec-MPa^{1/2} will be required in the automotive Stirling engine to minimize hydrogen recharging to acceptable intervals of 6 months. This figure indicates that all candidate substitutes for the cobalt-containing alloy N-155 (except 253 MA, W545, and 19-9DL), have permeability constants that are less than the required limit when H₂ + 1 percent CO₂ is used. This presents the possibility of using less dopant in the hydrogen since 1 percent CO₂ in the hydrogen lowers the calculated engine maximum power output by 7 percent. However, further studies are required to determine the optimum dopant level.

Some insight into the mechanism of reducing permeation by hydrogen doping is afforded by the compositions (table II) of the various tube alloys that were evaluated. Alloys with good resistance to hydrogen permeation, in general, contained significant quantities of strong oxide-forming reactive elements such as aluminum, titanium, niobium, and the rare earths. As discussed in previous CCM presentations, oxide film formation on the tube internal surface, as a result of doping the hydrogen with CO₂, and formation of an adherent oxide scale on the outer surface exposed to the combustion gases are the primary factors that contribute to reducing hydrogen permeation in the Stirling engine heater-head tubes.

Tests at Lewis have shown that the alloy 19-9DL has very poor oxidation resistance at 820° to 870° C and exhibits high rates of hydrogen permeation even when the hydrogen is doped with CO₂. To exploit the good mechanical properties of this lower cost alloy, 19-9DL was modified by adding two levels each of the reactive elements misch metal, niobium, and aluminum. Effects on cyclic oxidation resistance for times up to 500 hr are shown in figure 1. Additions of 0.5 wt % misch metal and 0.5 and 1.0 wt % aluminum improved the oxidation resistance of 19-9DL by reducing spalling, as a result of formation of an adherent oxide scale.

Figure 2 shows preliminary permeation data for the 0.5-wt % aluminum-modified 19-9DL alloy. After 20 hr of testing (under a NASA contract with Illinois Institute of Technology Research Institute), hydrogen permeation for 19-9DL + 0.5 wt % Al was lower than that for unmodified 19-9DL in H₂ + 1 percent CO₂. This figure also shows the effect of temperature on pure hydrogen and doped-hydrogen permeation for the modified 19-9DL alloy. These initial results suggest that alloy composition is an important factor in reducing hydrogen permeation in heater-head tubes and that minor additions of reactive metals may be used to reduce hydrogen loss from the engine.

Table I - Endurance Test Results
 [Temperature, 820° C; pressure, 15 MPa; gas, H₂ + 1 % CO₂ and helium.]

Time to failure, t, hr				
t > 3500	2500 < t < 3500	1500 < t < 2500	750 < t < 1500	t < 750
CG-27 Incoloy 901	Inconel 625 #545	12RN72 Cold worked 12RN72 Annealed	253 MA HS-188 Inconel 75u Sanicro 32	19-90L N-155 Inconel 718 Inconel 601 A286 Sanicro 31H Incoloy 800H

Table II. - Composition of Heater-Head Tube Alloys

Alloy	Fe	Cr	Ni	Co	Mn	Si	Mo	Cb	W	Al	Ti	C	Other
	Composition, wt %												
N-155	30	21	20	20	1.5	0.5	3.0	1.0	2.5	---	---	0.15	0.15 N
CG-27	35	13	38	---	.1	.1	5.5	.6	---	1.5	1.5	.05	0.01 S
Incoloy 901	34	14	43	---	.45	.40	6.2	---	---	.25	1.5	.05	0.015 S
Inconel 625	3	22	61	---	.15	.3	9.0	4.0	---	.2	.2	.05	---
#545	54	14	26	---	1.5	.4	1.5	---	---	.2	2.9	.08	0.08 B
12RN72	47	19	30	---	1.5	.29	1.4	---	---	---	.5	.1	0.02 N
253 MA	65	21	11	---	.4	1.7	.40	---	---	---	---	.09	0.7 N
HS-188	1.5	22	22	40	---	---	---	---	14.0	---	---	.08	0.08 La
Inconel 750	7	16	73	---	.5	.2	---	1.0	---	.7	2.5	.04	---
Sanicro 32	45	21	31	---	.6	.37	---	---	2.8	.4	.4	.89	---
19-90L	67	13	9	---	1.1	.6	1.3	.4	1.2	---	.3	.3	---
Inconel 718	19	19	52	---	.2	.3	3.1	5.0	---	.4	.9	.04	---
Inconel 601	14	23	50	---	.5	.2	---	---	---	1.4	---	.05	---
A286	53	15	25	---	1.4	.4	1.3	---	---	.2	2.2	.05	0.25 N
Sanicro 31H	46	21	31	---	.6	.55	---	---	---	.4	.5	.17	0.02 N
Incoloy 800H	46	17	33	---	.75	.5	---	---	---	.38	.38	.05	---

Table III. - Hydrogen Degradation of Pressurized Tubes
 [Pressure, 15 MPa.]

Ratio of life in H ₂ + 1 percent CO ₂ to life in He, R				
R	R > 1		R < 1	
CG-27 Incoloy 901	12RN72	Inconel 601	19-90L	(0.88)
	253 MA	A286	#545	(0.35)
	HS-188	Sanicro 31H	12RN72 cold worked	(0.83)
	Sanicro 32	Incoloy 800H	Inconel 750	(0.64)
	N-155	Inconel 625		
	Inconel 718			

No failures with either H₂ + 1 percent CO₂ or He.

Table IV. - Hydrogen Permeation
 [Temperature, 820° C.]

Permeability constant, ϕ , $\text{cm}^2/\text{sec-MPa}^{1/2}$		
$\phi < 0.1 \times 10^{-6}$	$0.1 \times 10^{-6} < \phi < 1 \times 10^{-6}$	$1 \times 10^{-6} < \phi < 10 \times 10^{-6}$
CG-27 12RN72 Inconel 601 Incoloy 901	Inconel 750 Inconel 718 HS-188 Sanicro 32 Inconel 625 Incoloy 800H Sanicro 31H N-155 A286	'253 MA W545 19-9DL

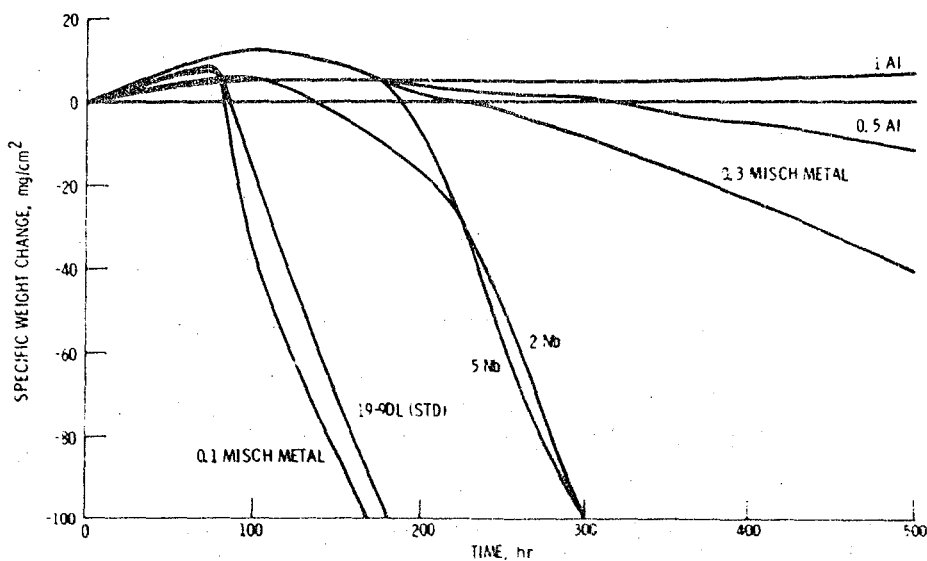


Figure 1. - Cyclid oxidation of modified 19-9DL alloys. Temperature, 300° C.

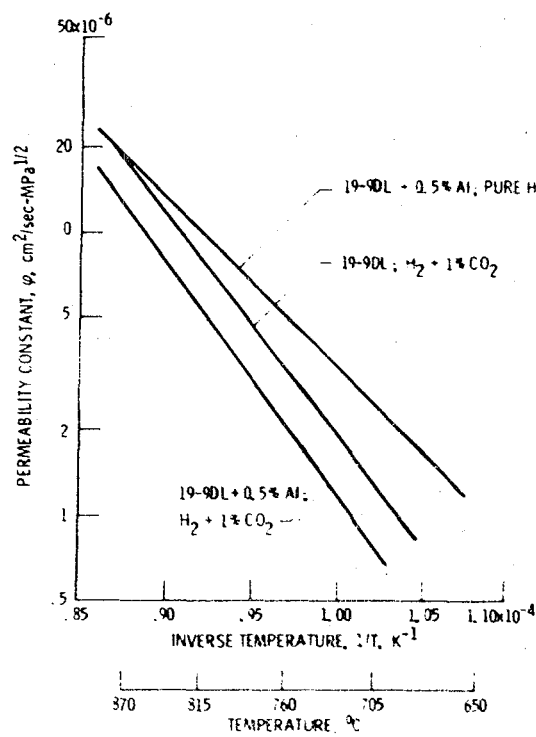


Figure 2. - Hydrogen permeation in modified-composition 19-90L alloys.

This factor will be taken into consideration when choosing an alloy for the heater-head tubes.

Creep Rupture - Several iron-base alloys are under evaluation at Lewis as possible substitutes for the high (20 percent Co) cobalt-containing alloy N-155, which is the heater-head tube material used in prototype and Mod I automotive Stirling engines. Figure 3 compares the 3500-hr rupture strengths of N-155 and two candidate iron-base alloys, CG-27 and 12RN72. The heater-head tube alloys will operate at approximately 820° C in the upgraded Mod I engine. At the proposed use temperature the rupture strength of the CG-27 alloy exceeds that of the currently used Mod I engine material by about a factor of 2. The CG-27 alloy affords a substantial growth potential and margin of safety. The 12RN72 alloy is not as strong as the other two alloys, but because of its low cost, adequate resistance to hydrogen permeation and oxidation resistance, 12RN72 is still under consideration for the upgraded Mod I engine.

Creep-rupture tests are under way in high-pressure hydrogen to evaluate hydrogen degradation of candidate heater-head tube alloys and cast cylinder and regenerator housing alloys. Some preliminary results are available from the high-pressure hydrogen tests, which are being conducted under a NASA contract with IIT Research Institute. Figure 4 shows the results of high-pressure-hydrogen (15 MPa) creep-rupture tests at 760° C on two heater-head tube alloys. The solid lines represent a multiple linear regression fit of the air creep-rupture data, which are used as a base line for comparison with hydrogen tests. These initial results indicate that hydrogen degradation has not occurred in these two heater-head tube alloys over the limited test duration. High-pressure-hydrogen creep tests are planned for CG-27 and 12RN72.

CYLINDER AND REGENERATOR HOUSING ALLOYS - Candidate commercial iron-base alloys and experimental iron-base alloys were evaluated at Lewis and MTI as potential substitutes for the cobalt-base alloy now in use for automotive Stirling engines.

Creep Rupture - Figure 5 shows a comparison of high-pressure-hydrogen creep-rupture data with base-line air data for two iron-base alloys, CRM-6D and XF-818 (table V), that do not contain the strategic metal cobalt. CRM-6D and XF-818 are under evaluation as substitutes for the cobalt-base alloy HS-31 (currently used as the cylinder and regenerator housing alloy in prototype engines). Hydrogen degradation has not occurred in these alloys over the time frame of testing. Another alloy being studied is SAF-11 (table V); however, creep-rupture data are not yet available for this material.

Tensile Properties - Candidate substitute alloys for the cobalt-base alloy HS-31 are under evaluation at MTI, with special emphasis on tensile strength and fatigue resistance. Figure 6 shows a comparison of the tensile properties of three cast iron-base alloys with those of HS-31.

All alloys were heat treated for 1/2 hr at 1125° to 1150° C and then for 50 hr at 800° C to simulate a brazing cycle and exposure at the proposed use temperature, respectively. Results show that HS-31 has superior strength over the temperature range investigated. At 800° C the order of decreasing tensile strength is HS-31, SAF-11, CRM-6D, XF-818. The ductility of all the alloys is low, remaining below 10 percent elongation up to 800° C.

Fatigue Life - The low-cycle fatigue lives determined by MTI for HS-31 and three cast iron-base alloys are shown in figure 7 for various strain amplitudes. The data were obtained at 800° C by applying various constant-strain-range $\Delta\epsilon$ or alternating-strain-range $\Delta\epsilon/2$ amplitudes about a mean stress of zero ($R = -1.0$) until material failure occurred. For random loading as experienced in actual engine operation, strain amplitudes and corresponding cycles must be grouped to establish a finite loading spectrum. The rain-flow counting method is one method for accomplishing this. The rain-flow spectrum (horizontal lines) represents the predominant cylinder-head manifold strain amplitudes and their corresponding frequencies expected over an engine lifetime of 3500 hr. The curve drawn through the end points of these lines is the limiting-life curve for the cylinder-head manifold. The higher parallel curve is the design-life curve, whose strain amplitudes have been increased by a safety factor of 2 above those of the limiting-life curve. Any material whose data points fall below the design-life curve is considered unacceptable. On the basis of the rain-flow spectrum of strain amplitudes anticipated in the cylinder manifold, all the alloys have sufficient lives to meet the design criterion.

Failure of cast cylinders and regenerator housings, due to high cycle fatigue (HCF) resulting from cycle pressure variations of the over-riding working fluid, is also of concern in the automotive Stirling engine. Failure analyses of P-40 heater heads by MTI have shown fatigue crack striations in the manifold areas of cast components. Relative fatigue properties determined by MTI are shown in the Haigh diagram, figure 8, for HS-31 and three iron-base candidate alloys. The Haigh diagram is a graphical method that is used to show the interaction of mean stress with alternating stress range. The stress values shown correspond to combinations of mean stress and alternating stress range that result in a fatigue life of 10^7 cycles to failure. The points for each of the three R values and a specific alloy are connected by straight lines to form upper bounds. Therefore, any combination of mean stress and alternating stress range that falls below a particular material curve will result in a life greater than 10^7 cycles for that particular material, while combinations falling above the curves will result in lives less than 10^7 cycles. A comparison of the data in figure 11 for the four alloys at 800° C shows that HS-31 has the highest HCF strength, with SAF-11 only slightly

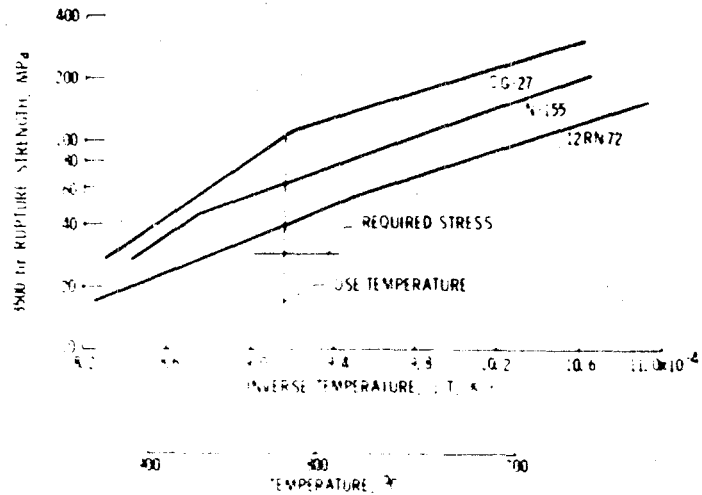


Figure 3. Stress rupture strength of candidate heater head tube alloys.

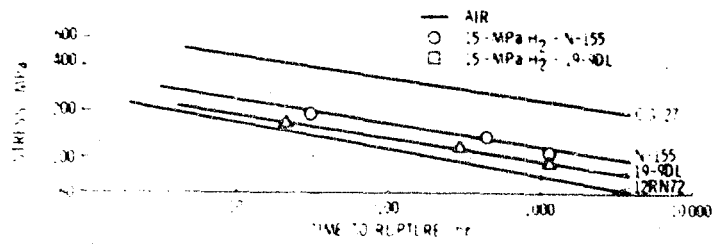


Figure 4. Rupture lives in air and hydrogen of candidate heater head tube alloys. Temperature: 500°C.

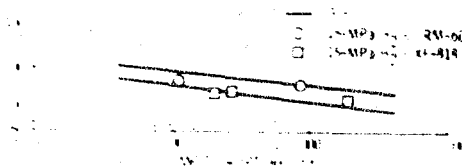


Figure 5. Rupture lives in air and hydrogen of candidate heater head tube alloys. Temperature: 500°C.

Table 4. - Compositions of Cast Cylinder and Regenerator Housing Alloys

Alloy	Composition, wt %										
	Fe	Cr	Ni	Co	Mn	Si	Mo	Cb	W	C	B
HS-31	1.5	25	10	55	0.5	0.5	---	---	7.5	0.5	----
CRM-60	63	22	5	---	5.0	.5	1.0	1.0	1.0	1.0	0.003
SAF-11	47	23	16	---	.5	.6	---	---	12	.6	.4
XF-818	55	18	18	---	.1	.3	7.5	.4	----	.2	.6

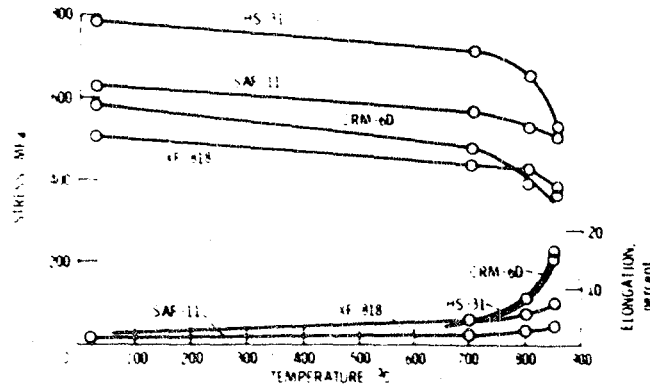


Figure 6. Tensile properties of candidate cylinder and regenerator housing alloys.

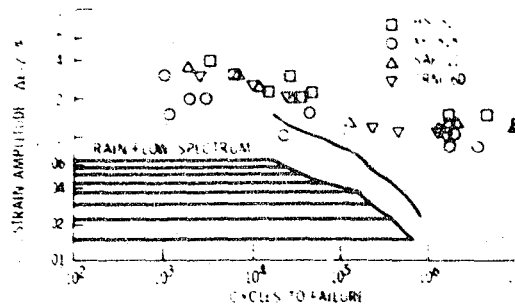


Figure 7. Fatigue properties of candidate cylinder and regenerator housing alloys. Temperature: 3000°F.

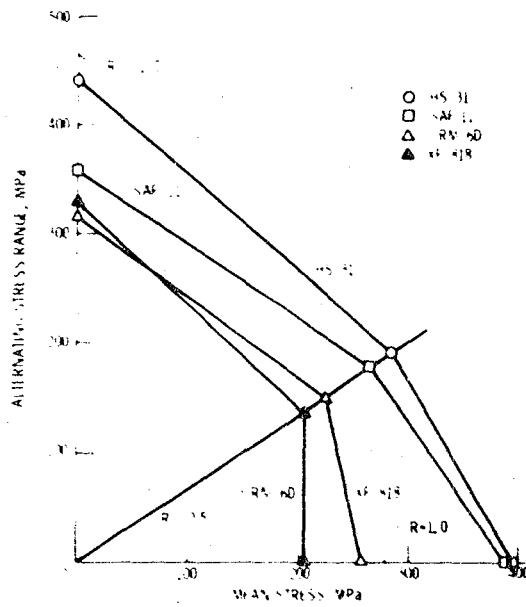


Figure 3. S-N diagram for candidate cylinder and regenerator processing alloys. Temperature: 400°C, 10⁷ cycles to failure.

lower. The remaining two iron-base alloys, XF-818 and CRM-6D, have lower HCF strengths.

Design changes in the Mod I engine, as compared with the P-40 engines, were focused on reducing the mean stress in the manifolds of the cylinder and regenerator housings. Success in substituting any of the three candidate iron-base alloys will depend in part on the resulting stress combinations that these components experience in Mod I engine testing.

Experimental Alloys - Candidate iron-base alloys are being evaluated by Lewis and MTI as substitutes for the cobalt-base alloy HS-31 now in use in Mod I engines. As shown by MTI, tensile strength and fatigue resistance are lower for the iron-base alloys than for HS-31. Figure 9 shows a comparison of the 3500-hr rupture strength at 775° C (the upgraded Mod I cylinder and regenerator housing use temperature) for HS-31 and the iron-base alloys SAF-11, XF-818, and CRM-6D. HS-31 also has better creep-rupture strength than these iron-base alloys. Results based on very limited data are also shown for two experimental alloys: EX-4G, under development at United Technologies Research Center (UTRC), and EX-76, under development at AirResearch Casting Company (ACC). Both programs are contractual with Lewis. The UTRC alloy is in the initial developmental stages and the alloy exhibits promising creep-rupture properties. The ACC program has been under way longer and the alloy has rupture strength superior to that of HS-31, although its rupture ductility is lower. Continued evaluation and alloy modifications are planned for these two programs.

ENGINE TESTING - Laboratory testing at Lewis and MTI is used to screen potential candidate alloys and to identify those alloys that offer the most potential as substitutes for currently used cobalt-base or cobalt-containing alloys. Actual engine operation gives a more critical evaluation of candidate alloys and can provide a means of ranking alloys under conditions that will be similar to those experienced in upgraded Mod I engines. USAB is also evaluating the candidate alloys that appeared most promising in laboratory testing by means of P-40 engine (a prototype engine) tests in one of their test cells located in Malmo, Sweden. Figure 10 shows the combinations of alloys that were selected for fabrication into eight quadrants for evaluation. Cylinder and regenerator housings were fabricated from the cobalt-base alloy HS-31 and three iron-base alloys CRM-6D, XF-818, and SAF-11. Heater-head tubes were matched with the corresponding cast alloys as listed in the figure. Tube alloys were a nickel-base alloy, Inconel-625, and four iron-base alloys, Sanicro 32, 12RN72, CG-27, and

Sanicro 31H. As of September 1982, a total of 1453 hr had been accumulated on the heater head of the P-40 engine. The test plan called for testing at 820° C and a pressure variation from 4 to 7.5 MPa for 1000 hr, with inspection of the four quadrants after 500 and 1000 hr of operation. If no severe failures occurred after 1000 hr, the pressure cycle was to be made more severe (variation from 4 to 9 MPa for an additional 500 hr). A further increase in pressure variation was to be chosen after 1500 hr operation if no severe failures had occurred. Test results to date (fig. 9) indicate that during the first 500 hr (pressure variation of 4 to 7.5 MPa) of operation, quadrants 1 and 4 were free from any detectable failures or cracks; quadrant 2 exhibited cracks in the manifold area of the regenerator housing, and there were some possible indications of cracking on quadrant 3. Testing was continued on all four quadrants. During the 500- to 1000-hr testing period, braze-joint failures occurred in quadrants 1 and 2. These quadrants were temporarily replaced by quadrants 5 and 6. After the pressure variation was increased (4 to 9 MPa), two tubes failed in quadrant 3, which was replaced with quadrant 7. In addition, it was determined that quadrant 3 was operating about 50° C higher than quadrant 4, so these quadrant positions were exchanged. To date, no problems have been encountered with quadrant 4. Engine testing is continuing as planned.

CONCLUSIONS

From Stirling engine materials research conducted at the NASA Lewis Research Center, Mechanical Technologies Incorporated, and United Stirling Sweden, the following conclusions were drawn:

1. The leading high-strength candidate heater-head tube alloys are CG-27, Inconel 625, and 12RN72 on the basis of Stirling engine materials simulator rig tests and stress-rupture tests performed at NASA Lewis.
2. The leading low-cost candidate iron-base cylinder and regenerator housing alloys all have shorter fatigue lives at 800° C than HS-31, the cobalt-base alloy now used in the Mod I engine, but some of these lives may be adequate on the basis of MTI-calculated strain amplitudes in cylinder manifolds.
3. Engine evaluation at United Stirling Sweden of candidate heater-head alloys under conditions simulating the upgraded Mod I engine has shown tube-manifold brazing to be a problem area. Tests in the P-40 engine at 820° C show that alloy 12RN72 may be stress and temperature limited.

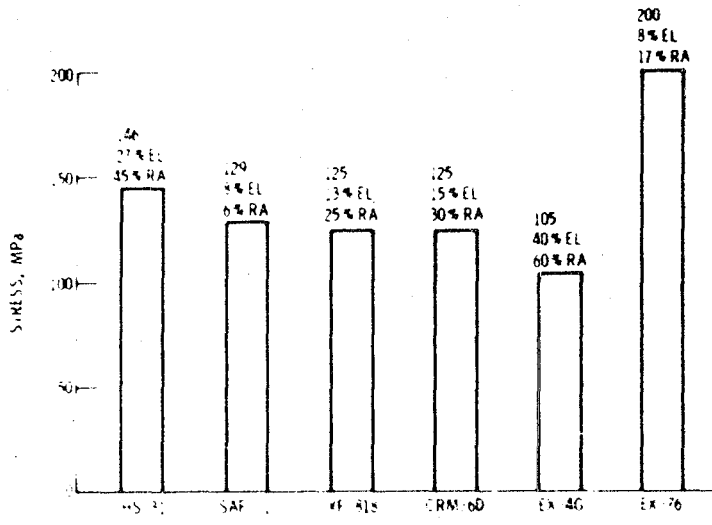


Figure 9. 1500-hour rupture strength for candidate cylinder and regenerator housing alloys. Temperature: 1150°C.

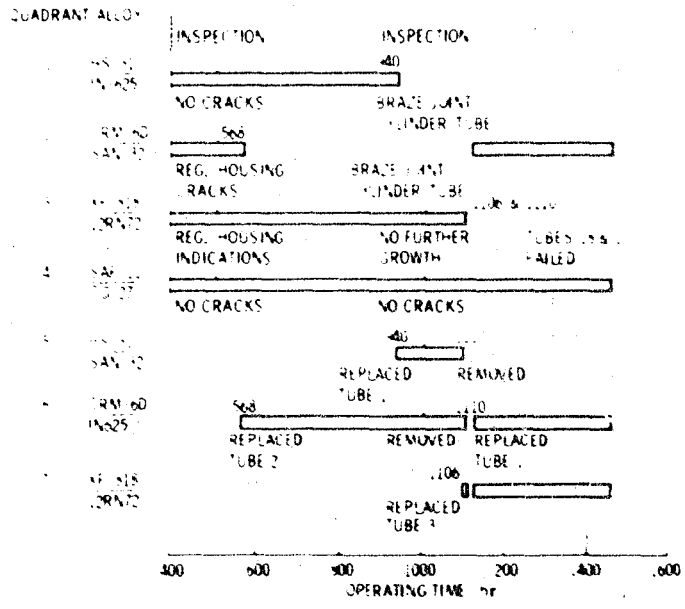


Figure 10. Status of high-temperature P-40 engine materials evaluation. Allow notation: cylinder/regenerator housing/tube.

Free-Piston Stirling Hydraulic Drive for Automobiles

Donald G. Beremand, Jack G. Slaby,
and David Miao

National Aeronautics and Space Administration
Lewis Research Center
Cleveland, OH

ABSTRACT

This analytical study compares the calculated fuel economy of an automotive free-piston Stirling hydraulic engine and drive system with a pneumatic accumulator to the fuel economy of both a conventional 1980 spark-ignition engine in an X-body class vehicle and the estimated fuel economy of a 1984 spark-ignition engine. The results of the study show that the free-piston Stirling hydraulic system with a two-speed transmission has a combined fuel economy nearly twice that of the 1980 spark-ignition engine - 21.5 to 10.9 km/liter (50.7 to 25.6 mpg) under comparable conditions. The fuel economy improvement over the 1984 spark-ignition engine is 81 percent. The overall engine and drive system efficiency (ratio of power to wheels to fuel in) is 36 percent. The study also includes the fuel economy sensitivity of the Stirling hydraulic system to system weight, number of transmission shifts, reduced drag coefficient, and varying vehicle performance requirements.

IN RECENT YEARS the NASA Lewis Research Center has conducted a number of Stirling engine investigations for a variety of potential applications. These activities have included the Department of Energy's Automotive Stirling Engine Development Project being conducted by the DOE Office of Vehicle and Engine R&D, Technology Development and Analysis Division, and the NASA Stirling Engine Technology effort sponsored by the NASA Headquarters Conservation and Fossil Energy Systems Branch of the Energy Systems Division. This NASA-funded effort was aimed at broadening the general Stirling engine technology base at Lewis and assessing its applicability to a variety of applications.

This study, "A Free-Piston Stirling Hydraulic Drive for Automobiles," was carried out as part of the NASA-funded effort. The study has

*Numbers in parentheses designate references at end of paper.

relied heavily on capabilities and information developed at Lewis under the various DOE- and NASA-funded activities. A significant part of the NASA-funded effort has been directed toward the free-piston Stirling engine. The free-piston Stirling engine is in an ever earlier state of development than the kinematic Stirling engine currently being developed under the automotive program. However, the free-piston Stirling engine inherently provides a high-payoff and high-risk type of advanced heat engine that offers the potential for high efficiency, simplicity, and long life.

Other studies (1)* have shown the potential fuel economy benefits of hydraulic drive systems for automobiles. However, a key drawback has always been the added complexity of these systems. The free-piston Stirling hydraulic engine and drive system addressed in this study offers a significant degree of simplification in the drive system. It avoids some fundamental problems inherent in kinematic Stirling engine development such as seal life and control complexity; and it also offers the potential for even higher efficiency. For these reasons, this study was undertaken to more carefully assess the fuel economy potential of such a free-piston Stirling hydraulic engine and drive system for the automotive application.

SYSTEM DESCRIPTION

The free-piston Stirling hydraulic drive system assessed in this study is shown schematically in figure 1. The free-piston engine generates hydraulic output directly by means of an integral hydraulic converter to supply hydraulic fluid to the accumulator, thereby compressing the gas in the accumulator. The accumulator serves as an energy buffer, isolating the engine from the vehicle drive system. High-pressure fluid from the accumulator is supplied to the variable-displacement motor-pump on demand by expansion of the gas in the accumulator. The hydraulic motor discharges the hydraulic fluid to the

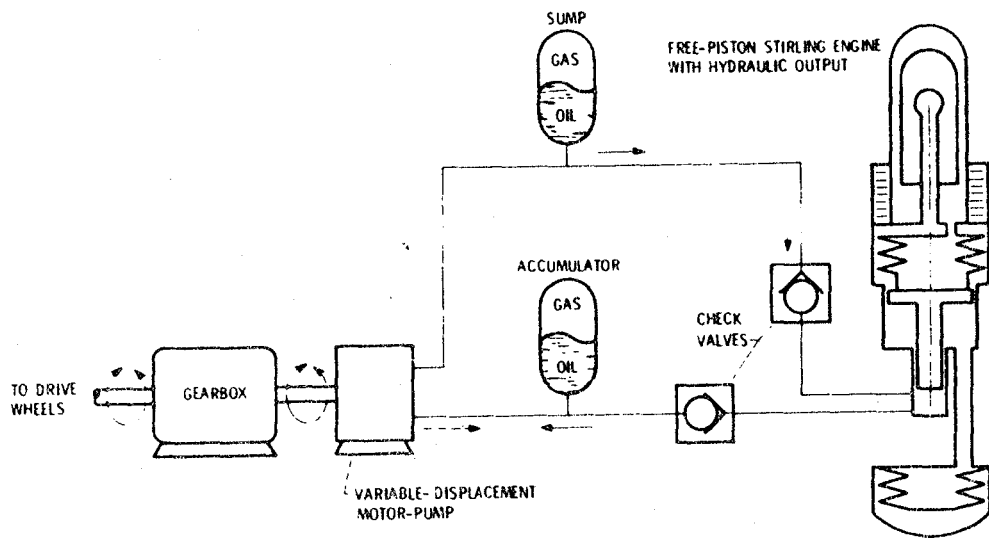


Figure 1. - Free-piston Stirling hydraulic engine and drive system.

sump, where it is again available to the inlet of the converter. Motor output is transmitted to the vehicle drive shaft through a gearbox, including an optional multispeed transmission. For regenerative braking of the vehicle the motor-pump unit is driven as a pump by the vehicle. The pump output is used to recharge the accumulator.

SYSTEM REQUIREMENTS

For this study it was decided to assess the drive system in a conventional "family car" type of vehicle with full normal performance capabilities. To this purpose the following performance criteria were selected:

- (1) Standstill to 30.5 m (100 ft) in 4.5 sec
- (2) Acceleration from 0 to 96.5 km/hr (60 mph) in 15 sec
- (3) Acceleration from 80.5 to 113 km/hr (50 to 70 mph) in 10 sec
- (4) Continuous 88.5 km/hr (55 mph) up a 5 percent grade
- (5) Maximum speed of 113 km/hr (70 mph) or greater on a level road

It was further decided that the system should be designed such that these requirements could always be met regardless of the immediately preceding operating history of the vehicle. This requirement was included to avoid unsafe driving situations such as attempting a high-speed pass maneuver without the normal expected acceleration capability.

A 1980 X-body vehicle was specified as the standard vehicle for the study. For the calculations, the X-body vehicle was assumed to have an inertia weight of 1361 kg (3000 lb) that included two passengers plus a full tank of fuel. A 272-kg (600-lb) weight penalty was calculated for the baseline hydraulic drive vehicle system at 1633-kg (3600-lb) inertia weight, which meets these requirements.

SYSTEM DESIGN APPROACH

The design approach chosen in this study was to size the accumulator system to store energy equal to the kinetic energy of the vehicle at maximum speed (113 km/hr, 70 mph) and to size the engine to provide all constant-speed power requirements (including continuous 88.5 km/hr (55 mph) up a 5 percent grade and 113 km/hr (70 mph) on a level road). In this approach the engine size can be reduced significantly and it operates in an off-off mode only. To assure that full vehicle acceleration capability would always be available, regardless of the preceding vehicle operating history, the accumulator differential pressure was scheduled with vehicle speed, as shown in figure 2, for the baseline case. The baseline parameters are shown in table I. This assured that there was always sufficient stored energy to provide the kinetic energy necessary to accelerate the vehicle to maximum speed (113

km/hr (70 mph) on a level road). The hydraulic motor was then sized to meet the acceleration rate criteria with the scheduled accumulator pressure. To avoid continuous on-off cycling of the engine, a +0.69-MPa (100-psi) dead band was added to the accumulator schedule so that the engine would cycle off at the top limit of the dead band and cycle on at the bottom limit. For example, for the baseline case shown in figure 2, at a speed of 80.5 km/hr (50 mph) the engine would turn on when the pressure fell below approximately 20.0 MPa (2900 psi) and would shut off when the pressure reached approximately 20.7 MPa (3000 psi). In view of the on-off engine operation, auxiliary power for both the vehicle and engine is provided by means of a separate hydraulic motor operating off the accumulator system. This assures the continuous availability of power for the vehicle accessories such as power brakes and air conditioning. It also provides for independent operation of the engine burner system, which will be required to maintain heater-head temperatures at design values while the vehicle is operating but the engine is shut off.

ENGINE SELECTION

At present, there are no known operating free-piston Stirling engines above about 3-kW (4-hp) output power. Nor have any design studies been prepared that would apply directly to the requirements of this study. Therefore, it was decided to estimate engine performance by extrapolating from existing large (30 to 60 kW, 40.2 to 80.5 hp) kinematic engine results and factoring in the results of design studies that did address hydraulic output for free-piston Stirling engines.

It was felt that the best basis for this was to extrapolate indicated efficiencies from the results of the DOE/NASA automotive Stirling engine program. The resulting method was to calculate the indicated engine efficiency as equal to 75 percent of the Carnot efficiency and add 1/2 efficiency point for optimizing the engine without any requirement for higher power, high-speed operation. (The Mod I engine incorporates only a portion of the automotive reference engine advancements, and still the predicted indicated efficiency of the Mod I engine is 50.1 percent, only 1/2 percentage point below a value of 50.0 percent obtained by using 75 percent of the Carnot efficiency.) Therefore, using a heater temperature of 762° C (1404° F) (assuming a continuous 15-MPa (2175-psia) charge pressure for 3500 hr of life) and a cooler temperature of 50° C (122° F) with 75 percent of Carnot efficiency yields an indicated efficiency of 51.6 percent. Adding 1/2 point for the optimization gives an indicated free-piston Stirling efficiency of 52.1 percent.

Overall engine efficiency was then calculated by applying a combustion efficiency of 92.4 percent (2) and a conservative hydraulic

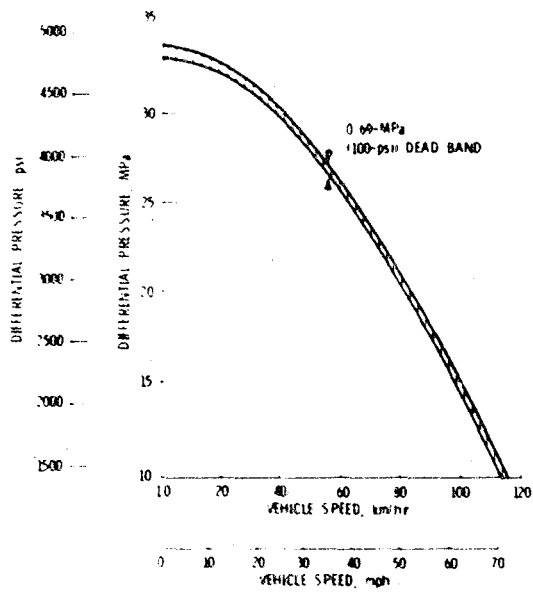


Figure 2 - Effect of vehicle speed on differential pressure accumulator minus signal for baseline vehicle.

Table I. - Stirling Hydraulic Baseline Input and Output Parameters

(a) Input conditions

Accumulator and sump	isothermal
Available engine power, kW (hp)	39 (52)
Average engine efficiency, percent	43
Maximum displacement of scaled Volvo V-20 hydraulic motor-pump, cm ³ /rev (in ³ /rev)	81 (4.94)
Maximum speed of hydraulic motor-pump, at 113 km/hr (70 mph), rpm	4000
Total vehicle inertia weight, kg (lb)	1633 (3600)
Accumulator maximum pressure, MPa (psi)	34.5 (5000)
Accumulator minimum pressure, MPa (psi)	13.8 (2000)
Sump maximum pressure, MPa (psi)	3.4 (500)
Accumulator and sump volume, m ³ (ft ³)	0.0683 (2.41) each
Motor-pump shaft speed over wheel speed:	
Direct connected	1.25
Single shift	4.08
Gear direct-drive efficiency, percent:	
Urban	96.0
Highway	97.4
Shift efficiency, percent	98
Tire efficiency, percent:	
Urban	93
Highway	98
Drag coefficient	0.417
Frontal vehicle area, m ² (ft ²)	1.98 (21.34)
Effective wheel radius, m (in.)	0.305 (12)

(b) Output conditions

Total hydraulic system weight, kg (lb)	174 (604)
Accumulator weight, kg (lb)	745 (1601)
Sump weight, kg (lb)	10 (22)
Oil weight, kg (lb)	58 (128)
Volvo motor-pump weight, kg (lb)	51 (113)
Vehicle weight less hydraulic system weight, kg (lb)	1359 (2996)
Clayton dynamometer EPA standard fuel economy, km/liter (mpg):	
Highway	24.03 (56.54)
Urban	14.55 (46.70)
Combined	21.54 (50.67)

converter efficiency of 94 percent (3). The resulting overall maximum engine efficiency of 45.3 percent (ratio of hydraulic power out to fuel in) does not include auxiliary power requirements, which are accounted for separately.

To better assess engine operation in the system, a hypothetical engine performance map was constructed (fig. 3) showing hydraulic power output as a function of engine stroke and hydraulic accumulator-sump pressure differential. Typically, the engine power output can be represented as a function of stroke raised to a power of 1.3 to 1.7. For the purpose of this study the exponent was chosen as 1.4, consistent with a 1-kW (1.34-hp) output free-piston Stirling engine tested at the Lewis Research Center. Stable system operation requires that the slope of the system load requirement be steeper than the engine output slope. To provide this characteristic, it was assumed that a null-center-band pump, similar to the design of Toscano et al. (4), was used in the converter. Although this is a very simplified approach, the resulting map does provide an indication of the range of operating conditions the engine might encounter in the system. The map indicates a stroke range from 70 to 100 percent of full stroke and a power range from 58 to 100 percent of full power for the differential pressure range of 10.3 to 33.1 MPa (1500 to 4800 psi). Examination of available Stirling engine maps, both free piston and kinematic, indicates that engine efficiency over this power range could vary as much as 10 percent. This 10 percent efficiency range was then applied to the 45.3 percent maximum efficiency previously estimated. This yielded an efficiency range of 40.7 to 45.3 percent, resulting in an average engine efficiency of 43.0 percent, which was then used throughout this study.

HYDRAULIC SYSTEM

The hydraulic system includes the high-pressure accumulator, the low-pressure sump, and the variable-displacement motor-pump, which is described below. In addition, the system requires some ancillary devices such as overpressure protection in the form of relief valves, filters, check valves, and a possible shut-off valve. Although it is recognized that these devices are necessary, flow losses associated with them should be minimal and were not accounted for in this report.

ACCUMULATOR - The accumulator system (accumulator and sump) was sized to store usable energy equal to the kinetic energy of the vehicle at 113 km/hr (70 mph). Accumulator maximum operating pressure, 34.5 MPa (5000 psi) for the baseline case, was selected on the basis of the current state of the art of hydraulic motor-pump technology. The baseline accumulator pressure ratio was selected as 2.5 (minimum accumulator pressure of 13.8 MPa, 2000 psi) to minimize volume and weight and at the same time limit the differential pressure range over which the motor-

pump must operate. Rifkin (5) indicates that the theoretical optimum accumulator pressure ratio for an isothermalized accumulator would be 2.72.

In the system arrangement addressed in this study almost all of the energy used by the vehicle must pass through the accumulator in charge-discharge cyclic operation. Thus it is important that the accumulator cyclic efficiency be as high as possible in order to achieve the best possible vehicle fuel economy. Near isothermal operation or operation at very low pressure ratios is necessary to achieve the desired high cyclic efficiency. For the drive-cycle calculations in this study the accumulator was assumed to be fully isothermalized. For isothermal operation the accumulator would be partially filled with a metal foam material to absorb heat during the compression process and to return heat to the gas during the expansion process. For simplicity of calculation, no weight or volume penalty for adding an isothermalizing foam material was included in the basic calculations. These penalties could vary over a very large range and depend on the degree of isothermalization required. The potential weight and volume effects of adding isothermalizing material and the degree of isothermalization desired are addressed in the RESULTS AND DISCUSSION section.

Although cylindrically shaped accumulators may be advantageous from installation and cost standpoints, this analysis was limited to calculating the weights of spherical accumulators. For simplicity all of the accumulator calculations were made by assuming an ideal gas. For a design stress of 206.9 MPa (30 000 psi) the volume determined from the stored energy requirement ranged from 0.057 to 0.085 m³ (2 to 3 ft³). The baseline system volume was 0.068 m³ (2.41 ft³). Accounting for the compressibility effects of a real gas would increase these values by approximately 12 percent. To minimize weight, the accumulator can be fabricated as a composite of a thin aluminum or steel liner with a glass- or Kevlar-wound outer covering. Such a construction would reduce the accumulator weight by one-half as compared with steel. Another advantage of the composite construction is its controlled failure mode with no fragmentation. The sump (low-pressure accumulator) was assumed to be the same size as the high-pressure accumulator with the same pressure ratio. Maximum sump pressure for the baseline case was set at 3.45 MPa (500 psi).

HYDRAULIC MOTOR - The variable-displacement type of motor-pump selected for this investigation was a Volvo Model V-20. Performance data generated by Volvo for a 178-cm³/rev (10.9-in³/rev) displacement unit was acquired under NASA contract (6). These data were scaled down, as recommended in (6), to the appropriate smaller motor-pump sizes used in this study. For the baseline system the operating pressure differential range, defined by accumulator and sump maximum and minimum pressures and the +0.69-MPa (100-psi) dead band, was 33.8 to 10.3 MPa (4900

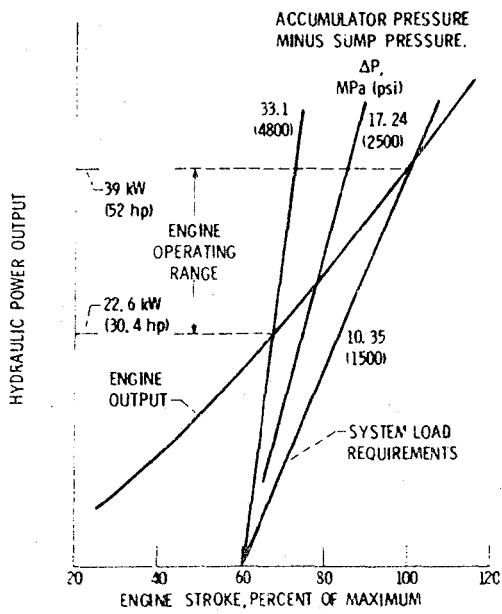


Figure 3. - Operating map of Stirling free-piston engine with hydraulic output. (Average engine efficiency, 43 percent.)

to 1500 psi). Motor-pump size was based on meeting the three acceleration criteria:

- (1) Standstill to 30.5 m (100 ft) in 4.5 sec
- (2) Acceleration from 0 to 96.5 km/hr (60 mph) in 15 sec
- (3) Acceleration from 80.5 to 113 km/hr (50 to 70 mph) in 10.5 sec

The first criterion was the most severe and thus determined the motor-pump size. For the baseline case this was a unit with $81\text{-cm}^3/\text{rev}$ ($4.9\text{-in}^3/\text{rev}$) maximum displacement.

RESULTS AND DISCUSSION

Fuel economy projections were calculated over the Federal urban and highway driving cycles and for the combined urban and highway driving cycle. These projections are presented in this section for the baseline system and for some of the variations investigated to assess sensitivity to various system and component design parameters. Included in these results are fuel economy sensitivity as a function of vehicle weight, number of gear shifts, and drag coefficient. In addition, runs were made to assess the changes in fuel economy resulting from varying the performance requirements. The baseline system component characteristics used in the study are presented in table II.

To make a meaningful comparison with the Stirling free-piston hydraulic baseline system, the performance of a 1980 spark-ignition Phoenix with a three-speed automatic transmission was computer calculated by using the same driving cycle and Environmental Protection Agency Clayton dynamometer computer program. The hot-start results for the free-piston Stirling hydraulic system and for the spark-ignition engine are shown in figure 4. The Stirling free-piston hydraulic system, though several hundred pounds heavier, showed almost a two-to-one improvement in combined fuel economy (21.5 to 10.9 km/liter, 50.7 to 25.6 mpg). Going one step further, the combined projected fuel economy for a 1984 spark-ignition engine also is shown in figure 4. The Stirling free-piston hydraulic system combined fuel economy showed an improvement of over 81 percent over this projected 1984 spark-ignition engine.

Figure 5 shows the effects of substantial vehicle weight reductions and a reduced aerodynamic drag coefficient. For this analysis the ratio of hydraulic motor size to vehicle weight was held constant to provide nearly constant 0 to 30.5 m (100 ft) acceleration times. White (7) projects a 907-kg (2000-lb) test weight as feasible in 1995 with current best technology. The Ford Thunderbird, to be introduced in January 1983, is projected to have a drag coefficient of 0.35 (8). The combined effect of a 907-kg (2000-lb) inertia weight with a 0.35 drag coefficient yielded a fuel economy of 31.4 km/liter (73.8 mpg), 46 percent higher than that of the baseline case.

For the baseline fuel economy calculations the total vehicle weight was taken to be 1633 kg (3600 lb), including a 272-kg (600-lb) hydraulic system weight allowance (accumulator, sump, hydraulic oil, and motor-pump). The baseline hydraulic system weight was then computer calculated as 273.9 kg (604 lb). No attempt was made to correct the fuel economy values for the 1.8-kg (4-lb) difference between assumed and calculated hydraulic system weights. This difference has an insignificant effect on the fuel economy. However, the use of composite materials for the accumulator and sump would reduce the hydraulic system weight for the baseline case by approximately 77.1 kg (170 lb), yielding about a 3-percent improvement in fuel economy to approximately 22.2 km/liter (52.2 mpg).

The effect on fuel economy of the number of transmission speeds and selected gear ratios is shown in figure 6. One interesting finding of the study was that the system can achieve the performance requirements with a single-speed (no shift) transmission. It is apparent that a two-speed transmission makes a significant improvement in fuel economy on the combined driving cycle of about 12 percent, as compared with a single-speed transmission. An additional shift (three speeds) only increases the fuel economy about 2.4 percent more. Thus there is not much of an incentive to go beyond a two-speed transmission. As a result, the baseline case was chosen with a two-speed transmission. It should be noted that these calculations were all made for the same vehicle inertia weight of 1633 kg (3600 lb). Some small reduction in the fuel economy benefits of the two- and three-speed transmissions would result if the appropriate weight differentials were included in the analysis.

All of the calculations in this study were based on an ideal gas and assumed the thermodynamic process to be isothermal in both the accumulator and the sump. This isothermalization can be achieved by filling the units with a high-surface-area material with high porosity and the appropriate thermodynamic properties. Obviously this requires larger total accumulator and sump volumes to compensate for the isothermalizing material volume in the accumulator and sump. This correction was not made in the computer calculations since the degree of isothermalization required was not defined. However, the results of the computer analysis provided additional information on the operation of the accumulator system. This allowed further assessment of the degree of isothermalization required and the associated efficiency and weight penalty. Even though an accumulator pressure ratio of 2.5 was chosen for the baseline case, the combination of pressure schedule versus speed, coupled with a +0.69-MPa (100-psi) dead band, resulted in a computer-calculated maximum pressure ratio over the combined driving cycle of 1.89. More importantly, the average pressure swing was only about 1.15. Table III calculated from (5) shows the

Table II. - Baseline System Component Characteristics

Vehicle	
Type	t-body
Inertia weight, kg (lb):	
base vehicle	1361 (3000)
hydraulic system	272 (600)
Total	1633 (3600)
Engine	
Type	Free-piston Stirling hydraulic
Maximum power, kW (hp)	29 (52)
Average efficiency, percent	41
Accumulator and sump	
Type	Spherical steel isothermal, perfect gas
Volume, m ³ (ft ³)	0.0014 (0.05)
Accumulator pressure, MPa (psia):	
Maximum	14.7 (214)
Minimum	11.2 (162)
Sump pressure, MPa (psia):	
Maximum	1.0 (14.7)
Minimum	0.1
Hydraulic motor and pump	
Type	Variable displacement
Maximum speed, m/s (ft/min)	4.0 (157)
Maximum displacement, cm ³ (in ³)	1.0 (0.061)
Transmission	
Type	Direct
Motor/pump shaft speed, rpm (rev/min)	1000
Direct/indirect	Direct
Single/multi	Single
Axles	
Type	Drum
Motor/pump shaft speed, rpm (rev/min)	1000
Engine hp, kW (hp)	29 (52)

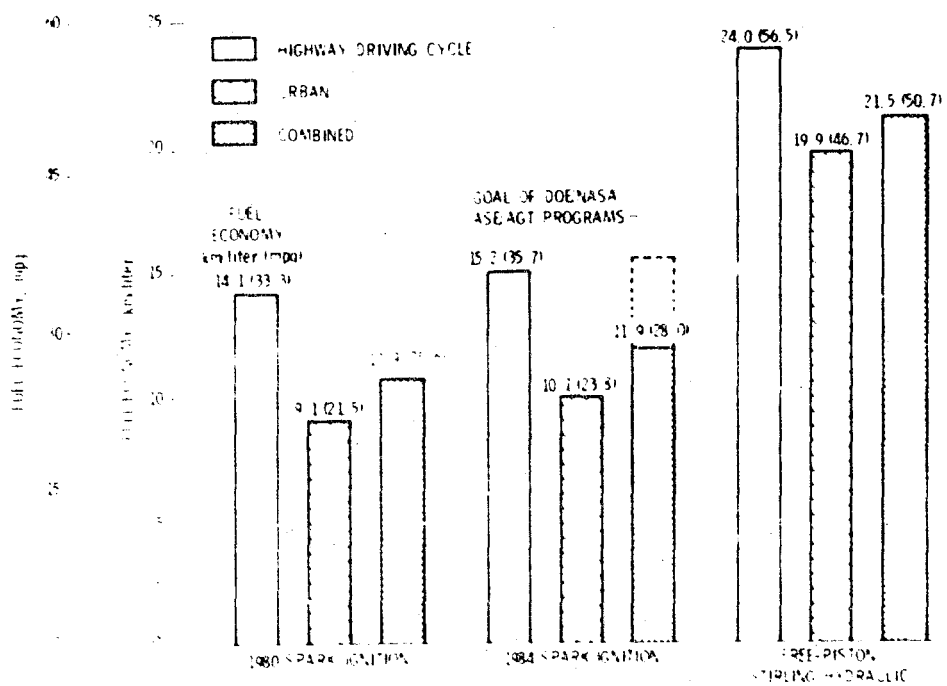


Figure 1 - Fuel economy of free-piston Stirling-Hydrolic system and spark-ignition engines in 1980-1984 vehicles.

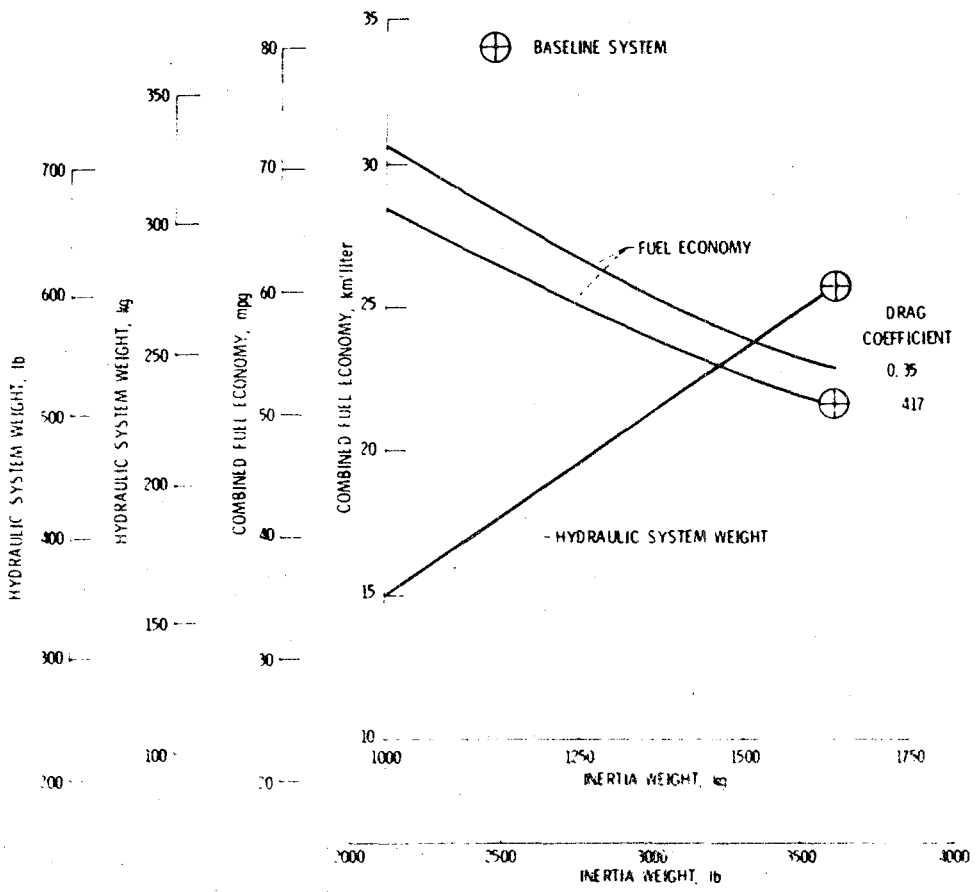


Figure 5 - Effect of vehicle inertia weight on combined fuel economy and hydraulic system weight for two drag coefficients

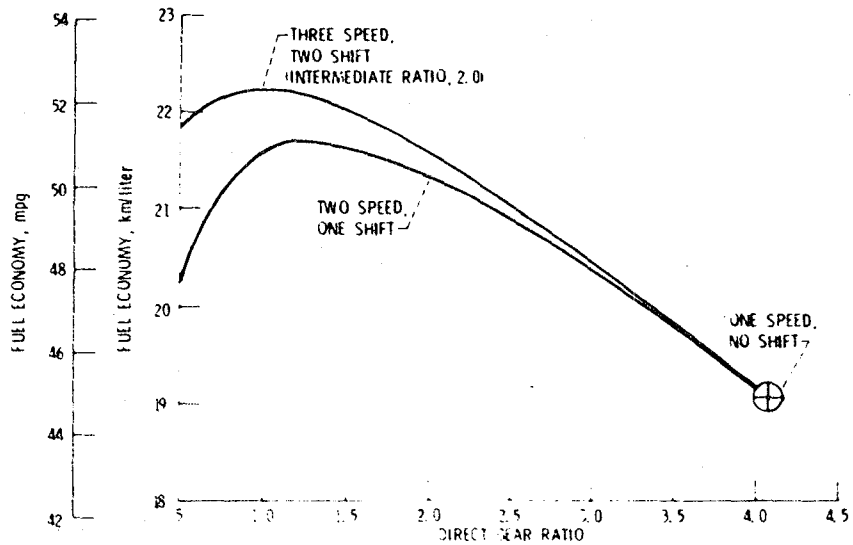


Figure 6. Effect of final gear ratio on fuel economy of baseline vehicle for combined cycle.

Table III. - Effect of Fill Factor on Accumulator Cyclic Efficiency (Calculated from (5)).

[Pressure ratio, 1.15.]

		Fill factor, percent	
		10	25
Accumulator cyclic efficiency, percent	26	45	39
Isothermization penalty, ³ weight, kg (lb)	--	20.4 (67)	59.3 (197)
Fuel economy, percent	--	+0.9	+0.6
Net fuel economy effect, percent	-4	+0.9	+0.6

³Including accumulator containment.

effect of various degrees of isothermalization (varying fill factor) on accumulator cyclic efficiency. Even with zero fill factor (pure adiabatic), the cyclic efficiency at the average pressure ratio (1.15) was about 96 percent. At a fill factor of 10 percent this increased to about 98 percent; and at a fill factor of 25 percent, to about 99 percent. These efficiencies, along with an estimate of the weight and fuel economy penalties associated with the addition of the isothermalization material, are shown in the table.

This first-order assessment indicates the optimum fill factor to be of the order of 10 percent. However, this yielded a fuel economy improvement of only about 1 percent, which may not be worth the added cost, increased accumulator volume, and complexity. Use of composite materials would have only a small effect on these results since only a third of the weight penalty (isothermalization material plus accumulator containment) comes from the increased containment weight. Isothermalization of the sump, which handles only 10 percent of the energy handled by the accumulator, would have substantially less effect on fuel economy and thus was not evaluated further.

As a final comparison the effects of relaxing the performance requirements were assessed. Since, in this system, motor size directly controls the acceleration torque available, two smaller and one larger variable-displacement motor-pump were investigated. The fuel economy results and the acceleration times associated with each performance criterion, along with the required time for each criterion, are shown in figure 7. The baseline system uses an hydraulic motor-pump with $81 \text{ cm}^3/\text{rev}$ ($4.49 \text{ in}^3/\text{rev}$). As shown in this figure, the 0 to 30.5-m (100-ft) standstill distance was met, and the 0 to 96.5 km/hr (60 mph) and 80.5 to 113 km/hr (50 to 70 mph) required acceleration rates were exceeded with the baseline system. Going to the extreme and decreasing the motor-pump displacement by about 26 percent ($60 \text{ cm}^3/\text{rev}$, $3.7 \text{ in}^3/\text{rev}$) had little effect on the highway fuel economy and increased the urban fuel economy about 3 percent. The combined fuel economy improvement was then only about 1.6 percent. Again, these results are all based on a vehicle inertia weight of 1633 kg (3600 lb). Adding in the small weight benefit effect of the $60\text{-cm}^3/\text{rev}$ ($3.7\text{-in}^3/\text{rev}$) unit (assuming unit weight is proportional to displacement) increased this to only about 2.2 percent. This modest fuel economy gain was made at the expense of substantial increases in the acceleration times, from 18 to 52 percent longer than with the baseline unit. On the other hand, increasing motor-pump size to $100 \text{ cm}^3/\text{rev}$ ($6.1 \text{ in}^3/\text{rev}$) yielded a relatively "hot" performing vehicle with a 0 to 96.5 km/hr (0 to 60 mph) time of 9.6 sec at a fuel economy penalty of 2.4 percent. Again accounting for the small weight penalty for the larger motor would increase the fuel economy penalty to only about 3 percent.

When this relative insensitivity of fuel economy is considered, cost, packaging, and the marketability of a "hot" performing vehicle may be more significant factors in considering any trade-offs in motor-pump sizes with acceleration capability.

The overall energy balances (including nomenclature) for the Federal urban and highways drive cycles are shown in figure 8. Some of the significant efficiencies for the system are as follows:

	Urban cycle	Highway cycle
Hydraulic drive efficiency (C/D) ^a , percent	75.4	84.1
Regenerative braking efficiency (A/B), percent	70.4	74.3
Overall hydraulic system efficiency (C/E), percent	84.4	85.1
Overall engine and drive system efficiency (C/F), percent	36.3	36.6

^aRefer to fig. 8

The 36.3 percent overall engine and drive system efficiency is 45 percent better than that projected as feasible (7) in the 1995 time period for an advanced diesel engine with a continuously variable transmission.

The question arises as to how much of the 81 percent improvement in fuel economy as compared with the projected conventional 1984 spark-ignition vehicle could be achieved by using a more conventional engine with the same type of energy-buffered hydraulic drive system used in this study. A detailed evaluation of this question was beyond the scope of this effort. However, preliminary estimates were made by simply ratioing the fuel economy results of the study on the basis of expected engine and hydraulic pump efficiencies. The results are presented in table IV. This approach ignores a number of specific differences such as auxiliary power requirements, idling or engine-off losses, and weight differences. However, these differences are unlikely to affect the following conclusions for engines utilizing this energy-buffered hydraulic drive system: (1) the free-piston Stirling hydraulic engine and drive system offers fuel economy improvements significantly greater than would be achieved with either a diesel or spark-ignition engine and (2) the kinematic Stirling engine offers a fuel economy improvement approaching that of the free-piston Stirling engine. However, factors such as cost, complexity, life, and reliability, in addition to the fuel economy differential, give the free-piston Stirling hydraulic engine and drive system a substantial advantage over the kinematic Stirling engine system.

CONCLUSIONS AND CONCLUDING REMARKS

The free-piston Stirling hydraulic engine and drive system has excellent payoff potential.

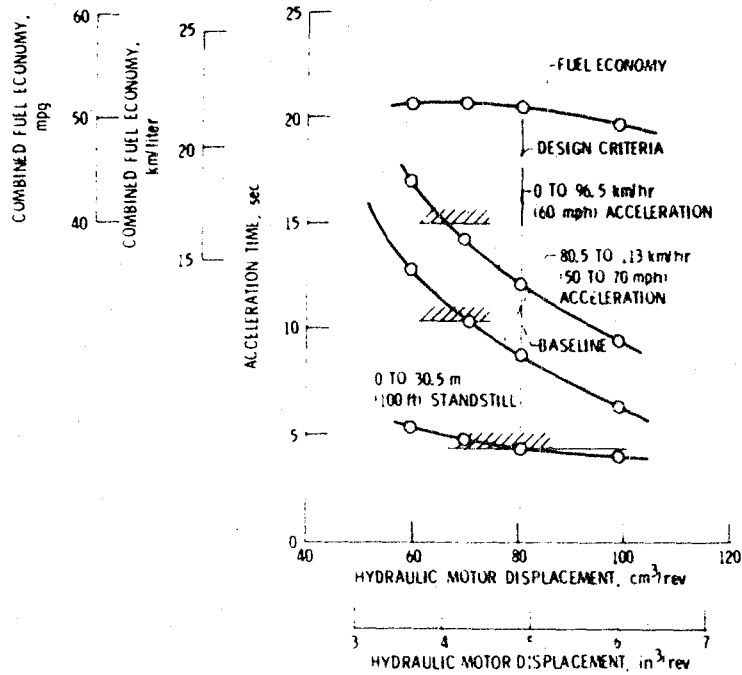


Figure 7. - Effect of motor size on combined fuel economy and performance. Inertia weight, 1633 kg (3600 lb).

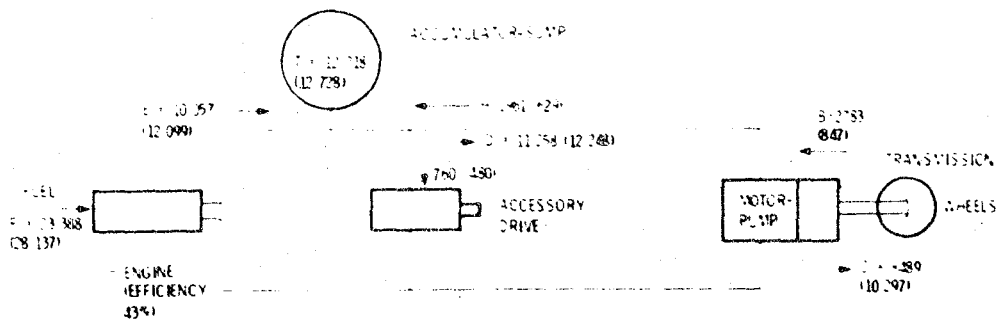


Figure 8. - Energy balances for urban and highway drive cycles. (Values shown are total integrated energy flows over drive cycle in horsepower-seconds. The first number in each location is for the urban cycle, the second number (in parentheses) is for the highway cycle)

Table IV. - Preliminary Comparison of Alternative Engines
with Energy-Buffered Hydraulic Drives

Engine and drive system	Engine efficiency, percent	Pump efficiency, percent	Combined fuel economy		Estimated improvement in combined fuel economy, percent
			km/liter	mpg	
Free-piston Stirling hydraulic engine and drive	46	94	21.5	50.7	37
Kinematic Stirling engine and hydraulic drive	48	95	22.0	51.0	53
Diesel engine ^a and hydraulic drive	34	95	16.2	38.1	26
Spark-ignition engine ^b and hydraulic drive	30	95	14.3	33.6	20
1984 spark-ignition engine with automatic transmission	--	--	11.9	28	c

^a1975 Chrysler-Nissan model 1N633 91.

^b1978 Ford 48 CID engine (10).

^cStandard.

The results show an overall engine-drive efficiency of 36 percent, as compared with about 12 percent for current automobiles, and a combined fuel economy 81 percent greater than that projected for the comparable 1984 spark-ignition engine vehicle. Further, high acceleration capability can be provided with minimal fuel economy penalty. The 0 to 96.5 km/hr (60 mph) acceleration time was reduced from 12.1 to 9.6 sec with only a 3 percent fuel economy penalty.

The fuel economy improvement results are sufficiently encouraging that simplifying assumptions used in the study should not significantly alter the projected fuel savings.

Although detailed evaluation has not been made, preliminary estimates also indicate that the free-piston Stirling engine should be significantly better than more conventional alternative engines (spark ignition, diesel, and kinematic Stirling) with the same type of hydraulic drive system.

No cost projections were made in this study. The hydraulic system arrangement used in this study was not optimized. Other arrangements and combinations of hydraulic components should be investigated further.

Free-piston Stirling engine technology is still in its infancy. Kinematic Stirling engines up to a few hundred horsepower in size have been built, and the DOE NASA Automotive Stirling engine program is currently developing one for automotive application at about 60 kW (80 hp). However, the largest free-piston Stirling engine built to date is about 3 kW (4 hp), and the only hydraulic output free-piston Stirling engine under development is a heart pump engine with about 8 kW (10.01-hp) output power.

The critical research and development need for this engine drive system then is to design, build, and test a free-piston Stirling hydraulic engine in the 30 to 40 kW (40 to 54 hp) output range in order to develop and validate this technology in the appropriate size range. The initial step in this process would be to conduct a preliminary engine and system design effort to generate a specific engine design, to refine the fuel economy and performance projections of this study, and to assess system costs and packaging.

Congress has mandated that the fleet of automobiles built for 1985 must achieve 11.7 km/liter (27.5 mpg) as measured by dynamometer tests administered by the Environmental Protection Agency. This paper presents a system concept

that conservatively would surpass that mandate by 84 percent.

REFERENCES

1. N. H. Beachley and D. R. Otis, "A Study of Accumulator Passenger Cars Based on the Ifield Hydrostatic Pump/Motor Unit," Lawrence Livermore Laboratory, University of California, Livermore, CA, UCRL-15390, August 24, 1981.
2. Automotive Stirling Reference Engine Design Report. Mechanical Technology Inc., Latham, NY, MTI-81-ASE-64DR-2, June 1981. (NASA CR-165381, 1981.)
3. M. H. White, "Conceptual Design and Cost Analysis of Hydraulic Output Unit for 15 kW Free-Piston Stirling Engine," University of Washington Joint Center for Graduate Study, Flow Industries Inc., Seattle, WA, NASA CR-165543, August 1982.
4. W. M. Toscano, A. C. Harvey, and K. Lee, "Design of Hydraulic Output Stirling Engines," Foster-Miller Inc., Waltham, MA, NASA Contract NAS3-22230.
5. W. D. Rifkin, "Free-Piston Stirling Engine Accumulator, Buffered Hydrostatic Vehicle Drive, Final Report," Energy Research and Generation, Inc., Oakland, CA, NASA Contract NASJ-21483, 1979.
6. M. Magi, A. Freivald, I. Andersson, and U. Ericksson, "On Variable Hydrostatic Transmission for Road Vehicles, Powered by Supply of Fluid at Constant Pressure," Volvo Flygmotor A.B., Trollhætten, Sweden, Rept. 301-7663, May 1981. (NASA CR-165246, 1981.)
7. C. L. Gray, Jr., and F. von Hippel, "The Fuel Economy of Light Vehicles," Scientific American, Vol. 244, No. 5, May 1981, pp. 48-59.
8. D. Sabath, "Aerodynamics to Dominate Ford's Future," Cleveland Plain Dealer, August 14, 1982, p. 12-D.
9. W. F. Marshall and K. R. Stamper, "Engine Performance Test of the 1975 Chrysler-Nissan Model CN633 Diesel Engine," DOD-TSC-OST-75-44, September 1975.
10. "Performance Characteristics of Automotive Engines in the U.S.," Energy Research and Development Administration, Bartlesville, OK, Department of Energy, Bartlesville Energy Technology Center, Bartlesville, OK, Rept. 7 - Third Series, BERCEP-78-34, July 1978.

A Look at a Cooled, Insulated Stirling Engine

William A. Tomazic

National Aeronautics and Space Administration

Lewis Research Center

Cleveland, OH

ABSTRACT

A simple analysis was made on a new Stirling engine design concept. The concept makes use of an insulating ceramic liner in a cooled metal structure to form cylinders and regenerator housings. The concept is intended to reduce greatly the need for expensive, strategic, high-temperature alloys and to improve efficiency. The analysis reported herein revealed that significant efficiency improvement is possible if cylinder inner-wall temperatures can be increased and made more uniform along the cylinder length. Potential efficiency gains as high as 20 percent for a 40-kW, 1000-rpm engine were calculated. The results of this analysis, which did not address potential practical problems related to the use of ceramic liners, suggest that this concept deserves a rigorous thermal and design analysis to define its potential benefits and limitations.

THE STIRLING ENGINE requires that cycle heat addition be brought to the working fluid by transfer across load-bearing boundaries and that the hot ends of the cylinder and regenerator housings be kept at temperatures close to the maximum working fluid temperatures to avoid unacceptable heat losses. This means that the maximum cycle temperature and, hence, efficiency are limited by the high temperature creep rupture strength of the engine hot end materials of construction. It is general practice for Stirling designers to employ costly, high alloy metals for these components. Such alloys as N-155 and HS-31 are typical. The concept of a cooled, insulated engine was suggested by Meijer and Ziph in their study of the Stirling engine for heavy-duty applications (1).^{*} They proposed glass-ceramic

insulation material enclosed in cooled external metal sheaths for the engine cylinders and regenerator housings. Since the metal load-bearing structure would be at low temperature, costly alloys would not be required. The glass ceramic insulation would greatly restrict the radial heat conduction out of the cylinder and regenerator housings. Meijer and Ziph proposed that the radial heat loss would be of the same order of magnitude as the axial heat conduction from the hot end down to the cold end of a conventional all-metal Stirling engine and that the efficiency levels would be equivalent. They assumed a thermal conductivity of 0.5 W/°C for the glass ceramic. This value, lower than that for commercially available glass ceramic materials, is for a proprietary material developed by Philips Research Laboratory. The concept of using glass ceramic insulation in this manner was introduced as part of the advanced Stirling engine technology work done at Philips Research Laboratory. It was one of the advanced concepts being examined in the Advanced engine project. Unfortunately, Philips chose to drop their Stirling engine program before the concept could be developed.

The cooled insulated Stirling engine (1) offers not only the potential of reducing cost, but also the possibility of improving efficiency if radial conduction losses could be reduced with more efficient insulation. A simple, preliminary study was undertaken at Lewis Research Center to compare heat losses for the cooled, insulated concept with those for conventional engines. The effects of engine power level and design speed were examined. The results of this analysis are presented herein.

ANALYTICAL APPROACH

The intent of this analysis is to compare heat losses for a cooled, insulated engine with those for a conventional engine such as the United Stirling P-40.

CYLINDER MODEL CONVENTIONAL ENGINE - Figure 1 shows a schematic cross section of a

^{*}Work performed for the U.S. Department of Energy under Interagency Agreement DE-A101-77CS510-0.

^{*}Numbers in parentheses designate references at end of paper.

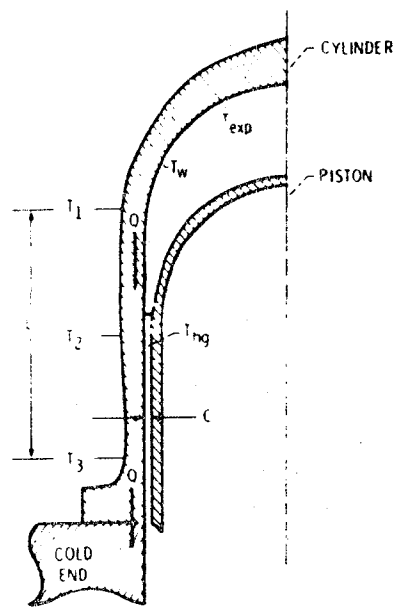


Figure 1. - Conventional engine cylinder.

cylinder for a typical conventional Stirling engine. Heat input to the cylinder is through heater tubes at the top of the cylinder. The outside of the cylinder is generally insulated. The bottom of the cylinder is fastened to the cold end of the engine. Conductive heat flow is primarily downward to the cooled lower end of the engine.

For this analysis it was assumed that all conduction was downward, that none was radial, and that T_1, T_2, T_3 were constant across the cylinder wall thickness and constant for any engine size ($\Delta T/L$ would then decrease with increasing engine size).

Four types of heat losses were assumed for the conventional engine cylinder:
Cylinder Conduction Loss - This loss can be described by an equation of the form

$$Q_{cc} = \frac{k\bar{A} \Delta T}{L}$$

where \bar{A} is the effective heat flow area, which must be derived for a tapered wall. For different engine powers and design speeds, $\Delta T (T_1 - T_3)$ is assumed constant, and k is then constant. Thus,

$$Q_{cc} \propto \frac{A}{L}$$

where

$$A = \frac{\pi}{4} (\bar{D}_o^2 - D_i^2) = \frac{\pi}{2} (\bar{D}_o + D_i) \bar{t}_w$$

where \bar{t}_w is the mean wall thickness corresponding to \bar{A} and the mean outer diameter \bar{D}_o . Assuming constant design stress and constant cylinder mean pressure as engine size is changed, mean wall thickness \bar{t}_w varies directly with cylinder diameter:

$$\bar{t}_w \propto D_i$$

Then $\bar{A} \propto [\bar{D}_o + D_i] D_i$ and $\bar{D}_o \propto D_i$, giving

$$A \propto D_i^2$$

It is assumed that engine proportions are maintained as engine size is changed and that $L \propto D_i$. Therefore,

$$Q_{cc} \propto D_i$$

Cylinder conduction heat loss is directly proportional to cylinder inside diameter.

Piston Conduction Loss - This loss can be described by the equation

$$Q_{cp} = \frac{kA_p \Delta T}{L_p}$$

where k and ΔT can be assumed constant. Hence,

$$Q_{cp} \propto \frac{A_p}{L_p}$$

where A_p is the piston wall cross-sectional area and is approximately equal to $\pi D_i t_{wp}$. The piston wall thickness t_{wp} should increase as diameter increases to maintain constant stress; therefore, A is proportional to D_i^2 , and L_p is proportional to D_i . So, finally,

$$Q_{cp} \propto D_i$$

Shuttle Loss - Heat transferred from the hot wall to the colder piston at the top of the piston stroke and then from the hotter piston to the cold wall at the bottom of the stroke can be described as

$$Q_{gs} = \frac{k\pi D_i S^2 \Delta T}{8CL}$$

As before, ΔT and k are assumed constant irrespective of engine size.

$$Q_{gs} \propto \frac{D_i S^2}{CL}$$

Since engine proportions are to be kept constant as engine size varies, S (stroke) and L (displacer length) are both proportional to D_i . Thus,

$$Q_{gs} \propto \frac{D_i^2}{C}$$

Pumping Loss - This loss is ascribed to the motion of working gas in and out of the radial clearance volume between the piston and the cylinder. It can be described using a relationship of the general form proposed by Rios (2) and Martini (3):

$$Q_{gp} = \frac{\pi}{4} \frac{\gamma - 1}{\gamma} \frac{S}{L} f(T, P) \frac{P_{\max} V_g}{r_p}$$

It is assumed in this analysis that all pressure and temperature relationships in this equation remain constant as engine size is varied; therefore,

$$Q_{gp} \propto \frac{S}{L} V_g, \quad S \propto L, \quad Q_{gp} \propto V_g$$

where

$$V_g \propto D_i L C$$

and where L_g is the length and C is the clearance. Since $L_g = D_i$,

$$Q_{gp} = D_i^2 C$$

Note that shuttle loss Q_{gs} is directly proportional to clearance, while pumping loss Q_{gp} is inversely proportional. Their sum is at a minimum when the two losses are about equal. The clearance at which this occurs is generally impractically small. At practical clearances, Q_{gp} will be substantially greater than Q_{gs} . This analysis assumes that clearance will be kept constant at the minimum practical value for all sizes of engines examined.

The regenerator housing is also subject to conduction losses in the same manner as the cylinder, and the same sort of equation applies. It is assumed that the regenerator is also scaled in direct proportion to the cylinder and, therefore, that the conduction loss Q_{cr} in the regenerator is proportional to engine size in the same manner as cylinder conduction loss.

$$Q_{cr} = D_i$$

Engine power R is proportional to displaced volume and engine speed if pressure, temperature, and the other design parameters that affect power are kept constant, irrespective of engine power level or design speed.

$$R = V_d N = \frac{\pi}{4} D_i^2 S N$$

Stroke is proportional to diameter. Therefore,

$$R = D_i^3 N$$

COOLED, INSULATED ENGINE CYLINDER MODEL - A schematic cross section of a cylinder for a cooled, insulated Stirling engine is shown in figure 2. The engine employs a cooled outer metal cylinder and regenerator housing lined with a low-conductivity, high-temperature glass ceramic, which will insulate the metal structure to prevent overtemperature and also minimize conductive heat loss. The analysis held the following assumptions:

The conductivity of the glass ceramic liner was $0.006 \text{ W/cm}^2\text{C}$, and the thickness for all engine configurations was 1 cm . The inner surface of the metal structural wall was kept at 100° C for all engine configurations by water cooling. Further, all conduction was radially outward over the whole cylinder surface, and no conduction occurred downward.

Cylinder Radial Conduction Loss - This loss can be expressed by

$$Q_{rc} = \frac{k A_s \Delta T}{t_w}$$

where k is the conductivity of the ceramic liner, A_s is the mean surface area of the ceramic liner, ΔT is the temperature drop across the ceramic liner, and t_w is the thickness of the ceramic liner. The surface area A_s is proportional to the square of the cylinder diameter D_i if the cylinder proportions are kept constant as engine size is varied. The conductivity k is assumed constant over the temperature range of interest. Typical commercial solid glass ceramics of similar composition vary less than 10 percent in conductivity from 450° to 600° C . The ceramic liner thickness t_w is kept constant for all engine sizes. Therefore, radial heat conduction can be shown as

$$Q_{rc} = D_i^2 \Delta T$$

The same relationships also apply to the regenerator housing, and

$$Q_{rr} = D_i^2 \Delta T$$

Conductive Loss - This loss is still proportional to D_i as for the conventional engine. However, ΔT may be higher. This analysis considered a range of possible ΔT 's. In any event, Q_{cp} is small enough that it can be dropped from the calculation of heat loss for both engines, since it adds only a constant relatively small loss.

Shuttle Loss - This loss is a function of engine dimensions for the ceramic-lined engine in the same manner as for the conventional engine. However, for the ceramic-lined engine, we must examine the effect of a range of possible inside wall temperatures and ΔT 's.

$$Q_{gs} = \frac{D_i^2 \Delta T}{C}$$

(Note: ΔT for both shuttle loss and pumping loss is taken as $T_{exp} - T_{hg}$).

Pumping Loss - This loss is also related to engine dimensions as for the conventional engine, but again ΔT will be examined as a variable.

$$Q_{gp} = D_i^2 C \Delta T$$

CONVENTIONAL ENGINE HEAT LOSSES - Calculations made for the United Stirling P-40 using the Lewis Stirling engine performance model at nominal design power and speed (40 kW at 4000 rpm) gave the following results for the various heat losses: $Q_{cc} = 503 \text{ W}$, $Q_{cr} = 1873 \text{ W}$, $Q_{cp} = 134 \text{ W}$, $Q_{gs} = 701 \text{ W}$, and $Q_{gp} = 5557 \text{ W}$. Differences in the piston conductive losses did not affect this analysis. For simplicity, it was not considered further. The total heat loss was then

$$Q_t = Q_{cc} + Q_{cr} + Q_{gs} + Q_{gp} = 8634 \text{ W}$$

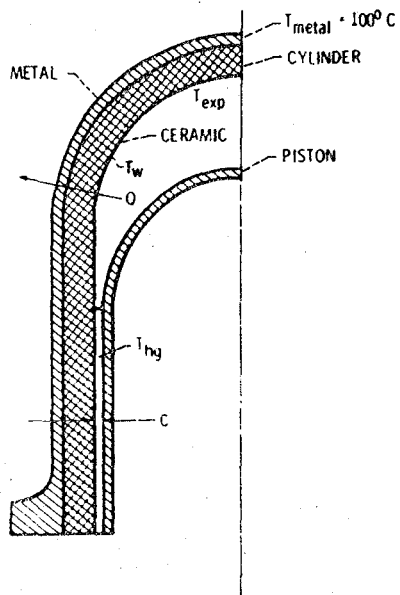


Figure 2. - Cooled, insulated engine cylinder.

The relative heat loss for different size engines was

$$Q_{tu} = \left(\frac{D_i}{D_{P-40}}\right) (Q_{cc} + Q_{cr}) + \left(\frac{D_i}{D_{P-40}}\right)^2 (Q_{gs} + Q_{gp})$$

where

$$\frac{D_i}{D_{P-40}} = \left(\frac{R}{40}\right)^{1/3} \left(\frac{4000}{N}\right)^{1/3}$$

and where R is the design power and N is the design speed.

The losses calculated for the P-40 engine with the Lewis performance program were extrapolated to design powers from 40 to 320 kW and design speeds from 1000 to 4000 rpm. Wall and hot-gap temperature were assumed constant for all configurations.

COOLED, INSULATED ENGINE HEAT LOSSES - It can be expected that using a glass ceramic liner in a cooled engine could result in a higher inner wall temperature in both the cylinder and regenerator housing. The temperature would also be more uniform from the top to the bottom of the cylinder. The higher wall temperature should result in higher radial conduction losses but lower clearance gap losses. Total heat loss appears to decrease as wall temperature T_w is increased above some nominal value.

Cylinder Radial Conduction Loss -

$$Q_{rc} = \frac{kA_s \Delta T}{t_w}$$

For a P-40 sized cylinder with a 1-cm-thick glass ceramic liner, $A_s = 158 \text{ cm}^2$. Conductivity for this liner is assumed as $k = 0.006 \text{ W/cm}^\circ\text{C}$. The outside liner temperature is taken as constant at 100° C . Therefore, for all four cylinders,

$$Q_{rc} = 4 \left[\frac{(0.006)(158)}{1} \right] (T_w - 100^\circ \text{ C})W$$

$$Q_{rc} = 3.79(T_w - 100^\circ \text{ C})W$$

In order to calculate Q_{rc} for different size engines, a correction for diameter is made which accounts for the change in surface area:

$$Q_{rc} = \left(\frac{D_i}{D_{P-40}}\right)^2 [3.79(T_w - 100^\circ \text{ C})]W$$

where

$$\frac{D_i}{D_{P-40}} = \left(\frac{R}{40}\right)^{1/3} \left(\frac{4000}{N}\right)^{1/3}$$

Regenerator Housing Radial Conduction -

$$Q_{rr} = \frac{kA_s \Delta T}{t_w}$$

For a P-40 sized set of two regenerators and a 1-cm-thick lining, $A_s = 223 \text{ cm}^2$. Conductivity is assumed as $k = 0.006 \text{ W/cm}^\circ\text{C}$, and liner outside temperature as 100° C . Therefore, for all four regenerator sets,

$$Q_{rr} = 4 \left[\frac{(0.006)(223)}{1} \right] (T_w - 100^\circ \text{ C})W$$

$$Q_{rr} = 5.35(T_w - 100^\circ \text{ C})W$$

To calculate Q_{rr} for different sized engines, correction is made for different surface areas, such that

$$Q_{rr} = \left(\frac{D_i}{D_{P-40}}\right)^2 [5.35(T_w - 100^\circ \text{ C})]W$$

where T_w for the regenerator is assumed to be the same as for the cylinder.

Shuttle Loss -

$$Q_{gs} = \frac{D_i^2 \Delta T}{C}$$

As noted previously, the Lewis performance program calculated Q_{gs} for the P-40 engine at nominal design conditions (40 kW, 4000 rpm) to be 701 W. This is for an effective wall temperature of 490° C . I have assumed that T_w is the same as the hot-gap temperature and that it applies to the shuttle loss as well as to the conduction loss. The mean expansion temperature T_{exp} is taken as 584° C for all cases. I have assumed that Q_{gs} will vary with T_w approximately as shown:

$$\begin{aligned} Q_{gs} &= \frac{701 \text{ W}}{584 - 490} (584^\circ \text{ C} - T_w) \\ &= 7.46(584^\circ \text{ C} - T_w)W \end{aligned}$$

The equation for Q_{gs} for different engine sizes is

$$Q_{gs} = \left(\frac{D_i}{D_{P-40}}\right)^2 [7.46(584^\circ \text{ C} - T_w)]W$$

(Note: Clearance C is held constant for all engine sizes at the minimum practical value.)

Pumping Loss -

$$Q_{gp} = D_i^2 C \Delta T$$

Using the Lewis performance program, an estimate of the effect of varying ΔT ($T_{exp} - T_{hg}$) was made (fig. 3). The effect of ΔT on Q_{gp} is very nearly linear and can be closely approximated by

$$Q_{gp} = 57.2 [(584^\circ \text{ C} - T_w) + 225]W$$

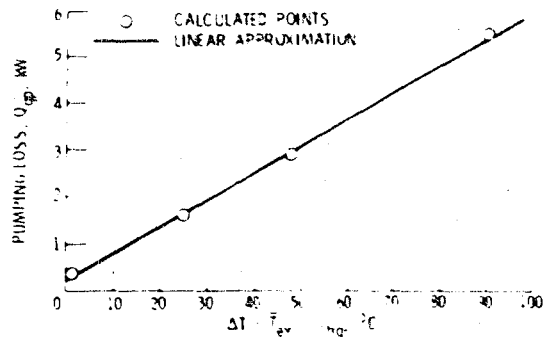


Figure 3. Hot-gas pumping loss as function of hot-gas temperature differential

where T_w is taken to be equivalent to T_{hg} . For different engine sizes,

$$Q_{kp} = \left(\frac{D_i}{D_{p-40}} \right)^2 [57.2(584 - T_w) + 225] W$$

Clearance is again assumed constant.

Total Heat Loss - The specific equation used to calculate total heat loss for various engine sizes is

$$\begin{aligned} Q_{TL} &= \left(\frac{D_i}{D_{p-40}} \right)^2 (Q_{rc} + Q_{rr} + Q_{qs} + Q_{kp}) \\ &= \left(\frac{D_i}{D_{p-40}} \right)^2 [3.79(T_w - 100^\circ C) \\ &\quad + 3.35(T_w - 100^\circ C) + 7.46(584^\circ C - T_w) \\ &\quad + 57.2(584^\circ C - T_w) + 225] W \\ &= \left(\frac{D_i}{D_{p-40}} \right)^2 [9.14(T_w - 100^\circ C) \\ &\quad + 64.7(584^\circ C - T_w) + 225] W \end{aligned}$$

Total heat-loss estimates for cooled, insulated engines of 40, 80, 160, and 320 kW nominal power and 4000, 2000, and 1000 rpm design speeds were made. Figures 4 to 10 show the relationship between heat loss and wall temperature for the range of power and design speed examined.

DISCUSSION OF RESULTS

Figure 4 shows specific total heat loss as a function of average wall temperature for several engine design power levels. As might be expected, specific heat loss decreased with increasing wall temperature. This is due to the preponderant effect of clearance losses, in particular, the pumping loss. Specific heat loss was also reduced as power was increased. Losses were related to effective surface area and increased by the square of the cylinder diameter, while power was a function of displacement and, hence, cylinder diameter cubed. Also plotted are the points representing total heat losses for conventional engines. Effective average wall temperature was assumed to be $490^\circ C$ for all power levels. If a line is projected horizontally to the corresponding cooled-engine heat-loss line, the wall temperature at which cooled engine losses are equal to conventional engine losses is defined. I call this the "break even" temperature. Above this temperature cooled engine performance should exceed conventional engine performance. Below, cooled engine performance will be lower. Figures 5 and 6 show the

same information for 2000 and 1000 rpm, respectively. The trends are essentially the same at all speeds, but the trend lines are steeper with lower design speeds. Interestingly, the break-even temperature tends to be higher with both higher powers and lower speeds. This can be seen clearly in figure 7 where break-even temperature is plotted as a function of design power for 1000, 2000, and 4000 rpm design speeds. For each speed, the break-even temperature increases with nominal power and appears to level off at powers above about 300 kW. The level of break-even temperature goes up as design speed is reduced.

The potential efficiency benefit of the cooled, insulated engine concept can be seen more directly in figure 8. Here is plotted the specific heat loss difference between uncooled and cooled engines as a function of average wall temperature for a range of engine power and a design speed of 4000 rpm. Specific heat loss difference is defined as total heat loss for the conventional engine minus total heat loss for the cooled, insulated engine divided by design power. This quantity is also numerically equal to the relative increase (or decrease) in thermal efficiency. For example, a specific heat loss difference of 0.1 denotes a one-tenth, or 10 percent, increase in thermal efficiency (such as going from 30 to 33 percent). The break even temperature can be seen clearly in this figure as the point at which each loss line crosses the zero line. The maximum gain is for a 40-kW engine with an effective average wall temperature approaching the average expansion temperature. This gain is progressively less as engine power is increased. A 320-kW engine gains only about 3 percent at the same temperature. This effect is due to engine power increasing more rapidly with engine size than cylinder and regenerator surface area. Since the losses are related to cylinder and regenerator surface area, they become a less significant fraction of output power as size increases. Therefore, any technique which tends to reduce surface-area related losses has less effect on performance as engine power is increased.

Figures 9 and 10 show the same relationships for engine design speeds of 2000 rpm and 1000 rpm, respectively. The same trends are observed. However, the slopes increase with increasing design speed. The maximum possible gains are approximately 14 percent at 40 kW and 2000 rpm and 20 percent at 40 kW and 1000 rpm. This, again, reflects the effect of surface area which increases with increasing design speed.

CONCLUDING REMARKS

The concept of using insulated, cooled cylinders and regenerator housings for a Stirling engine offers the possibility of largely eliminating the need for expensive, strategic high-temperature alloys. This is obviously desirable. The question of whether and under what circumstances this approach to Stirling engine

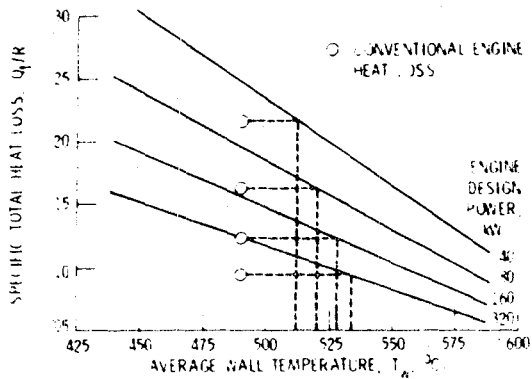


Figure 4 Cooled insulated engine specific heat loss. Design speed, 4000 rpm

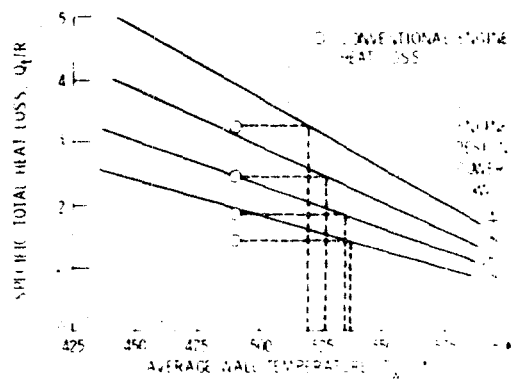


Figure 5 Cooled insulated engine specific heat loss. Design speed, 2000 rpm

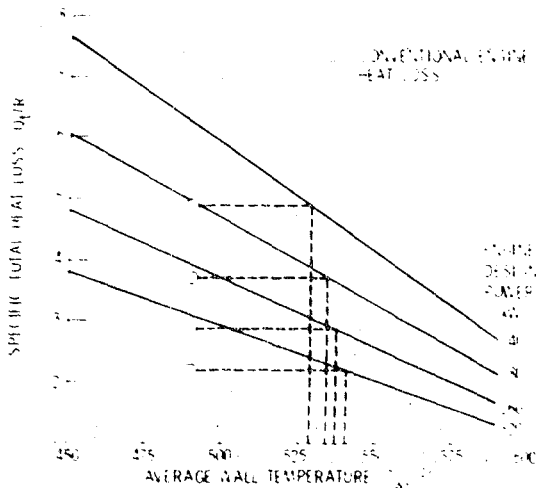


Figure 6 Cooled insulated engine specific heat loss. Design speed, 1000 rpm

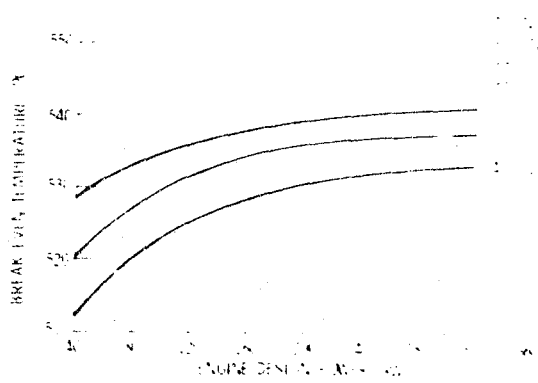


Figure 7 Break-even temperature vs. engine design power. Insulated mean wall temperature, $T_w = 525^\circ\text{C}$

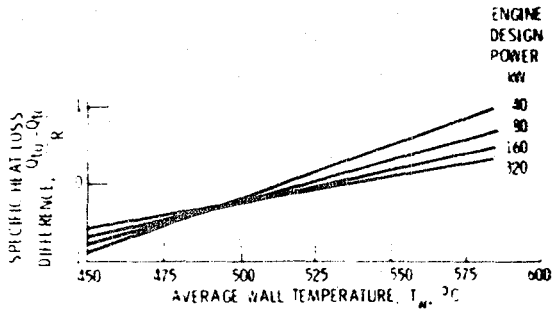


Figure 3. Specific heat loss difference between cooled and conventional engines. Design speed, 4000 rpm.

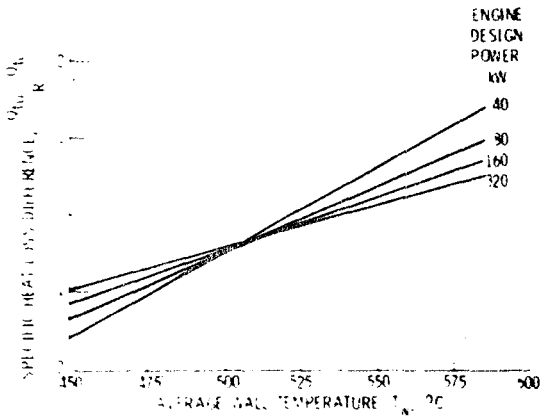


Figure 4. Specific heat loss difference between cooled and conventional engines. Design speed, 2000 rpm.

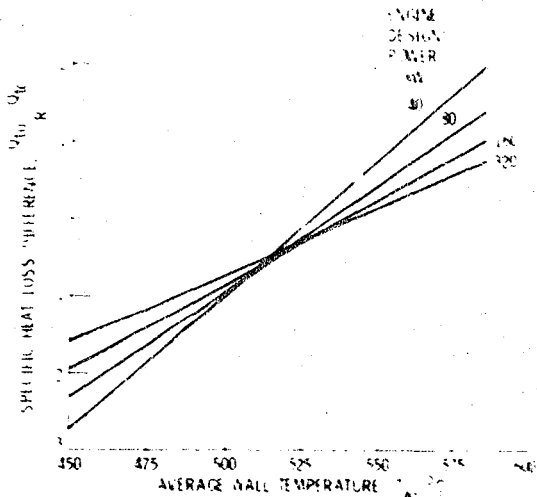


Figure 10. Specific heat loss difference between cooled and conventional engines. Design speed, 1000 rpm.

design could result in increased performance was examined in this simple analysis. This analysis does not attempt to address the practical problems which may be involved in the cooled, insulated engine concept. For example, the design of a small engine (of the order of 40 kW) may be severely compromised by inclusion of liners thick enough to do any good. And, no consideration whatsoever is given to the problems involved in installing and maintaining a glass ceramic liner in a practical engine of any size.

The results of this analysis indicate that performance gains can be made if appendix gap losses can be reduced. It appears that this can be done if higher cylinder inner wall temperatures can be achieved. Oddly enough, for the assumptions made in this analysis regarding the relative values of conduction and appendix gap losses (which are based on P-40 engine calculations made with the Lewis Stirling performance code) overall heat losses actually decrease as radial conduction losses increase with higher inner wall surface temperatures. The appendix gap losses dominate and are reduced substantially as wall temperature approaches the expansion temperature.

An engine with an active cooling system and appropriate insulation should provide the opportunity for control of the cylinder inner-wall temperature. Specifically how this would be done and what temperatures (and loss reductions) could be achieved should be the subject for a much more detailed and sophisticated analysis. This analysis should be carried out to define explicitly what the potential of this concept is. Furthermore, it would be desirable to examine the design and fabrication problems involved in achieving the design concept in practical engines.

NOMENCLATURE

A_p	piston wall cross section area
A_c	surface area for conduction
C	clearance between cylinder and piston
D_i	engine cylinder inner diameter
D_o	engine cylinder outer diameter
k	thermal conductivity
L	reference length of uncooled cylinder
L_p	piston length
N	engine speed, rpm

Q	heat flux
Q_{cc}	cylinder conductive loss, conventional engine
Q_{cp}	piston conductive loss, conventional engine
Q_{cr}	regenerator conductive loss, conventional engine
Q_{gp}	hot gap pumping loss
Q_{gs}	hot gap shuttle loss
Q_{rc}	cylinder conductive loss, cooled insulated engine
Q_{rr}	regenerator conductive loss, cooled insulated engine
Q_t	total engine heat loss
Q_{tc}	total heat loss for cooled engine
Q_{tu}	total heat loss for conventional engine
P	cycle pressure
P_{max}	engine cycle maximum pressure
R	engine design power
r_p	engine pressure ratio
S	engine stroke
T_1	uncooled cylinder reference temperature, top
T_2	uncooled cylinder reference temperature, middle
T_3	uncooled cylinder reference temperature, bottom
T_{exp}	average expansion temperature
T_{hg}	hot gap temperature
T_w	cylinder inner wall temperature
t_w	wall thickness
V_d	displaced volume
V_g	annular volume of hot gap between piston and cylinder
γ	ratio of specific heats

REFERENCES

1. R. J. Meijer and B. Ziph, "Evaluation of The Potential of The Stirling Engine for Heavy Duty Application," Stirling Thermal Motors, Inc., Ann Arbor, MI, Oct. 1981. (NASA CR-165473 1981.)
2. P. A. Rios y Cartaya, "An Analytical and Experimental Investigation of the Stirling Cycle," Ph.D. Thesis, Massachusetts Institute of Technology, 1969.
3. W. R. Martini, "Stirling engine Design Manual, Second Edition," (NASA Grant NSG 3194, University of Washington) in process of publication.

NOTICE

This report was prepared to document work sponsored by the United States Government. Neither the United States nor its agent, the United States Department of Energy, nor any Federal employees nor any other contractors, subcontractors or their employees, makes any warranty, express or implied, or assumes any legal liability or responsibility for the accuracy, completeness or usefulness of any information, apparatus, product or process disclosed or represents that its use would not infringe privately owned rights.

**GAS TURBINE
TECHNOLOGY SESSION**

Advanced Gas Turbine Technology Development (Systems and Components)

R. A. Rackley and D. M. Kreiner
Garrett Turbine Engine Co.

ABSTRACT

The Garrett/Ford AGT101 Program has progressed through initial design, fabrication, first generation aerodynamic component tests, and currently is focused on engine test bed development and ceramic component development. Many significant development activities have been accomplished, including successful full-speed operation of the AGT101 Mod I (1600°F) engine to 100,000 rpm.

A complete set of ceramic static structures, consisting of 49 parts, was assembled and successfully tested in the structures rig to the Mod I (1600°F) design conditions. Many ceramic structures have passed thermal screening tests to 2100°F. A silicon nitride rotor, produced cooperatively by ACC and Ford, has been spin tested at room temperature to 102,000 rpm, which exceeds the maximum power design condition.

Aerothermodynamic component testing of the first iteration AGT101 (2500°F) turbine design has been completed. Results of these tests show that final program goals have been exceeded in the low-power regime and initial goals have been exceeded at maximum power. The second compressor test has been completed with results showing that design flow and pressure ratio goals have been achieved. Combustion fuel nozzle development indicates that program emission goals are achievable within the program time frame.

All efforts indicate that AGT101 program goals are achievable. Over 3700 component rig test hours and over 90 hours and 185 starts of the engine have been accumulated in the development test program. Testing continues with emphasis on performance, incorporation of ceramic components, and higher temperature capability.

INTRODUCTION

An automotive Advanced Gas Turbine (AGT) technology program is being conducted by Garrett Turbine Engine Company and Ford Motor Company

under DOE/NASA Contract DEN3-167. This effort is a significant part of the Gas Turbine Highway Vehicle System Program established by the Department of Energy, with NASA-Lewis Research Center providing project management and administration. The Garrett/Ford AGT (designated AGT101) is a 100-horsepower, regenerated, single-shaft gas turbine engine. Ceramics are used extensively in the engine hot flow path. The status and technical progress through September 1982, which completes the third year of the project, is presented in this document.

The project was initiated October 1, 1979; the original program schedule is shown in Figure 1. The

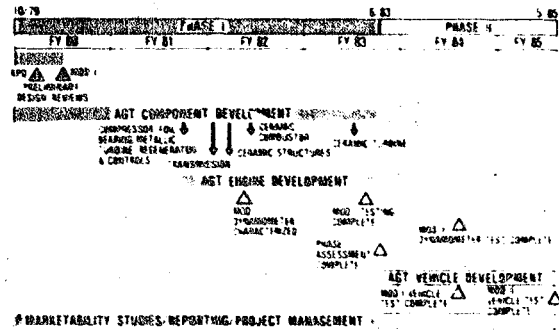


Figure 1. AGT101 Original Program Schedule.

Reference Powertrain Design (RPD) preliminary design review was successfully completed on January 30, 1980 and a second design review involving the Mod I powertrain and initial development engines was completed on April 30, 1980. These two reviews were held on schedule and successfully completed Contract Milestone 1. There have been no significant changes to the initial design since inception.

The Garrett/Ford project work plan was modified in FY1981 to accommodate budget constraints. Testing of several first-generation metallic compo-

nents was reduced, powertrain development (gearbox and transmission) was deferred, and vehicle activity terminated. These changes permitted concentration of resources toward continued development of higher technology components and ceramics necessary for the AGT101 engine. Significant progress was made in FY1981 as aerothermodynamic testing of the Mod I (1600°F) components was completed and the first engine was assembled and tested on July 31, 1981.

As FY1982 approached, the fiscal restraints caused restructuring of the AGT101 program as shown in Figure 2. Advancement of ceramic technology, improved component aerodynamic performance, and power section development as a "test bed

	FISCAL YEAR							
	82	83	84	85	86	87	88	89
CERAMIC DEVELOPMENT	ASSESSMENT OF PRODUCEABILITY							
STRUCTURES	2, 2100 F STRUCTURES							
COMBUSTOR	2, 2500 F TURBINE							
TURBINE								
REGENERATOR DEVELOPMENT								
COMPONENT UPGRADE								
POWER SECTION DEVELOPMENT	1ST CERAMIC PARTS ALL CERAMIC ENGINE 100 SHP 0.30 SFC EMISSIONS							
POWERTRAIN DEVELOPMENT	428 HP DEMO 50 HP DEMO							
PRODUCTION ENGINEERING AND MANUFACTURING DEVELOPMENT								

Figure 2. Restructured AGT101 Program.

for ceramics" were considered key objectives of this program. The power section performance objectives of 0.3 specific fuel consumption (sfc), 100 shp and low emissions were not changed from the original program. When these objectives are demonstrated, private industry will fund powertrain development.

AGT101 DESIGN FEATURES - The AGT101 engine, as shown in Figure 3, is flat rated at 100 horsepower, with a minimum sfc of less than 0.3. The single-shaft rotating group is composed of a turbine, compressor, and output gear supported by an air-lubricated, foil-journal bearing and an oil-lubricated ball bearing. Ambient air enters the engine through variable inlet guide vanes and passes through a single-stage compressor. The compressed air, at approximately 365°F, is routed around the full engine perimeter to the high pressure side of the ceramic rotary regenerator. This feature provides increased thermal efficiency by minimizing heat loss. The partially heated air passes through the regenerator core, where it is further heated to about 1940°F maximum temperature at idle, and then to the combustor.

The original combustor design utilized variable geometry to limit primary zone maximum temperatures to 3000°F to suppress NO_x formation, provide a prevaporizing/premixing zone to limit particulates and unburned hydrocarbons, and provide a high level of mixing along with minimal wall quenching to assure low CO formation.

Recent NASA and Garrett work indicates that a less complex design utilizing a lean-burn, low-emis-

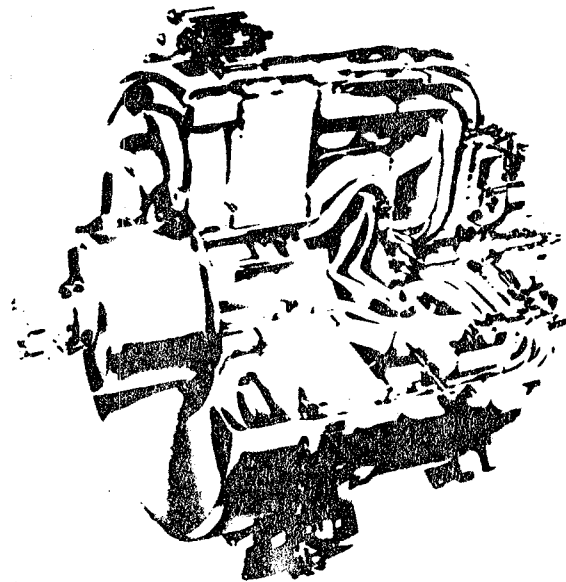


Figure 3. AGT101 Power Section.

sion, fixed-geometry combustion system has high potential of meeting the emission requirements. Hot gas exits the combustor at a maximum temperature of 2500°F to the turbine stator and then expands through the radial turbine rotor. The turbine exhausts the hot gas, at a maximum temperature of 2030°F at idle, to the low pressure side of the rotating regenerator and out the engine exhaust at a maximum temperature of 510°F at maximum power.

All ceramic hot section structural components are symmetrical except for one housing that separates high and low pressure regenerator flow. The symmetrical design provides a more uniform stress distribution and ease of manufacturing.

Key engine components have been undergoing performance testing in rigs during FY1982. These activities are summarized in the following paragraphs.

COMPRESSOR - Two additional compressor rig tests have been completed; Tests 2 and 2A. In Test 2, the modified impeller (increased tip and shroud recontour) was tested with a vaneless diffuser to establish impeller characteristics. Results indicated that, as desired, flow and work increased over Test 1.

In Test 2A, a three-stage diffuser, designed to match the modified impeller, was installed and full stage testing was completed at speeds from 40 to 100 percent of design corrected speed and IGV settings of 0, +20, +40, and +70 degrees. Axial clearance throughout the test was controlled to within 0.003 to 0.004 inch. Test results, comparing the original design (Test 1) with Test 2A, are shown in Figures 4, 5, and 6. This data indicates the following:

- o Design pressure ratio and flow were attained
- o Low speed efficiency was significantly increased from Test 1
- o A desirable efficiency envelope has been

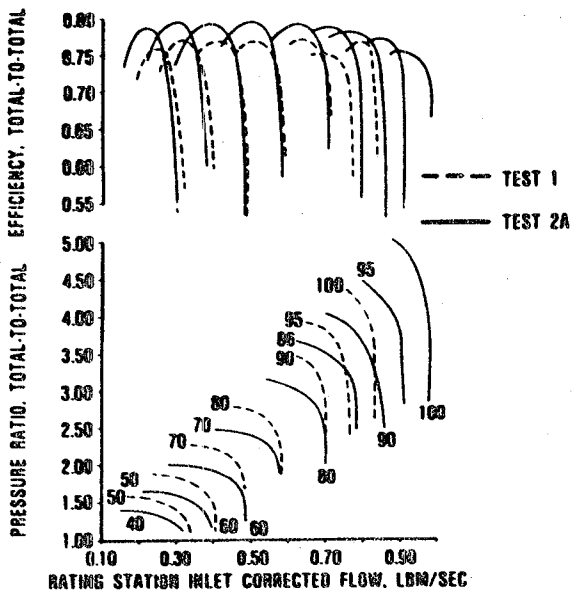


Figure 4. Full Stage Compressor Data, IGVs Open.

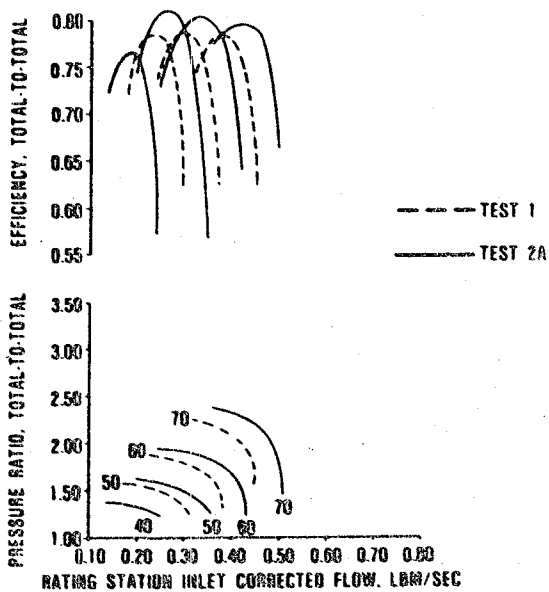


Figure 5. Full Stage Compressor Data, IGV = 40 Degrees.

achieved, which has the peak efficiencies increasing at the lower end of the speed range where most driving time occurs--this will result in improvements in overall fuel economy.

Diffuser performance was again very close to predicted levels. Additional improvements in range and efficiency can be achieved with a minor impeller-diffuser rematch.

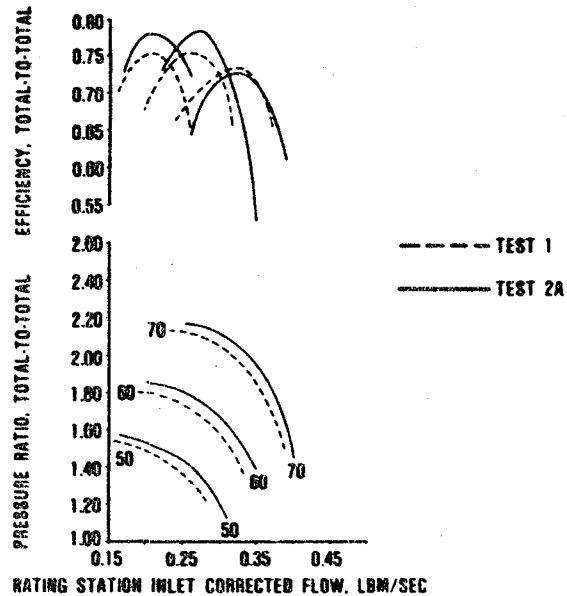


Figure 6. Full Stage Compressor Data, IGV = 70 Degrees.

The Test 2A map has been input into the Mod II cycle analysis and currently is being evaluated.

TURBINE - Cold air testing of the AGT101 ceramic design turbine stage has been completed. Metallic components were substituted for ceramic counterparts. Testing was conducted over a range of corrected engine operating conditions from idle to maximum power. The stage is rated (for cycle analyses purposes) from the combustor exit-to-generator LP inlet.

Testing was conducted using the same basic test rig as used during AGT101 Mod I turbine testing. Performance measurement techniques were identical to Mod I testing, which included a high-speed, direct-reading torquemeter and high-response thermocouples. Tare loss evaluations and dead weight calibrations were repeated prior to test initiation.

Test results, as shown in Figure 7, indicate the following:

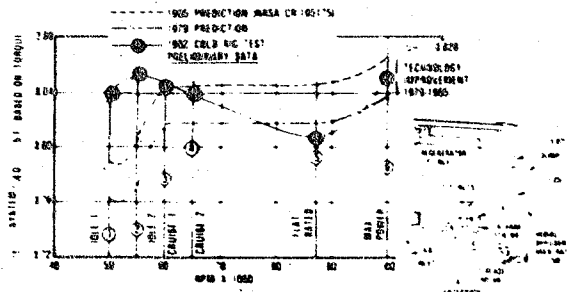


Figure 7. AGT101 Turbine Cold Rig Test (1982).

- o Initial design goals were exceeded at idle, cruise, and maximum power conditions
- o Program goals were exceeded at idle and cruise power points
- o Exhaust diffuser performance remained extremely good over the operating range

An 84 percent idle efficiency was achieved compared with the 79 percent program goal. Cruise performance was 84.5 percent versus 84.3 percent predicted. At maximum power, an initial design efficiency goal of 83.7 percent was projected; test results show that 85.2 percent was achieved. Table 1 presents a summary of the AGT101 turbine development testing conducted to date.

Table 1. AGT101 Turbine Development Test Summary

	Initial Goal	Initial Test	Program Goals
Idle 1600°F	0.718	0.763	--
Idle 2500°F	0.762	0.840	0.790
Cruise 1600°F	0.782	0.796	--
Cruise 2500°F	0.815	0.845	0.843
Maximum Power 1600°F	0.871	0.865	--
Maximum Power 2500°F	0.837	0.852	0.865

In an effort to assess tested turbine performance on powertrain operation, the tested turbine map is currently being input to the cycle analyses program.

Fabrication of the dual alloy turbine rotor for operation at a turbine inlet temperature (TIT) of 2100°F has continued. The rotor is comprised of a cast MAR-M 247 blade ring with directionally solidified blade tips and low-carbon, powder metal, astroloy hub hot isostatic pressure (HIP) bonded together. Figure 8 shows a rotor cut in half to examine the bond zone. An excellent bond was achieved. Additional rotors currently are being machined for engine use.

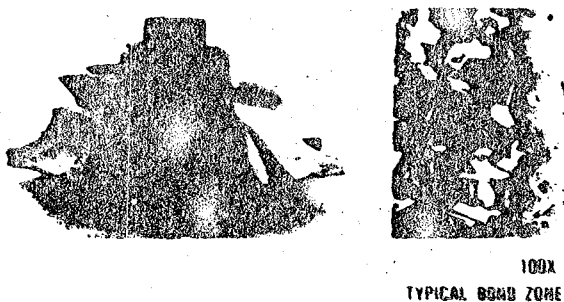


Figure 8. Successful Dual Alloy Turbine Fabrication Achieved for AGT101 Program.

COMBUSTOR - Development of the AGT101 ceramic combustor has concentrated on analytical modeling of a lean-burn, low-emission, fixed-

geometry combustion system and evaluation of candidate fuel nozzles.

Based on work conducted through NASA and Garrett in-house efforts, the AGT ceramic combustor design is evolving to a lean-burn, low-emission, fixed-geometry system. Numerous geometries have been analytically modeled using NASA information, Garrett in-house efforts, and cold flow nozzle tests of the Delevan Simplex and Duplex nozzles. Figure 9

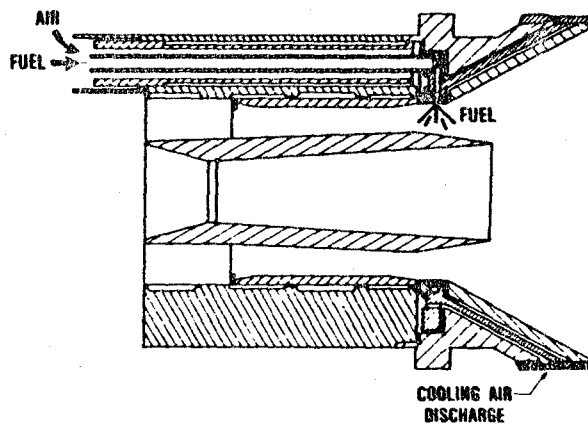


Figure 9. Modified Simplex Nozzle.

depicts the nozzle configuration selected for continued evaluation. Analysis and cold flow testing indicates that a fixed-geometry combustor, using a radial swirler, provides uniform flow fields and temperature profiles. Hardware has been ordered both for initial metal testing and ceramic testing.

Emissions testing of a Delevan Corporation Simplex fuel nozzle has been conducted at 1600°F combustor inlet temperature. Corrected combustor inlet flows were adjusted to yield the same pressure drop and fuel-air ratio as defined for engine operation. To assess the Simplex nozzle system potential at actual engine conditions, this data was corrected to compensate for different inlet temperatures and residence times. The correction factors applied to this data were based on information published in NASA TM 81640, "Ultra Lean Combustion at High Inlet Temperature". Idle emissions were not corrected for higher inlet temperature and residence time since NASA data, similar to this condition, was not presented. Results of these tests are summarized in Figure 10 for steady-state points. The emission indices shown are based on a 36 mpg urban estimate using DF-2, which is consistent with a predicted Combined Federal Driving Cycle of 42.8 mpg (DF-2) for the AGT101 installed in a 3000-lb inertia weight vehicle. These results show that the lean-burn fixed-geometry combustor has excellent potential of meeting program goals.

REGENERATOR SYSTEM - Regenerator system development efforts have concentrated on reduction of seal leakage, evaluation of high-temperature coatings, and engine test support. Ford has continued work on second and third generation

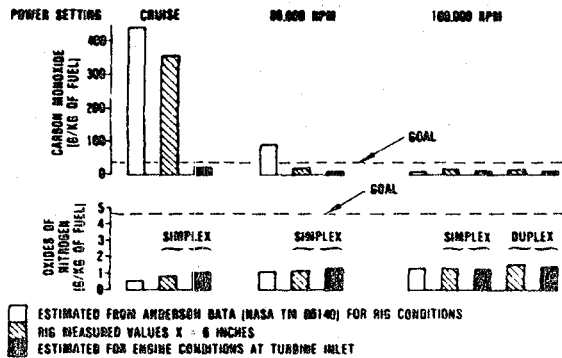


Figure 10. Element Rig Emission Results and Estimated Mod II Engine Emission Levels.

seals. Second generation (Phase 2) seals involved the addition of a third diaphragm to assist in preloading the upper diaphragm against the engine housing. Static seal leakage tests showed a minimal reduction in leakage for this configuration. Further investigations indicated a need to load the lower diaphragm and retainer against the metal substrate. This configuration, identified as Phase 3, shows a marked improvement in static seal leakage. Recent tests conducted at Ford show a leakage of 4.4 percent compared with a program goal of 3.6 percent.

Development of high-temperature coatings for 2000°F operation has progressed. Ford has evaluated 14 samples and has accumulated over 2000 hours of test time. Of the samples evaluated, the GE super-alloy substrate and Ford I-112 coating appear to satisfy the 2000°F objective. A summary of this regenerator development is provided in Table 2.

Table 2. Regenerator Hardware on Test

	State-of-the-Art	Test Result	Program Goals
Effectiveness, percent	90.1	93.6*	93.9
Temperature, °F	1832	2000	2000
Leakage, percent	7.2	4.4	3.6

*Projected from previous test.

ROTOR DYNAMICS - The rotor dynamics program task has developed a satisfactory rotating assembly for engine operation. This task was accomplished using a rotor dynamics rig that completely replicates all dynamic features of the rotating group. Using the Garrett rotor dynamics test facility, the replicated engine hardware, Figure 11, has been operated to full speed (100,000 rpm) 21 times, with 121 hours accumulated rig operating time.

The Teflon-coated foils presently being used have adequate temperature margin for the Mod I (1600°F) engine environment. Later engines will require higher temperature foil materials and coatings. Consequently, investigation of the high-temperature foil bearing (titanium carbide coated)



Figure 11. Rotor Dynamics.

has been initiated. This bearing has been successfully operated to full speed (100,000 rpm).

CERAMIC COMPONENT DEVELOPMENT - Ceramic components, as shown in Figure 12 have been received from the leading United States ceramic centers (Ford, ACC, Carborundum, and Corning Glass Works) and NGK in Japan. The good progress in material and processes development have made it possible to accomplish the component development activities described below. Material compositions include silicon nitride, silicon carbide and lithium aluminum silicate.

Ford and ACC have made good progress in development of ceramic turbine rotors. After successful spin testing without failure of non-bladed rotors to 115,000 rpm (ACC) and 134,000 rpm (Ford), efforts during the past year have concentrated on developing bladed rotors. Early bladed rotors with visible blade defects were spin tested at Ford. Although the defective blades fractured as low as 79,000 rpm, the rotor hub remained intact at 115,000 rpm. A recent rotor fabricated jointly by ACC and Ford was spin tested to 102,000 rpm exceeding the engine full-power design condition. Steady progress is expected to continue at ACC and Ford in development of reliable rotors for the AGT101 engine.

Ceramic structures have been undergoing mechanical screening tests, thermal screening tests, and structures rig tests in preparation for engine development testing. The first set (49 pieces) of ceramic components were assembled and successfully tested to 1600°F in the structures rig shown in Figure 13.

Entering into the next phase of development, several ceramics structures have been successfully tested in the thermal screening rigs to 2100°F. This effort is in preparation for structures rig and engine testing to 2100°F (Mod I Complete design goal).

COMPONENT TEST EXPERIENCE - Outstanding progress has been demonstrated on the aero-

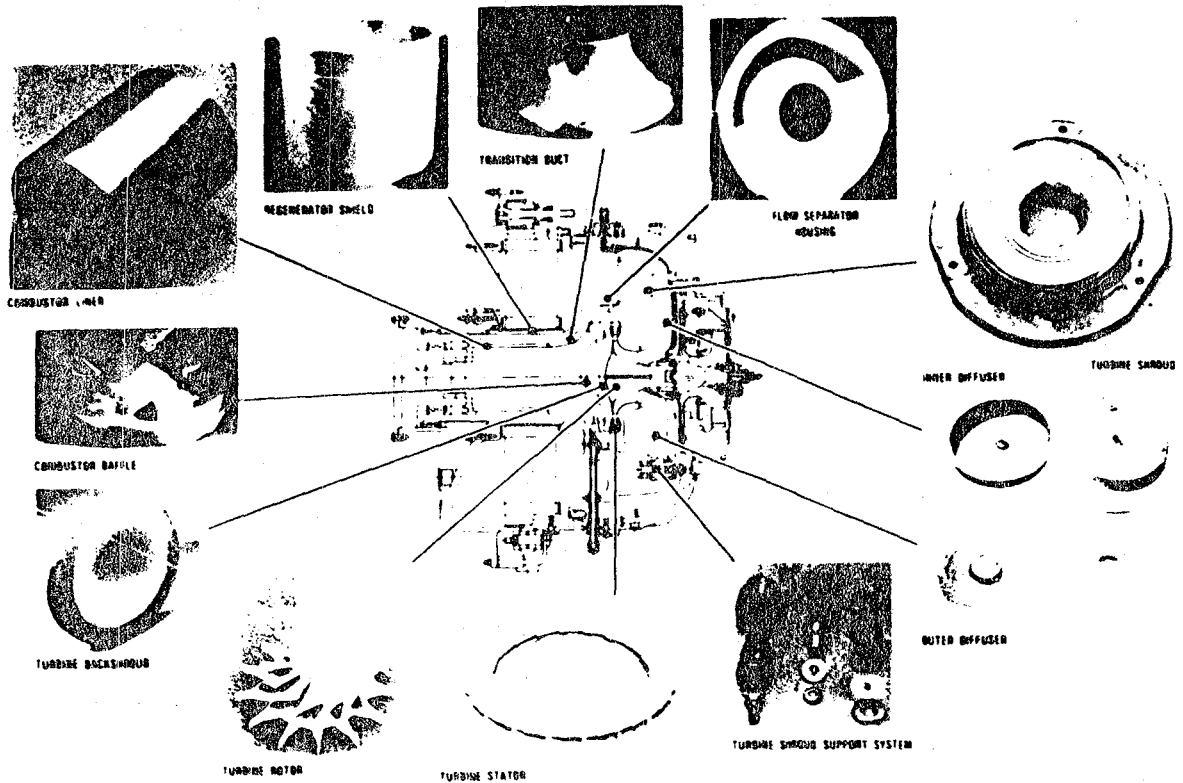


Figure 12. AGT101 Ceramic Parts.

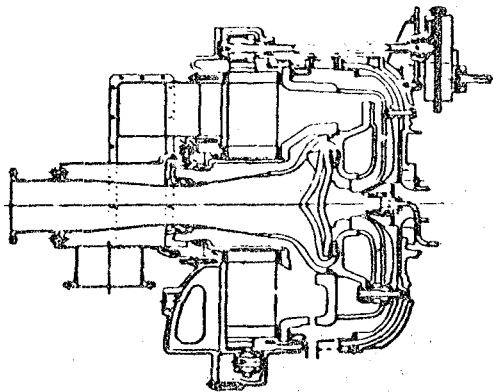


Figure 13. AGT101 Ceramic Structures Test Rig.

dynamic, thermodynamic and endurance test rigs. As shown in Table 3, over 3700 hours have been accumulated in AGT101 component development. As expected, the bulk of the test hours have been accumulated on the endurance regenerator seal wear rigs. Aerodynamic performance rig time has been limited to that necessary for data acquisition. Final performance and endurance capability must be demonstrated in the power section tests.

POWER SECTION DEVELOPMENT - Assembly of the parts as shown in Figure 14 for the first build

Table 3. AGT101 Component Test Experience

Rig	Accumulated Hours Through 9/30/82
Compressor	
IGV Flow Rig	42
Compressor Rig	67
Turbine Cold Flow Test Rig	122
Combustor	
Auto Ignition Rig	68
Element Rig	39
Main Combustor Rig	
Regenerator	
Cold Flow Regenerator Rig	102
Hot Flow Regenerator Rig	38
Ford Seal Wear Rig	2020
Ford Static Seal Rig	955
Rotor Dynamics	
Rotor Dynamics Rig	121
Hot Foil Bearing Rig	11
Foil Bearing Test Rig	167
Ceramics	
Thermal Screening Structures Rig	5
	9
TOTAL	3766

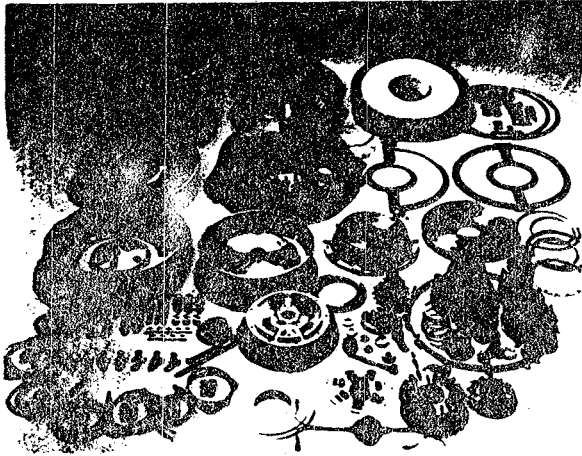


Figure 14. AGT101 Parts Display.

of AGT101 engine S/N 001 began in June 1981. The engine was motored to 30,000 rpm on July 30, 1981. Weeks of cold and hot motoring followed, to verify mechanical integrity and establish leakage from the high pressure (HP) to the low pressure (LP) portion of the engine.

With external ducts as shown in Figure 15, a leakage evaluation was conducted using a helium

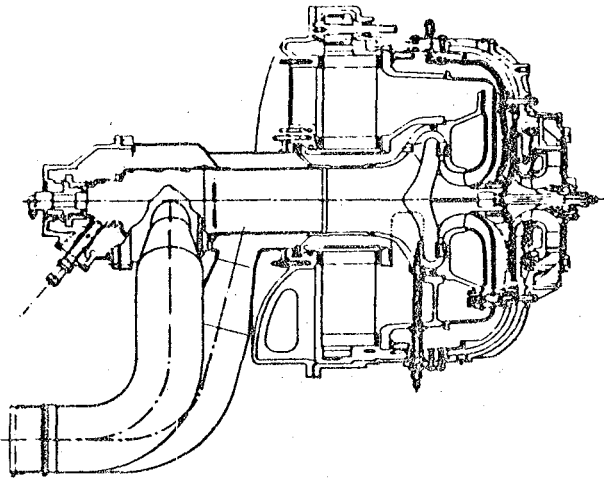


Figure 15. AGT101 Mod I Configuration With External Duct.

flow-seeding technique, shown schematically in Figure 16. When using this helium flow-seeding technique, the compressor and/or HP regenerator inlet flow is seeded with helium at selected injection ports. This seeded flow is ducted from the test cell after passing through the HP side of the regenerator core. Conditioned combustor inlet flow then is introduced to the burner. A proper compressor and turbine flow match is maintained and fuel is intro-

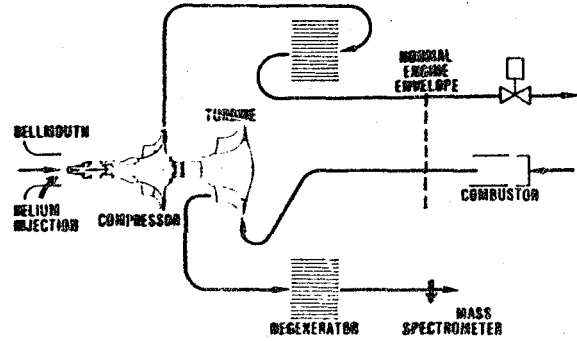


Figure 16. AGT101 Mod I Build 1 Test 1A, Regenerator Leakage.

duced, as required, to control turbine inlet temperature. Regenerator seal leakage from the HP side (seeded) to the LP side (unseeded) is determined by means of mass spectrometer measurements of helium concentrations in the exhaust.

During these tests, TIT was increased to a maximum of 1250°F at an engine speed of 50,000 rpm while leakage was monitored. Helium leak testing revealed that internal leakage was excessive; about 35 percent of compressor flow. Therefore, further testing was deferred until leakage could be decreased. Fuller's Earth then was introduced into the compressor inlet to provide visible indication of leakage areas. The engine was removed from the test cell for disassembly, inspection and analysis.

The engine was disassembled and progressively photographed. No evidence of damage was present. Internal leakage, as indicated by Fuller's Earth traces, was evident at the flipper seal, regenerator seals, turbine shroud piston seals, exhaust housing piston seal and numerous instrumentation penetrations. A comprehensive analysis and static leakage test of each suspected component was initiated. Twenty different potential leakage paths were identified and relative leakage values established for the points shown in Figure 17.

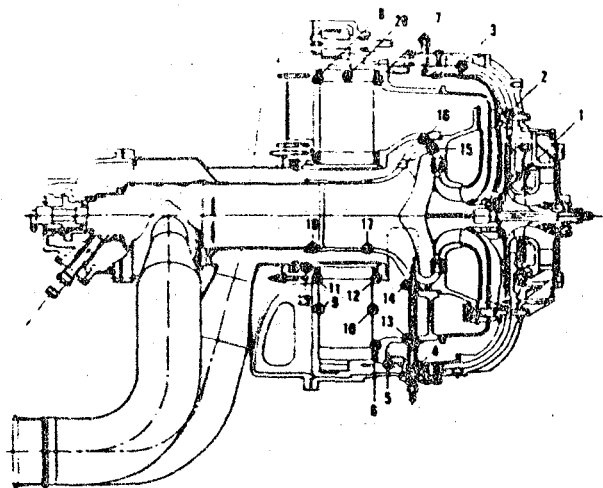


Figure 17. AGT101 Leak Path Designations.

Improving seals around instrumentation, adding springs to seat critical piston rings, and substituting an AS (alumina-silicate) regenerator core manufactured by Corning for the more porous MAS (magnesium alumina silicate) core allowed the static leakage to be reduced to approximately 15 percent of compressor flow on Build 4 of S/N 001 engine. This leakage would further reduce under the hot operating conditions and was considered adequate for initial engine operation.

The engine was installed in the test cell and a smooth start and acceleration to 50,000 rpm was made. The TIT was adjusted to 1000°F and helium leak testing initiated. Compressor flow and back pressure were adjusted to approximate corresponding turbine conditions, including the measured internal leakage. The TIT was increased to 1250°F while decreasing turbine pressure to maintain a steady-state speed of 50,000 rpm. A match of compressor flow and pressure ratio was obtained with the turbine by adjusting the compressor flowpath back-pressure valve. This match represented the engine self-sustaining conditions both for the turbine and compressor even though the flowpaths were separated. The engine was shutdown and external ducting separating the compressor and turbine flows was removed and replaced with a duct connecting the flowpaths as shown schematically in Figure 18.

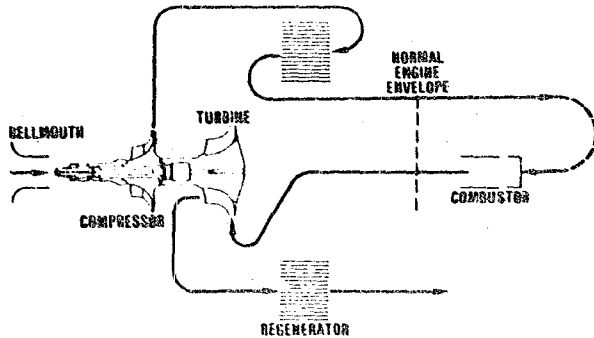


Figure 18. AGT101 Mod I Build 1 Test 1B, Self Sustain.

On December 15, 1981 the engine, shown in Figure 19, was started and accelerated to 50,000 rpm. Idle fuel consumption was approximately 3 lb/hr using JP-4 fuel. This test provided the first self-sustaining operation of the AGT101 as a complete unit. One hour and 58 minutes of self-sustaining operation was achieved on the first run.

Testing continued on the engine into January; electronic control functions were modified to improve lightoff and control functions. On January 5, 1982, some members of the House Science and Technology Committee and JPL visitors watched the engine operating near idle condition (53,000 rpm). Controls development continued through January. Testing was terminated after the engine reached 80,000 rpm and a speed control instability was observed. Teardown revealed that the turbine shroud had radially shifted touching the turbine rotor and

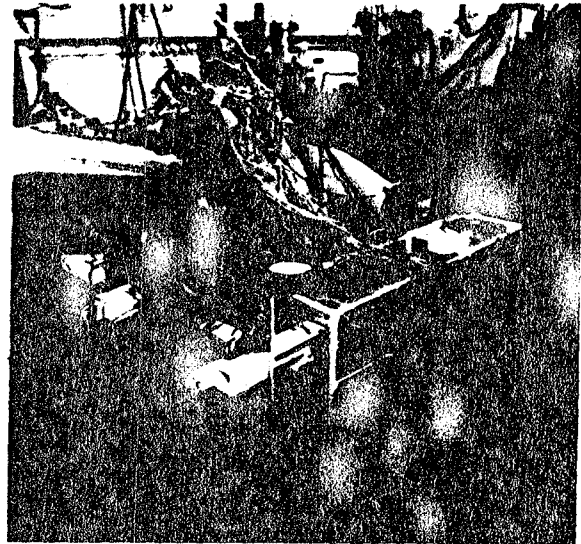


Figure 19. AGT101 Power Section in Test.

causing foil bearing distress. The turbine shroud support bolts were bent and had not slipped in the turbine shroud slots as intended during thermal expansion.

A redesign of the turbine support system was performed. The design features a radial flexure system consisting of nine beams supporting the turbine shroud as shown in Figure 20, which is representative of the present engine configuration.

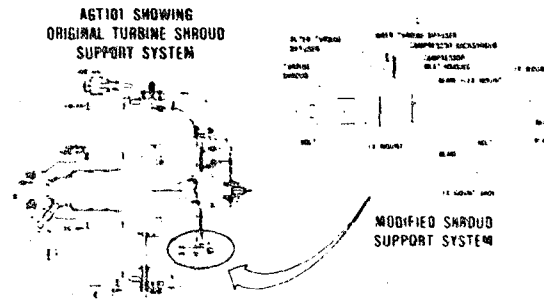


Figure 20. AGT101 Turbine Shroud Support System.

S/N 001 Build 5 was assembled with the redesigned turbine support system. Proximity probes were installed on the turbine shroud to monitor radial clearance from the turbine rotor. The engine was installed in the test cell on March 30, 1982, and subsequently completed 30 start/stop cycles of hot testing to verify turbine shroud concentricity during engine operation and after shutdown and cooling. The engine was accelerated to 75,000 rpm at the end of the test while monitoring rotor dynamic behavior which was excellent. The proximity probes indicated no shift of the turbine shroud during the test. Of significance, is that during this test, the lowest idle fuel flow (2.6 lb/hr, JP-4) was recorded on a dead

weight fuel measurement system. This is the lowest idle fuel flow known on any gas turbine and is already comparable to modern spark-ignition piston engines in the 100-hp class. A low idle fuel flow is necessary to meet the overall fuel consumption goals.

S/N 002 engine which incorporated radial and axial clearance probes for the compressor and turbine entered the test program in May 1982. Build 1 of this engine provided limited data as an abnormal rotor dynamic behavior was observed. Minor oil leakage in the compressor inlet was observed.

Between May and September 1982, tests of one build of S/N 001, three builds of S/N 002, and two builds of S/N 003 were conducted. Some abnormal rotor dynamics and minor compressor and turbine rubs were experienced. Inadequate clearances at the rub locations have been corrected. Additional stabilization of rotor motion is being evaluated both in the rotor dynamics rig and engine test beds.

On September 28, 1982 S/N 001 Build 7 was satisfactorily accelerated to full rated speed of 100,000 rpm. This unit provided further supportive data on running turbine clearances. By mid-October 1982, all three engines had been run to near full speed (97,000 to 100,000 rpm) and had accumulated over 90 hours and 135 starts (see Table 4).

Table 4. Testing Through October 15, 1982

Power Section Serial Number	Starts	Operating Time
001	101	71 hrs 47 min
002	50	19 hrs 24 min
003	34	8 hrs 58 min
Total	135	91 hrs 9 min

To verify proper operation, testing of these units, will continue during the next few weeks. Engines S/N 001 and S/N 002 then will be utilized as development test beds for ceramic components. After engine S/N 003 performance is verified, it will be shipped later this year to TPL as part of the Solar AGT program.

SUMMARY

Progress of the AGT101 ceramic development effort has been excellent. This is verified by the fact that all ceramic parts have been successfully fabricated; in some cases by more than one contractor. These parts are fabricated from different materials, and various manufacturing methods, which enhances the potential for successful ceramic applications.

Garrett test rigs have been valuable tools in this technology development. In fact, the structural parts already have been successfully tested as an assembly over simulated engine start and stop cycles. Ceramic bladed turbine rotor development by ceramic contractors has provided rotors capable of full operating speed. This was considered the most difficult technical challenge when the AGT101 program started three years ago. Some said it could not be done.

Compressor and turbine aerodynamic performance is another significant accomplishment. The excellent efficiencies demonstrated at idle and cruise will enhance the Combined Federal Driving Cycle gas mileage projections. Also of significance is regenerator development, which has provided leakage rates approaching program objectives; the combustor effort is equally impressive. At program initiation, variable geometry was thought to be required to meet future emission goals. However, development to date indicates that a simple, inexpensive, fixed-geometry combustor has the potential to meet all emission levels.

As previously stated, the AGT101 engine is now a test bed for evaluation of ceramic and other technologies being developed. Over the past year, testing has progressed to the point where metal engines have now demonstrated full speed operation. Although the engine test bed checkout period has been lengthy, the time spent has been worthwhile. Many problems experienced with the metal engines would have resulted in ceramic parts failures and resulting expensive repairs and failure investigations. The next step is to evaluate ceramics in the engine test beds under actual operating environments and experience actual interfaces between metal and other ceramic parts.

This AGT101 engine test bed is a summation of all significant program technology advancements. The go-forward program (through FY 1985) to develop this engine will technically be a challenging effort. Although excellent progress has been made in an environment of uncertain funding, the major challenge still lies ahead. Bringing ceramics and other technology elements to satisfactory operating levels in the engine test beds, and providing the predicted fuel economy, emission levels, and desired power levels, while maintaining the multifuel capability, is a difficult, but achievable task.

Based on program progress to date, the AGT101 team has confidence that overall program goals will be achieved. Thus, by 1986, the United States auto industry will be in a position to move towards production with the gas turbine technology developed in this program. In addition, the new technologies will be valuable national assets for many gas turbine applications.

QUESTION AND ANSWER PERIOD

Q: During the compressor rig test, was stall measured?

A: My answer to your question is that we did measure stall at each speed line that I showed on the compressor map all the way from 100 down to 50,000 rpm. We had good surge margin over all the range up to about 100,000 rpm. We would like to see just a little more surge margin at full speed than we showed. But overall, we met or exceeded our objectives as far as margin.

Q: What is the maximum turbine materials temperature you project in your runs?

A: The max temperatures we expect in the turbine rotor in the final engine (the 2500-degree turbine inlet temperature engine) are 2200 degrees on the turbine blade and 2000 degrees in the hub of the rotor. That is the max temperature shown by analysis.

Q: Could you tell us what the clearances were that you measured in serial number 1, 2, and 3 tests? You're talking about turbine clearance? The question was, what kind of turbine clearance was measured in the AGT engines run to date? Are you talking engine build clearance or component running clearance during engine operation?

A: During engine testing, we had instrumentation to measure the transient clearance during full-speed operation and at full temperature excursions. The clearance was seen to change out of the order of 30 thousandths from cold start to hot running conditions. So that means to achieve our target goal of 10 thousandths running clearance in the turbine, we had to

have a build clearance of approximately 40 thousandths. During the 20-minute transient, the clearance would decrease from 40 thousandths down to 10. In the compressor, the clearance change was much less in the order of 13 to 17 thousandths that it closed. So you can build within 13 to 17 thousandths of your desired running clearance on the compressor.

Q: Jim Napier from Solar Turbines. What materials were used in the rotor and do you have more than one supplier for the rotor? Are you talking about the metal rotors or the ceramic rotors? Ceramic rotor and rig test.

A: The rotor that we used in the rig test or aerodynamic testing was the metal rotor built to the same contour and profile as we would expect in the final design of the ceramic rotor. But as far as the ceramic rotor and the people who are working on that are concerned, we have Ford working on sintered reaction bonded silicon nitride for the rotor and we have AirResearch Casting Company working on sintered silicon nitride.

Q: Had those been spin tested and hot or cold tests?

A: Yes. Early in the program, a Ford rotor (one of the first units they processed) was cold spin tested. There were some flaws in the blades noticed before they even started the test and some of the blade tips let go during the test, but their rotor survived over 115,000 rpm indicating they had good material in the hub of the rotor. An ACC rotor recently was cold spin tested to 102,000 rpm.

Advanced Gas Turbine Technology Development: AGT 100 Systems and Components

H. E. Helms and R. A. Johnson

Detroit Diesel Allison, Division of General Motors Corp

ABSTRACT

Detroit Diesel Allison (DDA), Division of General Motors Corporation, is developing the advanced technologies to make the gas turbine a viable alternative to the spark ignition and diesel engines of the future. Goals, as shown in Figure 1, have been established for fuel economy, emissions, and reduction cost that could allow the gas turbine to be competitive with these engines in the 1990 time frame. High-risk new technology elements are ceramic engine components and high-efficiency small turbine aerodynamic components.

Current effort includes building the first AGT 100 engine, component qualification testing, and improvements to ceramic component strengths. The first engine with nine ceramic parts started shakedown testing in July. All major components and systems have passed qualification testing. Prototype silicon carbide rotors have been spin tested to 11,000 rpm at design speeds, and new ceramic coating is producing parts with higher strengths than those tested. Silicon nitride parts are also being developed.

AGT 100 SCHEDULE

KEY ELEMENTS IN THE AGT 100 ENGINE DEVELOPMENT PROJECT ARE:

- ceramic component development
- small turbine component development

Advanced technology in these two areas of gas turbine engines has the potential to produce an engine capable of serious consideration for automotive application. Ceramic components enable engines to operate at turbine inlet temperatures and regenerator inlet temperatures yielding very low specific fuel consumption when combined with aerodynamic components that have high efficiencies over a broad operating range. The initial work on this project has emphasized development of ceramic and aerodynamic components as shown in

the timing schedule. Experimental generation of data has now verified the DDA approach, and the fabrication of the engine needed to integrate these components into a useful device has now been completed.

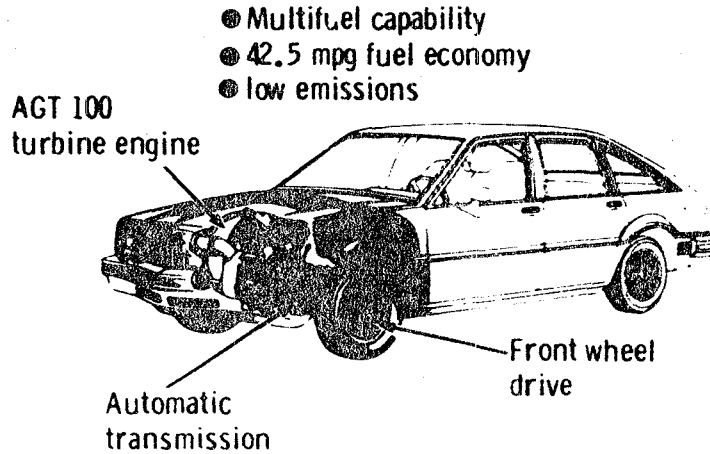
The modified schedule shown in Figure 2 reflects the elimination of penalties from the development plan. It is also noted that engines are now identified as "real engine" engines where emphasis is placed on "real engine environment" verification of ceramic components and integration of aerodynamic and ceramic components into a useful powerplant. It is believed that components tested and proven in the engine environment are valid demonstrations of new technology development as opposed to sterile component rig testing, which at best, never reproduces real transient and steady state operation representative of actual engine environment. Furthermore, engine performance and component reliability can be established directly from engine tests, as opposed to assumed data applicability from component tests, and iterative development can proceed based on the relative engine test results.

It is noted that engine evaluations of ceramic components, additional aerodynamic, and ceramic component development, and iterative design development cost reduction activities are planned for the coming year. Engine life testing, the first year of shakedown testing schedule and cost, and initial engine shakedown testing has successfully identified major design modifications required to proceed with planned component performance and durability evaluation.

AGT 100 ENGINE ACTIVITIES

The AGT 100 engine 501 is shown in Figure 3. This build was completed in early July 1981, and mechanical shakedown testing has proceeded since that date. Features of this engine are as follows:

1984 Pontiac Phoenix with Gas Turbine Power Train



Competitive: Reliability, life, costs,
performance, noise, safety

TE81-7023

Figure 1. 1984 Pontiac Phoenix with gas turbine power train.

- Ceramic components in hot section flow path
 - silicon carbide combustor
 - silicon carbide gasifier turbine vanes
 - silicon carbide power turbine vanes
 - lithium aluminum silicate (LAS) turbine exhaust/regenerator bulkhead
 - aluminum silicate regenerator
 - four zirconia thermal barrier rings-scroll mountings
 - insulation materials
- Metal components in hot section flow path
 - Mar-M246 gasifier and power turbine rotors
 - stainless steel 4188 gasifier and power turbine scrolls

The ODA approach to meeting program objectives is to incorporate state-of-the-art aerodynamic and ceramic components in the engine as they are available and to run to competitive turbine inlet temperature levels from the beginning of the testing (after shakedown testing). The planned turbine inlet temperature is 1975°F, and the inclusion of ceramic components initially is consistent with rig and engine experience in the CATE program and from the rig qualification testing on AGT 100 components. Future engine testing will introduce improved aerodynamic components and ceramic components as rig testing proves their engine readiness. Projections for the next year suggest completion of mechanical shakedown testing with the geometry described and at the 1975°F turbine inlet temperature. Ceramic component fabrication progress suggests gasifier rotor or scroll testing very late in FY 1983 or early in FY 1984 with all ceramic components and

turbine inlet temperature at 2350°F (reference power-train design level) in late FY 1984 or early in FY 1985.

Component efficiencies for the initial AGT 100 configuration are these:

	Initial	Closed clearances
Compressor	78%	90%
Gasifier turbine	83.4%	83.7%
Power turbine	87%	89%
Regenerator	94%	94%

Common development experience dictates "open" clearances while engine operating characteristics are mapped and transient behavior of parts is learned. These clearances are then closed to achieve optimum performance from the engine. Figure 4 shows a progression of horsepower and specific fuel consumption values expected with the 1975°F and 2350°F engine configurations.

ENGINE PERFORMANCE

Performance analyses were conducted to evaluate the effect of various engine parameters on fuel consumption. This information quantifies the effect of each parameter and, among other things, indicates where program resources and effort should be directed for maximum payoff.

The height of each bar represents the amount of parameter change required to produce a fuel economy (mpg) change of 1%. Fuel economy is thus least sensitive to the tallest bar and most sensitive to the shortest bar.

From Figure 5 it can be seen that a 0.25% change in regenerator effectiveness produces a

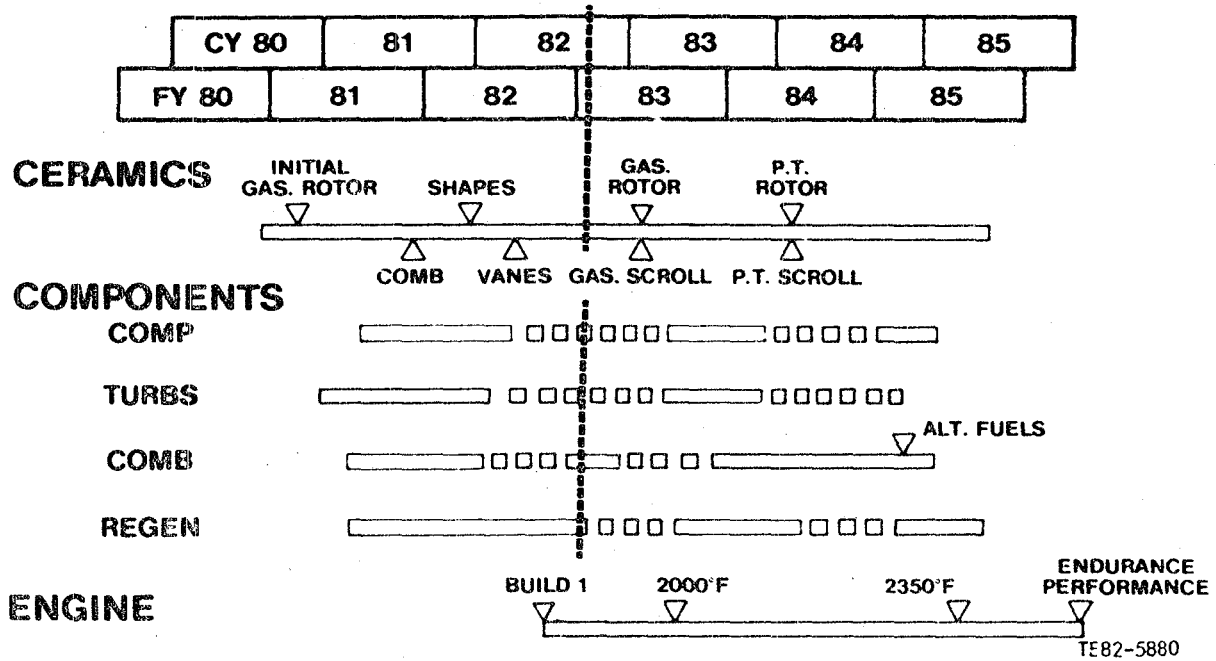


Figure 2. AGT 100 project schedule.

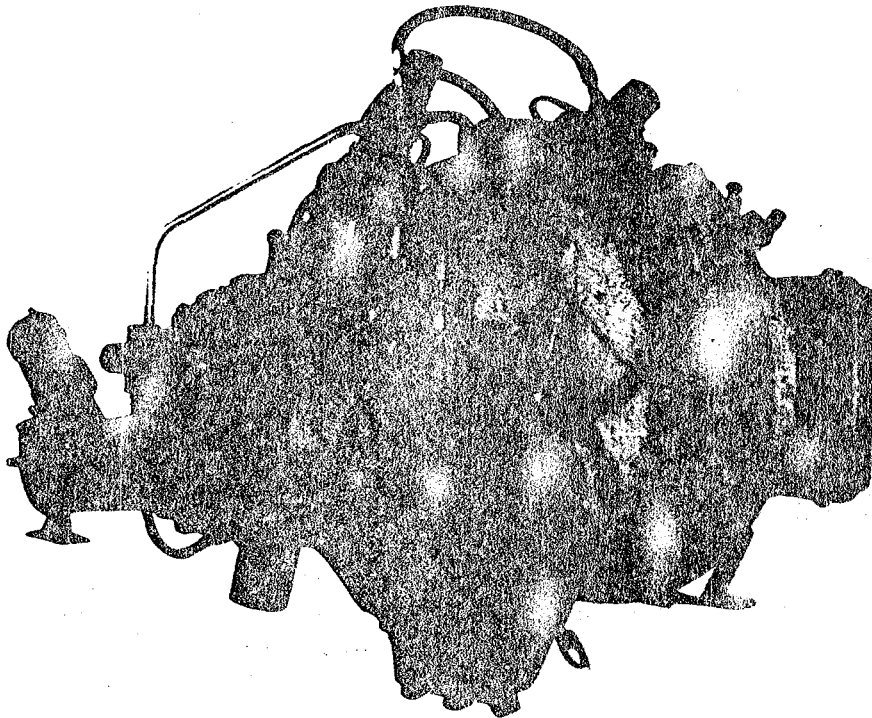


Figure 3. AGT 100 engine BU1.

TE82-5882

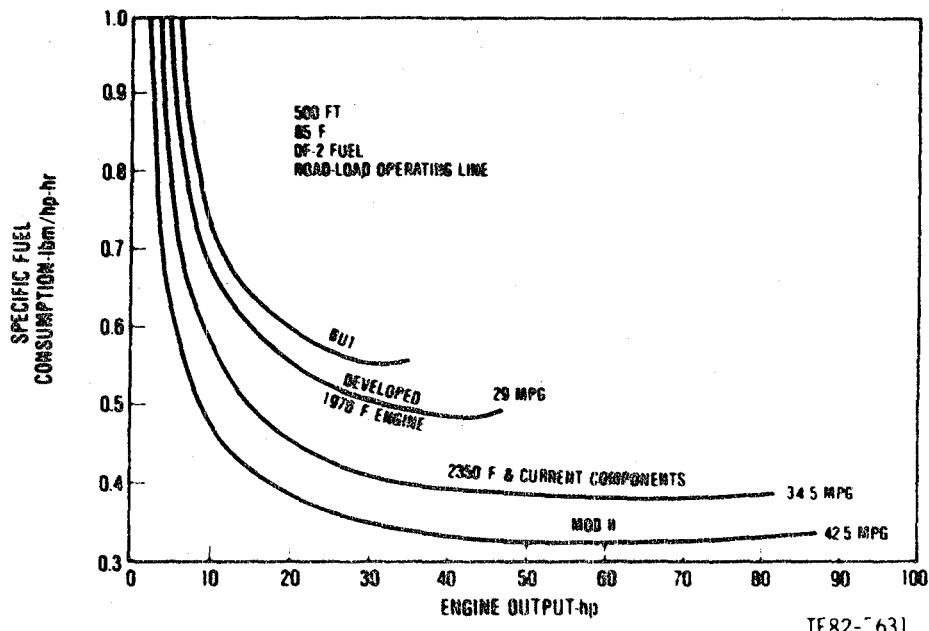
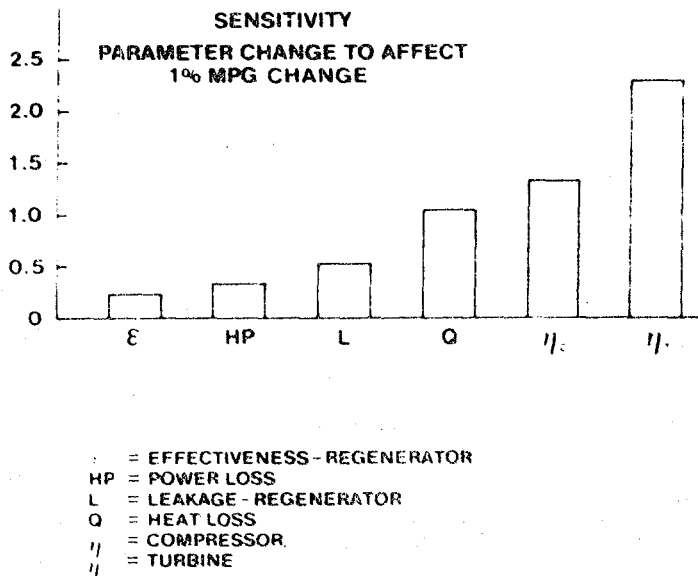
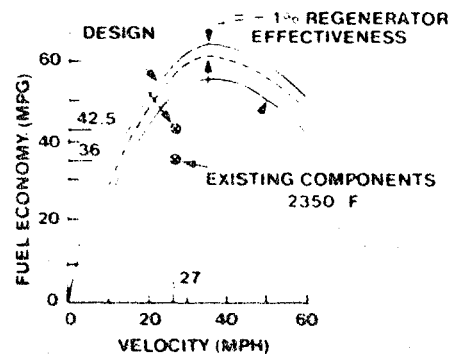


Figure 4. Predicted hp and sfc values for the 1975°F and 2350°F engine configurations.



- ε = EFFECTIVENESS-REGENERATOR
- HP = POWER LOSS
- L = LEAKAGE-REGENERATOR
- Q = HEAT LOSS
- η_c = COMPRESSOR
- η_t = TURBINE



TE82-5892

Figure 5. Performance parameters and effects.

1% change in fuel economy. This effect is illustrated somewhat differently in the fuel economy vs velocity curve. A 1% decrease in effectiveness gives about a 4% decrease in fuel economy. It should be noted that these effects are reversible; a 1% increase in effectiveness would give a 4% increase in fuel economy.

The fuel economy curve also shows the predicted engine performance using existing com-

ponents. These predictions are based on the aerodynamic performance values from rig tests in combination with the temperature (2350°F) allowed by ceramics. The results show a combined driving cycle fuel economy of 36 mpg.

CERAMIC COMPONENT DEVELOPMENT

Over three years of ceramic effort in the AGT 100 program has resulted in the components

shown in Figure 6. Success of the AGT 100 engine is dependent upon the success of these ceramic components; accomplishments over the last year have brought us closer to our goals.

The most difficult component to address has been the turbine rotor, largely because of the fabrication problems inherent with the thick hub, and the high service-strength requirements. This year we have seen rotors in cold spin tests exceed 110,000 rpm, or 127% of design speed.

Recent data from component samples show we are approaching test bar strengths in complicated shapes. This is a result of a new die incorporating features to improve the strength of the part. Bars from these new rotors show strengths greater than those of the rotors spun to 110,000 rpm. Additionally, proof tests cull out the lowest strength rotors to give increased confidence of a population with a higher average strength.

Advancements were made in other components. The injection molded SiC vanes successfully passed 10 thermal shock cycles at heating rates of 1000°F per second and were subsequently run in the engine. In this case, as well as in other component work, the success was attributable in a large degree to the experience

gained from the CATE program and applied to the AGT program.

The combustor (alpha SiC) design was modified to reduce the number of ceramic parts from five to four. In rig tests the emissions were a factor of 10 lower than goal, and the combustor operated exceedingly well in the engine test.

A new scroll has been designed and fabricated and awaits testing. Though basically slip cast, it is fabricated using pressed and injection-molded parts to its final assembled configuration.

Insulating rings (thermal barriers) of zirconia have also been fabricated and were installed in the engine for the testing. There have been no problems with these parts to date.

Finally, a large (14 lb) LAS exhaust diffuser and regenerator seal platform was fabricated by Corning, tested, and installed in the engine. Static deflection tests were run successfully, and the results agreed well with the analytical model.

The work has been a joint effort among DDA and the vendors. CBO has been the primary contributor on the SiC parts discussed, and AC and Kyocera have developed the zirconia rings.

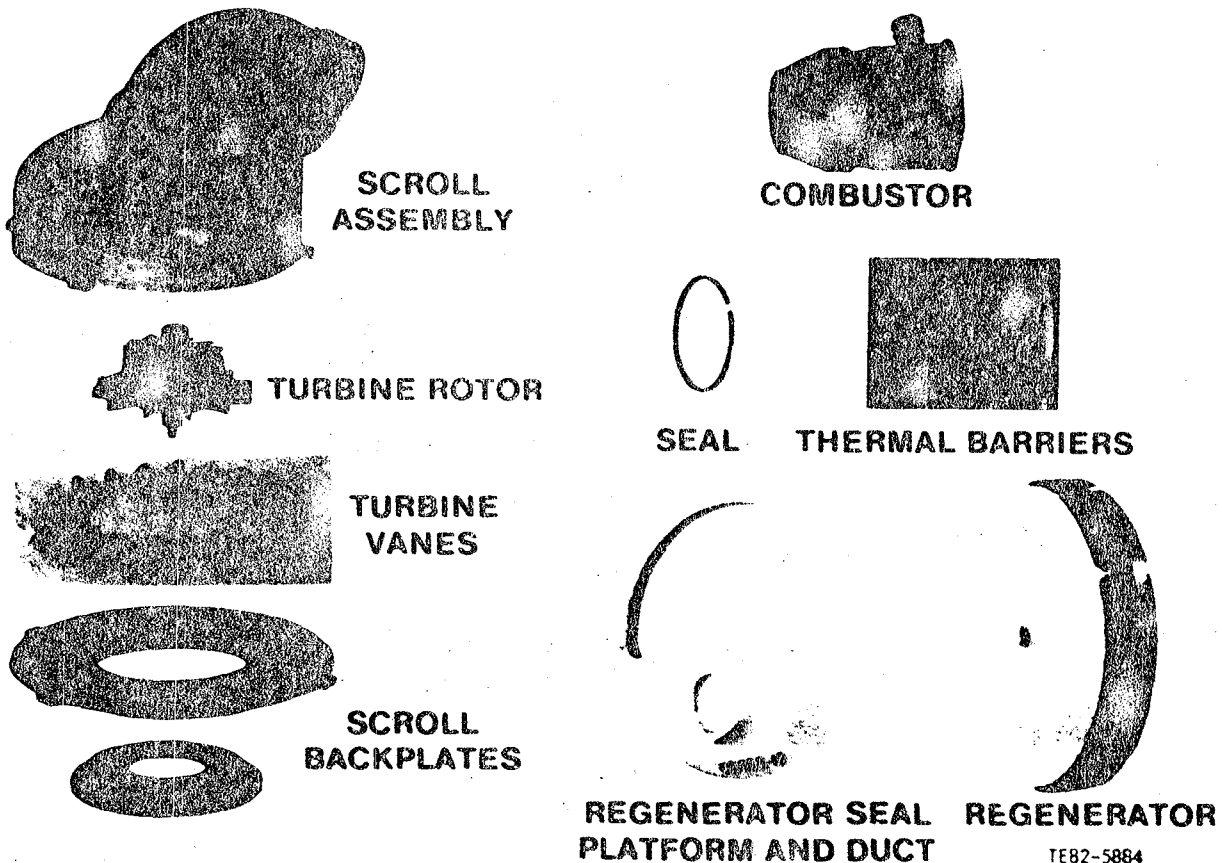


Figure 6. AGT 100 ceramic components.

Corning Glass Works continues to supply regenerator disks and LAS bulkheads. Much of the thermal barrier-rotor attachment work has been done by DDA and CBO, and GTE has made advances in silicon nitride rotor work.

ENGINE TESTING

Assembly of the first AGT 100 engine, shown in Figure 7, was completed in July 1982. This initial configuration contained the following ceramic components: silicon carbide vanes for both turbines, silicon carbide combustor, LAS seal platform, AS regenerator disk, and zirconia insulating spacers.

The engine was installed on a test stand equipped with a combination motoring, absorption dynamometer. Instrumentation lines connect to a remote data acquisition center. Data are recorded at approximately six readings per second. Pretest checkout included careful attention to the engine control system. All actuation systems were operated and calibrated; the fuel system was also checked and nozzle flow rates measured.

Motoring tests have been completed. Both the starter and the dynamometer were separately employed to drive the engine. Sound, vibration, shaft whip, and lubrication system checks were made during this running. Pilot nozzle light-offs have consistently been successful. They were followed by start nozzle tests during which combustor geometry positions and nozzle air-assist pressure level were varied. Schedules were identified that produced successful start nozzle light-offs.

The engine is currently being reassembled following minor modifications made as a result of mechanical shakedown testing.

AGT 100 COMPONENTS AND SUBSYSTEMS

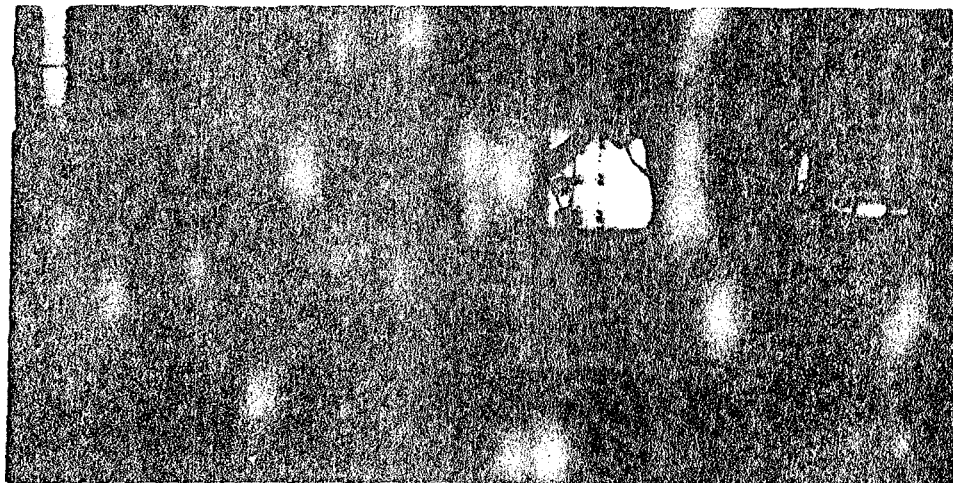
Technical challenges of the AGT 100 engine program involve various aerodynamic components as well as ceramic and other structural components and the electronic control system. In 1981 the primary component testing effort focused upon aerodynamics: compressor, combustor, turbine, and regenerator. Achievement in 1981 of the compressor and turbine goals required for the initial engine build allowed 1982 efforts to be devoted to further improvements in the combustor and regenerator, as well as to experimental evaluation of ceramic engine components and the electronic control system.

Figure 8 contains a summary of the testing now completed in each component area.

REGENERATOR DEVELOPMENT

Regenerator development effort has concentrated on the fabrication and qualification testing of the components required for the first engine build. Successful completion of these efforts resulted in the assembly of the regenerator system for the first engine build on schedule with rig-based performance characteristics matching the first build requirements.

An important function of the regenerator cover is to provide a smooth transition of flow from the compressor discharge air delivery tube to the regenerator with minimum pressure drop and a flow distribution compatible with that of the regenerator gas-side. Improper matching of these flow distributions can adversely affect regenerator effectiveness and engine sfc.



TE82-5883

Figure 7. AGT 100 BU1 on test stand.

COMPONENT	BUILDS	HOURS
COMPRESSOR	5	286
COMBUSTOR	7	132
TURBINES		
GASIFIER	2	204
POWER	1	26
INTERTURBINE DUCT	3	239
REGENERATOR		
COLD SIDE FLOW DISTRIBUTION	8	110
HOT SIDE FLOW DISTRIBUTION	1	72
SEAL LEAF LEAKAGE	4	35
HOT SIMULATOR RIG	2	220
CERAMIC SEAL PLATFORM	TWO UNITS	20
ELECTRONIC CONTROL SYSTEM	2 BUILDS	95
		1439
CERAMIC ROTORS	37 SPIN TESTS	
ENGINE STRUCTURAL ASSEMBLY	ONE UNIT	
CERAMIC TURBINE VANES		
GASIFIER TURBINE	ONE SET PLUS SPARES	
POWER TURBINE	ONE SET PLUS SPARES	

TE82-5885

Figure 8. Aerodynamic component and subsystem rig status.

Combining measured flow distributions with the disk characteristics, the regenerator effectiveness was calculated and a significant loss relative to uniform flow was identified. Modifications to the cover have been modeled and tested, as shown in Figure 9. The resulting flat velocity profile restored calculated effectiveness to within 1% of that for uniform flow with essentially no increase in pressure drop.

The first engine build of the AGT 100 will be used to evaluate starting characteristics and low speed operation at reduced temperatures. The regenerator system hardware selection reflected these operating goals by providing reduced low power leakage with a high clamp seal. The inboard seal incorporated O-ring backup at the miter joints and full perimeter O-ring backing of the outboard seal. The estimated regenerator system leakage and effectiveness are also shown in Figure 9.

Correlation and analysis of all available leakage data have resulted in the indicated breakdown. Future development efforts will be directed at those areas where potential for improvement exists. Immediate promising areas are disk internal leakage and the seal leaves, especially the miter joints.

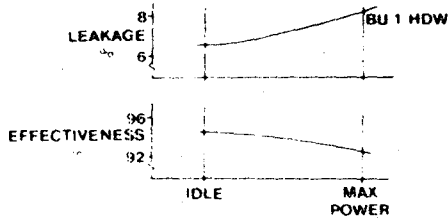
AGT 100 EXPERIMENTAL CONTROL SYSTEM

The control system utilized for dynamometer testing of the AGT 100 engine (Figure 10) will allow manual open-loop control of gasifier speed, inlet guide vanes, burner variable geometry, and power transfer clutch. It will also allow adjustment of the turbine outlet temperature limit and manual control of the timing of fuel flow transitions from the start nozzle to the main nozzle. Switches, lights, and meters are included in the control console to monitor the engine performance and to allow the control console operator to manipulate various engine conditions. Fuel flow is the only engine parameter that utilizes closed-loop control, where the amount of fuel flow is determined by the electronic control unit (ECU) software program.

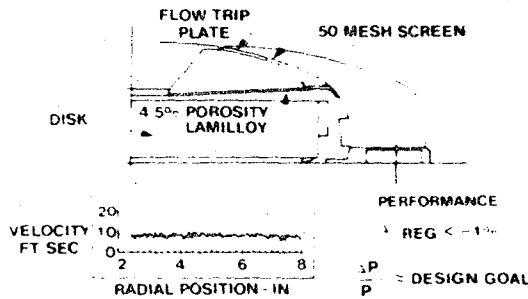
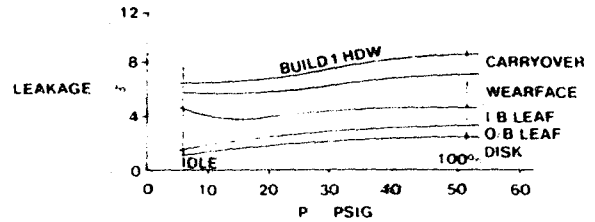
The ECU is a modification of an existing digital control unit. The software program was written using an in-house system that permits modifications to be made quickly and easily. This characteristic was desired to provide maximum flexibility to the AGT 100 engine development program.

All components of the system were individually tested on various test rigs. The fuel

HOT RIG RESULTS



LEAKAGE DISTRIBUTION



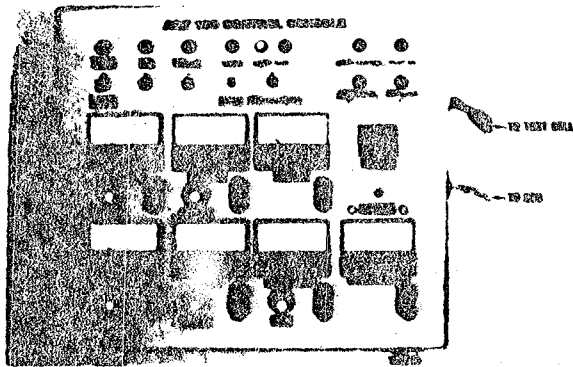
ACCOMPLISHMENTS

ACHIEVED INITIAL ENGINE LOW-POWER GOALS ON HOT RIG
 IDENTIFIED MODIFICATIONS TO MEET MAX POWER EFFECTIVENESS

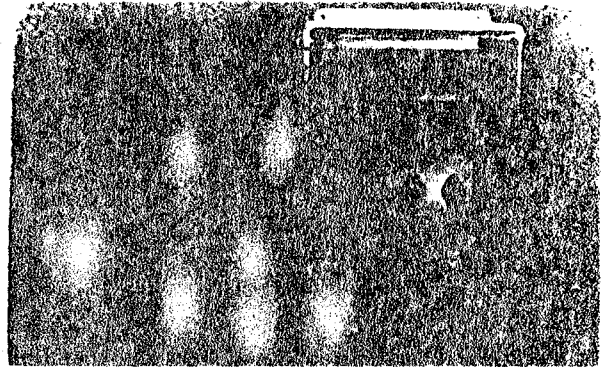
TE82-5886

Figure 9. Regenerator rig results.

CONTROL CONSOLE



ELECTRONIC CONTROL UNIT



COMPONENT	COMPONENT TESTS	SYSTEM TESTS		
		HYDRAULIC SYSTEM FLOW TESTS	STEADY STATE COMBINED SYSTEM	TRANSIENT COMBINED SYSTEM
CONTROL CONSOLE	•		•	
ELECTRONIC CONTROL UNIT	•		•	•
FUEL METERING CONTROL	•	•	•	•
PILOT FUEL CONTROL	•	•	•	•
PUMP	•	•	•	
BYPASS VALVE	•	•	•	
MAIN NOZZLE (CENTERBODY)	•	•	•	•
START NOZZLE	•	•	•	•
SOLENOIDS, REGULATOR VALVES, PRESS. CHECK RELIEF RESTRICTIONS	•	•		

TE82-5887

Figure 10. Control system test plan.

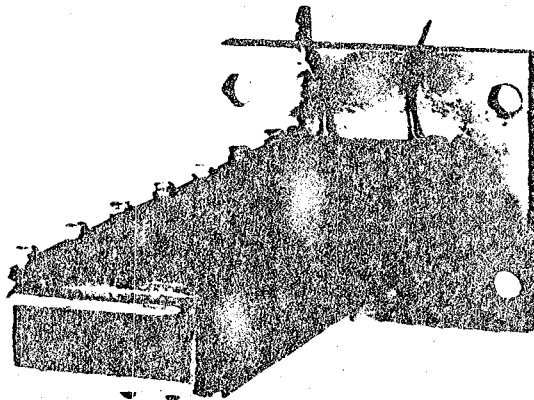
system components were next collectively tested on a flow bench. A successful checkout of the overall fuel and electronic systems was then completed. Steady-state engine operating points were tested, using the test simulator. Both actual fuel flow to the engine as well as transient fuel flows when switching from start to main nozzle were checked. Both tests show excellent correlation between predicted and actual fuel system performance.

THERMAL SHOCK TESTING OF CERAMIC TURBINE VANES

The AGT 100 engine design employs ceramic vanes for both the gasifier and power turbines (18 and 20 vanes respectively). The vanes fit into airfoil-shaped pockets contained in each of two endwall surfaces and thus direct the hot gases into the radial inflow rotors. The vanes have constant cross-sectional shape.

A test fixture shown in Figure 11 was designed to evaluate vane response to rapid temperature changes. The fixture, which holds three vanes in cascade fashion, fit into an already existing facility capable of rapidly changing temperature. A 4-minute cycle was selected in which temperature varied between 1200°F and 2000°F, the change occurring in approximately one second. Each three-vane set underwent 10 temperature cycles.

Eighteen gasifier and 21 power turbine vanes (all alpha SiC) were tested. All vanes survived the test without cracking or other damage and were approved for assembly into the first engine build.



PRESSURE TEST OF CERAMIC REGENERATOR SEAL PLATFORM

The largest structural ceramic part in the AGT 100 engine is the LAS regenerator seal platform. Twenty-one inches in diameter, this Corning-produced part also serves as an exhaust diffuser for the power turbine. LAS was selected as the material because of its low coefficient of thermal expansion. This material is expected to remain chemically stable because of the low surface-to-volume ratio (versus a high ratio typical of LAS regenerator disks used in some previous turbine engines).

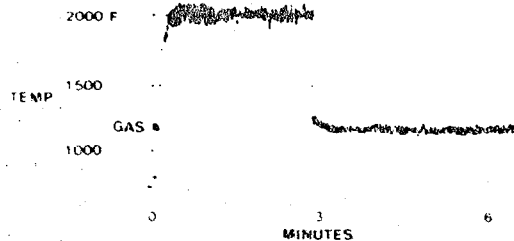
A three-dimensional finite element model was used as a tool in designing the seal platform. This model produced the estimated deflections indicated in Figure 12.

To check the seal platform prior to engine testing, a pressure test was conducted. As illustrated, a network of dial-indicator measurements were taken to define the actual deflections while under pressure. The measured deflections agree very well with the analytical predictions. During early testing, the part was covered with stress coat to identify areas of maximum stress. Strain gages were then attached at these areas during subsequent testing. The maximum measured tensile stress in the seal platform was 2900 psi.

ENGINE STRUCTURAL ASSEMBLY

A pressure proof test of the combustor case, inner gear case, and intermediate gear

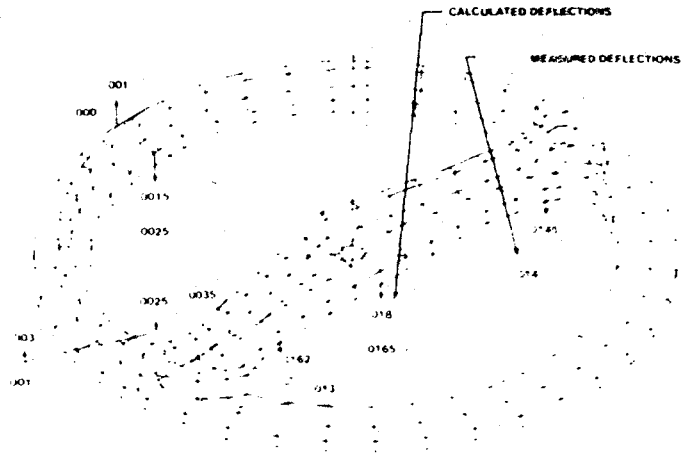
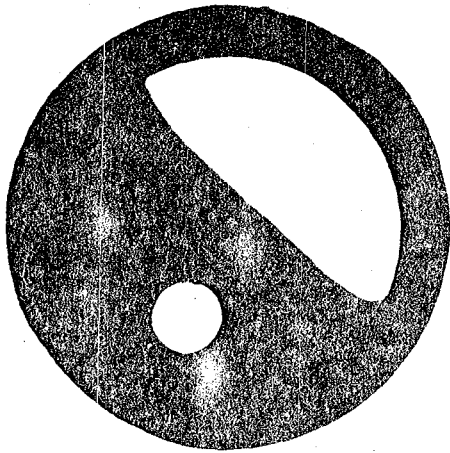
THERMAL CYCLE



SIC (α) VANES TESTED	RESULTS OF 10 THERMAL CYCLES
18 GASIFIER TURBINE	ALL PASSED
21 POWER TURBINE	ALL PASSED

TE82-5888

Figure 11. Ceramic vane thermal shock testing.



LAS SEAL PLATFORM

DEFLECTIONS @ MAX PRESSURE

**MAX MEASURED TENSILE
STRESS IN PLATFORM 2900 PSI**

TE82-5889

Figure 12. Ceramic regenerator seal pressure testing.

case was conducted. Together with the regenerator housing, these components form a pressure vessel that is the base structural load carrying path through the engine. The regenerator housing was pressure tested separately and therefore was not included in this test. The overall objective of the test was to subject the parts to the maximum pressure they would experience during engine operation.

The test setup is shown in Figure 13. The combustor housing, inner gear case, and intermediate gear case were bolted together with all of the associated engine seals and gaskets to form a pressure-tight structure. The dial indicators measure the inner gear case bearing pocket deflection and slope and compressor shroud deflection.

A total of 41 strain gages was installed in high stress regions. Pressure was applied to the combustion case in stepped increments up to the maximum pressure of 70 psig. The maximum measured combustor housing stress was 34 ksi. This and other measured stresses were in good agreement with calculated values.

The maximum stress in the inner gear case was 2.9 ksi and was located on the compressor scroll. The maximum deflection in the intermediate gear case was 0.012 in. located at the output shaft bearing pocket. Differential deflection between the inner gear case and the intermediate gear case at this same location was 0.0072 in. at maximum test pressure. All shafts have sufficient end play to accommodate

this reduction in clearance due to pressure loading.

COMBUSTOR DEVELOPMENT

The combustor for the BUL engine differed slightly in design from the prototype model previously tested. Following rig modification to accept the BUL combustor, 26 hr of burning time were accumulated on the combustion rig.

PILOT NOZZLE--Bench testing of the pilot nozzle investigated ignition and combustion characteristics. A photograph of this test fixture showing the pilot nozzle in operation at 0.3 lb/hr fuel flow is shown in Figure 14. The ignition limits were quite wide, and lean blowout was as low as 0.14 lb/hr fuel flow. Schedules picked for the BUL engine were 1 lb/hr during light-off and 0.6 lb/hr thereafter.

START NOZZLE--The centerbody start nozzle was tested to determine ignition characteristics and lean blowout limits at starting conditions. It was also tested over a range of inlet temperatures up to a burner inlet temperature of 1000°F to simulate operation during the warm-up period. Improvements made during this testing resulted in satisfactory start nozzle characteristics.

MAIN NOZZLE--Measured emissions and flame appearance during main nozzle operation were very similar to previous tests with the prototype combustor even though an appreciably different fuel injection design was used. Tran-



COMBUSTOR CASE
MAX MEASURED STRESS = 46 KSI

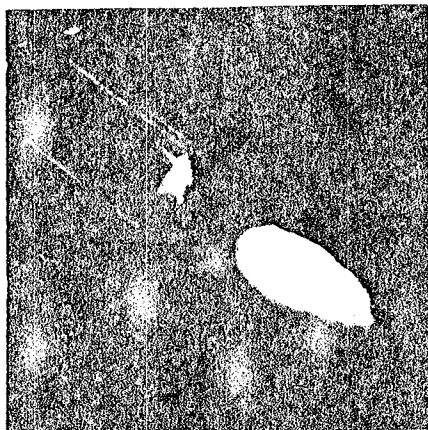
GEAR CASE
MAX MEASURED STRESS = 2.5 KSI

INNER & OUTER GEAR CASES

- **INNER GEAR CASE**
DEFLECTION = .012 INCHES
- **OUTER GEAR CASE**
DEFLECTION = .005 INCHES
- **REMAINED WITHIN**
PARALLELISM LIMITS

TE82-5890

Figure 13. Engine structural assembly pressure testing.

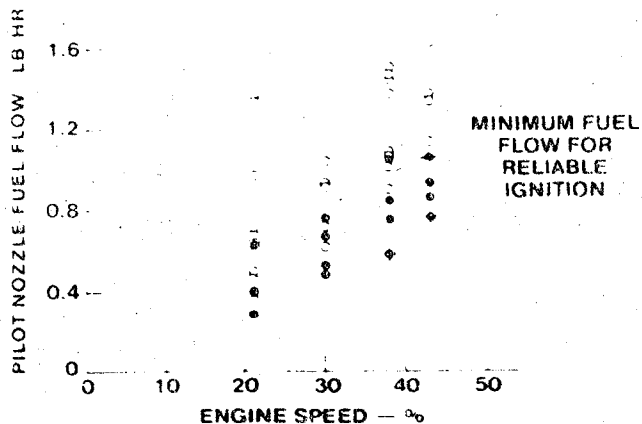


● **PROOF TEST OF TWO CERAMIC COMBUSTORS**

	BURNING TIME
● PILOT NOZZLE & IGNITION TESTING	5 HRS
● START NOZZLE DIFFUSION FLAME TESTING	8 HRS
● START - TO - MAIN NOZZLE TRANSITION	1 HR
● MAIN NOZZLE STEADY STATE EMISSION MEASUREMENTS AND SNAP FUEL TRANSIENTS	13 HRS
TOTAL BURNING TIME	26 HRS

AGT 100 PILOT BURNER IGNITION

- - IGNITION IN LESS THAN 10 SECONDS
- - IGNITION IN MORE THAN 10 SECONDS
- ◆ - NO IGNITION



TE82-5891

Figure 14. Combustor development.

sition from the start to the main nozzle was accomplished manually on the rig without difficulty at burner inlet temperatures from 800°F to 1100°F.

CERAMIC COMPONENTS--The combustor shown in Figure 14 has four ceramic components: the dome, the main body, the dilution band, and the pilot flame tube. After each day of testing, the combustor centerbody was removed and the interior surfaces visually inspected. No

damage was observed through the first six days of testing. A dome crack on the seventh day may have been caused by problems with test equipment (preheater air leak and coolant leak). Another assembly was installed in the rig for additional proof testing. Nearly 4 hr of burning time were accumulated on this assembly, including the snap fuel transient operation. No damage was observed in any of these ceramic components after the rig testing.

Ceramic Applications in Turbine Engines (CATE)

S. R. Thrasher

Detroit Diesel Allison, Division of General Motors Corp

ABSTRACT

The objective of the Ceramic Applications in Turbine Engines (CATE) program is to apply ceramic components in a highway vehicle gas turbine engine and reduce fuel consumption by improving engine cycle efficiency due to operation at higher temperatures. The Allison GT 404-4 is the test engine for this program.

As originally planned, ceramics were to be applied incrementally at successively higher operating temperatures, beginning with 1900°F, increasing to 2070°F and, finally, to 2265°F. Evaluation of the initial ceramic components at 1900°F has been successfully completed.

The 2070°F configuration has been concurrently designed, initial ceramic component process development and fabrication have been completed, and an advanced process development experiment is nearing completion. Rig and engine testing of the 2070°F-configuration ceramic components have been conducted.

Detroit Diesel Allison (DDA), Division of General Motors Corporation, has successfully engine tested the ceramic gasifier turbine nozzle and rotor assembly and the ceramic regenerator system to the maximum 2070°F-configuration operating conditions.

CERAMICS FOR ENGINES

THE CATE PROGRAM was the first of the three major DOE programs to develop structural ceramic components with the objective of significantly improving the fuel consumption in gas turbine engines. One of the CATE Program goals was to evolve the proper ceramic component development approach that would lead to application of ceramic components in a production engine, the DDA GT 404. Figure 1 is a representation of the CATE program development approach. The remainder of this paper provides background for the program and discussion for the major disciplines shown in the chart.

To successfully introduce structural ceramics into the hostile gas turbine engine environment, it is inadequate to merely manufacture components for engine test. Because of the brittle nature of ceramics, additional effort is required on the part of an engine manufacturer when addressing the problem of designing with ceramics. The key to the successful introduction of ceramics and the development approach taken in the CATE program is the establishment of a level of understanding of ceramics comparable to that which five or six decades of experience with metals have afforded industry.

This understanding begins with the ceramic material itself, the powders used, the process of generating complex shapes with acceptable strength, the elimination of variability (quality control), methods to nondestructively inspect components, cost-effective machining techniques, assessment of the materials' thermal and chemical stability, and methods of handling the brittle components without damage. The development of a useful ceramic material is directly linked to the engine that will use the material.

The design of ceramic components involves the analysis methods used; specifics such as the critical interface with metallic surfaces, accurate ceramic material characterization data, well-defined component environments, evaluation of the analysis results, and defining specifications for the material and components. Materials development and design efforts must proceed together and considerable coordination and iteration is required for the successful manufacture of a component that will satisfy design requirements.

After completion of the design/materials development phase comes the test evaluation. Here the proof-of-concept occurs. First, components are selected for engine testing by being subjected to realistic environments in rigs that provide the required maximum thermal

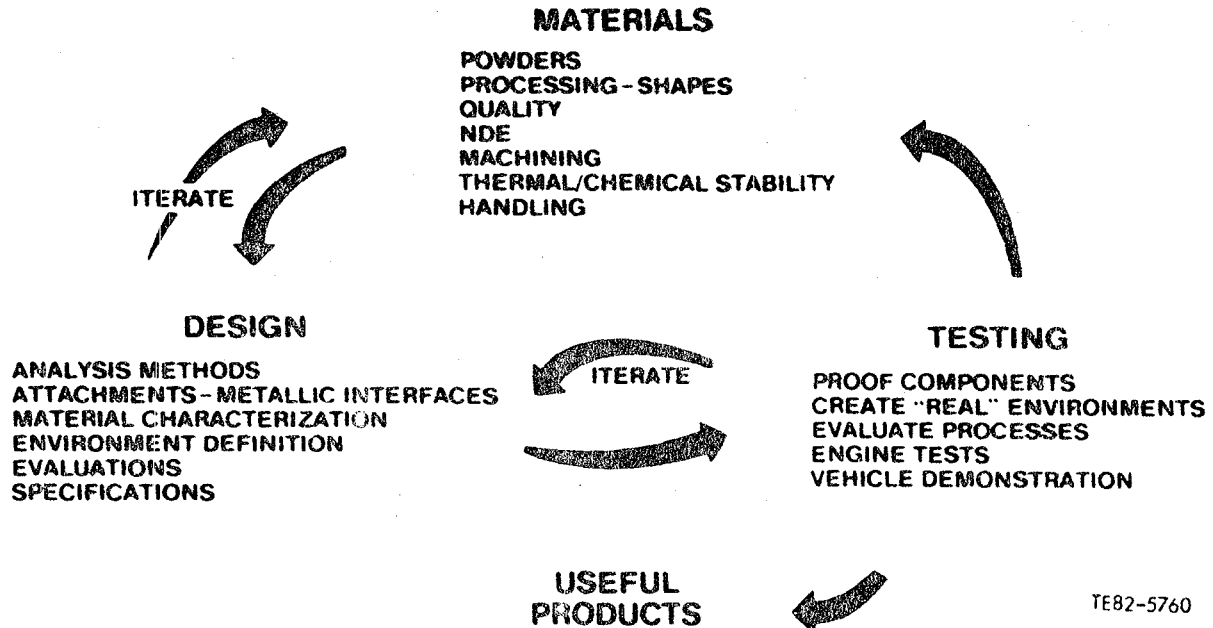


Figure 1. GATE program development approach.

stress. The proof testing in rigs will separate the flawed components from those worthy of engine evaluation.

During the proof testing, an evaluation of the manufacturing process and the design concept is obtained. The final proof-of-concept (and the only acceptable one) is engine testing of the ceramic components. The test phase must also undergo iterations with the design/materials development activities. These iterations refine all of the disciplines involved and ultimately lead to a useful product.

CERAMIC COMPONENT DEVELOPMENT

DDA has been under contract to NASA Lewis Research Center since July 1976 to demonstrate improved cycle efficiency of ceramic components by raising the operating temperature of the existing Allison GT 404-4 vehicular gas turbine engine. The program has been funded by the Department of Energy (DOE), Automotive Technology Development Division, Office of Transportation Programs.

The original plan was to apply ceramics incrementally at successively higher operating temperatures, beginning with 1900°F and increasing to 2070°F and, finally, to 2265°F. Evaluation of the initial ceramic components at 1900°F has been successfully completed.

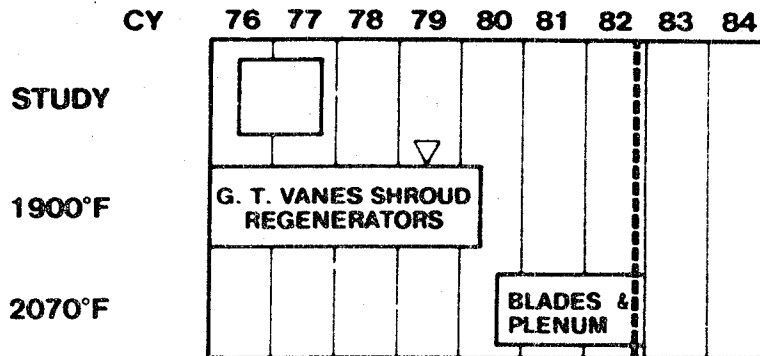
This evaluation included initial ceramic material process development, ceramic material characterization, ceramic component rig testing, engine test stand durability, and over-the-road demonstration in a gas turbine powered truck. A second ceramic engine configuration, to be operated at 2070°F, has been con-

currently designed. Initial ceramic component process development and fabrication have been completed, and an advanced process development experiment is nearing completion. Extensive rig testing of the 2070°F-configuration ceramic components has been conducted.

DDA has successfully engine tested the ceramic gasifier turbine nozzle and rotor assembly and the ceramic regenerator system to the maximum 2070°F-configuration operating conditions. FY 1982 changes in work scope deleted the 2265°F effort, halted development of the 2070°F-configuration ceramic plenum, and redirected the regenerator activity to laboratory scale ceramic regenerator core materials evaluations. Figure 1 shows the current schedule. The exclusive objective of the program has been to develop and engine demonstrate the ceramic components for the 2070°F-configuration. At each technological step, emphasis has been placed on durability of ceramic components on engine test stands operating at real engine cycle profiles.

Supporting the engine-oriented demonstration are: extensive ceramic component process development, ceramic material characterization, component nondestructive inspection, and rig qualification testing. The remaining activities for this year will emphasize completion of the ceramic blade process development experiment.

The baseline engine being used in this program is the Allison GT 404-4 Industrial Gas Turbine engine, which, in its all-metal configuration, operates at a turbine inlet temperature (TIT) of 1635°F. It is a two-shaft regenerative gas turbine with a power transfer system combining the advantages of single- and



▽ VEHICLE DEMONSTRATIONS
TE82-5761

Figure 2. CATE program schedule.

two-shaft engines, and is shown in cutaway view in Figure 3.

The 1900°F-configuration ceramic components were the gasifier nozzle vanes, gasifier turbine tip shroud, and regenerator disks with associated seals. These ceramic components have been successfully demonstrated at 1900°F (IT), while the 2070°F-configuration ceramic components were designed utilizing the ceramic technology available to date. The gasifier nozzle support rings, vanes and turbine tip shroud, the gasifier turbine blades, and gasifier inlet plenum are ceramic to withstand the 2070°F-gas stream temperatures.

The sequential introduction of components and materials at successively more severe operating conditions is intended to utilize each material fully while permitting parallel development of the design methodology and fabrication processes peculiar to high-strength structural ceramic materials technology.

1900°F-ENGINE CONFIGURATION

Engine durability testing of the 1900°F-configuration ceramic components has been completed, and the results are shown in Figure 4. The three ceramic components comprising the configuration were thoroughly rig qualified, and subsequent engine testing demonstrated the viability of the application of ceramic hardware in gas turbine engines. A total of 7,475 engine test hours was accumulated, which represents over 370,000 simulated vehicle miles. Although most of this test experience was on a test stand operating to a transient cycle representing a composite truck duty cycle, the ceramic gasifier turbine vanes and regenerator system were demonstrated in two truck installations featuring actual vehicle operation over highways, streets, and on

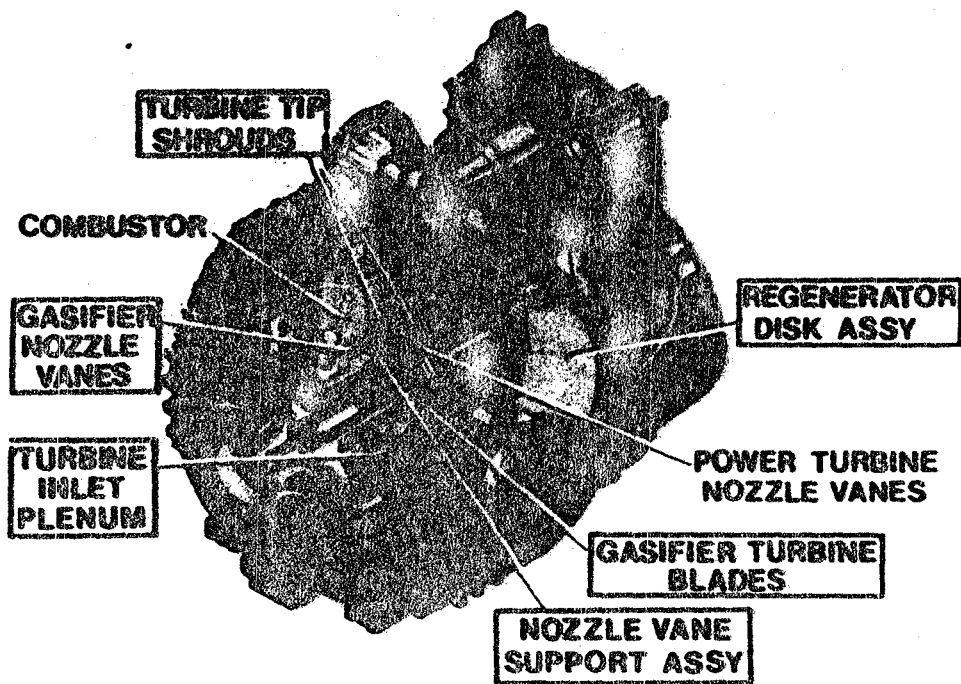
specially designed truck durability courses at the General Motors proving grounds. Throughout this testing, the ceramic part durability was excellent, underscoring the ability of ceramic materials to survive the violent environment of a vehicular gas turbine engine.

The reaction-bonded silicon carbide gasifier nozzle vanes were the primary components used for material process development for the 1900°F-configuration, and that processing was directly applied to the 2070°F-configuration, accommodating only geometrical differences. The results of these efforts and the initial development of test rigs and procedures established guidelines for later application to ceramic components.

The gasifier turbine tip shroud ring provided an early evaluation of the design concepts for ceramic rings for the 2070°F-configuration. The ring's structural requirements are moderate, but the abradable turbine tip shroud work that was applied to this component has resulted in promising materials and concepts aimed at addressing the problem of ceramic blade tips on ceramic rubbing surfaces.




The regenerator disks for the 1900°F-configuration were of two types: thick wall (0.0045-in. thick) and thin wall (0.0035-in. thick) alumina silicate--both rated at 1000°C (1832°F) maximum temperature. The aerodynamic performance of these disks has been excellent throughout the program. In addition to the engine durability testing, laboratory testing has concentrated on establishing those features of the disk that limit the strength and life characteristics. Development work continues on this family of compositions to provide a material suitable for the high-temperature engine configurations.

The total experience of these three initial ceramic components has demonstrated the structural and chemical stability of the cer-



TF82-5762

Figure 3. Ceramic components installed in GT 404/505-4 engine.

Vane	Material	Rig Tested	Engine Tested		
			Hours	High Time Part	Truck Installed
	Reaction Bonded Silicon Carbide	130	3138	1512	✓
	Reaction Bonded Silicon Nitride	67	81	81	
	Refel Silicon Carbide	4	435	435	✓
Turbine Tip Shroud 	Reaction Bonded Silicon Carbide	4	1546	985	
	Sintered Silicon Nitride	3	113	113	
	Lithium Alumina Silicate	3	11	11	
Regenerator 	Thick Wall 1000° C Alumina Silicate	5	2833	1808	✓
	Thin Wall 1000° C Alumina Silicate	16	3938	3050	✓
	Regenerator Inboard Seal	23	7475	2160	✓

Total 1900° F Configuration 7475 Hrs.
Vehicle Operation: 6656 Miles/231 Hrs.

Figure 4. Components and status of 1900°F-configuration CATE engine.

amic material candidates in an engine environment.

2070°F-ENGINE CONFIGURATION

The 2070°F-engine configuration design features a totally ceramic gasifier turbine and regenerator system, which is required for increasing the TIT. The turbine flow path is comprised of 78 ceramic parts, including the 28 gasifier turbine nozzle vanes and the 40 gasifier turbine blades. All of the ceramic components have been fabricated by at least two, and in some cases as many as four, ceramic suppliers, thus permitting the assessment of the candidate materials available and the potential component fabrication techniques that have been developed within the ceramics industry. With the exceptions of the gasifier plenum and the turbine tip shroud, all of the parts have been made with both silicon carbide and silicon nitride. Figure 5 shows a cross section of the hot section.

In addition to the ceramic gasifier turbine, two nonceramic engine design features are required to permit operation of the 2070°F-configuration: (1) the relocation of the temperature sensor for the fuel control system from the gasifier turbine inlet to the power turbine exhaust to keep temperatures within the limits of commercially available thermocouples, and (2) change in the engine block cooling. The resulting control uses microprocessor technology replacing the analog controls of the baseline engine.

The design goal for the ceramic parts was based on a probability of survival consistent with failure modes and effects analyses and on competitive warranty costs in a commercial truck application. The ceramic design methodology and material characterization, although changing with our understanding of the 2070°F-test experiences, were developed during the initial phase of the program and were applied during the design phase of the 2070°F-configuration. The test results correlate with and give credibility to the ceramic design methodology and material characterization.

The gasifier nozzle assembly is designed to isolate the vanes from all mechanical loading by capturing them in slots through the inner and outer ceramic vane support rings. The ceramic rings are held in place by a metal strut and support assembly, which is shielded from the hot gas path by the ceramic strut shells. The inner and outer vane support rings and the gasifier turbine tip shroud ring are similar in design to the 1900°F-configuration tip shroud. The ceramic gasifier tip shroud has an abradable layer requirement for compatibility with ceramic blades. Forty individual ceramic blades are attached to a metal turbine disk by a single dovetail. Around the dovetail shape on each blade is a 0.007-in. thick compliant layer of L605. The ceramic dovetail of the blade is coated with boron nitride to serve as a solid film lubricant and diffusion barrier.

The 2070°F-engine configuration has completed extensive rig testing, and the rotor and nozzle assemblies have been successfully subjected to engine testing at 2070°F-operating conditions. The ceramic component design technology developed during the CATE program is supported by the ceramic component test results and is being applied in other programs, such as the AGT 100.

CERAMIC COMPONENT ENGINE TEST EXPERIENCE

The experience of running ceramic components in engines has established the feasibility of common use of structural ceramic components. The incremental application of ceramic components with a corresponding increase in engine operating temperature has provided a sound technology base for the follow-on ceramic configurations. The first step was the introduction of the 1900°F-configuration ceramic components, which included ceramic gasifier turbine vanes, gasifier turbine tip shroud, and regenerator system. After rig running of the ceramic regenerator system and nozzle vanes, engine demonstrations were conducted. Included in the engine test hours shown in Figure 6 for the 1900°F-configuration

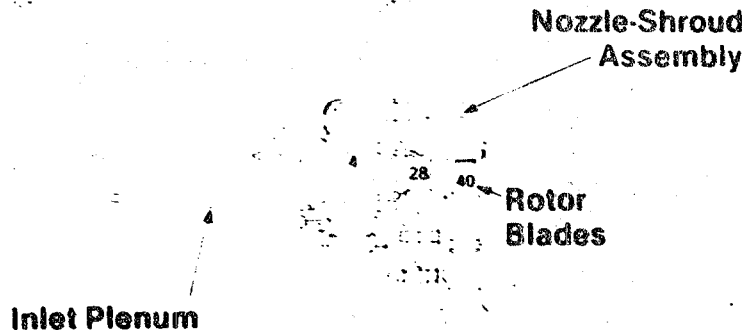


Figure 5. Ceramic components of the 2070°F CATE configuration.

CONFIGURATION	HOURS		
	1900°F	2070°F	TOTAL
VANES (VANE ASS'Y)	3406	894	4300
TIP SHROUD	1670	894	2564
REGENERATOR DISK	7814	1578	9392
BLADES	14	14
ENGINE	9392

TE82-5764

Figure 6. Ceramic component test times.

are two vehicle demonstrations with the ceramic components. The engine was installed in a truck that was subjected to severe duty cycle and operational testing, and the ceramic components withstood the severe vibrational and thermal shock loading without damage.

The second step in the incremental application of ceramic components is the 2070°F-configuration, which features a ceramic vane assembly (instead of ceramic vanes in a metal assembly), ceramic gasifier turbine blades and tip shroud, and an uprated ceramic regenerator system. Extensive rig testing of all the 2070°F-ceramic components has been conducted, qualifying parts for the engine testing shown in Figure 5. The 2070°F-configuration is the first introduction of a rotating ceramic component in the CATE program. The complete ceramic gasifier section, including all nozzle components and the ceramic blades, has been simultaneously engine demonstrated at 2070°F-operating conditions.

The total experience of these ceramic components has served to bolster the promise of ceramics as a viable material for a gas turbine engine.

BLADE DEVELOPMENT

Analytical and experimental test results on ceramic blades have identified the need to improve the overall strength of the blade, which will also improve reliability. The apparent weakness in the blade stalk and the yield from the initial process development definition signaled the need for second generation process development activity. The objective of such process development is to provide a better understanding of the influence processing variables have on strength, as well as to define the control necessary to reduce variability for each phase of the processing. A blade matrix process development experiment was initiated by DDA and Carborundum Co. (CBO)

to satisfy this objective and is nearing completion (see Figure 7).

The matrix experiment is a two-level factorial experiment featuring 13 processing variables, which involve compounding, molding, sintering, machining, and heat treatment. Thirty-two combinations of the 13 variables have been used to produce 4800 blade/bar pairs. The experiment is designed to isolate the most influential variables that will ultimately be chosen to maximize blade strength and processing yield.

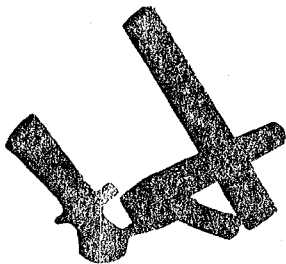
These parts have been inspected at each processing step by CBO and have been completely characterized by DDA. Laboratory characterization of these parts has provided information on defects, modulus of rupture (MOR) strengths (from both blades and comparison bars), process yield data, component microstructure, densities, and heat treatment. The laboratory evaluations employed several evolving nondestructive evaluation (NDE) techniques such as C-Scan, sonic velocity, and photoacoustic spectroscopy. Nine of the 32 experiments have been selected for spin testing. The laboratory characterization will be combined with spin test results in the final data evaluation and correlation.

A computerized data evaluation is designed to provide complete characterization of each of the steps in the manufacturing process and correlation with both NDE results and end product performance. The final result will be a better understanding of the processing variables' sensitivities and a definition of the control necessary for each phase of the critical ceramic processing.

INSTRUMENTED NOZZLE ASSEMBLY

The design analysis used for the ceramic nozzle components recognizes that control of thermal gradients is essential to ensure sur-

BLADE PROCESS DEVELOPMENT EXPERIMENT
GOAL: INCREASE STRENGTH — REDUCE VARIABILITY
BLADE/BAR PAIRS
32 VARIATIONS/13 VARIABLES
4800 BLADE/BAR PAIRS PRODUCED BY CARBORUNDUM



STATUS	% COMPLETED
LABORATORY CHARACTERIZATION	
BLADES	100%
FULL SIZE BARS	100%
BARS FROM BLADES	100%
SPIN TESTING BLADES	
SELECT BLADES	100%
DOVETAIL MACHINING	60%
SPIN TEST	—
DATA REDUCTION/CORRELATION	IN PROGRESS

TE82-5765

Figure 7. Ceramic blade status.

vivability of the ceramic parts. A more thorough understanding of the environment surrounding the 2070°F-configuration nozzle assembly is needed to allow better definition of these gradients. To this end, an instrumented all-metal nozzle assembly has been introduced into the thermal shock rig and engine test programs to obtain further information. The locations of the thermocouples and static pressure instrumentation designed to investigate the nozzle environment are shown in Figure 8. This instrumentation is designed to provide the following:

- o Verification of primary and secondary flow path environment.
- o Data for determination of local heat transfer coefficients for the ceramic rings.
- o Information regarding the effects of liquid and vaporized fuel during starts, accelerations, decelerations, and shutdowns.

These data were obtained for both rig and engine environments, and the resulting modifications were re-evaluated in the engine, which confirmed the anticipated corrections. The knowledge gained from this testing is as follows:

- o Secondary cooling air flowing over the outer ceramic rings caused excessive radial temperature gradients in the rings.
- o Higher than anticipated local heat transfer coefficients exist around the outer ceramic rings.
- o Leakage of cooling air under the inner ceramic ring caused excessive radial temperature gradients in the ring.
- o No adverse effects from fuel or circumferential temperature gradients were identified.

The following modifications were incorporated and tested in the engine with the instrumented nozzle:

- o The secondary cooling air was redirected to eliminate contact with ceramic components.
- o Leakage under the inner ring was eliminated with the addition of seals.

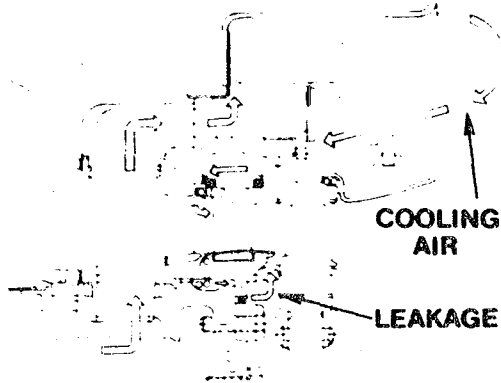
In addition to modifying hardware, design analysis inputs were updated to include the higher heat transfer coefficients and measured environmental conditions. This update resulted in analytical predictions of the previous failures encountered in the shock rig testing, plus predictions of success with the modified hardware, which was demonstrated with subsequent successful rig proof tests to 2070°F-conditions.

The utilization of the instrumented nozzle assembly permitted the necessary understanding of the environment and allowed proper modifications to be incorporated, which provided rig qualified nozzle components for the engine test program. Equally important was the confirmation of the design methodology used in the CAE program. Without good correlation between analytical predictions and test results, the design methodology and its resulting predictions would be questionable.

ENGINE TEST OF 2070°F-CONFIGURATION

The ceramic gasifier nozzle components that qualified in the thermal shock rig proof testing at 2070°F, and the ceramic gasifier turbine blades that qualified in the spin test program have been assembled into an engine. This assembly, shown in Figure 9, represents the com-

THERMAL SHOCK RIG AND ENGINE TESTING



RESULTS

- IDENTIFIED HIGH THERMAL GRADIENTS IN CERAMIC PARTS
- REDEFINED LOCAL HEAT TRANSFER COEFFICIENTS

MODIFICATIONS

- SECONDARY FLOW CIRCUIT
- SEAL LEAKAGE FLOW PATH

BENEFITS

- SUCCESSFUL PROOF TESTING
- CONFIRMATION OF DESIGN METHODOLOGY

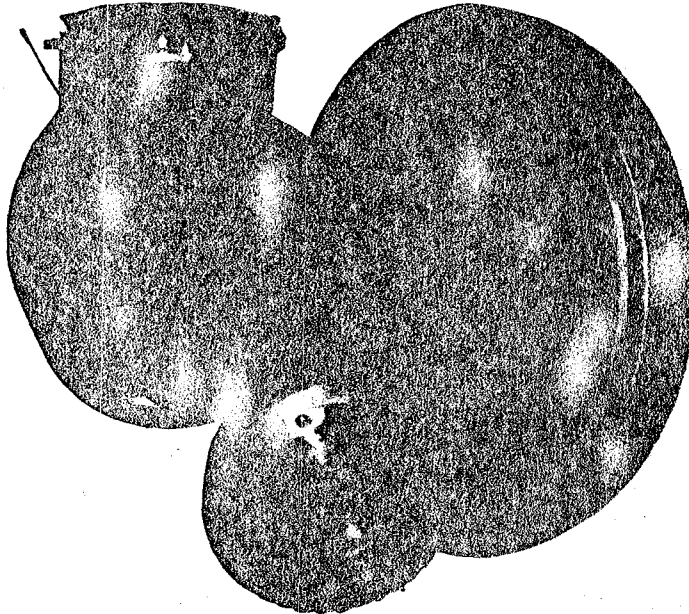
INSTRUMENTED NOZZLE

- STATIC PRESSURE LOCATIONS
- THERMOCOUPLE LOCATIONS

TE82-5766

Figure 8. Thermal shock rig and engine testing.

2070°F CONFIGURATION



2070°F ENGINE DEMONSTRATION

- 2106°F AVG. BOT
- 2070°F AVG. RIT
- 4 COLD STARTS
- 342 HP FROM CERAMIC BLADES

RESULTS

- SUCCESSFUL OPERATION
- NO VISIBLE DISTRESS
- SUBSEQUENT DURABILITY TEST FAILURE

TE82-5767

Figure 9. 2070°F engine configuration.

plete 2070°F-configuration, excluding the ceramic plenum, which has been eliminated from the project due to funding limitations. Also included in the engine were the 2070°F-configuration ceramic regenerator disks and seal system.

The ceramic nozzle components were reaction-bonded silicon carbide with the exception of seven vanes and the outer vane support ring, which were sintered alpha silicon carbide, all supplied by CBO. The vane retaining ring and three of the strut shells were Refel silicon

carbide supplied by Pure Carbon Co. The remaining strut shell was slip cast alpha silicon carbide by CBO.

All 40 ceramic turbine blades were sintered alpha silicon carbide supplied by CBO. The alumina silicate regenerator disks were supplied by Corning Glass Works. The testing conducted was a two-phase program. The first phase was the successful demonstration of the 2070°F-configuration at maximum rated operating conditions, 36,905 rpm and 2070°F rotor inlet temperature (RIT).

This is equivalent to 2106°F burner outlet temperature (BOT), which is cooled to 2070°F by secondary cooling air that enters the flow path ahead of the turbine rotor. During this first phase, two cold engine starts were made, and operation over the speed range from idle to 100% speed was accomplished while data were obtained. At the rated 2070°F RIT operating condition, the ceramic bladed gasifier turbine produced 342 hp. Post test inspection with a borescope revealed that all the ceramic components were in excellent condition.

The second phase of the test program was durability oriented. The objective was to accumulate approximately 50 hr operation at 2070°F RIT and 100% speed. Two cold engine starts were completed during this phase, but a failure occurred at 35,800 rpm (97% speed) during an acceleration. The failure resulted in extensive damage to the ceramic components. Approximately one-half of the ceramic nozzle assembly was severely damaged, and all 40 ceramic blades experienced loss of the airfoil with no failure of the blade attachment. Subsequent failure analysis identified two potential failure modes: (1) blade airfoil failure caused by a dislodged piece of ceramic Fiberfrax insulation used in the engine or (2) failure of the outer vane support due to vibration. Both of these modes are supported by ceramic blade spin test results, which is the topic for the next chart. Corrections have been incorporated for the next engine test to prevent reoccurrence of these failure modes.

SPIN TEST INVESTIGATION--CERAMIC BLADE IMPACT DAMAGE

As part of the engine ceramic bladed rotor failure investigation, a spin test program was conducted to evaluate the possibility of blade airfoil failure resulting from impact with objects originating in the engine upstream of the rotor (see Figure 10). Two potential failure modes were identified during the engine failure investigation. The first involved several pieces of moldable Fiberfrax insulation used to insulate the engine block. These pieces were missing following the test, and small particles of the insulation were found imbedded in the combustion liner walls. This insulation is a very hard, brittle material and may have dislodged, passed through the combustor and nozzle, and finally impacted the rotor.

The second potential failure mode involves the ceramic nozzle outer vane support ring. Assuming a vibration induced failure of that ring, a segment might pass downstream and impact the turbine rotor. Each of these materials was dropped on a alpha silicon carbide blade in the spin test facility spinning at 35,800 rpm (engine speed when failure occurred). Figure 10 shows the objects dropped and the resulting blade airfoil failures. These failures are identical to those encountered on the engine test rotor.

These results substantiate the potential failure modes and have precipitated two design changes. The engine block insulation has been changed to a soft fiber-type insulation in a blanket form. The second design change involves the configuration of the ceramic outer vane support ring. The ring tested in the engine featured a slotted leading edge intended to reduce stresses. Recent analysis, based on the instrumented nozzle data previously discussed, indicates these slots can be eliminated with little or no stress penalty. Therefore, the next test configuration will feature a reaction bonded silicon carbide unslotted outer vane support ring.

REGENERATOR MATRIX MATERIAL TESTING

A rapid, low-cost, experimental technique that duplicates the effect of engine accel and decel cycles on matrix strength and life has been developed for testing regenerator disk matrices. Engine accel temperature peaks are the primary determinants of regenerator disk life. Engine-exposed disks develop a loss in hot face strength roughly proportional to exposure time. Examination of the data showed that loss in strength could have been from either seal contact mass transfer or the accel/decel cycle.

These two variables were separated in a laboratory test. The test facility features an instrumented test section for a 1.5 x 2.5 x 3 in. core sample that is cut from a disk, as shown in Figure 11, and a natural gas burner with a cyclic-controlled, time-dependent, cooling-air supply to establish the test cycle. The time/temperature accel ramp, cyclic peak temperature, and decel ramp can be adjusted to match engine regenerator inlet cyclic conditions. Laboratory and engine testing has clearly established this cyclic thermal exposure as more damaging than steady-state operations.

The engine cycle selected for simulation in the laboratory test was full-power accel from stabilized idle (corresponding to about 1000°F-1050°F) to the selected cycle peak gas temperature, followed by immediate decel to idle. The tests have been conducted on the 1100°C (2012°F) alumina-silicate matrix at three peak temperature levels: 1950°F, 2050°F, and 2150°F (which includes the maximum temperature anticipated for the 2265°F-configuration). Following these rig cyclic thermal ex-

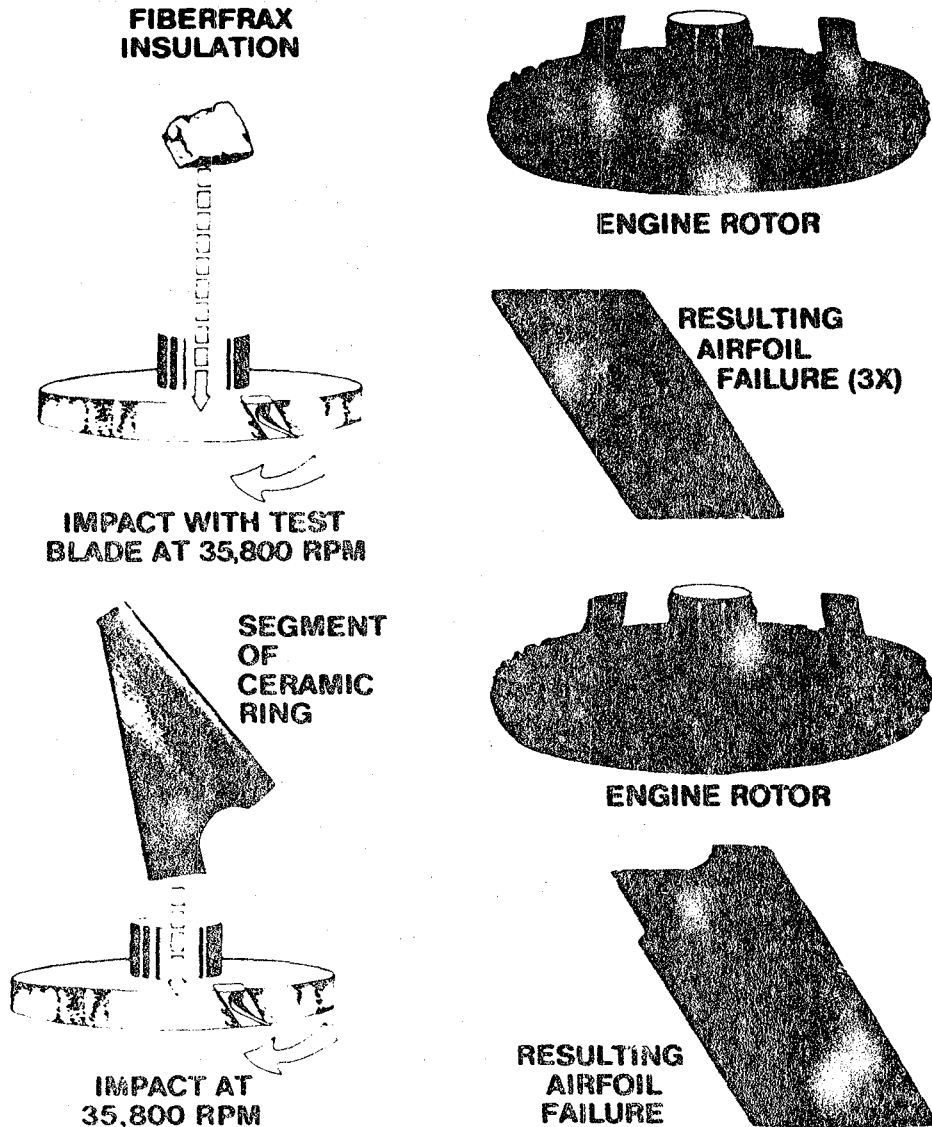


Figure 10. Ceramic blade impact damage tests.

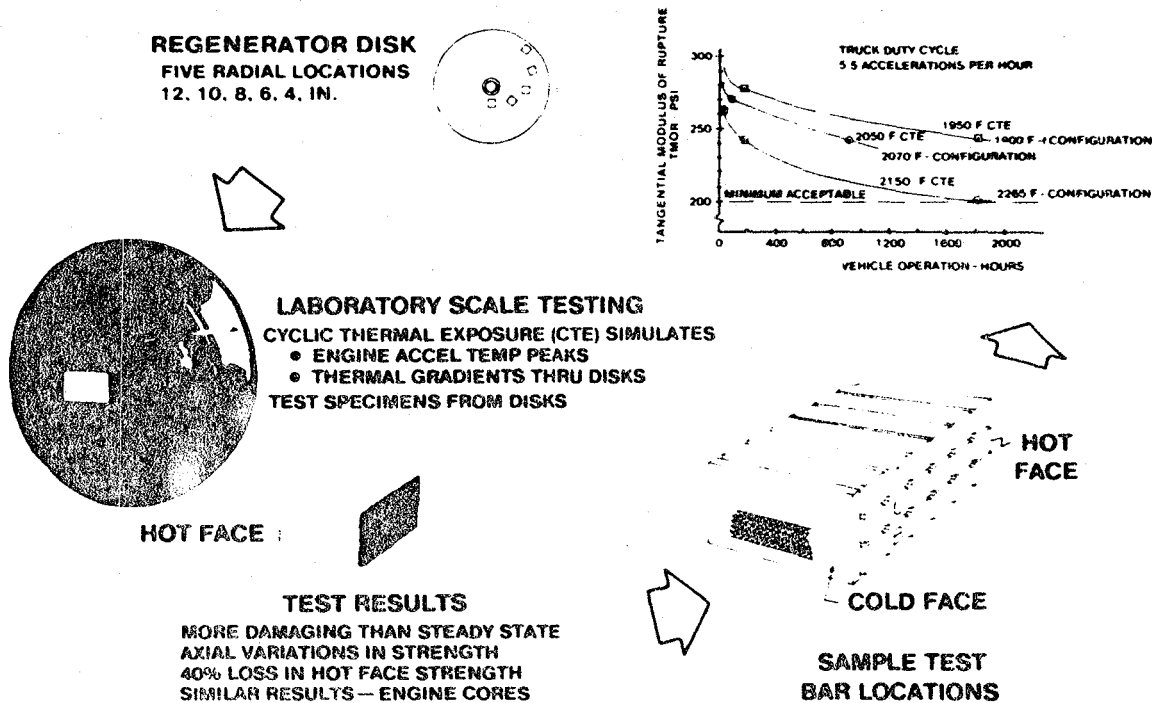
posure tests, the matrix core sample was cut into test bars for tangential MOR testing.

The MOR data in Figure 11 illustrate the effect of increasing peak temperature on disk life. The duty cycle represented involved a 70,000-lb gw truck, which makes 5.5 accelerations from idle to max power every hr. Automotive applications will increase the number of accel/hr to approximately 30, which will expose the regenerator to the peak temperatures at a much faster rate, thereby significantly reducing the useful life of the regenerator disk. The data shown indicate that for a peak temperature of 2150°F, the current regenerator disk matrix under the truck duty cycle will degrade to the minimum acceptable strength level in about 1800 hr. For an auto-

motive cycle, this degradation would occur in just over 300 hr.

The cyclic thermal exposure testing will continue to accumulate data at the 2150°F peak temperature. Additional testing at 2250°F peak temperature has been initiated to further define the capability and limits of the 1100°C matrix material. The data presented do not take into account the effect of road salts on matrix strength or that of stresses caused by mechanical drive system and aerodynamic loads.

The results of this work clearly establish the need for a regenerator matrix material with a temperature capability above the present 1100°C material. Though the 1100°C alumina-silicate is quite acceptable for engines with peak regenerator inlet temperatures below



1E82-5769

Figure 11. Regenerator material testing.

2050°F, and also permits engine development testing at peak inlet temperatures up to 2150°F, the life will be unacceptable above 2150°F.

CONCLUSIONS AND RECOMMENDATIONS

The CATE program will be concluded at the end of calendar year 1982. CATE was the first of three DOE ceramic programs and has lead the

1. PROGRAMS SHOULD DEVELOP CERAMIC COMPONENTS FOR ENGINES

- TRANSITION FROM OPTIMIZED TEST BAR PROPERTIES TO USEFUL COMPONENTS NOT YET POSSIBLE.
- ENGINE ENVIRONMENT DICTATES REQUIRED CERAMIC MATERIAL PROPERTIES.
- CERAMIC MATERIAL DEVELOPMENT MUST BE BASED ON ENGINE-DEFINED REQUIREMENTS.

2. CERAMIC COMPONENT DEMONSTRATION REQUIREMENTS

- PROOF TEST RIGS ARE REQUIRED TO ELIMINATE FLAWED COMPONENTS.
- TEST RIGS MUST APPROXIMATE ENGINE ENVIRONMENT.
- TEST RIG ENVIRONMENT MUST BE COMPLETELY DEFINED AND UNDERSTOOD TO CONDUCT SUCCESSFUL DEVELOPMENT TESTING.
- PROOF TEST RIGS WHICH COMPLETELY DUPLICATE ENGINE ENVIRONMENT CAN BECOME VERY EXPENSIVE.
- COST EFFECTIVENESS OF COMPLEX RIGS VERSUS ENGINE TESTING MUST BE STUDIED.
- ENGINE TESTING IS THE ONLY DEMONSTRATOR OF CERAMIC COMPONENT ACCEPTABILITY

way for development of ceramic materials and component technologies. Although funding constraints reduced the work scope of the original project, the CATE program still enjoyed great success.

It is appropriate now to reflect on the accomplishments of the program, to draw conclusions, and to make recommendations that will enhance the remaining DOE programs and future ceramic development efforts. Figure 12

3. MANUFACTURING PROCESSES AND NDE TECHNIQUES REQUIRE IMPROVEMENTS

- MANUFACTURING PROCESS DEVELOPMENT PROBLEMS
 - 1) EXCESSIVE VARIABILITY POOR REPEATABILITY
 - 2) INCREASED UNDERSTANDING OF VARIABLES
 - 3) INCREASED NDE CAPABILITY
- AVAILABLE NDE TECHNIQUES (NONDESTRUCTIVE EVALUATION)
 - 1) SMALL FLAW DETECTION REQUIRES ADDITIONAL DEVELOPMENT
 - 2) ADVANCED NDE TECHNIQUES MUST BE READY FOR PRODUCTION USE (QUICK AND EASY)

4. BUSINESS CONSIDERATIONS — CERAMIC COMPONENT DEVELOPMENT

- POTENTIAL PAYOFFS MUST BE EVIDENT TO CERAMIC SUPPLIERS AND ENGINE BUILDERS TO JUSTIFY
 - 1) COST SHARE OF GOVERNMENT PROJECTS
 - 2) CORPORATE INVESTMENT IN MANPOWER AND EQUIPMENT
- RETENTION OF PATENT RIGHTS IS A MAJOR CONCERN.

TE82-5770

Figure 12. CATE program: conclusions and recommendations.

presents these conclusions and recommendations, which are amplified by the following discussions.

1. Ceramic components, specifically designed for an engine with precise material properties required for that engine, provide the means to develop and demonstrate useful technology. Material for structural applications cannot be successfully developed using only test bars; high-strength test bars alone cannot demonstrate cost-effective producibility or structural integrity in an engine.

The goal for all ceramic component testing should be to demonstrate ceramics in an engine operating to its duty cycle. To conduct cost-effective engine testing, ceramic components must be selected for use that have an acceptable probability of survival. Available inspection techniques are inadequate, so proof testing in rigs is required to eliminate the unacceptable components. Rig testing also provides a means to learn from failures. Because the evidence is not destroyed, it can be used to advance the understanding of brittle material failure mechanisms and to develop design methodology and nondestructive (NDE) inspection techniques.

2. Rigs must have completely defined and understood environments, and they must approximate the engine to the extent that appropriate thermal stress is developed in the test parts.

However, rigs that completely duplicate engine environments can be extremely complex and expensive, and are not cost effective when compared with engine test cost. A properly designed rig is critical to successful ceramic component development, but it cannot be considered as the ultimate demonstration of acceptability. Only successful engine testing to the appropriate duty cycle can be considered a demonstration of ceramic component acceptability.

3. The successful development of NDE techniques and manufacturing processes can only be accomplished on ceramic components that can be engine tested and should be a significant part of a ceramic program. The CATE program has clearly demonstrated the requirements for reducing variability in manufacturing processes and for developing NDE techniques that discover very small flaws in a cost-effective way.

4. Ceramic suppliers and engine manufacturers must continue their multimillion dollar effort in labor, facilities, and cost sharing if viable competitive structural ceramics are to be developed. And the Government should continue to be a partner in this effort. Furthermore, these suppliers have a right to expect a fair return on investment and a protection of patent rights that may have commercial use.

CERAMIC TECHNOLOGY SESSION

Development of Ceramic Components for Gas Turbine Engines

Lance E. Groseclosa, Peter W. Heitman,
and Jenn Chang

Detroit Diesel Allison, Division of General Motors Corp.

ABSTRACT

Ceramic component activity under CATE and AGT 100 programs has focused on the development of material strength characteristics in full-scale hardware. Emphasis has been directed toward net-shape processing of silicon carbide components (most notably blades and rotors). Selected components have also been produced from a variety of silicon-based and zirconia materials.

State-of-the-art processing and strength characteristics have been realized in the 2070°F-configuration CATE turbine blades. To further improve these properties, a development study is currently being conducted with Carborundum (CBO). In addition, processing methodology for structurally sound AGT 100 gasifier rotors has been established. Full-scale rotors can now be produced with cold-spin capability consistently greater than 100% design speed. Additional studies are currently in progress. Extensive development activities focusing on applicable fixturing and joining technology required for the complex AGT 100 gasifier scroll assembly are also proceeding.

2070°F-CONFIGURATION CERAMIC BLADE DEVELOPMENT

THE CERAMIC ROTOR BLADE was identified as the most critical structural component in the CATE turbine flow path and has, therefore, been the subject of extensive development activities. During 1979-1980, the first process development program addressing the fabrication of injection-molded 2070°F-configuration blades from alpha silicon carbide was conducted at CBO. The focus of this early activity was to establish injection molding parameters conducive to the highest yields of defect-free blades. Upon completion of the program in late 1980, a complete process routing was established for fabrication of blades. Subsequently, a large "production" run of 641 blades was undertaken to quantitatively assess blade fabrication capability. Process yield, structural/dimen-

sional quality, and strength characteristics were evaluated. Figure 1 summarizes the results of this endeavor.

The total process yield of fully machined blades meeting both structural (NDE) and dimensional requirements was 28%. This was thought to be an acceptable level for this stage of the process development.

Initially, qualification test material molded simultaneously with each blade was evaluated to assess indirectly blade strength characteristics. Various surface finish conditions pertinent to the finished blades (longitudinally ground, as-fired, and transversely ground) were examined. Both the as-fired and transversely ground materials were oxidized for 24 hr in air at 2282°F. (Note: Previous experience has shown that such a treatment will restore strengths to a level comparable to that of the longitudinally

YIELDS

MOLDING	—	92%
BAKING	—	91%
SINTERING	—	43%
DIMENSIONAL	—	78%
TOTAL	—	28%

MATERIAL STRENGTH CHARACTERISTICS

LONGITUDINALLY GROUND	: 60.75 KSI
AS-FIRED/OXIDIZED	: 57.52 KSI
TRANSVERSELY	
GROUND/OXIDIZED	: 57.38 KSI

TE82-6110

Figure 1. Carborundum SASiC blade characteristics.

ground surface condition.) The average fracture strength for the longitudinally ground surface measured 60.75 ksi, with an associated Weibull modulus of 7.1. The average strengths for the oxidized as-fired and transversely ground surface conditions measured 57.52 ksi and 57.38 ksi, respectively. Spherical pores were observed as the primary strength-controlling defects, with occasional failures originating from surface flaws and large crystals. These strength characteristics are consistent with the state of the art for injection-molded silicon carbide in test bar form.

Overspeed spin testing was used to establish directly blade strength characteristics. Testing was conducted in a single slotted wheel using uniform thickness (± 0.0001 in.) L605 compliant layers. All blades were oxidized for 24 hr at 2282°F. The results of these tests along with those for blade proof testing are plotted in Figure 2. The straight line represents the predicted blade performance generated from the material strength determinations mentioned above. The correlation between predicted performance and actual performance is excellent. The types of defects that precipitate failure in the blades were identical to those observed in the companion test material. These results indicate that the companion test material is representative of the material in the components and that present-day material characteristics are being achieved in actual blades.

CERAMIC BLADE PROCESSING MATRIX

Because of the needs to increase the strength characteristics and improve processing yields in the 2070°F-configuration CATE blades, a second-generation process development study is currently underway. This effort is a two-level factorial study featuring 13

separate processing variables involving compounding, molding, sintering, machining, and heat treatment. Thirty-two separate processing schedules are used. The processing variables addressed in this experiment are those thought to be associated with the strength-controlling defects typically observed in the blades evaluated to date: spherical pores, large crystals, and machining flaws. Consideration was also given to variables pertaining to microstructure, particularly near the surface of the stalk.

Figure 3 illustrates the characterization procedures to be performed in the evaluation of each separate blade recipe. The shaded areas represent operations currently in progress. All other operations have been completed. All 4800 blade/bar pairs have been made at CBO, with inspections after each processing step. Laboratory characterization of these parts is completed, including microstructural evaluations, MOR strengths obtained from both blades and companion bars, and NDE characterizations (ultrasonic C-scan, ultrasonic velocity, and photoacoustic spectroscopy).

Nine of the thirty-two recipes have been selected for spin testing and are currently undergoing final machining. Correlation of these spin test results with laboratory data will then be made to define the sensitivities of the processing variables and to provide information pertaining to the processing control necessary for the fabrication of consistent, high-quality, high-strength blades. In addition, recommendations for further fine tuning of the process will be made.

Blade strength characteristics are to be evaluated using both companion test bars and miniature test bars cut from the blades. In addition, a sample of 10 blades from selected processing recipes will be subjected to an overspeed to failure spin test to further determine blade performance. A summary of the type of strength data generated in this processing study for one of the 32 individual recipes follows.

The companion test bars were molded simultaneously with the blades following an identical processing schedule. Three miniature test bars, measuring 1/16 in. x 1/8 in. x 1 in., were ultrasonically machined from the attachment/stalk region of each of 12 blades. Both sets of material were prepared with three types of surface finish: longitudinally ground, as-fired/oxidized, and transversely ground/oxidized. These surface conditions were selected to be representative of those surfaces present in the finish machined blades.

The average room temperature MOR of the as-fired/oxidized companion test material measured 70.41 ksi. This compares well with the strength of similar material cut from the blades of 95.03 ksi, when appropriate corrections for specimen size and loading factor in the Weibull statistical model are taken into account. Identical strength-controlling

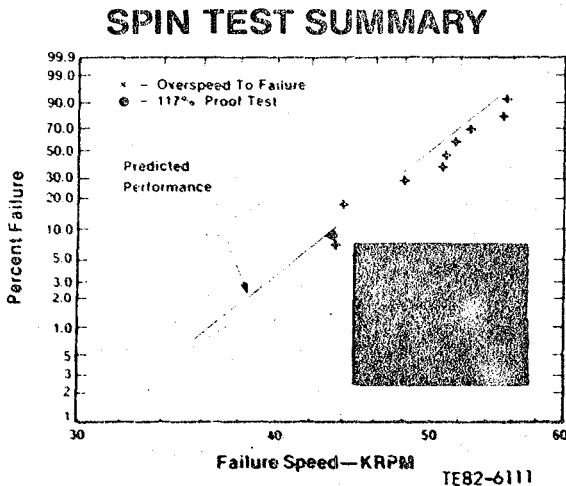


Figure 2. Blade spin test results.

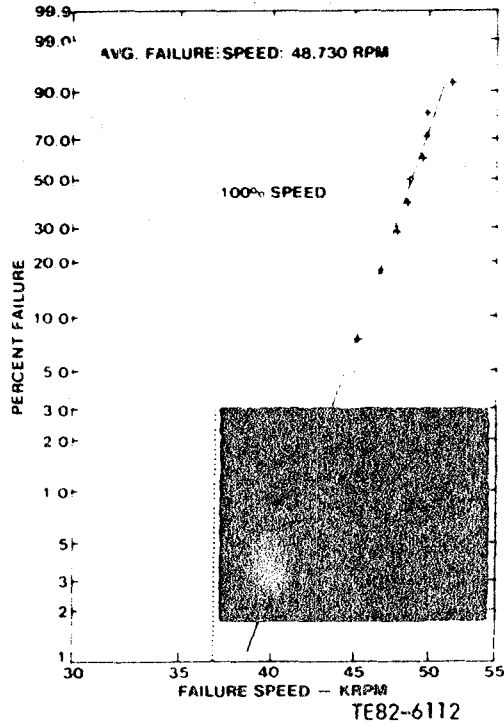


Figure 4. GTE Si_3N_4 blade spin test summary.

the surface indicated that additional development activities were required to enhance blade uniformity.

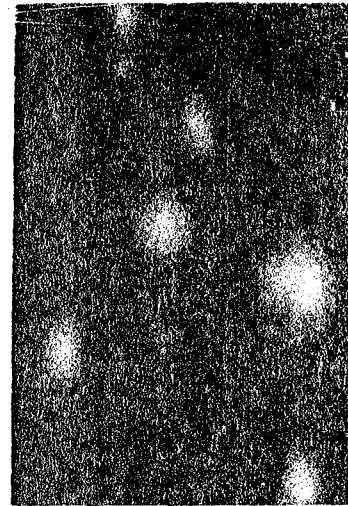
To address the difficulties encountered with internal low-density regions previously observed in first-generation injection-molded silicon nitride blades, additional process development studies were conducted by GTE Laboratories. An updated process specification (AY6-405) was developed, which incorporated a modified binder system with improved binder burnout characteristics.

Evaluation of test material fabricated by this process specification is currently proceeding, with encouraging results. The average room temperature MOR of longitudinally ground test material is 89.49 ksi, while the average as-fired strength is 78.72 ksi. These values represent the highest strengths obtained to date for any GTE injection-molded Si_3N_4 material.

One hundred-eighty blades to be produced from this new process routing are currently on order, with an anticipated delivery date in fiscal year 1982. A preliminary sample of three blades was received for dimensional evaluation. The dimensional stability of these blades was excellent, with all dimensions found to be within design specifications.

CERAMIC ABRADABLE SEAL DEVELOPMENT

The turbine tip shroud shown in Figure 5 was fabricated from reaction-bonded silicon



CARBORUNDUM RB SIC SHROUD

ABRADABLE COATING:

**86% ECCOSPHERES
14% YTTRIA-STABILIZED
ZIRCONIA**

TE82-6113

Figure 5. Turbine tip shroud with abradable coating.

carbide by the Alpha Silicon Carbide Division of CBO. This component was produced by green machining a compression molded ring to near net shape. Following siliconization, the critical dimensions were finish ground. To allow for tighter turbine blade tip clearances, a DDA-developed abradable seal material was applied to the inside diameter of the shroud by plasma spraying.

This abradable material contains equal weight percentages of prestabilized zirconia (with 8% yttria) and Type FA-A Eccospheres (hollow alumino-silicate spheres). In 1980-81 this composition, applied on a metal shroud, successfully ran for 288 hr at 1900°F conditions in CATE engine C-1. This particular ceramic shroud ring has been qualified at 2070°F conditions in the thermal shock rig and is planned to be installed in the next CATE engine build.

The abradability of the zirconia-Eccosphere system has been evaluated in an intentional rub situation on the abradability test rig. Using a CBO sintered alpha silicon carbide blade, twice proof tested to 43,000 rpm (117% design speed), a rub depth of 0.005 in. was achieved with no distress to either the blade or the shroud. The abradability demonstrated for this material system is considered suitable for engine applications.

CERAMIC ROTOR DEVELOPMENT--PROTOTYPE

Work continued during fiscal year 1982 at CBO on the definition of processing parameters for the production of injection-molded sintered alpha silicon carbide AGT 100 gasifier rotors. A limited processing matrix was designed and conducted to establish the process parameters necessary for the fabrication of high-strength prototype rotors. Variables addressed in this study included binder composition, binder removal technique, and sintering procedures.

The characterization of the prototype rotors received as a result of this effort has been completed. The room temperature spin test to failure has proved to be a useful tool in evaluating rotor performance. Figure 6 provides a summary of this testing for the latest 15 rotors. Of these rotors, 14 achieved burst speeds in excess of the 100% mark. The application of Weibull statistics in conjunction with finite element analysis enabled equivalent four-point MOR strengths to be inferred from these results. The median burst speed of 97,000 rpm converts to an equivalent standard bar strength of 49.3 ksi.

Test material cut from actual prototype rotors was also evaluated. The average MOR of 48.7 ksi measured for bars cut in the radial direction from the backface of the rotors correlates well with the predicted strength mentioned above. However, material cut from the interior of the rotors in the axial direction possessed an average strength of only 29.5 ksi.

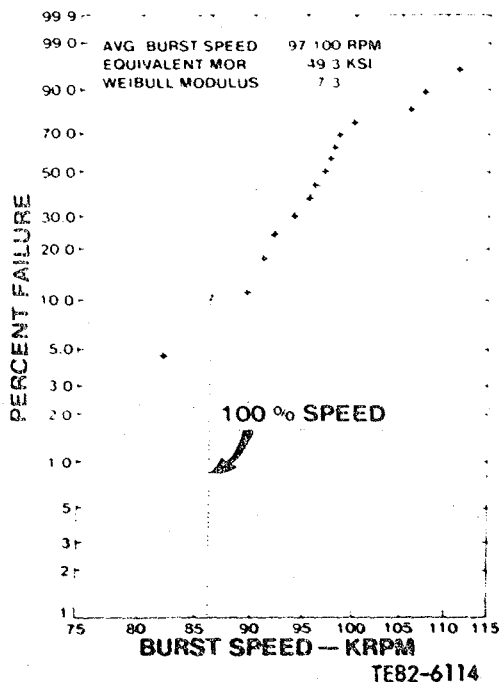


Figure 6. CBO SiC gasifier rotor burst test results.

The defects identified in the axial test bars are typical of the strength-controlling flaws observed in failures of early prototype rotors.

The results for the prototype rotor indicate that sound defect-free material is being achieved in the backface region where high stresses are developed during spin testing. Clearly, however, additional improvement in microstructure is needed in the central section of the hub.

CERAMIC ROTOR DEVELOPMENT--ENGINE CONFIGURATION

As a result of the initial processing study conducted on prototype rotors, a set of processing parameters was established for the fabrication of AGT 100 engine configuration rotors. The parameters selected were those observed to yield the highest average burst speeds in the room temperature spin tests. The engine configuration rotor differs from the prototype rotor in the direction of rotation (blade camber) and the thickness of the rotor shaft. In addition, the exducer blade tips were lengthened for aerodynamic consideration. A new injection molding tool was designed to accommodate these modifications and was delivered in May of 1982.

Rotors fabricated from this "optimal" process routing have been received. Approximately 70% have been judged to be of acceptable quality based on nondestructive inspection criteria. Preliminary strength evaluations of these rotors, determined from standard test bars cut from the components, as shown in Figure 7, indicate a more uniform material in all sections of the hub. Test material from the

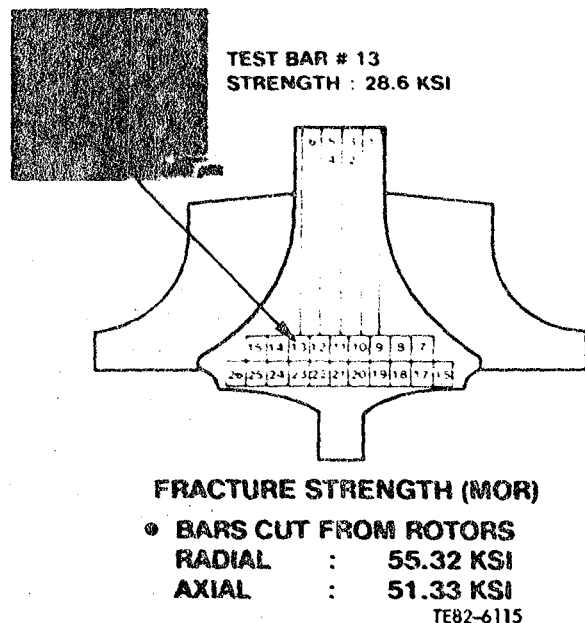


Figure 7. Engine configuration rotor material strength characteristics.

backface region in the radial direction registered an average strength of 55.32 ksi. An average strength of 51.33 ksi was observed for bars cut in the axial direction near the exducer. This represents a significant increase over the 29.5 ksi observed for the same region in the prototype rotors. Only a single low-strength bar (No. 13) with a defect similar to those prevalent in the hub region of the prototype configuration rotors was encountered. The frequency of these defects in the engine configuration rotors, therefore, appears to be greatly reduced. Additional process development activity will concentrate on the complete elimination of such flaws.

SILICON NITRIDE ROTOR DEVELOPMENT

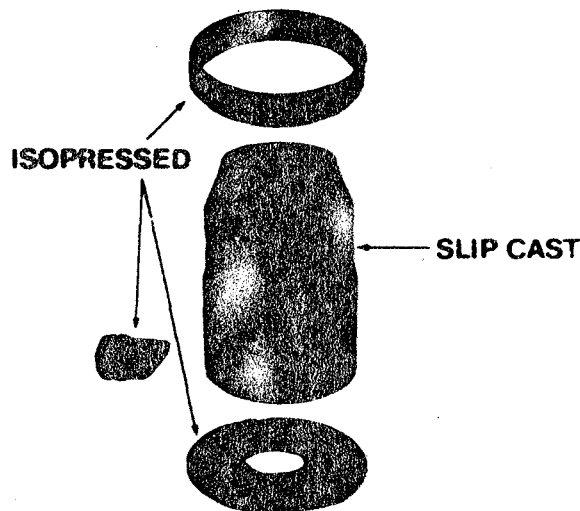
GTE Laboratories has made significant progress toward developing the technology necessary for fabrication of an injection-molded sintered silicon nitride (6% Y_2O_3 , 2% Al_2O_3) gasifier rotor.

This development effort, funded directly by DDA, has involved the evaluation of a variety of binder systems, as well as compounding methods, injection molding procedures, and binder removal techniques. A material system and associated process routing, designated AY6-100, have been established for the production of visually and radiographically flaw-free green rotors. Although these rotors can be sintered to greater than 98% of theoretical density, internal cracking remains a problem. A follow-on effort addressing this problem and associated optimization of the processing parameters is currently proceeding.

AGT 100 CERAMIC COMBUSTOR DEVELOPMENT

The AGT 100 combustor assembly shown in Figure 8 consists of four ceramic components. These parts are all produced from sintered alpha silicon carbide by CBO. The flame tube, swirl plate, and dilution band are fabricated from a standard grade of isopressed and sintered silicon carbide. General net shape is obtained by green machining. Only the most critical dimensions require diamond grinding after firing. All three of these components can currently be produced to a quality level that satisfies all material and dimensional requirements.

The main combustor body is produced by slip casting. A considerable development effort was required, in casting and sinter fixturing technique, before dimensionally acceptable components could be obtained. A nonstandard bimodal grain size starting powder is employed. This material system has a low shrinkage factor so that critical dimensions can be obtained without finish machining. The pilot tube and dilution holes are, however, ultrasonically machined after sintering. The slip cast combustor body material has a coarse-grained microstructure with a relatively uniform average grain size of 6.0 microns. The apparent poro-



TE82-6116

Figure 8. AGT 100 combustor assembly.

osity is approximately 10%. Despite this porosity level, test material slip cast simultaneously with the body registers strengths approaching those obtained from either dense isopressed or injection-molded sintered material. Bars with a longitudinally ground surface condition display an average room temperature MOR of 51.79 ksi, while the average strength of as-fired specimens measures 48.27 ksi. The primary strength-controlling flaws observed in both cases were small pores. The as-fired strength represents a substantial improvement over the 32 ksi previously recorded for earlier slip cast material. The elimination of surface blisters and pore agglomerates through modifications in casting procedure (found to be the primary failure origins in the early material) resulted in this strength improvement. Both rig and engine operating experience with the combustor assembly has been extremely successful to date.

AGT 100 GASIFIER SCROLL

The AGT 100 gasifier scroll assembly, shown in Figure 9, consists of four ceramic components, all produced by CBO from sintered alpha silicon carbide. The connecting duct and scroll are both fabricated by slip casting. The close tolerance shroud and adapter sleeves are made from isopressed silicon carbide, subsequently green-machined to final dimensions. The vane pockets in the shroud are ultrasonically machined after sintering.

The final scroll assembly is produced by sinter-bonding these individual components in sequential fashion. First, the slip cast connecting duct is sintered to full density using appropriate fixturing. Next, the green adapter flange is sinter-bonded to this duct. Then the green close tolerance shroud is bonded to

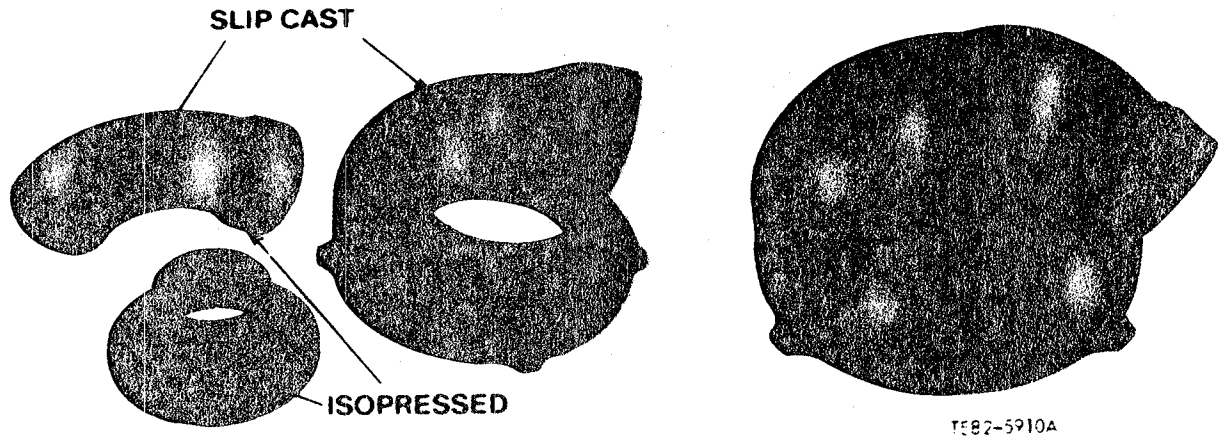


Figure 9. Ceramic gasifier scroll assembly.

the connecting part in yet another firing operation. Next, this assembly is joined to a green slip cast scroll during a final firing to produce a complete functional scroll assembly. Last, the second adapter sleeve is affixed to the scroll inlet. A total of five sintering operations is required.

Several assemblies have been successfully produced to date. While the general concept presently employed for producing this complex component seems sound, significant additional work is needed to consistently meet dimensional requirements and to achieve gas tight, struc-

turally sound joints between components. This work is proceeding on schedule.

ART 100 GASIFIER BACKPLATE ASSEMBLY

The gasifier backplate assembly, shown in Figure 10, comprises an inner backplate and an outer backplate; both are produced by SiC of sintered alpha silicon carbide. The inner backplate is fabricated from isopressed and green-machined billets. The outer backplate is injection-molded. This is the largest injection-molded component (at a weight of 1.8

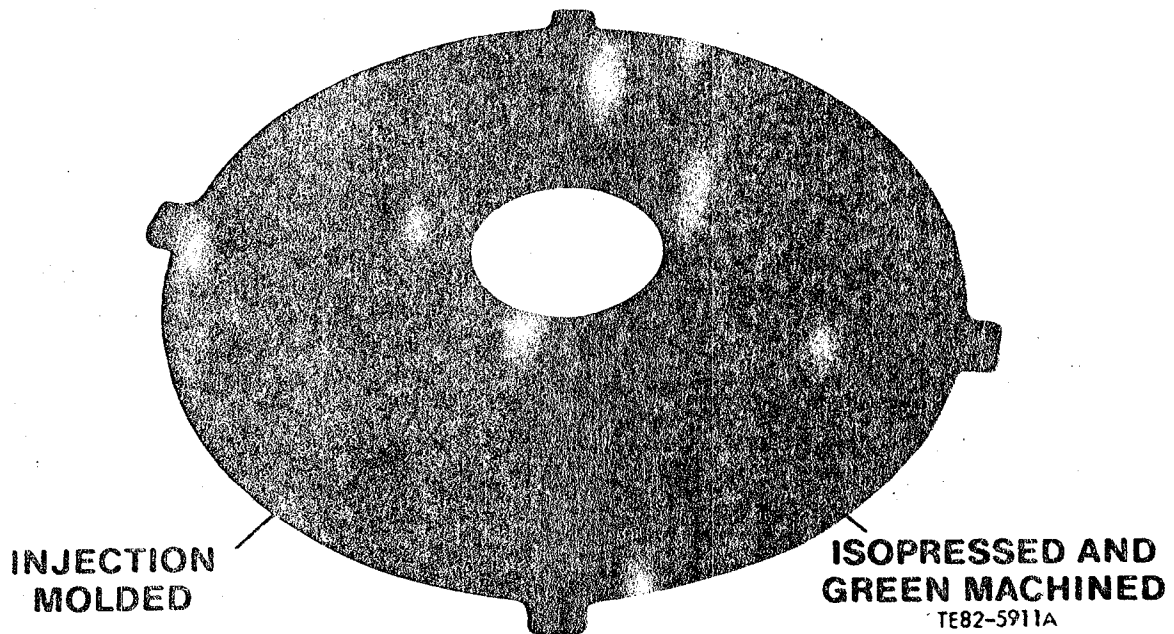


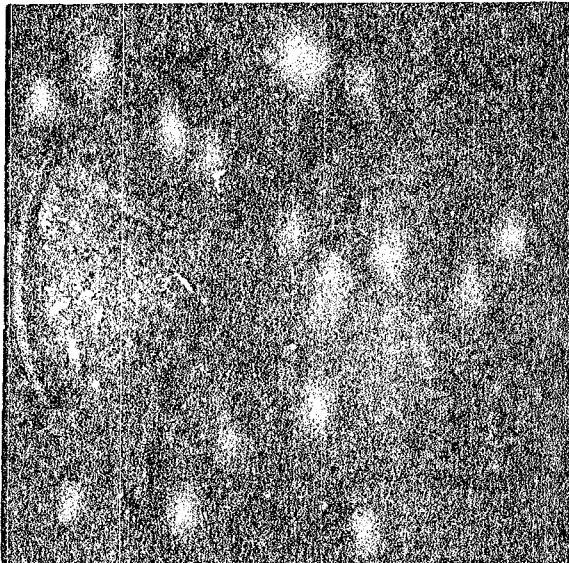
Figure 10. Gasifier backplates.

lb) in the AGT 100 engine. The vane pocket holes in the outer backplate are ultrasonically machined after sintering.

AGT 100 SEAL PLATFORM/EXHAUST DUCT

The seal platform/exhaust duct shown in Figure 11 is fabricated by Corning Glass Works from lithium aluminum silicate (LAS code 9458). At a weight of 17.6 lb, this duct, produced by slip casting, is the largest single ceramic component in the AGT 100 engine. After slip casting and sintering, only the bore and flange thickness require final machining to meet dimensional requirements. Nondestructive inspections of these components generally reveal no material discrepancies in high stress regions.

Evaluations of similar LAS 9458 material indicate an average room temperature fracture strength of 12.64 ksi with a Weibull modulus of 12.2. The primary strength-controlling defects observed in these test bars were surface pores. Preliminary elevated temperature tests indicate that this strength level is maintained to a temperature of 2192°F, although some plastic deformation was observed at this temperature. Further investigations to characterize this phenomenon and to determine the temperature level at which deformation occurs are currently underway.



TE82-6117

Figure 11. Slip cast Corning LAS seal platform/exhaust duct.

Rig and engine experience with these components has been extremely successful to date. All three parts subjected to a mechanical pressure test designed to simulate pressure differential loads at engine maximum power operation have passed, and the LAS seal platform/exhaust duct installed in the first AGT 100 engine build encountered no difficulties.

AGT 100 INSULATING SHIM DEVELOPMENT

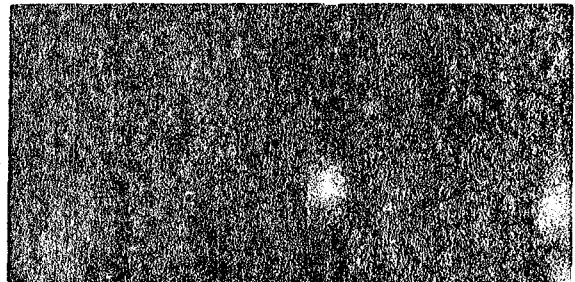
The use of structural ceramic components in the hot flow-path section of the AGT 100 engine, while allowing higher turbine temperatures to be employed, generates a need for insulating shims as a thermal barrier between these ceramic components and adjacent metal support structures. Zirconia (ZrO_2) is considered a leading candidate for insulating applications because of its refractoriness and low thermal conductivity.

The insulating shims shown in Figure 12 were produced by the AC Spark Plug Division of General Motors. The material is an isopressed and green-machined fine-grain partially stabilized zirconia (PSZ) consisting of both cubic and monoclinic phases. It is a derivative of the material used for the production oxygen sensor on all recent GM automobiles.

The average room temperature fracture strength measured on longitudinally ground bars is 49.80 ksi. The strength for the as-fired surface condition is 45.69 ksi. Fractures primarily originate from small pores for both surface conditions.

Preliminary elevated temperature tests indicate that this strength level is essentially maintained to a temperature of 1832°F. The thermal expansion and heat conducting capacity, of particular interest in thermal barrier materials, measured 3.9 in./in./°F and 0.088 cal/g/°F, respectively, at a temperature of 1472°F.

These insulating shims are being installed in AGT 100 engine build No. 3.



TE82-6118

Figure 12. AC Spark Plug PSZ insulating shims.

Advanced Gas Turbine Ceramic Component Development

G. L. Boyd, D. W. Carruthers,
J. R. Kidwell, and D. W. Richerson
Garrett Turbine Engine Co

ABSTRACT

The Garrett Ford AGT101 Program has progressed through initial design, fabrication, and first generation aerodynamic component tests, and currently is focused on engine test bed development and ceramic component development. Design A ceramic components of excellent visual quality have been received from the AiResearch Casting Company, Carborundum Company, Corning, Ford, and NGK. These components are being qualified for engine testing through a sequence of evaluations that include bulk density, NDE, dimensional inspection, visual examination up to 40x magnification, selected mechanical and thermal screening tests, and static structure rig tests.

Individual static structure ceramic components have been qualified up to 2100°F in thermal screening tests. The complete ceramic static structure, consisting of 49 components, has successfully been tested under cyclic conditions in the static structure test rig to the Mod I design conditions of 1600°F.

A bladed rotor, fabricated cooperatively by AiResearch Casting Company and Ford Motor Company, has been spin tested at room temperature to 122,000 rpm.

INTRODUCTION

The AGT101 engine test bed (Figure 1) was specifically designed around use of ceramic components in the hot flow path section. Except for the regenerator flow separator housing, all ceramic components are symmetrical; this provides a more uniform stress distribution and eases manufacturing.

AGT101 development, depicted in Figure 2, begins with a 1600°F turbine inlet temperature version. Testing of the 1600°F engine test bed is well underway using metallic structures. Initially, qualified ceramic structures will replace the metallic counterparts, beginning the ceramic component development.

Engine test bed development progresses to the

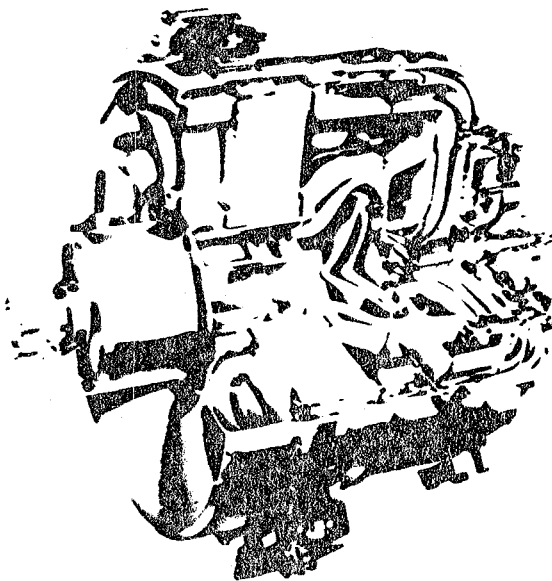


Figure 1. AGT101 Power Section.

2100°F version utilizing ceramic hot section hardware that will be qualified in separate test rigs. A metallic, dual-alloy turbine rotor will be used in this version.

Finally, the engine is upgraded to the 2500°F version. This is accomplished by introducing the ceramic radial turbine, thus permitting a turbine inlet temperature of 2500°F.

Substantial progress in ceramic technology has been accomplished on the Garrett/Ford AGT101 program during this past three years¹⁻⁴. Progress by ceramic manufacturers has been key to the successful demonstrations made to date⁵⁻⁷. Figure 3 shows a composite of the ceramic structural parts and turbine rotor successfully fabricated to the required engine dimensional envelope and delivered to Garrett for evaluation. All components are evaluated using bulk density measurements, NDE, 40x

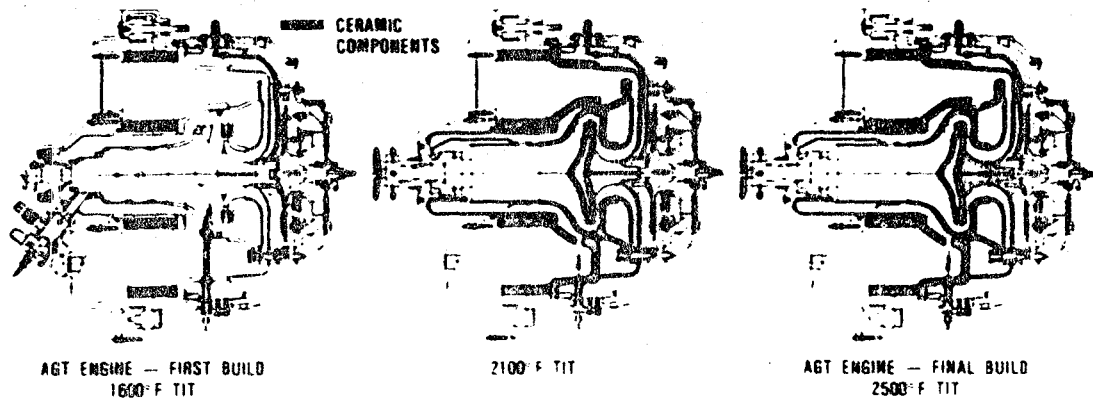


Figure 2. AGT101 Engine Evolution.

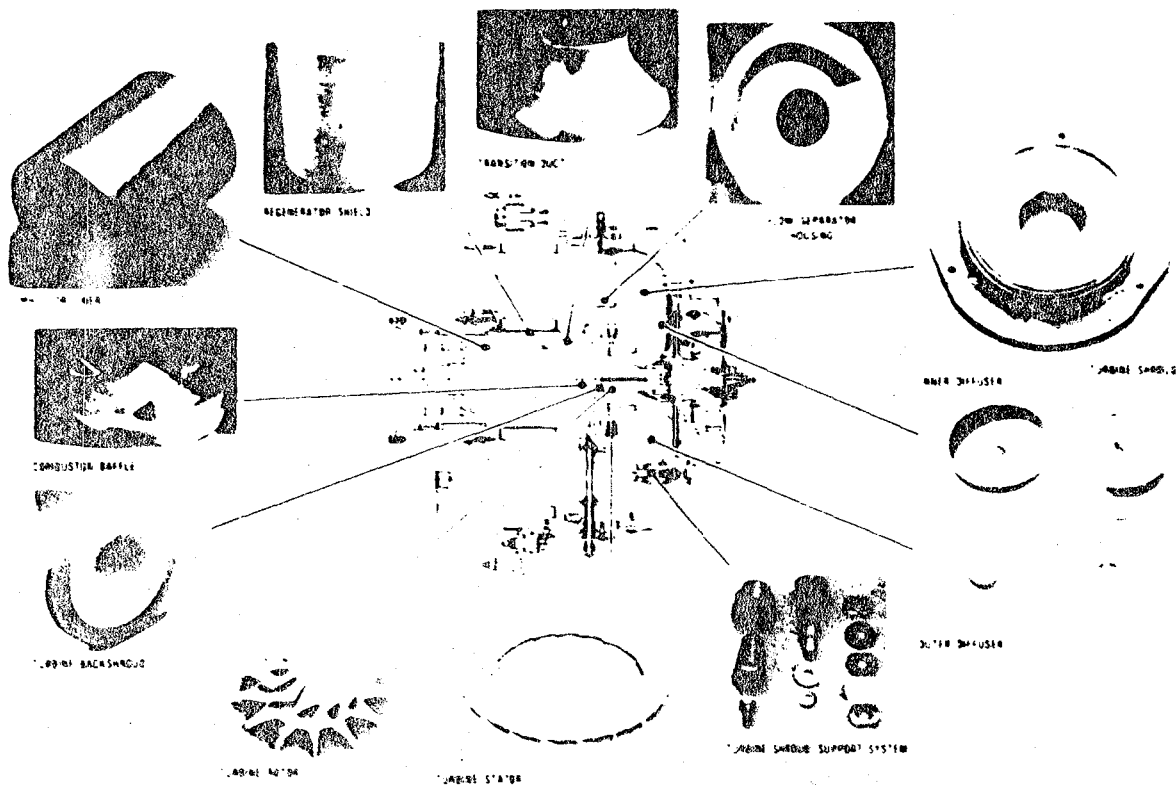
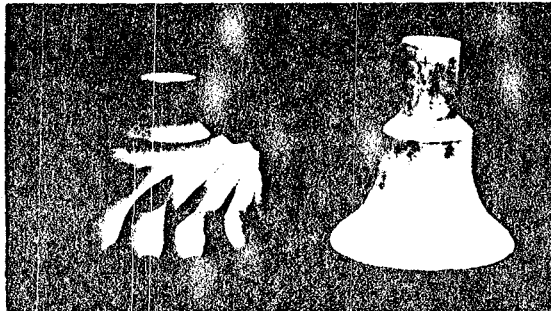


Figure 3. AGT101 Ceramic Parts.

visual examination, and dimensional inspection. Selected components are mechanically and/or thermally screened prior to static structures rig testing. This paper reviews the status of mechanical and thermal screening tests, static structures rig testing, rotor spin testing, and additional work conducted under the AGT101 ceramic component development tasks.

For clarity, the rotor development tasks will be separated from the structures development and will be discussed first.

TURBINE ROTOR DEVELOPMENT - MECHANICAL SCREENING - Cold spin testing of non-bladed and bladed rotors (Figure 4) has been utilized as a method of gauging developmental progress and iden-



BLADED ROTOR SIMULATED ROTOR

Figure 4. AGT101 Turbine Rotor Approach.

tifying strength-limiting flaws to support processing iterations. Initially, non-bladed rotor spin tests were used as a developmental stepping stone for the ceramic manufacturers to concentrate efforts on achieving the necessary material strength and uniformity in the rotor hub. Peak stresses were predicted to be 43 ksi at this condition. Through iterative development, both Ford Motor Company and AirResearch Casting Company (ACC) achieved the design overspeed goal of 115,000 rpm (115-percent design). A Ford sintered reaction bonded silicon nitride non-bladed rotor was spin tested to 134,000 rpm (peak stress 58 ksi) without failure, and an ACC sintered silicon nitride non-bladed rotor was spin tested to 115,000 rpm without failure. Having successfully passed non-bladed rotor spin test goals, both ceramic manufacturers were approved to initiate bladed rotor development.

Efforts during the past year at ACC and Ford have been concentrated on bladed rotor development. Early bladed rotors with visible blade defects were spin tested to evaluate rotor hub integrity. Although portions of blades fractured from these known defects at speeds as low as 79,000 rpm, rotor hub survival to 115,000 and 95,000 rpm was respectively achieved for Ford and ACC rotors. The ACC rotor may have attained higher speed except for a crack, that initiated in the blade, and propagated into the hub. These early spin test results demonstrated that the high hub strength achieved in non-bladed rotors also is being achieved in bladed rotors.

Rotors recently received from Ford and ACC show a marked improvement in blade quality and currently are being prepared for spin test evaluation. A rotor fabricated cooperatively by Ford and ACC has been successfully spin tested to 80,000 rpm and thus, is qualified for initial hot turbine rig testing. A similar rotor (Figure 5) was spin tested to failure at 102,000 rpm exceeding the maximum design speed of the AGT101.

TURBINE ROTOR DEVELOPMENT - THERMAL SCREENING TESTS - Following successful cold spin testing, the turbine rotor will be thermally screen tested to evaluate blade integrity. A simple, hot turbine test rig (Figure 6) has been fabricated for this evaluation. The rig utilizes common AGT101-metallic hot flowpath hardware and will be operated

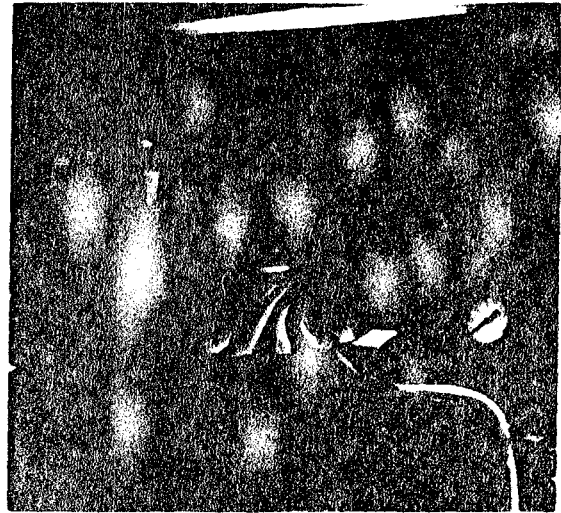


Figure 5. ACC Ceramic Turbine Rotor.

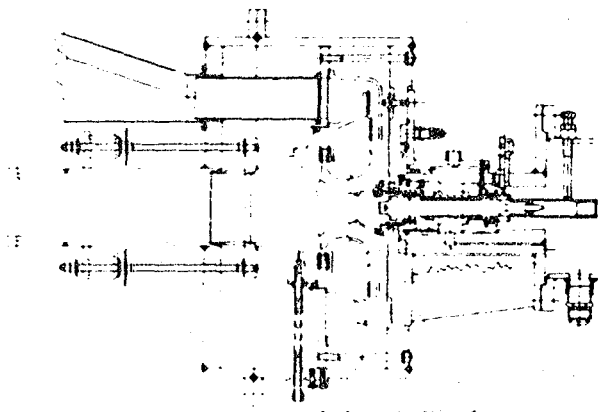


Figure 6. AGT101 Hot Turbine Test Rig.

to simulate a shutdown transient (the worst stress case for blading). Preparations are underway to initiate testing; when successful in thermal screening tests, a rotor then will be qualified to begin engine testing.

STATIC STRUCTURES - MECHANICAL SCREENING TESTS - Selected static components are mechanically tested at approximately 120 percent overstress conditions using either pneumatic or hydraulic pressure⁸. The flow separator housing, regenerator shield, turbine backshroud and turbine alignment bolt system all have been successfully tested. Results of these tests are encouraging and indicate that the quality of hardware received to date is very good; over 90 percent of those tested, have passed.

STATIC STRUCTURES - THERMAL SCREENING TESTS - Analytically, the predicted stress distribution for most static components is largely thermal and peaks during an engine start transient. In an

effort to screen inadequate parts and later thermally map satisfactory hardware for analytical validation, several thermal screening rigs have been designed and fabricated. These test rigs were designed to expose ceramic components to thermal transients up to 2100°F under normal engine start transients. Hot flowpath geometry is simulated and an AGT diffusion flame combustor supplies heated air to the rig. Engine mass flow and temperature ramp cycles are simulated during a start transient. Real time temperature, mass flow and acoustic emissions are monitored throughout testing.

To correlate a fracture event to a particular start transient condition (temperature versus time), a real-time fracture sensing mechanism is required. An acoustic emission system has been adapted, consisting of a high frequency response acoustic transducer mounted on a metallic waveguide. The waveguide is inserted through the rig sidewall and is in close contact with the component. During a fracture, a high level of energy is dissipated due to the breaking of material bonds as the crack propagates through the ceramic. This is detected by the transducer as a higher decibel output, than typical background flow noise, plus a large number of acoustic events. Testing to date indicates that acoustic emission can be used to determine ceramic fractures during test, and further, can aid in determining if rig/engine disassembly is warranted following a test sequence. Figure 7 illustrates some comparative characteristics observed during test.

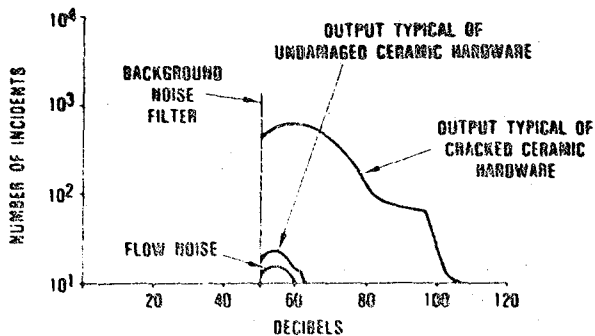


Figure 7. Acoustic Emission Output As Recorded by a Distribution Analyzer.

Thermal screening tests have been conducted on the transition duct/combustor baffle, and turbine shroud/turbine stator/turbine backshroud. An initial test of the turbine shroud alone is conducted prior to assembling the stator and backshroud in this rig.

Testing has been accomplished in two stages. First, a set of components was screened to 1600°F for initial structures rig testing. Subsequently, a second set of components was screened to 2100°F. A minimum of five lightoff cycles to temperature, hold for 3 minutes, and shutdowns were accomplished. Figures 8 and 9 show components qualified for 2100°F structures rig testing.

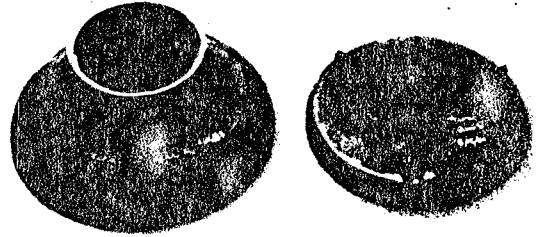


Figure 8. Ceramic Thermal Screening Test (Transition Duct/Baffle, 2000°F Cycles).

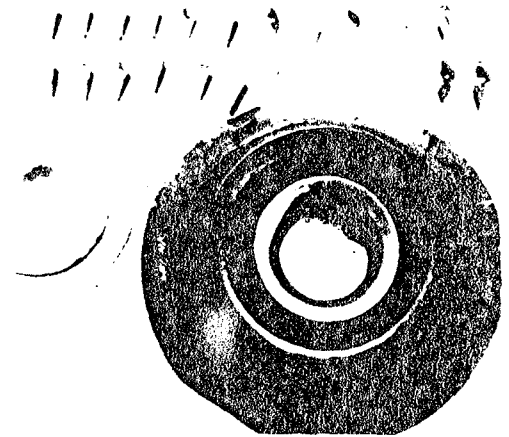


Figure 9. Ceramic Thermal Screening Test (Turbine Shroud, Turbine Backshroud, and Turbine Stators; 2100°F, 5 Cycles).

STATIC STRUCTURES RIG TESTING -

Although a set of components may pass a mechanical and/or a thermal screening test, a more important qualification remains — how does the assembly interact? The AGT101 ceramic structures rig was designed to subject a full complement of static structural components to simulated engine thermal and mechanical loads, transients, and to allow important diagnostic work to be accomplished prior to engine testing. The rig, shown in Figure 10, is essentially an AGT101 engine without a rotating group. The regenerator has been retained such that simulation of the asymmetrical mechanical and thermal loads imposed on the flow separator housing could be evaluated. The high pressure (HP) and low pressure (LP) regenerator flows are independently controlled, and heated LP flow is provided by an AGT101 diffusion flame combustor.

Assembly of the test rig, and later the engine, is depicted in Figures 11 through 18. Starting with

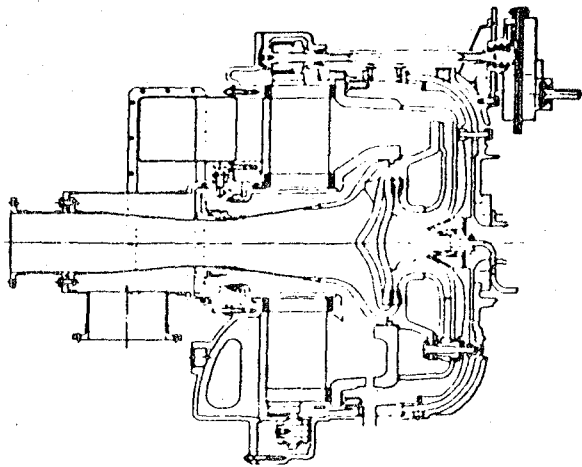


Figure 10. AGT101 Ceramic Structures Test Rig.

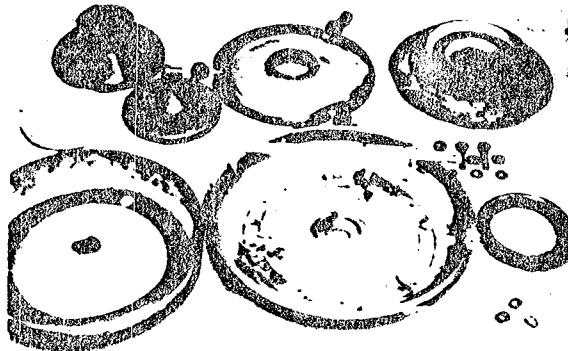


Figure 11. Ceramic Module - Hardware Layout.

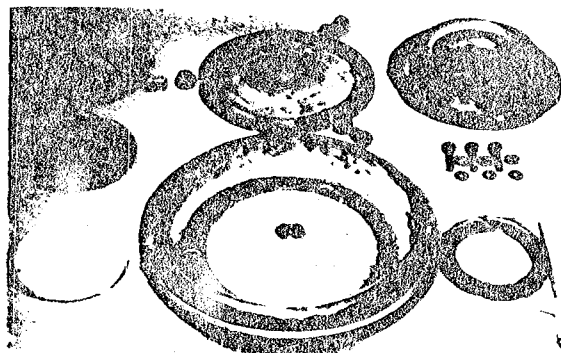


Figure 12. Ceramic Module - Install Inner Diffuser and Spacer.

the metal compressor backshroud, a ceramic module is assembled on the workbench. The module consists of the spacer assembly, inner diffuser housing, rocker assembly, outer diffuser housing, turbine shroud, and ceramic bolt assembly. The concentricity and nor-

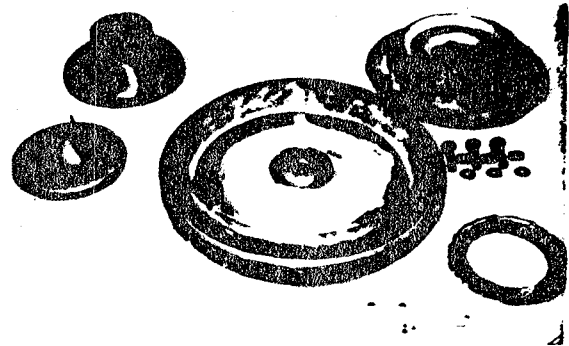


Figure 13. Ceramic Module - Install Outer Diffuser and Rocker Assembly.

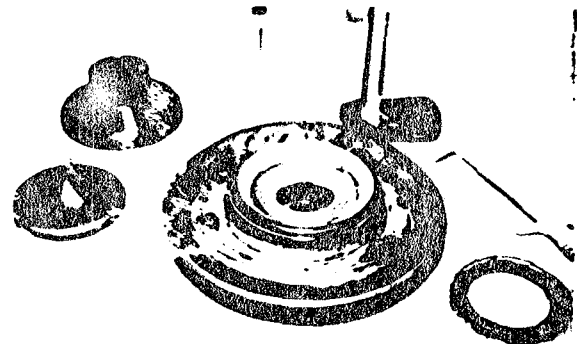


Figure 14. Ceramic Module - Install Shroud and Bolts.

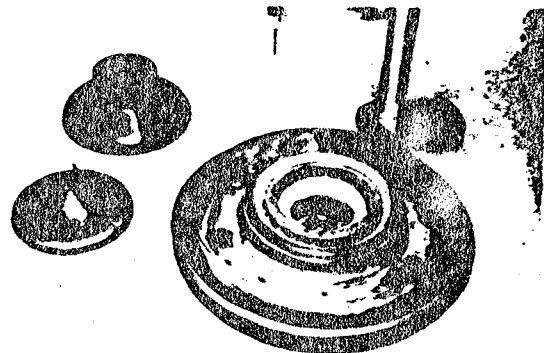


Figure 15. Ceramic Module - Install Segmented Stator.

mality of hardware is checked during build to assure proper fit and to maintain alignment (thus maintaining proper turbine clearance). This module then is installed in the outer casing, and stator vanes, turbine backshroud, combustor baffle and transition duct are installed. Figure 19 shows the rig installed in the test cell. Instrumentation includes thermocouples,

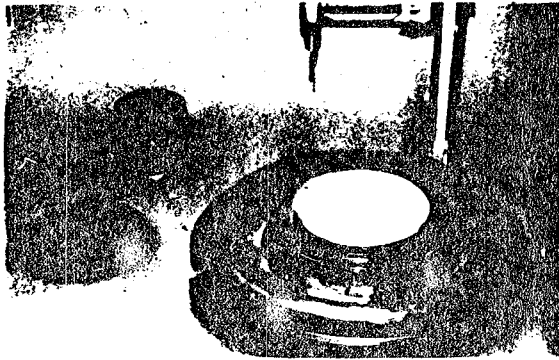


Figure 16. Ceramic Module - Install Backshroud.

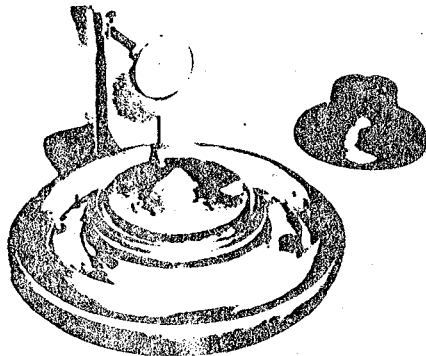


Figure 17. Ceramic Module - Install Combustor Backshroud.

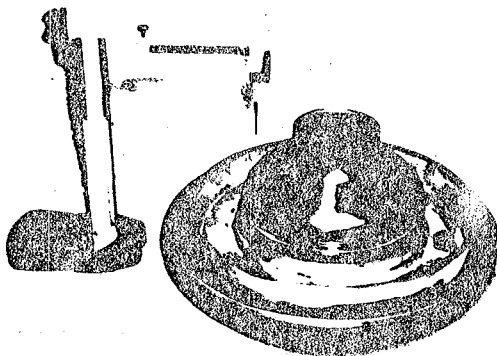


Figure 18. Ceramic Module - Install Transition Duct, Assembly Complete.

pressure transducers, and two acoustic emissions probes: one located on the flow separator housing and one on the turbine shroud alignment bolt.

Several short-lived or aborted test runs occurred prior to achieving stable operation of the test rig. During one such test, a 13-second lightoff to 1400°F was conducted. An excessively high acoustic emission (over 10,000 counts greater than 60 dB)

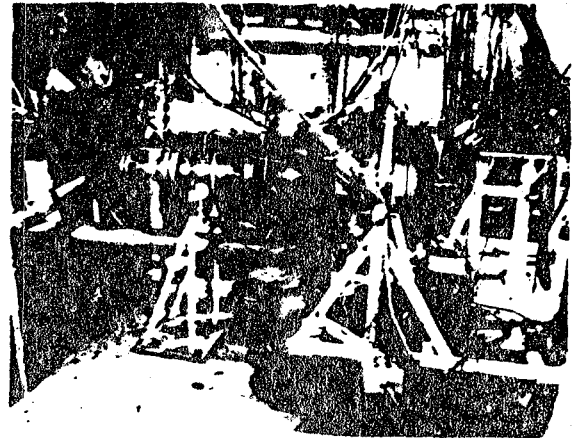


Figure 19. Ceramic Structures Rig Installed in Test Cell.

was noted two minutes into the start, indicating the potential of ceramic component fracture. Disassembly of the test rig revealed a fractured outer diffuser housing as shown in Figure 20. Analysis,

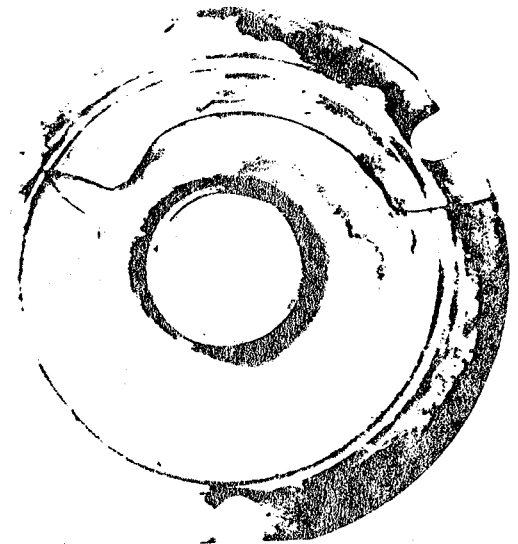


Figure 20. AGT101 Ceramic Outer Diffuser Housing Fractured During Rig Testing.

under the transient cycle performed, showed a peak stress (above 26 ksi) in the region of the fracture. Several corrective options were explored. Similar metal parts for the AGT101 650°F engine had been radially slotted to prevent a hoop stress buildup and subsequent warping. Using this concept, the part was reanalyzed with a 0.050-inch radial slot from the ID to OD; predicted stresses dropped to 3 ksi. In an effort to continue testing, a second part was recon-

figured as stated above. The fact that this "fix" is not permanent and that other solutions do exist (i.e. alternate materials or turbine exhaust diffuser redesign) is recognized. The rig was rebuilt and testing continued.

As shown in Figure 21, a temperature cycle (compressor discharge at idle) to 1600°F (simulated

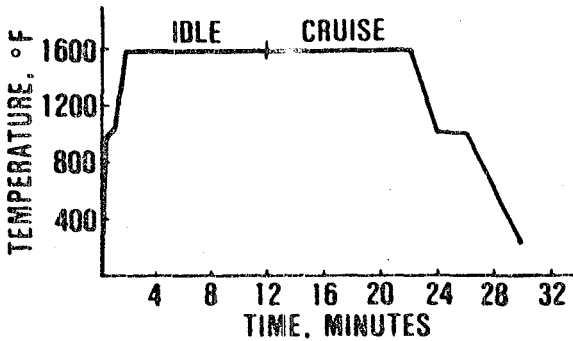


Figure 21. Ceramic Structures Rig Test Cycle.

TIT) was achieved over a 120-second time span. Mass flow was maintained at 10 lb/min (idle condition). This condition was held for 10 minutes; then was increased to 50 lb/min (cruise) while holding 1600°F TIT for 10 minutes; the system then was shutdown.

The 49 ceramic components were subjected to fifteen thermal cycles as described above without incident. The unit was removed from the test cell and disassembled. All ceramic components were undamaged and qualified for initial engine test and evaluation at 1600°F. This is the key initial step in ceramic component development and begins to demonstrate viability of the AGT101 design.

INTERFACE TESTING - In conjunction with ceramic component tests, an interface compatibility study currently is being conducted. All interface conditions for the AGT101 have been identified, as shown in Figure 22, along with respective stress and

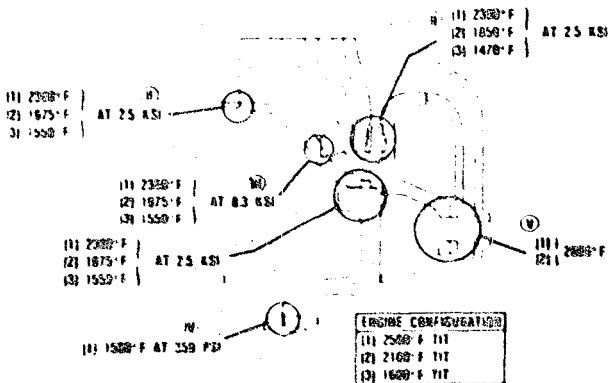


Figure 22. Interface Compatibility Testing.

temperature environments for the three engine operating conditions (1600, 2100 and 2500°F TIT). To date, the study has partially evaluated interface conditions I, II, and III for all combinations of material choices. Test bars of as-machined or as-processed material were stacked with a 0.25 x 0.25-inch contact area for conditions I and II, and a 0.01 x 0.25-inch contact area for condition III. The specimens were heated to the appropriate temperature while dead weight loaded at a minimum simulated engine assembly load. Once at temperature, additional dead weight loads were applied, as required, to simulate engine aerodynamic or mechanical loads and held for 20 hours. Unloading and cool down followed. The specimens then were inspected for sticking phenomena. Three classifications were assigned: no stick, no reaction (NSR); light sticking (LS) upon cool down, i.e., came apart during handling; and hard sticking (HS), not separable by hand. Concern is raised for LS and HS conditions due to the following:

- o LS - longer exposure may result in hard sticking
- o HS - could result in component fracture if the parts thermally expand or cool down at differing rates

Table I summarizes the testing for interface conditions I, II, and III. Testing at condition III, depicted in Figure 23, was conducted under a constant 9.3-ksi load (engine assembly preload) and results showed no sticking or reaction.

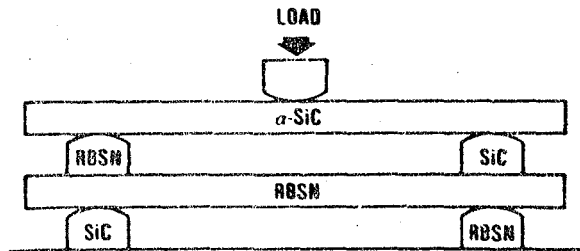


Figure 23. Compatibility Test Condition Number III - Interface Material Combinations.

As noted in Table I, several material combinations result in sticking under conditions I and II. Additional testing was conducted for these combinations using flame-sprayed mullite coating on one interface surface. Preliminary results indicate that no sticking or reaction occurred with flame-sprayed mullite-coated surfaces.

Although additional testing is planned, and warranted, these preliminary results indicate that the AGT101 ceramic development can proceed under the following guidelines:

- o Attention must be given to material combination selection
- o Coated α -SiC or RBSN can be used for selected interface combinations

Table 1. Ceramic Interface Test Summary

Material Combination	Interface ¹ I			Interface ¹ II			Interface ² III		
	1470°F	1850°F	2150°F	1550°F	1970°F	2300°F	1550°F	1970°F	2300°F
1	-	-	-	NSR	NSR	NSR	NSR	NSR	NSR
2	-	-	-	NSR	NSR	NSR	NSR	NSR	NSR
3	-	-	-	HS ³	HS ³	HS ³	NSR	NSR	NSR
4	-	-	-	NSR	NSR	HS ³	-	-	-
5	-	-	-	NSR	NSR	NSR	-	-	-
6	NSR	NSR	NSR	-	-	-	-	-	-
7	NSR	NSR	HS/Chip	-	-	-	-	-	-
8	-	-	-	NSR	Disk	NSR	NSR	NSR	NSR
9	-	-	-	NSR	Disk	NSR	-	-	-

¹ Evaluated at 0.2, 1.1, and 2.5 ksi
 NSR = No stick or reaction
² Evaluated at 8.3 ksi, crowned
 HS = Hard Stick
³ Mullite coated - NSR
 LS = Light Stick
 Disk = Discolored

Material Combination	Interface		
	I	II	III
1 RBSN/RBSN		X	X
2 RBSN/α-SiC		X	X
3 α-SiC/α-SiC		X	X
4 α-SiC/SiSiC		X	
5 SiSiC/RBSN		X	
6 RBSN/LAS	X		
7 LAS/α-SiC	X		
8 α-SiC/SN-50		X	X
9 SN RBSN		X	

Test Cycle
 Heat at 0.2 ksi
 Load
 Hold 20 Hrs
 Unload
 Cool at 0.2 ksi

- o Detailed inspection after test will be conducted to ascertain problem areas
- o Crowned surfaces appear to help in alleviating sticking phenomena

TURBINE ROTOR SHAFT ATTACHMENT - The ceramic turbine/coupling attachment study also has shown very encouraging results. A concept using a double-walled cylindrical coupling, shrunk fit on the ceramic turbine rotor shaft, has been evaluated under cyclic thermal testing. Results of these tests indicate that the ratcheting phenomena can be predicted and controlled. IN907 material was selected for the coupling due to low thermal expansion characteristics and strength properties at higher temperature. A 0.0045 to 0.005-inch diametral interference fit is used to affix the coupling to the ceramic turbine shaft.

A series of tests have been conducted on specimens in a furnace. The specimens (ceramic stub shaft/coupling) were subjected to thermal cycles from below 300 to over 1000°F. After 200 cycles, total movement was 0.0006-inch aft (toward the turbine). An additional 150 cycles currently are being conducted to verify initial test results.

Following the second test series, the coupling will be assembled on the turbine rotor for hot turbine rig testing. These test results then will be assessed and used to qualify a ceramic rotor for engine evaluation.

SUMMARY - AGT101 ceramic component development has progressed from the design and process fabrication phase to screening evaluation and initial feasibility rig testing. Significant accomplishments achieved during the last year include:

- o Ceramic bladed turbine rotors have been spin tested to greater than 100,000 rpm, exceeding the maximum speed requirement for engine operation
- o Individual ceramic components have been qualified for 2100°F in the thermal screening test rig
- o A complete set of ceramic static structures consisting of 49 components has been successfully tested under cyclic conditions in the structures test rig to 1600°F—this set now is ready for engine testing.

Achievement of these accomplishments continues to demonstrate the feasibility of the Garrett/Ford single-shaft, single-stage engine, from the standpoint both of design and materials.

ACKNOWLEDGEMENTS

The authors would like to thank DOE and NASA for support of this work under contract DEN3-167. They would also like to thank the individuals at AiResearch Casting Company, Carborundum Company, Corning, Ford Motor Company, NGK, and Pure Carbon for their efforts which have yielded substantial ceramic component fabrication progress.

REFERENCES

1. "Advanced Gas Turbine (AGT) Powertrain System Development for Automotive Applications", Progress Report No. 1, October 1979-June 1980, DOE/NASA/0167-80/1, NASA CR-165175, November 1980.
2. "Advanced Gas Turbine (AGT) Powertrain System Development for Automotive Applications", Progress Report No. 2, July 1980-December 1980, DOE/NASA/0167-81/2, NASA CR-165329, July 1981.
3. "Advanced Gas Turbine (AGT) Powertrain System Development for Automotive Applications", Progress Report No. 3, January 1981-June 1981, DOE/NASA/0167-81/3, NASA CR-167901, December 1981.
4. "Advanced Gas Turbine (AGT) Powertrain System Development for Automotive Applications", Progress Report No. 4, July 1981-December 1981, DOE/NASA/0167-82/4, NASA CR-167983, July 1982.
5. Storm, R.S., "Net Shape Fabrication of Alpha SiC Turbine Components", presented at the Automotive Technology Development Contractors Coordination Meeting, Dearborn, Michigan, October 26-29, 1981.
6. Mangels, J.A., "Sintered Reaction-Bonded Si₃N₄ for the AGT 101 Turbine Rotor - An Update", presented at the Automotive Technology Development Contractors Coordination Meeting, Dearborn, Michigan, October 26-29, 1981.
7. Styhr, K., "Fabrication of Silicon Nitride Turbine Engine Components", presented at the Automotive Technology Development Contractors Coordination Meeting, Dearborn, Michigan, October 26-29, 1981.
8. Kreiner, D.M. and D.W. Richerson, "Advanced Gas Turbine Ceramic Component Development", presented at the Automotive Technology Development Contractors Coordination Meeting, Dearborn, Michigan, October 26-29, 1981.

Ceramic Technology Progress Report - DOE/AMMRC Ceramic Materials Program

R. Nathan Katz and Edward M. Lenoir
Army Materials and Mechanics Research Center

ABSTRACT

During the past seven years, AMMRC has been actively engaged with the Department of Energy and its predecessor organizations, in building a ceramic materials technology base aimed at the vehicular gas turbine. The focus of this work has been the various DOE, Advanced Gas Turbine (AGT) efforts. Figure 1 lists several of the significant achievements attained both in-house at AMMRC and on contract, under DOE/AMMRC Interagency Agreement IAG DE-AE-101-77-CS51017. Many of these achievements are currently contributing to the AGT programs.

However, as the AGT programs near demonstration, the window for supporting materials research and development to impact these programs is closing. Accordingly, AMMRC and the DOE, Office of Vehicle and Engine R&D have decided that it is appropriate to redirect the AMMRC efforts to contribute to a more generic ceramic materials technology base aimed at both the gas turbine and diesel, for both light and heavy duty application.

MAJOR ACHIEVEMENTS UNDER THE DOE/AMMRC IAG
• INITIAL TECHNOLOGY ASSESSMENT ON CERAMIC MATERIALS AND COMPONENTS FOR SMALL AUTOMOTIVE GAS TURBINES - 1975
• INITIAL DEMONSTRATION OF N_2 OVER PRESSURE SINTERING OF Si_3N_4 - 1979
• DEVELOPMENT OF RAPID HIGH-RELIABILITY LOW-COST TEST PROCEDURES TO MEASURE LIFE DEPENDENCE OF CANDIDATE ENGINE CERAMICS - 1977
• DATA BASE ON LIFE DEPENDENCE OF Si_3N_4 CERAMICS - 1977 TO 1980
• DEVELOPMENT OF TWO-STEP SINTER AND MODERATE PRESSURE COLD-CHAMBER HIP TECHNIQUE - 1980
• FIRST TENSILE STRESS-RUPTURE DATA BASE FOR FULL DENSITY Si_3N_4 AND SiC - 1979 TO 1982
• ADVANCED PROCEDURES FOR STATISTICAL DATA EVALUATION AND LIFE PREDICTION - 1979 TO 1982

Figure 1

This presentation will outline our future plans, under the continuation of IAG DE-AE 101-77 CS51017, which address the above goals.

FY83 PROGRAM DIRECTIONS

During the coming year, AMMRC, in close coordination with the Oak Ridge National Laboratory, the NASA-Lewis Research Center, and DOE's contractors, will carry out R&D which exploits the technology base previously developed, is consistent with the available resources, and addresses pacing ceramic materials technology issues for advanced engines.

As outlined in Figure 2, the DOE/AMMRC Ceramic Materials Technology Program for FY83 will encompass 5 tasks. The life prediction, sintered Si_3N_4 , and time-temperature dependence of advanced ceramics tasks will contribute to both future gas turbine and diesel programs. The toughened ceramics task will be dedicated to diesel engine materials. Support to the IEA implementing agreement will continue to facilitate data exchange and technical communication on ceramic gas turbine programs between the U.S. and the Federal Republic of Germany. We hope that during FY83, that this agreement will be expanded to include other IEA member nations.

During the past year, work was initiated or continued on all five tasks. A large portion of the past year's progress on the sintered Si_3N_4 task is being presented by Pasco and Greshovich in their presentation. Therefore, this presentation will emphasize plans and preliminary progress on tasks relating to life prediction, time-temperature dependence of advanced ceramics, and toughened ceramics.

FY83 DOE/AMMRC PROGRAM DIRECTIONS		
TASK	APPROACH	GOAL
Life Prediction	Continue to Develop Methodology Extend Methodology	Accuracy in Extrapolation Account for New Materials and Failure Modes
Sintered SiC	Continue Development of Sinter and Coatings HIP Technology	Improve Reliability and Properties of Components
Advanced Ceramics	Study Overlapping of SiC Ceramics Continue Development of AlN/CrN SiC/SiC Ceramics	Define Limits of Problem Develop Test Systems for Descriptive Statistics
High Temperature Dependence of Advanced Ceramics	Stress Reliability of New and Improved Ceramics	Screen New Materials and Input into Materials Selection
Support to USA	Continue to Act as Agent for Engineering Agreement	Facilitate Exchange of Information and Experience

TASK I - LIFE PREDICTION METHODOLOGIES

In order to address the goals for life prediction shown in Figure 2, AMMRC's FY82-83 emphasis is on the areas of statistical data evaluation procedures and the determination of failure modes and life prediction parameters of selected materials.

STATISTICAL DATA EVALUATION PROCEDURES - Over the past few years, AMMRC has expended considerable effort to further extend its computer code for statistical data evaluation procedures for six statistical functions; normal, lognormal, Weibull 2, 3, & 4 parameter, and radical, as well as, incorporating non-parametric techniques. For these functions, the code now includes the capabilities listed in Figure 3.

AMMRC COMPUTER CODE STATISTICAL DATA EVALUATION PROCEDURES
• BEST FIT FOR PROBABILITY DENSITY FUNCTIONS - SIX FUNCTIONAL REPRESENTATIONS
• PARAMETER DETERMINATION (MAX. LIKELIHOOD METHOD)
• DATA RANKING OPTIONS
• PLOT ROUTINE
• CENSORED DATA EVALUATION (UPPER AND LOWER TRANSACTIONS)
• A 99% CONFIDENCE AND 8.99% CONFIDENCE DESIGN ALLOWABLES
• NON-PARAMETRIC METHODS
• RELIABILITY COMPUTATION PROCEDURES
• SIGNIFICANT DIFFERENCE OF SMALL DATA SETS
• QUANTILE BOX PLOTTING

Figure 3

During FY82, the AMMRC in-house code was extended to include Robustness and multi-modality procedures. The Robustness procedures are based on Huber's M-estimate method and: obtain outliers in a formal manner; have single and multi-variable capability; do not require the assumption of normality; improve the functional representation of data; and provide improved inferential statistics.

Thus, the AMMRC code is now able to systematically determine outliers, indicate whether or not, multi-modality exists (i.e., mixed mode failure), provide formal determination of best probability distribution fits, and provide confidence limits. In the case of small data sets, numerical simulation procedures are provided to enhance reliability computation.

DETERMINATION OF LIFE PREDICTION PARAMETERS FOR SINTERED SiC - The static fatigue resistance of 1980 vintage, sintered alpha silicon carbide has been assessed at 1200 and 1300°C by stress rupture experiments. Figure 4 shows the results obtained by Dr. Govila at Ford (under AMMRC Contract DAAG-46-77-C0028). To the best of our knowledge, this is the first tensile stress rupture data on sintered alpha silicon carbide. At 1200°C, the loss of strength with time can be modelled on a log stress log time plot by a line with a slope of 1/27. This result is remarkably close to the value of 1/25 obtained by Quinn at AMMRC who utilized four point flexural stress rupture testing. Fractographic examination of samples from both studies revealed that slow crack growth was the mechanism of failure, however, and the n values derived from the slopes should not be interpreted as slow crack growth (SCG) exponents. Nevertheless, life prediction estimates may be made using these slopes as "effective" SCG exponents. That the strength degradation slopes obtained in separate studies of the same material in separate laboratories, using different experimental techniques coupled with the fact that both studies included tests in excess of 1000 hours duration, should give a high degree of confidence to designers.

TASK II - SINTERED SILICON NITRIDE

Figure 5 lists several of the major highlights attained in the DOE/AMMRC sintered Si₃N₄ task. The work under contract at GE has produced a sintered silicon nitride with unexcelled high temperature properties (1). Work on this contract to be performed in FY83 will concentrate on reducing the percentage of the beryllium containing additive (SiBeN₂) while maintaining the materials unique high temperature behavior.

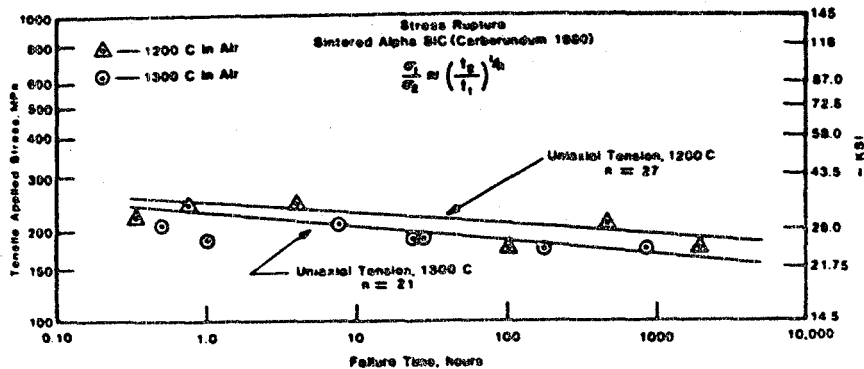


Figure 4 - Tensile Stress Rupture Behavior of Sintered α -SiC, with Inferred SCG Exponent, N (R. Govila, Ford Motor Co.,) - Contract DAAG46-77-C0028

Work recently completed under contract at the University of Washington (2) has provided valuable information on the wetting behavior of liquids in the $Y_2O_3-Al_2O_3-SiO_2$ system on Si_3N_4 . $Y_2O_3 + Al_2O_3$ used as a sintering aid reacts with native SiO_2 on the Si_3N_4 powder to form the liquid glass which enables the $\alpha-Si_3N_4$ solution- Si_3N_4 reprecipitation reaction required to produce high strength material. Thus, understanding the wetting behavior of $Y_2O_3-Al_2O_3-SiO_2$ melts on Si_3N_4 , can aid in obtaining more homogeneous microstructures. It was observed that only liquids in a limited compositional range between 42 Y_2O_3 -38 Al_2O_3 -20 SiO_2 and 67 Y_2O_3 -13 Al_2O_3 -20 SiO_2 produced wetting. The best wetting was obtained with a 60 Y_2O_3 -20 Al_2O_3 -20 SiO_2 composition.

The AMMRC in-house program in FY83 will focus on the use of nitrogen pressures (up to 100 ATMOS) on the sintering and resultant properties of the $Si_3N_4-Y_2O_3-Al_2O_3-SiO_2$ systems. Silica content is adjusted by controlled oxidation of the Si_3N_4 starting powders. Figure 6 illustrates the different oxygen content obtained from four different starting powders as a function of oxidation time. Thus, it can be seen that each different starting material will require a different process to yield an optimal end product. Work performed in FY82 demonstrated that it was not possible to fully densify compositions in the $Si_3N_4-Y_2O_3 + SiO_2$ system at pressures up to 20 ATMOS of N_2 (at 1800 to 1850°C). In FY83 a 100 ATMOS capacity furnace will be available at AMMRC, and it is believed that this pressure of N_2 will be sufficient to obtain full density. Work will also continue on sintering time-temperature-pressure cycles to optimize properties of materials in the $Si_3N_4-Y_2O_3-Al_2O_3-SiO_2$ system.

AMMRC SINTERED Si_3N_4 - TASK HIGHLIGHTS

CONTRACT (DAAG46-81-C-0029):

- N_2 GPS OF Si_3N_4 WITH NON-OXIDE ADDITIVE ($SiBeN_2$)
- ANDR ESSENTIALLY FLAT RT - 1400°C
- UNEXCELLED STRESS RUPTURE AND CREEP BEHAVIOR
- 1400°C OXIDATION 2-3 ORDERS OF MAGNITUDE LOWER THAN HPSN
- AIRSEARCH/GE DEMO OF INJECTION MOLDABILITY AND SINTERABILITY

UNIVERSITY OF WASHINGTON, CONTRACT (DAAG46-79-C-0054):

- DEFINED REGIME WHERE $Y_2O_3-Al_2O_3-SiO_2$ LIQUIDS WET Si_3N_4

AMMRC, IN-HOUSE:

- N_2 GPS OF Si_3N_4 WITH $Y_2O_3-Al_2O_3$ ADDITIONS
- DEMONSTRATED FULL DENSITY AT P_{N_2} AS LOW AS 20 atmos.

Figure 5

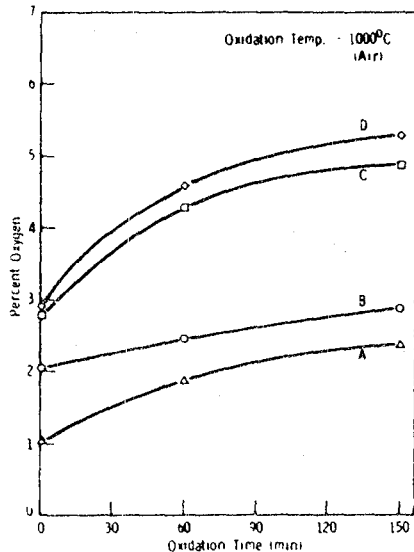


Figure 6

TASK III - TOUGHENED CERAMICS

Because of their unusual combination of properties (E steel, K 1/5 to 1/50 that of Si_3N_4 or SiC, an α steel, MOR 100 KSI, and a high K_{IC} 10), transformation toughened zirconia (TTZ) are leading candidates for cylinder liners, piston caps, head plates, valve seats, etc., for the Adiabatic Diesel engine. These materials are age-hardened ceramic alloy systems and as such they are likely to be susceptible to overaging and loss of strength at long times at high temperatures (i.e., close to the age hardening temperatures). The possibility of overaging with its likely negative impact on materials performance was identified as a critical area of ignorance in the preliminary technical assessment on ceramics for diesel engines presented by AMMRC at last year's CCM meeting (3). Accordingly, a task was initiated to: (a) define the extent and magnitude of the overaging (if any), and (b) develop toughened ceramic alloy systems which would not be susceptible to overaging at temperatures likely to be encountered in advanced diesels (1100-1200°C). The first subtask is being carried out in-house at AMMRC, while the second subtask will initiate this month, at the University of Michigan. Figure 7 gives an overview of the objective and approach of these two subtasks.

TOUGHENED CERAMICS	
SUBTASK I - AGING STUDIES OF TTZ	
P I	SCHICKLER - AMMRC
OBJECTIVE	DEFINE EXTENT OF AGING PHENOMENA, IF ANY
APPROACH	PHASE I - EXPOSE COUPONS FOR VARIOUS "T" AND EVALUATE CHANGES IN PHASE CONTENT, DENSITY, MICROSTRUCTURE, K _{IC} , DIMENSIONS
	PHASE II - EVALUATE MOR AND FAILURE MODE AFTER EXPOSURE
SUBTASK II - TOUGHENED Al_2O_3 BASED CERAMICS	
P I	PROG TIEN - UNIVERSITY OF MICHIGAN
OBJECTIVE	DEVELOP OVERAGING RESISTANT ALLOY SYSTEMS UP TO 1200°C
APPROACH	SCREEN $\text{Al}_2\text{O}_3\text{-Cr}_2\text{O}_3$, $\text{ZrO}_2\text{-MgO}$ ALLOY SYSTEMS SCREEN MULLITE $\text{ZrO}_2\text{-MgO}$ ALLOY SYSTEMS EVALUATE IN TWO PHASES AS IN SUBTASK I

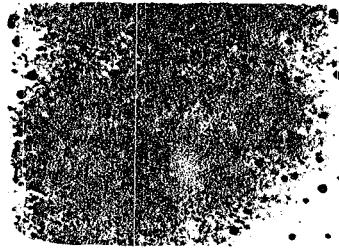
Figure 7

PRELIMINARY RESULTS OF TTZ AGING STUDIES - Five commercial zirconias, of which four are TTZ, are currently undergoing aging studies at AMMRC. As seen in Figure 8, some of these materials show no apparent change in microstructure after 50 hours aging in air at 1300°C while others showed considerable microstructural change (grain coarsening and pore agglomeration). Preliminary results showed that materials doped with Y_2O_3 and produced by sintering in the two phase region are more stable at high temperatures than those doped with MgO and produced by sintering in the cubic region followed by annealing in the tetragonal region. Material N of Figure 8 is an example of the first type of material, while material F is an example of the second.

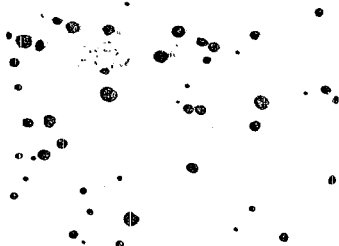
The situation with regard to the other experimental parameters is less clear. While evidence for phase and thus density changes exists, it is not presently clear what portion of this may be attributable to phase transformations occurring during specimen polishing. Future testing on unpolished samples to be subjected to MOR tests should help to resolve this ambiguity.

What can be stated with certainty, however, is that all TTZ's studied thus far, exhibit some degree of phase transformation and microstructural or dimensional change with even brief (50 hour) exposure with no load at 1300°C.

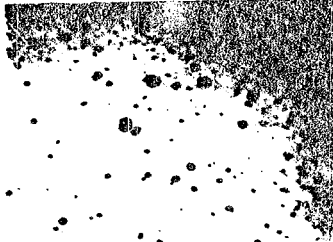
PRELIMINARY RESULTS OF STSR TESTS ON TTZ - Since a major portion of the Task on Toughened Ceramics will entail stepped-temperature stress-rupture (STSR) testing (4), it was decided to obtain early experience in this area by conducting such tests on a proprietary MgO stabilized TTZ. This material is currently under evaluation at AMMRC for a military application. The results of this study, shown in Figure 9, clearly indicate a significant reduction in the load carrying



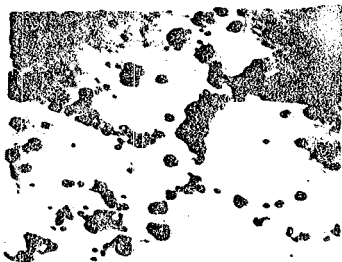
Material N As-Received, 24% Mono Phase



Material F As-Received, 27% Mono Phase



Material N Exposed in Air
1300°C 50 hr 33% Mono Phase

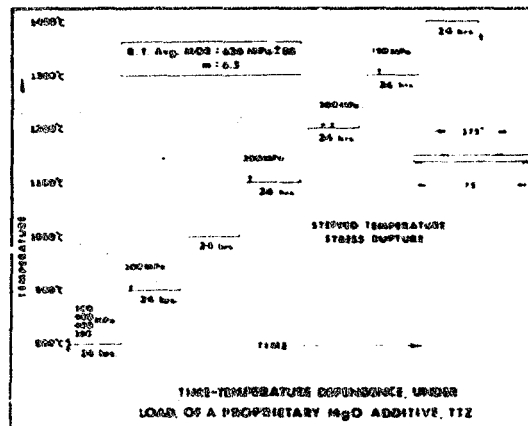


Material F Exposed in Air
1300°C 50 hr 29% Mono Phase

Figure 3 - Microstructural Appearance of Two Commercial Zirconias Before and After Aging

capacity of this material with time at temperatures as low as 800°C (in air). Several conventional stress rupture tests have also been performed. Two S-R tests at 1100°C and 150 MPa load resulted in failure at 205 and 188 hours. Both samples had large permanent deformations and failed in the creep rupture mode (i.e., many cracks on the tensile surface). One sample has continued to surface SR testing in excess of 2300 hours at 900°C and 200 MPa load.

While our preliminary results confirm the validity of our concerns about the aging behavior of TZ, it is important to maintain a balanced perspective. By defining the limitations of these materials, the manufacturers will undoubtedly be able to address and alleviate many of the problems. It should be kept in mind that even at the present state of development there are many applications in Adiabatic Diesel technology for a tough, low thermal conductivity ceramic which has a tensile stress rupture life at 900°C in air and 200 MPa (29 KSI) of over 2300 hours.

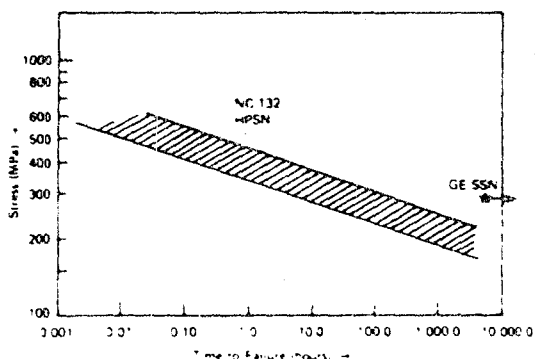


TASK IV - TIME-TEMPERATURE DEPENDENCE OF ADVANCED CERAMICS

During the past year, a task to evaluate the time-temperature dependence of the strength of new candidate heat engine ceramics was re-initiated at AMRC. The effect of pre-oxidation on the stress rupture of fully dense silicon nitride was evaluated in a joint study with the Ford Scientific Research Laboratory (5). It was shown that pre-oxidation at <1250°C can lead to reduced stress rupture life times if the oxide scale is left intact. Stress rupture tests of GE-sintered silicon nitride (Si₃N₄ densification aid) were also conducted. Based on a 1200°C stress rupture test of this material in air at 275 MPa (40 KSI) which has been running for over 5500 hours, this material shows the

potential for high temperature stress rupture life far beyond conventional hot pressed materials (Figure 10).

During the coming year, in addition to S-R evaluations of various TTZ's, new versions of both GE and Carborundum sintered SiC, and GTE sintered Si₃N₄ will be carried out. Where feasible, it is planned to coordinate materials and testing with the Air Force/ITTRI test program to assure maximum commonality of data bases.



FLEXURAL STRESS RUPTURE DATA FOR NC 132 HPSN AND GE SSN AT 1200°C

Figure 1

SUMMARY

The FY83 DOE/AMMRC Ceramic Materials Program is targeted at significantly advancing the state-of-the-art in critical areas of:

- Ceramic Life Prediction Methodology and Data
- New Ceramic Materials Development
- Process Development
- New and Improved Materials Screening

for advanced gas turbine and diesel engine application.

We look forward to reporting significant results in each of these areas at the next Contractor's Coordination Meeting.

REFERENCES

1. Pasco, W. D. and Greskovich, C. D., "Sintered Si₃N₄ for High Performance Thermo-Mechanical Applications", AMMRC TR 82-22.
2. Miller, A. D., "The Wetting Behavior of Yttria-Alumina-Silica Additives for Pressureless Sintering of Silicon Nitride", AMMRC TR 82-23.
3. Katz, R. Nathan and Leno, Edward M., "Ceramics for Diesel Engines: Preliminary Results of a Technology Assessment", presented at DOE Automotive Technology Development Contractor's Coordination Meeting, 28 October 1982, Dearborn, MI (to be published in the proceedings).
4. Quinn, G. D., and Katz, R. N., "Stepped Temperature Stress-Rupture Testing of Silicon Based Ceramics".
5. Quinn, G. D., and Swank, L., "Static Fatigue of Preoxidized, Hot Pressed Silicon Nitride", to be published in the communications of the American Ceramic Society.

Sintered Si₃N₄ for High Performance Thermomechanical Applications

Wayne D. Pasco and Charles D. Graskovich
General Electric Co.
Corporate Research and Development
Schenectady, NY

ABSTRACT

The gas pressure sintering (GPS) process for dense (>99%) Si₃N₄ containing ~7% BeSiN₂ and ~3.5 w/o oxygen as sintering aids was scaled-up to develop a property data base for use in thermomechanical applications at high (~1300°C) temperatures. The fracture strength in 3-pt bend for test bars ~0.6 x 0.6 x 4.5 cm was ~440 MPa (63,700 psi) for a span length of 3.8 cm. There was little drop (<15%) in high temperature strength at 1400°C in air. The creep resistance was outstanding at 1300°C to 1400°C, as evidenced by creep rates of ~4 x 10⁻⁵ h⁻¹ for a stress of 207 MPa (30,000 psi) at 1400°C and ~2 x 10⁻⁵ h⁻¹ for a stress of 345 MPa (50,000 psi) at 1300°C, and a total creep strain of 0.11% for a Si₃N₄ bar exposed for 650 h under an applied stress of 345 MPa at 1300°C in air. The oxidation rates in oxygen were very low and were 7.4 x 10⁻¹³ and 2.1 x 10⁻¹² Kg m⁻² S⁻¹ at 1300 and 1405°C, respectively.

I. INTRODUCTION

GENERAL ELECTRIC CORPORATE Research and Development, under contract with AMMRC (DAAG46-81-C-0029), is developing sintered Si₃N₄ for high performance thermomechanical applications. In a previous contract (DAAG46-78-C-0058) a 2-step gas pressure sintering (GPS) process was developed to yield sintered Si₃N₄ with a density of >99% of theoretical. Typical application of the 2-step GPS process consists of first sintering the sample to closed porosity at ~2100°C under 2 MPa N₂ for ~30 minutes followed by a second step at 1950-2100°C under 6.9 MPa N₂ for ~30 minutes. Those sequences yield Si₃N₄ with a density >99% and weight loss of ~2%. The purpose of this current contract was to scale-up the process to produce test bars (~0.6 x 0.6 x 4.7 cm) to generate a data base for this material. The composition which was studied contained Si₃N₄ + 7% BeSiN₂ + 3.5% oxygen. Another objective of this

contract was to more fully understand the GPS process which is becoming more widely used by other institutions.

II. PROPERTIES OF GPS Si₃N₄

Table I presents a comparison of properties achieved for small (0.2 x 0.2 x 1.9 cm) and large (0.6 x 0.6 x 3.8 cm) test specimens of GPS Si₃N₄. Small specimens were fired in a small high pressure sintering furnace with a 2.5 cm diameter x ~4 cm long hot zone. Large specimens were fired in a large, high pressure sintering furnace with a 9 cm diameter x 10 cm long hot zone.

TABLE I
Comparison of Properties of Small and Large Samples of GPS Si₃N₄

		Small (0.2x0.2x1.9cm)	Large (0.6x0.6x3.8cm)
Modulus of Rupture	25°C	597 MPa(m=8.3)	440 MPa(m=7.8)
	1300°C	553 MPa(m=12.9)	NA
	1400°C	NA	410
	1500°C	NA	279
Creep	1300°C	4.6x10 ⁻⁷ h ⁻¹ (69 MPa)	2x10 ⁻⁶ h ⁻¹ (345 MPa)
	1400°C	6.9x10 ⁻⁶ h ⁻¹ (69 MPa)	4x10 ⁻⁵ h ⁻¹ (207 MPa)
Oxidation	1300°C	1.1x10 ⁻¹² kg ² m ⁻² s ⁻¹	1.4x10 ⁻¹³ kg ² m ⁻² s ⁻¹
	1400°C	NA	2.1x10 ⁻¹² kg ² m ⁻² s ⁻¹
	1500°C	4x10 ⁻¹² kg ² m ⁻² s ⁻¹	NA
K _{IC}		2.9 MNm ^{-3/2}	
YHS (100g load)		~630kg/mm ²	

The room temperature modulus of rupture for the small specimens was 597 MPa with a Weibull modulus (m) of 8.3 as compared to 440 MPa with an m=7.8 for the large specimens. The decrease in strength with increasing size is consistent and in good agreement with stressed volume scaling theory. SEM examination of fracture origins revealed that porous regions <100 μm or inclusions in the bulk are responsible for failure. Improved processing will be required to eliminate these flaws. Approximately 90% of the room temperature strength is maintained up to

1400°C and above that the strength drops rapidly to ~50% of the room temperature strength at 1500°C in air. The oxidation resistance of the GPS Si_3N_4 was extremely low between 1000 and 1500°C. Typically, the parabolic rate constants ranged between 1×10^{-12} and $6 \times 10^{-12} \text{ kg}^2\text{m}^{-4}\text{s}^{-1}$ at temperatures between 1300 and 1500°C in air. The scaled-up material displayed virtually the same oxidation behavior. A thin oxide scale of alpha cristobalite was coherently bonded to the GPS Si_3N_4 and no catastrophic oxidation was observed at 1000°C in air after ~100 hours.

The fracture toughness of GPS Si_3N_4 measured by the microhardness indentation method was $2.9 \text{ MNm}^{3/2}$ and compares with $3.7 \text{ MNm}^{3/2}$ measured for NC-132 Si_3N_4 . The Vicker's hardness number was ~1650 Kg/mm² for a load of 500g.

The creep resistance of GPS Si_3N_4 was excellent and represented by steady-state creep rates of 4.5×10^{-7} and $6.9 \times 10^{-6} \text{ h}^{-1}$ at 1300 and 1400°C, respectively, for an applied stress of 69 MNm^{-2} (10,000 psi). No degradation in creep resistance was observed for the scaled-up material. In fact, a sample of the scaled-up material was stressed at 207 MNm^{-2} (30,000 psi) for 125 hrs at 1300°C, 91 hrs at 1350°C and 51 hrs at 1400°C. The temperature was then dropped to 1300°C and the load was increased to 345 MNm^{-2} (50,000 psi) and specimen survived for 650 hrs without failure, a result not previously demonstrated. The measured creep rate was observed to decrease with time and an average creep was determined to be $2 \times 10^{-6} \text{ h}^{-1}$ at 1300°C with a load of 345 MNm^{-2} . Figure 1 compares the creep rate, $\dot{\epsilon}$, of GPS Si_3N_4 with NC-132. It is apparent that the creep resistance of GPS Si_3N_4 is high. For example, stress rupture testing of GPS Si_3N_4 is currently being conducted at AMMRC by G. Quinn. One sample has been on test for over 5000 h at 1200°C with a load of 275 MPa (40,000 psi) in static air environment. The specimen is still on test and negligible creep (<0.1% strain) has been observed.

The creep mechanism was interpreted in terms of a creep stress exponent of ~2.1, an enthalpy of activation of ~600 KJ/mole. Microstructural observations showed the formation of isolated cavities in the glassy phase pockets at 3-grain intersections in the tensile region of creep specimens. Figure 2 shows that interconnection of these cavities occurs along grain faces as the total creep strain increases.

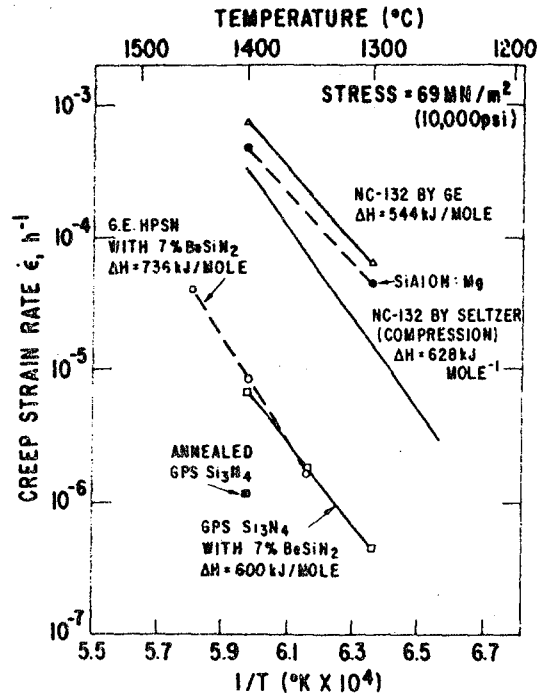


Figure 1 Steady state creep rate vs. $1/T$ for GPS Si_3N_4 and for hot pressed NC-132 Si_3N_4 used as a reference material. The creep data for several other compositions of Si_3N_4 are also plotted. $\text{SiAlON}:\text{Mg}$ (ref.), NC-132 in compression (ref.) and G.E. HPSN with 7% BeSi_2 (ref.).



Figure 2 - Link-up of intergranular cavities that cause grain boundary separation and crack growth in the tensile region of a creep specimen of GPS Si_3N_4 which ruptured at 1400°C after accumulating 0.37% strain. (TEM, mag. = 5,000X).

III. SINTERING OF GPS Si_3N_4

(A) POWDER PREPARATION AND PROCESSING - Batches of sinterable Si_3N_4 were prepared in ~200g amounts using Sylvania SN502 Si_3N_4 and 7 wt% addition of the densification aid, BeSiN_2 (prepared in-house by reacting an equimolar mixture of Be_3N_2 and Si_3N_4 at 1600°C under 2 MPa of N_2 gas). The powder batches were wet processed to yield final powder mixtures having specific surface areas ~10 m^2/g , oxygen contents ~1.8 wt% and other major impurities of Fe (~250 ppm) and Cl (<600 ppm). Powder compacts with relative green densities near 53% were prepared by isostatic pressing at ~200 MPa.

It was found that compacts of the initial composition require ~3 to 4 wt% oxygen for high sinterability. This increase in oxygen content was achieved by controlled oxidation at 1000-1050°C in air. Here, the weight gain of a compact is carefully measured and results primarily from the oxidation of BeSiN_2 and some Si_3N_4 .

(B) EFFECT OF TEMPERATURE IN THE SECOND STEP OF THE GPS PROCESS - In our earlier work a 2-step gas pressure sintering (GPS) process was developed which yielded Si_3N_4 with >99% density. Although the effect of pressure on the densification kinetics during the second step of the GPS process had been investigated, the effect of temperature had not been fully explored. To better understand the second step of the GPS process, a series of ~1g cylindrical specimens (0.9 cm dia. x 1.0 cm high) were fired. The conditions of temperature, pressure and time for the first step were kept constant at 2145°C in 2.2 MPa of N_2 for 30 minutes and yielded a final density of 92.3% and a weight loss of 0.44%. Specimens were fired individually with the parameters of the first step held constant and the parameters of the second step varied, but only with respect to temperature. The pressure was maintained at 2.2 MPa rather than increased and the isothermal soak time was 30 minutes. The soak temperature of the second step, final density and weight loss are summarized in Table II.

TABLE II

Sample #	Second Step T,P,t	ρ_f %	L/W, %
SN502-95-12	No second step	92.3	0.44
SN502-95-13	2145°C, 2.2 MPa, 30 min	93.6	0.83
SN502-95-14	2045°C, 2.2 MPa, 30 min	97.9	0.91
SN502-95-15	1995°C, 2.2 MPa, 30 min	98.7	1.23
SN502-95-16	1955°C, 2.2 MPa, 30 min	99.9	1.77
SN502-95-17	1905°C, 2.2 MPa, 30 min	93.8	2.18

The first step of the process yielded a density of 92.3% at which point closed porosity was obtained. By increasing the hold time from 30 to 60 minutes under the defined conditions of the first step, the density only increased to 93.6% and the weight loss doubled. By maintaining pressure constant and decreasing the temperature, the density reached a maximum of 99.9% at 1955°C. The density decreased as temperature was decreased to 1905°C.

The point to be emphasized is the unusual result of increasing density and weight loss with decreasing temperature. The first step of the sintering process requires heating the specimen containing ~7 wt%

BeSiN_2 and ~3.5 wt% oxygen to 2145°C, in 2.2 MPa of N_2 for 30 minutes. This treatment prevents the thermal decomposition of Si_3N_4 due to high N_2 pressure while permitting a liquid phase of unknown composition to form. The liquid is believed to be a beryllium-silicon-oxynitride initially, which promotes liquid phase sintering. As the Si_3N_4 dissolves, transports through the liquid and precipitates out, the compact densifies and decreases its specific surface area. It is believed that the precipitated β - Si_3N_4 is in fact a β - Si_3N_4 solid solution containing significant amounts of Be and O as confirmed by x-ray analysis. It has been observed that the densification proceeds to a "limiting" density of ~93.6% after 60 minutes at 2145°C. Further increases in temperature may provide additional liquid phase to permit further densification, but probably at the expense of the mechanical properties due to increased grain size.

The sintered specimens shown in Table II were polished, chemically etched and examined with SEM. Figure 3 shows the microstructure of sample SN502-95-12 which had been fired at 2145°C, 2.2 MPa, 30 minutes. This contrasts with Figure 4 which shows the microstructure of SN502-95-13 which had been fired at 2145°C, 2.2 MPa, 60 minutes. The most prominent observation is the large increase in grain size caused by a 60 minute soak over the 30 minute soak. It is believed that the grain growth and concomitant pore coalescence are the cause of the observed "limiting" density (~93.6%) which occurs when the 2145°C isothermal hold is extended to longer times. The increase in grain size indicates that the time and temperature parameters of the first step of the GPS process are important in controlling the final grain size. Figure 5 shows the microstructure of SN502-95-14 which was fired at 2045°C, 2.2 MPa, 30 minutes in the second step and achieved a density 97.9%. The grain size is smaller than that shown in Figure 4 indicating that decreasing the soak temperature in the second step not only increases the fired density but serves to maintain a smaller final grain size. Smaller grain size was observed for sample SN502-95-15 (Figure 6) which was fired at 1995°C in the second step to a density of 98.7% and for sample SN502-95-16 (Figure 7) which was fired at 1945°C to a density of 99.9%. By decreasing the soak temperature in the second step to 1905°C, the density dropped to 93.8% and no further gains were available at lower temperatures.

The reason for the increase in fired density with decreasing soak temperature at constant pressure during the second step of the GPS process is still not fully understood. However, one possibility for the increased densification is the increased solubility of the N_2 trapped in the closed pores with decreasing temperature. If the N_2 solubility in the liquid phase increases with decreasing temperature, then the gas pressure in the pores will decrease and thus remove the barrier to pore closure and densification will proceed. The equilibrium composition of the liquid phase as a function of temperature is not known and therefore only speculation as to composition changes is possible at this time.

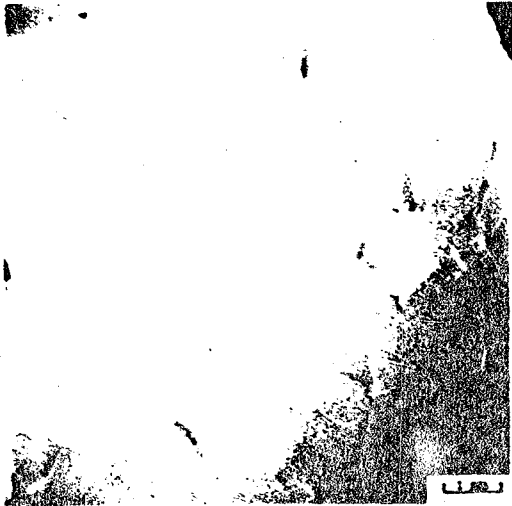


Figure 3 - SEM photomicrograph of sample SN502-95-12 which was fired at 2145°C under 2.2 MPa of N₂ for 30 minutes.



Figure 5 - SEM photomicrograph of sample SN502-95-14 which was fired at 2145°C under 2.2 MPa of N₂ for 30 minutes in the 1st step and 2645°C under 2.2 MPa on N₂ for 30 minutes in the 2nd step.



Figure 4 - SEM photomicrograph of sample SN502-95-13 which was fired at 2145°C under 2.2 MPa on N₂ for 60 minutes.



Figure 6 - SEM photomicrograph of sample SN502-95-15 which was fired at 2145°C under 2.2 MPa of N₂ for 30 minutes in the 1st step and 1995°C under 2.2 MPa for 30 minutes in the 2nd step.

Figure 7 - SEM photomicrograph of sample SN502-95-16 which was fired at 2145°C under 2.2 MPa for 30 minutes in the 1st step and 1955°C under 2.2 MPa of N₂ for 30 minutes in the 2nd step.

C. EFFECTS OF SOAK TEMPERATURE ON DENSITY IN THE FIRST STEP IN THE 2-STEP GPS PROCESS - Sintering experiments were conducted on Batch SN502-100 to determine how low the soak temperature in the first step of the GPS process could be and still obtain closed porosity. It is the sintering time and temperature in the first step which predominantly controls the final grain size of the sintered specimen. From the standpoint of achieving Si₃N₄ ceramics with high modulus of rupture, it is essential to minimize the final grain size. It was anticipated that if closed porosity could be achieved in the first step then the application of high N₂ pressure in the second step would result in pore closure and a high density specimen. Closed porosity occurs at ~92% density and the results of the sintering experiments are presented in Table III.

TABLE III
Effect of Sintering Temperature in the First Step of the GPS Process on Density

Sample #	Temp. °C	Pressure psi	Soak Time min	Rel. Den. %	Weight Loss %
SN502-100-2	2030	120	30	81.3	2.96
SN502-100-3	1980	115	45	81.2	2.93
SN502-100-5	1960	112	60	81	2.92
SN502-100-4	1940	105	90	83	2.90

A sintering temperature of at least 1980°C in the first step was required to obtain closed porosity. A specimen (SN502-100-9) was then fired at 2000°C for 30 minutes under 315 psi of N₂ in the first step and 1945°C for 30 minutes under 1000 psi of N₂. Although the fired specimen had achieved closed porosity in the first step, it did not go to full density upon application of high pressure. It was again observed that the weight loss increased with decreasing temperature in the second step. A series of experiments was conducted wherein the soak temper-

ature in the first step was increased and the conditions in the second step were kept constant at 1950°C for 30 minutes under 1000 psi N₂. The results are presented in Table IV which shows that by increasing the sintering temperature in the first step to 2095°C it is possible to attain a final density of > 99%.

TABLE IV

Sample	1st Step	2nd Step	Rel. Den. %	Weight Loss %
SN502-9	2000°C, 30 min, 310 psi	1945°C, 30 min, 1000 psi	93.0	1.52
SN502-10	2035°C, 30 min, 320 psi	1950°C, 30 min, 1000 psi	96.5	1.76
SN502-11	2060°C, 30 min, 320 psi	1950°C, 30 min, 1000 psi	98.8	1.91
SN502-13	2095°C, 30 min, 330 psi	1950°C, 30 min, 1000 psi	99.1	2.17

It was observed that the soak temperature in the first step must be ~100°C above the temperature at which closed porosity occurs if > 99% density is to be realized in the second step. The reason for this is not totally clear but it is believed to be associated with the amount and/or composition of the liquid phase developing at these high temperatures where no phase diagrams are available.

IV. SUMMARY

Sintering of Si₃N₄ with 7 wt% BeSiN₂ and ~3.5 wt% oxygen additions has been demonstrated to yield densities >99% of theoretical using a 2-step GPS process. The process has been scaled up successfully with no degradation in (1) the modulus of rupture at room temperature or elevated temperature, (2) creep resistance, or (3) oxidation resistance. Sintering studies have revealed that the chemistry of the system is complex and no phase equilibria data is yet available at the temperatures of interest.

V. FUTURE WORK

Future work will continue to address new additives which will enable reduction or elimination of BeSiN₂ from the system. The key issue will be to find an additive which will densify Si₃N₄ and still maintain the excellent properties which have been demonstrated with the BeSiN₂ additive. Other avenues of investigation will be improved processing techniques and a reduction in final grain size in order to increase the absolute strength of these Si₃N₄ ceramics.

ACKNOWLEDGMENTS

This work was sponsored by the Army Materials and Mechanics Research Center under AMMRC/DOE Interagency Agreement EC-76-A-1017-002 as part of the DOE, Division of Transportation Energy Conservation, Highway Vehicle Systems Heat Engine Program and carried out in the Physical Chemistry Laboratory of the General Electric Corporate Research and Development Center, Schenectady, New York, under Contract DAAG-66-81-0029. Mr. George Gazza was the Program Monitor.

The authors would like to acknowledge Dr. R. J. Charles for his overall guidance of the program, D. G. Polensky for considerable help with ceramic processing and heat treatments, C. O'Clair for ceramic processing skills, and the Materials Reactions and Characterization Laboratory for x-ray and microscopy work.

Highlights in the Development of the KTT Automotive Gas Turbine

Sven-Olof Kronogard
United Turbine
Malmo, Sweden

ABSTRACT

To provide some background and orientation, the main features of the KTT (Kronogard Turbine Transmission) System are reviewed and illustrated. Then a few comments are included about component and subsystems development before the Mark I engine and vehicle testing are summarized. The outlook for the Mark II engine is assessed.

FEATURES OF THE KTT SYSTEM

The KTT System is a very compact three-shaft regenerative gas turbine engine closely integrated with a very simple transmission. Fig. 1 is a photograph of the complete engine and transmission - the KTT Mark I engine.

A cross section of the engine-transmission system is shown schematically in Fig. 2. The arrangement is somewhat similar to a free power turbine with the very important exception that a third, auxiliary turbine is added after the power turbine. The auxiliary turbine provides additional torque through the planetary gear set back to the compressor turbine shaft and to the power turbine shaft.

This arrangement provides a number of advantages:

- It eliminates the need for a torque converter and a number of gears. Higher than 2:1 torque multiplication is achieved, hence, higher acceleration rates are achieved; acceleration lag is reduced.
- It leads to a smaller diameter turbine with reduced stresses in all three wheels particularly the high temperature first stage wheel. This allows for early application of ceramic materials in the high temperature turbine wheel. The whole arrangement leads to reduced size and

weight of the whole engine package.

- It moves the torque converter function out of the transmission and into the gas path allowing the recovery of some 80 to 90% of the torque converter losses which are usually dissipated in the transmission oil cooler. Thus, energy losses from the power turbine are recovered both in the auxiliary turbine and in the regenerator (see schematic diagram in Fig. 3).
- It permits more flexibility in the aerodynamic design of the turbines. This, plus use of variable geometry, gives higher efficiency particularly at part load.

Further comparison of the KTT three-shaft system with conventional single and two-shaft systems is given in the schematic sketches in Fig. 4. As indicated by the Roman numerals, there always seems to be the equivalent of three shafts regardless of the configuration. Having worked also with single- and two-shaft engines, it has been readily apparent that the three-shaft engine with the much simpler transmission has always led to a simpler, smaller, or more compact engine-transmission package. Further evidence of this is shown in Fig. 5 where all of the parts of the KTT Mark I engine are compared with all of the parts of a comparable production V-6 piston engine and transmission (taken out of the Volvo). A silhouette comparison of the two engines is shown in Fig. 6.

The fully equipped KTT Mark I engine installed in a standard Volvo 264 automobile is shown in Fig. 7. The size of the engine compartment could be reduced considerably, particularly since no radiator is required.

COMPONENT TEST AND DEVELOPMENT

A photograph of the compressor and diffuser is given in Fig. 8 showing the backswept

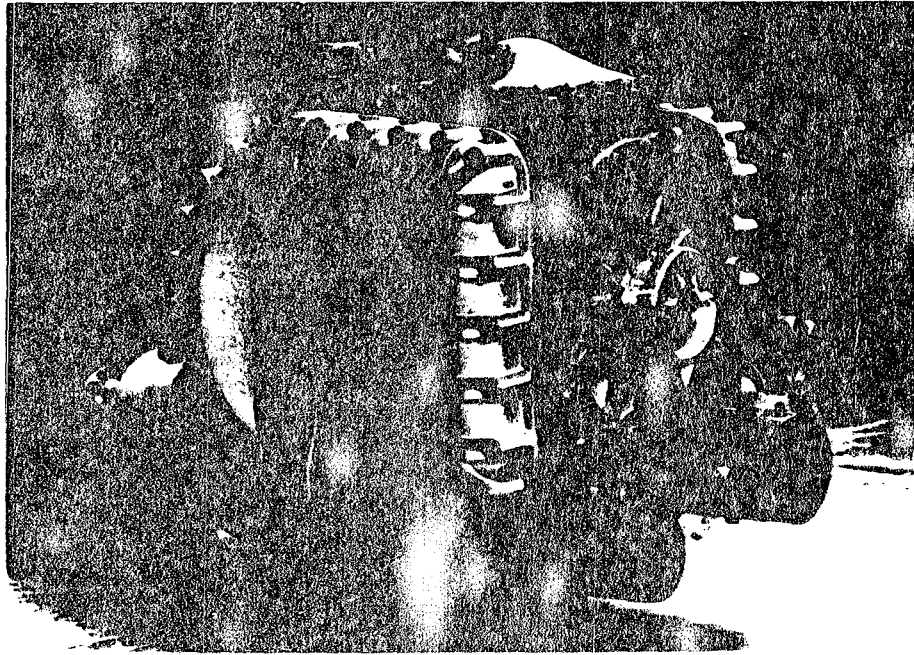
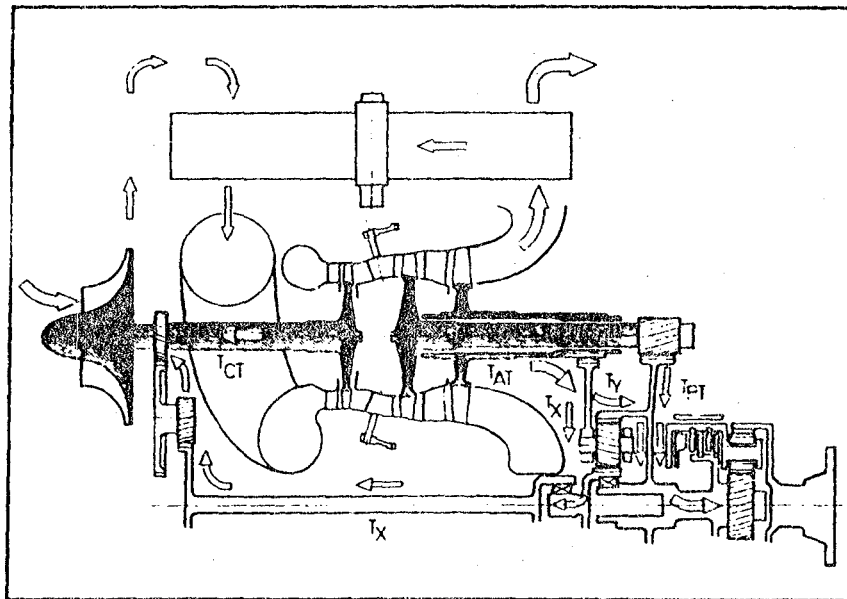


Fig. 1 - KTT Mark I Engine



- T_{CT} - torque from compressor turbine
- T_{PT} - torque from power turbine
- T_{AT} - torque from auxiliary turbine
- $T_{AT} = T_{X+Y}$
- T_X - torque transferred from auxiliary turbine to compressor turbine
- T_Y - torque transferred from auxiliary turbine to power turbine

Fig. 2 - Basic KTT System Configuration

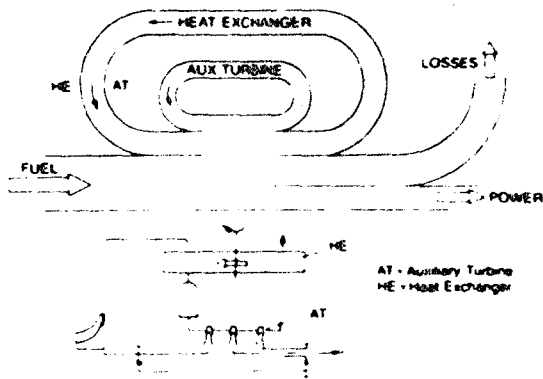


Fig. 3 - Schematic of KTT Dual Energy Recovery

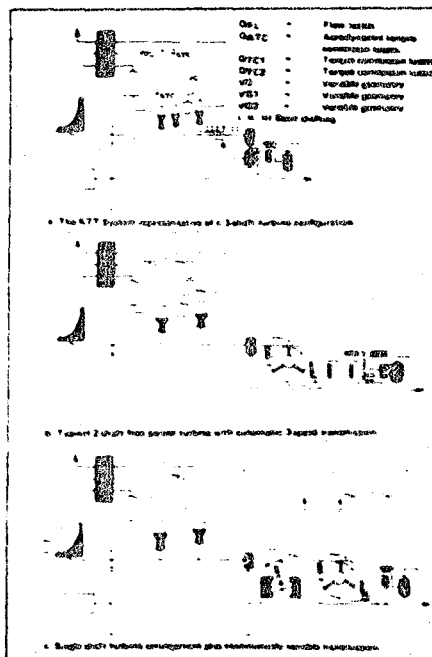


Fig. 4 - Different Automotive Gas Turbine Drive Trains

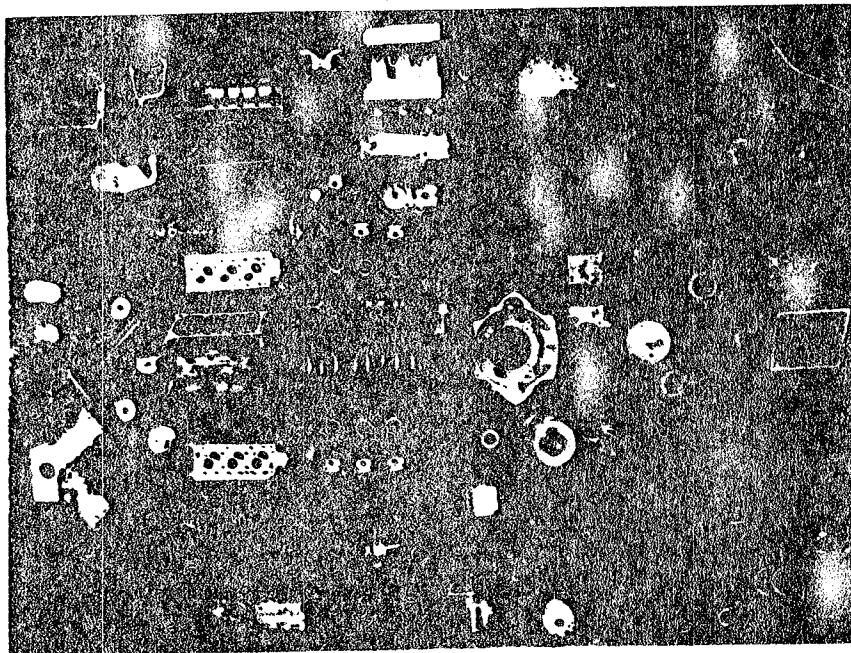
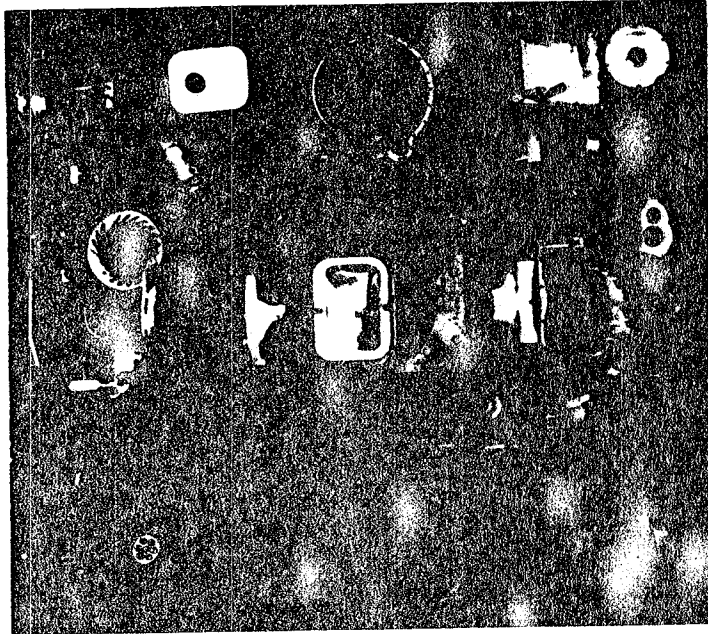


Fig. 5 - Parts of KTT System and of Production
6-Cylinder Piston Engine and Transmission

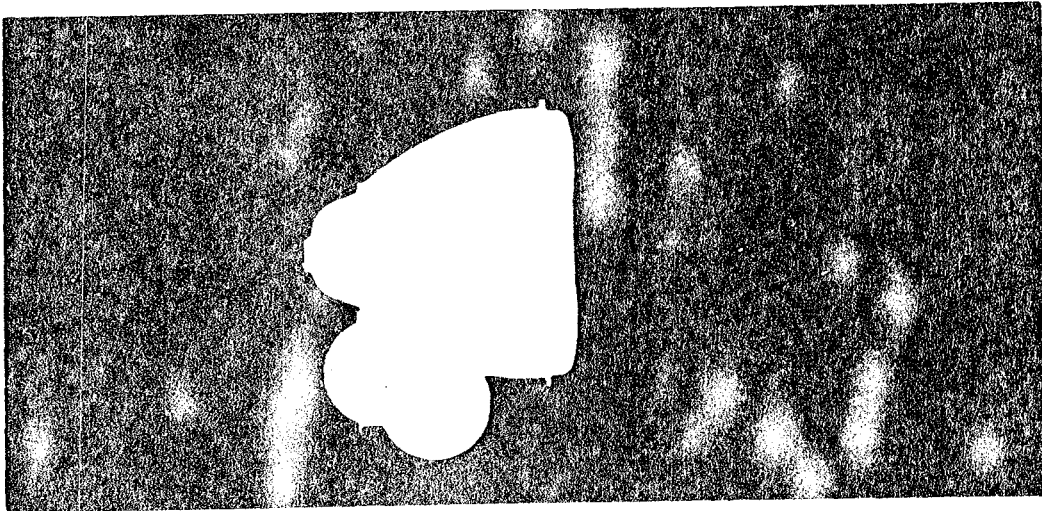


Fig. 6 - Profile Comparison of KTT Mark I
Engine and V-6 Piston Engine

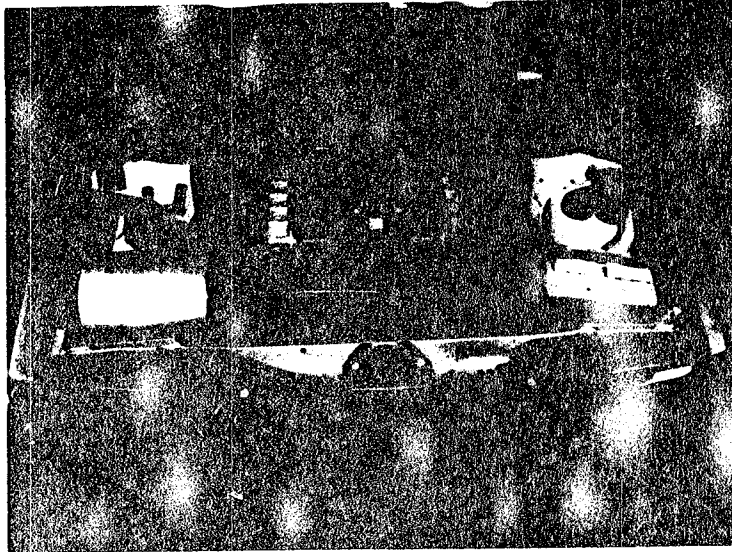


Fig. 7 - The KTT Mark I Engine Installed in a Volvo 264 Automobile

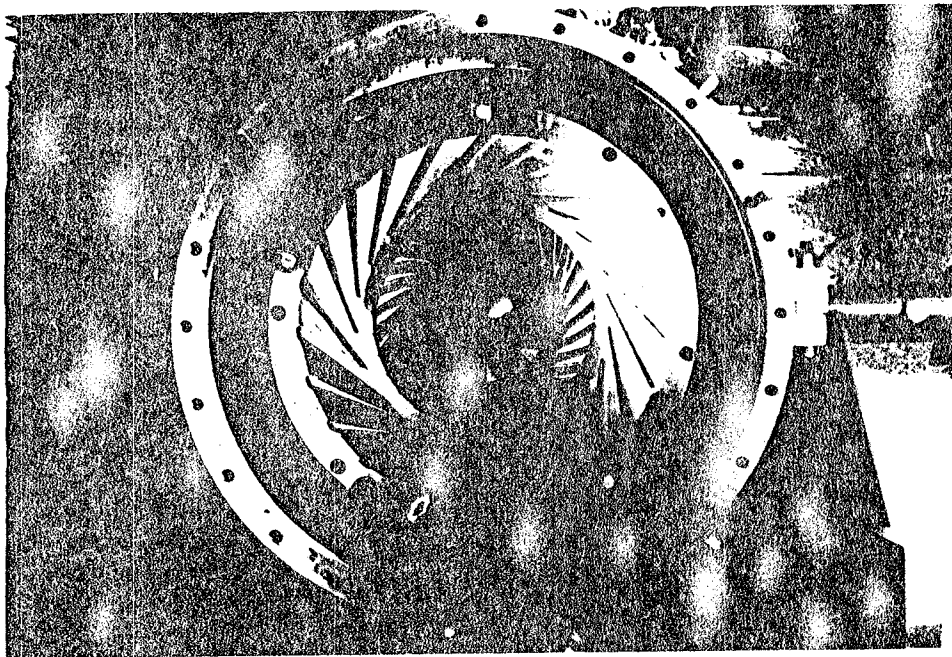


Fig. 9 - Compressor and Diffuser on Test Stand

impeller blades and straight diffuser vanes. Current peak efficiencies are typically in the 80% range (sometimes a few points more; sometimes a few points less) with a wide operating range. Continuous test and development are in progress to further broaden the range and improve part load efficiency.

Much time and effort have been devoted to instrumentation and measuring equipment to determine the details of flow and mechanical behavior in these tiny, very high speed components. Very small probes powered by servo-motors are moved in and out and rotated very precisely to accurately probe the flow in nozzles, ducts, and critical flow passages. Direct high speed torque measurement equipment and techniques were also developed with an English company. Also special test rigs were developed wherein subsystems such as the power turbine and the auxiliary turbine can be run and loaded independently and together, so that complete performance maps can be generated for each component and so that component interactions can be studied. Another test stand called the hot section test rig is set up with a motor and a burner so the speed and temperature of the first stage nozzle and wheel can be varied independently.

Two turbine test wheels are shown in Fig. 9 - one is a forged powder metal Pratt & Whitney Gatorized wheel; the other is a cast wheel. It should be noted that metal component developments are not standing still; there are many interesting improvements emerging. Ultimately, however, it is believed that ceramic materials will be necessary at least in stationary hot section parts. Ceramic material in the rotor is also very desirable. But, even though we have run a ceramic wheel in a turbine powered car, ceramics still have a long way to go.

Ceramics are expected to be used in several areas including: heat exchanger cores, insulation systems (such as that of FOSECO) for housings, ducting, shrouds (for clearance control), nozzles, and burner liners. Fig. 10 shows a KTT rotor system with a ceramic compressor turbine wheel (hot pressed silicon nitride, developed in cooperation with ASEA), a ceramic burner liner (REFEL Si C, developed with BNFL), a silicon carbide (developed in cooperation with Carborundum) nozzle ring, and an injection molded silicon nitride turbine wheel (also with ASEA). Fig. 11 shows two injection molded ceramic wheels, one in the green form (before processing); the other is a hot pressed silicon nitride wheel.

While many of these components are now running or scheduled for test, our efforts have concentrated primarily on the ceramic wheel, methods for fastening the wheel to the shaft, the nozzle ring, and the clearance control shrouds. Ceramic wheel development has evolved from rudimentary simulated wheels to a 24 blade aerodynamic wheel which actually drove the gas generator in the hot test rig, to a 33-blade

wheel which was used for engine test and for the first road tests which took place in February 1982. The car is shown in Fig. 12. With the limited testing to date, we have not experienced a ceramic turbine wheel failure in an engine. Of course in spin pits and test rigs, parts are tested to their limits. A new, 37-blade wheel is being prepared for hot rig testing. It has blading almost identical to that of the metal wheels. With this wheel we should begin to realize the full performance potential of the engine. Although the ceramic material still needs further improvement, it shows considerable promise.

The bar chart in Fig. 13 shows how the stresses, inertia, and size of the first stage turbine in a 3-shaft machine compare with those of a two-shaft machine. A 20 to 30% reduction in stress is possible - even more reduction is possible if compared to a single shaft machine. The reduced size also implies lower cost.

ENGINE AND VEHICLE DEVELOPMENT

The KTT, Mark I engine continues as the primary research and experimental engine for the routine test and development necessary to advance the technology and to demonstrate the integrated behavior of the KTT system not only on the dynamometer, but also in the full scale production vehicle on the chassis dynamometer and on the road. By the end of 1981, the vehicle had covered the equivalent of more than 10,000 miles of operation including more than 2000 miles of actual road tests.

It might be noted that many questions were raised at the beginning of this development about the need for special control elements for the auxiliary turbine and special balancing and vibration control for the three-shaft system. As we suspected, no special or added control elements are needed. The same control as that used for a conventional two-shaft, free power turbine satisfies the requirements. Also no special problems with rotor balancing or vibrations have been encountered. Development has been free of bearing and gear failures. Operation is smooth and automatic.

The KTT Mark II engine represents the next generation of the KTT system and it is expected to be a pre-production prototype. The Mark II contains all of the key features of the KTT system, however, it has many changes aimed at reduced cost, smaller size (down-rated) for a compact vehicle, and higher fuel economy. The closely integrated transmission is aimed primarily for front wheel drive. It includes a differential, but it also provides four-wheel or rear-wheel drive options. It has only one regenerator core. Fig. 14 shows both the Mark I (right) and Mark II engines along with the basic rotor system and a regenerator core. Figs. 15 and 16 show outline and cross-sectional sketches of the KTT Mark II engine. A mock-up of the Mark II is shown in a

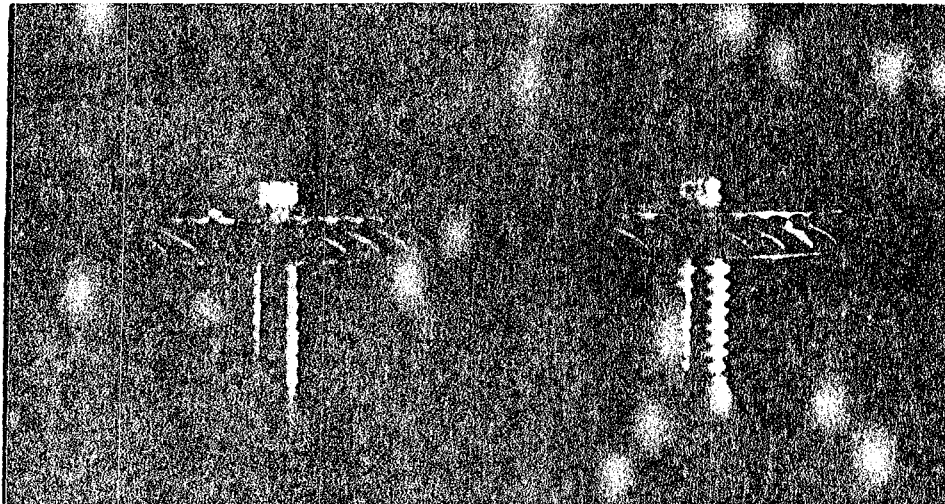


Fig. 9 - Two Turbine Wheels; Left is a Forged,
Powder Metal (Gatorized) Wheel; Right is a
Conventional Cast Wheel (INCO 713LC)

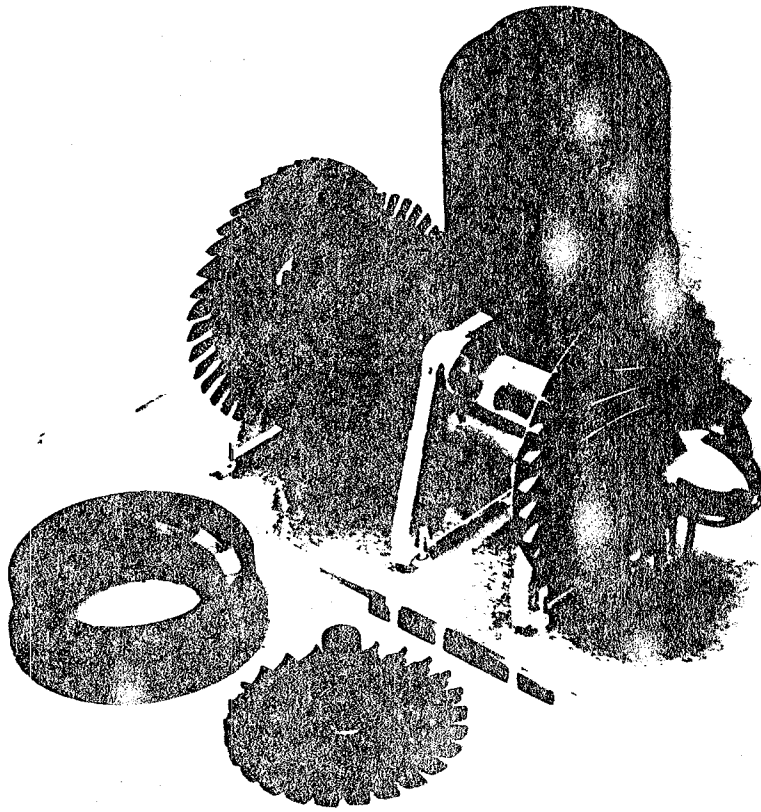


Fig. 10 - KTT Rotor System - First Stage
Turbine Wheel is Hot Pressed Silicon Nitride;
Nozzle Ring is Silicon Carbide; Burner REFEL
Silicon Carbide

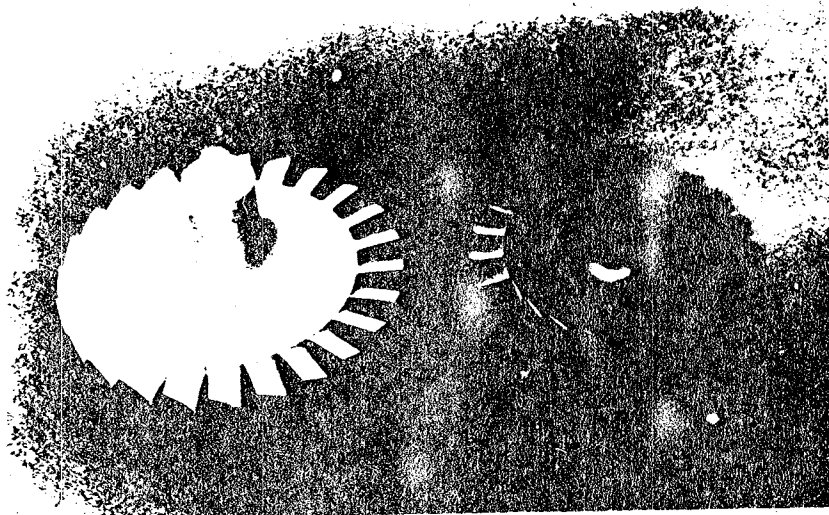


Fig. 11 - Two Turbine Ceramic Wheels; Silicon Nitride in Green Form (Left); and Hot Pressed Silicon Nitride (Right)

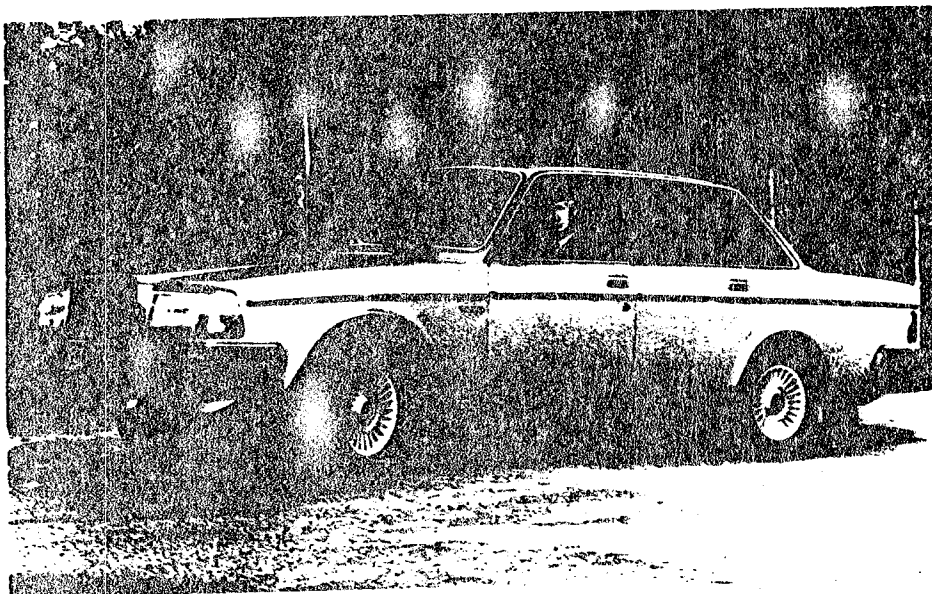


Fig. 12 - Volvo 264 Automobile with KTT Automotive Turbine Installed. This was the first car in the world to operate on the road with a ceramic turbine wheel in the engine.

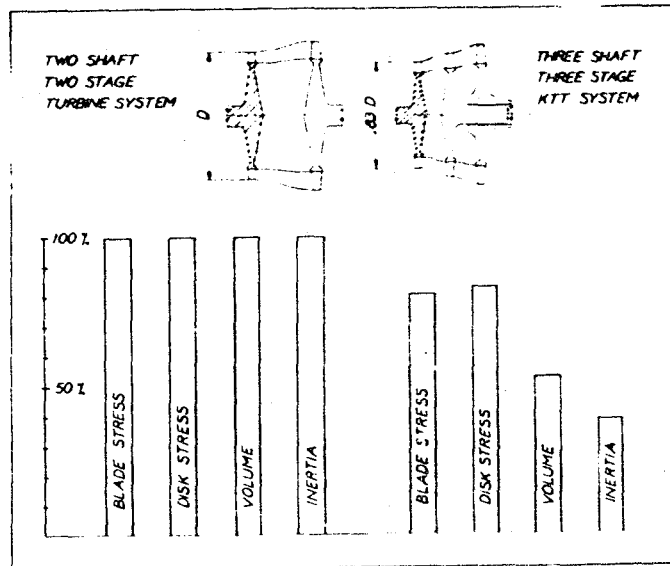


Fig. 13 - Relation Between Turbine Rotor Stress, Volume and Inertia for Two and Three Shaft Systems

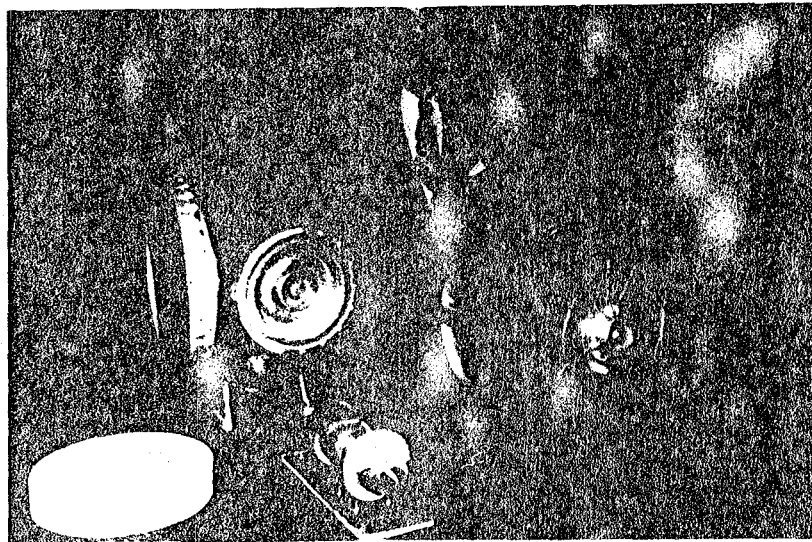


Fig. 14 - KTT Mark I (Right) and KTT Mark II Engines - Rotor System and Regenerator Core in Foreground

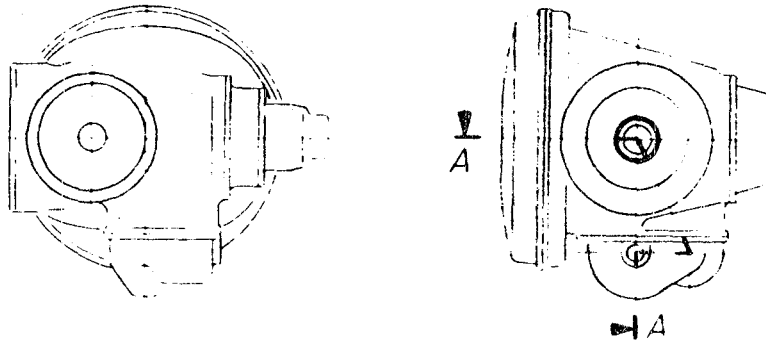


Fig. 15 - KTT Mark II Gas Turbine Engine with Integrated Transmission and Front Wheel Drive

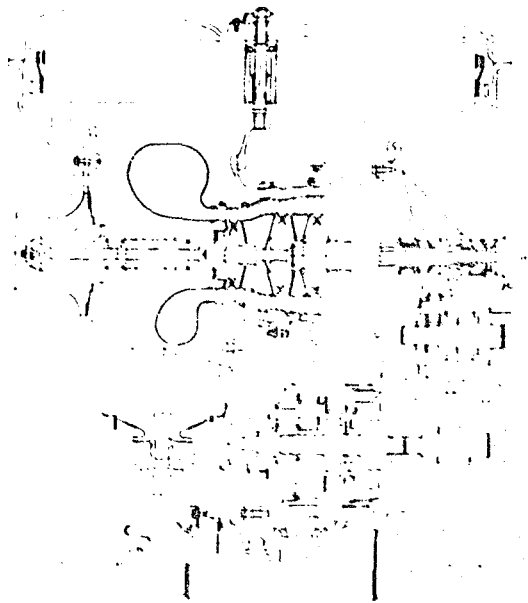


Fig. 16 - Advanced Version of KTT Mark II with Complete Drive Train (Section Line A-A of Fig. 15, H = Horizontal and V = Vertical Sections)

vehicle in Fig. 17. We are about ready to start detailed design of the KTT Mark II engine.

CONCLUSIONS

The KTT System, through close integration of the engine and transmission, leads to a very compact, light-weight, efficient drive train with fewer parts and very favorable torque characteristics. This small power package is compatible with even smaller compact vehicles. Cost estimates to date indicate that this engine will be in the same price class as comparable gasoline piston engines at the same annual production rates. The basic simplicity

and long life characteristics of the turbine engine should result in low maintenance costs. The three-shaft configuration gives high fuel economy, high specific power, and rapid acceleration (due to low inertia). The lower stresses will make it easier to introduce a high temperature ceramic turbine wheel at an early date further enhancing fuel economy. Ultimately the turbine is expected to provide diesel competitive (or better) fuel economy (Fig. 18).

The presentation concluded with a short movie showing operation of the KTT, Mark I engine installation in the Volvo 264 automobile operating in Malmo and surrounding countryside.

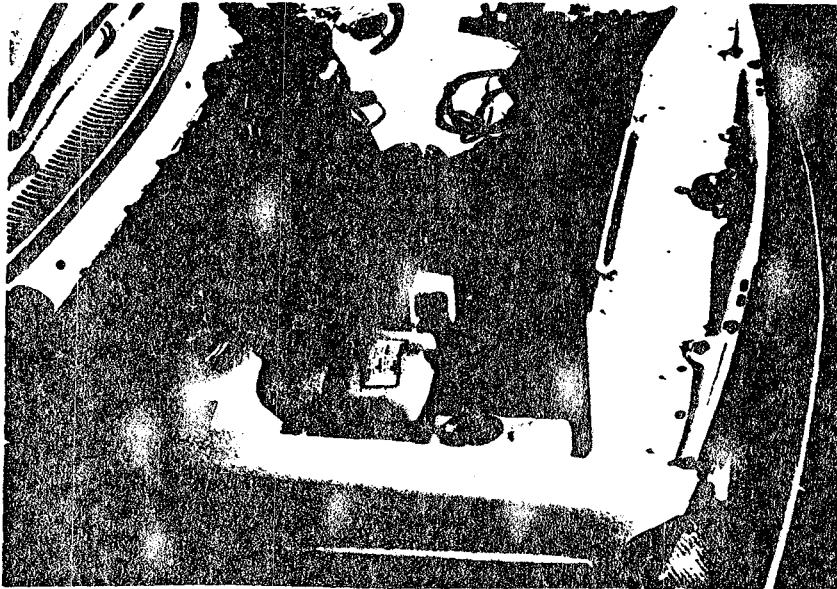


Fig. 17 - Mark II Gas Turbine Drive Train Mock
Up in Car

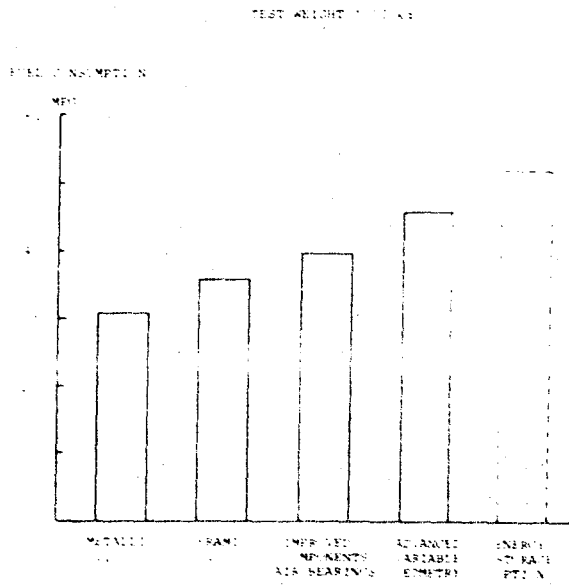


Fig. 18 - Fuel Economy Potential of KTT Gas
Turbine

QUESTION AND ANSWER PERIOD

Q: What is the power level of the KTT Mark I engine? Have you run any CVS cycle tests for fuel economy and emissions?

A: The Mark I is about a 100 KW engine. It is presently running at a somewhat lower level as yet. From in-house chassis dynamometer tests on the Federal Driving Cycle, we are getting relatively close to the spark ignition engine fuel economy levels. It is still too early to divulge specific numbers. Both types of engines are moving targets. Only certain types of emissions

have been measured. Detailed measurements have been postponed for future parts of the development program.

Regarding future fuel, based on component tests and studies, initial fuel economy will be competitive with conventional piston engine powered cars. In the long run, considering emissions, particulates, etc., we expect to equal and surpass diesel powered cars. The gas turbine should be a winner in many areas of application.

**HEAVY DUTY TRANSPORT
TECHNOLOGY SESSION**

DOE/NASA Heavy-Duty Transport Technology Program

Harry W. Davison

National Aeronautics and Space Administration

Lewis Research Center

Cleveland, OH

ABSTRACT

This new program is intended to provide a technology base for industry to use in developing heavy-duty transport engines. The program focuses on advanced diesel engine technology, waste heat utilization, materials, and tribology. Applications notices were sent to industry to encourage their ideas and participation. An excellent response was received as indicated by the receipt of over 80 proposals addressing various research activities applicable to heavy-duty transport. The program organization, current activities, and funding expectations are presented.

STUDIES BY THE DEPARTMENT OF ENERGY project the use of fuel in the year 2000 by medium- and heavy-duty trucks and by commercial buses to be approximately 60 percent higher than in the year 1980. Because of this trend there is a need to focus attention on methods of improving the energy efficiency of heavy-duty engines, which are typically diesel engines. Only about one-third of the fuel energy expended in current diesel engines is converted to useful work. One-third is rejected to the cooling system, and the remaining one-third is dissipated in the exhaust.

Current efforts are directed toward methods of increasing the fraction of useful work per unit of fuel energy consumed. A potentially attractive approach to achieving this objective is to extract additional useful work from the exhaust by using a turboexpander or other bottoming cycle. Further gains in useful work can be achieved by insulating the engine, where major heat losses occur, thereby eliminating the water cooling system, raising the exhaust temperature, and increasing the potential to extract more work from the exhaust. This is the concept of

Work performed for U.S. Department of Energy under Interagency Agreement EC-77-A-31-1011.

the adiabatic engine. Additional gains can be achieved by minimizing friction losses in mechanical components. This approach to improved diesel engine efficiency is being investigated by American and foreign engine manufacturers. Cummins Engine Company under contract with the Army Tank Automotive Command (TACOM) has achieved significant reductions in specific fuel consumption by eliminating water cooling in a turbocharged and turbocompounded engine. They project up to 40 percent fuel savings by reducing heat loss and friction loss. The Japanese Kyoto Ceramic Company in cooperation with Isuzu Motor Company has successfully operated an uncooled ceramic version of a diesel engine. In spite of these achievements, the adiabatic diesel is not yet ready for commercial development. To overcome the technological barriers preventing commercial development, DOE created the Heavy-Duty Transport Technology program.

OBJECTIVES

The objective of the Heavy-Duty Transport Technology program is to provide a technological base for industry to use in developing advanced heavy-duty transport engines. This program will focus on advanced diesel engine technology and will include the investigation of advanced concepts, component changes and improvements to basic engine concepts, and improved turbocompounding or bottoming system technologies required to maximize engine performance and fuel economy.

APPROACH

Although the planned program approach is to focus on adiabatic diesel engine technology for long-haul trucks, this technology is expected to be applicable to a wide variety of applications including marine, railway, and pipeline systems. Initial activities will include engine system studies and the beginning of long-lead-time

research and technological development. Contracts will be let for component and materials technology development and for evaluation of various waste heat utilization concepts. No engine testing is anticipated in the initial stages of the program. Industry participation in the identification of critical technological barriers is encouraged. Initially industry participation was sought through the use of applications notices.

The applications notices provide a notification of opportunities that may exist within a program area. They contain a "Dear Colleague" letter stating the program area, the approximate level of planned budget, and the persons to contact. The applications notices also describe the program and opportunity areas and the guidelines for submission of unsolicited proposals. Each unsolicited proposal is reviewed and evaluated on its own merits and is treated according to prescribed NASA procedures for unsolicited proposals. Research activities can be conducted under contracts, grants, or interagency agreements.

STATUS

In February 1982 two applications notices issued by the NASA Lewis Research Center were announced in Commerce Business Daily: "Heavy-Duty Diesel Engine Technology Program" - AN:LERC:82-B; and "Advanced Waste Heat Utilization Program for Heavy-Duty Transport" - AN:LERC:82-C. About 400 sets of these notices were distributed to industry and academic institutions. Over 80 unsolicited proposals (about \$23 million of research) have been received in response to these notices. These proposals, ideas, and suggestions were received from a broad spectrum of industry and academic institutions. However, acceptance of the large number of superior ideas would greatly exceed our funding capability. The current plan is to let about 15 contracts with \$3 million of fiscal year 1982 funding.

ORGANIZATION

The ideas, concepts, and suggestions received from the applications notices, along with a requirement to conclude demonstration activities funded previously under the Vehicle Systems program, led to the formulation of the Heavy-Duty Transport Technology project organization illustrated in figure 1. The DOE/NASA Heavy-Duty Transport Technology project managed by the NASA Lewis Research Center consists of three primary tasks: project management, advanced engine technology, and supporting research and technology. Project management tasks include planning and reporting requirements to support the DOE program and concluding the current contract activities at Cummins on the turbocompounded diesel and the Thermo Electron Corporation (TECO) organic Rankine bottoming cycle. Status reports on these activities are also presented in this meeting.

The advanced engine technology task will include new contract activities to develop technology in support of adiabatic diesels, engine components, and waste heat utilization systems.

A contract awarded to Cummins will identify critical technology needs for a low-heat-rejection diesel engine for automotive application, and the status of that effort will be reviewed at this meeting.

The third task, supporting research and technology, contains more basic research activities that will be started with fiscal 1982 funding in specific areas such as tribology, materials technology, systems analysis, and heat transfer. Contract negotiations and final evaluations are still in progress, and procurement regulations prohibit disclosure of proposers and ideas at this time. However, activities will be started in each of the areas indicated in figure 1.

The funding for future activities in heavy-duty transport technology is uncertain. However, the activities begun with fiscal year 1982 funding will provide fundamental pieces of technology and serve a beginning.

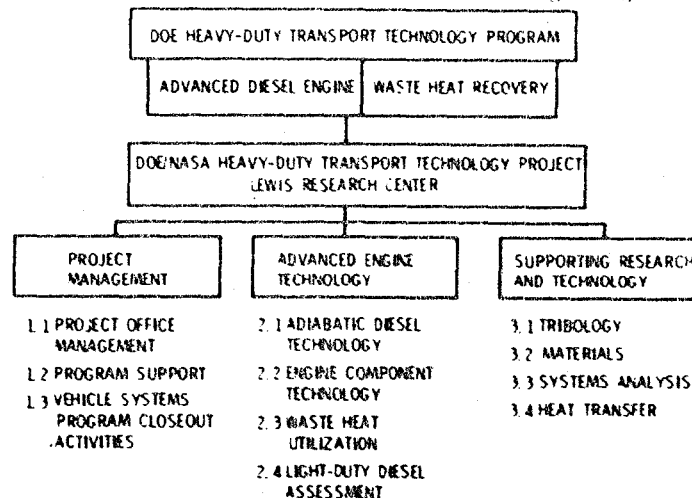


Figure 1. - Organization of DOE Heavy-Duty Transport Technology Program.

The Cummins Advanced Turbocompound Diesel Engine Evaluation

John L. Hoehne and John R. Werner
Cummins Engine Co., Inc.

ABSTRACT

The turbocompound diesel engine has been under development at Cummins Engine Company since 1972. Development reached a mature stage following the evolution of three power turbine and gear train designs. In 1978, the Department of Energy sponsored a program for comprehensive vehicle testing of the turbocompound engine. Upon successful completion of the vehicle test program, an advanced turbocompound diesel engine program was initiated in 1979 to improve the tank mileage of the turbocompound engine by 5% over the vehicle test engines. Engine improvements could be realized by increasing the available energy of the exhaust gas at the turbine inlet, incorporating gas turbine techniques into improving the turbomachinery efficiencies, and through refined engine system optimization. This paper presents the individual and cumulative performance gains achieved with the advanced turbocompound engine improvements.

A PROGRAM has been underway at Cummins Engine Company, Inc. since 1972 to develop the turbocompound diesel engine. This engine is a hybrid diesel reciprocator which is augmented in power by a pressure power turbine. The turbine power generated by means of exhaust gas expansion is transferred to the drive train by mechanically gearing the power turbine to the rear of the crankshaft at a fixed speed ratio. A fluid coupling is utilized to separate the crankshaft torsional vibration from the high speed gearing and turbine shaft.

The laboratory engineering development of the turbocompound engine reached a mature stage following the evolution of three power turbine and gear train designs. The next logical evaluation involved vehicle performance testing. Thus, Cummins Engine Company entered into a

contract with the Department of Energy in 1978 which called for a comprehensive vehicle test evaluation to ascertain the viability of the turbocompound engine for trucks and buses of the 1980's.

Within this effort, two turbocompound diesel engines were assembled and dynamometer tested. Both engines met the California 6 gram (BSNOx+BSHC) combined gaseous emissions limit and achieved a minimum fuel consumption of .313 lb/bhp-hr and a value at rated power of .323 lb/bhp-hr. These engines were then installed in Class VIII (73,000 GVW) heavy-duty trucks to determine their fuel consumption potential and performance characteristics. One turbocompound engine powered vehicle was evaluated at the Cummins Pilot Center facility where detailed engine-transmission-vehicle tests were conducted in a controlled environment. The other engine was placed in commercial service operating between Florida and California for 50,000 miles. The results of these tests are reported in the NASA technical report CR-159840 and SAE paper No. 810073. The most salient finding was that the turbocompounded engines in both locations showed a fuel consumption reduction of 15-16% over the production NTC-400 horsepower reference engine.

During these tests, a number of component modifications were incorporated in the turbocompound engine which resulted in fuel consumption reductions exceeding the expected benefit from turbocompounding alone. Through previous laboratory testing, it was established that a benefit of 6% reduction in fuel consumption over an equivalent turbocharged and aftercooled NH engine was achieved along the engine's torque curve. As the load is reduced, the gain reduces in value as the available exhaust energy decreases. Using these test results, the incremental fuel consumption improvement due to the turbocompounding alone was 4.2% to 5.3% for the interim turbocompound engine, depending upon the terrain or mission load factor.

The vehicle testing activity described above was conducted with the interim turbo-compound diesel. The interim nomenclature is primarily a distinction regarding the development status of the engine at the time of the vehicle test activity. That is, the vehicle test engines had known aerodynamic deficiencies and utilized modified production components to turbocharge the engine. Improvements could be realized by increasing the available energy of the exhaust gas at the turbine inlet, incorporating current aerodynamic design practices into improving the turbomachinery efficiencies, and through refined engine system optimization. The combined effects of these improvements were expected to increase the tank mileage by 5% over the interim turbocompound diesel engines. Therefore, in September of 1980, the Department of Energy extended the contract with Cummins to continue the development of an advanced turbocompound diesel engine. The primary objective of this program was to improve the tank mileage of the advanced turbocompound diesel engine by 5% over the interim turbo-compound diesel engine. A five-phase program was established to achieve these goals and enhance the fuel conservation potential of the turbocompound diesel:

- Task I Baseline Performance Mapping
- Task II Engine Performance Testing and Upgrading
- Task III Advanced Engine Preparation
- Task IV Advanced Engine Dynamometer Testing
- Task V VMS Analysis

Task I included engine removal from the Pilot Center test vehicle and installation in a dynamometer test cell to establish baseline data repeatability. Steady-state performance mapping consisting of a matrix of engine speed and load conditions was completed along with measurement of gaseous emissions.

Task II included an improvement in the fuel injection system along with flow path design changes to the exhaust manifold to reduce the pumping losses and minimize the exhaust gas mixing losses.

Task III entailed the implementation of existing design practices typically employed in gas turbine power plants into the turbo-compound engine turbomachinery, engine system optimization, and insulation of the exhaust system components.

Task IV was the dynamometer testing of the advanced turbocompound engine developed in Task III. This included performance mapping to assess the performance achieved against the interim engine performance at equivalent gaseous emission levels.

Task V utilized the performance map generated in Task IV as input to Cummins' Vehicle Mission Simulation (VMS) computer program. VMS is an analytical model which predicted the tank mileage for the advanced turbocompound engine.

These results were, in turn, compared to the reference tank mileage predictions of the interim turbocompound vehicle test engines.

TURBOCOMPOUND ENGINE DESCRIPTION

The turbocompound engine was developed from the Cummins NH engine. The bore and stroke of the NH engine are 5.5 and 6.0 inches, respectively. The engine is an inline-six, four cycle of 855 cubic inch displacement. Fuel is supplied to the engine by the Cummins PT high pressure injection system. The turbocompound engine was turbocharged, aftercooled, and conventionally cooled.

A number of component modifications have been made to improve the engine system performance under turbocompounding conditions. These include design changes of the camshaft, valves, cylinder head exhaust ports, exhaust manifold, and turbocharger. Primarily, these modifications were initiated to reduce the blowdown energy losses during the exhaust phase of the cycle and to improve the transmission efficiency of the exhaust gas from the cylinder to the first stage turbine.

The turbocompound system consists of a radial inflow low pressure power turbine to recover the exhaust gas energy. This, along with its bearing cartridge, is one of three separate modules. The modular concept was selected to provide for ease of assembly and maintenance. The second module consists of the high speed gearbox using involute spur gearing to achieve part of the necessary speed reduction from the power turbine to the crankshaft. Lubrication is provided by the engine oil system and directed by internal oil drillings. The third module is the low speed gearbox which completes the speed reduction required. A fluid coupling is an integral part of this module which performs the function of separating the high speed gearing from the crankshaft torsional vibration. The flywheel housing is an S.A.E. No. 1 housing constructed of cast iron to support the weight of the gear train. The overall increase in engine length is one inch and the entire system is designed such that it may be installed in most high horsepower engine applications. The design provides for 5% overspeed capability and 100% overspeed burst containment. A schematic of the Cummins turbo-compound diesel engine is shown in Figure 1.

The turbocompound engine was rated 450 brake horsepower at 1900 rpm engine speed with 15% torque rise to 1440 lb-ft at 1300 rpm. A lower operating speed rating was selected to take advantage of the low speed torque characteristics of a turbocompound engine. The increase in power rating at a lower engine speed was achieved without increasing the thermal or structural loading of the reciprocator.

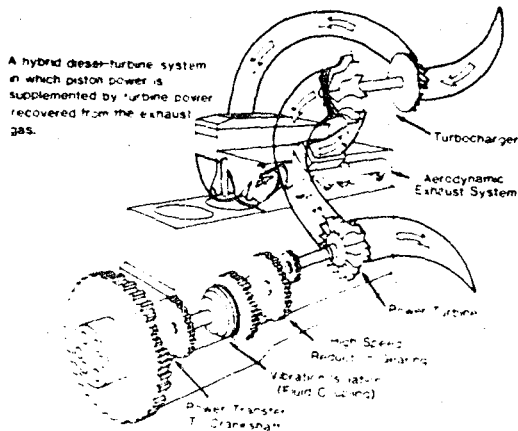


Fig. 1 - Cummins NH turbocompound diesel engine

BASELINE TESTING: Task I

The interim turbocompound engine was removed from the Cummins Pilot Center test vehicle in April of 1980. This engine and the associated turbocompound gear train were disassembled and examined for any undue or unusual wear. Inspection revealed that the high speed gear housing bushing had seized on the fluid coupling shaft. The bushing seizure was caused by the fluid coupling shaft bottoming in the gear housing bushing bore due to improper stackup of the shaft fluid coupling assembly. Due to this problem, it was decided to update the test engine with a revised turbocompound gear train housing which corrected this problem and also eliminated external oil drillings for lubrication of the gears.

Following the completion of the installation of all necessary instrumentation, steady-state performance mapping consisting of a matrix of engine speed and load conditions was completed along with measurement of gaseous emissions. Repeatability was achieved with a measured brake specific fuel consumption (BSFC) of .323 lb/bhp-hr at the California 6 gram combined emission level.

ENGINE PERFORMANCE TESTING AND UPGRADING Task II

A new cast exhaust manifold was designed to improve the pulse conservation of the exhaust blowdown. The junctions at each port connection were designed to maintain a constant area such that the exhaust pumping work was minimized. This manifold provided BSFC improvements of .003 lb/bhp-hr at rated power and a .005 lb/bhp-hr at torque peak power. The most significant BSFC improvements were made at part load in the 1300-1600 rpm engine speed range.

A new injector camshaft lobe was designed to provide improved injection characteristics for the advanced turbocompound engine. The new cam reduced the injection duration by 0.5

crank angle and increased the injection pressure by approximately 3000 psi over the interim baseline cam. The higher injection pressure and resultant shorter duration accelerates the air-fuel mixing rate. Performance testing at the same emission level resulted in a .002-.003 lb/bhp-hr BSFC reduction along the torque curve.

At this point, a performance map was generated which showed a BSFC achievement of .318 lb/bhp-hr at rated power, .307 lb/bhp-hr at torque peak power, and a minimum of .305 lb/bhp-hr at 1500 rpm. The fuel map is shown in Figure 2. It should be noted that while a gain of .005 lb/bhp-hr was achieved over the interim TCPD engine at rated power, significantly larger BSFC gains were achieved at part load and at the lower engine speeds (1300-1600 rpm) where an engine would typically operate on a level road at 55 mph.

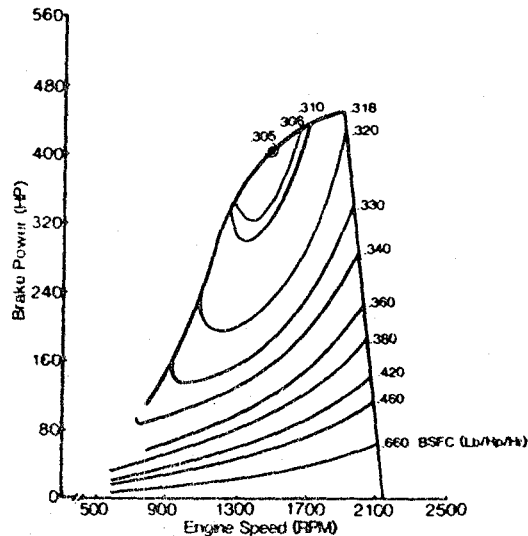


Fig. 2 - Upgraded turbocompound engine operating speed and load range - November, 1980

A 13-mode gaseous emission cycle was also conducted to determine the injection timing required to conform to the California 6 gram (BSNOx+BSHC) gaseous emission limit. The mechanical variable timing was set at 14° BTDC dynamic timing for normal operation and advanced to 21° BTDC dynamic timing during light load operation. This produced a 5.86 gm/bhp-hr combined (BSNOx+BSHC) emission level.

The new performance map was put into Cummins' Vehicle Mission Simulation (VMS) computer program to ascertain the tank mileage improvement over the interim turbocompound engine. The VMS program input requirement consists of a detailed description of the vehicle and selection of a route. The model is capable of adjusting to varying ambient operating conditions such as temperature plus prevailing wind velocity and direction. The VMS can predict both steady-state

performance as well as transient engine behavior. Output data under steady-state operating conditions includes startability, gradeability, and vehicle performance in all the transmission gears. The route simulation summary includes trip time, average speed, fuel consumption, gear shifts, time spent at full throttle, and average engine load factor.

A high degree of confidence in the predictive accuracy of the VMS model was achieved by comparing the interim turbocompound vehicle test results with the calculated results of VMS. Therefore, the VMS program was utilized for predicting performance gains of the advanced turbocompound engine.

A VMS run was made for the Pilot Center fuel economy route at the completion of Task II. This route consists of public roads beginning at the Cummins Technical Center in Columbus, Indiana, going south through Louisville, Kentucky, turning east to Cincinnati, Ohio, and returning to Columbus. VMS predicted a tank mileage of 5.59 mpg for the upgraded engine versus 5.40 mpg for the interim engine, or a 3.5% upgraded turbocompound engine tank mileage improvement.

ADVANCED ENGINE PREPARATION: Task III

ENGINE SYSTEM OPTIMIZATION - The engine cooling system during the vehicle tests utilized a two-pump, two-circuit cooling system providing a 140°F intake manifold temperature on an 85° day at rated power. A further reduction in intake manifold temperature to 110°F is possible with a chassis mounted air-to-air aftercooling system. A Class VIII truck engine currently in production utilizes this type of cooling system.

The comparison between engine fuel consumption along the torque curve for intake manifold temperatures of 140°F and 110°F is seen in Figure 3. The fuel consumption benefit of .001-.004 lb/bhp-hr was due to an increase in air-fuel ratios, resulting in improved combustion efficiency. The air-fuel ratio changed from 24.8 to 26.3 at torque peak power with 110°F IMT while the air-fuel ratio changed from 30.1 to 30.5 at rated power.

Insulation of the exhaust system to provide increased available exhaust gas energy to the turbines was evaluated. The externally applied insulation consisted of an alumina-silica refractory fiber blanket. The alumina-silica material chosen was suitable for continuous exposure to 2400°F in a normal oxidizing atmosphere.

Insulated versus non-insulated engine performance testing was completed using the blanket to externally insulate the exhaust manifold, charge air turbine volute, and interstage duct. The temperature increase at the charge air turbine was 10°F while the power turbine inlet showed an increase of 15°F. This was due to the cumulative effect of heat loss reduction over the exhaust manifold, charge air turbine and interstage duct. The increase in exhaust

gas enthalpy provided a reduction in fuel consumption of approximately .002 lb/bhp-hr along the engine's torque curve. The fuel consumption for the turbocompound engine is shown in Figure 4 for the insulated and non-insulated configurations.

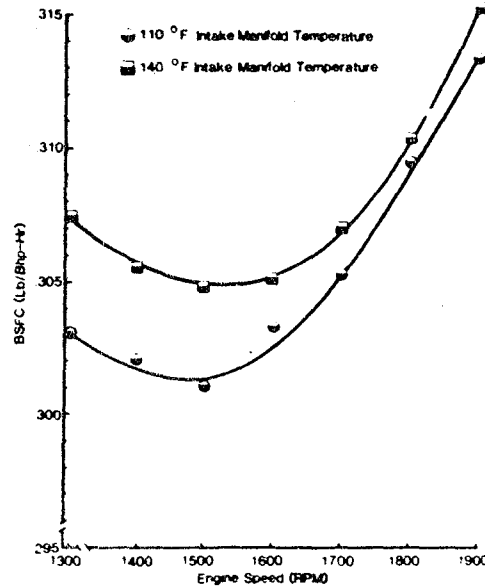


Fig. 3 - Intake manifold temperature comparison torque curve: BSFC vs. engine speed

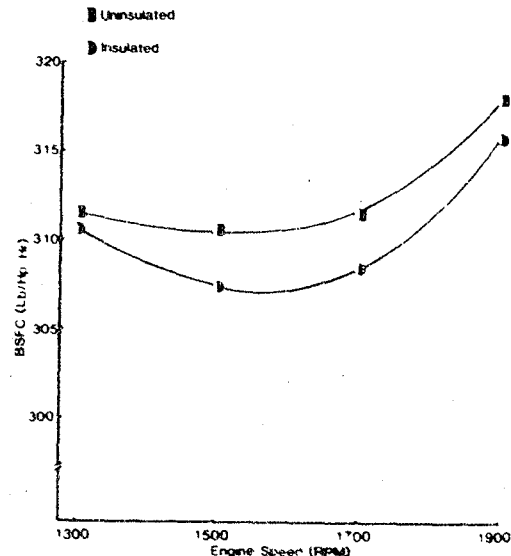


Fig. 4 - TCCP - 450 performance data: Insulated vs. non-insulated exhaust system

FREE POWER TURBINE - The Phase III turbocompound power turbine shaft was supported by semi-floating journal bearings. The journal

bearing power turbine was tested on the turbine map stand. Bearing losses were measured by determining the heat rejection to the oil from the bearing housing. This is accomplished by accurately measuring the oil flow to the bearing housing and the bulk oil temperature rise across the housing. Heat transfer effects were minimized by using a turbine inlet temperature which was approximately 250 F resulting in a minimum temperature differential between the test unit and the incoming oil.

A prototype ball bearing supported power turbine shaft was designed to determine the potential reduction in shaft mechanical losses compared to the journal bearings. The ball bearing arrangement incorporated spring loaded, angular contact ball bearings. The design used a modified aluminum bearing housing with an increased bore to accommodate the larger bearing carrier. The bearing carrier is steel and does have radial clearance within the housing to provide oil film damping. The carrier also incorporates lube orifices which target a jet of oil on the inner race of each bearing. The lube jet method requires accurate targeting of the flow to get the oil into the bearing working against the aerodynamic resistance of the spinning balls and cage. The oil is then carried through the balls and into the bearing housing cavity. The center cavity is drained or vented to the housing by holes in the bottom of the carrier. A pair of stacked wavy washers is used to provide axial preload. The inner races were fixed to the shaft against rotation by an axial clamp from the high speed pinion nut. The unassembled unit is shown in Figure 5. The benefit to be gained through the utilization of ball bearings includes not only a reduction in friction, but also a possible improvement in turbine efficiency made possible by a reduction in operating clearances due to the more stable shaft orbit.

After the initial journal bearing arrangement was evaluated, the turbine rotor and shaft were modified by reducing the diameter to accept the ball bearings. The comparison test of the ball bearing power turbine was performed using the same turbine volute, turbine rotor load compressor, collector, and rotor to shroud clearances.

A summary of the friction loss (as measured by heat rejection to the oil) data is depicted in Figure 6. A graph of the ball bearing versus journal bearing mechanical efficiency is shown in Figure 7. Figure 6 also shows the parasitic loss in horsepower of the journal bearing and the ball bearing unit at rated and torque peak speeds. This difference in horsepower is available as shaft power for the engine.

Further testing was to have been carried out to evaluate the gains from reduced operating clearances made possible by the ball bearing system, however, bench testing indicated that the shaft stiffness was not sufficient to avoid a flexural mode. This type of motion would not allow an evaluation of the ball bearing power turbine with reduced clearances. A second

design iteration would be required to provide sufficient bearing life, satisfactory shaft dynamics and oil film damping, minimum shaft flexing, and consideration for cost and complexity. A second design iteration was not pursued due to the design and procurement lead times.

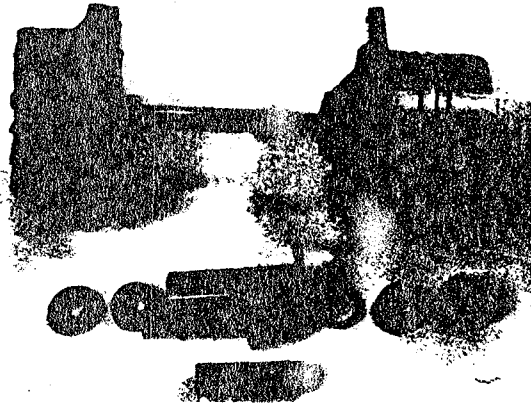


Fig. 5 - Ball bearing power turbine arrangement-exploded view

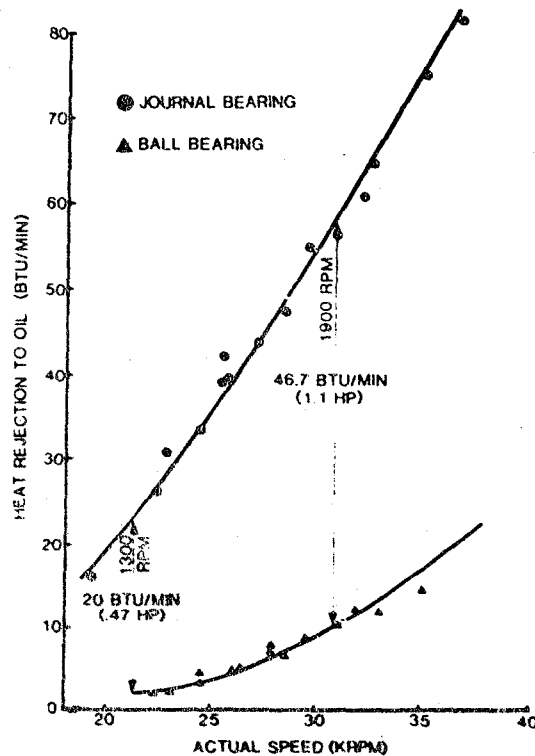


Fig. 6 - Power turbine bearing heat rejection to oil

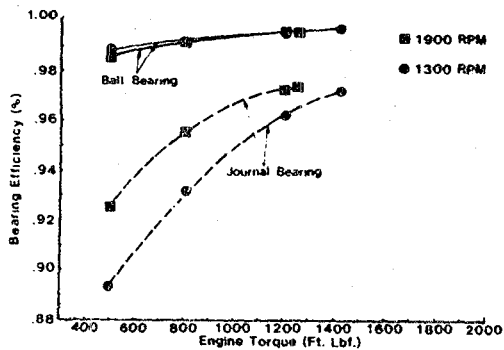


Fig. 7 - Power turbine journal vs. ball bearing efficiency

POWER TURBINE SPEED OPTIMIZATION - In an effort to improve the aerodynamic efficiency of the power turbine, an increasing speed was required. This was accomplished by varying the gear ratio with resultant changes in the operating line of the turbine shown in Figure 8. The interim turbocompound power turbine operated at a gear ratio of 15.78 times the engine speed. Operating lines are shown for engine speeds of 1900 and 1300 RPM at three gear ratios: 15.78, 16.42 and 17.12 times the engine speed. At 1900 RPM, as the gear ratio is increased the power turbine efficiency remains relatively constant at full load, but decreases slightly at part loads. At 1300 RPM, however, the power turbine efficiency improves significantly over the full operating range. Hardware was procured to increase the gear ratio to 16.42 and 17.12 times the engine speed.

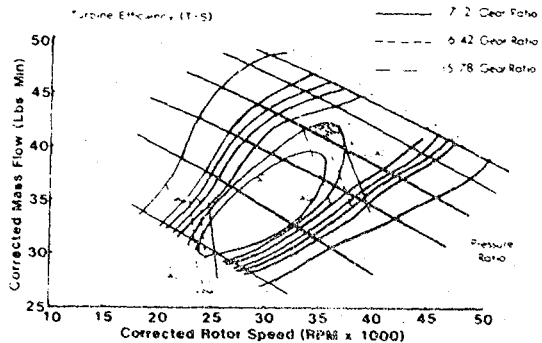


Fig. 8 - Radial power turbine efficiency map

Engine performance tests were completed with all three gear ratios throughout a matrix of engine speed and load conditions. The intermediate ratio of 16.42 was selected as the optimum ratio after evaluation of the full and part load fuel consumption data shown in Figure 9 and Figure 10. An average fuel consumption benefit of .001 lb/bhp-hr was measured along the torque curve over the interim gear ratio

of 15.78. This is consistent with the predicted benefits at full load using the improved efficiencies shown in Figure 8.

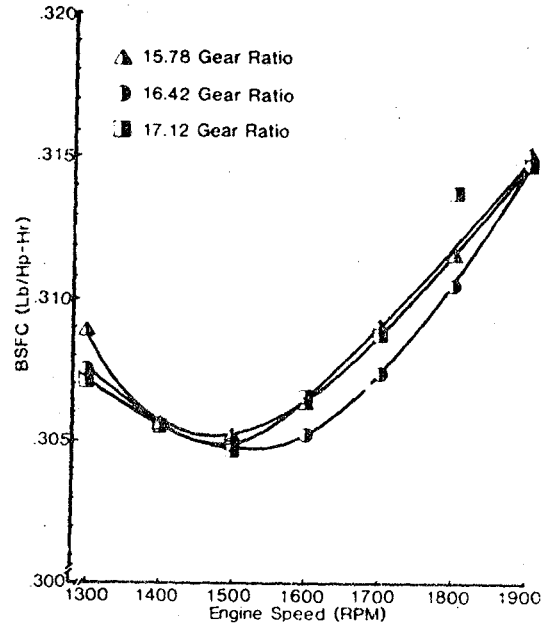


Fig. 9 - Gear ratio optimization torque curves: BSFC vs. engine speed

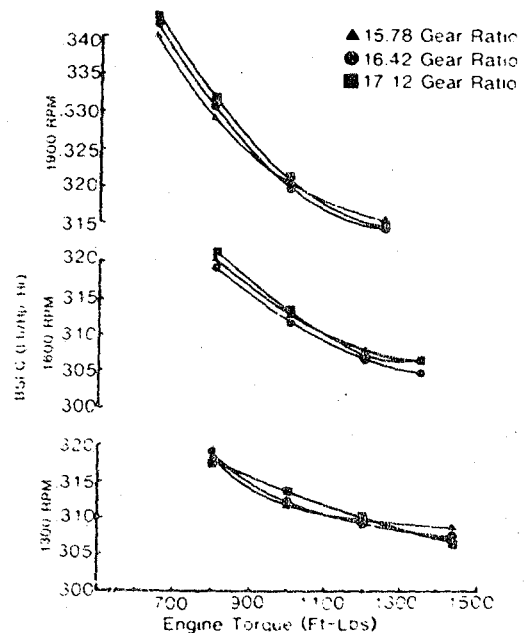


Fig. 10 - Gear ratio optimization: BSFC vs. engine torque

ABRADABLE SHROUDS - As stated previously, Task III involved implementing practices and techniques typically employed in gas turbine power plants into the turbocompound engine turbomachinery. One of these practices for increased efficiency levels is the utilization of abradable materials in order to reduce clearances between the rotor and shroud.

An abradable nichrome/polyester composite coating was applied to the charge air turbine shroud. The nichrome/polyester coating has a temperature capability of 1500° F. The abradable turbine shroud was initially evaluated on the engine. Performance testing was completed for the abradable versus baseline turbine shrouds. The cold clearance for the turbines evaluated are shown below:

	<u>Axial Clearance</u>	<u>Radial Clearance</u>
Baseline	.030	.010
Abradable	.015	(Minimum)

Test data along the torque curve did not indicate any fuel consumption advantage for the abradable turbine shroud.

Bench testing was subsequently completed to more accurately quantify the effect of clearances on turbine efficiency. Two turbine volutes were evaluated: a baseline shroud with no abradable coating and the turbine shroud with the abradable nichrome/polyester coating. Axial clearances for the abradable shroud were varied from .027 inch to .010 inch with minimal radial clearance. The baseline turbine shroud axial and radial clearances were set at .027 inch and .010 inch, respectively. The bench test results are summarized as follows:

	<u>Axial Clearance</u>	<u>Radial Clearance</u>	<u>Abradable Contour</u>	<u>Peak Turbine Efficiency</u>
Baseline	.027	.010	No	79.8
Build 1	.027	Minimum	Yes	80.9
Build 3	.018	Minimum	Yes	80.5
Build 4	.010	Minimum	Yes	80.3

The abradable charge air turbine shroud contour is shown in Figure 11 after the bench tests. The turbine efficiency versus rotor speed at a constant pressure ratio is shown in Figure 12. Taking into account test stand accuracy and repeatability, the abradable turbine shroud showed no difference in efficiency when the axial clearance was reduced from .027" to .010".

However, the data indicates a slight gain in turbine efficiency due to the lowering of the radial clearance. This improvement in performance, for this particular turbine, can be traced to the fact that a reduction in radial clearances reduces the blade to blade leakage in the area where a large portion of the work is being done.

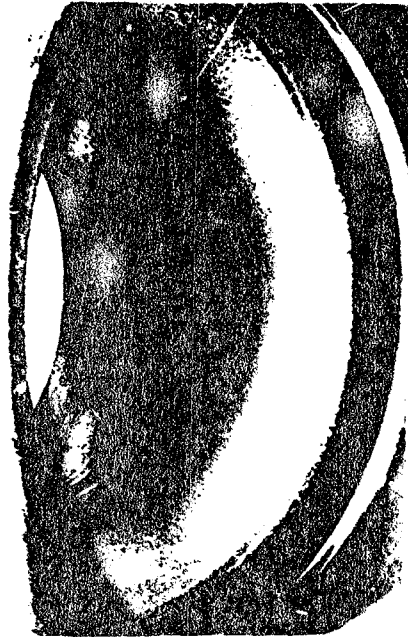


Fig. 11 - Turbine abradable shroud

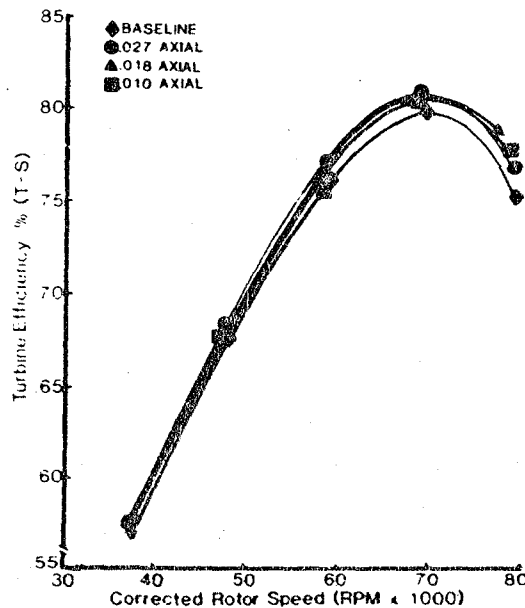


Fig. 12 - Turbine abradable shroud bench test - pressure ratio 2.2

ABRADABLE COMPRESSOR SHROUD - For the compressor shroud, an aluminum-graphite composite coating was evaluated as this material is compatible with an aluminum compressor rotor.

The turbocharger compressor with the abradable shroud was first tested on the bench test stand with minimum radial clearance at the inducer region and .024 inch axial clearance between the rotor and the contour of the exducer region. The axial clearance was reduced in .005 inch increments to a final .004 inch clearance at room temperature. The abradable shroud shown in Figure 13, after the last bench test, displays the coating abrasion due to the compressor impeller. The performance data shown in Figure 14 shows the peak compressor efficiency increasing from 81.7 percent to 83.3 percent for the minimum clearance build and a 1-2% efficiency improvement at a constant pressure ratio. This illustrates both an improvement in peak efficiency and an increase in the width of the efficiency islands with use of the abradable compressor shroud. Thus, not only does the compressor work at higher efficiency levels, but it will also operate in these regions a greater percentage of the time.

Engine performance testing was completed with the abradable compressor shroud at .024 inch and .004 inch axial clearance and minimum radial clearance. The engine test data shown in Figure 15 verified the 1-2% efficiency improvement measured on the bench test. A reduction in fuel consumption of .001-.003 lb/bhp-hr was measured along the torque curve.

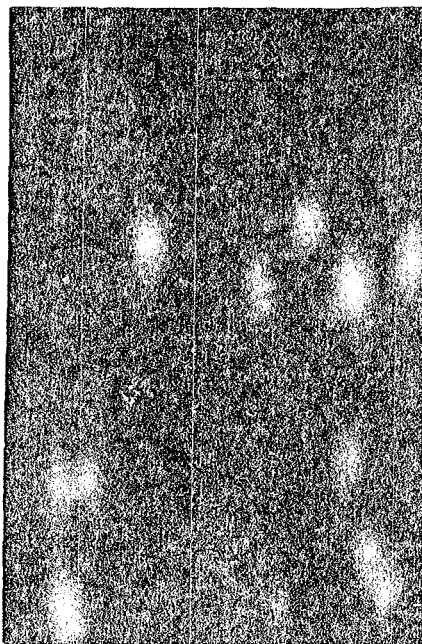


Fig. 13 - Abradable compressor shroud

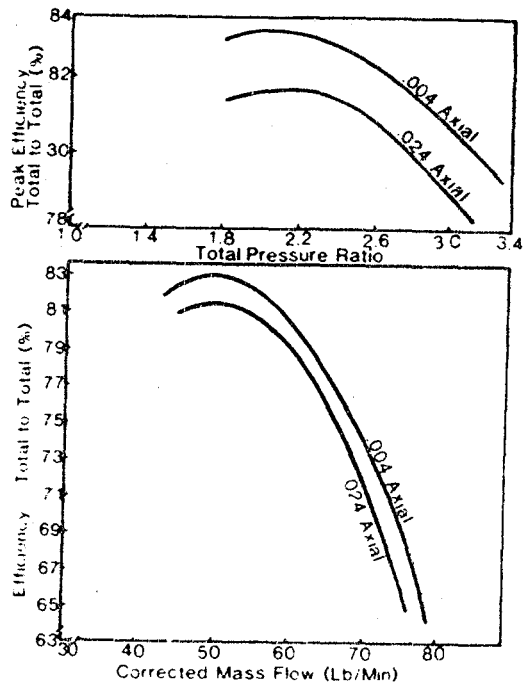


Fig. 14 - Effect of clearance on peak efficiency vs. total pressure ratio and compressor efficiency vs. mass flow at 2.2 pressure ratio

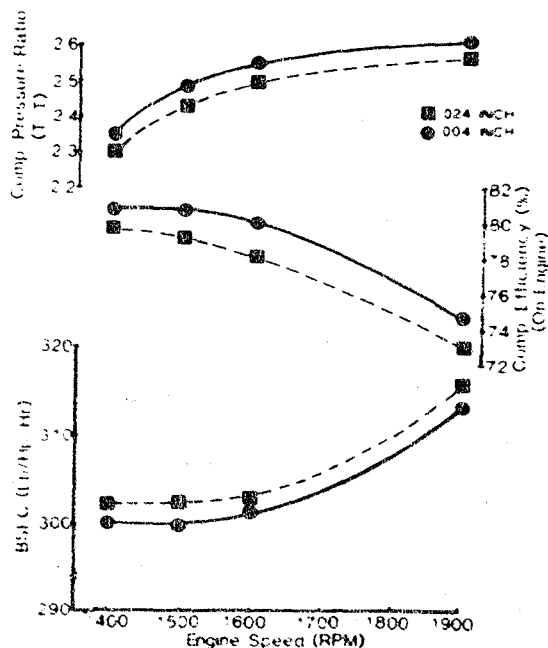


Fig. 15 - TCFI-450 performance data - abradable compressor shroud

ADVANCED ENGINE DYNAMOMETER TESTING: Task IV

The advanced turbocompound engine was equipped with the following hardware which differed from the interim turbocompound configuration to measure the cumulative performance gains of the advanced engine:

- . Redesigned 1.8 inch diameter pulse exhaust manifold
- . New injector camshaft lobe with improved injection characteristics
- . Insulated exhaust manifold, charge air turbine volute, and interstage duct
- . Simulated air-to-air aftercooling (11% IMT)
- . Simulated ball bearing system for the power turbine
- . Optimum power turbine gear ratio
- . Abradable compressor shroud with .004 inch axial clearance

Emissions were examined using the 13-mode gaseous emission cycle to verify that the engine was operating at the combined gram level. A 13-mode BSNOx of 5.00 gm/bhp-hr and BSHC of .27 gm/bhp-hr was measured at 14% BTDC dynamic injection timing with advanced injection timing to 21% BTDC in the light load modes.

A steady-state dynamometer performance map was generated with the advanced turbocompound engine at the 6 gram combined emission level. Figure 16 shows the BSFC consumption islands as a function of engine speed and power. Brake specific fuel consumption at rated power was .311 lb/bhp-hr. The minimum brake specific fuel consumption of .296 lb/bhp-hr occurred at 1500 rpm, which is equivalent to a thermal efficiency of 46.4 percent. Fuel consumption at torque peak power was .303 lb/bhp-hr. A comparison of fuel consumption along the torque curve for the advanced versus interim turbocompound engine is shown in Figure 17.

VMS ANALYSIS: Task V

The advanced turbocompound performance map was put into Cummins' VMS program to predict the tank mileage of a vehicle for comparison to the results of the interim turbocompound engine installed in the same vehicle and simulating the same route. A summary of the VMS calculations presented in Table 3 shows a predicted tank mileage of 5.75 mpg for the advanced turbocompound engine while the interim turbocompound engine prediction was 5.40 mpg. Thus, a VMS predicted tank mileage improvement of 6.5% was achieved. This produced a fuel savings of 2.9 gallons over the simulated 100.17 mile course.

A VMS comparison was also made for the interim turbocompound field test route from Florida to California. The southern route across the United States includes sections of I-75, I-10, I-20 and I-8. This route, shown in Figure 18, provides a variety of terrains including plains, rolling hills, and mountainous grades. The VMS predictions are shown in Table 2. The

advanced engine achieved tank mileage improvements of 6.9 and 6.1 percent over the interim engine at maximum cruise speeds of 60 mph and 65 mph, respectively. A VMS data summary for five types of terrains is presented in Table 3 for the advanced turbocompound engine and interim turbocompound engine. VMS predicted tank mileage improvements for the advanced turbocompound engine range from 7.0 percent on level terrain to 8.2 percent on a mountainous route.

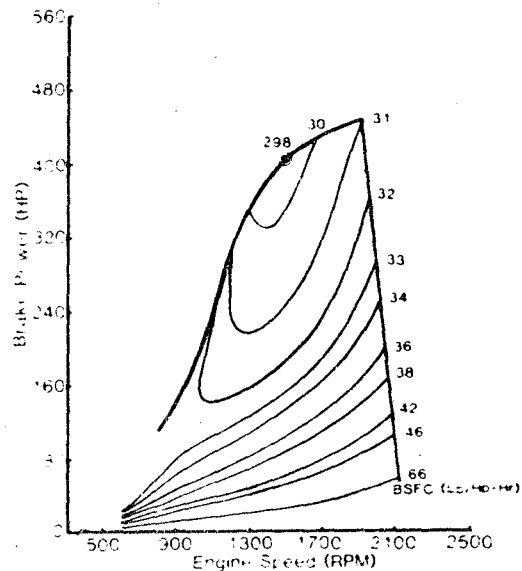


Fig. 16 - Performance curve - Advanced TCPC-450

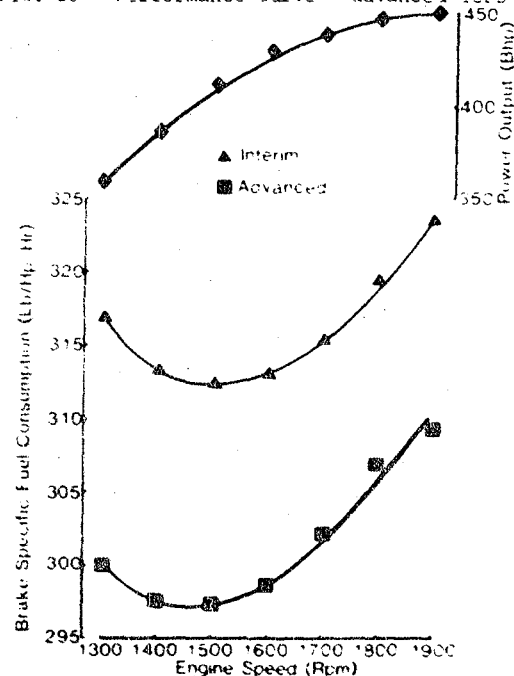


Fig. 17 - Interim and advanced TCPC engine performance



Fig. 15 - Turbocompound field test route

TABLE 1.
TMS DATA SUMMARY FOR
CUMMINS FUEL ECONOMY ROUTE
ADVANCED TCPD-450 vs. INTERIM TCPD-450

ENGINE	INTERIM	ADVANCED
MAXIMUM CRUISE SPEED (MPH)	55	55
AVERAGE VEHICLE SPEED (MPH)	43.3	43.3
FUEL USED (GALLONS)	48.2	47.3
AVERAGE FUEL RATE (LB/HR)	57.0	53.5
TANK MILEAGE (MPG)	5.40	5.75
% ADVANCED TCPD-450 MILEAGE IMPROVEMENT		6.5

VEHICLE TEST INPUT CONDITIONS:

W (LB) 73,000
 CRUISE SPEED (MPH) 55
 WIND SPEED (MPH) 0
 WIND DIRECTION (DEG.) 010
 TEMPERATURE (DEG.F.) 51
 TRUCK: PILOT CENTER UNIT 30
 KENWORTH CONVENTIONAL

TABLE 1.
TMS DATA SUMMARY
TCPD-450 FIELD TEST ROUTE
ADVANCED TCPD-450 vs. INTERIM TCPD-450

ENGINE	INTERIM	ADVANCED	INTERIM	ADVANCED
MAXIMUM CRUISE SPEED (MPH)	55	55	55	55
AVERAGE VEHICLE SPEED (MPH)	43.3	43.3	43.3	43.3
FUEL USED (GALLONS)	48.2	47.3	48.2	47.3
AVERAGE FUEL RATE (LB/HR)	57.0	53.5	57.0	53.5
TANK MILEAGE (MPG)	5.40	5.75	5.40	5.75
% ADVANCED TCPD-450 MILEAGE IMPROVEMENT		6.5		6.5
TRUCK SPECIFICATIONS				
TCPD-450, BASH STEEL, 74.4 RPM - 1,000 HP AN				

INPUT CONDITIONS: W = 73,000 LB
 RADIAL PLY TIRES
 STILL AIR
 AMBIENT TEMPERATURE 51°F
 KENWORTH CONVENTIONAL TRUCK
 ACCESSORIES: AIR CONDITIONING AND LOCKED PAN
 ROUTES SIMULATED BY M TAMPS, WILMINGTON, DE
 U.S. GOVERNMENT PRINTING OFFICE

TABLE 3.
VMS DATA SUMMARY FOR VARIOUS TERRAINS
ADVANCED TCPD-450 VS. INTERIM TCPD-450

ROUTE	ENGINE	TANK MILEAGE (MPG)	% ADVANCED TCPD TANK MILEAGE IMPROVEMENT
LEVEL INTERSTATE	INTERIM	6.17	7.0
	ADVANCED	6.60	
ROLLING PLAINS	INTERIM	6.20	6.8
	ADVANCED	6.62	
.2 PERCENT UP INTERSTATE	INTERIM	5.66	6.9
	ADVANCED	6.05	
HILLY INTERSTATE	INTERIM	5.99	6.7
	ADVANCED	6.39	
MOUNTAIN PASS	INTERIM	5.20	6.2
	ADVANCED	5.52	

INPUT CONDITIONS: 18 HP ACCESSORIES, BEARED SPEED = 66 MPH,
RADIAL PLY TIRES, 73,000 LB GW, 85°F,
STILL AIR

SUMMARY

The primary objective of the advanced turbo-compound diesel engine program was to improve the tank mileage by 5% over the 1980 vehicle test (interim) turbocompound diesel engines. The technical approaches used to develop the advanced turbocompound engine were:

- I. Increase the turbine available energy in the exhaust gas with a more efficient exhaust manifold and by insulating the exhaust system components.
- II. Improve the fuel injection characteristics by providing higher pressures and shorter durations.
- III. Improve the turbocompound system by optimizing the power turbine speed for maximum turbine efficiency and by reducing the turbine shaft bearing mechanical losses.
- IV. Lower the intake manifold temperature from 140°F to 110°F to reduce nitric oxide emissions, and increase engine thermal efficiency.
- V. Improve the compressor efficiency 1-2% by reducing the operating clearances with an abradable shroud.

The combined effect of these improvements resulted in a rated power BSFC of .310 lb/bhp-hr with a minimum BSFC of .298 lb/bhp-hr while meeting the California 6 gram (BSNOx + BSHC) gaseous emission level.

The advanced engine performance map was put into Cummins' Vehicle Mission Simulation (VMS) program to predict the tank mileage over the Cummins' Pilot Center fuel economy route for comparison to the interim engines. In the course of the vehicle testing program completed in 1980, it was proven that an excellent correlation exists between VMS predicted fuel consumption - and actual vehicle test results. The VMS calculations predicted a tank mileage of 5.75 mpg for the advanced turbocompound engine while the interim turbocompound engine prediction was 5.40 mpg. Thus, a predicted tank mileage improvement of 6.5% was achieved with the advanced turbocompound diesel engine.

In summation, the advanced turbocompound diesel engine program met and exceeded all tank mileage goals, further enhancing the potential fuel consumption savings of the turbocompound diesel engine. The turbocompound engine provides an opportunity for the future by offering increased thermal efficiency, reduced exhaust emissions, and improved driveability while maintaining present standards of durability.

Status Report on Diesel Organic Rankine Compound Engine for Long - Haul Trucks

Michael D. Koplow, Luco R. DiNanno,
and Francis A. DiBella
Thermo Electron Corp.

ABSTRACT

Among the efforts in this year's Truck Bottoming Cycle Program was the installation and testing of an organic fluid throttle valve located at the outlet of the vapor generator. The second Test Bed Vehicle (TBV No. 2) equipped with this mechanism and advanced bottoming cycle hardware was operated over the Mack fuel economy course and resulted in a 13.2-percent fuel savings in the 1100-mile test. This fuel savings is a major accomplishment towards the program goal - a 15-percent reduction in fuel consumption. Component development has continued with testing of the vapor generator and evaluation of a soot-blowing scheme for maintaining long-term vapor generator heat transfer effectiveness. Further development of the microprocessor-based control system has emphasized the optimization of the Bottoming Cycle System performance. Other work included stability testing of Fluorinol-85 in a specially constructed fluid loop. Baseline tests at a fluid temperature of 550°F have shown no decomposition in 1600 hours of operation.

THE TRUCK BOTTOMING CYCLE PROGRAM was initiated as an energy conservation project about a year after the oil embargo of 1973, with the objective of developing the technology for reducing the consumption of petroleum fuel in the transportation sector of the U.S. economy. Since that time, substantial progress has been made in improving the fuel economy of automobiles through vehicle downsizing, reduced engine size, dieselization, and technological advances in engine, powertrain, and aerodynamic design. In heavy-duty transportation some fuel savings have been accomplished through substitution of small trucks for larger ones (e.g., Class 7 for Class 8), using lower powered engines, some measurable improvements in engine efficiency, and the more widespread use of energy saving options such as fan clutches, wind

deflectors, and radial tires. Overall, the fuel saving improvements in heavy-duty transport are less - both proportionately and absolutely - than in the automotive sector. It has been projected by DOE that by mid-decade the aggregate fuel consumption of trucks and other heavy-duty vehicles will exceed that of automobiles. Fuel efficiency improvement is more difficult with trucks than automobiles because it is largely prime mover efficiency improvements that are needed, and these are difficult to accomplish. The Truck Bottoming Cycle System, with a projected fuel savings of 15 percent, represents the largest single gain in prime mover efficiency available for long-haul trucks.

One area of diesel engine research that holds substantial promise for efficiency gains is the development of an uncooled (adiabatic) diesel engine. It is noted that the potential for waste heat recovery with an Organic Rankine Bottoming Cycle System from this more efficient engine is even greater than with a conventional diesel engine.

Domestic petroleum consumption is off sharply from the peak of 1978 when imports reached 8 million barrels per day. Currently we are averaging imports of under 5 million barrels per day. This reduction in petroleum usage is due mostly to reduced automobile fuel consumption coupled with the depressed state of the National economy and the increased cost of fuel since the days of peak consumption. The oil glut we are now experiencing is also a product of the depressed world economy.

One factor that has remained unchanged over the last decade is the dependence of the transportation sector on petroleum fuels. No economically viable substitutes for petroleum show much promise. Thus, while the present petroleum supply picture is bright and prices are stable, there is little reason to be complacent about the longer view. The price of this depleting energy resource will inevitably rise. Efforts to reduce petroleum consumption are still very much in the National interest.

Our work in this program has applied advanced organic Rankine-cycle technology to mobile diesel engine waste heat recovery and has carried the development of the Bottoming Cycle System from concept to complete operational hardware. We have two roadworthy Bottoming Cycle System equipped vehicles, both of which have demonstrated more than 12 percent fuel savings in actual highway tests. In previous years we demonstrated the technological feasibility of the Truck Bottoming Cycle System. In the current program we have made improvements, refinements, and modifications to the system components to gain increased performance, better reliability, and reduced maintenance - efforts directed at the expressed concerns of the truck industry that a Bottoming Cycle System must be as reliable, maintenance free, and easy to operate as the diesel engine itself.

A full description of the work accomplished in the past year is given in the following sections of this paper.

SYSTEM DESCRIPTION

Operation of the bottoming cycle is outlined in the system flow schematic shown in Figure 1. Hot exhaust gas, at approximately 950°F at full power and speed of 2100 rpm, passes through a vapor generator where the organic working fluid (a Fluorinol-water mixture) is vaporized to obtain conditions of 550°F and up to 800 psia at the nozzle entrance of the turbine. The vapor expands through this small single-stage turbine, delivering additional power to the engine output shaft through a set of reduction gears.

After partial cooling in the regenerator, where some of the useful energy remaining in the turbine exhaust vapor is recovered, the remaining low-grade heat in the working fluid is transferred to cooling water in the condenser. Waste heat is rejected to the atmosphere by means of a separate radiator core mounted integrally with the diesel engine coolant radiator. The feedpump then pumps the condensed working fluid through the liquid side of the regenerator, where the Fluorinol regains part of the cycle heat, before it once again enters the vapor generator, completing the cycle.

In the current truck bottoming cycle system, waste heat is extracted from the exhaust of a standard 285 horsepower turbocharged and inter-cooled four stroke diesel engine (Mack Model ENDT676). The bottoming cycle system package incorporates all components of the organic fluid loop into two subsystems: the power conversion unit (including the turbine, gearbox, feedpump, and integrated condenser-regenerator) and a vapor generator module. The third module for cooling functions consists of the fan and compound radiator and has only water connections to the organic fluid system. This packaging arrangement allows the organic fluid system to be located entirely at the rear of the diesel engine.

POWER CONVERSION UNIT (PCU) - Arrangement of the PCU components is shown in Figure 2. This PCU, which includes the turbine, gearbox, feed-pump, and integrated condenser-regenerator, is packaged around a power take-off unit that has been designed and fabricated specifically for the Bottoming Cycle System to facilitate integration of the system.

Shaft power is produced by a 5-inch-diameter, single-stage, partial admission, axial impulse turbine. Five nozzles with a 7.5 to 1 expansion ratio deliver organic vapor to the turbine wheel and the turbine power is delivered to the diesel engine output shaft through a 17.7 to 1 gear ratio.

Pressurization and circulation of the organic fluid is accomplished by a specially designed three cylinder radial piston feedpump driven at engine speed. The working fluid flow rate is adjusted to engine load by varying the stroke (and hence the displacement) of the feedpump. The condenser, which is a water-cooled plate-fin heat exchanger, and the regenerator are combined in a single integrated unit.

CONTROL SYSTEM - The bottoming cycle control system shown in Figure 3 maintains proper temperatures and pressures in the organic working fluid as the speed and power of the diesel engine are varied in response to driving conditions.

Flow rate of the organic fluid is maintained in constant proportion to fuel flow rate in the diesel engine fuel injectors. This simple open-loop controller is augmented by two additive closed-loop error signals. One signal is proportional to the difference between actual turbine inlet temperature and the design point temperature. The second error signal, based on the rate of change of turbine inlet temperature, prevents instabilities that would otherwise occur due to thermal delays.

Engine fuel flow is proportional to the product of engine speed and the engine injection pump rack position (i.e., driver's throttle setting). Engine tests have shown that fuel flow rate is also proportional to compressor discharge pressure at the turbocharger, and this signal is more convenient to apply in the actual control system. The working fluid flow rate is proportional to the product of feedpump speed and feedpump displacement. Since the feedpump is driven at a fixed ratio to engine speed, feedpump displacement is made proportional to compressor discharge pressure divided by engine speed, with the added correction signals.

WORK EFFORTS AND ACCOMPLISHMENTS

During the past year, Thermo Electron Corporation has made significant progress in the development of the Truck Bottoming Cycle System. Work efforts were directed towards the following major task areas.

- Working Fluid Studies - The goal of this task is to study and develop methods that enhance trouble-free operation of a Rankine-cycle system with the use of the Fluorinol organic working fluid.

- Vapor-Generator Development - The objective of this task is to study, evaluate, and gather data through tests that will lead to the development of a compact vapor-generator heat exchanger with long-term heat transfer effectiveness and mechanical integrity.
- Control System Development
 - System efficiency optimization
 - Working fluid throttle valve
 This task emphasizes the development of a control system that optimizes the Bottoming Cycle System performance across the widest applicable range of operating parameters.

The specific efforts and advances made in the above work areas are described in the following sections.

WORKING FLUID STUDIES - Measurements of the formation of decomposition products are being made by testing under controlled conditions; methods are being developed for the removal of these decomposition products from the working fluid, Fluorinol.

The initial part of this program task was the construction of a dynamic test loop to measure the formation of decomposition products with subsequent development of a method to remove the decomposition products from the working fluid. The dynamic loop shown in Figure 4 consists of a boiler, pump, expansion valve, condenser, and related hardware. The fluid loop incorporates the following features.

- A leak tight system for contamination-free operation.
- System controls for continuous and long-term stable operation of the loop with minimum attention.
- The loop incorporates features that simulate conditions encountered in the Truck Bottoming Cycle System.
- The loop is instrumented to measure key temperatures, pressures, and fluid flow rate.

Rationale - Although working fluid inventory and condition have been documented in prior compound engine system testing (i.e., 1000-hour endurance tests), the tests were not geared for controlled Fluorinol working fluid tests. The fluid was subjected to transient temperature levels during the course of testing for any number of reasons (i.e., control system operation, startup and shutdown conditions, etc.). Also, testing was interrupted and the fluid system vented because of both scheduled and unscheduled downtimes (i.e., hardware changes, etc.).

The dynamic test loop has been designed to expose samples of working fluid to the conditions that are encountered in operating systems so that the fluid can be chemically examined and its decomposition rate ascertained. The idea of the loop is to expose the fluid to very prescribed conditions over fixed periods of time, and chemically measure any changes in the fluid composition.

The fluid circulating loop is designed to expose the working fluid to the operating conditions so that time at high temperature and pressure and the number of cycles which the fluid is put through are maximized.

Test Results - In order to ensure that the Fluorinol-85 (Fl-85) wetted surfaces were contamination free, an initial cleaning procedure was followed. Prior to starting the tests, the loop was first cold rinsed with Fl-85 for 1 hour. The loop was then charged with a 2500-ml inventory of Fl-85 and put through a 4-hour shakedown run at fluid conditions of 550°F and 500 psia. After cooling, the working fluid was drained out, the loop was pumped down and a virgin 2500-ml inventory of Fl-85 was added for the start of the 1000-hour test.

The test series were performed on the Fl-85 at the baseline conditions of 550°F and 500 psia at the inlet of the expansion valve which simulates the turbine in this loop. A total of 1600 hours were run in the two separate tests with approximately 600 hours accumulated during the first baseline series before this test had to be aborted, and a full 1000 hours accumulated during the second baseline test series.

The initial baseline test was terminated after 587 hours of operation due to excessive loss of the working fluid inventory through a fitting in the sampling system. Following the repair of the leak, the system was again charged with 2500 ml of virgin Fl-85 and the second series of tests was started.

The second test series was run for the planned 1000 hours. During both series of tests, liquid and gas samples were taken with the liquid samples analyzed for acidity level. Figure 5 shows the acid level as a function of running time for both tests performed. The neutralization number of each liquid sample is plotted as a data point in this figure. The neutralization number is an indication of a fluid's acidity, expressed in milligrams of potassium hydroxide necessary to neutralize 1 gram of the fluid sample. The methodology followed is that described in ASTM Method D974-64, Neutralization Number by Color-indicator Titration. The allowable acid level for Fl-85 in a Rankine-cycle system determined by prior laboratory experimentation at Thermo Electron, is 0.040. Figure 5 shows that this limit has not been exceeded in the tests performed to date.

During the second series of baseline tests, there were three distinct peaks in the acid level of the working fluid. The first of these peaks in neutralization number occurred within the initial 300 hours of operation and is believed to represent the formation of trifluoroacetic acid (TFAA) from the reaction of oxygen and trifluoroethanol. Although the loop is evacuated with a vacuum pump and the fluid inventory is extensively sonicated before changing the system, some dissolved gases remain in the Fl-85. It appears that once all the acid formed (due to the remaining oxygen in the system) has reacted with the loop materials the neutralization number decreases and reaches an equilibrium condition.

At 748 hours the loop shut itself down due to an electrical circuit interruption. When the unit shuts down, the condenser pressure drops to the vapor pressure of the Fl-85 at room temperature which is approximately 1.3 psia. Some leakage of air apparently occurred during the downtime because after restart, the sample neutralization number at 755 hours showed an increase from 0.013 at the 635-hour mark to 0.023 showing the second peak in Figure 5. The neutralization number dropped to 0.013 at 815 hours and remained low at 932 hours at a value of 0.014. Following a scheduled shutdown at 929 hours, there was a third peak in acid level with a subsequent downtrend at the end of the 1000-hour test.

Gas chromatographic analysis was performed on the virgin Fl-85 prior to the start of the test and again on the final 1000-hour sample. The analysis shown in Figure 6 indicates that no major degradation products were formed. Also, the figure shows that the working fluid essentially remained at the proper fluorinol-water mixture changing from Fl-85 (prior run sample) to only Fl-83.5 at the 1000-hour mark. This change is due to the "pumping-off" which acts as a distillation process, removing the trifluoroethanol with its higher vapor pressure at a faster rate than the water.

Another series of tests have begun with the working fluid at an operating condition of 600°F.

VAPOR GENERATOR DEVELOPMENT - Work efforts on this task are being directed toward effectiveness improvement of the Bottoming Cycle System vapor generator through design modifications and testing in the system dynamometer facilities.

More than 200 hours of testing have been performed on the present vapor generator (VGII). These tests included the verification of fouling characteristics of the heat exchanger and the effectiveness of a soot cleaning scheme.

The other major effort in this program phase is the design, fabrication, and testing of a new vapor generator (VGIII). This heat exchanger has been designed and is now being fabricated.

Vapor Generator (VGII) Tests - The initial work in this task consisted of testing the present vapor generator (VGII) in the system dynamometer facilities as shown in Figure 7. The VGII core shown in Figure 8 consists of 14 finned-tube coils, each 22 feet in length and assembled into a cylindrical package 17 inches in diameter by 48 inches in height. The coils are connected, both on the inside and outside core diameters, to form a single organic fluid circuit. This vapor generator also has added insulation and improved shrouding between the outside portion of the core and surrounding shroud to prevent exhaust gas bypass.

A set of laboratory diesel-ORCS engine tests were initiated to quantify the amount of diesel soot fouling in the vapor generator and to test any soot cleaning mechanisms that were thought to be effective, particularly for the truck's waste heat recovery system. Such tests were conducted with the intention of incorporating any significant results of this testing into the design of the advanced vapor generator wherever possible.

The soot cleaning device selected for testing from the several designs reviewed consisted of an air pressure actuated, butterfly valve which is installed in the exhaust (outlet) stack of the vapor generator.

The operational principle for this soot blowing mechanism or "Burp Valve" is fairly simple. When the vehicle decelerates or descends a hill in a "no load" condition at high engine speed, the valve is closed. With the burp valve closed the diesel engine will pressurize the exhaust system including the vapor generator enclosure. A pressure level of 15 to 18 psig can be attained in this manner in a very short time (less than 5 seconds). Having reached this pressure level, the valve is opened and the sudden expansion of the pressurized exhaust gas should dislodge soot particles from the heat exchanger's finned tube surface and carry them out of the vapor generator.

The diesel-ORCS testing proceeded by first quantifying the degree of soot fouling that occurs within the vapor generator during 100 hours of operation. A 100-hour test interval was found in two earlier endurance tests to be of sufficient duration to measure the effects of fouling on the heat exchanger. No soot blowing was performed during this first 100-hour test. Measurements during this first test, later verified by a subsequent test, indicated as much as a 25-percent reduction in heat exchanger efficiency when soot blowing is not performed. When soot blowing was performed a reduction in vapor generator efficiency of 20 percent was measured. This small difference does not suggest that the soot blowing mechanism described above is successful in completely preventing heat exchanger fouling. In fact, several aspects of the laboratory diesel-ORCS engine test are different from an actual vehicle installation and on-highway test. For example, the soot blowing was performed when the diesel engine was being powered and not when it was under no load (i.e., no fuel injection) and high-speed conditions - as it would be during on-highway applications. The laboratory setup could not duplicate these on-highway conditions and still expect to adequately pressurize the vapor generator enclosure. The pressurization of the enclosure was, in fact, further limited by retrofitting the new burp valve onto a previously used heat exchanger; a heat exchanger not originally designed for high-pressure containment. The vapor generator cylindrical enclosure was sufficiently sealed against leaks to record a maximum pressure of 12 psig at peak engine loads but typically 6 to 10 psig during part load operation. Leaks did occur during the 100-hour test that resulted in maximum pressure levels of only 3 to 5 psig. The significance of containment pressure in providing enough expansion force was quantified during one test at the 100-hour mark. It was found that an improvement in the heat transfer coefficient of at least 10 percent and as much as 25 percent could be obtained if the heat exchanger's containment pressure was maintained at 12 psig instead of 8 psig.

A similar burp valve will be installed in the advanced vapor generator (VGIII) which is designed for 15 to 18 psig pressure containment service. The improvement in vapor generator performance will be measured with soot blowing at these elevated pressure levels.

In addition to the soot blowing tests, the laboratory testing has verified conclusively that a water wash procedure for cleaning the vapor generator does work effectively in restoring the performance of the vapor generator to an "as new" condition. Figure 9 displays the results. For this reason, the advanced vapor generator design will include water spray nozzles located at the top of the finned tube core. These nozzles will allow for periodic but thorough water washings of the core during routine vehicle maintenance periods.

Advanced Vapor Generator (VGIII) - A new vapor generator is now being fabricated for subsequent testing in the system dynamometer facilities. The design features of VGIII, shown in Figure 10, include:

- Post test design modifications developed through VGII testing
- Simplification and cost reduction of fabrication
- Incorporation of soot cleaning device

Several design modifications have been incorporated into the new heat exchanger based on the test results of VGII. To prevent exhaust gas bypass and heat loss from both the outside and inside surfaces of the core, insulation has been placed in these areas. A cylinder valve has been added to the diverter mechanism to close off the upper port when the vapor generator is operating in the bypass mode. Together with the inside stack insulation, this valve prevents any overheating of the working fluid that might occur when bypassing the system. (Overheating was observed on a few occasions during prior road tests on TBV No. 1.) The above feature of VGIII also aids in the energy storage capability when operating the organic fluid throttling valve.

This new vapor generator design contains new features that are aimed at reducing both the material costs and labor efforts to construct this heat exchanger. A major design change is the core which now consists of 15 sets of spirally wound ("pancake") finned tube coils, as shown in the drawing of Figure 11. This vapor generator core has the following features.

- The tube and fin material are constructed of low carbon steel.
 - Ten "pancake" coils are 5/8-in.-o.d. tubes (as in previous vapor generators)
 - Five "pancake" coils are 3/4-in.-o.d. tubes. This set of coils are in the vapor phase region of the vapor generator and the larger tubes will decrease the flow resistance of the working fluid in this section where most of the pressure drop occurs.
- The center core tube is an integral part of each "pancake" coil.

- This center core tube is used as the mandrel to wind the tube coils when fabricating the core.

- Each center tube core has a helix baffle (see Figure 11) to guide the finned tube when initiating the winding procedure and this metal helix also acts as a gas baffle to prevent exhaust gas bypass of the inside core surface.

- The pancake coil design has all tube end connections on the outside diameter of the core. This feature eliminates the inside connections of the previous vapor generator and also the two-step brazing operations. Tube connections are straight through rather than U-bends, reducing the pressure drop on the fluid side of the vapor generator.

VGIII also will contain soot cleaning mechanisms. As shown in Figure 10, there is a built-in water spray manifold with an outside connection that will make water washing of the heat exchanger more efficient. The soot blowing valve will also be mounted at the stack exit, as in VGII, for testing on this vapor generator.

In the recent tests on VGII with the soot blowing (burp) valve, the pressure level buildup in the vapor generator upon closure of the burp valve was limited due to inherent leak paths in the heat exchanger (VGII was not originally designed to withstand appreciable internal gas pressure levels). Since the capability to build up pressure (internal to the vapor generator without appreciable gas leaks) is necessary to properly test the effectiveness of the burp valve, particular attention was given to adequate sealing of VGIII.

This new vapor generator is currently being fabricated and will be tested during the current program.

CONTROL SYSTEM DEVELOPMENT - Developmental work has continued on the microprocessor-based control system during this program phase. Initial efforts consisted of modification and installation of the control system (updated version as it exists in TBV No. 2) into the system dynamometer facilities to serve the function of general control of the compound engine for all testing (i.e., vapor generator tests) and also to serve as the "baseline" unit for further development work on the control system efficiency optimization.

An automatic data acquisition system has been designed and built for the control system and this capability has been incorporated into the TBV No. 2 control system. This feature eliminates the need for manual recording of the Bottoming Cycle System parameters during operation.

Another major effort this year is the frequency response tests, which are still in progress in the system dynamometer facility, to optimize the temperature error gain and establish control system stability during transient operating conditions.

Data Acquisition System - The second Test Bed Vehicle (TBV No. 2) is equipped with a microprocessor-based digital control system with added automatic control features including a data acquisition system. When a set of data is desired during a run, the operator actuates the data button and all pertinent parameters of the bottoming cycle system (temperatures, pressures, etc.) are automatically stored in memory of the on-board computer. The system is now also equipped with self-diagnostics which alert the operator to various problems (i.e., low organic fluid flow, high condenser pressure, low lube oil pressure, etc.).

The schematic of Figure 12 shows the interfacing of the various features of the control system and sequence of events from the data taking command to the final data printout. Figure 13 is a photograph of the CRT display, showing the page 1 data (there are two pages of data) being monitored during actual operation of the system. When the data button is actuated, the parameters being displayed on the CRT are stored in the on-board computer located in the control system unit shown in Figure 14. After a run or series of trips, the data are then transferred from the on-board computer memory to tape and/or to a data terminal for printout as shown in Figure 15.

Frequency Response Tests - Another major effort on the control system is to establish the maximum gain on the "set temperature" control loop to optimize response time and prevent instability during transient conditions. Some frequency response tests have already been performed to record the control system response to sinusoidally varying input signals. From this data mode, plots of gain and phase angle are being developed to show the optimum temperature error correction and rate error correction while maintaining a proper stability margin.

In the initial frequency response tests performed on the control system, the temperature error gain, $K_1 (T - T_{SET})$ of the control equation shown in Figure 3, was investigated. Although the conclusions from these tests are valid only for linear systems, the thermal inertia of the vapor generator should mask the other nonlinearities.

The steady-state temperature gain was determined by changing pump stroke a fixed increment and recording the two steady-state temperatures at a specific operating load and speed condition on the engine.

The temperature feedback loop was then opened and a voltage signal was imposed on the control summing junction with a sine wave generator. The signal level was then adjusted at extremely low frequencies to provide the same temperature swing that was obtained during the steady-state test. Signal frequencies were then increased with both input and temperature output being recorded on a strip chart.

The stability criteria for a linear system are:

- A phase margin of no greater than 45° (degrees from -180°) must exit at the 0 db attenuation curve.
- At the phase shift of -180° the gain (attenuation) must be no greater than -10 db.

Figure 16 is a Bode plot of the data from this steady-state test and shows the two stability criteria to be met for this condition. As a test, the temperature error gain of the control system was increased by approximately 20 percent; this resulted in an oscillatory system with a turbine temperature limit cycle of $\pm 30^\circ\text{F}$, thus indicating the gain for the system was optimum at the initial test point. This test was performed at an engine operating condition of 274 horsepower (1800 rpm and 800 ft-lb). Additional dynamic tests at other power levels will be performed during this program phase.

WORKING FLUID THROTTLE VALVE - An organic working fluid throttle valve has been installed on TBV No. 2 at the outlet of the vapor generator. This mechanism improves fuel economy by containing heat energy for use in an optimized schedule in the operation of the Bottoming Cycle System. The ORCS control system automatically operates the throttle valve according to the "load" or "no load" condition of the diesel engine. The valve remains in an "open" position when the engine is under a loaded condition and "closed" (energy storage mode) when the engine is not loaded (i.e., driving down grade).

The throttling valve is positioned in the organic fluid line between the vapor generator exit and the turbine inlet. The signal to close the valve is generated by the control system when the compressor discharge pressure falls below a set value. A small orifice in a line parallel with the valve acts as a bypass circuit to allow a small amount of fluid flow, thereby preventing local hot spots in the vapor generator.

Rationale - The Test Bed Vehicle (TBV No. 2) is the ultimate laboratory for testing the throttle valve because of the exposure to real road transient conditions (grades, etc.) and the ability to run the same route with and without valve operation for comparison of fuel economy difference. During previous road testing on TBV No. 1 at the Mack facility in Allentown, PA, the idea of controlling the energy flow from the vapor generator was formulated. The energy transferred to the organic fluid when climbing a grade was being expended at a time of low system demand; namely, during the descent from the preceding grade. It was felt that optimizing the match between energy demand and stored energy would improve the system performance.

The organic flow rate is controlled by a reciprocating feedpump with variable stroke. The stroke is modulated by a command equation which includes compressor discharge pressure, a measure of the diesel operating point. During a period of high demand from the diesel (e.g., climbing a grade), the feedpump stroke increases to match the increase in exhaust gas temperature and flow rate. As the demand falls to zero, the vapor

generator is still capable of transferring considerable energy to the organic working fluid. This energy transfer is reflected as an increase in turbine inlet pressure, which subsequently delivers power to the diesel power train at a time of low or zero demand. In the worst case, the energy created by climbing one grade is completely expended on the succeeding downgrade and the next upgrade is met with no stored energy in the vapor generator.

TBV No. 2 Throttle Valve Tests - The second test bed vehicle (TBV No. 2) is equipped with the advanced power conversion unit (PCU) shown in Figure 2, a microprocessor-based control system, and the working fluid throttle valve. Under this task a nominal 750 miles of road testing on TBV No. 2 was to be performed to test the effectiveness of the throttle valve. These initial tests were run on TBV No. 2 (Figure 17) at the Mack Engineering Development and Test Center (ED&TC) in Allentown, PA. These TBV No. 2 tests are being operated over the same basic 278 mile "roller-coaster" fuel economy and endurance road test course that TBV No. 1 had previously run.

Due to several construction projects on the route (over both the mountain and highway portions), there were a few detours which lengthened the overall course from 278 miles to 280 miles. Also, there were numerous "slow-down" areas and starts and stops over the course of a run that did not exist during prior tests and prevented the TBV No. 2 bottoming cycle system from operating as effectively as in previous tests with TBV No. 1.

Performance and fuel economy results have been established on TBV No. 1 in two prior tests performed at Mack in side-by-side tests with a control vehicle. The second series of tests with TBV No. 1 (4.98 mpg average fuel economy) showed a 12.53-percent fuel savings over the control vehicle (4.35 mpg average fuel economy).

These present throttle valve fuel economy tests on TBV No. 2 were performed over the course without the use of a control vehicle. Mack has dismantled the control vehicle and no others are available that can be used as a comparison vehicle for this test series. The test results of fuel economy data on the control vehicle during the two separate test series with TBV No. 1 were consistent and showed similar fuel economy.

Mack considers that a valid fuel economy number to use for the control vehicle for the comparison of the TBV No. 2 test results is 4.35 mpg. The tests were otherwise run in an identical manner as was done with TBV No. 1. The same two trailers were used and alternated during each test run for the entire series of tests and, at least, two different drivers operated the vehicle.

A total of 1120 miles were run on TBV No. 2 with the throttle valve operating. The overall fuel economy was 5.01 mpg which represents a fuel savings compared to the control vehicle fuel economy (4.35 mpg) of 13.2 percent. This TBV No. 2 fuel savings is to date the largest improvement attained over the Mack course by a test vehicle

equipped with a bottoming cycle system. TBV No. 1 in the last test series showed a 12.5-percent fuel savings.

The results of these road tests on TBV No. 2 are summarized in Table 1 and are highlighted below.

● Tractor-Trailer Combination Gross Vehicle Weight (GVW)	72,000 lb
● Test Mileage	1120 miles
● Minimum Fuel Economy for a Single Run	4.81 mpg
● Maximum Fuel Economy for Single Run	5.15 mpg
● Average Fuel Economy	5.01 mpg
● Improved (Fuel Savings Compared to Control Vehicle)	13.2%

These tests exposed TBV No. 2 to formal road use for the first time. Prior to these tests, the vehicle was essentially garaged with only occasional local operation. Although in this limited mileage test TBV No. 2 did show an improvement in performance over TBV No. 1, more road use of TBV No. 2 is necessary to shake out the infant mortality type failures and to "fine tune" the vehicle for optimum performance.

It is somewhat difficult from the results of these tests to determine exactly what amount of improvement is due to the throttle valve, but all ORCS data observations during the runs indicated that the throttle valve was operating as designed.

FUTURE PLANS

It is Thermo Electron's objective to finish the development of the Truck Bottoming Cycle System in as complete a fashion as possible, given the constraints on available resources. We want to reduce or eliminate the remaining technical problems of the system and have fully functional operating hardware (e.g., Test Bed Vehicles) that can attract venture capital when the market for energy conservation improves.

Our best chance for accomplishing our objective is to continue working on the two Test Bed Vehicles (Figure 18) which are really our laboratories on wheels. We are arranging with DOE to maintain control over the use of these vehicles through a cost-free lease arrangement. We plan to support continued testing and development of the trucks by using them in commercial service to defray operating expenses while testing them. TBV No. 1 will be used by our Marine Engine Division in Detroit to deliver its products to East and West Coast distributors. TBV No. 2 will be loaned to selected commercial carriers and companies within the truck industry for operation on revenue routes and testing for periods of about 1 month each. Thermo Electron will provide training and equipment support during these loan periods. The response of users and test data will be collected and reported to the government. In this way we will keep the trucking industry informed of progress with the Truck Bottoming Cycle System and test the vehicles at the same time.

Thermo Electron will also be participating in several other projects that involve Organic Rankine-Cycle Systems similar to that of the Truck Program. Our Japanese licensee, Mitsui Engineering and Shipbuilding is just completing its first year of operation of a 14-megawatt Bottoming Cycle System at a Nippon Steel Corporation facility. We will be reviewing technical data on the system's operation that will provide us information on long-term system performance, especially with respect to materials stability. Also, in December we will deliver a nominal 100-kW waste heat recovery system to a wastewater treatment plant in Rochester, Minnesota. This system uses Truck Program related hardware including turbomachinery and controls, and it too will provide operational data useful for the development of Truck Program hardware.

We expect to participate in the NASA/Lewis Advanced Waste Heat Recovery for Mobile Applications Program where we will be designing and costing a high-temperature Organic Rankine Bottoming Cycle System employing RC-1 as a working fluid. This work will build from and improve upon our earlier Rankine-Cycle designs, and will also contribute to the advancement of Truck Bottoming Cycle System technology.

However, working directly on the development of the Truck Bottoming Cycle hardware will have the greatest impact in bringing the Truck Bottoming Cycle to the marketplace. Prototype hardware designs must be improved in terms of function and simplicity now that we have learned their shortcomings. Electronic controls must be reduced from hundreds of components down to a relatively few custom-made chips that will provide the ruggedness and reliability needed for truck use. Packaging of the Bottoming Cycle System must address the requirements of long-haul truck manufacturers today, both their conventional cabs and cab-over models. This can be done, but it requires substantial work.

Some of this work we will be able to accomplish on our own, but clearly some important work will go undone, as things now stand.

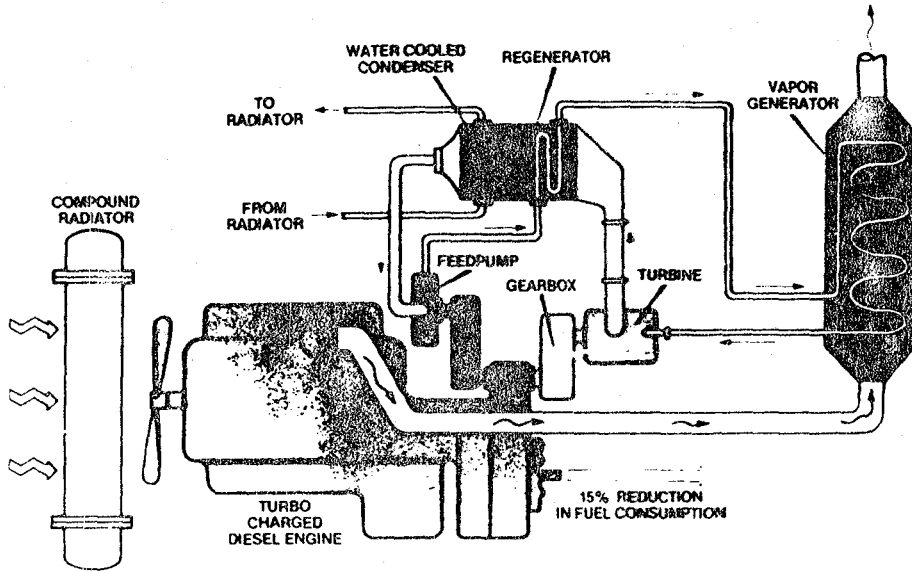
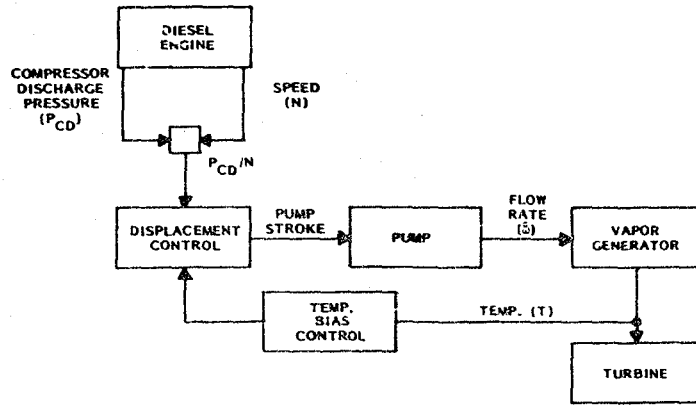


Figure 1. System Outline



Figure 2. Advanced Power Conversion Unit Assembly



CONTROL SYSTEM EQUATION

$$\dot{P}_{CD} = K_1 \frac{P_{CD}}{N} \left[1 + K_2(T - T_{SET}) + K_3 \frac{\partial T}{\partial T} \right]$$

Figure 3. Control Schematic for Bottoming Cycle System

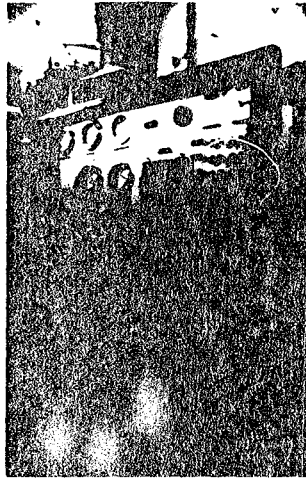


Figure 4. Dynamic Loop for Fluorinol Working Fluid

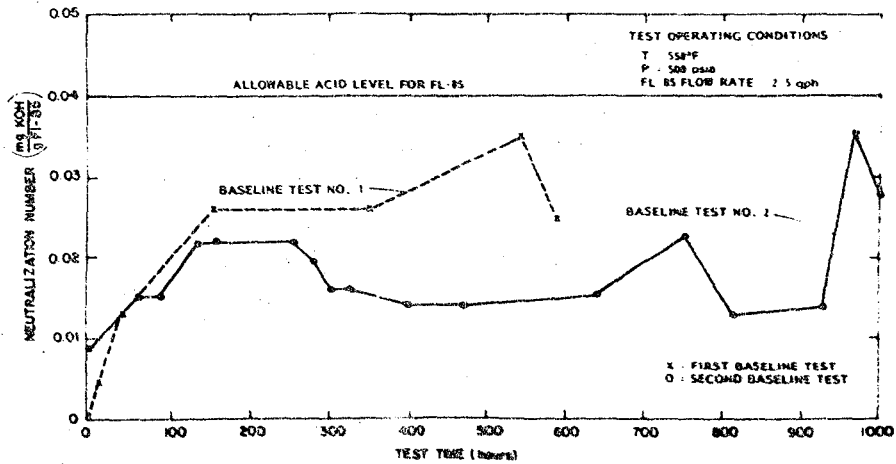


Figure 5. Fluorinol-85 Acid Level vs Test Time in Dynamic Fluid Loop

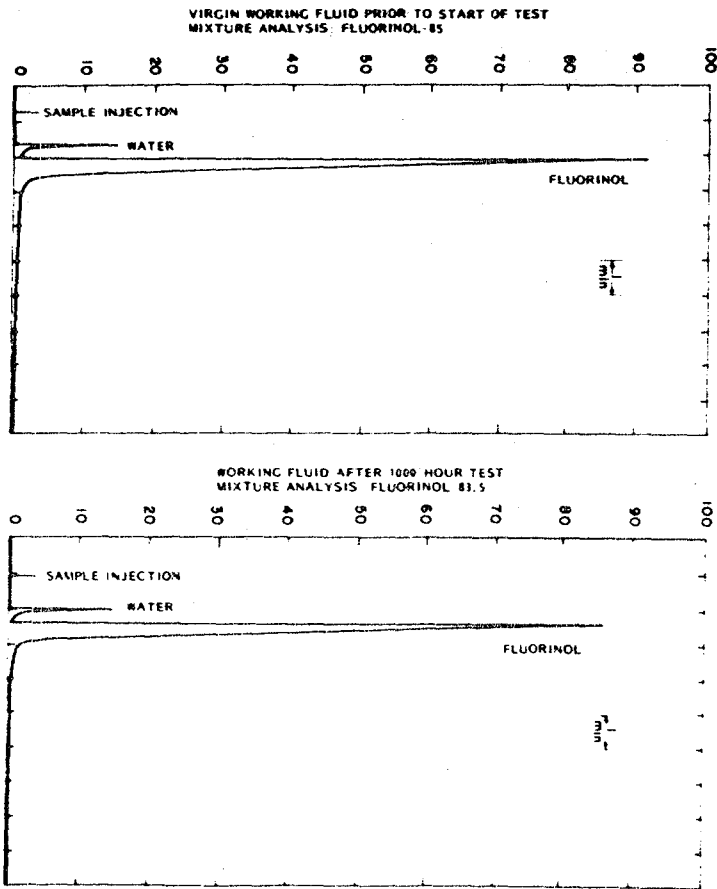


Figure 6. Gas Chromatograph of Working Fluid for Dynamic Loop Baseline Test Series

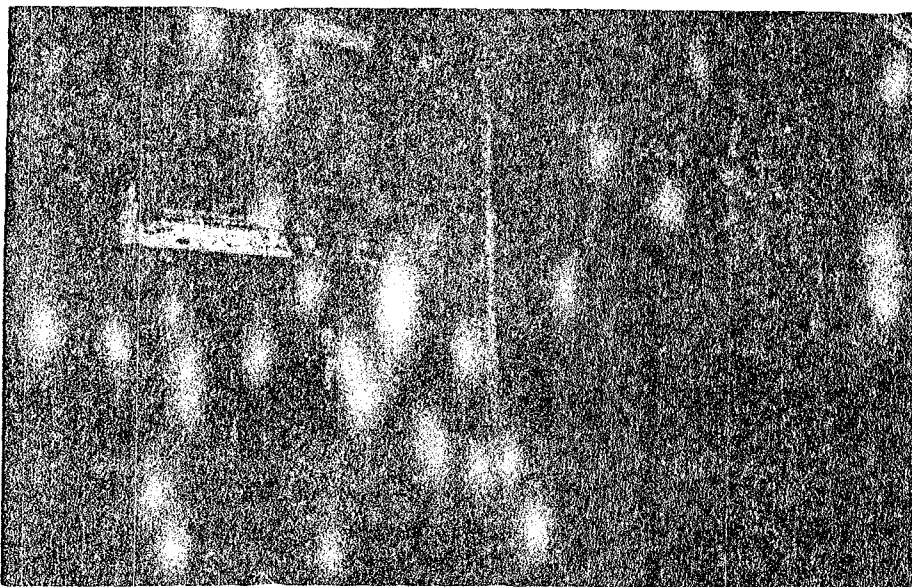


Figure 7. Vapor Generator (VGII) on Test in System Dynamometer Facilities

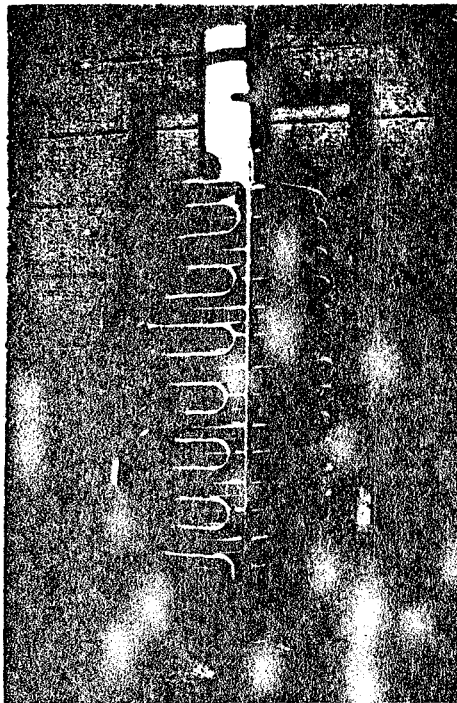


Figure 8. Vapor Generator Core

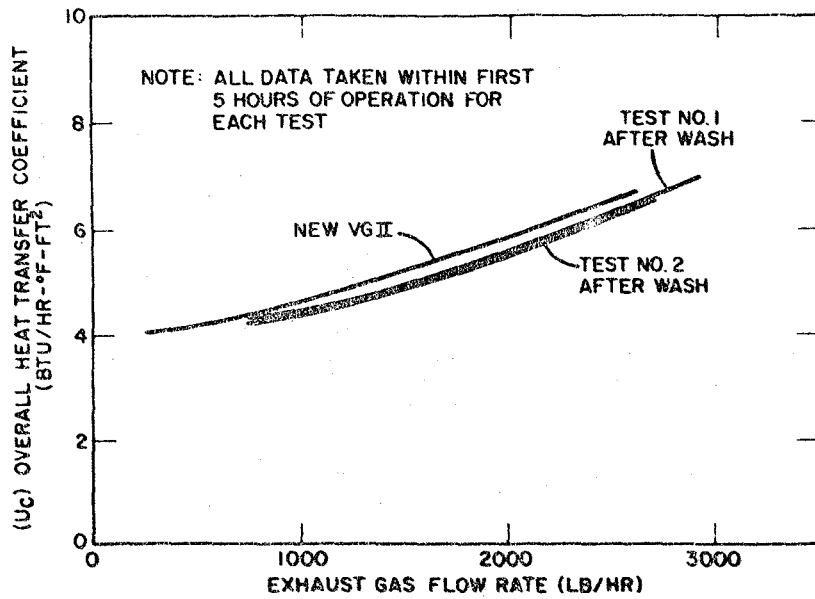


Figure 9. Vapor Generator (VGII) Performance Shown When "New" and After Water Wash Procedure

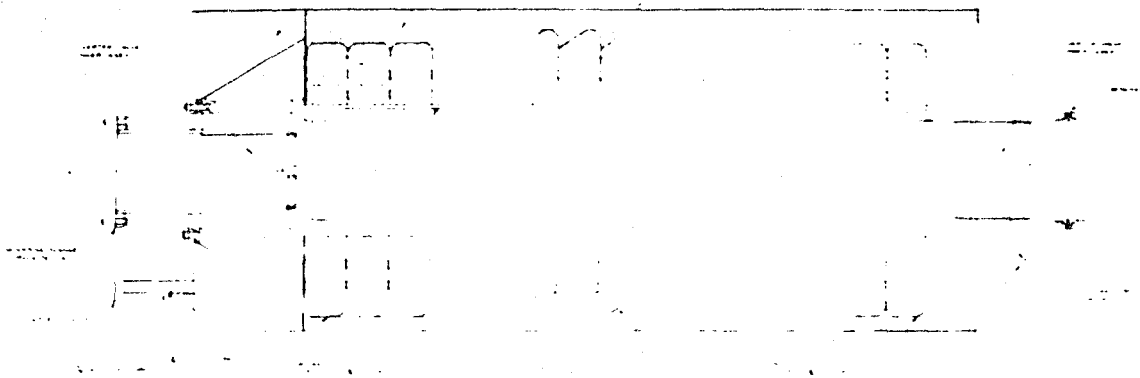


Figure 10. Advanced Vapor Generator (VGIII)



Figure 11. Spiral "Pancake" Coil for Advanced Vapor Generator (VGIII)

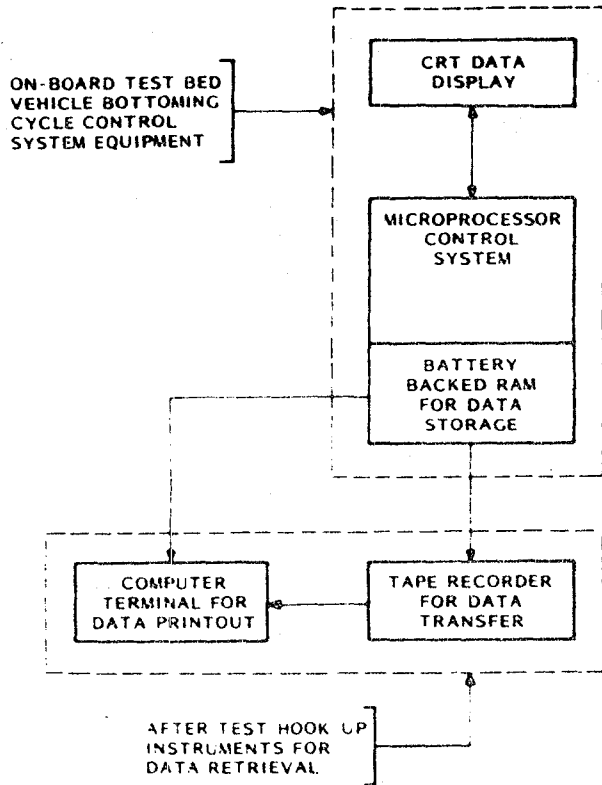


Figure 12. Schematic for Data Acquisition System



Figure 13. CRT Data Display of Truck Bottoming Cycle System in Operation

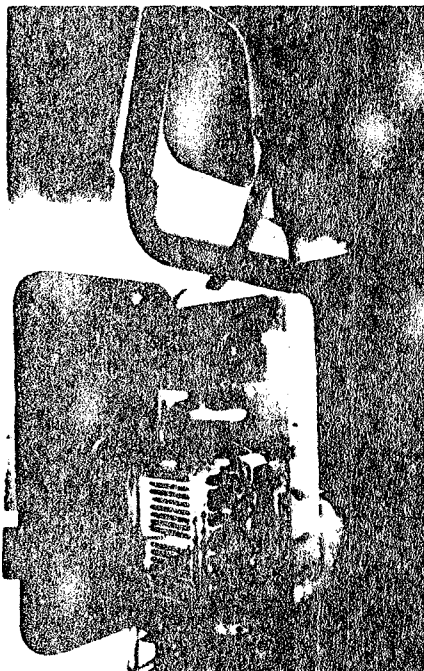


Figure 14. TBV No. 2 Control System Module

8-SEPT-82 15:28:35
 RUN NO 003
 CDP = 19.9 PSI NDE = 1710. RPM FTI = 650. PSI TTI = 517. DEG
 PTU = 654. PSI FCO = 26.3 PSI FLO = 94.2 PSI STR = 81.2%
 TAM = 71.7 DEG TCO = 164. DEG TSO = 141. DEG TUG = 524. DEG
 TGI = 959. DEG TGO = 298. DEG TLO = 138. DEG

8-SEPT-82 15:10:27
 RUN NO 002
 CDP = 18.5 PSI NDE = 1870 RPM FTI = 612. PSI TTI = 470. DEG
 PTU = 618 PSI FCO = 19.9 PSI FLO = 98.2 PSI STR = 78.7%
 TAM = 72.8 DEG TCO = 164. DEG TSO = 140 DEG TUG = 481. DEG
 TGI = 995. DEG TGO = 305. DEG TLO = 135 DEG

8-SEPT-82 14:47:10
 RUN NO 001
 CDP = 19.0 PSI NDE = 1790. RPM FTI = 598. PSI TTI = 465. DEG
 PTU = 606. PSI FCO = 20.5 PSI FLO = 98.6 PSI STR = 82.5%
 TAM = 71.5 DEG TCO = 165. DEG TSO = 140. DEG TUG = 470. DEG
 TGI = 942. DEG TGO = 295. DEG TLO = 131. DEG

DATA PRINTOUT KEY

CDP = Engine Compressor Discharge Pressure (psig)
 PTU = Organic Working Fluid Pressure at Throttle Valve Inlet (psia)
 TAM = Ambient Temperature (°F)
 TGI = Exhaust Gas Temperature at Inlet of Vapor Generator (°F)
 NDE = Diesel Engine Speed (rpm)
 PCO = Organic Working Fluid Pressure in Condenser (psia)
 TCO = Organic Working Fluid Temperature in Condenser (°F)
 TGO = Exhaust Gas Temperature at Outlet of Vapor Generator (°F)
 FTI = Organic Working Fluid Pressure at Turbine Inlet (psia)
 PLO = Turbine Lube Oil Pressure (psig)
 TSO = Turbine Seal Oil Temperature (°F)
 FLO = Turbine Lube Oil Temperature (°F)
 TTI = Organic Working Fluid Temperature at Turbine Inlet (°F)
 STR = Organic Working Fluid Pump Stroke (°)
 TVG = Organic Working Fluid Temperature at Throttle Valve Inlet (°F)

Figure 15. Printout of Data Sets Taken During Operation of Truck Bottoming Cycle System

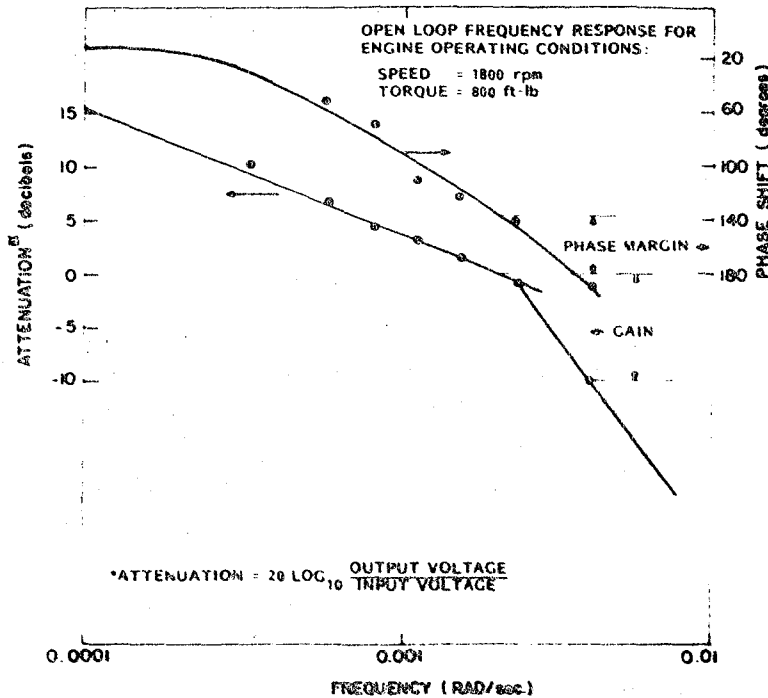


Figure 16. Bode Plot for Bottoming Cycle Control System

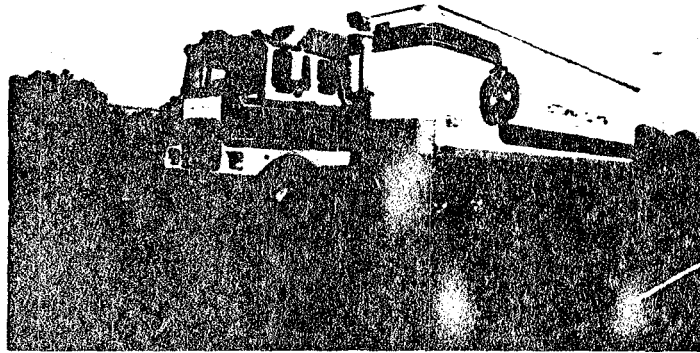


Figure 17. Test Bed Vehicle (TBV No. 2) Throttle Valve Fuel Economy Road Test

TABLE 1
SUMMARY OF TBV NO. 2 THROTTLE VALVE FUEL ECONOMY TESTS
AT MACK TRUCKS, INC. (FALL 1982)

Run No.	Test Mileage (miles)	Fuel Used (gal)			Fuel Economy (mpg)			Fuel Savings (\$) *		
		Mtn.	Hwy.	Total	Mtn.	Hwy.	Total	Mtn.	Hwy.	Total
1	280	21.8	11.4	33.2	4.38	8.42	6.07	16.07	11.47	27.54
2	280	21.8	11.4	33.2	4.38	8.42	6.07	16.07	11.47	27.54
3	280	21.8	11.4	33.2	4.38	8.42	6.07	16.07	11.47	27.54
4	280	21.7	11.7	33.4	4.40	8.36	6.15	16.52	11.47	27.99
Avg.	280	21.8	11.5	33.3	4.34	8.34	6.12	16.50	11.49	27.99
	DATA FROM PRIOR TESTS	TBV NO. 1			4.38	8.42	6.07	16.07	11.47	27.54
		CONTROL VEHICLE			4.38	8.42	6.07	16.07	11.47	27.54

* Fuel Savings = (Fuel Economy (mpg) - Fuel Economy (mpg) Control Vehicle) x Test Mileage (miles) x Fuel Price (\$/gal)

* Fuel Savings = (Fuel Economy (mpg) - Fuel Economy (mpg) Control Vehicle) x Test Mileage (miles) x Fuel Price (\$/gal)

- Fuel Price = \$2.50/gal
- Fuel Price = \$2.50/gal
- Fuel Price = \$2.50/gal

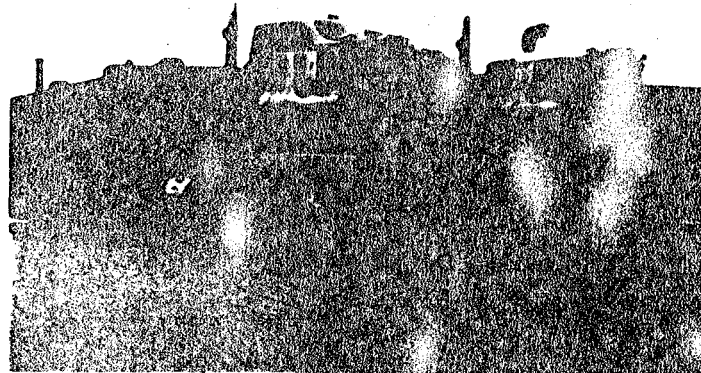


Figure 18. Test Bed Vehicles (TBV No. 1 and TBV No. 2)

QUESTION AND ANSWER PERIOD

Q: Is there either competition or compatibility between this approach (bottoming cycle) and the previous talk in terms of turbo-compounding? Do you see these as being competitive or do you see them as being complementary in some cases?

A: I'd say they are both competitive and complementary. There is certainly the potential to do both waste heat recovery and turbo-compounding on the same engine if there is enough energy in the exhaust gas. The two energy recovery systems would be in series, first turbo-compounding and behind it a Rankine cycle unit. In the near term - as far as commercialization is concerned

- we might find that they are competing systems. It takes a little imagination to envision selling both packages with the conventional diesel engine. But with the adiabatic diesel engine, in fact, I think some of the studies the Army did showed projections with the two (energy recovery) systems in series. With the adiabatic engine, there is a lot of heat in the exhaust gas so it is probably quite reasonable (to use both systems). Because we don't recover the blowdown energy in the exhaust gas, just the sensible heat, the sum of the energy recovered by the two systems in series would be greater than either one alone.

Light Duty Vehicle Diesel Engine Assessment Program Passenger Car Diesel Engine of the Future

Roy Kamo, Luigi Tozzi,
and Raj Sekar
Cummins Engine Co.
Columbus, IN

ABSTRACT

This paper outlines the objectives of the Light Duty Vehicle Diesel Engine Assessment program and the work tasks required to accomplish the same. The power plant and vehicle requirements for the future automobile are presented. The important related economic and technical parameters are ranked. The potentially promising engine concepts and advanced technologies available to meet those requirements are identified and discussed. Conceptual evaluation has disclosed a moderate speed, four stroke, high BMEP diesel engine which is compounded by a positive displacement screw expander and compressor. The power plant will be adiabatic with no cooling water and a minimum friction design with no oil for lubrication. Reliance on advanced materials and technologies is stressed.

The Diesel Engine has made rapid entry in the Light Duty Vehicle market during the last decade, due mainly to its superior fuel economy. In the future, the changing environmental requirements as well as the competition of alternate engines will force changes in the diesel based power plants. It will be to remain in the running.

What are some of the trend changes that could continue to keep the diesel engine as a major competitor? The TACOM/Cummins adiabatic-turbocompound engine, the TACOM/Cummins minimum friction engine, the DOE-TECO/Mack Rankine bottoming cycle, as well as a host of other development activities underway in the heavy duty diesel truck engine sector could very well pave the way for the Light Duty Vehicle diesel engine of the future.

In retrospect, the forces making these

developments possible are advancements in materials, turbomachines, heat transfer technology, and design techniques.

The purpose of this LDV Diesel Assessment program, funded by NASA/DOE, is to identify the potentially promising concepts and approaches which will advance the LDV diesel engine technology. These concepts and approaches will be quantified where possible, and analysis of its influence on engine and subsequently on vehicle performance will be determined. The program will also identify the technological areas where R/D work is required to bring these concepts and approaches to fruition.

LDV SPECIFICATIONS

The baseline vehicle in which an advanced LDV diesel engine will be installed is:

Weight	3000 lbs
Aerodynamic Drag Coefficient	0.30
Frontal Area, ft ²	21.5
Drive Axle	Front
0-60 MPH Acceleration	15 seconds
Emissions	1992 Levels
Transmission	Automatic
Noise	90 dBA @ 1 meter
Roominess Index	1.73 in.
MPG	35

The vehicle and drive train specification and analysis will be provided by the Ford Motor Company of Dearborn, Michigan, which is a

subcontractor to this program.

RANKING OF ENGINE CHARACTERISTICS

Although each engine application places different weighting on each engine characteristic, the LDV diesel engine requirements were decided jointly with NASA. The engine requirements and their ranking in the order of importance were as follows:

1. Fuel economy on Federal combined driving cycle shown in Figure 1
2. Emissions
3. Cost
4. Driveability
5. Size and weight
6. Noise
7. Reliability and durability
8. Multifuel

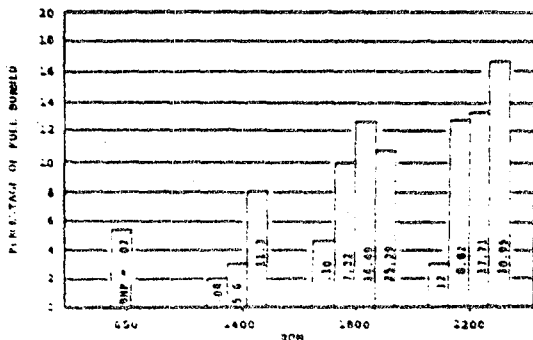


Fig. 1 - Distribution of the engine power as a function of the percentage of fuel burned over the federal driving cycle

ENGINE TECHNOLOGY CANDIDATES

Based on past and current diesel engine technology, many options are available for consideration. Notable among them are:

- . Engine cycles and configurations
- . Prechamber vs. direct injection
- . Adiabatic
- . Turbocompounding
- . Miller cycle (Atkinson cycle)
- . Spark assist
- . Turbochargers
- . Compres
- . Positive displacement
- . Ceramics

- . Injection system
- . Variable displacement
- . Antifriction bearings
- . Gas lubricated piston/liner
- . Oil-less operation
- . Preheat cycle
- . Variable inlet and exhaust valve timing
- . Higher air utilization

ENGINE CYCLES & CONFIGURATIONS

The conventional four-stroke cycle engine was compared to the two-stroke design. In the future, the adiabatic concept is expected to emerge as a reliable low maintenance power plant with no cooling system. Further, the utilization of waste heat from the exhaust can further increase the engine efficiency. The loop scavenged two stroke or the opposed piston uniflow design has much to offer since poppet valves are not required.

The opposed piston two-stroke design has the most to offer because it does not have the complexity of the cylinder head. Heat loss is minimal for this design. When the minimum friction gas bearing for the piston and cylinder liner is considered, the opposed piston design with no side thrust on the engine is ideal. Figure 2 shows the cross-section of a swing beam two-stroke opposed piston engine under development by Sir W. J. Armstrong Whitworth and Company.

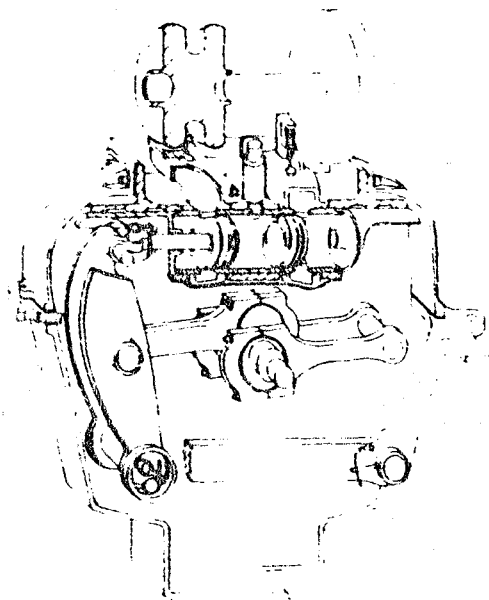


Fig. 2 - Sketch of a two-stroke opposed piston engine

The use of advanced ceramic materials is expected to overcome the major problem facing the two-stroke design, i.e. thermal loading. Absence of lubricating oil passing through the ports will enhance its emissions characteristics. Indeed, the advanced technology, i.e. adiabatic concept, minimum friction, etc., certainly favors the opposed piston two-stroke design. The other features which favor the two-stroke engine design are:

- . High specific output
- . Lower torque fluctuation
- . No valves or gear timing
- . Variable compression ratio (opposed piston design)
- . Variable air flow through ports

The four-stroke engine has served us well over the years. However, to take advantage of the new emerging engine technology, additional complications may be necessary to compete with the two-stroke design. A case in point will be the complexity in the cylinder head design with ceramics or its equivalent. Another will be the gas bearing piston and liner. A cross-head piston design (see Figure 3) through additional crank, Scotch yoke, Rhombic drive, pressurized gas, or any other approach will simply add to its complexity. Nonetheless,

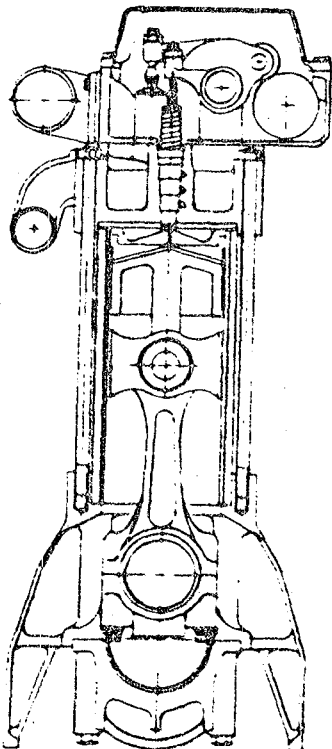


Fig. 3 - Sketch of a four-stroke cross-head diesel engine

a four-stroke engine can be made to operate satisfactorily in the adiabatic form as in the TACOM/Cummins design shown in Figure 4.

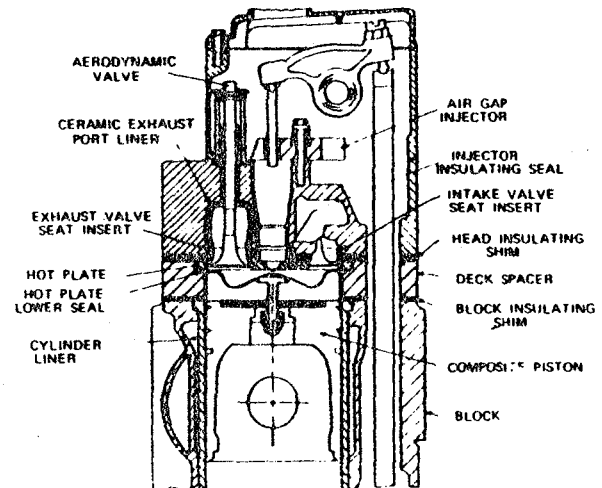


Fig. 4 - Cross section of the TACOM/Cummins insulated diesel engine

It appears at this stage that the emerging advanced engine technology will be more useful to the two-stroke engine than the four-stroke design. It has very favorable impact on overcoming the basic problems of the two-stroke engine of the past:

1. Thermal loading
2. Oil consumption
3. Emissions
4. Fuel consumption in some cases
5. Smoke

ADIABATIC ENGINE CONCEPT

The waterless adiabatic engine has received considerable attention in recent years and for a good reason. The engine operates without water or air cooling and simplifies the design and installation of the engine into a vehicle. Absence of a cooling system improves the overall thermal efficiency and reduces the cost, size, weight, and most importantly, improves the reliability and durability of the engine.

Considerable progress has been made by TACOM/Cummins on the adiabatic engine for the 400 to 700 HP size range. Adequate use of ceramic materials is made to overcome some of the technological difficulties. At this point, the high temperature lubrication problem in the adiabatic engine is the most severe one. Thus, the main problem in the efforts toward minimum friction engine with gas lubricated piston and cylinder liner becomes obvious.

Lower carbon monoxide and hydrocarbons as well as particulates can be expected in the high temperature combustion of an adiabatic engine. However, the favorable NOx emission characteristic of the adiabatic engine was unexpected. Figure 5 shows the trade-off between BSNOx and BSFC for an adiabatic and a standard cooled engine. Figure 6 shows the expected drop in particulates as compared with a standard water-cooled engine.

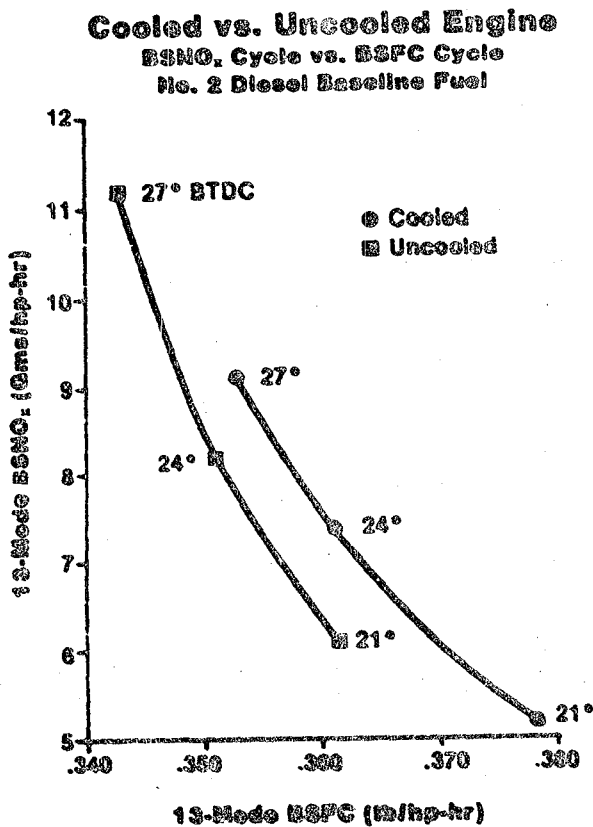


Fig. 5 - Comparison between cooled and uncooled engines on a BSNO_x-BSFC trade-off basis

Adiabatic vs Conventional Engine Relative Carbon Particulate Levels

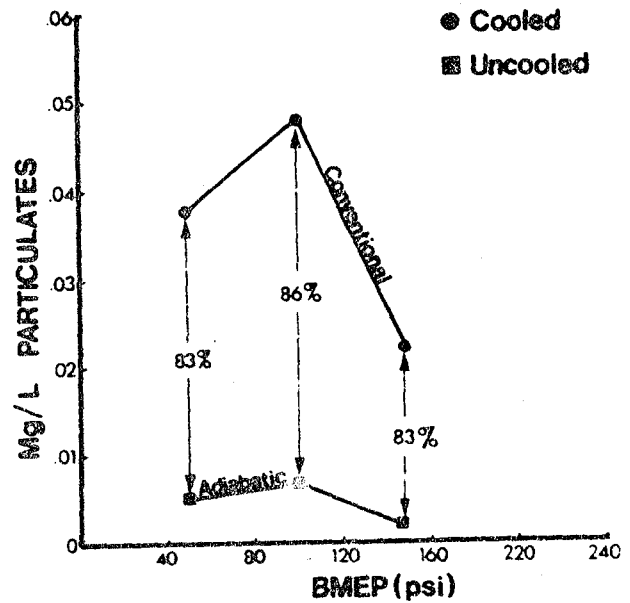


Fig. 6 - Comparison between cooled and uncooled engines on a particulate emissions basis

One of the important fail outs of the adiabatic engine has been its multifuel capability. The hot cylinder walls and cylinder head walls exceeding 1000° F contribute to the combustion of low cetane fuel. Figure 7 illustrates the excellent multifuel characteristics of the adiabatic engine.

Efficiency Comparison House Fuel vs. Synthetics 1900 RPM .085 Static Timing

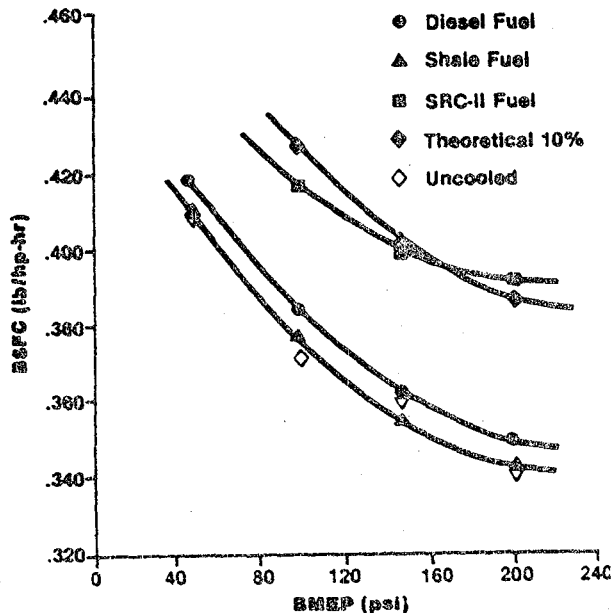


Fig. 7 - Fuel tolerance evaluation of an uncooled engine on an efficiency basis

MINIMUM FRICTION TECHNOLOGY

The objective of a minimum friction engine is to operate without oil and keep the frictional losses low. Gas lubricated piston and liner without piston rings can contribute the most to the overall mechanical friction reduction. High temperature lubrication problems of an adiabatic engine will also be minimized.

The most severe problem facing the gas lubricated piston and cylinder liner is the side thrust induced by the connecting rod angularity. To remedy this situation, a cross-head piston may be necessary in a conventional crank, four-stroke or two-stroke engine. The opposed piston, swing beam, two-stroke engine described earlier has no side thrust on the piston.

Another approach toward overcoming the side thrust force on the piston is to provide a passage for the combustion gases through the piston to obtain pressurized gas bearing. This approach, however, is more complex and probably less efficient. Reliability may be affected by the combustion products.

The crankpin, wrist pin, and the crankshaft main bearings can be made from ceramic antifriction bearings as shown in Figure 8.

These bearings are expected to operate at minimum friction without oil.



Fig. 8 - Picture of a crankpin with ceramic roller bearing

The camshaft, rocker arm, and gears will be solid lubricated in conjunction with low friction materials. Considerable progress has been made in the field of solid lubricants. A recent development is the use of micropockets in bearing materials filled with solid lubricants such as CaF_2 and MoS_2 , as shown in Figure 9.

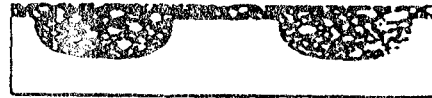


Fig. 9 - Cross section of an antifriction bearing with micropockets

COMBUSTION CHAMBER

In the past, it was considered that a prechamber engine was necessary for high speed operation. Since direct injection offers 10 to 15% improvement in fuel economy over the prechamber, a considerable amount of development efforts is directed toward DI. Furthermore, high BMEP operation with slower engine speed to reduce friction, such as the Cummins Formula concept, is bound to enter the LDV diesel engine field. A modern direct injection, high BMEP, small diesel engine is scheduled to be in production next year. This engine achieves a minimum fuel consumption of 0.338 lb/bhp-hr and the specific weight of the package is only 4.5 lb/hp. The six cylinder version weighs 4.0 lb/hp.

In order to achieve multifuel capability, a spark assist will be quite helpful. The adiabatic engine has demonstrated its capability to burn low cetane fuel down to CN10, as shown in Figure 7. A spark assist can further improve this as demonstrated on a DOE Coal Utilization Branch program. Figure 10 shows improvement in combustion diagram with spark assist when burning middle distillate SRC-2 coal-derived fuel oil with CN18.

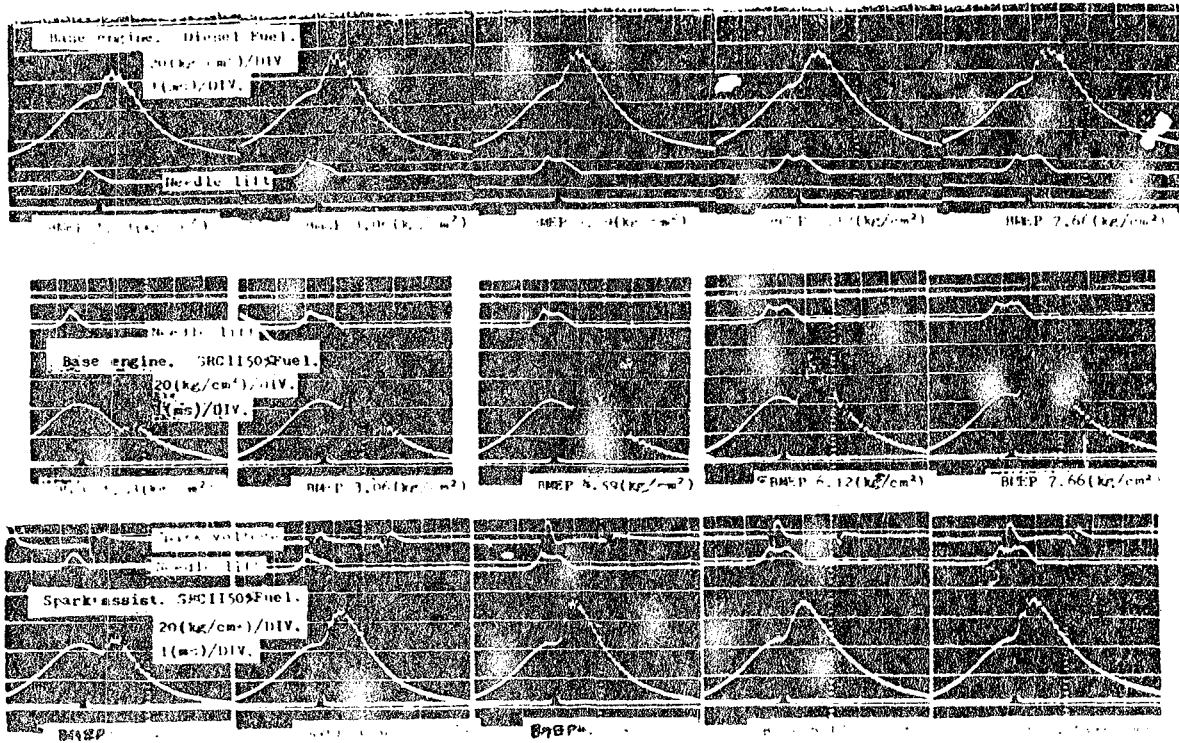


FIG. 10 - Comparison of combustion pressure diagrams for spark assisted diesel engine

AIR HANDLING SYSTEM

The present trend toward turbochargers has subsided, mainly because of its simplicity and low cost. However, for the LDV engine, the turbochargers are exceptionally high speed (100,000 - 200,000 rpm) machines with low aerodynamic efficiencies. For practical reasons, it is not adoptable to turbocompounding as developed by Cummins on the slower speed heavy duty truck engine as shown in Figure 11.

**CUMMINS NH
TURBOCOMPOUND
DIESEL ENGINE**

A hybrid diesel-turbine system in which piston power is supplemented by turbine power recovered from the exhaust gas.

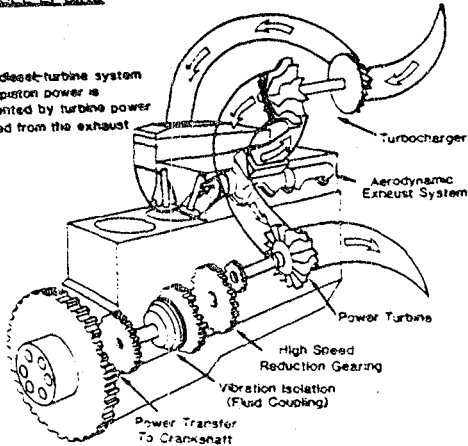


Fig. 11 - Sketch of the Cummins NH turbo-compound diesel engine

If waste heat utilization from the exhaust and high response are desired, the positive displacement machine has much to offer. It is slower in speed and more efficient in some cases. An internal expanding type machine is highly desirable from the standpoint of efficiency. An entire system using such a unit is shown in Figure 12.

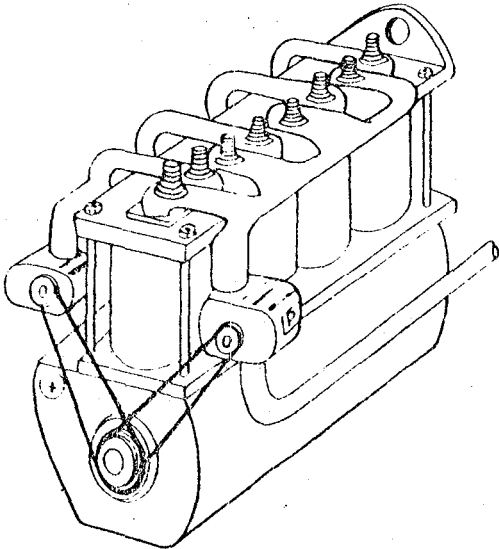


Fig. 12 - Conceptual sketch of the Cummins LDV adiabatic PD compound engine

The projected adiabatic efficiencies of the highly efficient screw compressor and expander are shown in Figure 13. The predicted performance by use of these machines for the PD compound system is shown in Figure 14. It is compared to a similar turbocharged engine. It must be noted that the PD compound system also has excellent response characteristics.

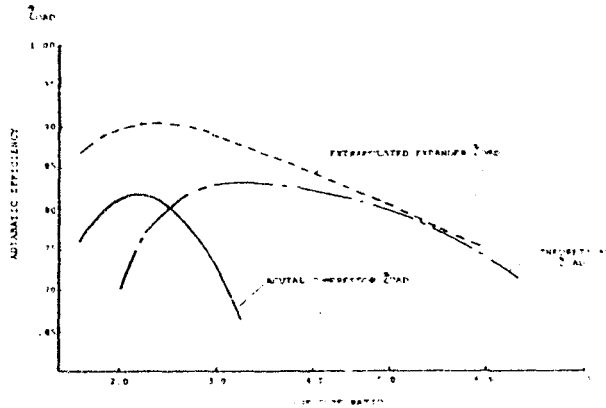
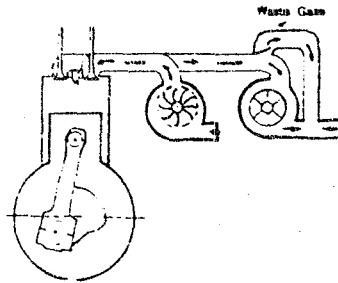


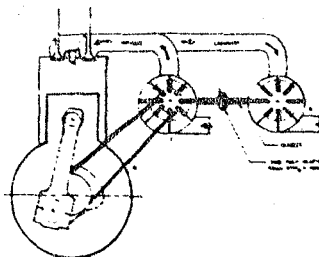
Fig. 13 - Positive Displacement Expander Adiabatic Efficiency (Projected)

CONVENTIONAL WASTE GATED TURBOCHARGER SYSTEM



Waste Gate
 $\eta_c = 0.69$
 $\eta_t = 0.60$
 $\eta_m = 0.96$
 BHP = 88
 BSFC = 336

CUMMINS POSITIVE DISPLACEMENT COMPOUND SYSTEM



$\eta_c = 0.80$
 $\eta_{ext} = 0.90$
 $\eta_c = 0.85$
 BHP = 102.2
 BSFC = 299

Fig. 14 - Predicted performance improvements for the positive displacement expander and compressor over a conventional turbocharged system

Another air handling system considered was the Comprex. The Comprex matches the requirement of the LDV duty cycle quite well. The response characteristics are conducive to excellent driveability. A combined efficiency vs. load for a Comprex and a turbocharger is shown in Figure 11. The performance of a Comprex on a LDV diesel engine is quite obvious from this figure. One of the problems of the Comprex is the inability to utilize waste exhaust energy to obtain useful work.

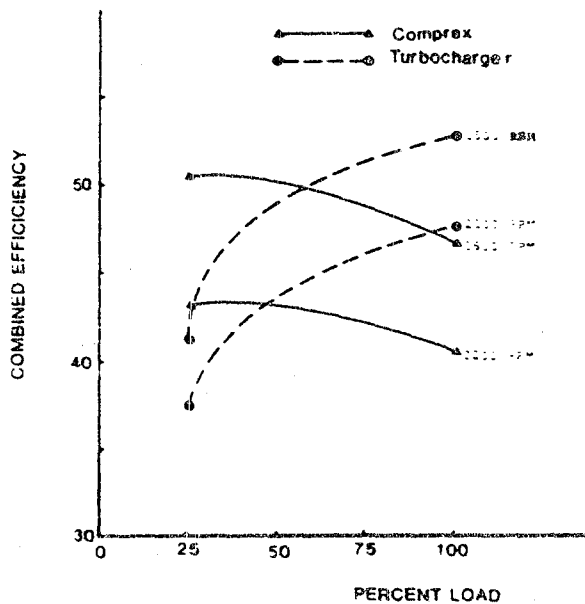


Fig. 11 - Performance comparison between Comprex and Turbocharger

NOISE

The limited available LDV noise data compares many new design concepts directly unknown to the engine design field. The Institute of Sound and Vibration Research (ISVR) has been selected to join forces with Daimler-Benz to assist in completely redesigning the conventional engine block-head assembly by a structural approach consistent with low noise. Over many years of experience with noise emitted by conventional passenger car diesels are shown in Figure 12. The advanced LDV engine is expected to reduce the noise level as indicated by the dashed line. This improvement in noise is expected through:

- Low speed-high BMEP design
- Structural design
- Spark assisted combustion

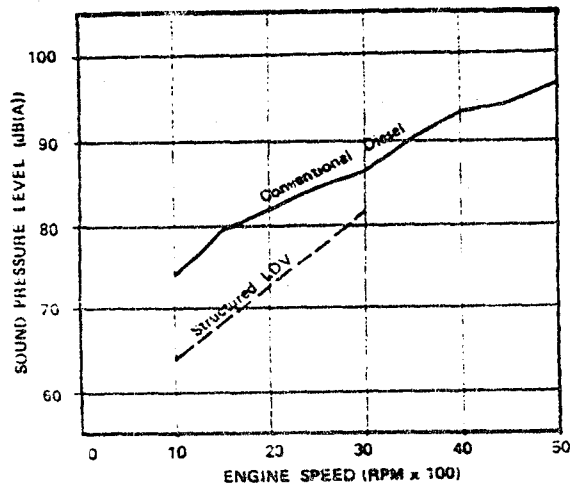


Fig. 12 - LDV noise comparison to the conventional diesel.

OTHER ADVANCED TECHNOLOGIES

Other advanced technologies are still available for application to the diesel engine of the future. These are:

- Variable inlet and exhaust valve timing
- Ultra high injection pressures
- Preheat cycle

The variable inlet and exhaust valve timing can be achieved in a number of ways. At low levels of air flow, the use of variable engines, a spirally vane controlled electronics would be possible. Variable valve timing enables optimum timing as a function of engine load and speed. Furthermore, it is also possible for maximizing exhaust gas energy for the turbocharger. Ultra high injection pressures will reduce the variation of the spray pattern and improve the fuel-air ratio.

- Variable injection
- Miller cycle - Atkinson cycle
- Preheat cycle
- Exhaust gas preheating

The ultra high pressure ultra high injection system with a compatible combustion chamber could approach homogeneous combustion as the droplet sizes approach minimum levels. A higher air utilization can be achieved in the future engine with a reduced air inlet loss. Significant increases in horsepower are possible for a given peak pressure, if air utilization could be increased from 80% to 90% air fuel (A/F) ratio. The exhaust temperatures will approach those of a gasoline engine or even greater. This matches the requirements of a turbocompound system. Materials to withstand high temperature fatigue are essential in this

application.

The electronically controlled fuel injection and the electronic intake and exhaust valve control add up to a microprocessor controlled system which can give optimized fuel economy, performance, and emission characteristics at the entire operating range of the vehicle.

Finally, a method to improve the part load efficiency of the turbocompound engine would be highly desirable. One cycle being investigated now is the preheat cycle where the compressed air is heated by the waste exhaust energy. Figure 17 illustrates the cycle on the h-s diagram. The combustion temperature may be kept constant over a wide operating range and thus providing the turbocompound unit with adequate exhaust energy for its operation.

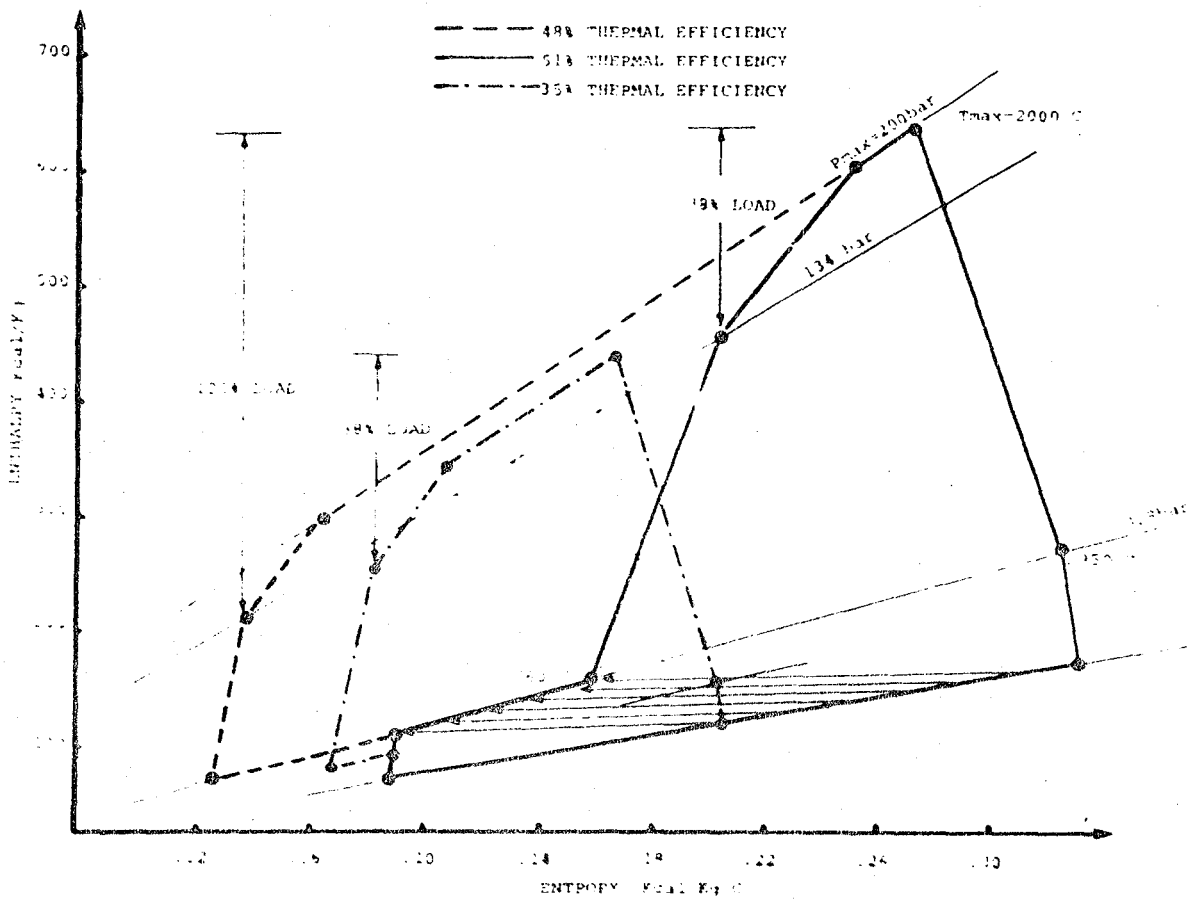


Fig. 17 - Comparison between a conventional part load diesel cycle and the proposed preheat cycle.

PERFORMANCE PREDICTION

The selected power plant for the Light Duty Vehicle Diesel Engine when installed in a vehicle with specifications described earlier is expected to give the following miles per gallon fuel consumption when fully optimized, starting with the prechamber diesel-powered vehicle as the baseline.

Possible Improvements in Fuel Economy

Over Combined Federal Driving Cycle
Shown in Figure 1

Baseline-Indirect Injection Engine	37.7
Direct Injection Combustion System	43.2
Formula Concept (High BMEP, Low Engine Speed)	45.8
Adiabatic Concept	50.1
. Thermal Efficiency Improvement	
. Elimination of Fan	
. Absence of Pulley and Belts	
. Ceramic Components	
High Injection Pressure, Fast Combustion	53.0
Optimized Variable Valve Timing & Injection	57.0
Minimum Friction Concept	61.4
. Gas Bearing	
. Ringless Piston	
. Rolling Element	
. Antifriction Camshaft, Rocker	
. Elimination of Oil Pump	
Positive Displacement Compounding	65.1
High Efficiency Part Load Air System	67.6
Water Pump Elimination	68.9
Weight Reduction of Engine/Accessories	69.4
Drag Reduction of Vehicle	70.6

CONCEPT EVALUATION

Although all the technical information from the various subcontractors is not in, they will be considered concurrently during the power train analysis task. Based on the present information, data, and thinking, the LDV Diesel Engine will have the following specifications and features:

Specifications

- Engine Configuration	D.I., FD Compounded
- Engine Cycle	4-Stroke
- Bore and Stroke	77 mm x 77 mm
- Number of Cylinders	4
- Compression Ratio	14
- Rated Engine Speed	3000 rpm

- Horsepower 80
- Engine Displacement 1.44 liters

Features

Adiabatic - Uncooled (waterless)

- Insulated Piston
- Insulated Liners
- Insulated Cylinder Heads
- Insulated Exhaust Ports
- Insulated Intake Ports
- Insulated Exhaust Manifolds
- Insulated Valves

Minimum Friction (oil-less)

- Gas Bearing, Piston/Liner
- Antifriction Ceramic Rollers
 - . Wrist Pin
 - . Crankpin
 - . Main Bearings
- Solid Lubricants
 - . Valve Guides
 - . Cams
 - . Gears

Multifuel Combustion System

- Spark Assisted Diesel
- May-Type CC
- Fast Combustion
- Low Noise
- Low Emissions

Low Noise Design

- Lower Engine Speed
- Structured Design
- Smooth Combustion

FD Compound System

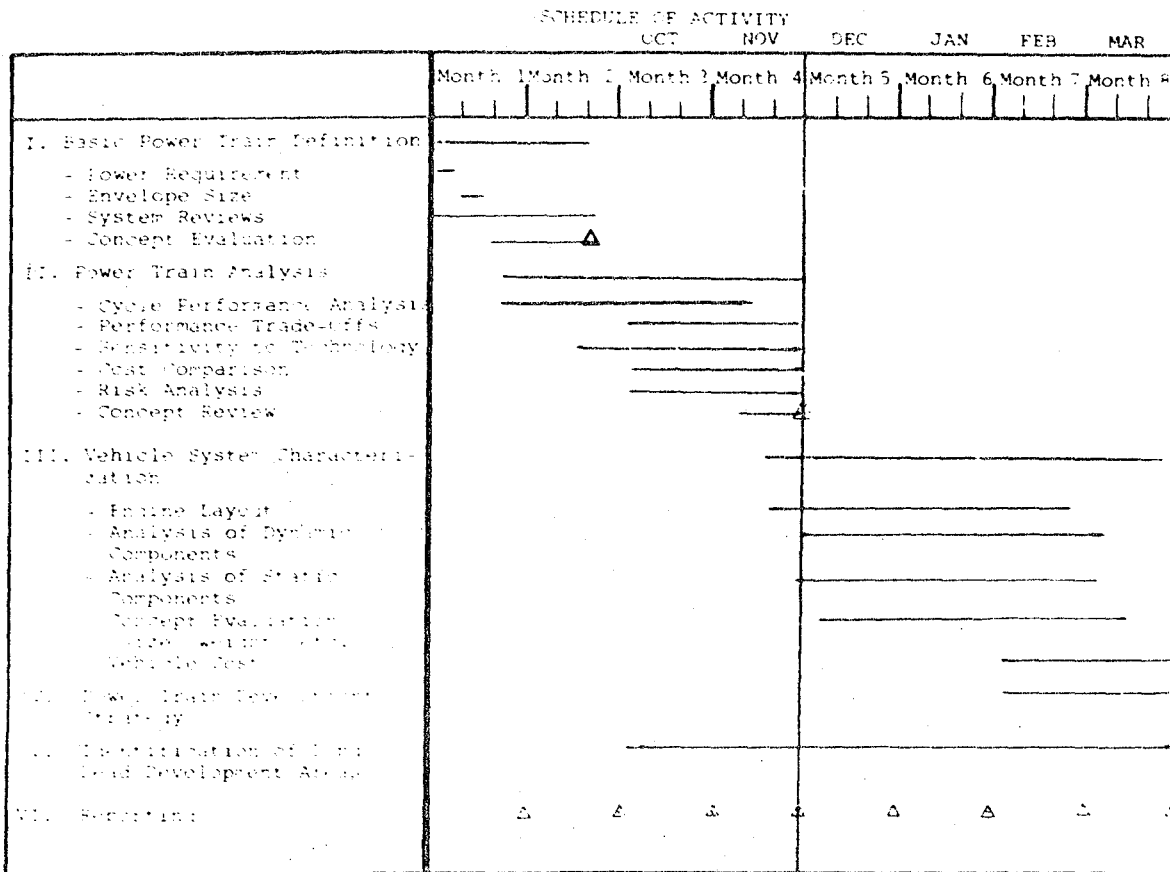
- Efficient Screw Compressor and Expander (VCR)
- Exhaust Gas Waste Utilization
- Outstanding Response

WORK SCHEDULE

The work schedule outlining the tasks of this DE NASA-sponsored program is shown in Table I. We have completed Task I, Basic Power Train Definition, and are now beginning Task II, Power Train Analysis. Upon completion of Task II, the power plant performance and emission map should be forthcoming.

The Ford Motor Company has been subcontracted to conduct the Vehicle System Analysis. Ford will be provided with the new LDF Diesel Engine performance and emissions characteristics. Ford will aid in conducting power train analysis, vehicle system characterization, vehicle cost analysis, power train development strategy, and in the identification of long-lead technology requirements.

FIGURE 1
ADVANCED ALTERNATIVE DIESEL ASSESSMENT PROGRAM



QUESTION AND ANSWER PERIOD

- Q: I have two questions. First you showed that you wanted to go with the two stroke concept and then with the four stroke. But wouldn't both of those detract a little bit from performance? It seems to me that customers want a lot of acceleration performance nowadays at least, and wouldn't you be detracting from that? Second, for all these improvements, once you get past 50-60 MPG your gallons per mile savings are pretty small. Are these going to be cost effective at all in any way?
- A: This engine number one has a positive displacement compressor and their response would not be slow. You know they have faster response than a turbocharger. And as for the last question, your guess is as good as mine right at the moment.
- Q: Roger Storm, Carborundum. Roy, I have a comment rather than a question. We agree wholeheartedly with your assessment of the potential for two-stroke, particularly with regard to incorporating ceramics into the engine. And as you are aware, we recently ran the opposed piston two-stroke engine which you were describing and were able to eliminate any lubrication or cooling and still got a very dramatic reduction in friction. We will be presenting that in conjunction with Professor Timoney and Mr. Flynn as an SAE paper in February, 1983.
- A: Thank you Roger. I think that's a good point and for those of you who don't believe that you could run these engines without coolant or oil, ask Roger. They have done it. They have done it with Professor Timoney's opposed piston two-stroke engine and we see as long as you don't have any side thrust, it's a very simple way of doing it.
- Q: You showed several curves, Roy, of performance and some other curves on emissions with alternate fuels and particulates and so forth. Are those projections for one of these small engines, or measurements on one of your previous ones?
- A: Those are actual data from a single cylinder 5-1/2" bore 6" stroke NH engine. We think we could obtain similar results for this passenger car engine, but since we don't have an engine, I gave you the data from the NH engine.
- Q: Could you comment on how you think these figures might change with the smaller displacement for each cylinder?
- A: The smaller engine will have higher surface to volume ratio. I don't think it will get worse. If anything, it might get better. You shouldn't ask me that. I'm too optimistic.
- Q: It seems to me this is a rather long term project. When do you think you can commercialize this engine?
- A: That is a good question, but I have no answer because you need R&D funds. That push now is the dollar sign.

TACOM/Cummins Adiabatic Engine Program

Walter Bryzik

US Army Tank Automotive Command

ABSTRACT

This paper discusses the goals, progress, and future plans of the TACOM/Cummins Adiabatic Engine Program. The Adiabatic Engine concept insulates the diesel combustion chamber with high temperature materials to allow hot operation near an adiabatic operation condition. Additional power and improved efficiency derived from this concept occur because thermal energy, normally lost to the cooling and exhaust systems, is converted to useful power through the use of turbomachinery and high-temperature materials. Engine testing has repeatedly demonstrated the Adiabatic Engine to be the most fuel efficient engine in the world with multi-cylinder engine performance levels of 0.285 LB/BHP-HR (48% thermal efficiency) at 450 HP representative. Installation of an early version of the Adiabatic Engine within a military 5 ton truck has been completed, with initial vehicle evaluation successfully accomplished. Design and procurement of long lead time items for the next generation of Adiabatic Engine in the 600-750 HP power range is continuing. Work on the minimum-friction Adiabatic Engine version continues.

Advantages of the Adiabatic Engine include virtual elimination of the conventional cooling system, a minimum of 30% improvement in fuel economy over current diesel engines and a 40% reduction in engine size and weight. Elimination of the engine cooling system including cooling fans, radiators, hoses, shrouds, water pump, cooling jackets, cooling fins, etc., would produce a quantum jump in reliability and maintainability as over 50% of engine failures in both military and commercial heavy duty vehicles are attributed to cooling system related items. The Adiabatic Engine would not be sensitive to conventional cooling system damage. Because of high temperature engine operation, smoother combustion, less engine noise, improved multifuel characteristics and enhanced cold start capability result. With this engine concept the entire philosophy of combat vehicle design becomes far less restrictive with regard to space claim

and location of cooling system components. Cost of the engine is expected to be less than its cooled counterpart on a \$/HP basis.

AS WORLD-WIDE ACTIVITY in the area of Adiabatic Engine technology accelerates, it becomes increasingly apparent that the diesel engine is undergoing a dramatic technological transformation. Future Adiabatic Engine characteristics will include improved efficiency, wider fuel tolerance, reduced size and weight, improved reliability, reduced noise, reduced cost, and greater vehicle/engine design freedom. The Propulsion Systems Division of the US Army Tank-Automotive Command (TACOM) and the Cummins Engine Company continue to aggressively pursue an innovative high-payoff concept called the Adiabatic Engine. This work effort began in 1975 as a paper study and has progressed through full scale engine feasibility evaluation and preliminary vehicle demonstration. As a result of the pioneering efforts in the area of adiabatic engine technology performed by the US Army Tank-Automotive Command and the Cummins Engine Company, many worldwide Government, industry and academic sources have begun work in this general area. This paper discusses the overall strategy and definition, progress, future plans, and implementation of the TACOM/Cummins Adiabatic Engine Program.

DESCRIPTION AND ADVANTAGES OF THE ADIABATIC ENGINE

In the study of thermodynamics, the adiabatic process is defined as a no-heat loss process, hence, the adiabatic engine name implies a no-heat-loss engine. It should be noted that this engine is not adiabatic, or without heat loss, in the true thermodynamic sense; however the engine is without conventional forced cooling and strives to minimize heat loss. The Adiabatic Engine insulates the diesel combustion chamber

with high temperature materials to allow "hot" operation with minimized heat transfer. The "hot" or insulated high temperature components, include piston, cylinder head valves, cylinder liner, exhaust valves, and exhaust ports. Additional power and improved efficiency derived from an Adiabatic Engine are possible because thermal energy, normally lost to the cooling water and exhaust gas, is converted to useful power through the use of turbomachinery and high temperature materials.

A simplified schematic of the Adiabatic Engine is shown in Figure 1. Following the engine flow path, air enters the turbocharger (is compressed) and then enters the insulated, high-temperature combustion chamber of the piston unit. Insulated combustion chamber components include those previously noted. Combustion occurs and useful energy is extracted from the piston unit. The high-temperature, high pressure exhaust gas is then expanded through two turbine wheels to extract as much as possible of the remaining energy. One wheel is used to drive the compressor, and the second is connected by gears (turbocompounding system) to the engine crankshaft to further increase the useful power output of the engine.

Fundamentally, the Adiabatic Engine is more efficient than a conventional diesel because it converts the fuel heat energy into additional, useful output. Three pie-shaped energy balances of various configurations are shown in Figure 2. The first shows a conventional, turbocharged diesel engine with one third of the fuel energy being absorbed by the coolant, one-third going to the exhaust, and one-third going to useful energy (or power). The center chart represents an engine that utilizes turbocompounding. Here the fraction of exhaust energy decreases, while useful energy proportionately increases. The last chart represents an engine that uses insulated, high-temperature components, combined with turbocompounding, to further increase the useable energy while proportionately decreasing waste energy. Thus, the potential for increasing the useful work of the same fuel is greater for adiabatic, turbocompounded engines. Obviously, the availability of such an engine would have great positive impact on future vehicle designs, particularly upon the design of military tactical and combat vehicles.

By greatly reducing lost energy and essentially eliminating the need for a conventional cooling system, the Adiabatic Engine dramatically improves fuel economy and provides approximately a 40 percent reduction in weight and volume for the same horsepower fuel. Further, from a military system standpoint, the component volume of the total "under armor" propulsion (Fig 3) system could be reduced by 40 percent overall. Elimination of the engine cooling system, including cooling fans, radiators, hoses and shrouds would produce a remarkable increase in reliability and maintainability. The engine would not be sensitive to most conventional cooling systems damage and extreme environmental

conditions. Fuel economy improvements translate into increased vehicle range and reduced logistics concerns. Specific weight reductions allow improved vehicle response, while less vehicle volume allows reduced armor cover requirements, reduced vehicle weight, and new innovative designs with improved survivability characteristics. The Adiabatic Engine's high temperature operation also gives smoother combustion and a wider range of acceptable fuels. With this engine, the entire philosophy of combat vehicle design becomes far less restrictive. Concerns regarding satisfactory locations for cooling grilles, air passages, and associated equipment are eliminated. The cost of the engine is expected to be equal to or less than its cooled counterpart since engine radiators, cooling fans, water pump, seals, hoses, and costly water jackets would be eliminated. Application of the Adiabatic Engine to commercial activities provides advantages similar to those discussed above and in addition includes improvements in the areas of emissions, simplicity, vehicle aerodynamics, operating cost, and maintenance. It should be noted that 50% of the commercial and military engine field failures are cooling system related.

OBJECTIVES AND STRATEGY

The program seeks to develop adiabatic engine technology and demonstrate principles and payoffs from feasibility through vehicle implementation. The Adiabatic Engine has applicability over a wide range of power levels and vehicle types. Feasibility demonstration performed to date has been concentrated within the 250-500 HP range. Figure 4 shows potential applications within the military area. Starting with a commercial 250 HP engine which is in the military 5 ton truck, an uncooled version of this engine incorporating some ceramics and turbocharged could be applied to 5 ton and 10 ton trucks. By adding the turbocompound unit and more ceramics, it is technically feasible to build a 500-700 HP engine, based on a highly modified commercial engine block. This version of Adiabatic Engine is currently being developed in the 500-700 HP range for application to tracked combat vehicles. In the main battle tank category (1500 HP), the Adiabatic Engine would begin with an all new design and discard the conventional cast iron engine block in order to compete with the power density of gas turbine and rotary engines. Adiabatic Engine studies are currently underway in the 1500 HP range for possible future main battle tank application.

PROGRESS (OVERVIEW)

A great deal of feasibility demonstration has been accomplished within the program to date utilizing both single-cylinder and multi-cylinder engine testing phases. Engine testing has repeatedly demonstrated the Adiabatic Engine to be the most fuel efficient engine in the

ADIABATIC DIESEL ENGINE

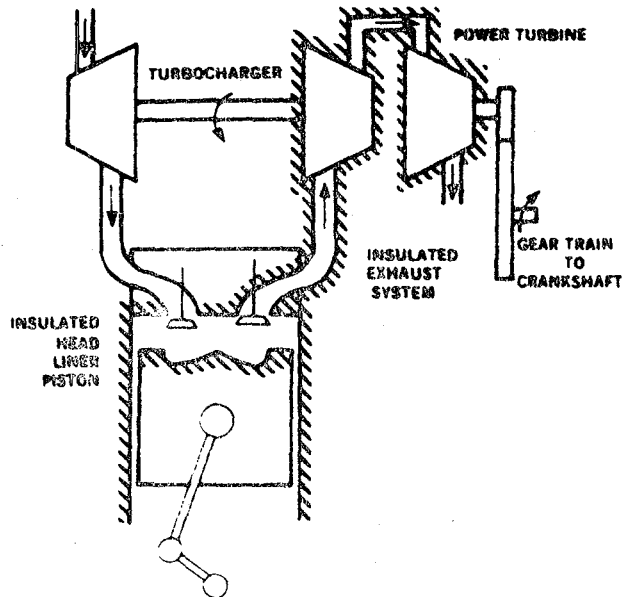


Figure 1 -- Adiabatic Diesel Engine

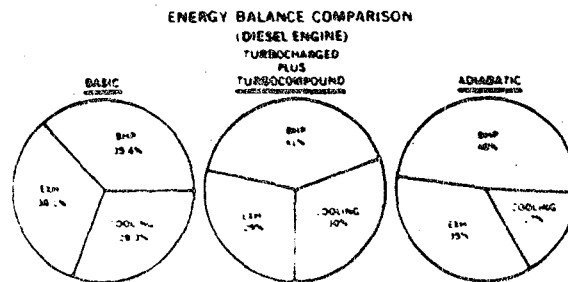


Figure 2 -- Energy balance comparison

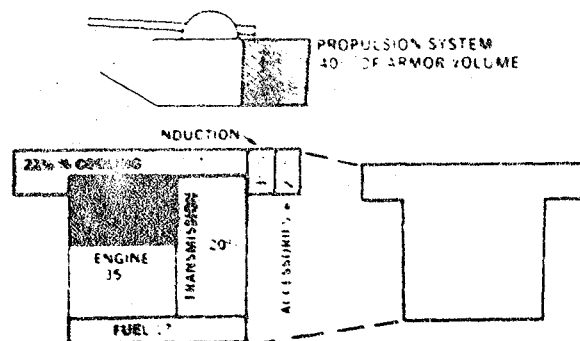


Figure 3 -- Military vehicle volume reduction with Adiabatic Engine

ADIABATIC DEVELOPMENT STRATEGY

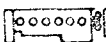



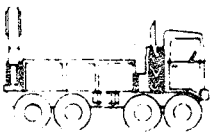
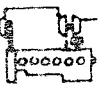

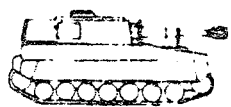
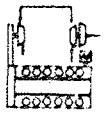
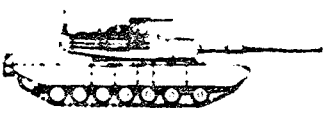
ENGINE	CONFIGURATION	TYPICAL HP-RANGE	POTENTIAL VEH APPLICATION	GVW (TON)
COMMERCIAL (BASELINE)	 ↓	250	 5T	15
UNCOOLED (COMMERCIAL BLOCK)	 ↓	250	 5T  10T	15-30
ADIABATIC TURBOCOMPOUND (COMMERCIAL BLOCK)	 ↓	500-750	 M2  M109/ESPAWS	25-35
ADV ADIABATIC (NEW DESIGN)	 ↓	1500-2000	 FUTURE MBT	40 +

Figure 4 - Adiabatic development strategy

world with multi-cylinder engine performance levels of 0.285 LB/BHP-HR (48 percent thermal efficiency) at 450 HP representative. Over 500 hours of multi-cylinder operation have been successfully accomplished to date. Installation of an early version of an uncooled engine within a military 5 ton truck has been completed with initial vehicle evaluation complete. This vehicle installation represents an early spin-off demonstration of the type of adiabatic engine technology which has been pioneered at TACOM. Design and initial fabrication of long lead time items for the next generation of Adiabatic Engine in the 600-700 HP power range is continuing, with emphasis on compactness, performance, and manufacturing practicality. An on-going active basic support effort within the Adiabatic Engine Program involves "minimum friction" adiabatic technology. This engine work emphasizes minimization of friction through the use of components such as gas bearings, "ringless" pistons, low friction "dry" ceramic bearings and solid lubricants.

UNCOOLED ADIABATIC ENGINE/5 TON TRUCK INSTALLATION

An early version of adiabatic engine technology has been demonstrated in a military 5 ton truck. Figures 5 and 6 show the truck as modified to incorporate improved aerodynamics, driver visibility, and packaging characteristics. Figure 7 shows the installed uncooled Adiabatic Engine. Note its uncluttered appearance which results from the elimination of 361 individual pieces (Figure 8) including the radiator. Advantages of the uncooled Adiabatic Engine are listed in Table 1, with listed fuel economy savings a conservative estimate based on full load engine operation. Part load truck operation (unloaded truck bed) revealed outstanding fuel economy or over 9 miles per gallon during a round trip between Detroit and Washington DC. The current production military 5 ton truck utilizing the Cummins NHC 250 engine averages approximately 6 miles per gallon in an unloaded test bed condition. To date, this uncooled Adiabatic Engine/5 ton truck installation has accumulated over 3000 miles of road testing on the highways of the eastern United States with no incidence of failure. In addition, the last 500 miles of road testing was successfully accomplished in an overloaded condition with 13 tons of cargo in the bed.

Tables 2 and 3 show characteristics of the uncooled Adiabatic Engine. Note that the engine is based on the current Cummins NHC 250 engine and utilizes ceramic coatings throughout its combustion chamber areas. In addition, an uncooled Adiabatic Engine has been successfully endurance tested on a dynamometer for 250 hours, with one third of the test at full load. Figures 9 and 10 show coated zirconia-based pistons and head taken from this engine after 250 hours of operation.

Table 1 - Uncooled Adiabatic Engine Advantages

• Lifetime Fuel Savings*	\$7,089
• Volume Savings (ft ³)	20
• Parts Eliminated	361
• Weight Savings (lbs net)	338
• Elimination of Engine Coolant (qts)	42

*Based on 2500 Hrs of Operation: \$1.25 Per Gallon

Table 2 - Uncooled Adiabatic Engine Components

The following components are coated with plasma sprayed ceramics:

Component	Coat Surface
•Pistons (ductile iron)	Piston Dome
•Cylinder Liners (ductile iron)	Inside Diameter
•Cylinder Heads (cast iron)	Combustion Surface
	Exhaust Ports
	Intake Ports

Table 3 - Uncooled Adiabatic Engine

- Based on Current 240 HP NHC-250 Engine in Military 5 Ton Truck
- In-line 6 Cylinder, Turbocharged
- 5½" Bore, 6" Stroke, 855 cu. in. Displacement
- 230 Brake Horsepower @ 2100 RPM
- Elimination of Water Cooling System (Radiator, Fan, Water Pump, Hoses, Belts, etc.)
- Combustion System Insulation via Ceramic Coatings

Table 4 - AA750 Adiabatic Engine

Specification

- 750 BHP @ 3200 RPM
- Minimum Fuel Consumption: 0.28 LB/BHP-HR
- Bore x Stroke: 5 1/2" x 4 3/4"
- V-8, High Speed Diesel

Configuration

- Turbocharged and Air-to-air Aftercooling
- Turbocompound Configuration with Radial In-flow Power Turbine
- Intake Ports Outboard of Vee - Designed for Tuned Induction System
- Insulated Combustion Chamber, Cylinder Ports, Manifold, and Turbine Housing
- Pulse Exhaust Manifold with Pulse Converter
- New Cylinder Head Design
- Advanced Fuel System Design

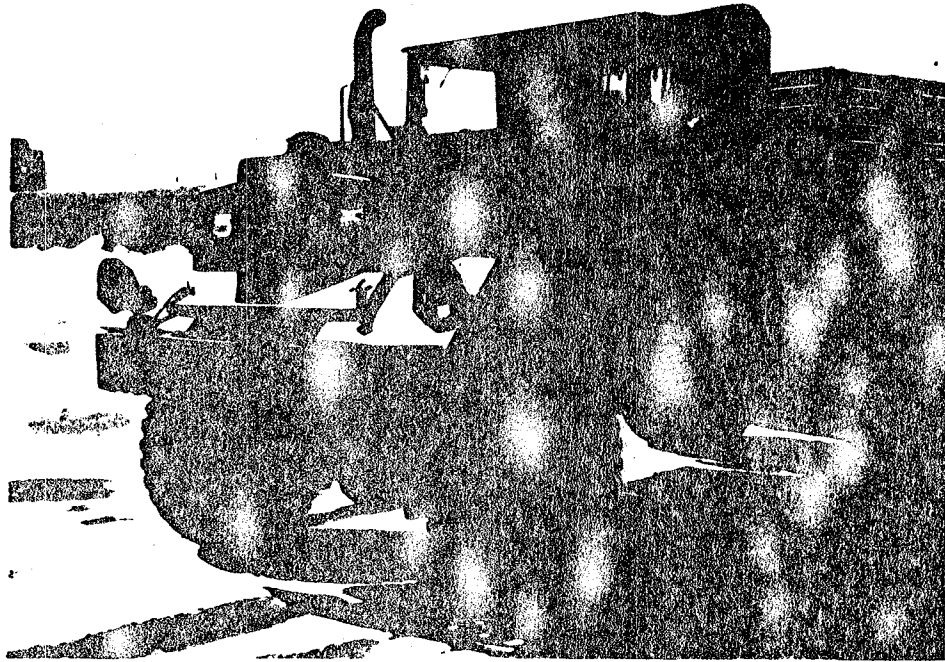


Figure 5 - Uncooled Adiabatic Engine vehicle
installation

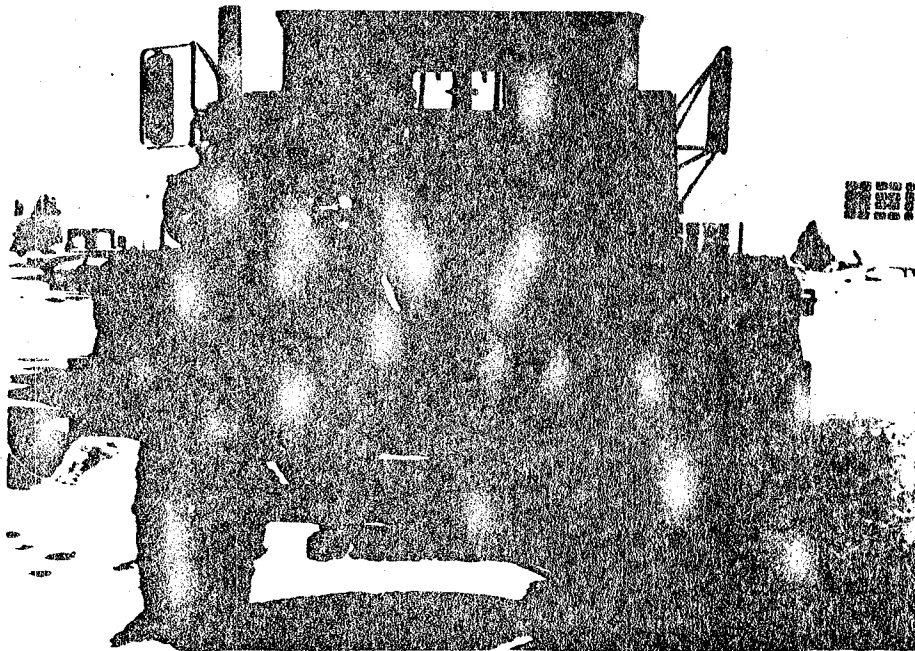


Figure 6 - Uncooled Adiabatic Engine vehicle
installation



Figure 7 - Uncooled Adiabatic Engine

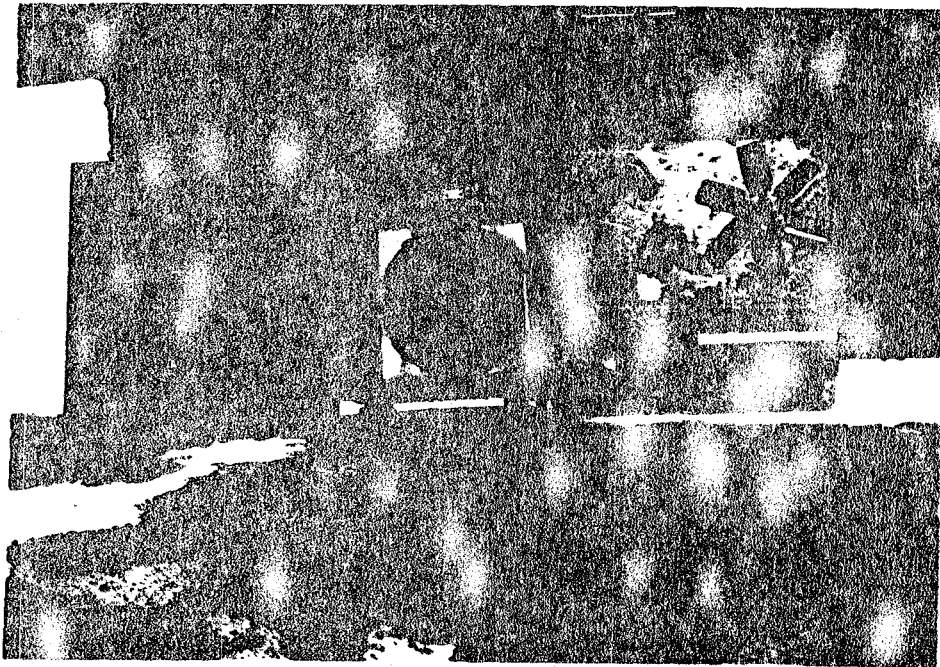


Figure 8 - Eliminated production hardware -
uncooled Adiabatic Engine

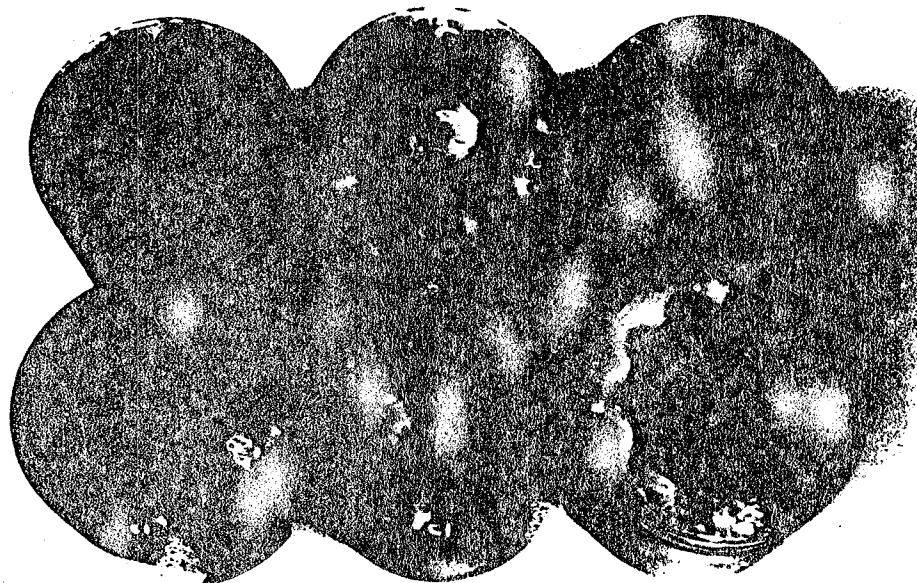


Figure 9 - Pistons - uncooled Adiabatic Engine
(after 250 hr endurance test)

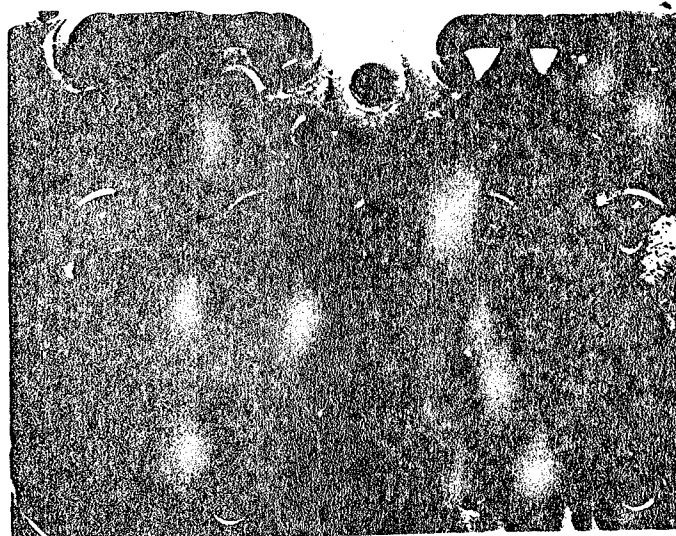


Figure 10 - Cylinder head - uncooled Adiabatic
Engine (after 250 hr endurance test)

AA750 ADIABATIC ENGINE

Work continues on the next generation of Adiabatic Engine, with application to tracked combat vehicles in the 600-750 HP range targeted. The effort currently involves design, initial fabrication, and basic component development. The specifications and configuration of this engine are shown in Table 4. A preliminary cross-section of the AA750 Adiabatic Engine is shown in Figure 11.

COMPONENTS - Basic component development of the AA750 Adiabatic Engine continues, with emphasis being applied to both monolithic and coated zirconia based materials. Zirconia based materials have been found to be desirable for Adiabatic Engine application because of their excellent insulating characteristics, adequate strength characteristics, and thermal expansion characteristics which are relatively close to some metals. A representative cross-section of a single-cylinder engine used for AA750 component development is shown in Fig. 12. The composite metal/ceramic approach is used throughout, with ceramic materials generally designed to operate in a compressive mode. Results utilizing both monolithic and coated zirconia-based materials have been quite encouraging to date, with both types remaining viable options for the final AA750 Adiabatic Engine.

Pistons - Various piston configurations continue to be evaluated. Figure 13 shows an interference-fitted partially stabilized zirconia (PSZ) insert within a ductile iron piston. Figure 14 shows a second monolithic PSZ insert which is interference fitted and brazed to a ductile iron piston to provide more complete insulation of the piston top. Figure 15 shows a thick (0.100 inch) coated and surface treated zirconia based/ductile iron composite piston.

Liner - Various liner concepts continue to be evaluated. Figure 16 shows a monolithic partially stabilized zirconia (PSZ) insert interference fitted into an iron sleeve. Figure 17 shows a thick (0.100 inch) and surface treated zirconia based coating applied to an iron liner sleeve. In addition, work using a monolithic alumina-iron composite liner continues to be evaluated.

Head Related Components - Work continues in the headface insulating plate, valve, valve seat, valve guide, and exhaust port areas. A headface plate with integral valve seats and made of partially stabilized zirconia (PSZ) is shown in Figure 18, with extensive test of this component particularly successful at brake mean effective pressures of up to 200 PSI. The shown headface plate was interference fitted into a metal head. An installation of PSZ valve inserts into a metal head is shown in Figure 19, with significant heat transfer reduction measured relative to the rather small ceramic insulating area of the inserts. Figure 20 shows PSZ valve guides currently being evaluated for the AA750 Adiabatic Engine. Exhaust port work involves continued

evaluation of a zirconia-metal form composite casting in a metal cylinder head and an aluminum titanate casting (Figure 21) in a metal cylinder head.

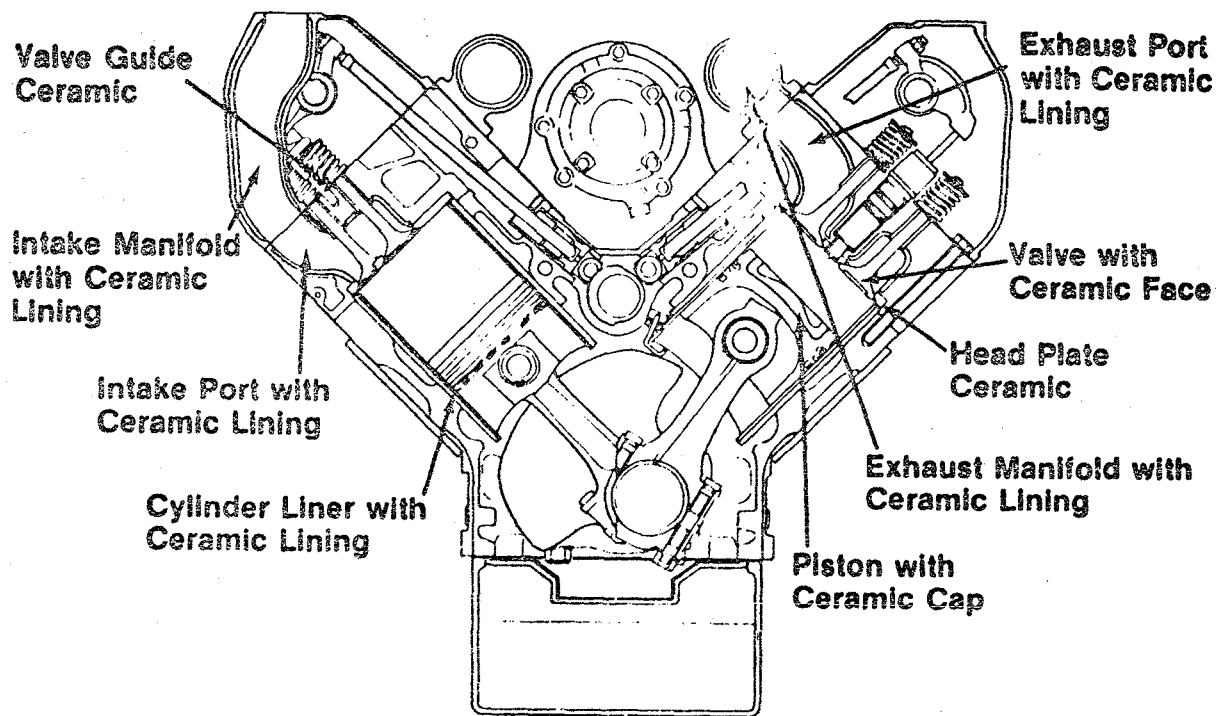
MINIMUM-FRICTION ADIABATIC ENGINE

An on-going, active, basic support activity for the Adiabatic Engine Program is the "minimum-friction" adiabatic engine technology effort. This effort emphasizes minimization of friction through the use of components such as gas bearings, "ringless" pistons, low friction "dry" ceramic bearings and solid lubricants. The engine is projected to incorporate all the advantages of the current Adiabatic Engine types, plus further improve fuel economy to 0.25 LB/BHP-HR (54 percent thermal efficiency) and eliminate the engine oil system. A representative schematic diagram of this concept is shown in Figure 22. Progress to date has included 1) initial fabrication and rig testing of various piston/liner combinations, 2) evaluation of low friction bearings, 3) completed design and initiated fabrication of an advanced camshaft/valve train concept, and 4) initiation of multicylinder integration of the components discussed above. Initial component integration of the minimum-friction Adiabatic Engine into a multicylinder configuration is scheduled for 1983. Beginning in 1983, this basic support effort will incorporate additional advanced development areas including variable valve train, porting/manifold system, and cylinder block and head.

FUTURE PLANS

It is important to note that an Adiabatic Engine can be applied to a wide range of military vehicles, ranging from trucks to main battle tanks. In addition, adiabatic engine technology can be applied commercially to ground vehicles from trucks to automobiles and to such applications as helicopters, winged aircraft, locomotives, marine use, etc.

Figure 23 shows projected production availability dates of various spinoffs of adiabatic technology and the fuel economy of these various configurations. Turbocompound diesels have been demonstrated with fuel economy as shown, and will be available for production in 1985. The US Army has demonstrated an uncooled engine in 1982, and it appears that this type of engine could be available for production by 1987. The full Adiabatic Engine with turbocompounding is projected to be available for production in 1992. These dates could be accelerated with increased funding levels for applications from automobiles to main battle tanks, and in fact recent accelerated activities by various international concerns may well prove these availability projections to be extremely pessimistic.



AA-750 Cross Section End View

Figure 11 - AA-750 Cross section end view

Zirconia Insulated Engine

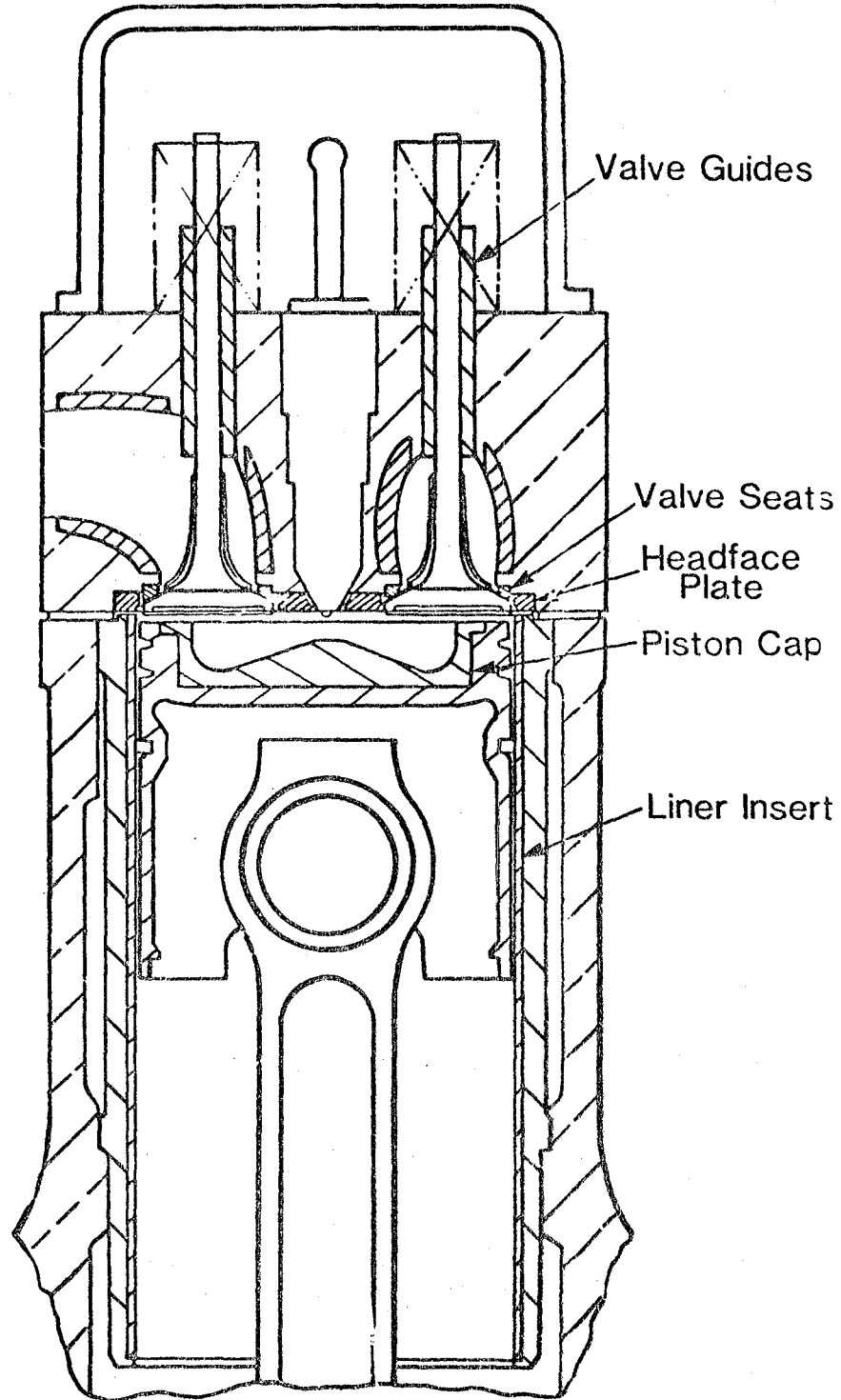


Figure 12 - Zirconia insulated engine

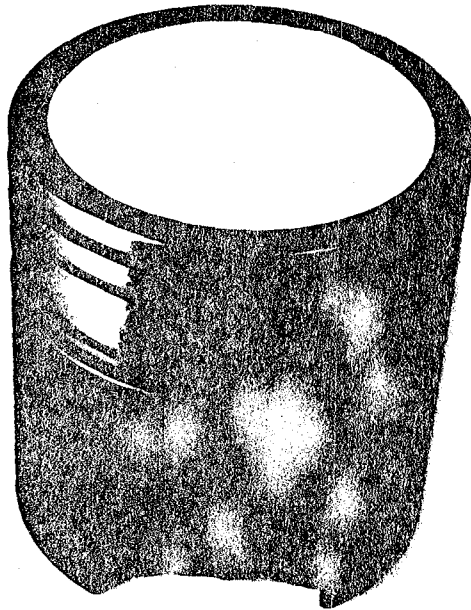


Figure 13 - Partially stabilized zirconia/
ductile iron piston (design 1)

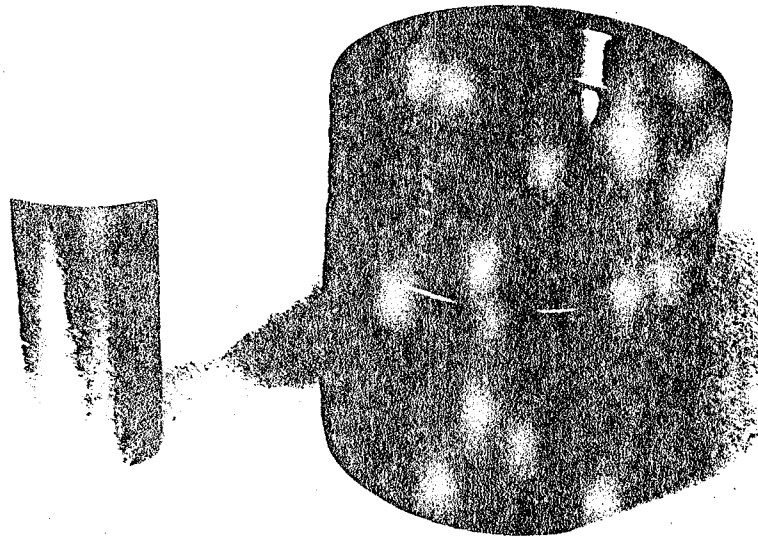


Figure 14 - Partially stabilized zirconia/
ductile iron piston (design 2)



Figure 15 - Thick (0.100 inch) zirconia coated piston

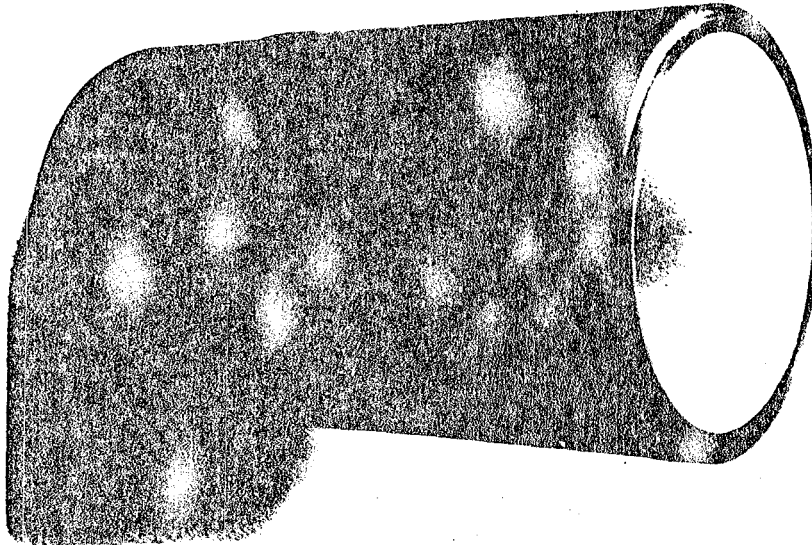


Figure 16 - Partially stabilized zirconia/iron cylinder liner

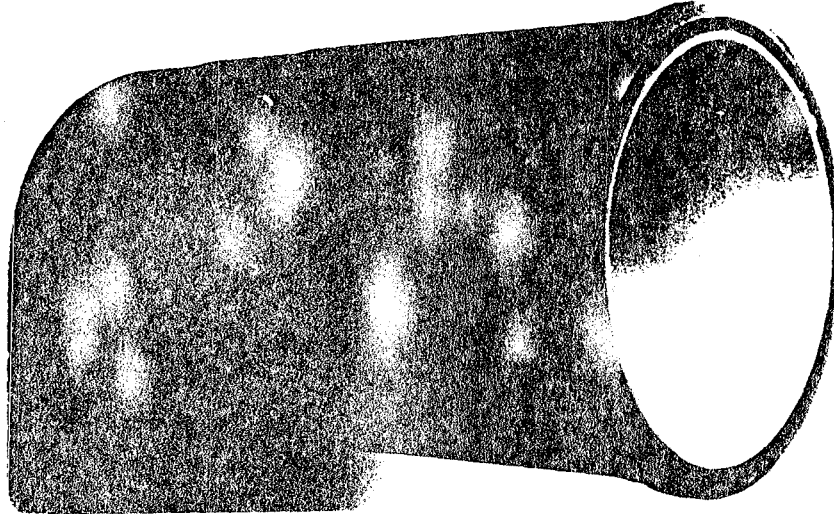


Figure 17 - Thick (0.100 inch) zirconia coated cylinder liner

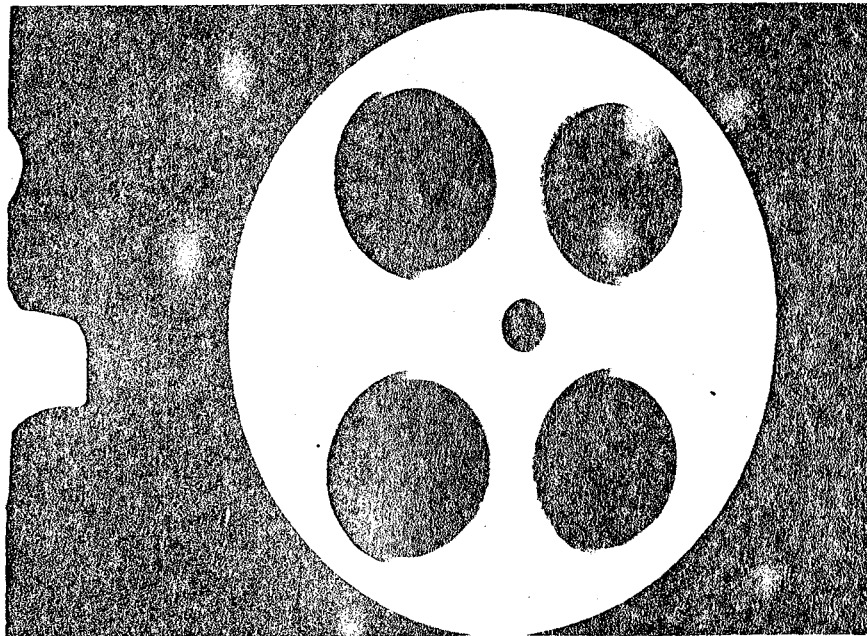


Figure 18 - Partially stabilized zirconia head face with integral valve inserts

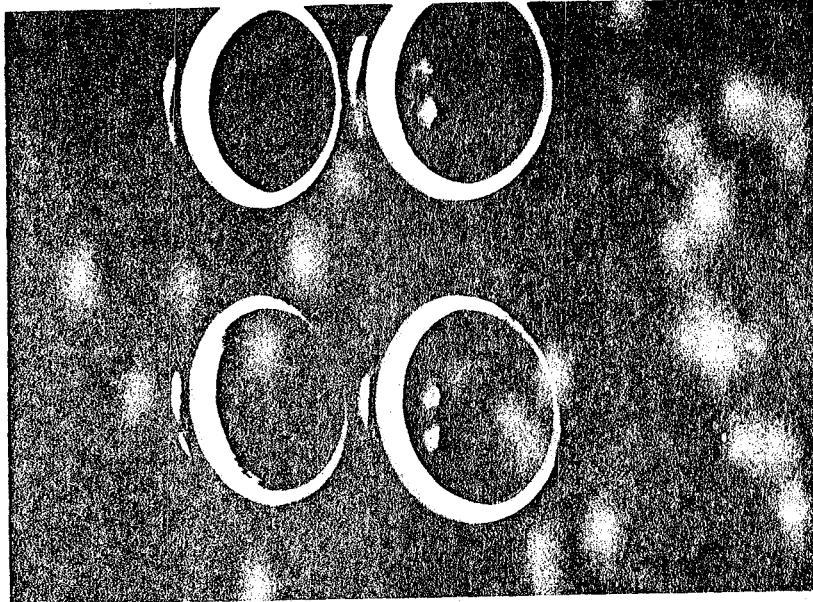


Figure 19 - Partially stabilized zirconia valve inserts

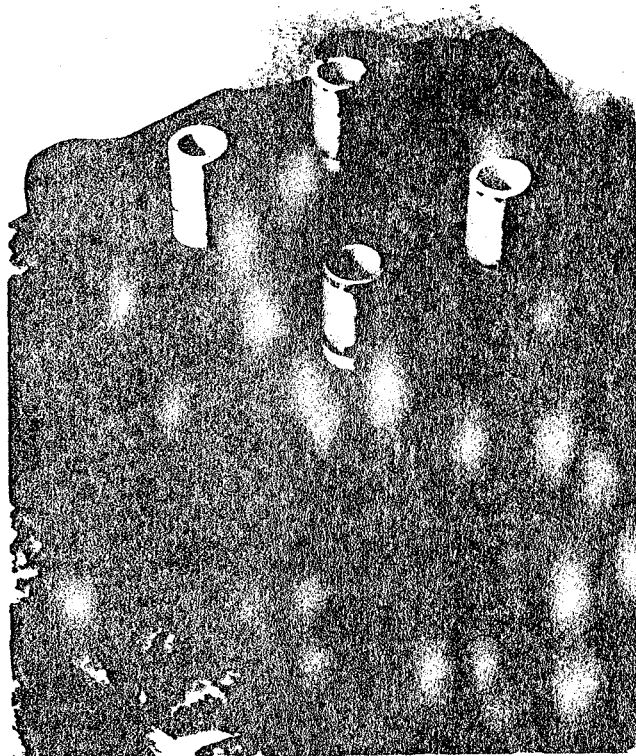


Figure 20 - Partially stabilized zirconia valve guides

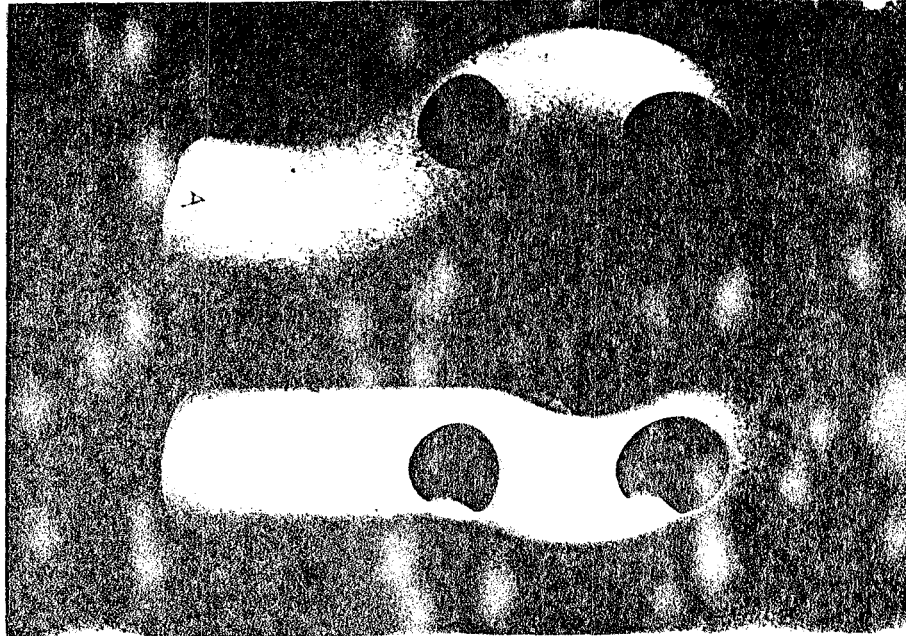


Figure 21 - Aluminum titanate exhaust ports

MINIMUM FRICTION ADIABATIC DIESEL ENGINE

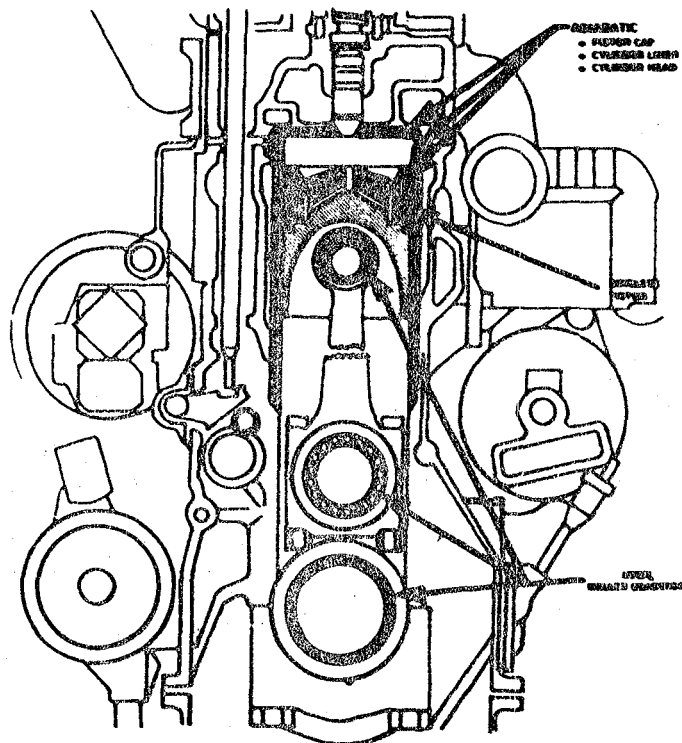


Figure 22 - Minimum - friction Adiabatic Engine

PREDICTED PRODUCTION DATE ADIABATIC ENGINE SPIN-OFFS ENGINE PROGRAMS

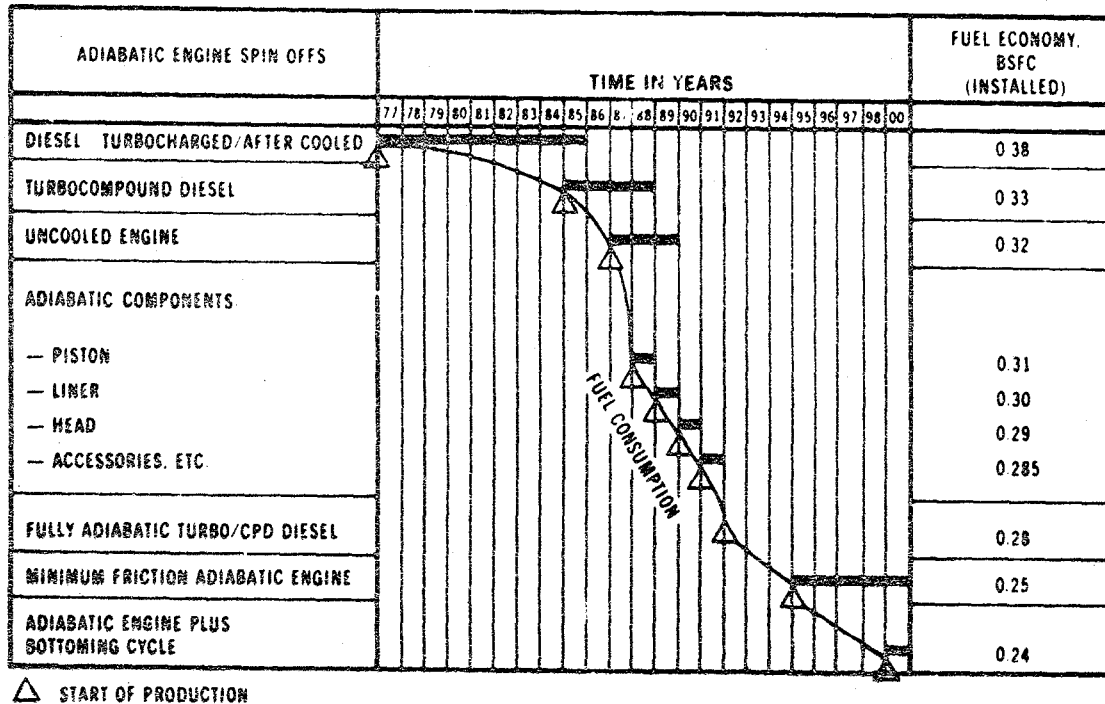


Figure 23 - Predicted production dates Adiabatic Engine spin-offs

CONCLUSION

Work to date has demonstrated the feasibility of the TACOM/Cummins Adiabatic Engine concept, and has shown many dramatic results including the world's best fuel economy. The uncooled Adiabatic Engine, utilizing a metal composition and application of minimal ceramic coatings on critical engine components emerges as a breakthrough in engine technology. The potential of high performance ceramics in an Adiabatic Engine has only begun to be explored, with many international concerns greatly accelerating efforts in this field. One should expect continued dramatic results in the area of adiabatic engine technology to surface on an international scale in the near future.

ACKNOWLEDGEMENT

Acknowledgement is made for the valuable contributions made by the TACOM/Cummins Adiabatic Engine Team. The cooperation from the various ceramic manufacturers in the U.S.A., Japan, Germany, England, and Australia is also acknowledged. The overall support of the Cummins Engine Company and the US Army Tank-Automotive Command is genuinely appreciated.

REFERENCES

1. W. Bryzik, "Adiabatic Engine Program", National Department of Energy Automotive Technology Meeting, Dearborn, Michigan, 11-14 November 1980.
2. W. Bryzik, "Adiabatic Engine Program", National Department of Energy Automotive Technology Meeting, Dearborn, Michigan, 25-28 October 1981.
3. W. Bryzik and R. Kawo, "Adiabatic Turbo-compound Engine Program" 1981 SAE International Congress and Exposition, SAE Paper 810070, Detroit, Michigan 23-27 February 1981.
4. R. M. Ogorkiewicz, Design and Development of Fighting Vehicles, Doubleday and Company, Inc., Garden City, New York, 1968.

Fabrication, Testing and Brazing of Dispersed-Metal Toughened Alumina

A. J. Moorhead, P. F. Becher,
and R. J. Lauf
Oak Ridge National Laboratory

C. S. Morgan
Oak Ridge National Laboratory (retired)

ABSTRACT

An aluminum oxide based material that contains approximately 1 vol % finely dispersed platinum or chromium was developed for use in high temperature, thermal-shock resistant electrical insulators. These composites are produced by hot-pressing Al_2O_3 -Pt or Al_2O_3 -Cr powders containing fine metallic particles obtained by in situ reduction of platinum chloride or chromium nitrate. These materials: (1) have high fracture toughness (about twice that of conventional alumina), (2) are excellent electrical insulators (resistivity comparable to that of aluminum oxide up to at least 800°C), (3) are highly resistant to repetitive thermal transients of 300°C/s, (4) have greater than 97% of theoretical density, and (5) are readily joinable by brazing to metal components. The improved toughness and thermal shock resistance of these materials are evidently attributable to both the metal particles (that impede and divert cracks) and to a mixed morphology of the alumina grains that also causes crack deflection and branching. Both of these mechanisms are significant as they lead to stable crack growth.

ONE OF THE MOST SIGNIFICANT FACTORS limiting the use of ceramics in structural applications is the low fracture toughness of these materials. In general, ceramic materials are brittle; they fail from the elastic propagation of flaws or cracks with very little, if any, plastic deformation generated at the crack tips. Thus, ceramics fracture with a very small strain to failure and because little strain energy is absorbed before fracture (with the exception of the transformation toughened ceramics and the fiber reinforced glass-ceramics which contain small [5-10 μ m] diameter SiC fibers).

A series of Dispersed-Metal Toughened (DMT) aluminum oxide based materials are being studied

that exhibit greater fracture toughness and are much more thermal-shock resistant than conventional ceramics and are also impermeable to liquids in high temperature oxidizing atmospheres.(1,2) These new materials were developed for use as long-lasting electrical insulators and have performed well in large simulated pressurized water nuclear reactors during loss-of-coolant experiments. However, they also show potential in valve and pump components for chemical processing, cutting tools and abrasive grains, electronic tube envelopes, and advanced heat engine components.

DMT ceramics are produced by pretreating a fine-grained alumina powder with a dilute solution containing a metal compound. The metallic compound is subsequently reduced to leave a small amount of a very fine dispersion of tough, ductile metallic particles throughout the alumina matrix. The dispersed metal phases studied to date include chromium, platinum or iron, but a wide range of metals could be used depending on a particular application. The basic shapes of the ceramic are fabricated by hot-pressing in a graphite die or by pressureless sintering. The material can subsequently be joined to itself or to metal components by brazing to make larger or more complex parts.

FABRICATION

The ceramic-metal powders are prepared by coating the ceramic particles with a metal precursor compound, then decomposing the precursor under conditions that result in fine metal particles dispersed on the ceramic particle surface. Alumina was used in the initial work as the ceramic matrix because it is an electrical insulator, is essentially insoluble in hot water, is resistant to steam corrosion, can be brazed to metals, and is readily available. Platinum and chromium were extensively tested as the dispersed metal, and Al_2O_3 -Pt and Al_2O_3 -Cr composites containing about 1 vol % of finely dispersed metal were found to have

significantly improved thermal shock resistance.

The first step in the production of Al_2O_3 -Pt composites consists of the formation of a slurry of alumina powder in a methanol solution of a soluble platinum compound, PtCl_4 or H_2PtCl_6 (Fig. 1). The solvent is evaporated with continuous stirring. The platinum compound is reduced with hydrogen, depositing finely dispersed platinum particles on the Al_2O_3 powder. Composite powders made from reagent grade alumina or from Alcoa A-17 alumina containing 0.5-1.5 vol % metal were hot pressed 15 minutes at 1610°C and about 55 MPa to obtain near-theoretical density. Special graphite dies permitted higher pressing pressures that were needed to achieve adequate density with small-diameter composites.

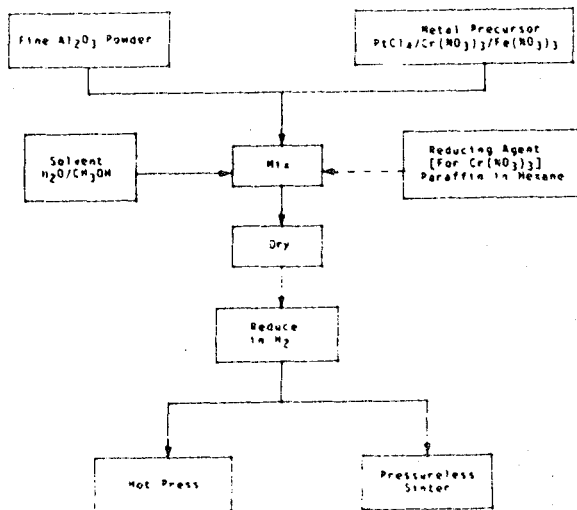


Fig. 1. Processing flow diagram for Dispersed-Metal Toughened Alumina.

Composites of alumina with chromium metal were prepared and tested to provide a less expensive substitute for platinum-containing material. The reduction of chromium compounds to the metal is very difficult and could be accomplished only when an additional reducing agent was present. Paraffin served satisfactorily in this capacity and was added in an amount equal to one-half the weight of the chromium compound. A solution of paraffin in hexane was slurried with the alumina powder. The hexane was removed by gently heating with stirring. The compound $\text{Cr}(\text{NO}_3)_3 \cdot 9\text{H}_2\text{O}$ was then deposited on the paraffin-coated Al_2O_3 powder from a methanol solution by evaporating the solvent with stirring. After the powder appeared dry, it was further dried in an oven at 110°C. The chromium nitrate was usually added in amounts equivalent to 2 wt % Cr (~1.1 vol %). Substantial or complete conversion to metal was accomplished by heating in a hydrogen atmosphere

atmosphere at about 1300°C for 10 min. No deleterious effect of possible residual carbon was detected. Hot pressing conditions for Al_2O_3 -Cr powders were similar to those for Al_2O_3 -Pt, (i.e., 1600°C, 10 minutes and 55 MPa.)

Samples of the DMT material are black in color both on the surface and through the body after hot pressing. We observed only a very limited surface reaction (between the graphite die and the powder) that did not extend an appreciable distance into the composite. Hot pressing of Al_2O_3 -powder with a molybdenum liner isolating the powder from the graphite made no detectable difference in composite properties. Composite pieces with lengths greater than about 13 mm were hot pressed with a Grafoil* liner to facilitate removal from the die. Composite tubes as large as 47.6 mm OD by about 44.5 mm long were produced by hot pressing. Hot-pressed bodies 10.2 mm in diameter by 31.7 mm long had no appreciable density gradient. A selection of some of the sizes of the DMT material that have been fabricated by hot pressing is shown in Fig. 2.

RESULTS

The microstructure of an Al_2O_3 -Pt composite is shown in Fig. 3. The apparent grains outlined by the platinum particles actually represent agglomerates of small particles in the original alumina powder. Grain growth occurring during hot pressing causes grain boundaries to sweep past the metal particles leaving the particles distributed through the grains. An example of this, along with fairly extensive exaggerated grain growth is shown in the etched Al_2O_3 -Pt sample of Fig. 4(a). Transmission electron microscopy [Fig. 4(b)] shows that the platinum particle size is in the range of 0.1-2 μm . Figure 5(a) shows the microstructure of an Al_2O_3 -Cr composite in reflected light and Fig. 5(b) shows a transmission micrograph. The latter illustrates that the chromium particles are occasionally rod- or disk-shaped and are larger on the average than the platinum particles.

COMPOSITE PROPERTIES

THERMAL SHOCK BEHAVIOR - The DMT materials were originally developed as electrical insulators for sensors exposed to the severe thermal transients of a simulated loss-of-coolant accident in a pressurized water nuclear reactor core. Thus, the resistance of these materials to thermal shock was a very important property. Rather than trying to develop data on the thermal stress resistance parameter ΔT_c of these materials, we were forced by constraints in time to use a simple test that was directly related to the initial application. Hot-pressed samples were heated in air to 500°C and dropped into water at 80°C. The approximate rate of cooling, determined by attaching a thermocouple to a small specimen and recording the temperature

*Trademark, Union Carbide Corporation.

Y-169960

Y-181621

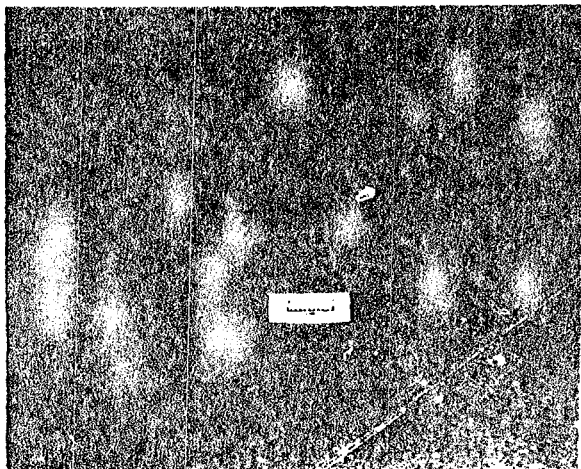


Fig. 2. Hot-pressed samples of DMT alumina before and after machining.

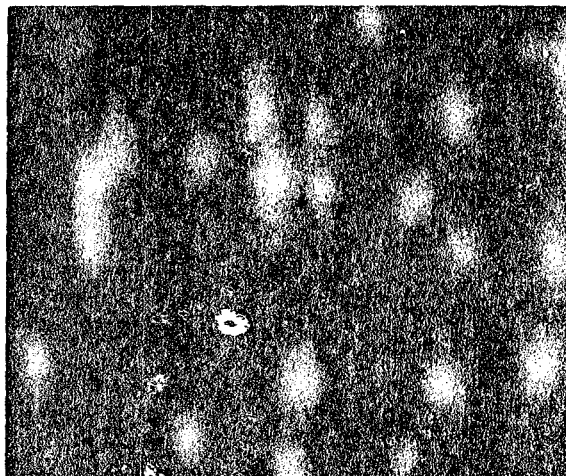
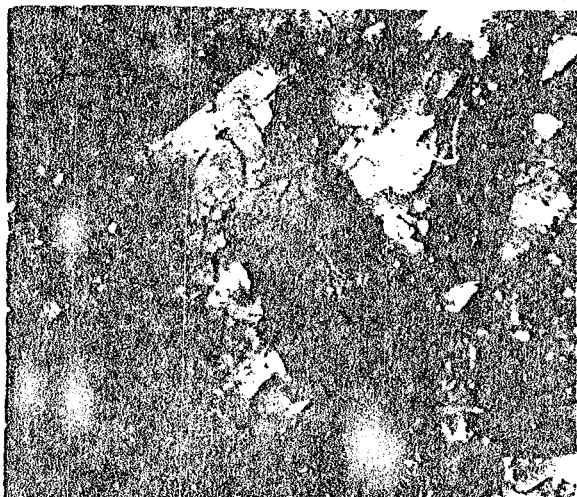


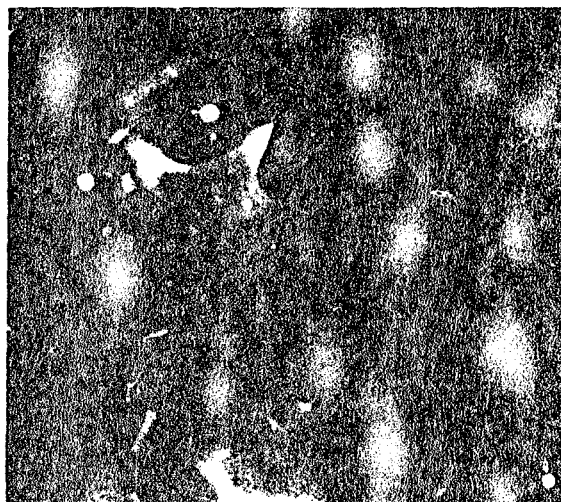
Fig. 3. As-polished structure of the dispersed-platinum toughened alumina (Al_2O_3 -1 vol % Pt).

Y-174611

E-29312



(a)



(b)

Fig. 4. Al_2O_3 -1 vol % Pt ceramic. (a) Polished surface etched with H_3PO_4 showing mixed microstructure and (b) transmission electron micrograph showing Pt particles (arrows) and voids (white spots).

during quenching with a transient recorder, was about $600^\circ\text{C}/\text{s}$. The helium permeability was measured by clamping the specimen in the end of a rubber tube, applying 0.17 MPa (25 psi) helium to the enclosed side, and then monitoring helium leakage. The helium permeation was usually detected by observation of bubble formation in ethanol, and in some cases this was qualitatively

calibrated by comparison with mass spectrometer measurement of helium leak rates. The required thermal shock resistance of composites as indicated by helium leak tests was arbitrarily set at $5 \times 10^{-7} \text{ cm}^3/\text{s}$ after 15 quenches for 10- and 15-mm-diam samples. Quenched specimens were not used in production of actual sensors, but quenching results were used to evaluate adequacy

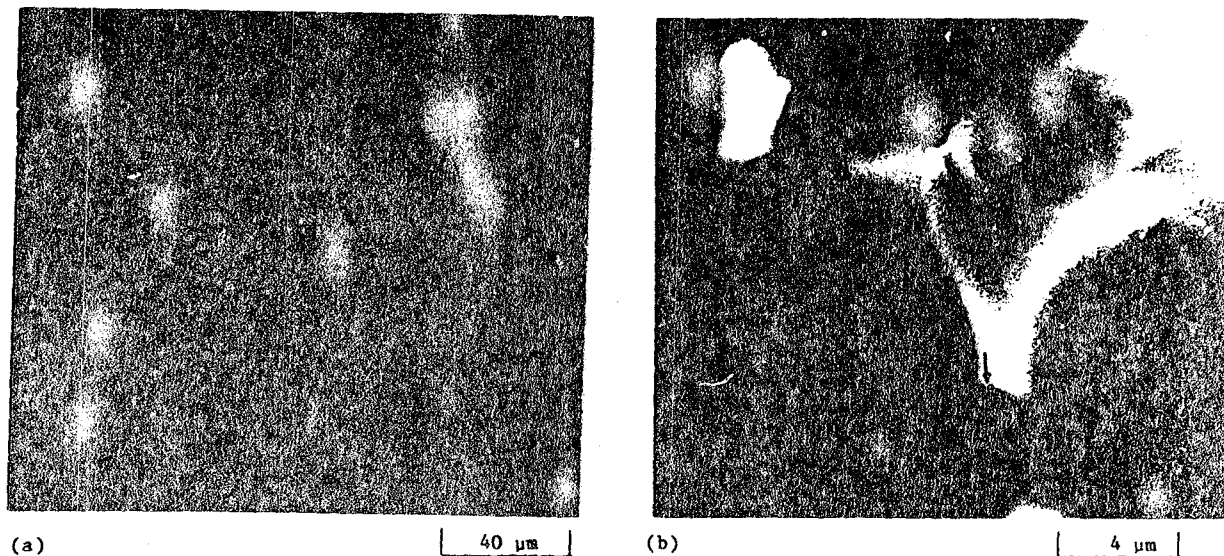


Fig. 5. Al_2O_3 -1 vol % Cr ceramic. (a) As-polished surface of specimen quenched 50 times, exhibiting frequently diverted crack (arrows); and (b) transmission electron micrograph showing faceted Cr particles (arrows).

of other samples hot-pressed in the same operation.

Most composites produced met the thermal shock resistance requirement. Small specimens (3 mm diam) were not regularly subjected to quenching tests because they consistently passed. The thermal shock resistance tests were useful for evaluating the composites in the 10 to 15 mm size range.

A comparison of the thermal shock resistance of these composites with that of commercial ceramics, and with alumina specimens produced similarly but without the metal dispersion demonstrated that the composites were significantly superior. This particular thermal shock test determines in effect how much stable rather than catastrophic crack growth occurs during the transient thermal cycling. A variety of conditions can affect stable crack growth during thermal shock. It can be increased by the introduction of microscopic voids or cracks in the main crack tip zone or by localized plastic deformation. The dispersion of fine metal particles which have thermal expansion coefficients less than the matrix and/or deform plastically can produce such effects. In Fig. 5(a) a crack can be seen in a Al_2O_3 -Cr composite that has been quenched 50 times. The crack grew stably and followed a tortuous path with diversions and splits, finally disappearing from the surface of the specimen. It is evident that the energy to propagate such a crack must be greatly

increased compared with a smoother crack in conventional materials without the metal particle dispersion. The moderate amount of exaggerated grain growth observed in these composites may also add defects, such as tiny cracks, that further increase the thermal shock resistance.

Evidence suggests that the metal particles in the composite may also increase thermal shock resistance by plastically deforming. The transmission micrograph of Al_2O_3 -Cr in Fig. 6 shows what appears to be a crack in the ceramic bridged by a chromium particle that has extensively deformed plastically.

MECHANICAL BEHAVIOR — Although the principal requirements for the dispersion enhanced ceramics were superior resistance to thermal shock, some of the material has been characterized as to mechanical behavior as will be discussed below. Although admittedly the results are somewhat preliminary, we think that the general trends in the data are encouraging enough to justify more extensive studies on these materials.

A limited test of mechanical strength was made by three- and four-point bending tests. The average values obtained for samples with various alumina grain sizes and morphologies (e.g., large plate-like grains in fine grained matrix) are given in Table 1. The breaking force of the fine grained material was 700 MPa for the Al_2O_3 -Cr (2 wt % Cr); that for the Al_2O_3 -Pt was 630 MPa; and that for pure Al_2O_3

E-30839

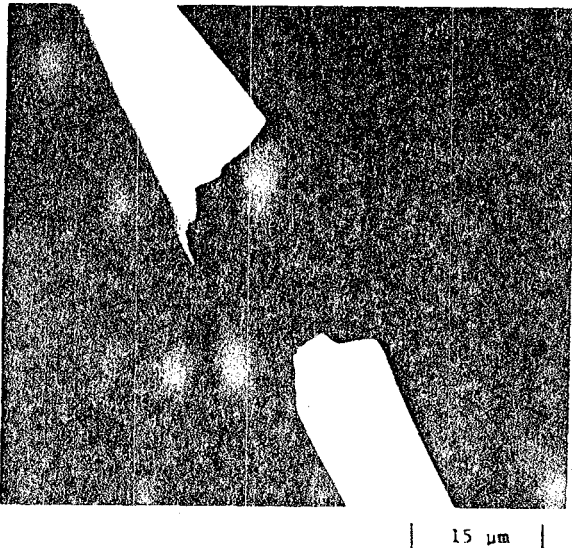


Fig. 6. Transmission electron micrograph of $\text{Al}_2\text{O}_3\text{-Cr}$ showing Cr particle that appears to have been deformed during passage of crack that it bridges.

cylinders, prepared similarly except without the metal dispersion, was 670 MPa. It is obvious that changes in grain size and morphology (i.e., formation of plate-like grains) are detrimental to the fracture strength of the composites. However, as will be seen later in this report, the fracture toughness of the alumina with mixed grain morphology is significantly greater than that of the fine-grained material.

Table 1. Fracture stress of alumina with and without dispersed metal particles

Sample	Fracture stress, MPa		
	Grain		Mixed Morphology
	Fine ²	Medium ²	
$\text{Al}_2\text{O}_3\text{-1.1 vol } \%$ Cr	700	290	160
$\text{Al}_2\text{O}_3\text{-0.7 vol } \%$ Pt	630	-	-
Al_2O_3 (pure)	670	320	-

¹Three-point bend test of 3.18 mm diam cylinders.

²Four-point bend test of ~2 mm thick rectangular bars ground parallel to long axis of specimen.

The compressive strength of 6.25-mm-diam cermet cylinders is given in Table 2. As with breaking stress, the $\text{Al}_2\text{O}_3\text{-Cr}$ sample was the strongest. Diamond pyramid hardness values determined with a 50-g load are also contained

in Table 2. These values follow the same order of three-point breaking strength, $\text{Al}_2\text{O}_3\text{-Cr}$, Al_2O_3 (pure), $\text{Al}_2\text{O}_3\text{-Pt}$.

Table 2. Compressive strength and hardness of dispersed-metal toughened ceramic

Material	Strength (0.002 in./min) (MPa)	Diamond pyramid hardness (50-g load)
$\text{Al}_2\text{O}_3\text{-1.1 vol } \%$ Cr	3040	2311
$\text{Al}_2\text{O}_3\text{-0.7 vol } \%$ Pt	2632	2137
Al_2O_3 (pure)	2582	2158
ZrO_2^a (partially stabilized)	—	1280

^aCommercial material.

The DMT alumina ceramics have significantly greater fracture toughness than commercial alumina or advanced structural ceramics such as SiC or Si_3N_4 . Typical room temperature fracture toughness values (as determined using applied moment double cantilever beam specimens) for these new materials and some commercial materials are given in Table 3. The values demonstrate that our materials, although containing only one vol % or less of dispersed metal, can have significantly superior fracture toughness.

Table 3. Fracture toughness of dispersed-metal toughened alumina and some commercial structural ceramics

Material	Volume % metal	Fracture Toughness $\text{MPa}\cdot\text{m}^{1/2}$		
		Fine grain	Mixed morphology	Commercial
Al_2O_3	-	4.7	>5.3	-
$\text{Al}_2\text{O}_3\text{-Cr}$	1	4.7	<9	-
$\text{Al}_2\text{O}_3\text{-Pt}$	0.7	-	<7	-
PSZ ²	-	-	-	5.3
Si_3N_4 , SiC	-	-	-	2-6

²Partially stabilized zirconia.

The increased toughness demonstrated in the composites could greatly enhance the use of ceramics in structural applications.

1. The size of discontinuities (flaws or cracks) which control the tensile strength must generally be kept very small in order to achieve good strengths. This is seen from the relationship of tensile fracture strength (σ_f) to flaw size (C) and fracture toughness (K_{IC}).

$$\sigma_f = YK_{IC} C^{-1/2} \quad (1)$$

where Y is a geometric factor.

For example, for a typical alumina ceramic with $K_{IC} = 4 \text{ MPa}\cdot\text{m}^{1/2}$ and with Y assigned a value of 0.8 (typical for a semicircular flaw in flexure) and a fracture stress $\sigma_f = 700 \text{ MPa}$ (~100 ksi), the critical flaw size is only 21 μm .

Producing complex ceramic components while maintaining flaw size below such a small value is extremely difficult, and the problem is complicated further by the lack of nondestructive examination (NDE) techniques capable of readily detecting such small defects even in simple shapes.

One can see from Eq. (1), however, that if a material's fracture toughness (K_{IC}) can be doubled, the allowable discontinuity size is increased by four times while maintaining the same fracture strength. Thus, increasing K_{IC} has a very practical advantage in that these larger flaws are much more readily detectable.

For example, if all values for the alumina ceramic considered above are the same except that $K_{IC} = 8 \text{ MPa}\cdot\text{m}^{1/2}$, the critical flaw size is increased to a more readily attainable (and detectable) 84 μm .

2. Associated with the above, ceramic materials with enhanced toughness could be used at higher service stresses (because of higher fracture strengths) if components were produced with small flaws that were detected by improved NDE techniques.

If, in the case of the ceramic with $K_{IC} = 8 \text{ MPa}\cdot\text{m}^{1/2}$, discontinuities can be shown to be less than 21 μm , then the tensile fracture strength will be >1400 MPa (>200 ksi). This would allow the material to be used at a significantly higher service stress or provide a greater working margin between service stress and fracture strength.

3. In addition most, if not all, ceramics are susceptible to the slow growth of cracks at applied stresses well below their fracture strengths. The rate of flaw growth increases until failure occurs, either as the applied stress approaches the fracture strength or as the length of the flaw increases in size at a fixed low applied stress. This process controls the time to cause failure in a component at applied static stresses less than the fracture strength. By increasing the fracture toughness of the material one can increase the stress level at which such slow crack growth limits the lifetime of a component.

PHYSICAL PROPERTIES - There are only limited data on the physical properties of the dispersion toughened ceramics. The thermal expansion of $\text{Al}_2\text{O}_3\text{-Cr}$ (1.1 vol %) is little changed from that of Al_2O_3 . In the temperature range of room temperature to 1000°C, a value of $8.7 \times 10^{-6}/^\circ\text{C}$ was obtained. Electrical resistance measurements up to 700°C showed the resistivity was inversely proportional to the metal content (e.g., the $\text{Al}_2\text{O}_3\text{-7% Pt}$ had a 0.7% lower resistivity than pure Al_2O_3). The thermal conductivity of the cermet may show the same effect of a slight increase with metal content. We have not performed extensive long-

term stability tests on the composite materials. However a sample held 516 h at 940°C in air showed no deterioration in resistance to thermal shock and very little change in microstructure.

BRAZING OF CERAMICS - One of the key technologies that will enhance or restrict the use of ceramic materials in high performance applications (e.g., heat engines or advanced heat exchangers) is the ability to reliably join simple-shape components to form complex assemblies or to join unit lengths of material to form large systems. Although by careful selection of location or through judicious design a joint in such applications may not be required to withstand the full intensity of the various service conditions (such as temperature or stress) as the bulk ceramic material itself, it is of course highly desirable that a ceramic-to-ceramic or ceramic-to-metal joint be capable of operation at near peak conditions. Unfortunately, although ceramic joining technology has been highly developed over the past fifty years or so, most of the effort has been expended in developing materials and techniques for applications that will see service at "low" temperatures and with low structural requirements. The development of technology for joining ceramics for use at elevated temperatures, at high stress levels, and in dirty environments has been very limited.

At least three techniques appear to have at least some promise for joining of ceramics in high performance applications: (1) mechanical joining, (2) brazing, and (3) diffusion welding. However, based on careful consideration of the advantages and disadvantages of each technique, we have concluded that brazing has the most potential for meeting the ceramic joining requirements in heat engines such as the advanced heavy duty diesel or advanced gas turbine.

However, brazing of ceramics is considerably more difficult than brazing of metals because most commercially available brazing filler metals will not wet ceramic materials. This problem has been overcome in most applications of ceramic brazing by first applying a metallic coating to the ceramic substrate and brazing to this coating with a conventional filler metal. The large commercial ceramic-to-metal seal industry and many electronic applications are based on this technology. More recently a number of researchers have developed filler metals (based on active metal additions that wet some ceramic materials directly without the need for precoating, and that is the technique that was used to join a large number of the DMT alumina insulators into the various sensor subassemblies shown in Fig. 1). Direct brazing avoids the development and application of what is in many cases a very sophisticated coating or metallizing treatment. Also the bond strength and corrosion resistance of a coating does not have to be of concern. Filler metals used for direct brazing (as those used to braze precoated ceramics) will generally

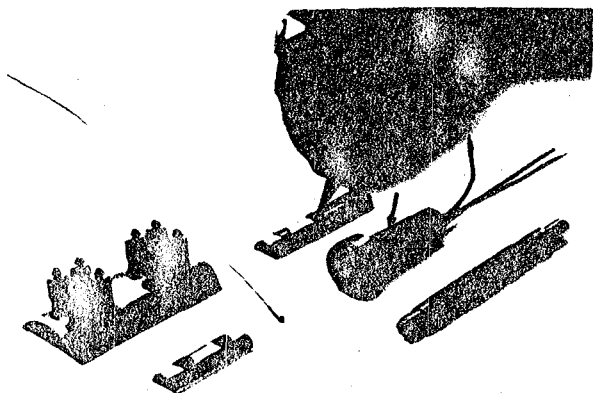


Fig. 7. Typical brazed sensor subassemblies incorporating dispersed-platinum toughened alumina insulators (black material in photo).

not have the oxidation resistance of many high purity ceramics at their maximum service temperatures, but of course many commercial ceramics must operate at lower temperatures because of the effect on properties of densification or sintering aids. On the other hand brazing of ceramics in general is in many cases made difficult by the mismatch between coefficients of thermal expansion of the ceramic and the generally metallic filler metal.

One final hindrance to direct brazing of ceramics is the fact that only a very few filler metals that will wet ceramics are sold commercially. Thus in most cases these important fillers are made by the user company or laboratory.

The wetting behavior of a liquid (brazing alloy) on a solid (ceramic in this case) is dependent on the surface energy of the solid, the surface tension of the liquid, and the solid-liquid interfacial energy. The phenomena of wetting, spreading and adhesion of molten materials onto substrates have been studied extensively through the years, primarily using the sessile drop method.^(3,4,5) These and other researchers have shown that although many metallic elements by themselves will not wet and bond to ceramic materials, wetting can be promoted by the addition of specific alloying elements. It is important to note that for a brazing alloy to be "successful" it is not sufficient that the surface tension of the molten material be minimized but also that the solid-liquid interfacial energy be decreased. Thus improved wetting can always be obtained by decreasing the interfacial energy and may be obtained in some cases by decreasing the surface tension of the liquid.

One of the most beneficial elements added to brazing filler metals to promote wetting of ceramics has been titanium. Titanium and other reactive metals such as zirconium and hafnium evidently aid in wetting and adhesion by decreasing the interfacial energy rather than by changing the surface tension of the molten filler. This change in interfacial energy is brought about by the reaction of the titanium or (other reactive metal) with the surface oxygen atoms (in the case of an oxide ceramic) so the degree of adhesion is a function of the free energy of oxide formation ΔF_f° of the additive. Thus the most beneficial brazing filler metal additions are those that are strong oxide formers (for brazing of oxide ceramics) or strong carbide formers in the case of carbon-base ceramics.

The sensors shown in Figure 7 were made possible by a unique ceramic-to-metal seal system based upon both the dispersed-metal toughened alumina insulator and an experimental brazing filler metal also developed at this laboratory. This seal system has been shown to be resistant to at least 100 h exposure to 700°C (1470°F) steam, and repetitive thermal transients of 300°C/s. For example, film sensor subassemblies (one is identified by an arrow in Fig. 7) containing a relatively large platinum-dispersion toughened ceramic insulator (12.7 mm diam) typically have helium leak rates of 10^{-6} cm³·s⁻¹ or less after 35 such thermal transients.

The sessile drop apparatus shown in Fig. 8 is being used to evaluate the wetting behavior of experimental brazing filler metals on various substrates. This particular unit uses induction heating with the ceramic substrate enclosed in a tantalum susceptor. Typical results from this apparatus are shown in Fig. 9 for the 49 Ti-49 Cu-2Be filler metal that was ultimately used to braze all of the high temperature sensors shown in Figure 7.

The sessile drop unit is presently being used in our task to develop a filler metal for brazing of partially stabilized zirconia to the ductile iron metallic components for one version of an adiabatic diesel engine. Work is also underway on a high temperature, oxidation resistant alloy for brazing of silicon carbide. Both efforts are supported by the small arc-welder shown in Fig. 10 that enables us to melt one gram buttons of experimental filler metals.

FRACTURE TOUGHNESS OF BRAZED JOINTS - The traditional engineering approach to design of fail safe structures has been the use of conservative nominal stresses. However, too often the existence of a critical defect has resulted in catastrophic failure. Therefore, the evaluation of fracture mechanics has become increasingly important to the designer, and methods of analytically describing the resistance of a material to fracture have been developed. Braze joints are generally designed on the basis of shear strength data, but it is our contention that many joints are loaded in

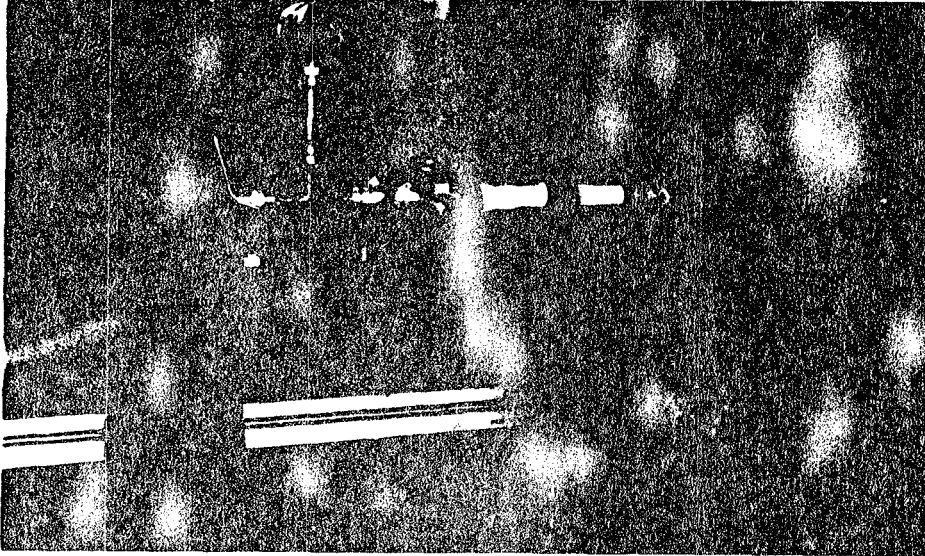


Fig. 8. Sessile drop apparatus used to monitor the wetting behavior of experimental brazing filler metals as a function of time, temperature and atmosphere.

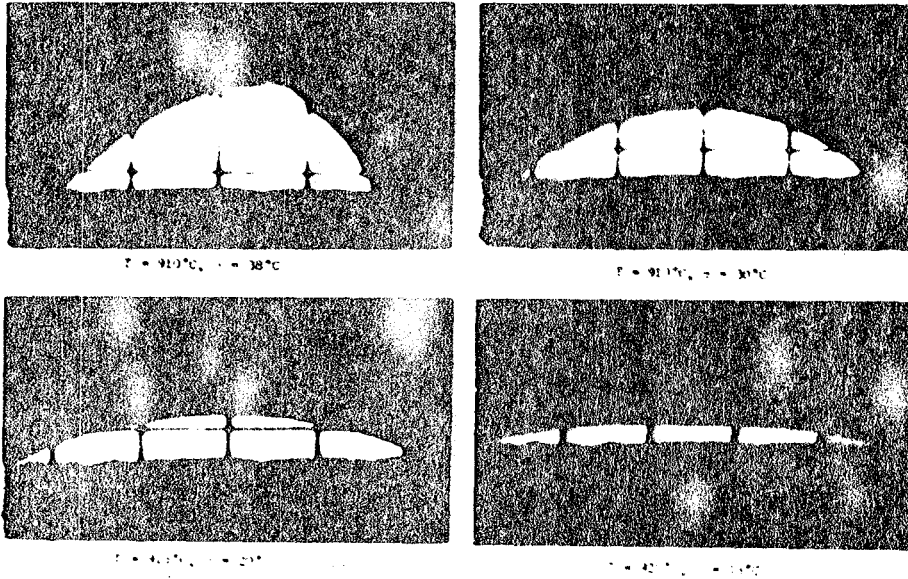


Fig. 9. Sessile drop of 49Ti-49Cu-2Be experimental brazing filler metal on a substrate of Al_2O_3 -1 vol % Pt.

Table 4. Critical fracture toughness values for braze joints in ceramics

System	K_{IC} , $\text{MPa}\cdot\text{m}^{1/2}$	Locus of fracture
$\text{Al}_2\text{O}_3/\text{Ti}\cdot\text{Cu}\cdot\text{Be}/\text{Al}_2\text{O}_3$	4.2 ± 0.2	Braze material
$\text{Al}_2\text{O}_3\text{-}0.7\% \text{ Pt}/\text{Ti}\cdot\text{Cu}\cdot\text{Be}/\text{Al}_2\text{O}_3\text{-}0.7\% \text{ Pt}$	4.7	Braze material

REFERENCES

1. A. J. Moorhead, C. S. Morgan, J. J. Woodhouse and R. W. Reed, "Brazing of Sensors for High-Temperature Steam Instrumentation Systems," *Welding Journal*, (Miami) 60(4), April 1981, pp. 17-28.
2. C. S. Morgan, A. J. Moorhead, and R. J. Lauf, "Thermal-Shock Resistant Alumina-Metal Cermet Insulators," *Ceramic Bulletin*, (Ohio) 61(9) September 1982, pp. 974-81.
3. R. M. Crispin and M. Nicholas, "The Wetting and Bonding Behavior of Some Nickel Alloy-Alumina Systems," *J. of Mater. Sci.* 11:17-21 (1976).
4. C. R. Kurkjian and W. D. Kingery, "Surface Tension at Elevated Temperatures," *J. Phys. Chem.* 60(7):961-63 (1956).
5. B. C. Allen and W. D. Kingery, "Surface Tension and Contact Angle in Some Liquid Metal-Solid Ceramic Systems at Elevated Temperatures," *AIIME Trans.* 215(2): 30-36 (1959).

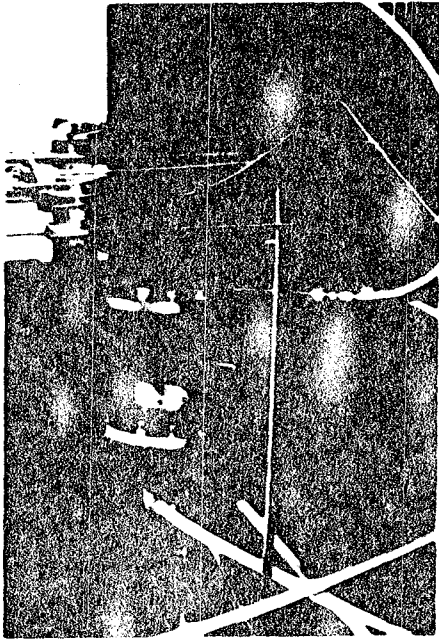


Fig. 10. Arc melter used to fabricate small quantities of experimental brazing filler metals.

tension at least part of their lives so that it is important to know how they behave under those conditions. Braze joints by their nature contain flaws that under crack-opening (tensile) conditions could lead to unexpected failure. We have recently initiated an effort to utilize fracture mechanics analyses to study the fracture behavior of braze joints between ceramic base materials and to develop data on the critical stress intensity factor, K_{IC} , in such brazements.

The specimen used in measuring the fracture toughness of the brazed joints is the same as that used for the bulk ceramic--the applied moment double cantilever beam (AMDCB). The composite specimen is made by brazing together two hot pressed ceramic bars such that the resulting braze joint is located in what eventually becomes the center of the AMDCB specimen.

As seen in Table 4, the critical fracture toughness, K_{IC} , of the brazed samples was at least as high as that for alumina ceramics. In all cases, the crack propagated primarily in the braze metal. The ceramic-metal interface did not control the braze joint toughness. The fracture toughness values suggest that in many cases the braze joint did not diminish mechanical performance of the system significantly, if at all.

Research sponsored by the Office of Nuclear Regulatory Research, U.S. Nuclear Regulatory Commission under Interagency Agreement DOE 40-551-75 and the U. S. Department of Energy, under contract W-7405-eng-26 with the Union Carbide Corporation.

**INDUSTRY PERSPECTIVES
PANEL DISCUSSION**

INDUSTRY PERSPECTIVES

PANEL DISCUSSION

A special panel session was convened on Wednesday afternoon, October 27, 1982, during the Twentieth Automotive Technology Development Contractors' Coordination meeting. The purpose of the panel discussion was to obtain feedback from certain sectors of the industry on past DOE achievements and for possible future consideration in its program planning.

The session took the form of a panel discussion with maximum audience participation. Dr. David E. Cole, Professor at the University of Michigan and President of Applied Theory Incorporated (ATI) served as moderator and chairman of the session. Panel members were selected from pertinent allied industries. The expressed opinions, however, were their own, and do not reflect their affiliations.

Professionals serving on the panel were:

Harold Brock, Private Consultant - John Deere Corporation, Waterloo, Iowa;

Claire Eatock, Pratt and Whitney of Canada, Longueville, Quebec;

Victor Suski, American Trucking Associations, Washington, D.C.;

Al Bellin, General Electric Corporation, Lynn, Massachusetts;

John Fobian, American Automobile Association, Falls Church, Virginia;

Stan Greene, General Aviation Manufacturers Association, Washington, D.C.

Subjects of discussion were centered around the following topics:

- Research and development emphasis
- Program design and management
- Information and technology transfer
- Future scenario and requirements

Positive feedback was received at this meeting and many pertinent technical discussions also took place. These topics will be the subject of a planned separate SAE publication.

ALTERNATIVE FUELS I SESSION

Utilization of Alternative Fuels in a Diesel Engine

S. S. Lestz, S. M. Geyer,
and M. J. Jacobus
The Pennsylvania State Univ.

ABSTRACT

A 1975 Oldsmobile 1.7 L-8 Diesel engine was operated on DF-2 and DF-M shale oil, and a single-cylinder Acco-Bernard engine was operated on DF-2 and various vegetable oils. The objective of the DF-2 study was to screen the DF-M fuel for its use in a more detailed single-cylinder engine study. The objective of the vegetable oil tests was to provide a detailed comparison of these oils and DF-2. In both cases, performance and emission data were obtained and biodegradability of the soluble organic fraction of particulate samples was determined using the Ames test.

Results of the DF-2 study show about equal performance and gross test efficiency for the fuels. At the vegetable oil tests, a slight increase in thermal efficiency was noted, but this was accompanied by slight increases in gas phase emissions and slight increases in total hydrocarbon and particulate emissions. The gross test efficiency of the vegetable oils was lower than that of the DF-2.

Interest in alternative fuels has led to an interest in utilizing alternative fuels, especially in some of the more remote areas of the world. The use of DF-M is desirable for a diesel engine which is available in great quantities. The fuels are available from the renewable sources of energy and have a particular interest among farmers as an alternative fuel. The properties of these fuels render them best suited for use in diesel engines.

Tests with DF-M in a marine diesel engine at Southwest Research Institute indicated that the topics of engine performance were acceptable

and comparable to DF-2 (1). Another series of tests at SWRI showed fuel efficiency increases averaging 2.4 percent for DF-M over DF-2 in a single-cylinder assembly from a Teledyne-Continental air-cooled Diesel engine (4). The same investigators found that the opposite occurred with their Detroit Diesel 6V-53T engine.

Numerous engine related problems are encountered with the use of vegetable oils as Diesel fuels (5,6). These include fuel system clogging, polymerization during storage, high viscosity leading to poor atomization and incomplete combustion, and blowby causing polymerization of the lubricating oil. Various additives to reduce polymerization have been tried, but with limited success (7,8). Nevertheless, these problems are not severe enough to prevent the use of vegetable oils in emergency situations.

DESCRIPTION AND RESULTS OF V-8 ENGINE TESTS

For purposes of comparison with operation on the baseline DF-2 (1), a 1975 Oldsmobile V-8 engine was run on DF-M shale oil at 1720 and 2000 RPM to obtain performance data and a limited amount of particulate data. Particulate samples drawn directly from the tailpipe were obtained at the 2000 RPM, 1.2 and 1.4 Rack and 1720 RPM, 1.2 Rack conditions. All samples have had the soluble organic fraction removed and have been assayed by the Microbial Assay Laboratory using the Ames test. Previous work with DF-2 and alcohols was done in this engine by Houser (9) and Brockhoff (10,11).

Selected properties of DF-2 and DF-M are presented in Appendix A. Performance data is presented in Table 1 for 1720 RPM and Table 2 for 2000 RPM. The 2000 RPM data for thermal efficiency, corrected brake horsepower, oxides of nitrogen emissions, and carbon monoxide emissions are presented graphically in Figs. 1 and 2. Pressure and needle lift histories were virtually identical; consequently, they have not been presented.

Numbers in parentheses designate references at the end of the paper.

Table 1 - Comparative Multicylinder Engine Test Data for 1720 RPM

Rack	1/4		1/2		3/4		Full	
	DF-M	DF-2*	DF-M	DF-2	DF-M	DF-2	DF-M	DF-2
FUEL								
BHPc (HP)	15.4	14.5	40.5	39.7	64.8	62.1	68.5	68.2
THEFF (%)	20.3	19.2	30.0	29.2	29.9	28.9	29.8	27.9
BSEC (BTU/HPHR)	12555	13235	8480	8702	8503	8797	8557	9113
AF	56.2	60.6	32.4	33.1	19.7	20.3	18.9	18.3
ϕ	0.266	0.246	0.46	0.451	0.76	0.735	0.79	0.815
CO (%)	0.032	0.020	0.020	0.019	0.030	0.030	0.055	0.039
CO ₂ (%)	3.72	3.60	6.87	6.54	11.53	10.53	12.10	11.64
NO (PPM)	90	91	190	199	260	256	250	253
NO _x (PPM)	105	104	220	223	270	264	265	258
HC (PPM)	70	63	53	45	100	318	100	51
O ₂ (%)	17.5	16.6	14.0	12.8	8.0	7.8	6.0	5.6

Table 2 - Comparative Multicylinder Engine Test Data for 2000 RPM

Rack	1/4		1/2		3/4		Full	
	DF-M	DF-2*	DF-M	DF-2	DF-M	DF-2	DF-M	DF-2
FUEL								
BHPc (HP)	10.7	12.5	39.6	40.6	65.1	65.7	76.0	77.5
THEFF (%)	13.7	16.2	26.7	27.3	29.0	29.2	28.5	29.0
BSEC (BTU/HPHR)	18659	15710	9515	9316	8770	8707	8913	8783
AF	67.8	68.3	34.7	35.2	23.6	22.0	18.5	18.6
ϕ	0.220	0.219	0.430	0.424	0.633	0.680	0.804	0.804
CO (%)	0.042	0.029	0.022	0.019	0.016	0.023	0.029	0.038
CO ₂ (%)	3.29	3.42	6.18	6.04	9.54	9.43	11.77	11.79
NO (PPM)	45	61	163	188	276	267	275	270
NO _x (PPM)	79	72	198	206	292	274	285	274
HC (PPM)	125	91	88	50	83	129	70	69
O ₂ (%)	19.5	16.9	14.7	13.4	10.0	8.4	7.0	5.6

* All DF-2 values are from Ref. 10, pp. 98-105.

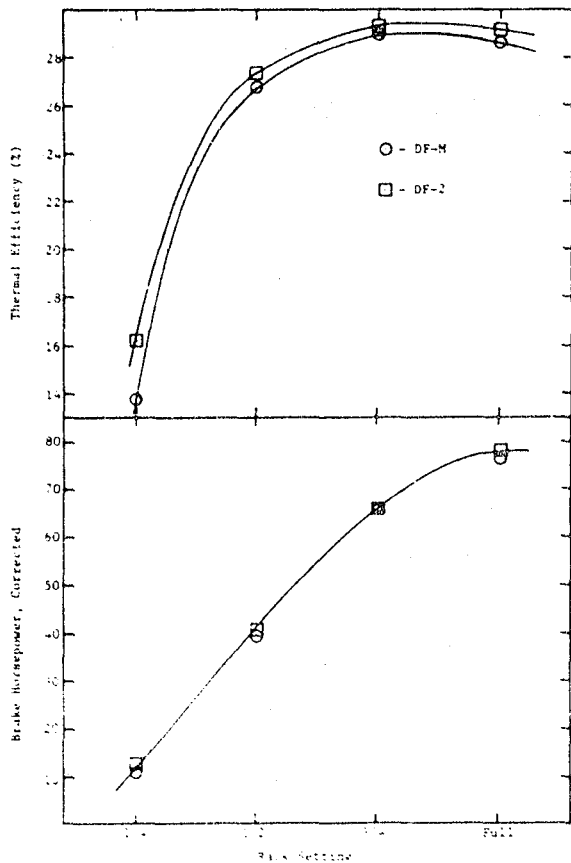


Fig. 1 - 2000 RPM Performance Data Comparison

The thermal efficiency with DF-M was similar to that of DF-2 oil at the same operating conditions. At 2000 RPM, the thermal efficiency for DF-2 oil was generally slightly higher than for DF-M. Conversely, the DF-M had a slightly higher thermal efficiency for all rack settings at 1720 RPM. Corrected brake horsepower followed the same relative differences as thermal efficiency. Except for the 1-4 Rack, 2000 RPM condition, differences are generally less than 6 percent which could still be attributed to experimental error. Therefore, the relative differences presented here should not be considered conclusive. A more detailed single-cylinder engine study has been undertaken to study these differences more fully. Ames test results as well as the SOF for all particulate samples are presented in Table 3. Standard deviations are presented where possible, but some of these results are based on a small number of samples - as low as only two; consequently, care should be exercised when interpreting these data. In all cases, the Ames results for DF-M and DF-2 overlap within one standard deviation, indicating no significant measurable difference; however, in all cases, the

DF-M did result in a lower mean value. The soluble organic fraction was consistently higher for DF-M than for DF-2, but again differences are not statistically significant.

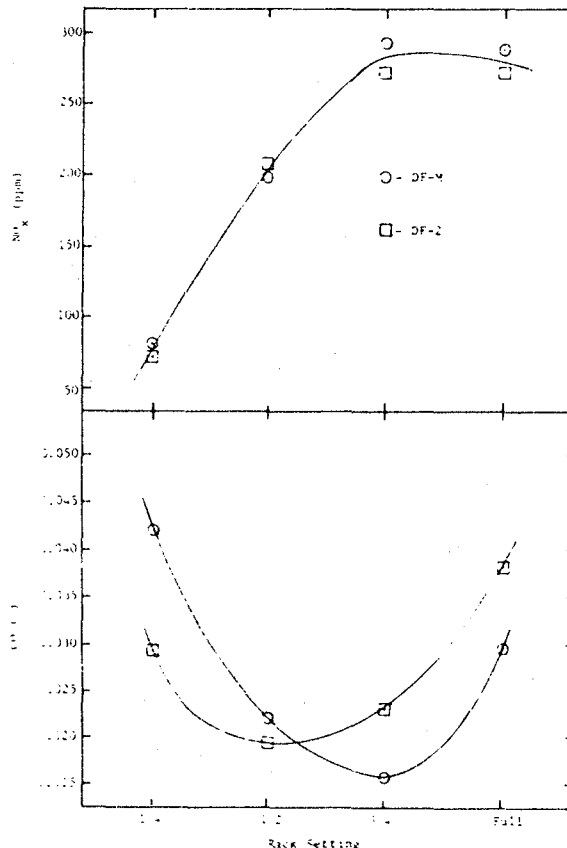


Fig. 2 - 2000 RPM Emission Data Comparison

DESCRIPTION AND RESULTS OF VEGETABLE OIL TESTS

The objectives for this phase of the project are as follows:

1. Establish a baseline for the engine on DF-2 using three load conditions at 2400 RPM.
2. At each load condition for sunflowerseed oil, cottonseed oil, soybean oil, and peanut oil, obtain performance data and gas-phase emission data for CO, HC, NO_x, and total aldehydes. Compare these data with that obtained for the baseline.
3. Collect exhaust particulate matter at each load condition to document the biological activity of these solid-phase emissions.

The single-cylinder direct-injected Diesel engine (Avco-Bernard W-51, 0.36 cc) being used for this phase of the study is fully instrumented to provide performance data (12,13). The instrumentation consists of:

Table 3 - Comparative Multicylinder Engine Particulate Data

	1/2 RACK, 1720 RPM		1/2 RACK, 2000 RPM		3/4 RACK, 2000 RPM	
FUEL	DF-M	DF-2	DF-M	DF-2	DF-M	DF-2
Soluble Organic Fraction (%)	43.0	30.3 ± 6.9	57.1 ± 7.6	40.2 ± 11.6	10.9 ± 0.9	7.5 ± 1.5
Ames Test Results of SOF*	0.94 ± 0.29	0.99	0.61 ± 0.25	0.77 ± 0.18	1.32 ± 0.05	1.75 ± 0.6

* Ames test results using TA98, slope at 100 micrograms per plate ± std. dev.

1. Thermocouples mounted at strategic locations on the engine.

2. Transducers mounted on the engine to sense needle lift, timing, and cylinder pressure.

3. On-line gas phase instrumentation consisting of a Beckman model 955 heated chemiluminescent analyzer for oxides of nitrogen, a Beckman model 864 infrared analyzer for CO, a Beckman model IR-15A infrared analyzer for CO₂, a Beckman model 741 for O₂, and a Beckman model 109 unheated FID for HC. Aldehydes are collected using the DNPH method outlined in Appendix B.

The outputs from the transducers are recorded on floppy discs using a Nicolet Explorer III memory oscilloscope for documentation and further processing.

A comparison of selected fuel properties is given in Appendix A. Shown in Figs. 3 and 4 are typical pressure and needle lift traces comparing DF-2 to cottonseed oil (CSO) performance. At 1/3 rack, the differences are more pronounced than at the higher rack settings since the CSO is burning later in the cycle. In this engine, as evidenced by the pressure traces presented, the combustion is smoother with vegetable oil than with DF-2. Hence, this could be one reason why slightly higher thermal efficiencies are experienced with vegetable oils, as shown in Fig. 5. The equivalence ratio is slightly higher for the vegetable oils because of the differences in heating values of the fuels combined with differences in the stoichiometry. The smaller heating values of the vegetable oils tend to decrease their

actual air-fuel ratio and the theoretical air-fuel ratio is also lower; these two factors combine to give an overall increase in the equivalence ratio.

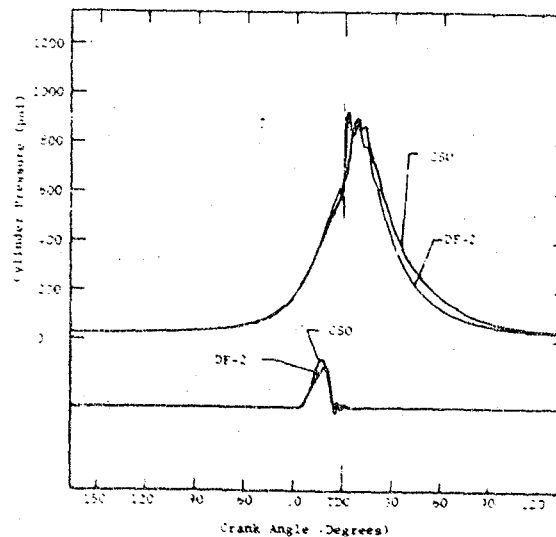


Fig. 3 - Comparative DF-2 and Cottonseed oil Pressure and Needle Lift Traces at 1/3 Rack, 2400 RPM

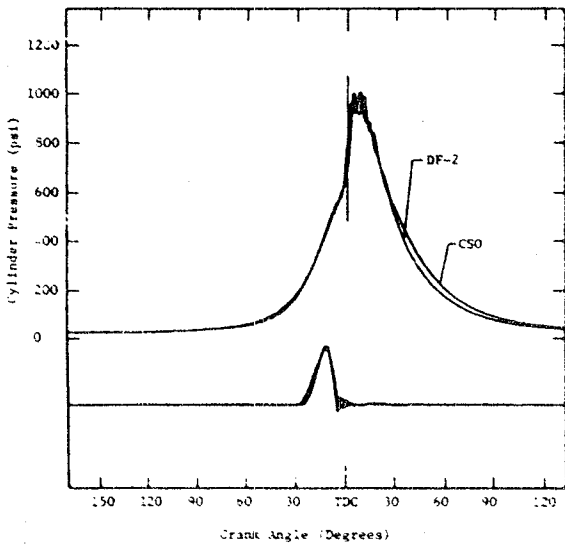


Fig. 4 - Comparative DF-2 and Cottonseed Oil Pressure and Needle Lift Traces at 2/3 Rack, 2400 RPM

The comparative emission data are shown in Fig. 6 and Table 4. Generally, the gas-phase emissions for the two vegetable oils tested are slightly higher. However, in the case of NO_x at 2/3 and full rack and total aldehydes at all rack settings, the vegetable oils show significantly higher values. Particulate mass loading rates increase for the vegetable oils. This is most pronounced at the full rack condition. Based upon a limited number of tests on the SOF, the biological activity as assayed by the Ames test is lower for vegetable oils than for the baseline DF-2.

SUMMARY

This program has just completed its fifth year. During the first four years, almost all activity centered upon alcohol utilization in light-duty Diesel engines. Since alcohols have such poor cetane numbers, it was realized that in the absence of an active ignition system and/or major engine modifications that burning these fuels neat was not possible. The goal of the program was not to develop new hardware, but rather to investigate how the alcohols might

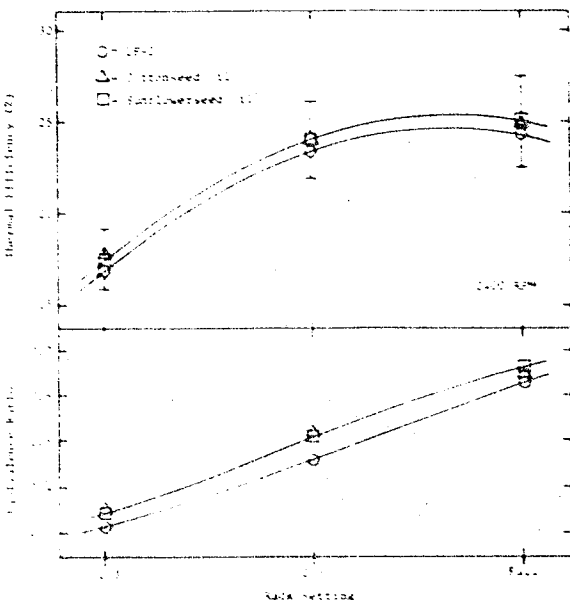


Fig. 5 - Single-cylinder Engine Performance Comparative Data

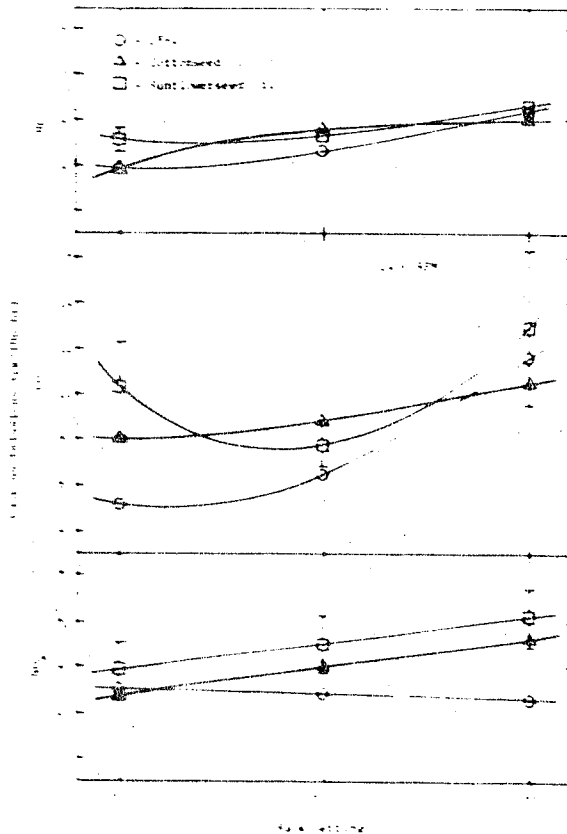


Fig. 6 - Single-cylinder Engine Emission Comparative Data

Table 4 - Comparative Single-cylinder Engine Particulate and Total Aldehyde Data

Fuel Rack	DF-2	Sunf. seed 11	Cottonseed 11
13	22700 44.7 -11.7 1.0 2.69	21742 23.4 12.4 1.64 6.12	21782 40.2 17.7 1.14 1.78
23	11620 119.1 14.0 2.11 2.93	21742 130.6 61.9 1.4 5.55	21782 131.1 111.1 1.26 1.75
Full	1971 191.2 4.4 1.68 1.07	19770 155.7 19.4 1.25 1.25	19224 133.7 14.5 1.27

*Data in each block is tabulated as follows:
 Total energy input BTU/hr
 Particulate deposition rate mg/min
 SOF-percent
 Ames test TA98 bean cell mutagenicity rev. 4
 Total aldehydes mg/m³ (total formaldehyde etc.)

best be utilized by the present generation of engines. Therefore, it was decided that the alcohols would be handled as fuel extenders and that the mode of introduction would be via fumigation.

During the fourth year, program emphasis began to shift in two respects. First, fuels other than the alcohols were now being considered, and second, the build-up of a neat-alcohol, Diesel-like engine test facility was begun. Shale oil, coal-derived oils, and various vegetable oils were selected for testing. The engine build-up consists of a single-cylinder fitted with a removable head of either DI or IDI configuration and an active ignition system.

The major findings of this study to date have been: 1) that while alcohol fumigation does reduce the mass of particulate matter formed, the bioactivity, as assayed by the Ames Test, of both the raw particulate matter and its soluble organic fraction is enhanced and 2) generally, the fumigation of aqueous alcohol degrades engine performance gradually until the onset of "wet misfire" is encountered; this seems to correlate reasonably well with the number of water molecules in the exhaust products and the latent heat of the alcohol-water-fuel oil combination supplied to the engine.

For the vegetable oils tested thus far (sunflowerseed and cottonseed), there appears to be small fuel-energy and bioactivity advantages when compared with DF-2 although the particulate mass emission rate is higher. The multicylinder-

engine screening tests of the shale-derived DF-M yielded results that were essentially the same as DF-2 operation.

ACKNOWLEDGEMENT

This work was supported by a NASA Grant (NAG 3-91) from the Department of Energy, Office of Transportation, administered through the Center for Air Environment Studies of The Pennsylvania State University. The assistance and cooperation of the project officers, John Clark (NASA) and Ralph Fleming (DOE), is greatly appreciated. The authors also thank Dr. William D. Taylor for performing the biological assays reported here.

REFERENCES

1. "The Role of Synthetic Fuels in the United States Energy Future," Exxon Corporation (May 1980).
2. Colucci, J. M., "Directions for Alternative Fuel Programs," Fuels and Lubricants Department, General Motors Research Laboratories, Warren, MI (1979).
3. "Alternative Fuels for Medium-Speed Diesel Engines Program," Southwest Research Institute, San Antonio, TX (1981).
4. Bowden, J. N., et al., "Military Fuels Refined from Paraho-II Shale Oil," U. S. Army Fuels and Lubricants Research Laboratory, SURL, San Antonio, TX (1981).
5. "The Biological Liquid Fuels Alternative Technology Status and Engineering Considerations," A Technical Report Developed through ASAE's Public Policy Issues Program, ASAE (Oct. 1981).
6. Korus, R. A., E. L. Moussetis and L. Lloyd, "Polymerization of Vegetable Oils," Chem. Eng. Dept., University of Idaho, Moscow, ID (1982).
7. Baldwin, J. D., H. Klimkowski and M. A. Keesev, "Compression Ignition Engines," Agr. Eng. Dept. Louisiana State University, Baton Rouge, LA (1982).
8. Vander Walt, A. N. and F. J. C. Hugo, "Attempts to Prevent Injector Coking with Sunflower Oil by Engine Modifications and Fuel Additives," Agr. Eng. Div., Department of Agr. and Fisheries, Silverton, South Africa (1982).
9. Mouser, K. S., S. S. Lestz, M. Dukovitch, and R. E. Yasbin, "Methanol Fumigation of a Light Duty Automotive Diesel Engine," presented at the SAE Fuels & Lubricants Meeting, Baltimore, MD, October 1980. Paper appears in Engine, Fuels and Lubricants - A Perspective on the Future, SAE SP471 (November 1980).
10. Broukhivan, E. M. H. and S. S. Lestz, "The Fumigation of Alcohol in a Light Duty Automotive Diesel Engine," NASA Report CR167915 (1982).
11. Broukhivan, E. M. H. and S. S. Lestz, "Ethanol Fumigation of a Light Duty Automotive Diesel Engine," Paper 811209 presented at SAE Fuels & Lubricants Meeting, Tulsa, OK, October

1981. Paper appears in Alternate Fuels for Diesel Engines, SAE SP503 (October 1981).

12. Heisey, J. B. and S. S. Lestz, "Performance and Emissions Characteristics of Aqueous Alcohol Fuels in a DI Diesel Engine," NASA Report CR167917 (1982).

13. Heisey, J. B. and S. S. Lestz, "Aqueous Alcohol Fumigation of a Single-Cylinder DI Diesel Engine," Paper 811208 presented at SAE Fuels & Lubricants Meeting, Tulsa, OK, October 1981. Paper appears in Alternate Fuels for Diesel Engines, SAE SP503 (October 1981).

APPENDIX A

Selected Fuel Properties

Fuel Property *	DF-2	DF-M	Sunflowerseed 011	Cottonseed 011
LHV (BTU/lbm)	19197	18318	15907	15941
Density (lbm/gal)	7.05	6.96	7.69	7.63
Initial Boiling Point (°F)	420	402	~420	~420
Final Boiling Point (°F)	640	593	Cracks	Cracks
Cetane No.	48	49	37	38
Stoichiometric A/F	15	14.6	13.7	13.7

* Values from the following sources:

A-1. Fuel Suppliers

A-2. CRC Handbook of Chemistry and Physics
61st Edition - CRC Press Inc., Boca Raton, FL
(1981).

A-3. Obert, E. F., Internal Combustion Engines
and Air Pollution (Harper and Row Publishers,
New York (1973)).

APPENDIX B

ALDEHYDE MEASUREMENTS

Aldehyde samples have been collected from the single-cylinder engine for Diesel fuel as well as cottonseed oil and sun oil. The aldehydes are collected by bubbling the exhaust gas through a solution of 2-4, dinitrophenylhydrazine (DNPH). This causes the highly reactive aldehydes to form their DNPH derivatives which have a much higher molecular weight and have greater stability. After collection, solid DNPH derivatives are filtered out and remaining derivatives which are in solution are extracted using pentane. Following extraction, the solid precipitate and

extracted derivatives are combined and analyzed gravimetrically to obtain an indication of total aldehyde emissions. As found in other literature, the total aldehydes are reported as mg formaldehyde per cubic foot exhaust. This was generally reasonable since formaldehyde accounted for 70-90% of the aldehydes present (B-1, B-2). However, there is evidence that the material analyzed gravimetrically contains more than just aldehyde-DNPH derivatives (B-1). For this reason, the values presented are likely to be too high; consequently, a gas chromatograph has been set up to analyze individual aldehyde derivatives to obtain a more accurate indication of aldehyde emissions. Preliminary indications have shown that for aldehyde emissions from DF-2 and vegetable oils, formaldehyde is a much lower percentage of the total than the 70-90% reported by others for gasoline and methanol. This could cause further errors in measuring total aldehydes as equivalent formaldehyde.

REFERENCES

B-1. Adt, R. R., et al., "Characterization of Alcohol/Gasoline Blends as Automotive Fuel -

Performance and Emissions Characteristics,"
Department of Mechanical Engineering, University
of Miami, Coral Gables, FL (September 1981).
B-2. Oberdorfer, P. E., "The Determination of
Aldehydes in Automobile Exhaust Gas," SAE Paper
No. 670123 (January 1967).

QUESTION AND ANSWER PERIOD

- Q: Bill Peters, Ricardo. One question. Were your oils raw oils or were they esters?
- A: Excuse me sir.
- Q: Were the vegetable oils raw vegetable oils or had they been esterized?
- A: All tests reported here were with the raw vegetable oils; however, we plan to do some tests where we are going to take one of the oils when we finish the tests (we will find out which one appears to have the biggest problem) and we are going to try ourselves to run it through an esterification process and look at that. That probably will be the extent of what we will do to try and adjust the composition.
- Q: My name is Lynn of Cummins. I would like to make a strong plea for future work in the alternate fuel. To provide the fuel specifications as much as possible. Now I notice you provide some. In one diesel application this will be a very helpful thing. And also, maybe you have presented it previously, I don't know, the chemical composition. And I wonder whether for the vegetable oil fuels you should do a test for nitrogen in the fuel. But I would just like to make a plea to provide as much of a complete fuel specification as possible and that would make the result more meaningful for the reader.
- A: Thank you Dr. Lynn. Can I just make one brief comment before we take the next question? In the SAE paper version of this presentation, the table includes cetane numbers as well as theoretical air-fuel ratios listed there. In some of our former work, we showed very conclusively the role of nitrogen as it affects the bioactivity of the soluble organic extracts. So we were keenly aware of what the nitrogen in the fuel might do as far as the NOx and the activity of the extract is concerned.
- Q: Bailey, Caterpillar. Did you heat both the diesel fuel and the vegetable oil, or just the vegetable oil? And was it really raw vegetable oil, crude degummed, fully refined, or what?
- A: That needs to be cleared up. I'm sorry that I confused you as far as the heating is concerned. Our standard procedure was to deliver the diesel fuel at 85°F when we were running a baseline. In our test cells, that requires some auxiliary heating, stirring, and making sure that that temperature is well controlled. The vegetable oils we heated and stirred and controlled the temperature to 160° before delivery. So there was that difference we found we needed. I used the term raw incorrectly as it is used in the answer to the former question. The vegetable oils were degummed and once refined and in the case of the sunflower seed oil, it was also bleached.
- Q: Ralph Fleming, DOE. The way the hydrocarbon procedure for diesel exhaust hydrocarbons was developed, it was pretty much empirical based around straight run petroleum diesel fuel. It would seem to me the numbers would be highly questionable because of the very significant difference in boiling points between these fuels and the products that might come out the exhaust stack. It would seem to me there needs to be a look at that. The second point is that I agree fully with Dr. Lynn that the more fuel data you have, the more we can interpret the results, but I would like to caution that cetane numbers on vegetable oils would be highly questionable as far as the testing is done in a CFR engine. So I think there needs to be some work in the future to develop a new procedure for rating fuels.
- A: I'll just comment on your first point and I agree with your second point. The distillation curves for the vegetable oils have an initial boiling point slightly above that of DF-2, at least with the ones we are working with, then they go up to about 600°F and then crack. They do not behave the same as a full boiling range DF-2. What we are doing concurrently with the development of our aldehyde procedures, is developing a GC technique to look at the hydrocarbons in the exhaust gas that we are collecting. It seems to me to be a little ambitious to find some correlation between this and what you do see with an FID total hydrocarbon detector. But at least that is the direction we are going, and I do agree with you Ralph that that is a concern.

The Ability for Conventional IC Engines to Run on Fuels Derived from Coal and Oil Shale

J. R. Needham, S. R. Norris-Jones,
and B. M. Cooper
Ricardo Consulting Engineers plc

ABSTRACT

to index

This paper provides an overview of the Department of Energy Contract, DE-AC01-80GS50021 aimed at studying the interaction between IC engines and fuels. Both indirect and direct injection diesel and spark ignited stratified charge combustion systems were addressed. Fuels covered regular D-2 diesel, low ignition quality diesel fuel, naphtha and naphtha/diesel fuel broadcuts.

Candidate combustion systems for future fuel groups are examined and the necessity for further research in specified areas highlighted for a full understanding.

IN ORDER TO AVOID reliance upon high importation levels of petroleum crude to satisfy future domestic energy requirements, the U.S. is embarking upon the development of a Syncrude industry to manufacture liquid hydrocarbon fuels from coal and oil shale. To help understand the impact of such fuels upon the operation of automotive internal combustion engines, Ricardo have been engaged upon a DoE sponsored project evaluating various fuels in conjunction with several types of combustion system.

The contract was initiated in January 1980 and the programme divided into four tasks namely,

- Task 1 - Literature Study
- Task 2 - Diesel Multi-cylinder Screening Study
- Task 3 - Diesel and Spark Ignited Stratified Charge Fundamental Study
- Task 4 - Final Report

Task 1 is not covered in this presentation since the results have been fully reported at the 1980 CCM and in the definitive report subsequently published (Ricardo Reference DP 81/539). Owing to the current status of Tasks 2 and 3, this presentation provides an overview of these tasks and the major conclusions and recommendations arising. Since data acquisition

and analysis is still ongoing the conclusions and recommendations given here should be regarded as preliminary. Full results from the available database and definitive conclusions etc. will be made available in the final report due for publication in December 1982. Since a synopsis of typical results is difficult to extract from the database, actual data are not contained in this paper.

OVERALL OBJECTIVES

The overall objectives of Tasks 2 and 3 may be stated as:-

- an assessment of the interaction between fuels and engines and the acquisition of a database to assist in the required trade-off studies between fuel production costs, specifications and implications in use.

EXPERIMENTAL DETAILS

TEST ENGINES - During the Task 2 screening study, both indirect (IDI) and direct injection (DI) diesel combustion systems were evaluated. Both incorporated swirling combustion chambers and the DI system utilized multi-fuel spray injection equipment.

For Task 3, the same IDI and DI diesel combustion systems were again examined in conjunction with three spark ignited, stratified charge systems. The latter covered one IDI and two DI systems (Texaco TCCS and MAN FM). The DI diesel and TCCS systems were evaluated in multi-cylinder form and the FM and both IDI systems in single cylinder form utilising a Ricardo Hydra designed and procured as an integral part of the Task.

All of the above combustion systems employed cylinder displacements and rated speeds commensurate with light duty applications.

FUELS - A synopsis of fuel inspection data for both Tasks 2 and 3 are provided in Appendices 1 and 2 respectively.

The rationale behind the fuel design

primarily brackets the future specifications of syncrude derived products when addressing a broadcast option. The inclusion of the alternative diesel fuel in Task 3 examines the impact of a heavy, low ignition quality, aromatic diesel fuel and attempts to cover an alternative candidate future fuel strategy.

ENGINE OPTIMISATION - For the screening study no optimization was carried out and the fuel injection pump was timed statically at the optimum compromise developed for regular diesel fuel. During the fundamental programme, the injection and ignition timing was varied as appropriate for each fuel primarily with the aim of identifying optimum fuel economy.

DATA GENERATION - During the Task 2 screening study, comparisons of performance, economy, smoke and gaseous emissions (HC, NOx, CO) were made over the load and speed range. During the Task 3 fundamental study these were again recorded with the inclusion of particulate emissions. Testing was concentrated over the load range towards selected test speeds (1500 and 2400 rev/min) as representative of light duty operation. Performance aspects were however also addressed at the rated speed for each combustion system in addition to observations on combustion details, startability, engine condition etc.

EXPERIMENTAL OBSERVATIONS

For expedience, the experimental observations are divided into two groups by combustion system. The comments made and the subsequent discussion and conclusions are mainly drawn from the fundamental study database since this covers the widest range of fuel specifications and includes particulate measurements and startability observations.

IDI AND DI DIESEL - In general terms, hot operability did not present a problem with the diesel engine/fuel combinations examined with performance and emission characteristics not consistently differentiating from operation with Phillips D-2 as reference. Indeed, the degree of fuel tolerance initially noted during the Task 2 screening study justified continued work with the diesel during the fundamental programme utilizing much wider ranging fuel specifications. These observations illustrate a degree of fuel tolerance with the systems evaluated although specific problem areas were highlighted as follows:-

Operability - a) Starting - At the time of writing, starting evaluations have only been made with the IDI diesel. Tests were only made down to typical laboratory ambient temperatures. Under these conditions D-2, naphtha and the two D-2/naphtha blends enabled immediate starts utilizing the standard heater plug with sustained idling also being achieved. With the low ignition quality alternative diesel fuel, starting was significantly worse and subsequent idling erratic. At lower temperatures more typical of true winter ambients it is anticipated that

the IDI diesel will not start successfully even with the other low ignition quality fuels, i.e. naphtha and the predominant naphtha/D-2 blend.

It is expected that the DI will behave in a similar fashion and starting with low ignition quality fuels remains as a potential problem.

b) Misfire - In the DI diesel only D-2, the predominant D-2/naphtha blend and the low ignition quality alternative diesel fuel were evaluated during the fundamental study. On these fuels, no misfire problems were encountered. With the IDI diesel, significant misfire was apparent at light load, low speed with the low ignition quality diesel fuel. To clear misfire, the injection timing needed to be advanced incurring significant HC and particulate penalties. This increase in HC is not fully understood. With the low ignition quality naphtha fuels, misfire was not prevalent except for very light load with retarded injection timing when using straight run naphtha.

c) Noise - Noise was only subjectively monitored during the programme. In this case, noise overall did not appear to be appreciably influenced. Possible exceptions however were increased harshness with the low ignition quality diesel fuel at higher load and straight run naphtha at light load in the IDI diesel tests during the fundamental programme. With the latter fuel, it should also be noted that the degree of injection advance required to clear misfire at light load, rated speed approached the subjective noise threshold. The lack of any subjective noise increase with the DI diesel when running on the low ignition quality diesel fuel proved somewhat surprising. The inaccuracy of subjective assessment should however be noted.

Preliminary analysis of the IDI diesel combustion diagrams broadly supports the subjective assessments made. It should also be noted that in the case of the IDI diesel, all of the test work with the very low ignition quality fuels was carried out with a relatively stiff single cylinder engine which tends to mask noise trends. It must be concluded without access to further data that low ignition quality fuels will impose a noise penalty in diesel combustion systems. This requires continued research with both IDI and DI variants.

d) Fuel Injection Equipment - During the programme, a fuel handling system for the suppression of fuel vapour with volatile fuels was utilized. Although this arrangement was successfully employed on several of the combustion systems throughout the programme, apparent vapour problems were encountered during the Task 3 DI tests. The problem arose when running with the predominantly naphtha/D-2 blend and resulted in severe instability of the dynamic injection timing and fuelling level throughout the operating range. Data was not collected with this fuel therefore and it was assumed that similar problems would have been prevalent with naphtha.

The reasons for this problem are not fully understood but it may be significant that of all

the combustion systems examined, the DI diesel has a relatively higher rate injection pump which may be a contributing factor.

Performance and Emissions - a) IDI diesel - With this combustion system, HC penalties were evident with low ignition quality fuels. Penalties were however restricted to high speed over the load range with straight run naphtha and low speed with the alternative diesel fuel. In the latter case the response was most significant and particulate emissions were also influenced adversely. These penalties were observed when advancing the injection timing to clear misfire. Retarding the timing largely overcame the emissions penalty towards the higher load factors at the expense of light load misfire.

In the important consideration of fuel consumption, adverse effects relative to D-2 operation ranging between c. 3-11% were apparent, the magnitude being dependent upon fuel, speed and load. The importance of these consumption penalties requires close review when studying the trade-off between the production costs of lower quality fuels and vehicle economy.

b) DI diesel - Preliminary analysis suggests that the major fuel effect in the DI diesel was increased smoke at low speed with the alternative low ignition quality diesel fuel. This trend penalised particulates and available torque.

SPARK IGNITED STRATIFIED CHARGE COMBUSTION SYSTEMS - As expected with positive ignition, the stratified charge systems evaluated have proved generally fuel tolerant but problem areas may be summarised as follows:-

Operability - a) Rated speed - With high ignition quality fuels of c. 40+ cetane number, the MAN FM system incurred combustion problems at high speed significantly limiting the available speed range. In this case, spark control was lost and heavy detonation occurred at rated speed (4000 rev/min) with load factors in excess of c. 1.5 bar BMEP. Realistic torque was only restored when reducing the rated speed to low levels (c. 3000 rev/min) not commensurate with light duty applications.

With the spark ignited, indirect injection (SIIDI) engine, spark management of the engine was not obtained with D-2 at high load, high speed, resulting in unstable, erratic combustion. This could only be overcome by reducing the rated speed on this fuel to low levels similar to that of the MAN FM system.

With all other fuels in these combustion systems, useable rated speeds of c. 4000 rev/min could be achieved up to relatively high load factors. The absence of any problems with the Texaco TCCS system in this respect reflects one of the major differences between the systems i.e. the TCCS utilizes a very high energy, multi-strike ignition source timed simultaneously with the injection and therefore ignites the 'wet' fuel spray, avoiding pre-mixing, self-ignition and detonation. With the FM and SIIDI, the TCCS philosophy cannot be achieved by

advancing the spark towards the front of the injection period since the relatively low energy, single strike ignition source does not successfully ignite the spray, presumably due to plug wetting.

b) Light load - With the FM and SIIDI systems very light load stable combustion frequently proved difficult to achieve. The experience of others suggests that this is not a fundamental characteristic of the systems but reflects the very limited development status of the actual engines tested.

c) Spark plug life - The SIIDI engine could not be run on naphtha at the lower speeds owing to rapid spark plug sooting and loss of correct ignition causing misfire and unstable running. Frequent spark plug failures were also encountered on all fuels with this system but it is reasoned that a fundamental design change to reduce the length of the electrodes whilst preserving the position of the gap within the pre-chamber may overcome this problem. With the FM system, running with detonation must be avoided or spark plug failures result whilst in the TCCS system, spark plug failures were not recorded but high rates of electrode erosion were encountered.

Whilst design/development should overcome these problems, the harsh environment for sparking plugs within the stratified charge engine should be noted.

Performance and Emissions - Unlike the diesel engine with a unique reference fuel, the influence of fuels upon performance and emissions with the multi-fuel, stratified charge engine is not so readily interpreted in a succinct manner. For all fuels, performance and emission trends were generally distinctly defined but in the case of the open chamber systems (FM and TCCS) it may be stated that there is a preference for the more volatile fuels. Such fuels encourage lower smoke and greater torque. Whilst such fuels do not overall assist in reducing the high HC characteristics of these systems, they do enable in conjunction with the smoke trends, lower particulates to be achieved. It is believed that with volatile fuels, lighter HC species are formed not conducive to particulate formation. In the case of fuel economy, volatile fuels returned the best consumption at high load factors but this was not always reflected at light load.

DISCUSSION

For the purposes of this overview, the discussion is restricted to the identification of likely candidate combustion systems for future fuel groups. Within each fuel group the likely candidate combustion systems are reviewed based upon two scenarios - relaxed environmental pressure with comparison of baseline characteristics using optimum economy timing plan; and continued stringent environmental standards.

HIGH IGNITION QUALITY DIESEL AND BROADCUT FUELS - Fuels of c.40+ cetane number ignition quality are considered here. For fuels of this class, it is judged that the diesel will remain dominant with hot and cold operability not presenting a major problem. When considering economy, the DI diesel has a c.10% advantage over the IDI and this will be an important consideration in the overall energy balance since high ignition quality fuels will be more costly to produce. The DI does however have lower torque potential than the IDI and higher baseline emission characteristics. With relaxed environmental pressure, it may be assumed that the selection of DI or IDI would depend upon individual requirements between economy and torque. Continued development of the DI should result in improved torque although the use of the high pressure fuel injection equipment required will increase first costs. In this context, other DI systems, such as the MAN Controlled Direct Injection (CDI) system appear promising.

With maintained stringent emission controls, the IDI is likely to remain dominant owing to lower baseline emission characteristics compared with the DI. Even in this case, particulate emissions may present a problem in the longer term. The multi-spray DI system evaluated during this programme is unlikely to achieve engineering HC, NOx and particulate targets commensurate with future legislation even when using such technology as valve covering orifice nozzles (VCO).

The spark ignited stratified charge engine is not thought to represent a candidate for fuels of this class. With such fuels only the TCCS system may be considered as the other two systems evaluated (FM and SIIDI) generally encountered operability problems in respect of rated speed. The TCCS system, however, exhibits significantly higher baseline HC and particulate emissions and low torque characteristics with respect to either the IDI or DI diesel and its adoption for such fuels is not thought to be justified.

LOW IGNITION QUALITY NAPHTHA AND BROADCUT FUELS - In this class, fuels of c.35 or lower cetane number are considered. When examining the baseline characteristics of the IDI diesel with these fuels, the emissions and available torque characteristics did not overall represent a major problem area relative to D-2 operation as reference. Instances of worse economy were however noted.

Doubt must however exist for the IDI diesel with fuels of this class based upon three reasons - cold operability, tolerance to retard for low NOx in respect of misfire and noise. With low baseline emissions, high torque and wide speed range in conjunction with the encouraging results from this programme, research should be encouraged to see whether the aforementioned problems and the instances of worse economy may be overcome by development. It must however be recognised that the suitability of the IDI diesel in conjunction with very low ignition quality fuels will be seriously in doubt with continued

stringent emissions standards requiring injection retard for low NOx. In this case misfire regimes are likely, with sharp HC trade-off responses.

Since the DI diesel was not evaluated on this class of fuel for the reason previously mentioned, the long term suitability of the DI diesel cannot be ascertained and resort to speculation will not be made.

With positive ignition the spark ignited stratified charge engine is able to avoid the cold operability etc. type of problem that will face the IDI diesel. The achievements of the TCCS system in these respects have been well reported in the past and it is reasoned that with equivalent development effort, the FM and SIIDI system should be capable of similar performance.

Spark ignited stratified charge engines must clearly represent candidates therefore for fuels of this class. Based upon this programme, the suitability of the SIIDI cannot be fully ascertained owing to the rapid spark plug fouling with naphtha as fuel. Of the two open chamber systems examined (FM and TCCS) both have good light load economy characteristics. Overall, the FM performed better with lower HC emissions and particulates, better torque and lower high load consumption. Baseline NOx emissions were however somewhat higher than the TCCS system presumably due to fuel/air pre-mixing prior to ignition.

Whilst the lower HC emissions of the FM compared with the TCCS are fundamental owing to the use of a pintle type of injector, an overall judgement of the selection of candidate between the FM and TCCS is withheld for two reasons as follows:- Firstly, the FM system was evaluated in single cylinder form. Whilst the friction factors utilized to predict multi-cylinder FM performance for comparison with the observed multi-cylinder TCCS data are entirely credible, the basic single cylinder performance may be enhanced owing to the lack of any cylinder to cylinder distribution problem of air flow, swirl or injection/ignition timing. Secondly, the single cylinder FM engine had excellent volumetric efficiency compared with the low breathing efficiency of the White TCCS engine. Required therefore, for a full understanding, are comprehensive multi-cylinder programmes comparing FM and TCCS systems with equivalent, well developed breathing characteristics, ultimately employing appropriate natural injection/ignition timing plans.

What is clear is that either of the two systems will have overall higher baseline emissions and lower torque compared with the IDI diesel. Furthermore, the extensive emissions controls required for continued stringent emission standards are likely to significantly erode the favourable light load baseline economy characteristics of the two systems.

In this context, the SIIDI system is worthy of continued evaluation. Although as expected its fuel economy characteristics are not as good as those of the open chamber design, the limited available evidence from this

programme suggests that the HC response overall is lower, approaching more closely that of the IDI diesel. Because of this, the differential in fuel economy trends between pre and open chamber systems may be narrowed when controlling emissions to stringent levels.

LOW IGNITION QUALITY DIESEL FUEL - Addressed here are fuels of c.35 cetane number ignition quality, high aromatic content and c.700^oF end point.

Such fuels have proved problematical in the IDI diesel programme owing to the misfire/HC/particulate trade-offs prevalent at light load, low speed and discussed earlier in this presentation. In this case, and somewhat surprisingly, the DI diesel appeared more tolerant with similar misfire regimes not being encountered. Corroborative support from the screening study was obtained when comparing low speed HC trends between the IDI and DI diesels with the low ignition quality D-2 fuel tested. In this case HC emissions were significantly elevated with the IDI diesel but remained more typical of D-2 operation in the DI.

This class of fuel also caused significant starting difficulties at typical laboratory ambient temperatures in the IDI diesel even compared with the lower ignition quality naphtha type fuels. Such data support the frequently exploited volatility/ignition quality trade-off in respect of starting. At the time of writing, starting tests have not been undertaken in the DI diesel although it is anticipated that the results will not be encouraging with this class of fuel.

In addition, low speed torque with the DI diesel was further curtailed with the low ignition quality diesel fuel due to a marked increase in smoke at higher load factors.

Outside of the aforementioned problem areas, baseline emissions and performance of the IDI and DI diesels generally remained competitive with the D-2 reference data. This would encourage further research although the suitability of the diesel, particularly of the IDI, does not seem assured based upon the available evidence with fuels of this class. With maintained environmental pressures, retarding for low NO_x will further this suspicion as starting problems will be exacerbated, further misfire regimes encountered and marked emission trade-off penalties incurred. In this case, the continued use of the diesel is thought unlikely.

The FM and TCCS combustion systems would appear suited to such fuels as they were successfully evaluated with good light load economy trends and cold starting and no apparent operability problems. Their inclusion in a future scenario utilizing such fuels would therefore appear justified although baseline emissions will be high. In this context, it should be noted that the superior HC characteristics of the FM compared with the TCCS were lost at low speed with this type of fuel,

presumably due to the adverse influence of the less volatile fuel upon mixing and evaporation from the wall of the combustion chamber under the low bowl swirl conditions prevalent at low speed. Compared with the demonstrated ability of the IDI diesel with such fuels, the torque curve of either the FM or TCCS systems will also be lower as a consequence of their inclusion to avoid operability problems.

Since these types of fuel further increase the HC and particulate emissions in the FM system and particulates in the TCCS, the demands upon emissions controls for maintained stringent standards will be increased. Again, this is likely to erode or nullify the favourable baseline economy trends of these systems.

For budgetary reasons, the low ignition quality diesel fuel was not evaluated in the SIIDI system and with spark ignition the systems suitability for such fuels may only be speculated. Such a system should again be examined in the continued research programmes required for a full understanding, in particular, when comparing well developed multi-cylinder FM and TCCS systems for the reasons previously discussed.

CONCLUSIONS

CANDIDATE COMBUSTION SYSTEMS FOR FUTURE FUELS

Relaxed Environmental Standards -

- a) High Ignition Quality Diesel and Broad-cut Fuels - IDI and DI diesel
- b) Low Ignition Quality Naphtha and Broad-cut Fuels - Spark ignited stratified charge or IDI diesel providing potential cold operability and noise problems can be overcome by development in the interests of minimising baseline emissions and maximising torque availability.
- c) Low Ignition Quality Diesel Fuels - Spark ignited stratified charge or adapted IDI/DI diesel providing cold operability etc. problems are not insuperable.

Maintained Stringent Emissions Standards -

- a) High Ignition Quality Diesel and Broad-cut Fuels - IDI diesel.
- b) Low Ignition Quality Naphtha and Broad-cut Fuels - Spark ignited stratified charge.
- c) Low Ignition Quality Diesel Fuels - Spark ignited stratified charge.

OVERALL - The interaction between fuels and engines is complex requiring extensive research from structured programmes for a full understanding. During these programmes, the following areas must be addressed:-

- a) Candidate Syngas fuels
- b) IDI and DI diesel development in respect of cold operability, noise and tolerance to retard with low ignition quality fuels.
- c) Well developed, multi-cylinder stratified charge comparisons.
- d) Other combustion systems, i.e. pre-chamber IDI diesel and MAN CDI DI diesel.
- e) Combustion systems with different cylinder sizes, speed ranges and methods of aspiration.

As dictated by the above programmes, the detailed optimisation of promising combinations must be carried out.

APPENDIX 1

Basic Specification of Test Fuels - Task 2

Fuel	Cetane No	Distillation °F				
		IBP	10%	50%	90%	FBP
Phillips D-2	48	378	432	505	568	603
50%/50% wt/wt Diesel/Naphtha	44	298	313	381	613	666
66%/34% wt/wt Diesel/Naphtha	47.5	306	324	435	617	676
Phillips D-2 +0.12% T.E.L.	38	363	426	502	565	601
Phillips D-2 +0.2% I.P.N.	51	363	430	502	565	603

- NB 1) The diesel used for the above diesel/naphtha blends is not Phillips D-2 but selected high cetane European diesel fuels.
- 2) The above blending naphthas are not the same as the straight-run naphtha utilised for Task 3.

APPENDIX 2

Basic Specification of Test Fuels - Task 3

Fuel	Cetane No	Distillation °F					Aromatic Content % vol
		IBP	10%	50%	90%	FBP	
Phillips D-2	48	378	432	505	568	603	30.3
73%/27% vol/vol Phillips D-2/straight-run naphtha	40	172	248	478	565	599	25
66%/34% vol/vol straight-run naphtha/Phillips D-2	35	153	208	289	538	597	21.2
Straight-run naphtha	27	151	196	237	307	354	16.2
50%/50% vol/vol light cycle oil/gas oil	34.5	170	446	505	603	675	45.6

Effective Values of Evaporation Constant for Hydrocarbon Fuel Drops

J. S. Chin

Beijing Institute of Aeronautics and Astronautics

A. H. Lefebvre

School of Mechanical Engineering

Purdue Univ.

West Lafayette, IN

ABSTRACT

Experimental values of evaporation constant for use in calculations of evaporation rates and drop lifetimes are fairly sparse and are usually confined to conditions of steady-state evaporation in quiescent mixtures at normal atmospheric pressure. The main objective of the present study is to provide "effective" values of evaporation constant that cover wide ranges of ambient air pressure, temperature and velocity, and which also take into account the influence of the heat-up period in lowering the overall evaporation rate. The average boiling point (50 percent recovered) is the physical property selected to characterize the volatility of the fuel.

KNOWLEDGE OF FUEL DROP EVAPORATION is of prime importance to the design and performance of liquid-fuelled combustion systems, including diesel engines and gas turbines. In a previous paper (1) attention was focussed on the effects of ambient pressure and temperature on the steady-state evaporation of fuel drops. A numerical procedure was described for calculating steady-state values of drop-surface temperature and evaporation constant, and the method was then used to examine the evaporation characteristics of n-heptane, aviation gasoline, JP-4, JP-5, and diesel oil (DF-2) in quiescent atmospheres. In a subsequent paper (2) the factors governing the duration of the heat-up period in fuel drop evaporation were studied analytically and an equation for estimating the duration of the heat-up phase was derived. Graphs were presented which showed, for selected fuels, the effects of air pressure, temperature and velocity, and fuel drop size, on the length of the heat-up period and on the ratio of the heat-up period to the total drop lifetime. It was shown

*Numbers in parentheses designate references at end of paper.

that neglect of the heat-up period can lead to serious errors in the calculation of drop evaporation rates and drop lifetimes. The extent of this error, and its dependence on drop size and ambient air conditions, was demonstrated quantitatively for several fuels.

The main drawback to these studies is that they were confined to a limited number of standard engine fuels. Consequently, the results obtained cannot be readily applied to alternative fuels, or fuel blends. The present study was undertaken to remedy this deficiency. Its objective is to provide the same type of information on fuel drop evaporation, but in a more general form, thereby extending its range of application to a fairly wide variety of hydrocarbon fuels. To achieve this goal it is necessary to select a correlative fuel property that will define to a sufficient degree of accuracy the evaporation characteristics of any given fuel. It is recognized that no single chemical or physical property is completely satisfactory for this purpose. However, the average boiling point (50 percent recovered) has much to commend it, since it is directly related to fuel volatility and fuel vapor pressure. It also has the virtue of being easy to measure, and is usually quoted in fuel specifications. For these reasons the average boiling point was chosen for the present study to characterize the fuel's propensity for evaporation.

BASIC EQUATIONS

The procedures employed to determine the variation of the effective evaporation constant with air pressure, temperature, and velocity, fuel drop size and average boiling point, follow closely those outlined in detail in previous publications (1, 2). Thus only the basic equations required for the study are presented below. For further information on the physical properties of fuels and fuel vapors, and methods for estimating reference values of temperature and species

concentration, reference should be made to these earlier companion papers.

According to Faeth (3) the heat transfer coefficient between a fuel drop and a surrounding quiescent gas is given by

$$Nu = \frac{h D}{k_g} = 2 \frac{\ln(1+B_M)}{B_M} \quad (1)$$

The heat transferred from the gas to the drop is

$$Q = \pi D^2 h (T_\infty - T_s) \quad (2)$$

Substituting for h from Eq. (1) into Eq. (2) gives

$$Q = 2\pi D k_g (T_\infty - T_s) \ln(1 + B_M) / B_M \quad (3)$$

The heat used in vaporizing the fuel is

$$Q_e = \dot{m}_F L \quad (4)$$

where L is the latent heat of fuel vaporization corresponding to the drop surface temperature, T_s . We have (1)

$$L = L_{T_{bn}} \left[\frac{T_{cr} - T_s}{T_{cr} - T_{bn}} \right]^{0.38} \quad (5)$$

Now the rate of fuel evaporation of a single drop of diameter, D , is given by (4)

$$\dot{m}_F = 2\pi D (k/c_p) \ln(1 + B_M) \quad (6)$$

Substituting for \dot{m}_F from Eq. (6) into Eq. (4) gives

$$Q_e = 2\pi D (k/c_p) L \ln(1 + B_M) \quad (7)$$

The heat available for heating up the droplet is obtained as the difference between Q and Q_e . From Eqs. (3), (6) and (7) we have (2)

$$Q - Q_e = \dot{m}_F L (B_T / B_M - 1) \quad (8)$$

where B_M , the mass transfer number, is given by (1)

$$B_M = \left[\frac{P}{\exp[a-b/(T_s-43)]} - 1 \right]^{-1} \quad (9)$$

and B_T , the heat transfer number, is defined as

$$B_T = c_p (T_\infty - T_s) / L \quad (10)$$

In Eq. (9) P is the ambient pressure, and M is the ratio of the molecular weights of fuel and air. Values of a and b for several commercial

fuels are listed in Table 1 of reference 2.

The rate of change of drop surface temperature, T_s , is given by

$$\frac{dT_s}{dt} = \frac{Q - Q_e}{c_{pF} m} \quad (11)$$

$$\text{or,} \quad \frac{dT_s}{dt} = \frac{\dot{m}_F L}{c_{pF} m} \left[\frac{B_T}{B_M} - 1 \right] \quad (12)$$

$$\text{where } m = \text{droplet mass} = (\pi/6) \rho_F D^3 \quad (13)$$

Also, we have,

$$\dot{m}_F = 2\pi D (k/c_p) \ln(1 + B) = \frac{d}{dt} [(-6)\rho_F D^3] \quad (14)$$

$$\text{hence} \quad \frac{dD}{dt} = \frac{4k \ln(1 + B_M)}{\rho_F c_p D} \quad (15)$$

CALCULATION OF HEAT-UP PERIOD

In order to calculate effective values of evaporation constant it is necessary first to estimate the duration of the heat-up period and the drop diameter at the end of the heat-up period, using Eqs. (12) and (15) respectively. The main drawback to these equations is that their solution entails iterative procedures that tend to be tedious and time-consuming. To simplify the process an alternative approach has been developed which is much shorter and forfeits little in terms of accuracy. The basis of the method lies in the designation of mean or effective values of \dot{m}_F and T_s for the heat-up period which, when inserted into the appropriate equations, allow the duration of the heat-up period and the drop diameter at the end of this period to be readily evaluated. The method has been fully described elsewhere (2), and only the resulting key equations are presented below.

For the mean, or effective value of \dot{m}_F during the heat-up period we have

$$\dot{m}_{F_{hu}} = \frac{8k_g}{c_{pF} \rho_F} \ln(1 + B_{M_{hu}}) \quad (16)$$

$$\text{where} \quad B_{M_{hu}} = M \left[\frac{P}{\exp[a-b/(T_{s_{hu}}-43)]} - 1 \right]^{-1} \quad (17)$$

In order to estimate the heat-up period Eq. (12) is rewritten, using Eqs. (6) and (13), as

$$\frac{dT_s}{dt_{hu}} = \frac{c_{pF} \rho_F c_p D_{hu}^2}{12k_g} \left[\frac{B_T}{B_{M_{hu}}} - 1 \right] \quad (18)$$

where $B_{T_{hu}} = c_{p_g} (T_{\infty} - T_{s_{hu}}) / L_{T_{s_{hu}}}$ (19)

D_{hu} is the effective mean diameter during the heat-up period. It is related to the initial drop diameter, D_o , by the equation

$$D_{hu} = D_o \left[1 + \frac{c_{p_F} (T_{s_{st}} - T_{s_o})}{2L[B_{T_{hu}}/B_M] - 1} \right]^{-0.5} \quad (20)$$

It is important that the physical properties contained in Eqs. (16) to (20) should be evaluated at the correct level of temperature. For c_{p_F} and L the appropriate temperature is $0.5(T_{s_o} + T_{s_{st}})$. For B_M the proper temperature is $T_{s_{hu}}$. The drop diameter at the end of the heat-up period is readily obtained as

$$D_l^2 = D_o^2 - \dot{m}_{hu} t_{hu} \quad (21)$$

and the drop lifetime is given by

$$t_e = t_{hu} + t_{st} \quad (22)$$

$$= t_{hu} + D_l^2 / \dot{m}_{st} \quad (23)$$

CONVECTIVE EFFECTS ON FUEL DROP EVAPORATION

Most published values of evaporation constant, \dot{m}_{st} , relate to steady-state evaporation conditions in quiescent mixtures. A method for estimating \dot{m}_{st} for any stipulated values of pressure, temperature and fuel properties, is described in reference 1. This same method has been used to examine the variation of \dot{m}_{st} with T_{bn} . The results are shown in Figs 1 to 4 as graphs of \dot{m}_{st} plotted against T_{bn} for ambient temperatures of 500, 800, 1200, 1600, and 2000K, at pressure levels of 100, 500, 1000, and 2000 kPa.

The values of \dot{m}_{st} contained in Figs. 1 to 4 are for quiescent mixtures only. The effects of forced convection on heat evaporation rates may be accounted for by multiplying \dot{m}_{st} by a correction factor which is a function of Reynolds number and Prandtl number. Frossling (5) proposed the factor

$$1 + 0.276 Re_D^{0.5} Pr_g^{0.33} \quad (24)$$

Another widely used correction factor is the following due to Ranz and Marshall (6),

$$1 + 0.3 Re_D^{0.5} Pr_g^{0.33} \quad (25)$$

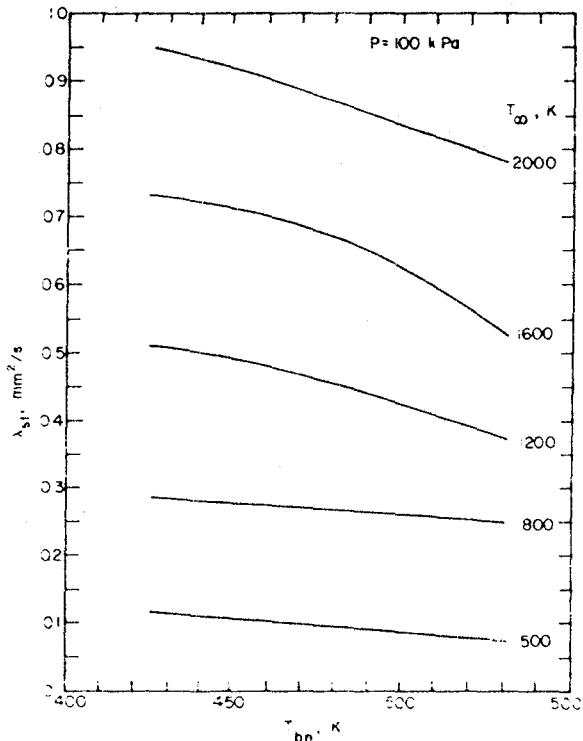


Fig. 1. Influence of ambient temperature and normal boiling temperature on the steady state evaporation constant for a pressure of 100kPa.

The relative merits of these and other correction factors for forced convection have been reviewed by Faeth (3). The velocity term in Re_D should be the relative velocity between the drop and the surrounding gas, i.e. $Re_D = U D_r / \nu_g$. However, both calculations and experimental observations suggest that small droplets rapidly attain the same velocity as the surrounding gas, after which they are susceptible only to the fluctuating component of velocity, u' . The appropriate value of Reynolds number then becomes $(u' D_r / \nu_g)$.

From a practical viewpoint it would be very convenient if the effect of the heat-up period could be combined with that of forced convection in a manner that could lead to the derivation of an "effective" value of evaporation constant for any given fuel at any stipulated conditions of ambient pressure, temperature, velocity, and drop size. This can be accomplished by defining an effective evaporation constant as

$$\dot{m}_{eff} = D_o^2 / t_e \quad (26)$$

where t_e is the total time required to evaporate the fuel drop, including both convective and transient heat-up effects. From Eqs. (21) and (25)

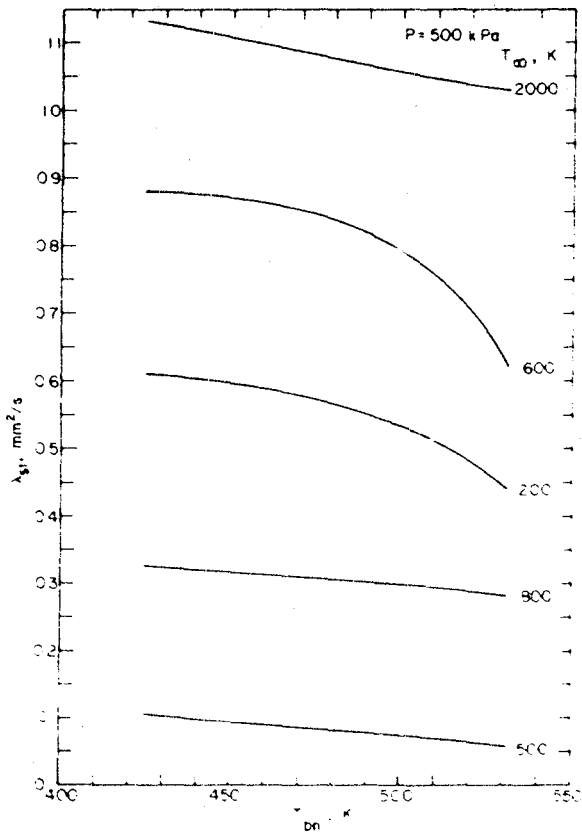


Fig. 2. Influence of ambient temperature and normal boiling temperature on the steady state evaporation constant for a pressure of 500kPa.

we have

$$t_e = t_{hu} + \frac{D_{st}^2 - D_{hu}^2}{4\alpha_{st}} \frac{t_{hu} (1 + 0.30 Re_{hu}^{0.5} Pr_z^{0.33})}{1 + 0.30 Re_{st}^{0.5} Pr_z^{0.33}} \quad (27)$$

in which Re_{hu} and Re_{st} are based on D_{hu} and D_{st} respectively. (Note that $D_{st} = 0.25D_{hu}$). Values of λ_{eff} , calculated from Eqs. (26) and (27), are shown plotted in Figs. 5 to 7. These figures represent plots of λ_{eff} versus T_{bn} for various values of UD_0 , at three levels of pressure, namely 100, 1000 and 2000kPa, and three levels of ambient temperature, namely 500, 1200 and 2000K. They show that, in general, λ_{eff} increases with increase in ambient temperature, pressure, velocity and drop size, and diminishes with increase in normal boiling temperature.

The concept of an effective value of evaporation constant considerably simplifies calculations on the evaporation characteristics of fuel drops. For example, for any given conditions of pressure, temperature, and relative velocity, the lifetime of a fuel drop of any

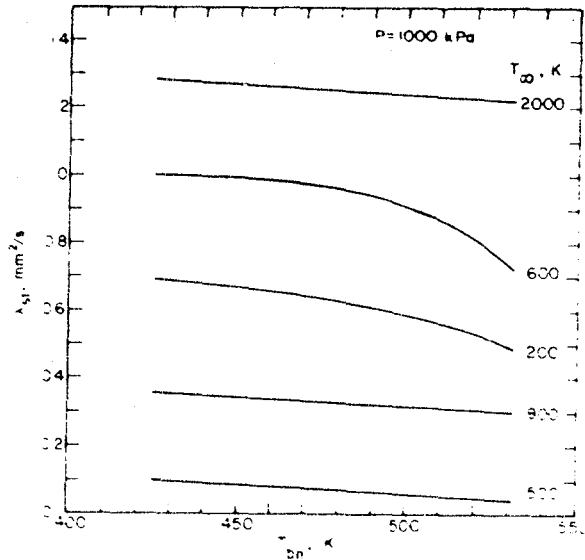


Fig. 3. Influence of ambient temperature and normal boiling temperature on the steady state evaporation constant for a pressure of 1000kPa.

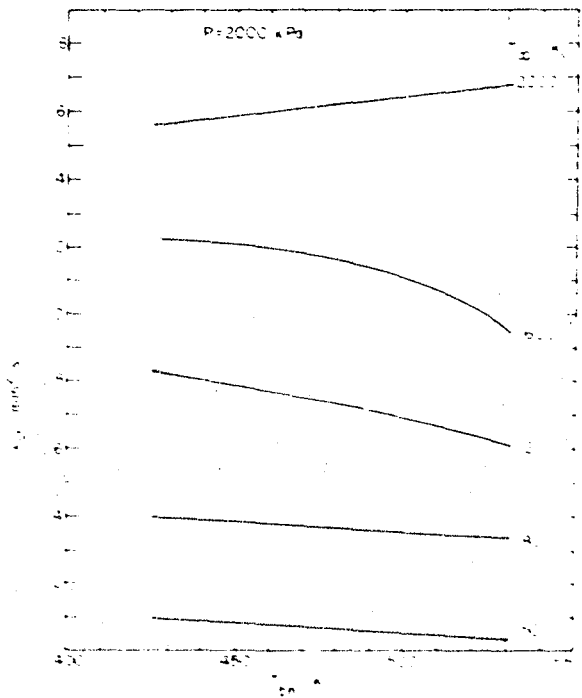


Fig. 4. Influence of ambient temperature and normal boiling temperature on the steady state evaporation constant for a pressure of 2000kPa.

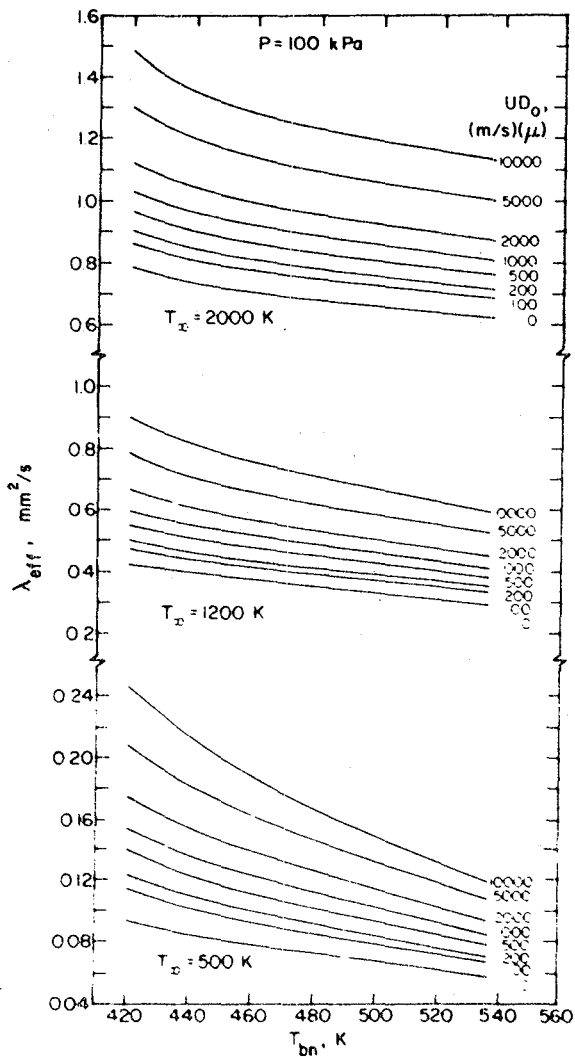


Fig. 5. Variation of effective evaporation constant with normal boiling point at a pressure of 100kPa.

given size is obtained from Eq. (26) as

$$t_e = \frac{D_0^2}{2 \lambda_{eff}} \quad (28)$$

while the average rate of fuel evaporation is determined by dividing \dot{m}_F from Eq. (13) by t_e from Eq. (28) as

$$\bar{m}_F = (-6) \cdot F_{eff} \cdot D_0 \quad (29)$$

CONCLUSIONS

In the spray combustion of liquid hydrocarbon fuels the heat-up period occupies a significant proportion of the total drop lifetime. In consequence the average evaporation

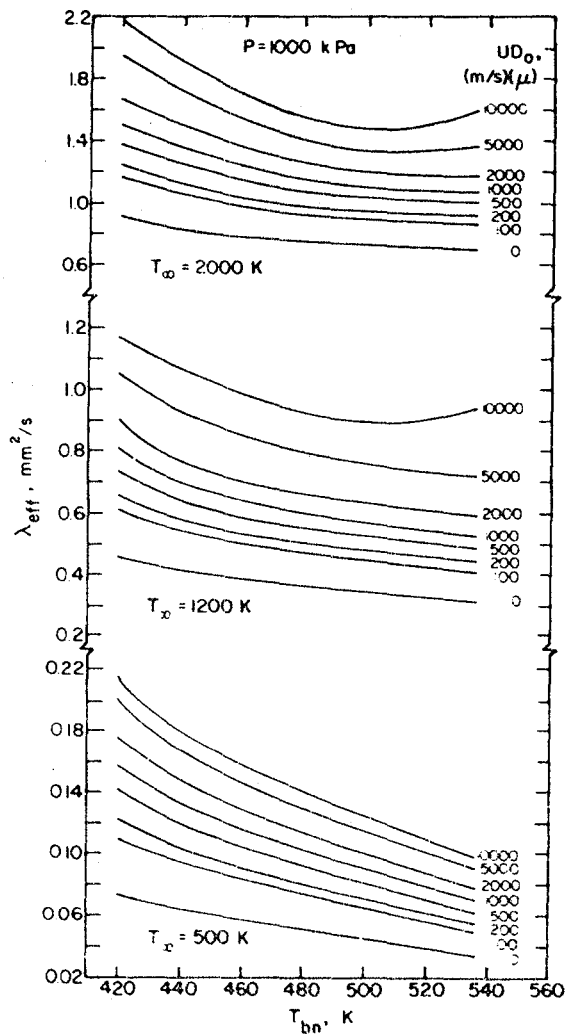


Fig. 6. Variation of effective evaporation constant with normal boiling point at a pressure of 1000kPa.

rate is lower than the steady-state value and the drop lifetime is extended. The effects of the heat-up period and those of forced convection can be accounted for quite conveniently by defining a mean, or effective, value of evaporation constant, λ_{eff} , such that the drop lifetime is obtained as

$$t_e = \frac{D_0^2}{2 \lambda_{eff}}$$

while the average rate of fuel evaporation during the drop lifetime is given by

$$\bar{m}_F = (-6) \cdot F_{eff} \cdot D_0$$

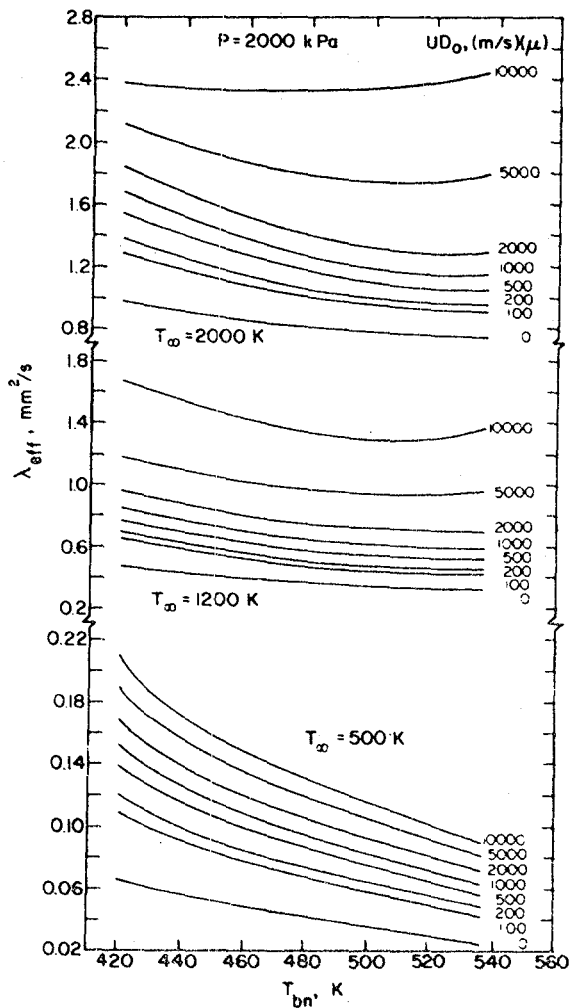


Fig. 7. Variation of effective evaporation constant with normal boiling point at a pressure of 2000kPa.

Calculated values of evaporation constant, corresponding to wide ranges of fuel type, drop size and ambient conditions, show that λ_{eff} increases with increase in pressure, temperature, relative velocity, and drop size, and diminishes with increase in normal boiling temperature.

NOMENCLATURE

a, b	constants in Eq. (9)
B_M	mass diffusion transfer number
B_T	thermal diffusion transfer number
c_p	specific heat at constant pressure, kJ/kg K
D	drop diameter, m

D_0	initial drop diameter, m
D_1	drop diameter at end of heat-up period, m
h	heat transfer coefficient, kJ/m ² s K
D_{hu}	effective mean drop diameter during heat-up period, m
k	thermal conductivity, kJ/ms K
L	latent heat of vaporization, kJ/kg
$L_{T_{bn}}$	latent heat of vaporization at normal boiling temperature, T_{bn} , kJ/kg
$L_{T_{s_{hu}}}$	latent heat of vaporization at temperature, $T_{s_{hu}}$, kJ/kg
M	ratio of molecular weights of fuel and air
m	mass of fuel drop, kg
\dot{m}_F	rate of fuel evaporation, kg/s
Nu	Nusselt number
P	ambient gas pressure, kPa
Pr	Prandtl number
Q	rate of heat transfer to drop from surrounding gas, kJ/s
Q_e	rate of heat utilization in fuel vaporization, kJ/s
Re_D	drop Reynolds number
T	temperature, K
T_{bn}	boiling temperature at normal atmospheric pressure, K
T_{cr}	critical temperature, K
T_s	drop surface temperature, K
T_x	ambient temperature, K
t	time, s
t_e	drop evaporation time, s
t_{hu}	duration of heat-up period, s
t_{st}	duration of steady-state period, s
U	relative velocity between air and fuel drop, m/s
λ_{eff}	evaporation constant, m ² /s
λ_{eff}	effective average value of λ_{eff} during drop lifetime, m ² /s
λ_{hu}	effective average value of λ_{eff} during heat-up period, m ² /s
μ	dynamic viscosity, kg/ms
ρ	density, kg/m ³

Subscripts

A	air
F	fuel
V	vapor
g	gas

- o initial value
- s value at drop surface
- st steady-state value
- hu mean or effective value during heat-up period
- ∞ ambient value

REFERENCES

1. Chin, J. S., and Lefebvre, A. H., "Steady State Evaporation Characteristics of Hydrocarbon Fuel Drops," to be published.
2. Chin, J. S., and Lefebvre, A. H., "The Role of the Heat-up Period in Fuel Drop Evaporation," to be published.
3. Faeth, G. M., "Current Status of Droplet and Liquid Combustion," Prog. Energy Combust. Sci., Vol. 3, 1977, pp. 191-224.
4. Spalding, D. B., "The Combustion of Liquid Fuels," Fourth Symposium (International) on Combustion, Williams and Wilkins Co., Baltimore, 1953, pp. 847-864.
5. Frossling, N., "On the Evaporation of Falling Droplets, Gerlands Beitrage zur Geophysik, Vol. 52, 1938, pp. 170-216.
6. Ranz, W. E., and Marshall, W. R. Jr., "Evaporation from Drops," Part I, Chem. Eng. Prog., Vol. 48, 1952, pp. 141-146; Part II, Vol. 48, 1952, pp. 173-180.

Identification and Evaluation of Optimized Alternative Fuels

Norman R. Sefer, John A. Russell,
Thomas W. Ryan, III, and Timothy J. Callahan
Southwest Research Institute
San Antonio, TX

ABSTRACT

Alternative highway transportation fuels were studied in three project phases. First, refining studies used linear programming models of composite regional refineries. Shale oils and coal liquids were included with petroleum crudes to make forecast 1995 product slates. Product variations included maximum diesel fuel and broadcut fuel in three regions. Methanol, ethanol, and MTBE in gasoline blends were explored in one region. In the second phase, fuels were formulated based on the refining studies, and blends were prepared using synthetic components. Products were shared with other laboratories for their evaluation. The third phase was engine testing of diesel fuels, broadcut fuels, and gasolines. Screening tests in single-cylinder CLR engines were applied to all fuels. Selected fuels were given durability tests in the same engines. Other fuels were tested in city and highway cycles in vehicles on a chassis dynamometer. The project identified potential fuel problems and promising fuel-engine combinations.

ALTERNATIVE FUELS for highway vehicles are being studied systematically in the Alternative Fuels Utilization Program. (1,2)* This report summarizes a three-year project to predict compositions of alternative highway transportation fuels, to produce quantities of fuels for testing, and to perform engine testing of those fuels. The final objectives were to identify problems in using those fuels and to characterize promising fuel/engine combinations for minimum energy consumption. The project was completed recently and most of the information has been reported in interim reports. The major findings are summarized in this report along with new information on a limited study of optimizing diesel engine operation on two fuels.

* Numbers in parentheses designate references at end of paper.

REFINERY MODELING STUDIES

In the first project phase refinery models were developed in cooperation with Bonner & Moore Associates using their Refinery and Petrochemical Modeling System to represent composite refineries. Three regional models were used with forecasts of 1995 crude supply and product demand to generate baseline cases. Representative shale oils and coal liquids were added to the data base along with processing schemes for synthetic crudes.

BASIS OF STUDY - The year 1995 was selected as the basis for forecasts. Shale oil and coal oil production was expected to be substantial by then. Also, fifteen years would give time for assumed changes in engine types to have significant effects on the vehicle population.

Three regions were selected where syncrudes were expected to have major impact (Figure 1):

- Rocky Mountains
- Mid-Continent
- Great Lakes

These regions were defined as areas with similar product quality and production objectives. Also, the refineries are near the source of shale oil production or are served by existing pipelines and barge transportation. The source of coal liquids was not as well defined, but coal is available in all three regions.

Baseline projections were made for each region assuming conventional crudes and products. Syncrudes were added as part of the raw materials to evaluate three alternate product slates:

- Conventional products -- 1995 forecast
- Maximum diesel fuel -- limit set by refinery capability
- Broadcut fuel -- limit related to engine availability

Broadcut fuel production was also evaluated with conventional crudes in each region. Four gasoline components, with potential for use in each region, were selected for evaluation:

- Methanol
- Ethanol
- Methyl tertiary-butyl ether (MTBE)
- Synthetic Naphtha from Methanol

Concentration of 10 volume percent in gasoline blends was used to provide a basis for comparison.

The four gasoline supplements were used only in the Rocky Mountains where synthetic crudes were at highest concentrations.

PRODUCT OPTIONS - Broadcut fuel is a wide-boiling product (100-650°F) without octane or cetane requirements. It requires less processing than gasoline or diesel fuel. It could be used in continuous combustion such as turbine or Stirling engines. It may also be usable in intermittent combustion engines such as stratified charge or spark-assisted diesel.

Product options for maximum diesel fuel and broadcut fuel cases were based on projections and estimation factors as follows:

Maximum Diesel Fuel - Increasing diesel fuel and decreasing gasoline production eventually reaches a limit. Four studies showed some level of diesel fuel production where further increases were uneconomical or impractical. (3-6) Based on those results, a replacement of 30% of the gasoline with diesel fuel was used to define maximum diesel fuel operation. In other words, it was assumed that 30% of the vehicles with gasoline engines on the road in 1995 had been built with diesel engines instead.

Broadcut Fuel - Hypothetical market penetration of engines to use broadcut fuel was assumed. If used in 6% of new vehicles in the 1985 model year and an additional 6% each following year, the new engine would account for 38.5% of vehicle miles traveled in 1995. This was rounded off to 40% of gasoline consumption to be replaced with broadcut fuel. Availability of a fuel distribution system was assumed to develop with the engine.

Replacement Volumes - A further assumption was made that vehicle miles driven would be constant in each region. Therefore, the volume of each fuel replacing gasoline was adjusted for vehicle fuel economy. Diesel-powered vehicles were assumed to average 35% more miles per gallon than equivalent vehicles with gasoline engines; this amount was based on better engine performance and higher energy content of the fuel. A mileage improvement of 24% was used for broadcut-fueled engines with similar assumptions on engine performance and BTU content of the fuel.

These factors were used to adjust the volume of the alternate fuels in the product options cases. The net volume reduction of 7.28% for maximum diesel fuel is very close to the 7.24% for broadcut fuel. This similarity was not planned, but it does allow comparison of results for the two fuel options at the same level of product reduction in the following section.

**PRODUCT VOLUMES TO REPLACE
GASOLINES, PERCENT OF BASE CASE GASOLINE**

	Base	Maximum Diesel	Broadcut
A. Relative Fuel Economy, MPG	1.00	1.35	1.24
B. Percent Gasoline Replacement, %	0	30.00	40.00
C. Replacement Volume, % (B + A)		22.22	32.26
D. Motor Fuel Reduction % (B-C)		7.28	7.24

Product Volumes - Highway transportation fuels were modified for three series of cases in each region. The ratio of gasoline to total distillate shifted from 0.93-1.36 in the base cases to 0.54-0.73 in the maximum diesel cases. All other products were held constant in each region except that LPG production was allowed to vary. Raw materials then were varied to make a given product slate by adjusting the swing crude, butanes, and natural gasolines.

RESULTS OF COMPUTER CASES - Results of the refining studies were reported in the first annual report (7) and in two presentations at DOE Contractor Coordination meetings. (8,9)

Synthetic crudes replaced petroleum on nearly a one-to-one basis. For example, in the Rocky Mountain Region, each barrel of shale oil replaced 0.95 barrel of petroleum. Each barrel of coal oil replaced 1.03 barrels of petroleum. In the Mid-Continent and Great Lakes Regions, shale and coal oils were processed together, although their components were tracked through the refinery separately. The combined effect on petroleum replacement was 0.97 and 1.02 barrels.

Maximum diesel fuel production saved varying amounts of raw materials when replacing 30% of the gasoline with a smaller amount of diesel fuel. These values are compared with the reduction of transportation fuel that occurs as a result of the better fuel economy for diesel fuel, as follows:

VOLUME % OF BASE RAW MATERIALS

Region	Diesel Savings	Product Reduction
I Shale	3.33	2.97
I Coal	2.62	2.97
II Both	3.92	3.63
III Both	2.74	3.07
Average	3.15	3.16

The average raw material savings for four cases was almost identical with the reduction in product volume. The variations above and below this reduction are a result of differences in processing and energy consumption within the refinery.

Broadcut fuel manufacture to replace 40% of the gasoline also resulted in raw materials savings. The savings in the syncrude cases were:

VOLUME % OF BASE RAW MATERIALS

Region	BCF Savings	Product Reduction
I Shale	3.27	2.97
I Coal	3.59	2.97
II Both	4.28	3.61
III Both	3.52	3.06
Average	3.67	3.15

Note that the transportation products were reduced because of improved fuel economy of the broadcut fuel. Broadcut savings were higher than the fuel reduction because of added benefits in processing and energy consumption in the refinery. Similar savings occurred for broadcut fuel made from petroleum.

Gasoline supplements were used at 10% concentration in the Rocky Mountain region. Methanol replaced slightly less than 1 barrel of petroleum per barrel of supplement. Ethanol and MTBE were somewhat more effective and saved over 1 barrel of petroleum per barrel supplement.

Synthetic naphtha from methanol was incorrectly assumed to be used as a gasoline supplement. Later information showed that Mobil MTG was a finished gasoline with well balanced volatility and could be marketed without further blending. The Mobil process is likely to be used in new plants independent of refineries.

Refinery energy consumption was accounted for in the total raw materials used. Investment costs were included in the refinery models for incremental facilities needed in each case. These factors were reported for each case in the first annual report. (7).

FUEL FORMULATION

The second objective of the project was to formulate and prepare blends of various types of fuels for laboratory and engine testing in the succeeding phase of the project. Many of these fuels were based on computer results from the refinery modeling phase discussed in the last section. Other fuels were synthetic fuels or blends provided by programs in fuel conversion research. The blends were prepared to utilize the components which were available to represent possible future products.

Formulation of eight diesel fuels and seven broadcut fuels was described in the second annual report (10) and a presentation at the DOE Contractors Coordination Meeting. (11) Gasolines for testing were described in detail in the project final report (12) and a coordination meeting presentation. (13)

DIESEL FUELS - Four shale-derived products were available. Two of these were Paraho DFM and Paraho JP-5 provided by the U.S. Navy and the Standard Oil Company of Ohio. (14) The Paraho materials were finished products, refined to meet Navy specifications. Two other blends were made with Paraho components and petroleum fractions to represent refinery products where shale oil was only part of the raw materials.

Four coal-derived diesel fuels were prepared using SRC-II middle distillate from the Pittsburg and Midway Coal Mining Company, a Gulf subsidiary. This component was not a finished engine fuel because high aromatics content gave it a low cetane number, and hetero compounds contributed to low stability. Blending with other components in this study allowed it to be used without further treating. Two refinery-type blends were prepared to diesel fuel quality, over 40 cetane number, using 13 and 16 volume percent SRC-II material. Two other blends were made at lower cetane levels using 35 and 50 percent concentrations of coal distillate.

BROADCUT FUELS - Seven broadcut fuels were patterned after blends with a variety of compositions in the computer study. These wide boiling range products were made without octane or cetane specifications, using components in both the gasoline and diesel fuel boiling ranges. Paraho shale oil naphtha was supplied by SOHIO. Coal-derived naphtha was simulated as described in the section on gasoline formulation. Diesel boiling range fractions from shale, coal, and petroleum were used as needed to match properties of the blends. Since there was no standard broadcut fuel for comparison, and testing was done in diesel engines, performance was compared with Phillips D-2 diesel fuel.

GASOLINES - Eight gasolines were tested in the project. Two of these fuels were supplied ready to use. Gulf Research and Development Corporation provided a blend of 5 volume percent methyl aryl ethers (MAE) in unleaded gasoline. The methyl aryl ethers were produced by extraction of phenolic compounds from solvent refined coal liquids followed by reaction to add a methyl group. (15) The mixture of ethers is in the gasoline boiling range and improves gasoline octane. The unleaded gasoline was also supplied for comparison of properties and performance, and was used as baseline fuel for comparison with all gasolines tested.

The second synthetic gasoline was supplied by Mobil Research and Development Corporation. This product was produced by Mobil's MTG (methanol to gasoline) process in a fixed-bed pilot plant at Paulsboro, New Jersey. It contained antioxidant and metal deactivator, but no other additives.

Six other gasolines tested were blends prepared at SwRI. Five of these were modifications of a simulated coal-derived (SCD) blend.

It was noted that naphtha and reformat from coal sources have significantly more bicyclic aromatics and naphthenes than petroleum in the same boiling ranges. Detailed compositions were reported by UOP, Inc., in a study of hydrotreating and reforming of naphthas from the H-coal process. (16) The plan was initiated to simulate those H-coal characteristics by addition of tetralin-naphthalene mixtures derived from coal, and/or pure tetralin and decalin, to petroleum naphtha or reformat. The simulated components were then blended with other petroleum fractions to make a final product for testing.

Five gasolines contained oxygenates in various

concentrations to evaluate their compatibility with an SCD type gasoline. The first blend was a simple addition of 6.9 volume percent methanol to the Gulf unleaded baseline gasoline. This methanol proportion was defined to provide the same oxygen content by weight as a 10 volume percent ethanol blend.

The final four oxygenate blends were made to use the beneficial properties of the alcohol or ether to produce a finished product of controlled octane and volatility. This approach was used in the refinery modeling study and represented probable refinery practice. With the high octane oxygenated compounds available as blend stocks, catalytic reformer operation would be adjusted to lower octane levels for yield and cost savings. The higher RVP contribution of alcohols would be offset by using less butane or other light components in the blends.

To accomplish the same approach for using alcohols and ethers in actual blends, the SCD reformate octane was modified by small increments of low octane SCD naphtha. The SCD naphtha was prepared for use in a broadcut fuel using the same approach as used in simulating coal-derived reformate.

PRODUCTS FOR OTHER RESEARCH PROGRAMS - The third phase in the project plan was making products available to other researchers for evaluation in various programs. The only obligations were to assume shipping charges and to provide results of the evaluations to DOE.

In addition, special blends were prepared for DOE projects at University of Miami and Purdue University.

Samples of various sizes, usually small, were shipped to the following laboratories:

Cummins Engine Company, Inc.
Environmental Protection Agency
(Projects at SwRI)
Ethyl Corporation, Research Department
Mobil Research & Development Corp.
NASA-Lewis Research Center
National Bureau of Standards
Naval Ship Research & Development Center
Pennsylvania State University
Perkins Engines, Inc.
Phillips Petroleum Company
Research & Development Department
Purdue University
Stanadyne Corp.
U.S. Army Fuels and Lubricants
Research Laboratory (SwRI)
United Technology Research Center

References to reports or testing results are given in the project final report. (12)

FUEL EVALUATIONS

The fourth phase of the project was to evaluate the fuel by engine testing. All fuels were subjected to screening tests in single-cylinder CLR engines. The direct injection, compression ignition configuration was used for diesel and broadcut fuels and was changed to carbureted, spark ignition for gasolines. Limited durability tests were run on two selected fuels

in the same engines. Full-size vehicle tests on a chassis dynamometer were made on two diesel and two broadcut fuels using a 1981 Oldsmobile Cutlass; four gasolines were run in a 1981 Volkswagen Rabbit. All tests compared performance and emissions with baseline fuels.

Most of the engine testing results have been presented in several interim reports. These reports will be cited as references, and new information not previously reported will be discussed in this report. A limited fuel/engine optimization study evaluated performance and emissions with a broadcut fuel and the baseline diesel fuel at optimum injection timings. A summary of all test results is given at the end of this section.

SINGLE CYLINDER TESTING - Screening tests in single-cylinder CLR engines were run to determine relative performance and emissions with a minimum amount of fuel. Fuel consumption ranged from 1 to 5 pounds per hour over the range of 1 to 8 brake horsepower. A complete screening of 5 load conditions at 3 different speeds was completed with about 10 to 12 gallons of fuel. Screening tests provided a basis for selection of fuels for other types of testing.

Diesel Fuels - CLR tests were reported for eight synthetic-derived diesel fuels in the second annual report. (10)

Broadcut Fuels - Results of single-cylinder testing of seven broadcut fuels are summarized in the second annual report. (10)

Gasolines - Single cylinder testing of eight gasolines and the base fuel was conducted in the third year of the project and is covered entirely in the final report. (12)

DURABILITY TESTING - The amount of durability testing was limited by the quantity of fuel available. Duration was set at 115 hours for diesel fuel and 100 hours for gasoline which were believed to be minimum times to detect differences in wear or deposits. About 50 gallons of diesel fuel and 70 gallons of gasoline were used in each of the tests described in this section.

Diesel Fuel - The single cylinder CLR diesel engine was used to perform two 115 hour durability tests. The first test was a baseline run using the Phillips D-2 diesel control fuel. The second test was performed using Coal Case 5A diesel fuel. Results are given in the project final report. (12)

Gasoline - Two 100-hour durability tests were performed using the same CLR spark ignition engine as used in the gasoline evaluations. The baseline test was performed using unleaded regular gasoline with properties similar to the MTG product. Mobil MTG was selected for evaluation in the durability test because of its unique synthetic origin. Details were reported in the final project report. (12)

VEHICLE TESTING - Selected fuels were tested in vehicles on a chassis dynamometer by the Emissions Research Department at SwRI. Testing was done in accord with the Federal Test Procedure (FTP) and Highway Fuel Economy Test (HFET). These tests are sometime referred to as city and highway driving

cycles, respectively.

Diesel and Broadcut Fuels - The multi-cylinder testing was done in a 1981 Oldsmobile Cutlass powered by a 350 CID diesel engine and automatic transmission. The engine was rated at 105 SAE net horsepower at 3200 RPM. Vehicle test weight was 3000 pounds. Odometer reading was 3,184 miles at the start of testing. Results in Table 1 in the Appendix are presented from the final report. (12)

Gasolines - A Volkswagen Rabbit with automatic transmission was used for testing gasolines. The 1.7 liter spark ignition engine was rated 74 SAE net horsepower at 3000 RPM. Vehicle test weight was 2500 pounds. Odometer reading was 8,627 miles at the start of testing. The catalyst assembly was removed from the exhaust system of the car and replaced with a section of equal pressure drop so that maximum emissions and differences were measured. The closed loop control system was operative during the dynamometer runs. Results are given in Table 2 in the Appendix; details were presented in the final report. (12)

LIMITED FUEL/ENGINE OPTIMIZATION - The single cylinder screening tests of the diesel and broadcut fuels were made with the intent of holding engine conditions constant, so that differences in results from baseline fuel could be ascribed to differences in the test fuel composition or properties. A few fuels ran poorly in the engine at certain conditions. Poor operation included inability to start the cold engine, knocking which varied with speed, and unstable operation (misfiring) at various speeds.

Since the engine operating conditions, as well as design, are generally based on the baseline fuel, it is not unexpected that any fuel which differed greatly from baseline fuel would perform poorly at some speed-load conditions within the engine operating range. One factor, which is fuel dependent, that could affect engine performance is ignition delay. Adjustment of injection timing could correct for ignition lag and improve performance of marginal fuels. Thus, injection timing optimization could keep a potentially useful fuel from being eliminated prematurely if tested at unsuitable conditions.

Fixed Air-Fuel Ratio - The technique used for this optimization involved defining the injection timing which produced maximum brake torque output of the engine. The test matrix included three speeds (1000, 1500 and 2000 RPM) and three rack settings. The rack settings were chosen so that they would correspond to air fuel ratios of 20, 30 and 40:1. Engine power output was recorded as injection timing was adjusted at each specific speed-rack setting. The optimum injection timing occurred when maximum power output was obtained.

One baseline fuel (Phillips DF-2) and one broadcut fuel (BCF-6), having properties and performance significantly different from each other, were chosen for optimization by the method indicated. The optimum injection timings were found for each fuel at each speed-rack setting. Typical optimization curves, shown in Figure 2, are plots of load versus injection timing for the broadcut and baseline fuels at 1500 RPM and an air-fuel ratio of 20:1. The optimum

timings for this speed-rack condition are 16 and 18° BTDC for Broadcut Fuel 6 and Phillips D-2, respectively.

In general the optimum timings for the broadcut fuel were retarded from that of the baseline fuel except the high speed condition (2000 RPM) where the optimum timings for the baseline and broadcut fuel coincided. For cases where the optimization curve was relatively flat, optimum timing was chosen as the most retarded injection timing which gave maximum brake torque.

A portion of the higher load generated by the broadcut fuel is due to a higher heat of combustion of the broadcut (19083 BTU/lb) as compared to the baseline fuel (18078 BTU/lb). In Figure 2, approximately half of the 11 percent increase in load is accounted for by a 5.5 percent increase in energy content.

In order to segregate the fuel effects on engine performance from the effects of the engine optimization, additional testing was conducted with each fuel at the optimum injection timing of its counterpart fuel. This essentially produced four sets of data.

1. Diesel fuel at its optimum injection timing
2. Broadcut fuel 6 at its optimum injection timing
3. Broadcut fuel 6 at the optimum injection timings for diesel fuel.
4. Diesel fuel at the optimum injection timings for broadcut fuel 6.

A comparison of the optimized performance of each fuel with the unoptimized performance reported in the second annual report (10) is shown in Figure 3, a plot of BSEC vs BHP at 1500 RPM. For both fuels, it is apparent that injection timing optimization improved performance. This plot also shows that while the broadcut fuel performs worse than the baseline fuel with standard timings, the performance of the broadcut fuel is significantly better than the baseline with timing optimization.

The effects of optimized injection timing are shown in Figure 4 at 1500 RPM. At each speed the lowest BSEC's are obtained with the broadcut fuel at its optimum timings. In addition the BSEC's obtained by the broadcut fuel at the optimum timings for the diesel fuel are significantly lower than those obtained by the diesel fuel.

Based on the results obtained, injection timing optimization appears to significantly enhance the performance of potential fuels which would otherwise be eliminated due to poor performance in standard engine tests. It is clear however, that optimization based solely on maximum brake torque is not sufficient to define the optimum timing due to knock limitations. The optimum timing could lie in a region in which the knock has a detrimental effect. Therefore optimization based on maximum power should be coupled with a quantitative estimate of knock. This estimate could simply be a measurement of the amplitude of pressure oscillation after ignition. Thus the method would allow maximizing power output while remaining outside the region of detrimental knock.

Other methods of optimization involve maintaining fixed power output or fixed energy input instead of fixed air-fuel ratio. The fixed power optimization method would involve maintaining a given load while adjusting the injection timing to obtain a minimum energy consumption. While all methods require precise measurement of fuel flow, this method would require relatively long measurement intervals so that the standard error of measurement would be a relatively small portion of the total fuel flow.

The fixed energy method involves adjusting the timing to obtain maximum power while energy input to the engine is held constant. This method requires that the energy content of the fuel be known accurately. One advantage of this method is that it accounts for differences in energy content. Thus any increase or decrease in maximum power would essentially be proportional to an increase or decrease in efficiency.

Fixed Power Output - In order to illustrate the other methods of optimization, the 1500 RPM and 20:1 AFR test point was selected as a basis for further timing optimization runs. The fixed power output scheme was run first. Figure 5 is a graph of BSEC versus timing for the baseline and broadcast fuels, respectively. These data were obtained by varying the timing while adjusting the fuel flow to maintain constant loads of 21.2 ft-lb for the base fuel and 25.7 ft-lb for the broadcast fuel. The optimum timing occurred at the minimum fuel flow, hence minimum BSEC. As indicated by the figure, the optimum timings were 20° BTDC and 22° BTDC for Broadcast fuel 6 and Phillips D-2, respectively. These timings were advanced from those obtained by maximizing power output which were 16° and 18° BTDC for the Broadcast fuel and Phillips D-2, respectively. At the optimum timings, the energy consumption of the broadcast fuel was 16 percent less than the base fuel.

It should be noted that the load set points for the constant power optimization were lower than the loads obtained at the corresponding test point (1500 RPM, 20:1 AFR) and optimum timings (16° BCF, 18° Base) for the fixed air fuel ratio optimization. For the broadcast fuel, the 25.7 ft-lb set point was 6.2 percent lower, while the set point for the base fuel, 21.2 ft-lb, was 10.9 percent lower. One possible explanation attributes a decrease in load for the base fuel to increased clearance between injection plunger and barrel due to wear. Therefore, in order to maintain the same fuel flow rate, the length of the injection event was increased, thus compromising the combustion process and decreasing efficiency. It was suspected that the marginal lubricity of the heavy naphtha comprising 50 percent of the broadcast was responsible for the injection pump wear. The hypothesis was that the plunger expanded due to excess heat generated by an increase in friction. This was evidenced by freezing of the rack position during operation with the broadcast fuel. It appears that the increase in friction in the injection pump raised the friction horsepower requirement of the engine thus reducing the brake horsepower.

This is only a hypothesis. In order to obtain a definitive explanation, it would have been necessary to

make indicated horsepower measurements. Thus any change in friction horsepower could be calculated by the difference of the brake and indicated measurements. A change in the combustion process could also be detected by a change in the apparent heat release.

Fixed Energy Input - The fixed energy input scheme involved matching the energy input of the broadcast to that of the base fuel, thus accounting for differing heats of combustion. The test conditions was 1500 RPM and the load obtained at the 20:1 AFR. The injection timing was then adjusted to find maximum power output. Figure 6 shows the load versus timing curve for the broadcast fuel when the energy input was matched to that of the base fuel during the fixed air-fuel ratio optimization. As indicated by the figure, the optimum timing for the broadcast was 16° BTDC; the same optimum timing obtained by the constant air-fuel ratio method. Under the same test conditions, the optimum timing was 18° BTDC for the base fuel.

Although the curves fall close together it should be noted that at the time when the broadcast fuel test points were run, it is hypothesized that an increase in friction horsepower decreased the brake measurements by 6.2 percent, while the base fuel data were collected before any appreciable wear in the injection pump. Allowing for this difference, the broadcast fuel produced a 6.2 percent increase in power output. As with the fixed air-fuel ratio method, both the fixed energy input method and the fixed load methods of optimization produced results which were affected by the degree of engine knock occurring during the test.

ENGINE TESTING RESULTS

The following comments summarize all of the major results of engine testing which have been presented in previous reports. (10, 11, 12, 13).

Diesel fuels derived from Paraho shale oil were well refined products. Their performance and emissions were similar to the base fuel and the minor differences were explained by differences in boiling range or other properties. Two blends with petroleum fractions indicated that the straight materials were compatible in blends.

The SRC-II coal-distillate was a product from the coal liquefaction process and not further refined. It was unstable and had a strong odor. Two blends were made at low SRC-II concentrations to represent products from Rocky Mountain Case 5A and Case 12. Both fuels ran well in the CLR diesel engine with energy consumption close to the base fuel. Particulate emissions were high for both fuels, and hydrocarbon emissions were high for Case 5A. These effects may have been related to high 90 percent distillation temperature and viscosity as well as the presence of SRC-II.

Coal Case 5A was also tested in a 115-hour durability run. Deposits found in the combustion chamber were believed to have caused a piston ring to stick. This in turn caused higher wear rates. Carbon residue of the lubricating oil also increased faster than with the base fuel.

The same Coal Case 5A diesel fuel exhibited much better performance in the Oldsmobile vehicle tests. Fuel economy and particulates were practically identical with the base fuel. Only nitrogen oxides emissions were high which may be related to hydrocarbon types or organic nitrogen in the fuel.

Higher concentrations of SRC-II were used in Medium Cetane (31.4 CN) and Low Cetane (25.4 CN) blends. Further problems were identified in the CLR engine with these two lower cetane number fuels. The Medium Cetane blend caused knock at all speeds and unstable operation at some speed and load conditions. The Low Cetane blend caused severe knock, unstable operation, and would not allow cold starting. Particulates and nitrogen oxides emissions were high for both fuels.

The Medium Cetane diesel fuel ran surprisingly well in the Oldsmobile vehicle, with no increase in knocking. Fuel economy was down slightly in the city cycle. Particulates were less than the base fuel, but all gaseous emissions were higher.

Coal-derived diesel fuels were evaluated in blends over a range of properties, and problems were identified above for certain blends. The results and fuel properties can provide a basis for estimating the minimum degree of treatment of SRC-II distillate for acceptable performance.

Broadcut fuels were tested in the same diesel engines and ran reasonably well without engine modifications. In the CLR engine, fuel consumption was generally more than the base fuel and was higher with more naphtha in the blends. Hydrocarbon emissions followed a similar pattern. Particulate emissions were high for blends with high 90% distillation temperatures. Knocking was moderate to severe with all fuels. The two lowest cetane fuels would not provide stable operation at all speeds or cold start ability.

The Oldsmobile diesel was more fuel tolerant than the CLR for knocking tendency with two fuels, BCF-2 and BCF-4. Fuel economy in MPG was lower than the base fuel and emissions of hydrocarbons and carbon monoxide were higher. BCF-4 with higher naphtha content exhibited the lowest combustion efficiency. The only modification required was a booster pump to provide positive suction for the engine fuel pump.

A series of tests was run to optimize injection timing for one broadcut fuel (BCF-6) and the baseline fuel. Injection timing was adjusted in 2° increments to find the point of maximum power output. The tests showed that fuel consumption (in BSEC) was improved for both fuels by timing optimization. The broadcut fuel performance improved more than the base fuel, and changed its ranking from "worse than" to "better than" the base fuel. Emissions at optimum timing for the broadcut fuel were higher NO_x, lower CO, and only slightly higher hydrocarbons. The main impact of the test results was that timing or other optimization can substantially improve the relative performance of a test fuel.

The results of these limited optimization experiments point out the need for standard test methods for alternative fuels. The procedures should

be developed to give each fuel a fair test, and should not be based on an engine optimized for petroleum fuels. Two advantages would accrue from such procedures. First, test results from various laboratories would tend to standardize and be more comparable. Second, data needed for future engine design would be provided.

Gasolines tested in the CLR spark ignition engine showed only minor variations in performance and emissions from the base fuel or among the eight test fuels. The fuels were made to unleaded regular gasoline specifications and had similar properties, but with differences in composition, both hydrocarbon types and oxygenated compounds. Therefore, any differences were primarily composition effects. This effect showed with the measurable increase in average energy consumption (BSEC) for SCD gasoline. Use of ethanol in the modified SCD blend improved energy consumption; and methanol made a somewhat larger improvement. MTBE in a modified SCD blend did not change energy consumption.

Although test results were similar for all gasolines, the SCD gasoline with 6.9 percent methanol appeared to have slightly lower emissions and higher thermal efficiency than the other fuels, and in particular than the similar SCD blend with 10 percent methanol. Additional work may be worthwhile to verify the results and to find reasons for the deleterious effects of the additional 3.1 percent methanol.

Mobil MTG gasoline showed good performance in all three types of engine testing. In the single cylinder CLR engine, the MTG emissions were lower than the baseline gasoline. The CLR durability runs resulted in less wear during the MTG test which was consistent with less lubricating oil wear metals, viscosity reduction, and fuel dilution. In the multi-cylinder tests in a Volkswagen Rabbit, the MTG produced 3.6 to 5.5 percent better MPG and slightly lower emissions.

The SCD gasoline gave 4.6 and 6.4 percent better MPG than base fuel in the Volkswagen Rabbit. The SCD blends with 10 percent methanol and 10 percent MTBE had slightly lower fuel economy than base fuel on an MPG basis, but were about equal in miles per MM BTU. The methanol blend produced higher CO and HC emissions, but lower NO_x. The MTBE blend emitted more CO than baseline. Emissions from all gasolines would be controlled to 1982 EPA standards by use of catalyst.

CONCLUSIONS

This report has covered the project in condensed form except for the more detailed description of recent work on optimized fuel injection timing. The following conclusions and recommendations apply to the overall project, essentially as presented in the project final report. (12).

REFINING STUDIES - The linear programming models explored maximum diesel fuel, broadcut fuel and oxygenate gasoline blend cases in the Rocky Mountain, Mid-Continent, and Great Lakes regions. The main conclusions were:

- o Product compositions in the several cases provided patterns for blending transportation fuels in the experimental phase of the project.
- o The amount of raw materials saved or replaced in each case was a measure of economic benefit, since purchase of raw materials is the largest refinery operating cost.
- o Maximum diesel fuel saved an average 3.2 percent of raw materials, the same amount as the reduction in product demand as a result of better fuel economy for diesel engines.
- o Broadcut fuels cases saved an average 3.7 percent of raw materials, slightly more than the 3.2 percent reduction in product demand because of better engine fuel economy.
- o Refinery energy savings were greater for broadcut fuel than for maximum diesel production.
- o Broadcut fuel production could be increased but diesel fuel was at its limit.
- o Early development of engines to use broadcut fuel (or any fuel requiring less processing) would avoid building facilities to make conventional fuels (such as more unleaded gasoline).
- o Oxygenated compounds in gasoline saved raw materials in amounts proportion to the volume of gasoline supplements used, as follows:

Methanol	0.83 to 0.96
Ethanol	1.01 to 1.21
MTBE	1.16 to 1.19
- o Diesel fuels of somewhat lower quality can be utilized with penalties in emissions. Potential savings in refining were not evaluated.
- o Paraho shale-derived distillates which were adequately refined performed well in diesel engines. Results with straight DFM and JP-5 and with blends showed only minor differences from petroleum.
- o SRC-II coal-derived distillate at less than 20 volume percent in blends performed well in single-cylinder and vehicle tests.
- o Broadcut fuels blends were evaluated in diesel engines with variable results depending on properties and composition. Results were better in a vehicle than in single-cylinder tests. Fuel consumption and HC emissions generally were higher than diesel fuel, and overall performance was better for blends with more than 32 cetane number. (See the later comment on single-cylinder engine optimization).
- o Gasolines of varying composition showed little variation in the single-cylinder engine tests because of similarity in properties.

Problems - Various problems in use of the fuels were identified as follows:

- o SRC-II distillate at 16 percent of the blend was tested in a CLR engine durability run. Deposits in the combustion chamber caused a piston ring to stick. Lubricating oil degradation and higher wear were observed.
- o Blends with 35 and 50 percent SRC-II operated poorly in the CLR engine with high particulates emissions. The 35 percent blend ran well in a multi-cylinder vehicle engine, but showed high gaseous emissions.
- o Broadcut fuel consumption and hydrocarbon emissions were generally higher with both CLR and vehicle engines. The effects were greater in fuels with lower cetane number and higher naphtha content.

Potential - Promising fuel-engine combinations that were found in the engine phase included:

- o Broadcut fuels could be used in diesel engines with minor fuel system modification and an increase in HC and CO emissions. Refining savings are equivalent to those obtainable by making additional diesel fuel, and potential production levels are higher.

The original forecasts and modeling premises were reviewed and found to be valid, with one exception. The 1.4 percent annual growth rate in product demand projected in 1979 might be replaced by about 0.5 percent annual decline in 1982. Therefore, the original conclusions about investment costs for new facilities would change and have been omitted in this discussion.

ENGINE TESTING - Results from engine testing provide a basis for numerous conclusions in three categories.

General Conclusions - Findings with broad applications in the first group are as follows:

- o Diesel fuels of normal specification quality continued to show good fuel economy and reasonable emissions. Savings in refining raw materials and energy use are available up to some limiting diesel production.

- o Broadcut fuel performance can be improved by higher cetane number, lower naphtha content, and perhaps other property changes. Effect on product economics is unknown.
- o The limited optimization study with one broadcut fuel in the CLR engine showed marked improvement in performance and emissions. This approach made the fuel more usable and offers encouragement for further development.
- o The fixed energy input method appears to be most advantageous for optimizing injection timing. It accounts for heating value differences and allows more direct comparison of the fuels than fixed air-fuel ratio and fuel flow. It also allows shorter tests than fixed power output with measurement of small variations in fuel flow.
- o Gulf gasoline with methyl aryl ethers performed well in limited testing. More extensive testing had already been done by Gulf (15) and others.
- o Mobil MTG gasoline compared favorably with baseline fuel in all three types of engine tests in this study.
- o Three oxygenated compounds were apparently compatible with simulated coal-derived gasoline and caused no adverse effects.
- o Simulated coal-derived gasoline with 6.9 percent methanol appeared to have advantages in engine performance and emissions.

RECOMMENDATIONS

The results and conclusions presented led to the following recommendations:

1. Coal-derived distillate or synthetic crude evaluation should be based on an adequately treated diesel fraction. The processing would probably be hydrogenation at two or more levels of severity. Data for evaluation of manufacturing and enough fuel for engine and vehicle testing should be provided.
2. Broadcut fuel quality variation should be explored to develop specifications more suited to needs of actual engines and fuel

systems. This step would be related to the following three proposals.

3. Broadcut fuels optimization studies in diesel engines could explore performance and emissions under test conditions best suited to the fuel. Systematic variation of fuel properties would permit generalized conclusions. Minor engine modifications could also be considered.
4. Other types of engines should be used to explore use of broadcut fuel from petroleum or synthetic sources to establish desired quality parameters. Candidate engines could include Stirling, turbine, stratified charge, spark-assisted diesel, or diesel engines with other combustion chamber designs.
5. With modified specifications from recommendations 2 through 4 above, refinery models could be used to evaluate the effect of the new quality levels.
6. Shale-derived and coal-derived gasoline components should be obtained or prepared to make blends for engine and vehicle testing. The most likely components would be reformate and catalytically cracked gasoline.
7. A standard test procedure should be developed for evaluating alternative fuels. The procedure would define methods to optimize spark advance for SI engines or injection timing for CI engines for the include severity of engine knock, heat release rate, indicated power, and possibly wear of engine and components.

ACKNOWLEDGMENTS

The project work was done on DOE Contract No. DE-AC01-79CS-50017 under the direction of Dr. Ralph D. Fleming, DOE, Project Manager, and Mr. George M. Prok, NASA-Lewis, Technical Manager. Joe C. Dickson and Franklin P. Frederick of Bonner & Moore Associates were instrumental in the planning and execution of the refinery modeling studies. Robert A. Rightmire and Warren T. Wotring of SCHIO participated in the early planning and supplied blend stocks. The authors appreciate the contribution by many other SwRI staff members, in particular the technical personnel who performed the laboratory and engine testing. Analytical work was done in the Army Fuels and Lubricants Research Laboratory with the concurrence of MERADCOM.

REFERENCES

1. "Program Planning Document, Highway Vehicle Alternative Fuels Utilization Program (AFUP)," U.S. Department of Energy Report No. DOE/CS-0029, April 1978.
2. "Project Planning Document, Highway Vehicle Alternative Fuels Utilization Program (AFUP)," U.S. Department of Energy Report No. DOE/CS-0093, July 1979.
3. F.P. Frederick, J.F. Moore, J.S. Bonner, J.C. Dickson, and L.P. Karvelas, "The Impact of Automotive Fuel Changes on the U.S. Refining Industry," Bonner & Moore Associates, Inc., FE-2216-1, Energy Research and Development Administration, ERDA 76-40, February 1976.
4. T.O. Wagner, "Economics of Manufacturing Automotive Diesel Fuel," Amoco Oil Co., SAE Paper 770758, October 1977.
5. D.K. Lawrence, D.A. Plautz, B.D. Keller, and T.O. Wagner, "Automotive Fuels-Refinery Energy and Economics," Amoco Oil Co. SAE Paper 800225, February 1980.
6. F.H. Kant, A.R. Cunningham, and M.H. Farrier, "Effects of Changing the Proportions of Automotive Distillate and Gasoline Produced by Petroleum Refining," Exxon Research and Engineering Co., PB-236 900, Environmental Protection Agency, EPA-460/3-47-018, July 1974.
7. N.R. Sefer, and J.A. Russell, "Regional Refining Models for Alternative Fuels Using Shale and Coal Synthetic Crudes," Report No. DOE/CS-50017-1, November 1980, (First Annual Report).
8. N.R. Sefer, "Identification and Evaluation of Optimized Alternative Fuels," Status Report and Project Outline for Automotive Technology Development Contractors Coordination Meeting (ATD CCM), October 23-25, 1979.
9. N.R. Sefer, "Alternative Highway Fuels from Shale and Coal Syncrudes," Status Report for ATD CCM, November 11-14, 1980.
10. N.R. Sefer, and J.A. Russell, "Formulation and Evaluation of Highway Transportation Fuels From Shale and Coal Oils," Report No. DOE/CS-50017-2, December 1981, (Second Annual Report).
11. N.R. Sefer, "Formulation and Evaluation of Fuels from Shale and Coal Oils," Status Report for ATD CCM, October 26-29, 1981.
12. N.R. Sefer, J.A. Russell, T.W. Ryan, III, and T.J. Callahan, "Refining Studies and Engine Testing of Alternative Highway Transportation Fuels," Report No. DOE/CS/50017-3, September 1982. (Final Project Report).
13. N.R. Sefer, "Engine and Vehicle Testing of Alternative Gasolines," Status Report for ATD CCM, April 14, 1982.
14. E.T. Robinson, "Refining of Paraho Shale Oil Into Military Specification Fuels," Twelfth Oil Shale Symposium, Colorado School of Mines, April 1979.
15. G.M. Singerman, "Methyl Aryl Ethers From Coal Liquids as Gasoline Extenders and Octane Improvers," SAE Paper 810443, SAE Special Publication SP-480, Alternate Fuels, February 1981.
16. G. Tan, and A.J. deRosset, "Hydrotreating and Reforming H-Coal Process Derived Naphthas," UOP, Inc., DOE Report No. FE-2566-12, March 1978.
17. "Identification of Emissions From Gasolines Derived From Coal and Oil Shale," EPA Contract No. 68-03-2377 (in progress at SwRI). Project Officer: Robert J. Garbe, EPA, Ann Arbor, Michigan. Project Leader: Lawrence R. Smith, SwRI, San Antonio, Texas.

APPENDIX

Table 1. Summary of Emissions and Fuel Economy Tests in a 1981 Oldsmobile Cutlass with a Diesel Engine

Fuel	Federal Test Procedure (FTP)					Highway Fuel Economy Test (HFET)				
	Emission, gm/mile				Fuel Econ.	Emission, gm/mile				Fuel Econ.
	HC	CO	NOx	Part.	MPG	HC	CO	NOx	Part.	MPG
Baseline D-2	0.26	1.14	1.05	0.383	22.44	0.15	0.71	0.60	0.216	33.65
BCF-2	0.58	2.17	1.00	0.220	18.55	0.34	1.24	0.55	0.121	28.34
BCF-4	0.53	1.80	0.85	0.389	20.94	0.27	1.01	0.50	0.177	30.27
Coal Case 5A	0.18	1.06	1.27	0.389	22.38	0.10	0.64	0.72	0.204	33.22
SRC-II Med. Cetane	0.37	1.37	1.61	0.359	21.66	0.19	0.84	0.95	0.195	33.22
1981 Fed. Standards	0.41	3.4	1.0	0.60	-	-	-	-	-	-

Table 2. Summary of Emissions and Fuel Economy Tests in a 1981 VW Rabbit with SI Engine and Without a Catalyst

Fuel	Federal Test Procedure (FTP)				Highway Fuel Economy Test (HFET)			
	Emission, gm/mile			Fuel Economy	Emission, gm/mile			Fuel Economy
	HC	CO	NOx	MPG	HC	CO	NOx	MPG
Baseline	1.16	8.56	4.92	24.45	0.92	8.03	5.44	31.28
Mobil MTG	1.09	8.24	4.39	25.32	0.84	7.72	4.75	32.99
Sim. Coal Derived SCD +	1.13	8.37	4.78	25.57	0.85	8.24	5.26	33.27
10% Methanol	1.21	9.91	4.52	23.33	1.00	12.66	5.21	29.81
SCD + 10% MTBE	1.16	9.16	4.83	23.64	0.92	8.59	5.21	31.15
1982 Fed. Standards	0.41	3.4	1.0	-	-	-	-	-

NOTE: Results in Tables 1 and 2 are averages of duplicate tests on each fuel.

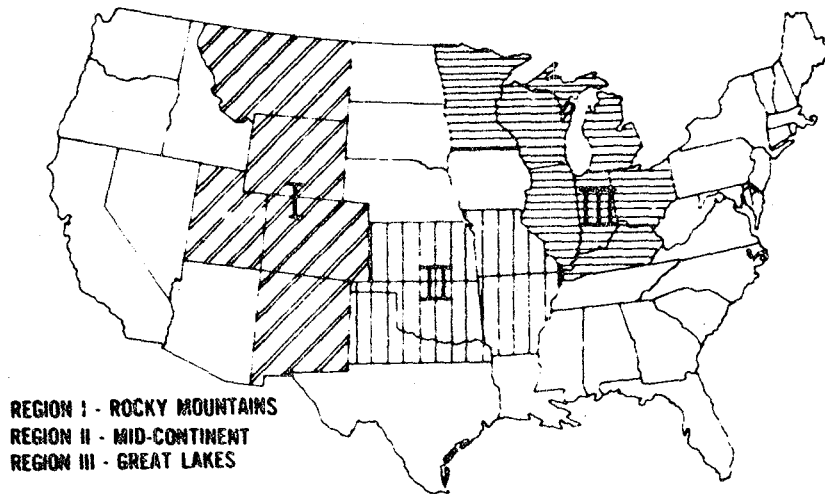


Figure 1. Regions for Composite Refinery Models

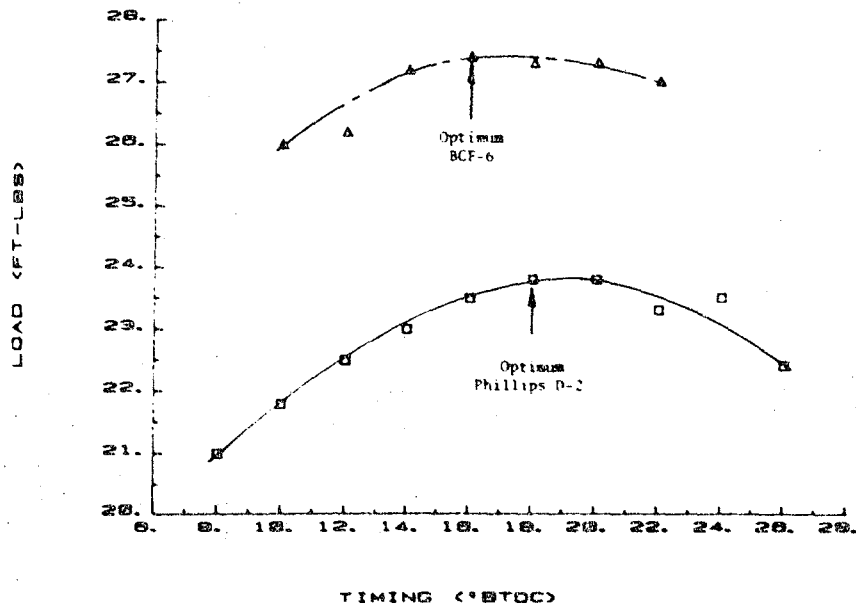


Figure 2. Load vs. Injection Timing for 1500 RPM and 20:1 Air-Fuel Ratio

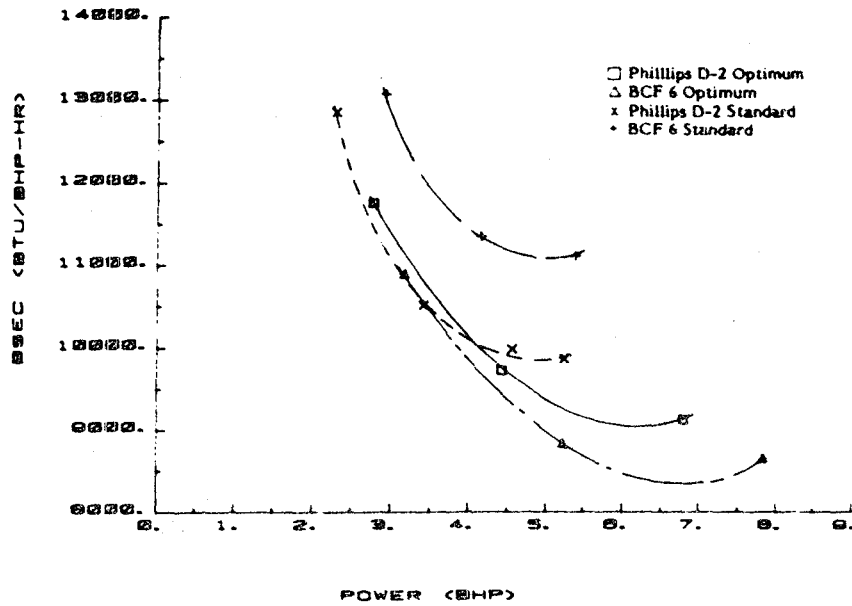


Figure 3. BSEC vs. Power at 1500 RPM, Optimum and Standard Injection Timings for Phillips D-2 and BCF-6

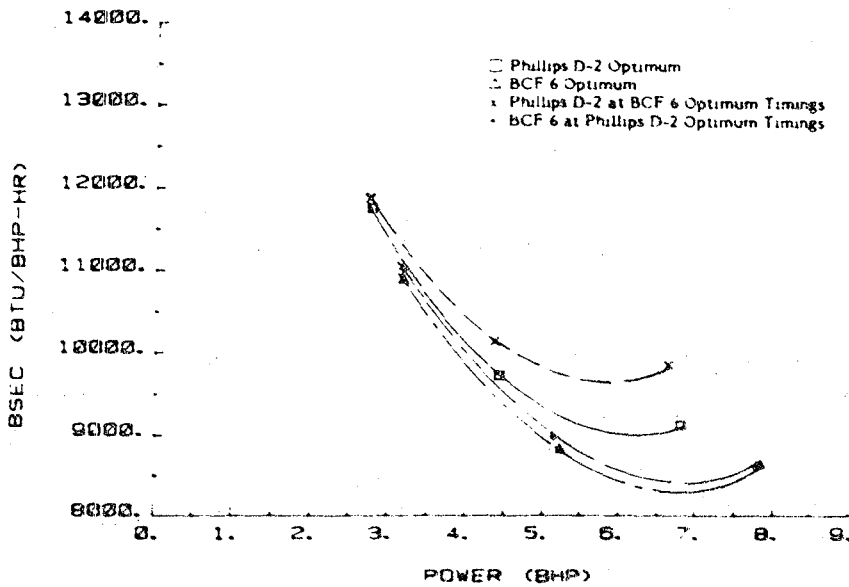


Figure 4. BSEC vs. Power at 1500 RPM for Phillips D-2 and BCF-6 at Optimum Injection Timings of Both Fuels

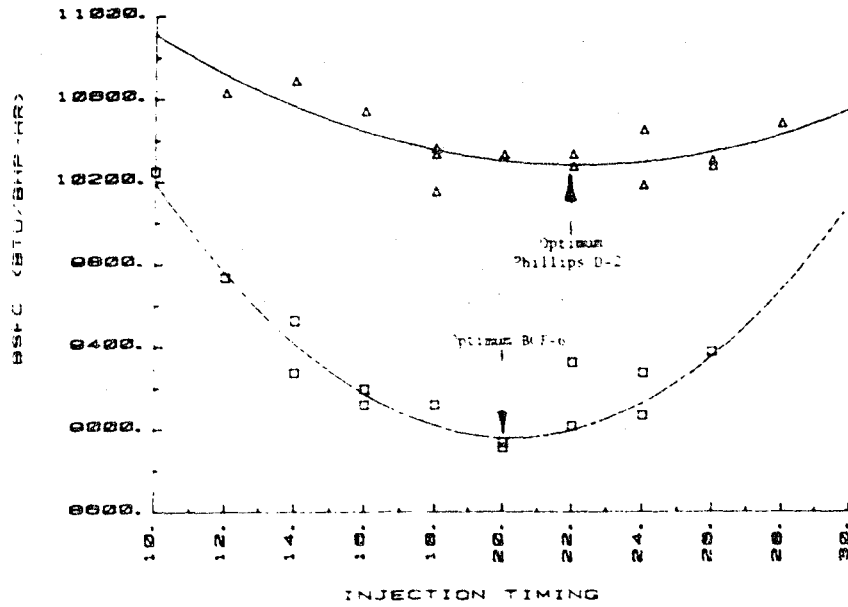


Figure 5. BSEC vs. Injection Timing at Fixed Load (1500 RPM)

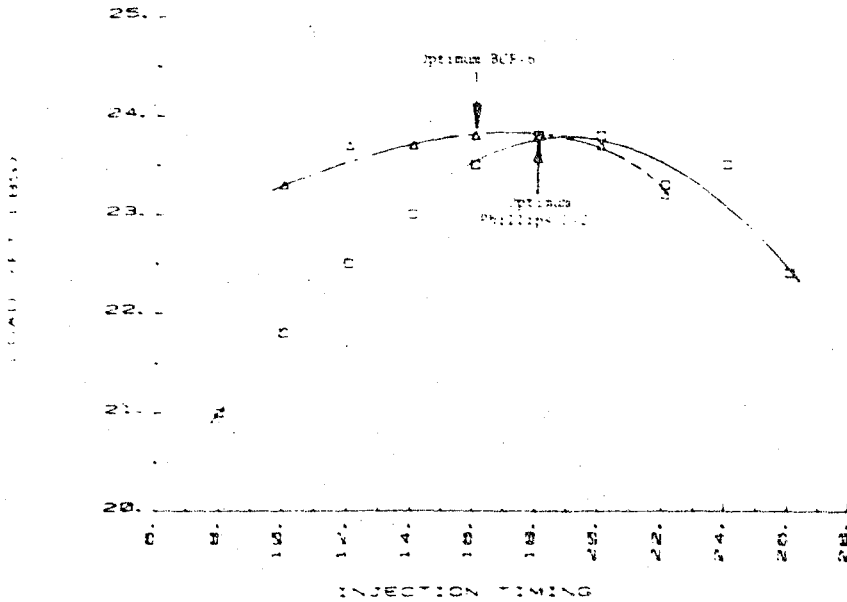


Figure 6. Load vs. Injection Timing at Fixed Energy Input (1500 RPM)

ALTERNATIVE FUELS II SESSION

Summary: Report of Hydrogen SI Engine Research

Robert R. Adt, Jr. and Michael R. Swain
Univ. of Miami

John M. Pappas
Hawthorne Research and Testing Inc.

ABSTRACT

The objective of the project reflected in this paper is to document an experimental design data-base on hydrogen-fueled automotive engines. The effort, sponsored by the U.S. Department of Energy, is directed toward possible future designs of airbreathing piston engines using hydrogen. To this end, pertinent performance and emissions (NO_x only) characteristics of 19 engine configurations are presented.

Configurational variations of a 1600 cc automotive test engine included: throttled and unthrottled operation (i.e., quantity and quality power level control); central manifold, port, direct cylinder injection; single and divided combustion chambers; exhaust gas recirculation (EGR), water induction and air injection; and certain other features.

Comparisons of these hydrogen-engine characteristics with the stock gasoline-fueled reference case are made at the same displacements, and at a (stock) compression ratio of 9.0:1.

PROSPECTS AND PROBLEMS of hydrogen-fueled internal combustion engines have been reviewed in the past few years (1,2)*. As a consequence of interest and activities in hydrogen as a candidate alternative fuel beginning about 1970, the absence of a comprehensive engine design data-base became apparent. The 4-year project reflected in the present summary paper was established in 1976 to provide an initial contribution to such a data-base in order to provide technical

guidance in possible future engine design involving hydrogen fuel.

The project was carried out by the University of Miami's Department of Mechanical Engineering under Contract E(04-3)-1212 with the U.S. Department of Energy (DOE). Hawthorne Research & Testing, Inc., conducted the experimental activities in the University's facilities under subcontract. Escher: Foster Technology Associates, Inc. (E:F) technically monitored the project and assisted the project via supporting liaison (also under DOE contract).

Comprehensive documentation for the project is available in its annual and final reports (3-5). The basic objective was to determine engine performance and emissions characteristics, as well as to explore, and where feasible to investigate, the unique problems associated with hydrogen-fueled engines. These were known to be, speaking generally: low specific power and induction manifold backfiring (naturally aspirated), rough or abnormal combustion and high oxides of nitrogen (NO_x) emissions at high loads, and complex interfacing with the fuel containment system (particularly metal hydrides).

On the other hand, the project was to explore and to capitalize on the unique features of hydrogen operation, e.g., very wide fuel/air operating range including the "ultralean" range, lack of hydrocarbon (HC) and carbon monoxide (CO) emissions and ability to operate at high compression ratios.**

*Numbers in parentheses designate References at end of paper.

**Not reported herein; a fixed compression ratio of 9.0:1 was used.

Although the thrust of the project was directed toward the automotive powerplant field now served by gasoline and light-duty diesel engines, the results are also applicable to both smaller and higher-power engine designs.

PROJECT TECHNICAL APPROACH

BASIC CLASSES OF ENGINES CONSIDERED - Two basic classes of hydrogen-fueled piston engines are

manifold or in the vicinity of the intake valve. The injection can be continuous or timed, the latter being used exclusively in this project. With the Pre-IVC engines, sparkplug ignition is used. In addition to using the conventional throttle to control charge density, Pre-IVC engines can be operated with the load being controlled by changing the fuel/air ratio. This method of operation, termed the unthrottled or quality-controlled mode of operation, is made possible by the

Engine Config. No.	Type of Combustion Chamber				Mixture Formation Method				Airflow Control		Additional Mixture Components		
	Open (Single)	Divided (Prechamber No. 1)	Divided (Prechamber No. 2)	Divided (Prechamber No. 3)	Single Mixer 4-Cyl	Single Mixer 1-Cyl	Timed Port Induction 4-Cyl	Direct Cylinder Injection	Throttled	Unthrottled	EGR (15%)	Water Injection	Air Injection
1	•				•								
2	•				•								
3	•				•								
4	•				•								
5	•				•								
6	•				•								
7	•				•								
8	•				•								
9	•				•								
10	•				•								
11	•				•								
12	•				•								
13	•	•			•								
14	•		•		•								
15	•			•	•								
16	•				•								
17	•				•								
18	•				•				•*				
19	•				•				•*				

• Early compression stroke injection •• Near top-center injection

considered: (1) engines in which hydrogen is admitted into the cylinder prior to Intake Valve Closure (referred to as Pre-IVC engines) and (2) engines in which hydrogen is admitted following intake valve closure (Post-IVC engines). Airbreathing operation and ambient-temperature gaseous hydrogen was employed throughout the project.

Pre-IVC Engines - These engines are similar to conventional gasoline-fueled engines in that both hydrogen and air are introduced into the cylinder during the intake stroke. They can be introduced as a mixture, the mixture being formed by a carburetor-like device (a gas-mixer), or they can be introduced separately, as in a fuel-injection gasoline engine, with the hydrogen being injected (induced) in the intake

high flame speed of hydrogen over a wide range of fuel/air ratio.

Post-IVC Engines - These engines are similar to compression-ignition engines, but some positive source of controlled combustion initiation is needed, such as a spark-plug (single or multiple spark discharge) or a glow plug. Gaseous hydrogen is injected directly into the cylinder, commencing during or near the end of the compression stroke and continuing on into the expansion stroke. Mechanical, electrical and hydraulic pulse-actuated hydrogen injectors have been used.

ENGINE CONFIGURATIONS - Table 1 delineates the 19 engines to be covered in this paper. The various test engine configurations are grouped first, as follow: (1) type of combustion chamber

design (open or pre-chamber), (2) method of mixture formation (direct injection Post IVC, gas-mixer Pre IVC, part admission Pre IVC), (3) air-flow induction control (if any), and (4) use of additional mixture components (EGR, water, air injection). In dealing with the design basis for Engines 1 through 19, Table 1 is basically self-explanatory. However, it is helpful to further break down the Table by "natural groups" as follows:

Engine Configurations Nos. 1-3

- The first three engines are best described together as being quite equivalent to conventional throttled, carburetted gasoline engines. A single air-throttled central gas-mixer of the conventional "propane carburetor type" provided the hydrogen-air mixture to four-cylinder of the test engine via a stock intake manifold. Single, open, spark-ignited combustion chambers were operated at approximately stoichiometric conditions over the throttled-controlled load range, at commensurate levels of manifold vacuum (i.e., quantity control).

Whereas Engine Configuration No. 1 is just as described, No. 2 adds Exhaust Gas Recirculation (EGR amounts to be specified) and No. 3 adds water induction. For the latter, several admission techniques were explored with a simple single-orifice injector in each intake port continuously directing water into the valve pocket, intake manifold and/or combustion chamber being selected for the data runs. Typically, the average water/hydrogen mass-flow ratio was about 5. The effect of varying this parameter is brought out in the Project reports (3-5). Water induction in hydrogen engines is a rather widely practiced means of both (1) ameliorating the intake manifold backfiring problem and (2) suppressing the production of NO_x .

Engine Configuration Nos. 4-6

- In a similar sequence with regard to the inclusion of EGR and water induction, this series of test engine configurations again used a single, central gas-mixer feeding four stock combustion chambers. However, air-throttling was not used, i.e., the throttled plate remained in the wide-open position. Load control was accomplished by varying the fuel/air mixture, often referred to as quality governing, quality control, etc.

This mode of control is, of course, basically similar to that of a typical diesel engine in that, although fuel quantity varies, manifold vacuum does not for a given load and speed. However, for a conventional homogeneous fuel/air charge Otto-cycle engine, it is only feasible because of hydrogen's uniquely wide flammability limits, due in turn to its exceptionally high flame speed. (the order of 4-times hydrocarbon fuels at stoichiometric conditions; see "Some Theoretical Considerations of Hydrogen as an Internal Combustion Engine Fuel," Appendix D (1).)

In this project, engines thus operated in the unthrottled mode ranged in operation fuel/air equivalence ratio (PHI) from 1.0 (stoichiometric) down to as low as 0.20 ("ultralean"). But, as will be seen (Engine Configuration No. 16), some air throttling at the extreme lean-end was found beneficial. Engine Configuration No. 4, analogous to No. 1, employed neither EGR nor water injection; No. 5 used EGR and No. 6, water.

Engine Configurations Nos. 7-9

- This sequence of 4-cylinder engine types all used timed-port fuel induction, rather than the central gas-mixer approach employed in the previously described engines. An individual sleeve-valve arrangement for admitting flow-controlled hydrogen fuel was integrated with each intake valve. This fixed-geometry set-up beginning 45 degrees after TDC and ending 135 degrees after TDC in the intake stroke. Hydrogen flow was thereby started after, and terminated before the initiation and termination of air flow into the cylinder, respectively.

Engine Configuration No. 7, again analogous to previously described Nos. 1 and 4, had neither EGR nor water induction. No. 8 had EGR and No. 9, water induction. All three (Nos. 7-9) were operated in the unthrottled mode like Nos. 4-6.

Engine Configuration No. 10 - No. 10 employed a special unthrottled/throttled mode NO_x -control operating strategy. It was unthrottled in the low-load range up to a PHI where NO_x generation began its typical steep rise, on the order of 0.7 or thereabouts for the test engine series. At that point, step-function air-throttling was initiated and fuel-flow commensurately increased to match the unthrottled load. Operation was then

sufficiently rich (PHI was on the order of 1.2) such that NO_x emissions were again low.

Thus Engine No. 10, labeled the "discontinuity engine" was so operated as to enable a step across the characteristic PHI vs NO_x peak from a given low level on the ascending slope to an equivalent level on the descending slope (going from lean to rich). As will be seen, there is a penalty in fuel economy (related here as Brake Thermal Efficiency) for this approach for achieving low NO_x operation without EGR or water.

Engine Configuration No. 11

- This configuration tested the effect of air injection into the intake manifold runners of a central gas-mixer 4-cylinder test engine operating in an unthrottled mode without EGR or water induction. (In effect, No.4 with the air injection feature.) The objective here was to determine the contribution of forced-air induced mixture turbulence on backfire alleviation, if any.

Engine Configuration No. 12-16

- The final set of 5 engine configurations were alike in that they utilized a single-cylinder version of the basic stock 4-cylinder design. The leading (front) cylinder remained active and the remaining pistons and valve operating-components were removed. The crank-shaft was equipped with compensating weights and an increased moment-of-inertia flywheel replaced the stock item. Testing was at a constant (rpm i.e., the 1800 rpm condition reported on in this paper).

These configurations each used a single, smaller gas-mixer mounted close-coupled to the intake port. (The previously used central gas-mixer with the unused 3 cylinders' intakes blanked-off was initially tested as well.) In an actual multi-cylinder engine, based on the selected configuration, each individual cylinder would be fueled and controlled by its own close-mounted gas-mixer.

Engine Configurations No. 12-15 were operated unthrottled (quality governed), differing only in combustion chamber design. No. 12 used the stock open-chamber hemispherical design; Nos.13, 14 and 15 used pre-chamber designs of varying geometry as supplied by the engine manufacturer (R & D hardware). The pre-chamber geometries varied as follows:

Eng. Config. No.	Portion of Total Clearance Volume	Pre-Chamber Volume-to-Orifice Area Ratio
13	15%	10:1
14	15%	6.5:1
15	9%	6.5:1

Engine Configuration No. 16 - used the open chamber and principally unthrottled operation. At light-load conditions, air-throttling was initiated to improve thermal efficiency.

Engine Configuration No. 17 - used an open chamber and unthrottled operation. Hydrogen was injected during the compression stroke and ignited by a multiple spark ignition system. Four different injection timings and lifts were investigated.

Engine Configuration No. 18 - was identical to Configuration No. 17 except at light-load conditions, air throttling was initiated to improve thermal efficiency.

Engine Configuration No. 19 - employed direct injection of the hydrogen into the combustion chamber near top dead center. Ignition was accomplished with a platinum wire glow plug.

PREPARATION OF DATA

In an effort to present the considerable amount of data in a compact form the following methods for comparison were used. An attempt was made to make comparisons at engine speeds and loads typical of the EPA city (CVS) driving cycle.

PEAK POWER - Comparisons of power output were made at 1800 r.p.m. The comparable gasoline fueled engine with EGR and stoichiometric air-fuel ratio was assumed to produce 113 bmeP.

FUEL CONSUMPTION - Comparisons of fuel consumption were made on a BTU per mile basis. Three mini mapping points characteristic of the speeds and loads encountered over the city driving cycle were chosen at the suggestion of Carl Kukkonen of Ford Motor Company. They were 1000 r.p.m. at 15 psi. bmeP for .49 Hp-Hr, 1250 r.p.m. at 37 psi. bmeP for 1.35 Hp-Hr, and 1700 r.p.m. at 75 psi. bmeP for 1.16 Hp-Hr. The three points were weighted by their respective number of horsepower-hours. The entire 7.5 mile course required the equivalent

of 3 horse power-hours to navigate.

EMISSIONS - Comparisons of emissions (NO_x) were made on a grams per mile basis. The same three data points as were used to make fuel consumption calculations were used for oxides of nitrogen. The base line gasoline engine was assumed to produce .48 grams per mile oxides of nitrogen.

PRESENTATION OF DATA

Table 2 shows the results of the aforementioned comparisons. Peak power is presented as a percentage of the gasoline fueled engine value. Fuel consumption is presented as a percentage of the gasoline fueled engine (greater than 100% indicating poorer fuel economy). Total oxides of nitrogen are presented as a percentage of the gasoline fueled engine (greater than 100% indicating higher emission levels).

SUMMARY OF TECHNICAL RESULTS

PERFORMANCE AND DESIGN

Pre IVC Engines - (1) Unburned hydrogen was found in the exhaust during normal operation. During richer operation ($0.8 < \text{PHI} < 1.2$), the unburned hydrogen in the exhaust can be accounted for by dissociation and a slow down of oxidation reactions

during the expansion stroke. During operation at $0.4 < \text{PHI} < 0.8$, the unburned hydrogen may be accounted for by: (1) wall quenching of the flame; (2) preferential flow of hydrogen during blowby; (3) small-scale nonhomogeneity in the combustion chamber. During operation at $0.2 < \text{PHI} < 0.4$, it can be accounted for by bulk quenching.

(2) Consistent with the results of others, the unthrottled engine, vis-a-vis the throttled engine, exhibited higher brake thermal efficiency, except at light loads where some throttling is beneficial.

(3) Peak power output calculations show that the potential, nonflashback-limited power output of Pre IVC engines can be larger than had been previously reported if advantage is taken of the properties of hydrogen as a fuel. Test results with Engine 12 where a peak power bmeq of 100 psi was found compared to the 115 psi value attainable with a gasoline engine supports the results suggested by these calculations.

(4) Except for Engine Configuration No. 7, 10, 12 and 16, under ideal conditions (i.e., with limited deposits in the combustion chamber), power was limited by flashback for all engine configurations tested without EGR and water injection.

Engine No.	Max. Power (%)	Fuel Consumption (%)	NO_x (%)	Notes
1	100	100	100	
2	100	100	100	
3	100	100	100	
4	100	100	100	
5	100	100	100	
6	100	100	100	
7	100	100	100	
8	100	100	100	
9	100	100	100	
10	100	100	100	
11	100	100	100	
12	100	100	100	
13	100	100	100	
14	100	100	100	
15	100	100	100	
16	100	100	100	

* Max. Power, Fuel Consumption, and NO_x for a standard gasoline engine with EGR, stoichiometric Air-fuel Ratio and 10:1 Compression Ratio.
 ** 10:1 Compression Ratio.
 *** It denotes that flashback prevented operation at lower levels required to complete the driving cycle, i.e., insufficient power developed by engine.
 - MEI denotes Maximum Power was limited by engine cylinder filling, volumetric efficiency.
 - 10:1 Compression Ratio.
 - denotes that Maximum Power limited operation with 10:1 Compression Ratio.
 - denotes that Maximum Power limited operation with 10:1 Compression Ratio.

The use of EGR and water injection, however, allowed for wide-open throttled operation at near peak-power PHI (for the levels of EGR and water injection used).

(5) Comparison of the results of the present study with those performed by the authors in the past indicates that charge stratification can increase or reduce the lean limit of operation for the unthrottled engine.

(6) Proper carburetor (gas-mixer) selection can reduce cylinder-to-cylinder variation in fuel-air ratio with subsequent improvement in performance.

(7) For residence times in normal operating engines, the diffusion rate of hydrogen is not sufficiently high to make homogeneous mixtures from initially heterogeneous mixtures.

(8) Two independent methods were used to generate indicated quantities from brake measurement: (a) performance map method; (b) Bishop/Taylor method. The methods gave results consistent with each other when applied to the present-study data. The Bishop/Taylor method was used to make the comparison of the present-study data with those of others, and good agreement was found, eliminating much of the apparent conflict of results as reported by others.

(9) The lithium-filled exhaust valves did not attain their performance potential, a result recently found by industry.

(10) By choosing the proper displacement, it should be possible to design an unthrottled Pre IVC hydrogen engine with some throttling at light loads that can operate over a driving cycle with performance and energy conversion efficiency (BTU/mile) equal to that of a gasoline-fueled engine and emission levels below the 0.4 gm/mi level.

(11) The BTE of the dual-chamber Pre IVC engine is about the same as that of the single-chamber design at light loads. At high loads, as a result of heat loss, the dual-chamber engine yields a lower BTE.

Post IVC Engines - (1) The B1 for the Post IVC engines is not as strong a function of PHI as was found with the Pre IVC engines; the BTE for the Post engines was found to be more a function of injector valve design, lift and fuel pressure.

(2) The Post IVC engine could be throttled at light loads to increase the BTE there. This increase is

suspected of being due to better fuel penetration and mixing at the throttled condition.

(3) The peak power output for Post IVC Engines 17 and 18 was higher than that of the corresponding gasoline engine. However, it was necessary to operate these engines with an unacceptably-low coolant temperature. Engine 19 yielded approximately the same peak power output as the corresponding gasoline engine with normal coolant temperature. It is suspected that the burn-after-injection Post IVC engine can be made to operate with even higher peak power if the fuel injector design can be optimized.

FLASHBACK - (1) Hot spot-induced flashback was found to be predictable and therefore, subject to characterization. There is a period preceding hot spot-induced flashback (Period PHIF) during which the charge is ignited by the hot spot at progressively earlier crank angles until it occurs prior to closing of the intake valve, resulting in flashback. During the Period PHIF, NO_x emissions rise very rapidly and the RPM drops.

(2) Decreased valve overlap was not found to decrease flashback tendencies negating the hypothesis that flashback was being caused by communication of the fresh charge with still-burning exhaust gases during the valve overlap period, when employing common valve overlaps.

(3) Lean mixture operation can cause flashback, raising the lower engine speed limit of the carburetted (uniform-charge) unthrottled engine.

(4) Evidence was found to substantiate the hypothesis that oil in the residual gas can cause flashback.

(5) Partial ignition failure (misfire, flame initiation failure) does not result in flashback.

(6) Hydrogen/air induction methods influence, somewhat, flashback limits.

(7) Flashback-free operation does not seem possible without EGR or water injection with stock water-jacketed cylinder heads operating at stock water temperature unless extreme care is taken to continuously clean the combustion chamber. Changes in cylinder head coolant passage design, however, can definitely improve this situation.

(8) Proper cylinder head coolant passageway design is a necessity for flashback-free operation.

(9) Throttling of the homogeneous-charge Pre IVC engine with the concomitant mixture enrichment helps to eliminate flashback at light loads.

OXIDES OF NITROGEN EMISSIONS

Pre IVC Engines - (1) Consistent with the results of others, NO_x emissions were found to be a strong function of PHI.

(2) The use of EGR while maintaining constant load, constant engine speed and BESA did not affect NO_x emissions for the unthrottled engine as a result of reduced air flow with increasing EGR rates.

(3) The use of EGR while maintaining constant load, constant engine speed and BESA resulted in a decrease in NO_x emissions for the throttled engine operated at constant PHI = 1.0.

(4) The use of water injection while maintaining constant load, constant engine speed and BESA was found to decrease the initially low NO_x emission level at low PHI.

(5) The use of water injection while maintaining constant load, constant engine speed and BESA was found to decrease the NO_x emission level of the throttled engine operated at PHI = 1.0.

(6) For the same diluent heat capacity flowrate, EGR and water injection were found to decrease NO_x emissions by a similar amount.

(7) For practical operating conditions, a given volume of air has essentially the same effectiveness in reducing NO_x emissions as an equal volume of exhaust gas.

(8) An unthrottled engine designed to give good performance over a driving cycle (Federal Register Vol. 35, No. 136) gives off NO_x emissions well below 0.4 g/mi without using EGR or water injection.

(9) NO₂, possibly a worse pollutant than NO, is found to be the major oxide of nitrogen emitted over a driving cycle (Federal Register Vol. 35, No. 136).

(10) NO_x emissions at high loads can be reduced using the discontinuity mode of operation with a loss in thermal efficiency.

(11) Compared to gasoline-fueled operation, humidity has a negligible effect on NO_x emissions.

(12) Throttling Engine 16 at light loads increased both the BTE and NO_x concentration (ppm) but resulted in a decrease in brake specific NO_x (gm/hp hr) emissions.

(13) All of the prechamber Pre IVC engines produced less NO_x emissions than the single-chamber ones.

Post IVC Engines - (1) The NO_x versus PHI curve emissions for Engine 17 had the same appearance as the Pre IVC engine curves. Throttling the engine at light load (PHI = 0.65) to increase the BTE there, was done with Engine 18, caused the NO_x emissions to increase. Less throttling, of course, could be used which would still cause an increase in BTE with a smaller increase in NO_x emission.

(2) Engine 19 yielded very low NO_x emissions high loads and high NO_x emissions at low loads. Instead, the emission level was found to be a strong function of injector lift and injection pressure. Changing the lift resulted in the NO_x emission level changing by a factor of up to three.

OTHER CONSIDERATIONS - (1) FID HC were found to be a function of manifold vacuum (VCF) with increasing levels at higher vacuum.

(2) The previously-used KMnO₄ titration method of measuring H₂O₂ emissions was found to give erroneous results due to interference with NO. The phenol-ferrous sulfate solution method was subsequently employed for the present study.

(3) H₂O₂ emissions were found to increase with decreasing PHI. There was good correlation between the drop-off in the Hydrogen Utilization Coefficient and the rise in H₂O₂ emissions during lean-mixture operation.

NOMENCLATURE

In this section, symbols and terminology used in the paper's text, tables and figure are defined. Excluded is additional nomenclature used in the project reports (3-5) but not in this paper. (The more extensive nomenclature is presented in the reports.)

Symbol	Meaning
BESA (°)	Best Efficiency Spark Advance (before top dead center, BTDC)
BMEP (kPa)	Brake Mean Effective Pressure
BSNO _x (g/kWh)	Brake Specific Oxides of Nitrogen (NO _x) Emissions
BTE (%)	Brake Thermal Efficiency
EGR	Exhaust Gas Recirculation
Backfire	Combustion of the hydrogen-air mixture in

the induction system. Backfiring or flashback in the induction system occurs when the hydrogen-air fresh charge ignities prematurely prior to the closing of the intake valve. The flame thus generated propagates through the fuel-air induction system producing a report of varying severity.

Equivalence Ratio PHI Fuel/air equivalence ratio is the actual fuel/air ratio divided by the stoichiometric ratio, i.e., values less than one represent fuel-lean operating conditions.

Throttled Operation Operation during which the load is changed by varying the density of the fresh charge with a convention throttle plate producing varying levels of intake manifold vacuum.

Unthrottled Operation Operation during which the throttle plate is left in the wide-open position (or is eliminated) and the load is controlled by changing the flowrate of hydrogen. The result is power-level control through varying PHI. The total volume flowrate of fresh charge is essentially constant for a fixed speed.

Hawthorne for designing and constructing much of the special test apparatus and instrumentation, as well as his data-taking and presentation efforts.

The cooperation of Toyota Motor Co., Ltd., Secaucus, NJ, and especially Mr. Tushiro Yoshida, Staff Engineer, in providing special data and experimental hardware is acknowledged with gratitude.

REFERENCES

1. W.J.D. Escher, "The Hydrogen-Fueled Internal Combustion Engine, A Technical Survey of Contemporary U.S. Projects," U.S. Energy Research and Development Administration Report "EC 75/005, September 1975.
2. W.J.D. Escher and E.E. Ecklund, "Recent Progress in the Hydrogen Engine," paper 760571 presented at the Society of Automovite Engineers Fuels and Lubricants Meeting, St. Louis, Missouri, June 1975.
3. R.R. Adt, Jr., M.R. Swain, and J.M. Pappas, "Hydrogen Engine Performance Analysis Project," University of Miami First Annual Report under U.S. Department of Energy Contract E(04-3)-1212, Report SAN-1212-1, August 1978.
4. R.R. Adt, Jr., M.R. Swain, and J.M. Pappas, "Hydrogen Engine Performance Analysis Project," University of Miami Second Annual Report under U.S. Department of Energy Contract E(04-3)-1212, Report SAN 1212-T1, January 1980.
5. R.R. Adt, Jr., M.R. Swain, and J.M. Pappas, "Hydrogen Engine Performance Analysis Project," University of Miami Third Annual Report under U.S. Department of Energy Contract E(04-3)-1212 (in publication).

ACKNOWLEDGMENTS

The effort reported on in this paper was supported by the U.S. Department of Energy (DOE) through Contract E (04-3)-1213 (University of Miami, Hawthorne) and DE-AC01-80CS50093 (E:F). The DOE Project Manager is Mr. E. Eugene Ecklund. The authors extend their appreciation for this support and personal thanks to Mr. Ecklund for his continuing interest and counsel during the conduct of the work. The authors also express appreciation to their colleagues at the University for general support and assistance, and especially to Mr. M. N. Swain of

QUESTION AND ANSWER PERIOD

- Q: At what minimum equivalence ratio could the engine run?
- A: Equivalence ratio of .18.
- A: The minimum equivalence ratio run was approximately 20% of stoichiometric down to an equivalence ratio of .18. At that point, bulk quenching occurred in the combustion chamber and half the hydrogen was passing through the engine in the unburned state. That was for a homogenous charge engine. For a stratified charge engine, we could go down to an equivalence ratio of .1. But in that case we had a locally rich mixture.
- Q: .18?
- A: Yes, yes, absolutely. It's consistent with the oxygen concentration in the exhaust and the amount of hydrogen measured when we used the mass spec to determine if in fact there was hydrogen in the exhaust.
- Q: Would you be more specific on the fact that in the case of pre-IVC engines you had an increase in efficiency for lower equivalence ratios and for post-IVC engines you had the opposite?
- Q: Sounds strange to me but that's what you measured.
- A: The trends were not opposite for pre-IVC and post-IVC operation. Perhaps there has been a misunderstanding here. But in general, as you increased air fuel ratio, you got an increase in thermo efficiency up to a maximum of about 80-85% of stoichiometric and then it began to flatten out and eventually taper off thereafter. I'm not too sure of what you're referring to.
- A: Yes, and it's not at all unusual for hydrogen engines to run that lean.
- Q: I think you said that there were two opposite trends, but . . .
- Q: .18?
- A: Yes .18 to 2.0.
- A: In terms of NO_x ?
- Q: Dave Renfrew from GMI Engineering Management Institute. I was curious as to what the spark timing was when you were running the engine?
- Q: No, in terms of efficiency.
- A: It depended. Of course spark advance is a strong function of air fuel ratio. For a pre-IVC engine running with an equivalence ratio about 20% of stoichiometric, about 94 degrees of spark advance was required. The spark advance went to about 4-5 degrees after top dead center ignition at mixtures slightly rich. So it was as I said, a very strong function of air fuel ratio.
- A: I certainly didn't mean to say that.
- Q: Okay, those are the things we were getting at GMI. Also, could you explain again why the late injection produces NO_x in the light loading condition?
- Q: Well okay. How did you control and how did you measure the equivalence ratio?
- A: At this point I'd have to take a few guesses. Basically, you're burning a jet of hydrogen in the combustion chamber. You have already compressed all the gases and you have a spray of hydrogen that passes through about 3/4" of air and then impinges upon the glow plug. Now the flame speed of hydrogen continues to increase at equivalence ratios greater than one on up to 30-40% rich. So if the jet ignites, it is very likely that the flame will propagate up the jet to a relatively rich region. Once it begins to propagate up the jet, it will go well past the stoichiometric region because the flame speed is continuing to increase. So you can sort of envision a jet of hydrogen burning close enough to its source to where it's a very rich mixture. This can be compared to the flame in a pre-IVC engine in which the first burned portion of the charge creates the highest concentrations
- A: The equivalence ratio was measured by measuring the flow rate of the hydrogen and the flow rate of the air that entered the engine.
- Q: So you had two flow meters?
- A: Two flow meters. The air flow meter was changed back and forth. We had two separate air flow meters and they changed back and forth and both gave us the same readings. The hydrogen flow meters were rotometers and a turbine meter for the case of the high pressure injection. They were calibrated by a group in Denver, Colorado on hydrogen.
- Q: You are absolutely sure that you ran the engine at an equivalence ratio of .18?

of NO_x . In the case of the post-IVC engine, the first burned portion of the charge is blown into air only and quenched and this portion is now brought to a low enough temperature that it shouldn't be producing large concentrations of NO_x . It would appear that there are two possible reasons why the NO_x at full load is so very low. One, at the flame front itself, we are burning a richer mixture than would normally be burned with another type of operation because the flame speed continues to increase at the very, very rich mixture hydrogen. Secondly, the first burned charge is then blown by the hydrogen behind it out into a portion of the combustion chamber where its temperature will drop and not produce as much NO_x as it would were it left at a higher temperature.

Q: Bill Escher, EF Technology. Mike, first just a clarification on your bar chart presentation with all those good colors; the blue really was not BTE relative to gasoline, but the fuel energy used for the cycle. Is that right?

A: Right, exactly.

Q: So lower then is good? I got confused myself on that one.

A: Yes. Lower is good in that case. That is the relative amount of BTU it takes to drive around a cycle. I'm sorry for the confusion. I realize now that that's easily confused.

Q: On the NO_x side of life the gasoline . . . your reference against the hydrogen was a good one. Now the thing that might be raising a few eyebrows here on the post-IVC engines is this business of 1,000 psi hydrogen and where one might get that on a car or vehicle. It might be worth pointing out that the approach the Japanese and Germans are looking at is to use liquid hydrogen in the very small low power pump to almost in-diesel like fashion to develop those high pressures at low energy expense. The Japanese, for example, have operated a demonstration car, Mike, as you well know, with that system using

engine number 19 in effect. I'd like to make the last point and I'm asking you for a response. It may be viewed that those 19 engines, in effect, were proposed engines to be taken on out into some use application. But wouldn't you rather put it that this is a system of sort of matrix of data gathering for a later engine designer to now pick and choose what combination of things he might like to use? Is that a good interpretation?

A: Yes. One point in particular I might make, because it wasn't covered in the slides, is that while we were trying to run engine number 19 we started out with a very small glow plug. It's the same glow plug that you find in aircraft engines. The small model airplane engines. It's screwed in the bottom of a fitting and screwed in the regular spark plug hole and we could then, by putting current across the plug, make it glow. We were completely unable to get any response from the injected hydrogen in terms of oxidation. So we hooked the carburetor back up and we found that you could run virtually stoichiometric hydrogen through the engine with the glow plug glowing and not have any preignition take place. But should the temperature of the glow plug become high enough to produce the first sign of preignition, then the engine would rattle and bounce for a number of crankcase rotations until we eventually reduced the supply of hydrogen. It occurred to me at the time that there are two things that are causing preignition in the hydrogen engine. You must supply a hot spot, and we had gone to a lot of work to reduce this hot spot enough to where we could get 100 BMEP out of the engine. But additionally, you need the leftover radicals from the previous cycle. They can exist as we have seen in quite high concentrations. In the case of lean operation, we had 1,000 PPM hydrogen peroxide. So this would mean there are two ways to approach the problem of reducing preignition. One way would be to alleviate all the hot spots. The second way would be to provide some method of superior scavenging of the combustion chamber to get the residuals left over from the previous cycle out of the combustion chamber.

Gaseous Fuel Safety Assessment Status Report

M. C. Krupka, F. J. Edeskuty,
J. R. Bartlit, and K. D. Williamson, Jr.
Los Alamos National Laboratory
Los Alamos, NM

ABSTRACT

The Los Alamos National Laboratory, in support of studies sponsored by the Office of Vehicle and Engine R and D in the US Department of Energy, has undertaken a safety assessment of selected gaseous fuels for use in light-duty automotive transportation vehicles. The purpose is to put into perspective the hazards of these fuels relative to present day fuels and delineate criteria for their safe handling. Fuels include compressed and liquefied natural gas (CNG and LNG), liquefied petroleum gas (LPG), and for reference, gasoline and diesel. This paper is a program status report. To date, physicochemical property data and general petroleum and transportation information were compiled; basic hazards defined; alternative fuels were safety-ranked based on technical properties alone; safety data and vehicle accident statistics reviewed; and accident scenarios selected for further analysis. Methodology for such analysis is presently under consideration.

THE USE OF ALTERNATIVE AUTOMOTIVE FUELS other than those derived primarily from petroleum were considered for many years and in fact were used in relatively minor quantities. More recently a rekindling of interest in the utilization of these fuels has emerged. The impetus for this is derived from a variety of reasons including:

- o a mandate to reduce exhaust pollution
- o escalating fuel costs
- o concern over potential petroleum supply reduction
- o a desire for self-sufficiency (import reduction)
- o potential technical advantages.

The alternative fuels under consideration are by no means new energy sources. However,

because their use in the automotive transportation sector is limited, an extensive commercial infrastructure such as exists for petroleum and its refined products has not been developed.

The expected increased usage of these fuels for routine automotive transportation has also elicited an increase in concern over their relative safety. A degree of risk is always associated with the use of energy sources. Acceptance of large scale usage of new energy sources and technologies by both government and the public-at-large can be expedited if it can be demonstrated through adequate assessment, safety testing, and operational experience that the intrinsic risk is either equivalent to or less than that associated with the energy source presently used. Liquid petroleum products such as gasoline and naphtha are flammable, in selected situations explosive, yet are safe and acceptable when handled properly.

The United States Department of Energy (DOE) has already established an Alternative Fuels Utilization Program (AFUP). To implement selected facets of the Methane Transportation Research, Development, and Demonstration Act of 1980, P. L. 96-512, some funding from AFUP was diverted and a Gaseous Fuel program with primary emphasis on methane (natural gas) was developed. The program is managed by the Office of Vehicle and Engine R and D (VERD). In support of VERD, the Los Alamos National Laboratory is undertaking a safety assessment of selected gaseous fuels for use in light-duty automotive transportation vehicles.

The purpose of the assessment is to put into perspective the relative hazards of these fuels compared to gasoline and diesel fuels and to delineate criteria for their safe handling in the transportation sector.

This paper represents a status report. Completed efforts are described herein but significant analysis remains to be accomplished.

TRANSPORTATION SECTOR

In 1980, the transportation sector consumed approximately 50% of the total US petroleum use. Of this quantity, approximately 80% was used for highway motor fuels (1).^{*} Motor fuel consumption amounted to about 1.2×10^{11} gallons (gal) (gasoline, diesel, and LPG). Gasoline alone accounted for about 1.0×10^{11} gal (2). LPG sold for internal combustion engine use amounted to about 5.0×10^9 gal although not all was used for mobile transportation purposes (3). On-highway transportation use of distillate fuel oil (diesel) amounted to about 1.4×10^{10} gal (3). The quantity of natural gas used as a motor fuel was very minor relative to these quantities.^{**}

Of the 1.2×10^{11} gal of motor fuel consumed, about 8.0×10^{10} gal were used by personal passenger vehicles and motorcycles, about 4.0×10^{10} gal were used by trucks (all gross vehicle weight (gvw) classes) and approximately 0.1×10^{10} gal by buses (4). A discussion of resource availability and the impact upon fuel production is given by Fleming (5).

A total of about 1.6×10^9 vehicles were registered in 1980 (6). This number can be subdivided as follows:

o passenger vehicles	1.1×10^9
o trucks	3.5×10^7
o buses	5.5×10^5
o motorcycles	5.8×10^9

Light trucks (< 10,000 lb gvw) represent about 65% of the truck fleet.

The use of diesel fuel in passenger vehicles has increased recently and in 1980, diesel-powered passenger vehicles represented about 4.4% of new vehicle registrations.

Approximately 1.5×10^{14} vehicle miles were traveled in the US in 1980 (6).

A brief discussion of the number of vehicles, injuries, and fatalities involved in vehicular accidents will be presented later.

PHYSICO-CHEMICAL PROPERTY DATA

The comparative safety assessment of the alternative automotive fuels considered herein relies heavily upon the fundamental physico-chemical properties of the fuels. Selected property data for these fuels were compiled and are shown in Table 1.^{***}

^{*}Numbers in parentheses designate references at end of paper.

^{**}Total mileage accumulated by natural gas-powered vehicles is assumed to be about 2.1×10^8 miles over the years 1970-1981. Using conversion factors of 15 miles per gallon and an average 125 ft^3 per gallon of gasoline equivalency, about $17.5 \times 10^8 \text{ ft}^3$ of gas were used over this time period.

^{***}Additional property data will appear in the final report to be published at a later date.

The properties of natural gas and methane are considered to be equivalent in this report. Methane is the primary constituent of the natural gases used as fuels although they may contain small quantities of other hydrocarbons. Impurities such as moisture and a small amount of sulfur are also present. Similarly, the properties of LPG and propane are considered to be equivalent. For the automotive fuel application, a special grade under tight ASTM specifications, MU-5, is used. This grade contains propane in excess of 90%.

HAZARD IDENTIFICATION

In any comparative safety analysis or risk assessment, it is necessary to define within reasonable limits the boundary conditions for the given system. The choice of parameters is critical. For the alternative fuels under investigation, those hazards contributing to the risk of using the specific fuel are identified herein as primary hazards. They include:

- o fire
- o degradation/deterioration
- o cryogenic damage
- o physiological damage

On a secondary level, the hazard of explosion definition, one can derive a set of conditions or generalized properties that lead to the primary hazard. This sublevel analysis is on a basis and is derived from an interactive matrix of fundamental physicochemical properties. The latter in turn represents a minimum hard technical data level required as a basis for selected techniques. Selected safety and health selected sublevel hazards are shown in Table 2.

HAZARD, PROPERTY, INTERRELATIONSHIPS

The interrelationships between the hazards of several fuels (natural gas, methane, gas, fuel, diesel) and the fundamental physicochemical properties of these fuels have been discussed in significant detail by Lewis and others and others (7,8,9,10). Comparisons between LPG, The fundamentals of combustion, flames, and detonation are thoroughly discussed in many texts, e.g., Lewis and others (9). It is stressed here to briefly mention a couple of examples of potential pitfalls when determining the safe safety based upon hazard property considerations alone.

Analogous to the case of liquid hydrogen, spillage of other cryogenic fuels, e.g., ethane, can cool a volume of air immediately surrounding the cryogen (11). If the vapor density of the cryogen/air mixture approaches or becomes greater than that of air, the cryogen/air mixture becomes nonbuoyant and can spread to distances beyond the immediate spill zone. In time, the cryogen/air mixture will warm and rise creating a hazard over greater distances as well as lengthening the time period for the existence of the hazard.

Table 1
Selected Physicochemical Properties of Automotive Fuels

	Natural Gas*		LPG*	Gasoline	Diesel
	LNG	LNG			
Expansion Ratio, Liquid to Gas		600-650	270-310	156	(Est. ~ 125)
Specific Gravity Relative to Air (1.29)	0.70	--	1.45-1.56	3.4-3.9	--
Energy Content, Btu/lb Lower Heating Value	4,700	16,300 * 111.6 kJ, 1atm	82,450	115,000 (Av)	130,000 (Av)
Energy Content, Btu/lb Lower Heating Value	11,300	31,300	19,770	18,920 (Av)***	19,200-19,500 (Est.)
Flammability Limits, vol. %	5-15.5	--	2.4-9.5	1.0-7.6	0.5-4.1
Detonation Limits, vol. %	5-15.5	--	3.1-7.0	1.1-3.3	--
Autoignition Temp., °C	513	--	165-875	501-744	~520
Ignition Energy, Millijoules	100	--	10.24-0.30	0.24	(Est. 0.25)
Flash Point, °C	gaseous	--	gaseous	230	310-340
Flame Temp., °C	2100	--	2245	2470	--
Diffusivity, cm ² /sec with air***	0.15	--	0.34	0.17	--
Relative Density to Air	0.70	--	nonbuoyant	nonbuoyant	nonbuoyant
Heat of Vaporization, kcal/mole	--	168	--	352	560
Boiling Point, °C	100	--	40-47	37-43	34 (Est.)
Freezing Point, °C	--	-160	-130	-100	(Est. -100)
State at 15°C	gas	liquid	liquid under pressure	liquid @ ambient T&P	liquid @ ambient T&P
State at 15°C and 1 atm	compressed gas	liquid @ 1atm	liquid @ 0-6 atm, ambient	liquid @ ambient T&P	liquid @ ambient T&P

*Values are given for the most common commercial grades of these fuels. LNG and propane are still only used in limited quantities.

**Values are given for the most common grades of these fuels. LNG and propane are still only used in limited quantities.

***Values are given for the most common grades of these fuels. LNG and propane are still only used in limited quantities.

Table 2

Selected Secondary Hazards

	Fundamental Property
Leakage	Absolute Viscosity, Molecular Weight
Mixing, Dispersion	Diffusivity, Buoyancy
Volatility, Boiling	Thermal Diffusivity, Density, Vapor Pressure
Ignition	Heat of Vaporization, Ignition Energy, Flash Point, Autoignition Temperature
Flammability	Flash Point, Vaporization Rate, Thermal Conductivity, Heat Capacity, Composition
Radiation	Burning Velocity, Emissivity, Heat Release Rate
Mechanical Containment	Chemical, Metallurgical, and Engineering Properties Various

The greater buoyancy of natural gas (versus gasoline, diesel, and LPG) becomes advantageous in unconfined areas by permitting rapid dispersion and dilution. Confinement, on the other hand, can reverse the assessment since a fire and possible detonation hazard is produced quickly. Hence the importance of defining boundary conditions for a given application or scenario.

SAFETY RANKING OF FUELS

A preliminary comparative safety ranking was accomplished based upon consideration of the absolute technical properties of each fuel. Each property is considered and the fuel ranked accordingly. Effects of property interactions and other boundary conditions are not considered here. Rankings are essentially qualitative. It is recognized that the methodology is relatively simple and that realistically the final assessment must ultimately take other factors into account. It does demonstrate however, that

- o certain properties contribute more to hazard generation than others
- o certain properties are neutral, i.e., fuel rankings are equivalent
- o certain properties reverse the rankings generated by others
- o safety ranking becomes a more complex problem

Comparative safety rankings are shown for a selected number of properties in Table 3.

SECONDARY HAZARD CRITERIA - Fuels may also be ranked according to secondary or sublevel hazard designations noted in Table 2. This was done in part by Bowen for nine fuels including methane, gasoline, and diesel (8). Rankings were made on the basis of 1-9, the largest number indicating the greatest hazard. Our analysis has produced similar results with LPG included. Selected results of our analysis on the basis of 1-4, the larger number indicating the greater hazard, are presented in Table 4 (see footnote in Table 4).

Once again, it is apparent that safety ranking of this type will yield various results although there is a trend to classify LNG and LPB as more hazardous materials. These rankings also suggest diesel fuel to be the safest. Toxicity or emission data (not shown) may however change the above. It should be emphasized again that rankings are based solely upon technical data. Stringent boundary conditions, applications, scenarios, and risk abatement strategies are not involved.

The ranking methodology so far detailed yields some idea of the relative hazards of these fuels, but only in a most general sense. In basic agreement with the general conclusions of Hord, a relative safety analysis of alternative fuels will now require the generation of specific accident or application scenarios (7).

SAFETY DATA, TESTING, AND OPERATIONAL REVIEW

General motor vehicle accident data as well as those applicable to LPG-, CNG-, and LNG-powered vehicles have been compiled and reviewed.

GENERAL MOTOR VEHICLE ACCIDENT DATA - Some pertinent motor vehicle data are presented. These data were obtained from several sources (2,6,10). It can be assumed that the great majority of vehicles involved were gasoline-powered plus a small percentage under diesel power.

In 1980, motor vehicle accidents resulted in 51,077 fatalities and approximately 2.0×10^6 nonfatal injuries of all types. The fatality rate per 1×10^8 vehicle miles was 3.38, per 10^3 registered vehicles 0.3, and per 10^4 licensed drivers, 3.5. Vehicles involved in fatal accidents numbered 63,477 of which fire was reported in 1,720 or 2.7%.* we do not to date have details on fuel type or whether explosions occurred. Fire involvement data in all types of accidents can only be estimated. Some old data suggest that fires occur in approximately 0.1% of all accidents (11). This translates to approximately 12,000 vehicles. Passenger vehicles and light trucks were the major vehicle types involved in accidents, ~80%. Approximately 12×10^6 vehicles of all types were involved in accidents.

Head-on and various angular collision accidents represented the two most prominent multivehicle fatal accident scenarios, each causing approximately 40% of the accidents. (near end collisions accounted for approximately 30%.) Over 60% of fatal accidents involved a single vehicle. The majority of fatal accidents occurred on rural roads, approximately 55%.

Finally, the risk of death occurring in a passenger motor vehicle accident was estimated at 21-26 per 10^9 persons per year (averaged over 25 years).

LPG MOTOR VEHICLE ACCIDENT DATA - Statistics applicable to LPB-powered vehicles are more difficult to acquire and subsequently assess. Although some risk assessments are available for large volume usage of LPG (marine snipping and terminals, storage, rail, and tanker truck shipments, such assessments may not be applicable to individual motor vehicles although selected effects and characteristics of large scale accidents may be pertinent. These large scale accident data and those data concerned with consumer products (stoves, campers, etc.) are not given here.

Ford Motor Company personnel estimate that there are approximately 100,000 LPB-powered vehicles on the US highways (12). Some older studies on the use of LPB as an engine fuel covering a 30-year period listed 18 accidents, 16 injured, and two fatalities. Another

*Communication with National Highway Traffic Safety Administration (August 1982).

Table 3

Safety Ranking of Fuels-Selected Properties

	Ranking Order* >(more hazardous than)
Flammability Range	NG > LPG > G > D
Ignition Energy	Equivalent
Autoignition Temperature	G > NG D > LPG
Diffusion Coefficient	NG > G or G > NG**
Energy Content-Volume	D > G > NG > LPG
Energy Content-Mass	Equivalent
Heat Release Rate	D > G > LPG > NG

*NG, natural gas (methane); LPG, liquefied petroleum gas (propane); G, gasoline; D, diesel.
**Dependent upon confinement.

Table 4

Relative Safety Ranking of Fuels based Upon Secondary Hazard Criteria*

	Leakage	Flammability	Radiation	Volatility (Spill)	Dispersion (Unconfined)
CNG	4	3	1	--	1
LNG	4	3	1	4	3
LPG	3	1	2	3-4	2
Gasoline	2	2	3	2	1
Diesel	1	1	4	1	4

*The assignment of numbers to rank fuels under a given secondary criterion is done qualitatively with the higher numbers suggesting greater degrees of hazard. No mathematical relationship between these numbers exists. Thus, for example, the use of the number 4 does not mean or imply that the fuel so rated is 4 times more hazardous than the fuel rated number 1.

13-year period study listed 174 accidents, most relatively minor. In the Netherlands have approximately 100,000 LPG-powered vehicles in operation. Safety records as reported very good. A number of vehicle fires were reported but no explosions. Full scale safety crash tests on LPG-powered vehicles were accomplished with compact European cars and some city buses. Vehicle storage tanks withstood these tests well with leakage generally contained from other components of the fuel system.

CNG Motor Vehicle Accident Data - Data on CNG-powered vehicles are minimal primarily due to the very few vehicles that were or are in operation. The Atlanta Gas and Light Company operates about 100 vehicles. The company reported four collisions in 1976-78 (two rear end, two side angular, no fire/explosion, no injuries, no fatalities). The company also reports three cryogenic burn incidents during transfer operations. LNG-fueled vehicles have traveled approximately 2.5×10^6 miles since 1975. Full scale safety crash tests on CNG vehicle storage tanks were conducted in 1971 by the US Department of Transportation (DOT) (14).

component testing has been done by Beech Aircraft Corp.

CNG Motor Vehicle Accident Data - Estimated total mileage accumulated by natural gas fueled vehicles since 1970 in the US is approximately 2×10^6 miles. Most of these have been accumulated by the Southern California Gas Company operating approximately 2000 vehicles on CNG. Something over 20,000 vehicles total are reported to be operating on natural gas (CNG and LNG). The total number of accidents involving CNG-powered vehicles is not available but is estimated to be approximately 1500. Very few injuries, no fatalities, a few fires, and no explosions were reported.

Safety impact testing on full scale vehicles of 1959-1968 vintage was accomplished by the US DOT (14). It should be noted that today's American vehicles are constructed quite differently. The Canadian Government has recently completed a series of impact tests (15). Several private concerns have conducted tests on fuel system components, e.g., Gulf Fuel Services.

Operational experience to date as reported by several organizations (in excess of 40) is

said to be very good although many note some technical and psychological disadvantages and have suggested selected improvements (16).

Irrespective of the physical state in which natural gas is stored in the vehicle, vapor leakage into the vehicle is a potential problem. A study by NBS was made concerning vapor seepage into vehicle interiors and recommendations made to minimize this hazard (17).

Additional reviews of safety-related issues concerning CNG-, LNG-, and LPG-powered vehicles are planned. Partial reviews will also be made of large volume LPG and LNG spill tests. The data obtained may prove useful in our final scenario analyses.

SELECTION OF CREDIBLE ACCIDENT SCENARIOS

To pursue the relative safety ranking of alternative fuels further and to assess the hazards due to operation of gaseous-fueled vehicles, it becomes necessary to introduce additional degrees of realism, i.e., boundary conditions. The selection of credible accident scenarios with subsequent analysis is one method of accomplishing the above.

Consensus of opinion was used to select five general scenarios that warrant further analysis. These are believed to be credible in major detail. Although not precisely defined at this time, such definition will be completed shortly. It is recognized that the scenarios can assume worst case situations without definitive boundary conditions or the inclusion of specific risk abatement techniques that either already exist or can be applied. These will be taken into consideration in the final analysis.

The five scenarios include:

- a. Fuel leakage - enclosed garage, parking and vehicle storage
Case A - Residential, attached
Case B - Public, ventilated
- b. Transfer line rupture, break or leak
Case A - Delivery truck station
Case B - User vehicle station
Conditions of venting,
drive-off with nose attached,
leakage will be examined.
- c. Vehicle collision/Fuel loss - Urban
head-on/near end, angular
collisions at major inter-
change or business district
- d. Vehicle collision/Fuel loss - Rural
highway speed and single vehicle
vehicle collision/Fuel loss - Tunnel
high density traffic in jam,
ventilation conditions

For each of the above scenarios the probabilities of the primary hazards occurring as a function of the fuel used will be examined.

RISK ANALYSIS

The operation of gaseous fueled vehicles presents some unknown degree of risk to the

general public. Our efforts will be to determine whether or not such risk is equivalent to, better or worse than that already acceptable using the conventional fuels.

The program effort thus far has not yet reached the analysis stage. Our preliminary thoughts will be to consider existing levels of risk, these to be modified by constraints imposed by the chosen scenarios, and finally to estimate the risks imposed by the use of alternative fuels within those scenarios.

To assist in the risk estimations, it is tentatively planned to elicit information and judgment by convening or mail surveying a group of experts.

Four methods of elicitation of expert judgment will be examined to determine which one is the best for our purpose. The simplest is the staticized group method in which a questionnaire is filled out individually by the members of the group and the results averaged by routine statistical methods. This method is simple, but the results are generally poorer than the other three methods.

The second method is the Delphi method in which the experts reply to a mail survey. The survey results are then circulated anonymously to the group, and the group is asked to submit second round replies to the questionnaire. This process is repeated until the desired consensus is reached. The Delphi method is very time consuming.

The structured interactive group method can be likened to a face-to-face Delphi in that each expert presents his judgment to the group which remains silent to prevent spontaneous interaction. After each expert has made his presentation, the group discusses the judgments and each expert is allowed to modify his judgment in the next round of presentation. The process is repeated until the desired consensus is reached. Like the Delphi method, the structured interactive group method is time consuming.

The fourth method is the group consensus method in which the experts interact face-to-face to arrive at a consensus judgment. Although this method is the simplest in time, careful control by the discussion leader is needed to keep the group on course and careful monitoring is necessary to insure consistency and to insure judgment is not based on groupthink or other factors.

Two analytical approaches to reduce the statistical data, group responses, and expert judgment into an overall risk analysis will be considered. If there is sufficient data to support a fault tree analysis, this well known technique might be chosen. The inadequacy of the problem in the manner pioneered by Fiat could also be used where more weight must be placed on subjective expert judgment (18).

The fault tree analysis is a logical graphical and logical representation of possible fault and normal events for a system which can result in a predefined unwanted event (accident). The unwanted or final top event is

analyzed for various ways by which it may occur. Each subevent is similarly analyzed. One arrives finally at a basic level of events or information where probabilities of occurrence or values are known with a high degree of confidence.

The Saaty pair-comparison technique considers a partitioning of the analysis into several sublevels aimed at generating a specific index value (which can be intercompared) for each fuel within a given scenario. It is basically a scoring methodology. The technical properties of the fuel provide the basis for the buildup of several levels to the final determination of the index value, viz., technical property information--secondary sub-level hazard--primary hazard--index value.

Our current thoughts lean strongly to the use of the group consensus method for elicitation of information and the Saaty technique as a scoring methodology.

ASSESSMENT STATUS

In review, assessment status is as follows:

0. Physicochemical property data assembled
1. General petroleum and vehicle usage data compiled
2. Primary hazards defined
3. Secondary sublevel of hazards defined
4. Fuels ranked based upon both properties alone and on interactive matrix
5. Safety data reviewed
6. Accident scenarios selected
7. Interfuel safety analysis and comparison to be initiated.

REFERENCES

1. Transportation Facts and Trends, 17th Ed. and Supplements, dated April, 1981 and August, 1981, Transportation Association of America, December, 1981.
2. Highway Statistics, US Department of Transportation, Federal Highway Administration, 1980.
3. Petroleum Supply Annual-1981, U.S. DOE, 1981.
4. National Transportation Statistics, US Department of Transportation, report no. DOT-HS-80898, 1981.
5. R. D. Fleming and R. L. Sednoid, "Natural Gas, Methane, Synthetic Natural Gas, and Liquid Petroleum Gases as Fuels for Transportation," West Coast International Meeting, Paper No. 82084, San Francisco, in August 1981.
6. Transportation Safety Information Report, US Department of Transportation, report no. DOT-TSC-RSPA-81-7 (June 1981).
7. J. Hord, "Is Hydrogen Safe?" NBS Technical Note 690, National Bureau of Standards (October 1976).
8. T. L. Bowen, "Hazards Associated with Hydrogen Fuel, Eleventh IECEC Meeting Proceedings, V. 1, Lake Tahoe, CA (September 1976).
9. B. Lewis and G. von Elbe, Combustion, Flames and Explosions of Gases, 2nd Ed., Academic Press, New York (1961).
10. Fatal Accident Reporting System, 1980, US Department of Transportation, National Highway Traffic Safety Administration, report no. DOT-HS-805953 (October 1981).
11. Symposium on Nonpetroleum Vehicular Fuels II, Institute of Gas Technology, Detroit, MI (June 15-17, 1981).
12. D. Schuitz, "LPG-Engine Fuels," Symposium at 75th ASME Meeting, ASME Special Techn. Publ. 825, Los Angeles, CA (June 25-30, 1972).
13. G. van der Weide, "Safety Testing of LPG and Gas-Fueled Vehicles," Symposium on Nonpetroleum Vehicular Fuels, Institute of Gas Technology, Arlington, VA (February 11-13, 1980).
14. Dual-Fuel Motor Vehicle Safety Impact Testing, US Department of Transportation report no. DOT-HS-800622, Dynamic Science, Division of Marshall Industries (Nov. 1977).
15. Transport Canada, Motor Vehicle Traffic Safety Branch, Field Safety Impact Test Program, Winter 1981-1982. (Cited in Canadian Consumer June 1982).
16. T. L. Loyce, "Assessment of Research and Development Needs for Methane-Fueled Engine Systems," Final report for Gas Research Institute, Contract No. 601-81-1-1, March 1981.
17. J. M. Arvidson, G. Hord, G. B. Mann, "Efflux of Gaseous Hydrogen or Methane Fuels from the Interior of an Automobile," NBS Technical Note 600, March 1981.
18. T. L. Saaty, The Analytic Hierarchy Process, McGraw Hill, Inc., New York (1980).

QUESTION AND ANSWER PERIOD

Q: Ralph Fleming, Department of Energy. I'm wondering how you are going to guard against the situation that one of the speakers mentioned this morning, namely, that in referencing property data, have you listed older literature? I suspect some of these numbers you have were determined in the 1920's. How do we know how good those numbers are?

A: This is an unfortunate occurrence in the scientific literature. I have run into this with my own experimental work, in that data tends to get reproduced continually and is actually out of date. Our best bet here is to really go to what you consider your best sources, e.g., people who are working in the field, and attempt to acquire the latest data available, if it's available at all. I might find information through my contacts, I might go to the latest meetings, for example, a particular

fuels and combustion meeting and attempt to contact various people be they in universities or industry.

Q: I wondered how rigid your programmatic restrictions are. Is there any possibility this study might encompass other fuels like methanol? Methanol seems to be emerging these days as the most likely candidate alternative fuel to become available in substantial quantities in this country in this century.

A: I'm not certain to date whether there is a similar study going on with methanol. It certainly should be done sooner or later. But this again becomes a function of both interest and available funding. The Department of Energy should be contacted as to whether or not we will do a program like that.

Research Investigation of Alcohol Usage in Spark Ignition Engines

L. H. Browning, J. F. Nebolon,
and R. K. Pefley
University of Santa Clara
Mechanical Engineering Research
Santa Clara, CA

ABSTRACT

Research investigations of alcohol fuels for automobile engines continues to show alcohols as viable alternative fuels to gasoline. However, some technical problems still need continued research before alcohol fuels enter the public sector. These problems are cold starting, increased engine wear, increased aldehyde emissions and the unknown impact of these fuels on the environment. Research at the University of Santa Clara has continued to center on these problems and a description of this research is presented here.

THROUGH 14 YEARS OF CONTINUED RESEARCH on the use of alcohol fuels in automotive spark ignition engines, the basic alcohol fuels (methanol and ethanol) have been shown to be efficient, clean burning fuels for automotive use [1,2,3].* However, before these fuels can become totally commercialized, there are still some problems that need to be solved. These problems are cold starting, engine wear, aldehyde emissions and the unknown impact of these fuels on the environment. Each of these problems has been identified and research is continuing to solve them. The following paper will explain some of the research being done at the University of Santa Clara relative to these problems.

COLD START STUDIES

Cold startability of alcohol fueled vehicles is an important issue since the method used for starting can effect cold start emissions, engine wear and warm-up driveability. Cold starting of a spark ignited alcohol vehicle without auxiliary starting aids is presently limited to

about 7 C due to the low vapor pressure of these fuels[2,3]. In order to enhance the cold starting of alcohol fueled vehicles, several auxiliary starting aids have been tried. These include gasoline injection, iso-pentane and di-methyl-ether as fuel additives, ether injection, electric heat addition (vaporizers), and dissociation of methanol into carbon monoxide and hydrogen.

Three observations can be drawn from the study of these auxiliary starting techniques. The first and most important is that the period immediately following a successful cold start, the warm-up period, is the most difficult to improve. Even with exhaust heating of the intake mixture, there is a short period of time during which intake temperatures drop instead of rise and a smooth idle is difficult to obtain. This fact leads to point two: an auxiliary fuel system (i.e., gasoline or related fuel) cannot be a simple one-shot device. Rather it must be capable of fuel delivery through at least part of the warm-up period and this greatly complicates the necessary hardware. Thirdly, no reasonable, single, auxiliary cold starting technique was capable of satisfactory start and warm-up performance other than auxiliary fuels such as dissociated methanol, gasoline, di-methyl-ether or butane tailored for cold starting and warm-up operation. From these statements, one concludes that the best solution to the cold starting problem has not yet been developed.

Droplet transport and vaporization may be part of the solution to cold starting and warm-up problems with alcohol fuels and is currently our area of emphasis. This area is being studied through both computer models of the cold start engine processes and an experimental study in which an engine is mounted in a refrigeration chamber with instrumentation to measure the vaporization process.

* Numbers in brackets designate references at end of the paper.

COMPUTER MODELS - In order to study droplet transport and vaporization, a sophisticated one-dimensional, two-phase flow computer model which simulates the gas exchange and compression processes occurring in a spark-ignition engine has been developed. The model solves the basic unsteady conservation equations for both gaseous and liquid components at each node in the intake runner and engine cylinder at each time step. Thus 13 derivative equations are solved at each of 20 nodes during each time step during a cold starting event. While the time intervals are determined by an error criteria, the average time step is approximately 0.0025 crank angle degrees. This model is written in Fortran and executes one complete cranking cycle on a CDC 7600 computer in approximately 200 CPU seconds. A color graphics display is then used to visually study the droplet transport and vaporization processes occurring in the intake runner and engine cylinder during a cold start event.

Initial studies, however, have broken this model into two sub-models. These are droplet transport down the intake runner, and compression of the gas and droplet mixture in the engine cylinder. The results from these two sub-models are presented here.

The droplet fall-out and sling-out sub-model is used to examine the fate of droplets in the intake manifold. In this model, plugged flow along a two-dimensional intake runner was assumed and the conservation of momentum equation was solved in Lagrangian form. Droplet transport was calculated from drag forces imparted to the droplet, while gas velocity was assumed constant along the intake runner. In Figure 1, a gas velocity of 275 cm/sec was used to simulate a cranking speed of 200 RPM. Droplet trajectories for various sized droplets are plotted within the runner.

As can be seen from this figure, the 10 and 25 micron droplets will enter the cylinder while a 50 micron droplet will fall out of the air stream before entering the cylinder. The 100 micron droplet is shown to be slung out in the manifold corner. This is due the fact that the larger droplets have higher downward momentum during travel in the down-draft portion of the intake runner.

Figure 2 shows the effect of air stream velocity (or cranking speed) on the trajectory of a 50 micron droplet. As can be seen from this figure, the slower the air stream velocity (slower cranking speeds), the larger the chance of the droplet entering the cylinder.

The second sub-model examines the fate of droplets during the compression process. It assumes that all the fuel is in droplet form at the beginning of the compression stroke. Both heat transfer and droplet vaporization are allowed to occur during the compression process. Figure 3 shows the cylinder pressure during the compression stroke for air only, air plus methanol, and air plus ethanol. The starting conditions are 298.15 K, 0.775 atm, a compression ratio of 10 to 1, a cranking speed of 200 RPM and a stoichiometric mixture of liquid fuel droplets and air. Initial droplet size is set at 50 microns. As can be seen in this figure, there is a substantial reduction in final cylinder pressure due to fuel vaporization in the air plus fuel cases. As expected, methanol shows the greatest reduction in final cranking pressure due to its very large heat of vaporization and its larger fuel mass for a stoichiometric mixture in comparison to ethanol.

Figure 4 shows the cylinder temperature versus crank angle for the same comparison. As expected methanol shows the greatest reduction in final cylinder temperature due to its high heat

INTAKE MANIFOLD DROPLET FALL-OUT AND SLING-OUT MODEL
AIR STREAM VELOCITY: 275 CM/SEC

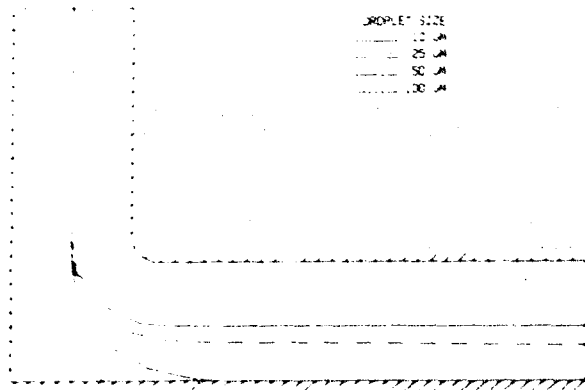


FIGURE 1. DROPLET SIZE EFFECTS ON DROPLET TRAJECTORY

INTAKE MANIFOLD DROPLET FALL-OUT AND SLING-OUT MODEL
DROPLET SIZE: 50 MICRONS

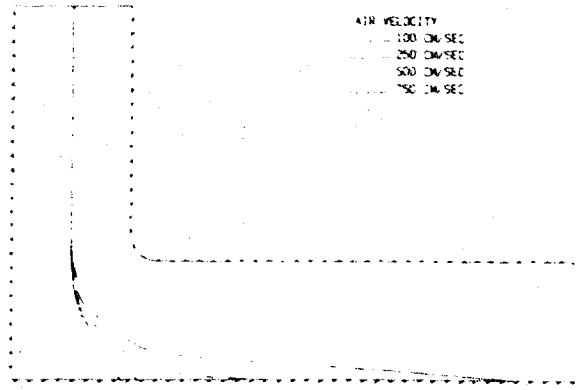


FIGURE 2. CRANKING SPEED EFFECTS ON DROPLET TRAJECTORY

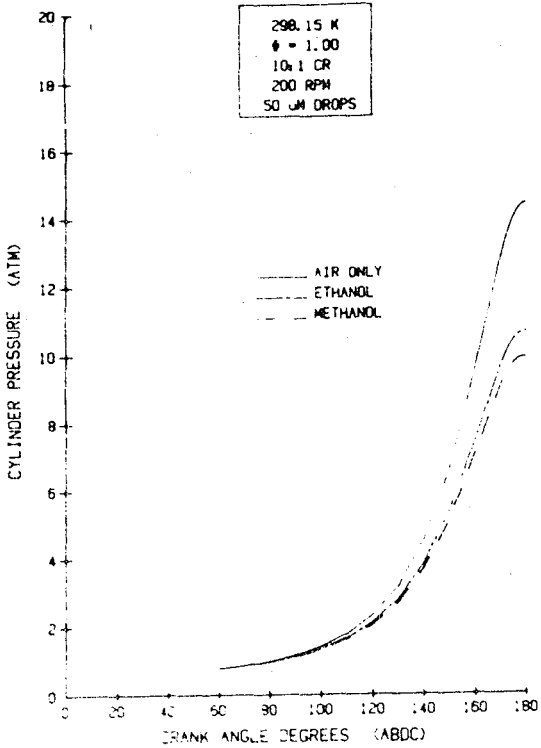


FIGURE 3: CYLINDER PRESSURE FOR ROOM TEMPERATURE CRANKING

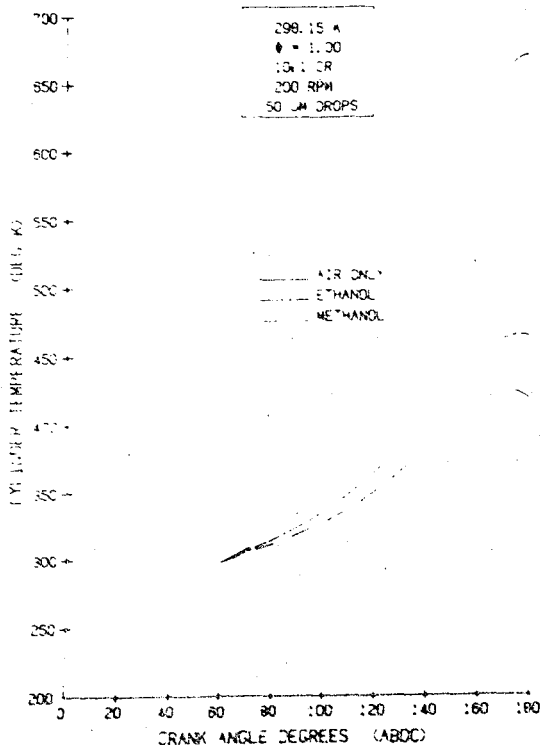


FIGURE 4: CYLINDER TEMPERATURE FOR ROOM TEMPERATURE CRANKING

of vaporization and increased fuel mass. Figure 5 shows fuel vapor/air equivalence ratio (lower curves) and droplet size (upper curves) during the compression process for the above comparison. As can be seen both methanol and ethanol are above the lean flammability limit (approximated here as 0.63) at the end of the compression stroke for room temperature cold starting. It also shows that ethanol droplets vaporize more readily due to the lower heat of vaporization and lower fuel mass.

The same comparison is shown in Figure 6, but for a starting temperature of 0 C instead of room temperature as in the previous graphs. As shown in this figure, the methanol vapor/air equivalence ratio is below the lean flammability limit at the end of the compression stroke while ethanol is above. Thus a methanol fueled engine cannot be started under these conditions without additional starting aids.

Figure 7 shows the effects of various droplet sizes on fuel vapor/air equivalence ratio during the compression stroke at a starting temperature of 0 C. As can be seen from this figure, droplet size is very important in the startability of a spark ignition engine. The figure shows startability of a methanol engine with 10 micron sized droplets, while the 30 and 50 micron droplets do not provide a flammable mixture at the end of the compression stroke.

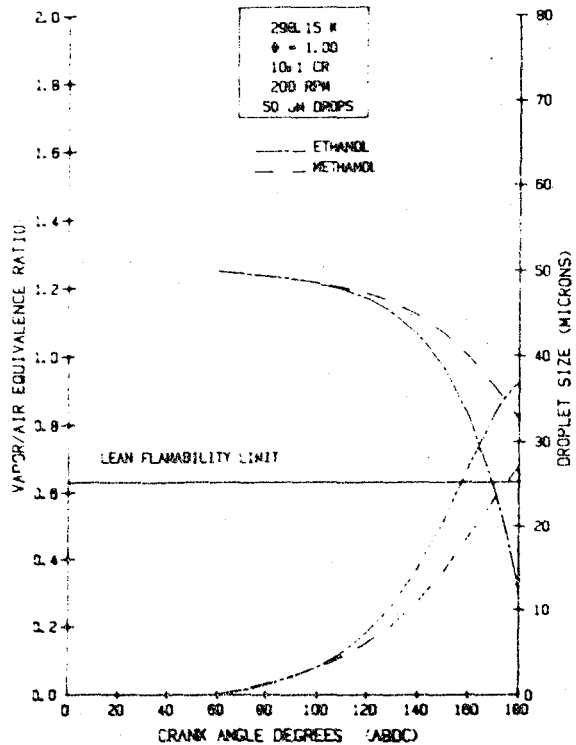


FIGURE 5: FUEL EFFECTS FOR ROOM TEMPERATURE CRANKING

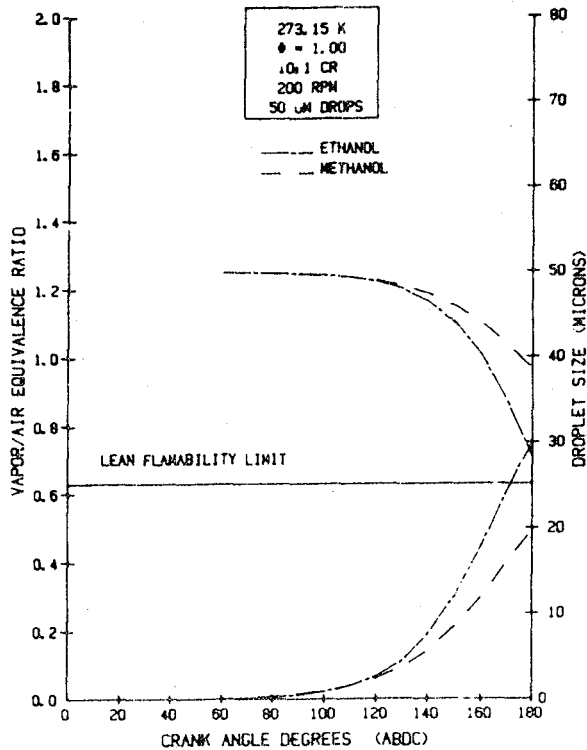


FIGURE 6: FUEL EFFECTS AT 0 C CRANKING

Figure 8 shows the effects of cranking speed on droplet vaporization. As can be seen from this figure, the slower the cranking speed, the more time there is available for droplet vaporization. Still, even with a cranking speed of 100 RPM, the 50 micron droplets do not provide a flammable mixture at the end of the compression stroke with a starting temperature of 0 C.

Figure 9 shows the effects of compression ratio on startability of a methanol mixture of 50 micron drops with a starting temperature of 0 C. As can be seen from this figure, modest changes in compression ratio have only a slight effect on final vapor/air equivalence ratio. However a very high compression ratio like those seen in diesels, can provide a flammable mixture while normal compression ratios can not, especially with the fine atomization of the diesel injector.

EXPERIMENTAL STUDY - In order to provide experimental verification of the findings thus presented, an engine mounted in a refrigeration chamber is instrumented to record cylinder pressure and temperature during a cold starting event. Figure 10 shows a schematic of this experiment.

The theory behind the cold chamber experiment is based upon a simple energy and mass balance of the mixture trapped in the cylinder during the compression stroke. The energy balance includes cylinder leakage and heat transfer to the

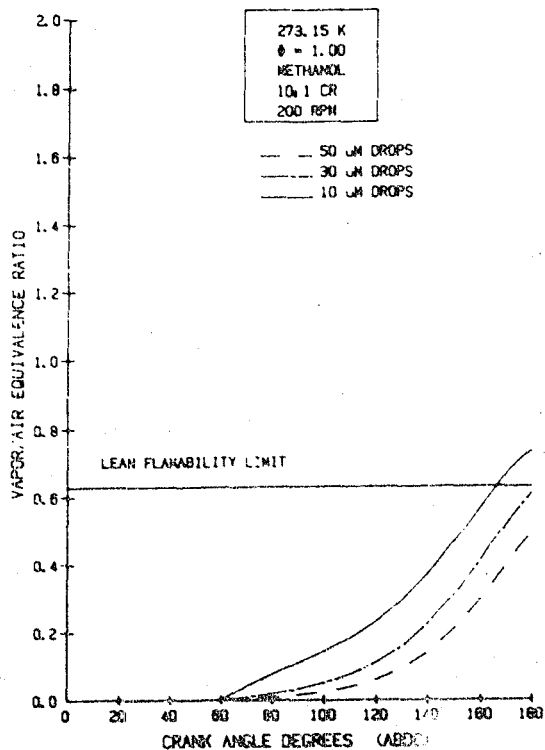


FIGURE 7: DROPLET SIZE EFFECTS AT 0 C CRANKING

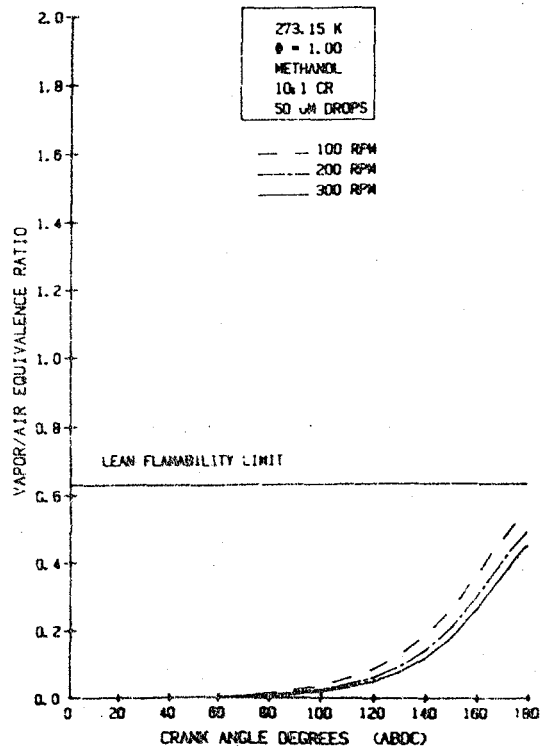


FIGURE 8: CRANKING SPEED EFFECTS FOR 0 C CRANKING

cylinder walls. Droplet fall-out and vapor condensation are not modeled at this point. Leak rates are determined from a dynamic pressure measurement in which the cylinder is charged with compressed air at constant piston position. Once the leak rate is known, an estimate of heat transfer can be obtained by comparing the measured air-only cycle to a cycle computed using the calculated leak rate and the conservation equations. With the leak and heat transfer rates quantified, the quantity of fuel vaporized per unit time is backed out of the calculations by comparing the calculated pressure trace to the air plus fuel cycle. While this approach is less sophisticated than the one-dimensional, two-phase computer model mentioned above, the two approaches work hand-in-hand in providing a better understanding of the fuel vaporization process.

Measurement of droplet vaporization during the compression stroke opens a number of interesting research possibilities. The first application is

to be an investigation of droplet behavior to reduce the temperature at which pure alcohol engines will start and warm-up satisfactorily. Other applications include the effect of droplet vaporization upon the compression work of a running engine. It has been hypothesized that with alcohol fuels this effect upon efficiency can be significant. Regarding combustion modeling, with the state of the mixture known at the time of ignition, more accurate modeling of warm-up performance and exhaust emissions is possible.

ENGINE WEAR

Engine wear resulting from the use of alcohol fuels has been documented by several researchers [4,5,6,7]. It appears that alcohol increases wear in automotive engines from 2 to 10 times that in gasoline engines depending on engine type, driving and climactic conditions. The reason for this increased wear is not well understood, although many speculations of possible wear mechanisms have been made. Research at the University of Santa Clara has examined wear by examining the major factors which relate to wear and corrosion in automotive engines.

The most serious engine corrosion and wear problems appear related to the differences in the products of combustion among the alcohols and gasoline. The effects of excessive cylinder wear, rust colored compounds formed on iron parts bathed in oil and crankshaft bearing failures are believed to stem from two sources:

(1) The increased water formed by combustion of the alcohols which elevates the dew point temperature of the exhaust products.

(2) The increased acidity of the condensate formed on cold surfaces.

The calculated dew point temperatures for methanol, ethanol and gasoline when burned stoichiometrically in dry air at one atmosphere are shown in Table I along with the measured pH values of the condensate. The condensate was obtained by passing exhaust gases from the engine exhaust (ahead of the catalys through a carbon dioxide cold trap.

The high dew point temperature for methanol combined with its high heat of vaporization clearly indicates that the warm-up time for a gasoline engine converted to methanol will be significantly extended. In addition, the amount of combustion condensate and unburned fuel collected on the cold cylinder walls, valves and piston faces is estimated to be twice that of gasoline because of the extended warm-up time and elevated dew point temperature. When these factors are combined with the measured pH values of the condensate, a major source of corrosion and wear in methanol engines is identified.

One last mechanism which needs to be explained is the fact that the presence

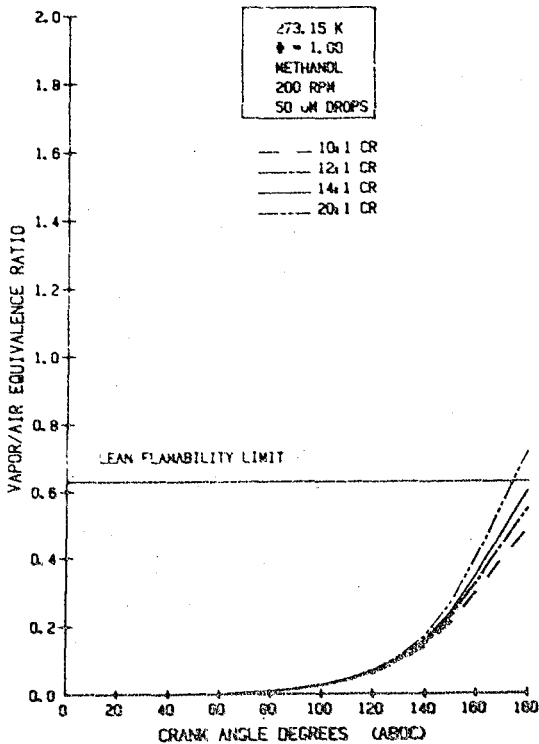


FIGURE 9: COMPRESSION RATIO EFFECTS FOR 0 C CRANKING

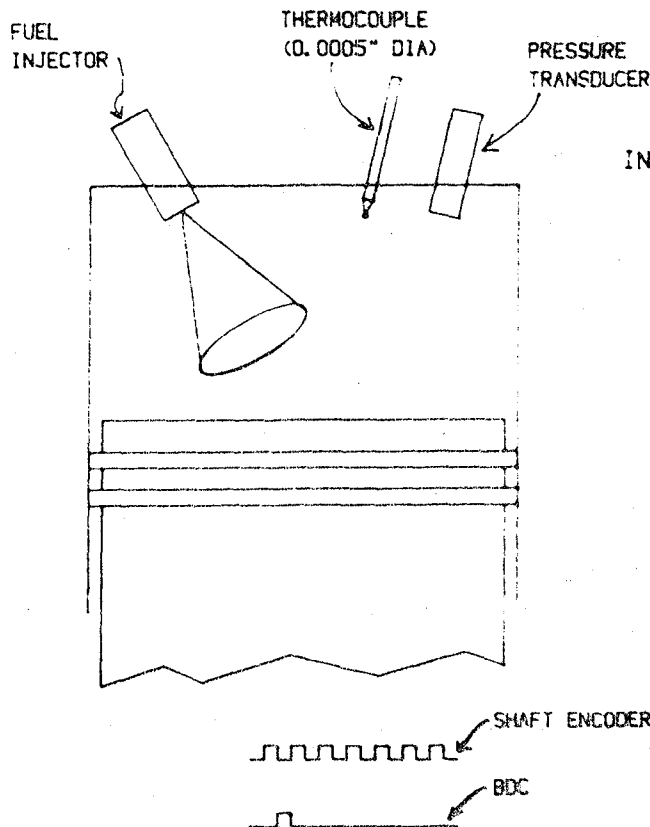
TABLE I: COMBUSTION CONDENSATE FACTORS

FUEL	COMBUSTION CONDENSATE PROPERTIES	
	DEW POINT TEMPERATURE (C/F)	pH
METHANOL	23.5/146.5	1.94
ETHANOL	58.5/137.5	2.24
GASOLINE	52.0/126.0	2.76

of alcohol in the condensate significantly reduces the surface tension of the condensate. Simple experiments with watch glasses coated with engine lubricating oil indicate that methanol added to a drop of water enables it to spread on the oil film possibly reaching the glass surface. With acid added to this condensate, a corrosion theory can

be developed which can explain the severe corrosion and wear encountered in alcohol engines. The alcohol in the water may provide a conduit through the thin oil films plated on the iron cylinder which will allow the acids in the condensate to attack the bare iron surface. Acids, such as nitric and formic which produce hydrogen ions, can cause local cell corrosion forming compounds such as $Fe(OH)_3$, $Fe(HCOO)_3$ and $Fe(NO_3)_3$ which are of lower density than the base metal. These compounds are easily removed by the sliding surfaces, thereby causing rapid wear.

In order to understand the high pH values in the methanol condensate, equilibrium calculations of methanol, ethanol and gasoline exhaust were done using a NASA chemical equilibrium program[8]. This study showed that formic acid ($HCOOH$) was formed at high temperatures and was highly temperature dependent. Figure 11 shows comparisons of the exhaust of methanol, ethanol and gasoline at 1800 K as this represented the high end of exhaust temperatures. As can be seen in this figure, equilibrium



INSTRUMENTS AND MEASURED QUANTITIES

- CYLINDER GAS PRESSURE
- CYLINDER GAS TEMPERATURE
- THROTTLE & CHOKE ANGLE
- MANIFOLD VACUUM
- ENGINE SPEED
- ENGINE TEMPERATURES
- MASS FUEL INJECTED/STROKE
- SHAFT ENCODER
- PDP 11/03 DATA ACQUISITION SYSTEM

FIGURE 10: 2.3 LITER TEST ENGINE IN COLD CHAMBER

calculations do not show significant differences between the three fuels but do show that formic acid formation favors rich mixtures.

Another possible acid existent in the exhaust from these fuels is nitric acid (HNO₃). It can be formed from NO₂ at low temperatures and the equilibrium exhaust concentrations for the three fuels are shown in Figure 12 at 600 K as this represents the low end of exhaust temperatures. Nitric acid is shown to form in lean mixtures, but again there is little difference between the three fuels. However, high NO₂ concentrations (far above equilibrium concentrations) are found in the blow-by gases which might promote the formation of nitric acid at the low temperatures found in crankcase conditions. Further studies which involve chemical kinetics need to be done fully understand the mechanisms of corrosion and wear.

ALDEHYDE EMISSIONS

Aldehyde emissions from alcohol fueled spark ignition engines are typically higher than those from gasoline fueled engines. It is generally accepted that aldehydes are formed from lean partial combustion of alcohols and are primarily formed in the exhaust system (9,13). An exception to this rule

is when alcohols are burned at rich stoichiometry in an engine with an exhaust catalyst and an air pump. Under these conditions, the catalyst can actually form aldehyde emissions from the unburned fuel and injected air particularly under lower exhaust temperature conditions such as during extensive idling. These conditions duplicate the standard methods for making aldehydes in the chemical industry. These conditions occurred with several U.S. Postal Service vehicles converted to alcohol which led to a temporary suspension of fleet operations. The difficulty stemmed from the previously mentioned factor and the fact that the mixture of the vehicles was inadvertently set too rich. This latter condition has since been corrected. Additionally the driving cycles for these vehicles (10 miles/day) are such that the catalyst never gets above warm condition. Studies of this phenomenon and solutions to this problem are currently underway.

The experience the U.S. Postal Service is having should be noted for two reasons:

(1) Aldehyde emissions (and more importantly carbon monoxide emissions) from alcohol fueled and gasoline vehicles can become serious problems for the vehicle operator.

(2) Long before this level is reached,

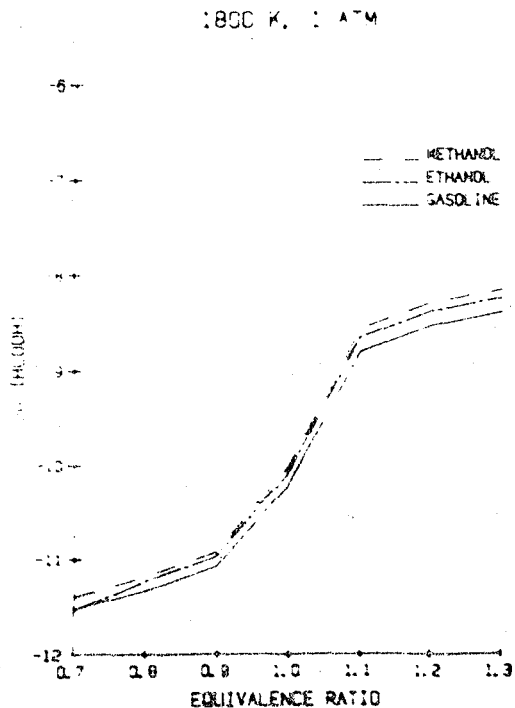


FIGURE 11: EQUILIBRIUM FORMIC ACID CONCENTRATIONS

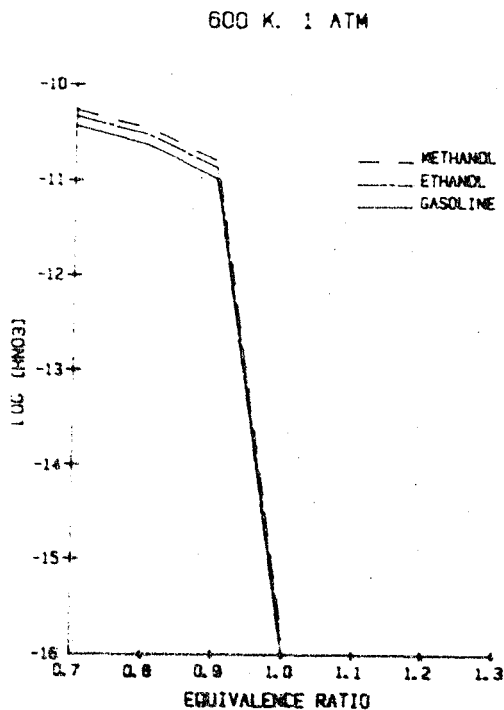


FIGURE 12: EQUILIBRIUM NITRIC ACID CONCENTRATIONS

lower levels of formaldehyde and carbon monoxide may pose health problems to operators exposed to partially reacted exhaust for extended periods as they may exceed OSHA carbon monoxide safety standards or aldehyde levels above 1 ppm where health effects are noted[11].

Figure 13 compares aldehyde emissions from an in-tune vehicle (PS #2) to an out-of-tune vehicle (PS #10) from the U.S. Postal Service alcohol fleet. As shown in this figure, PS #10 emitted 2 to 3 times the aldehyde emissions of PS #2. The over-rich condition was due to both the sinking of the carburetor float due to methanol absorption and to an overly rich idle speed carburetor jetting. When both these problems were corrected the emissions from PS #10 were brought into line with PS #2.

While carbon monoxide emissions are not shown in Figure 13, PS #10 emitted 3 to 4 times the carbon monoxide emissions of PS #2. Replacement of the carburetor float, however, made little difference in carbon monoxide emissions in comparison to PS #10 as received.

ENVIRONMENTAL IMPACT

The storage, distribution and use of chemically pure methanol fuel appears to have a beneficial environmental effect in comparison with the storage, distribution and use of gasoline or distillate fuels. However, more detailed modeling studies are needed to account for the net changes in emissions inventories under various end-use scenarios in the stationary and transportation sectors. In addition, the photochemistry of methanol should be validated when hydrocarbon emissions and methanol emissions are combined in computer models to predict urban ozone pollution effects.

The interactive photochemistry of methanol emissions with the existing

fossil fuel emissions is currently being studied in a photochemical smog chamber at the University of Santa Clara. Earlier studies with this smog chamber have shown methanol and ethanol to be relatively unreactive in creating photochemical smog. Aldehyde emissions, however, increase the photochemical reactivity of the alcohols[2].

A cryogenic trapping and gas chromatography technique has recently been developed to measure hydrocarbon concentrations down to a few parts per billion. Chamber characterization studies are underway in parallel with a series of baseline urban mixture experiments. Multi-client support is being sought for the experimental work and subsequent photochemistry validation and computer modeling studies.

In contrast to the anticipated atmospheric benefits from the use of pure alcohol, blending of volatile hydrocarbons into methanol for cold start and driveability reasons, may increase the mass emission rate and the reactivity of the blended fuel's evaporative and exhaust emissions. These effects are also currently under study for the most likely fuel blends of methanol and iso-pentane or gasoline.

CONCLUSIONS

Alcohol fuels are clean burning, efficient fuels for automotive use. The alcohols provide some continuity in international fuel supplies since alcohols can be produced by even underdeveloped nations. Production of alcohol as an alternative fuel to gasoline is already begun in Brazil and is the top most choice of several other nations. However before complete commercialization of alcohol fuels can begin, some technical problems need to be solved. These problems are cold starting, increased engine wear, increased aldehyde emissions and the unknown impact of alcohol fuels on the environment. Research is continuing to study these problems and solutions are within reach.

ACKNOWLEDGEMENTS

This work was funded under NASA-Lewis Research Center Grant No. NAG 3-143.

REFERENCES

1. R.K. Pefley, L.H. Browning, W.E. Likos, M.C. McCormack and B. Pullman, "Characterization and Research Investigation of Methanol and Methyl Fuels," ERDA Contract No. EY-76-S-02-1258, University of Santa Clara Report No. ME-77-2, 1977.
2. R.K. Pefley et al., "Characterization and Research Investigation of Alcohol Fuels in Automobile Engines," Final Report, DOE Contract No. DE-AC03-78CS, University of Santa Clara Report No. ME-81-1, 1981.

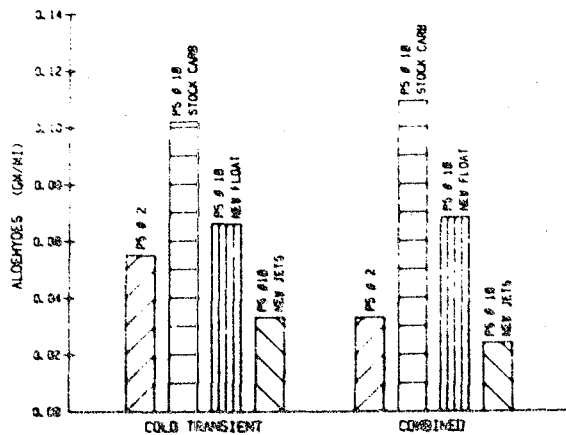


FIGURE 13: FTP ALDEHYDE EMISSION RATES

3. R.K. Pefley et al., "Research and Development of Neat Alcohol Fuel Usage in Automobiles", a Six-Month Progress Report, NASA-Lewis Contract No. NAG 3-143, July 1981.
4. R.K. Pefley, "Alcohol Fuel Corrosion and Wear Effects," presented at the UNIDO Conference in Dehra Dun, India, October 1982.
5. W. Baisley and C.F. Edwards, "Emission and Wear Characteristics of an Alcohol Fueled Fleet Using Feedback Carburetion and Three-Way Catalyst," Proceedings of the IV International Symposium on Alcohol Fuels Technology, Guaraja, Brazil, October 1980.
6. E.C. Owens et al., "Lubrication Requirements for Alcohol-Fueled Spark Ignition Engines," Proceedings of the IV International Symposium on Alcohol Fuels Technology, Guaraja, Brazil, October 1980.
7. G.K. Chui and R.E. Baker, "Lubrication Behavior in Ethanol-Fueled Engines," Proceedings of the IV International Symposium on Alcohol Fuels Technology, Guaraja, Brazil, October 1980.
8. S. Gordon and B.J. McBride, "Computer Program for Calculation of Complex Chemical Equilibrium Compositions, Rocket Performance, Incident and Reflected Shocks and Chapman-Jouquet Detonations," NASA Report No. SP-273, 1971.
9. L.H. Browning and R.K. Pefley, "An Analytical Study of Aldehyde Formation During the Exhaust Stroke of a Methanol-Fueled SI Engine," Proceedings of the IV International Symposium on Alcohol Fuels Technology, Guaraja, Brazil, October 1980.
10. K. Ito and T. Yano, "Formaldehyde Emissions from a SI Engine Using Methanol," Proceedings of the III International Symposium on Alcohol Fuels Technology, Asilomar, California, May 1979.
11. "Formaldehyde and Other Aldehydes," Report to the National Research Council, National Academy Press, 1981.

QUESTION AND ANSWER PERIOD

- Q: Robert Potter, General Motors. Regarding your slide 4, I believe isn't one of the major factors in the cylinder temperature the mass of methanol compared to the mass of ethanol? I mean since the stoichiometric air/fuel ratio of ethanol is 9:1 compared to 6.5:1 for methanol, approximately 40% of the reduced cylinder temperature effect could be due to the differences in the fuel mass as well as their differences in latent heat of evaporation.
- A: Certainly that is true. There is a difference in mass agreeably and when you are talking about stoichiometric mixtures, you definitely have less ethanol than methanol in the cylinder. But the latent heats of vaporization are also distinctly different. I think both effects are there.
- Q: Jerry Panzer, Exxon Research. Maybe I missed something in what you said, but when you talked about the concentration of nitric acid in the exhaust, I was wondering why it didn't peak a little lean of stoichiometric like nitrogen oxides do?
- A: These calculations were equilibrium concentrations at a constant exhaust temperature and thus the adiabatic flame temperature trend with equivalence ratio was removed from the trends. If nitric acid concentrations were calculated at the adiabatic flame temperature, you would see a peak slightly lean of stoichiometric.
- Q: Roberta Nichols, Ford Motor Company. On your lean flammability limit, is that at atmospheric pressure?
- A: It's actually figured at ten atmospheres, i.e. end of compression type pressures. The data was taken from a minimum ignition energy study figuring approximately the amount of energy a typical spark would generate under typical conditions, i.e. end of compression type conditions.
- Q: Second question. Have you looked at the possible effects, and correct me if I'm wrong, of the fact that you are starting the postal fleet with ether on aldehyde formation? Since ether is injected whenever you turn on the key, is it possible that the increased aldehydes you found were due to the use of ether?
- A: I don't believe so. We have done tests on standard driving cycles and basically the vehicles showed very high aldehydes even for a combined driving cycle including the hot transient. In fact, the differences between the in-tune and out-of-tune vehicle for this situation were almost three-fold on the combined cycle. So it existed both when the catalyst was hot and cold. The postal service situation was a little different. The postal workers were driving the vehicles up against the loading dock and leaving them at idle for a considerable period of time. Under these conditions the CO would probably cause them headaches anyway but at least the aldehydes told them it was time to get out of the area. In that sense maybe it's a safety feature but it's not a very good one.
- Q: The methanol used in the postal fleet, was it primed with butane or higher alcohols or anything?
- A: No it was neat methanol. We only use ether injection for cold starting.
- Q: Granger Chui, Ford Motor Company. What is the driving force for vaporization rate in your model? Does temperature or pressure have the more significant effect?
- A: Basically the evaporation rate in the model is driven off the saturated vapor pressure. But the amount of fuel vaporized during the compression stroke is nowhere near the saturated state. The evaporation rate is slow enough during the compression stroke, such that the saturated vapor pressure is never reached.
- Q: David Elliot, Ontario Ministry of Transportation. I'd like to refer to slide 2 where you talked about the effects of air velocity on the stability of the drops. I guess that because they're turning a corner, the heavier drops are slung-out against the wall. Is that right?
- A: That's right. It's basically the downward velocity in that case. Heavier droplets maintain the downward momentum through the turn and hit the bottom of the manifold.
- Q: Does the cranking speed really have any benefits on cold starting?
- A: Basically it was found that cranking speed made very little difference on whether the droplets entered the cylinder or not. You are going to need very fine droplets to even enter the cylinder under cranking conditions and thus cranking speed need not be considered as a primary variable in transporting fuel into the cylinder. Practically, as we all know, cranking speed has a great deal to do with cold starting but not in the transport of the fuel droplets.

Evaluation of Fuel Additives to Reduce Engine and Fuel System Material Problems with Methanol-Gasoline Blends

C. F. Rodriguez and J. P. Cuellar, Jr.
Southwest Research Institute

ABSTRACT

Commercial fuels were screened for inhibition of material incompatibilities with methanol-gasoline blends. The additives, chosen to provide a diversity of applications and chemical types, were tested at four methanol concentration levels. Corrosivity tests were conducted on metals commonly used in automotive applications. Polymeric materials—elastomers, plastics and cork—were tested for compatibility with the methanol blends. As a result of these tests half of the additives were subjected to further testing in search of optimal application conditions. The completed screening phase indicated three additives which inhibit corrosive effects of the blends on some metals; no effects were noted in the polymeric materials. Optimization continues with a reduced number of additives, materials, and methanol blends.

METHANOL produced from coal has the potential of becoming a major contributor to this country's alternative fuels inventory. Methanol blended with gasoline has already been and is being tested in automotive fleets of various types. The Department of Energy's Alternative Fuels Utilization Program (AFUP) provides the planning base upon which the compatibility of methanol-containing fuels and other related methanol applications questions may be investigated. (1,2)* The results to date have been encouraging; however, some technical problems have arisen. Among these problems are those associated with corrosion of metal engine parts and deleterious effects on polymeric materials used in automotive fuel systems. This report summarizes the progress made up to this time of the project having the main objective of

identifying, obtaining and evaluating commercially available fuel additives that might be applicable to reduction or elimination of engine and fuel system material deterioration in methanol fuel blends.

Although in new vehicles it may be possible to use improved materials that are not subject to attack by methanol-gasoline blends, it is necessary to seek protection for existing systems. The use of currently available fuel additives to overcome these material compatibility problems is apparently a more realistic approach available at this time. A methanol/t-butyl alcohol mixture containing a corrosion inhibitor has been developed for use with unleaded gasoline in blends which must meet the EPA legal limit for oxygen content. Concern arises because of the waiver requests which have been made for an increase in oxygen content. Knowledge of the material effects of blends of higher methanol content is incomplete, and this investigation was initiated to seek such information.

PROJECT ORGANIZATION

The project was organized into two main parts: the screening task in which six additives were obtained and evaluated followed by the optimization task in which three additives exhibiting some apparent protective effects were further evaluated. The two tasks were further divided into subtasks as shown below:

TASK I - Initial screening tests were conducted with the six additives in methanol-gasoline blends.

SUBTASK IA - Fuel blends were prepared containing methanol, gasoline, 2-butanol, and the six additives.

SUBTASK IB - Metal corrosivity tests were conducted according to recommendations of applicable ASTM and NACE standards. Elastomer and plastic compatibility tests and physical property determinations were conducted according to the appropriate ASTM standards.

*Numbers in parentheses designate references at end of paper.

SUBTASK IC - Results of the corrosivity and compatibility tests were evaluated relative to results from baseline unleaded gasoline neat and blended with methanol.

SUBTASK ID - Three additives were chosen for further testing in the optimization task.

TASK II - The three additives chosen in the preceding task were formulated singly and in binary combinations with methanol-gasoline blends for testing to determine if higher concentrations or combinations of additives would produce the desired optimum protective conditions.

SUBTASK IIA - Fuel blends containing the additives chosen in subtask ID were prepared for further corrosivity and material compatibility testing.

SUBTASK IIB - Corrosivity and compatibility testing are being conducted with the materials and fuel blends formulations chosen in Task I.

SUBTASK IIC - At the end of the test period the effectiveness of the three additive formulations in methanol fuel blends will be evaluated with respect to reference unleaded gasoline and methanol blends.

EXPERIMENTAL PROGRAM

The program was divided into six 30-day periods during which two 30-day periods were required for corrosivity determinations. The materials compatibility testing periods require shorter periods and were conveniently conducted during the corrosivity test periods. These two test periods began at approximately the one-third and two-third points of the program term. The remainder of the time went to acquisition of reagents and materials; preparation of test specimens, fuel blends, and testing equipment; and the evaluation of results.

ADDITIVES - A broad range of applications and chemical types of corrosion inhibitors was sought by canvas of 16 major suppliers of fuel additives. The suppliers were requested to recommend candidate materials and provide any available technical information. The suppliers proposed 13 commercially available corrosion inhibitors for which they would provide formulating instructions and other technical information. In consultation with the NASA Project Manager we chose the six additives described below. The concentrations listed were recommended by the suppliers, all of whom indicated some corrosivity testing had been conducted with their additives but only one provided the results of tests with ethanol. The cost of formulating these additives ranged from \$3.50/1000 bbl for A to \$232.50 for C and \$7,635.00 for F. The suppliers also said that no modification of incompatibilities between fuel and polymeric materials could be expected. They suggested the one thing we could look for was that the additives would not worsen the deleterious effects of the fuel blends.

ADDITIVES

Test Code	Inhibition Type	Chemical Type	Concentration lb/1000 bbl
A	Corrosion	Organic Acid	5
B	Rust-Fuels and Lubricants	Acylated Amines in Organic Hydrocarbons	3
C	Corrosion	Organic Acid	100
D	Corrosion	Substituted, High Molecular Weight Succinic Acid	2 x vol % Methanol
E	Rust and Anti-icing	Organic Acid	15
F	Rust-Circulating Oils	Fatty Acid Amine	1,936

The additives chosen for further testing in Task II, B, D and E were formulated in the following manner:

ADDITIVE CONCENTRATIONS

Formulation Number	Additives Used	Concentration lb/1000 bbl
1	D	2 x vol % Methanol
2	B	9
3	B D	3 2 x vol % Methanol
4	B D	9 2 x vol % Methanol
5	B E	3 15
6	D E	2 x vol % Methanol 15

The additives formulated in this way will allow us to observe any effects of increased concentration and/or combination of the additives in addition to conducting confirmatory repetition at previous additive concentrations.

FUEL BLENDS - Methanol-gasoline blends were not expected to exhibit highly corrosive effects on most metals under the proposed test conditions. In order to make it more likely that some effects would be induced, we chose a broad range of methanol concentration, 2.5 - 20 vol %, for the initial series of tests. The unleaded gasoline (24% aromatics) containing only antioxidant and metal deactivator additives is a typical South Texas fuel

obtained locally. Technical (99.98%) grade methanol used to make the fuel blends contained traces of acetone and formaldehyde and 0.06% (vol) water. Isobutanol was chosen as the cosolvent since it provides good water solubility properties with methanol and gasoline containing 15% aromatics.

Fuel blends for the screening tests were made in the following proportions as volume percentages:

TEST SOLUTIONS

<u>Gasoline</u>	<u>Methanol</u>	<u>2-Butanol</u>
76	20	4
88	10	2
94	5	1
97	2.5	0.5

Additives were dissolved in the baseline gasoline at twice the desired final concentration and diluted with the appropriate amount of gasoline to achieve a 1:1 dilution of the additive when mixed with the alcohols. The alcohols were mixed in the proper proportions and water was added to give a final concentration of 1.25% by volume in the test solution. The alcohol mixture was then added slowly to the gasoline with constant agitation to ensure complete mixing and keep the water from separating.

Test solutions for Task II were made in the same manner except the methanol concentrations were decreased to three levels, 5, 7.5, and 10% by volume. Greater care was taken in mixing the alcohols and gasoline in order that the higher concentrations of additives did not cause the water to separate.

SOLUTION CORROSIVITY - Ten metals used in automotive fuel systems were used for the corrosivity determinations. Aluminum, zinc, carbon steel, stainless steel, terneplate, cast iron, brass, bronze, magnesium and copper were obtained in 1-mm thick coupons, 50-mm long by 13-mm wide. The metal specimens were prepared for testing by washing in a volatile organic solvent, polishing with a fine grit abrasive cloth, rinsing with the organic solvent, and drying. Although there are no standard methods available for corrosion testing, there are recommendations (3-8) which were followed wherever applicable to these experiments. Each specimen was suspended halfway in 250 ml test solution contained in a glass bottle sealed with a screw cap. This arrangement gave a fluid volume to specimen surface area ratio of 0.35 ml/mm². Each bottle contained only one metal specimen to avoid any dissimilar metal ion effects. Any effects of the fuel vapors could be observed on the part of each specimen not immersed in solution. The bottles containing the test specimens partially immersed in the test solutions were

placed in a constant temperature chamber maintained at 43°C for a 30-day period. In order to maintain a nominally constant level of available oxygen, the solutions were re-aerated by sparging with compressed air at the halfway mark of the test period.

The solution corrosivity tests were conducted in Task II in the same manner except the number of metals was reduced to six. Zinc was apparently not affected by exposure to the test solutions in Task I and was used as a confirmatory control. The other metals: copper, brass, bronze, terneplate and magnesium were all apparently affected to some degree in Task I.

MATERIAL COMPATIBILITY - Polymeric materials for compatibility testing were chosen from the two major classes of synthetic elastomers and plastics, in addition to a naturally occurring compound. These materials represent as broad a range of applications and chemical types as could reasonably be tested within the scope of the program. The twelve materials used in the compatibility tests are:

1. Nitrile (NBR) - high acrylonitrile elastomer, a butadiene-acrylonitrile copolymer,
2. Nitrile (NBR) - low acrylonitrile elastomer, a butadiene-acrylonitrile copolymer,
3. Fluorocarbon elastomer, a vinylidene fluoride and hexafluoropropylene copolymer,
4. Neoprene elastomer, a chloroprene (chlorobutadiene) polymer,
5. Epichlorohydrin elastomer, a chloropropylene epoxide polymer,
6. Fluorosilicon elastomer, a fluorinated silicon oxide polymer,
7. Acetal resin, a copolymer of a formal and glycol,
8. Polypropylene-high density, a propylene polymer,
9. Polyethylene-high density, an ethylene polymer,
10. Nylon, a polyamide made from dicarboxylic acids and diamines,
11. Perfluorocarbon, a fully fluorinated linear polymer, and
12. Cork gasket material made from cork oak.

These materials, obtained as sheets, were cut into coupons with a size C die and the physical properties of tensile strength, ultimate elongation, volume swell, dimensions and hardness were determined where appropriate according to the provisions of the pertinent ASTM standards. (9-12)

The Task II testing of these materials was conducted in the same manner except that the number of substances was reduced to six. These six materials consisted of three elastomers: fluorocarbon, nitrile-high acrylonitrile and Neoprene; two plastics: Nylon and perfluorocarbon; and the cork gasket material.

TASK I RESULTS

Results of exposure of test specimens immersed in blends containing the test additives were compared with control exposures. Control determinations consisted of the corresponding material specimens exposed to gasoline containing 0-20% methanol and no test additives. All comparisons were made within a material group only. In no case were observations or ratings made on one material compared with those made on another; the results made any such comparisons difficult if not impossible in most instances.

CORROSIVITY - Within the first week of the test the magnesium specimens immersed in the 20% methanol solutions had completely disintegrated. Only the specimen in the blend containing additive D remained intact for the duration of the test as did those in solutions containing the lesser amounts of methanol. Brass, bronze, copper and terneplate exhibited visible effects—for the most part color changes—at the end of the 30-day test period. The other metals had no detectable changes and neither did any of the metals in the gasoline control solutions.

Except for occasional, randomly occurring pits there was no evidence that pitting would be of any use in assessing the extent of corrosion. There was no measurable weight change on any of the randomly selected metal test specimens. Even the magnesium coupons which had been immersed in the 10% methanol blends apparently neither lost nor gained any weight.

Changes in coloration were left as the only apparent effect of corrosive action of the methanol-gasoline blends. Assuming that these effects were corrosion related, the test strips were ranked by visual inspection relative to the control within each methanol-concentration group. Ranking the brass test strips in this manner resulted in the following ratings table:

CORROSION INHIBITION RANKING

Methanol, vol %	Inhibition						
	Best						Worst
2.5	C	K	E	A	B	D	F
5.0	K	C	B	D	A	F	E
10.0	D*	B*	K	C	E	A	F
20.0	A*	B*	D*	K	F	E	C

The control in each group is designated "K". The asterisks designate distinctly less corrosion noted on the specimens immersed in these additive solutions as compared to the controls.

These subjective evaluations indicated only additives B and D seemed to have any significant inhibitory effects on corrosion of the brass

and bronze specimens. Likewise, additive E apparently inhibited the corrosive effects on terneplate. These three additives, B, D and E, were chosen for further testing in Task II.

COMPATIBILITY - Technical information obtained from the additive suppliers had indicated there would be no modification of any incompatibilities between the methanol fuel blends and polymeric materials. Since it is known that alcohols generally aggravate incompatibilities between gasoline fuels and polymeric fuel system materials, these tests were conducted to ascertain that the candidate additives would not create any additional compatibility problems. The properties measured to determine compatibilities were tensile strength, ultimate elongation, volume swell and hardness for the elastomers. Dimensional change was substituted for volume swell determinations in the case of the plastics and was the only determination that could be made on the cork gasket material.

Change in tensile strength is expressed as percent retained after immersion in test solution compared to the value before immersion. According to the pass criterion for elastomers, "shall not lose more than 20% of original tensile strength," epichlorohydrin and fluorosilicone failed at all concentrations of methanol and NBR-low acrylonitrile was marginal. Examination of the tabulated results of the tensile strength measurements seemed to indicate that the additives had neither a beneficial nor a detrimental effect in any instance but this was not readily apparent.

Since it seemed that the percent retention was decreasing as a function of the methanol concentration, all of the results within each material group were normalized with respect to the corresponding value in unleaded gasoline. The normalized values for the six additives within a methanol-concentration group were averaged and compared to the controls as shown in Fig. 1 with the control result designated by "K" and the test average by "T." In the example shown for epichlorohydrin the K and T values are essentially identical since in all cases the variability of the T values defined by either the range or standard deviation includes the corresponding value of K.

These results were essentially the same for the other five elastomers except that the loss of tensile strength was approximately equal for all four methanol concentrations. Only with the fluorocarbon did the retention seem to decrease as methanol concentration increased. There was no detectable difference in the tensile strength of the plastics after immersion in the test solutions. Apparently, the presence of additives in the test fuels had no effect beyond that of the methanol on the tensile strength property of the elastomers and plastics.

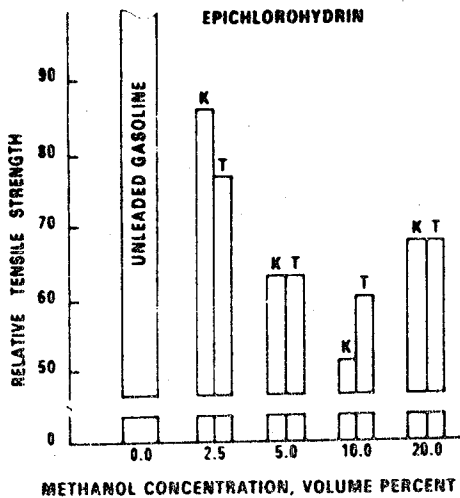


FIGURE 1. RETENTION OF TENSILE STRENGTH RELATIVE TO UNLEADED GASOLINE

Elongation measurements are also expressed as percent retention after immersion in test solution. Only epichlorohydrin failed to meet the pass criterion, "shall not lose more than 50% of original elongation." The elongation data were normalized in the same manner as tensile strength. The results from the epichlorohydrin data are shown in Fig. 2.

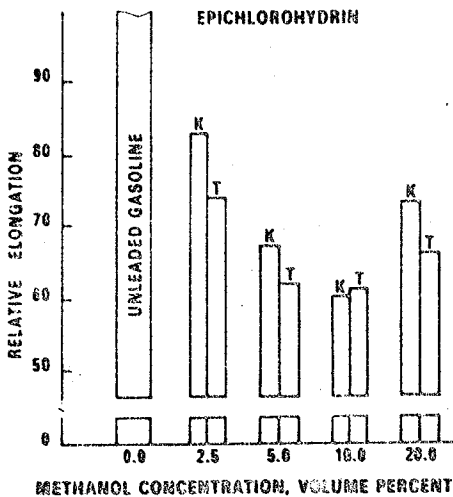


FIGURE 2. RETENTION OF ELONGATION RELATIVE TO UNLEADED GASOLINE

These results closely parallel those from the tensile strength determinations; the elastomers are apparently affected by alcohol in the fuel with no apparent modification by the additives. The plastics exhibited no noticeable effect from the alcohol or additives in the fuel solutions. As with the tensile strength, these

data led to the conclusion that the additives had no effect beyond that of the alcohol on the retention of elongation.

According to the criterion that there be "no shrinkage or a maximum volume increase of 25%," only the fluorocarbon elastomer passed the volume swell test. Only a slight volume increase was noted for the plastic, Nylon 6/6, and slight shrinkage for high-density polypropylene. The results of normalization of the volume swell data are illustrated by the epichlorohydrin example in Fig. 3. The volume change apparently is a function of the methanol content of the fuel, and as with the other properties, the additives do not modify this effect.

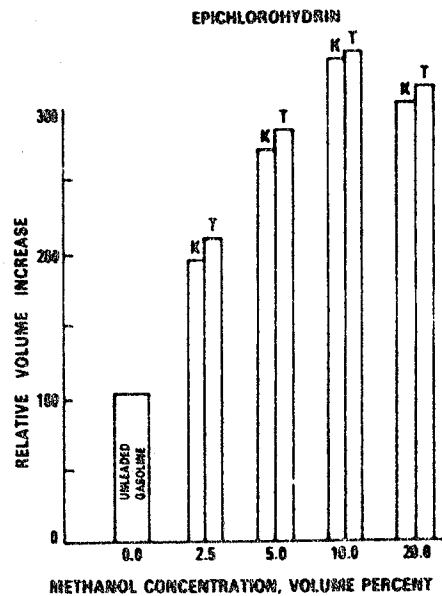


FIGURE 3. INCREASE IN VOLUME RELATIVE TO UNLEADED GASOLINE

Difficulties in cutting the cork test specimens made it possible to accurately measure only the thickness of the coupons. There was no change in this dimension detected after immersion in the test solutions.

PROJECT STATUS

As reported here, Task I, Screening, has been completed and Task II, Optimization is underway and near completion. The Task I corrosion and compatibility tests were completed on a test matrix including six additives, ten metals, six elastomers, five plastics, and cork gasket material in fuels containing four concentration levels of methanol in unleaded gasoline. The evaluation of Task I results led to reduction of the Task II experimental matrix to three additives used singly and in combination, six metals, three elastomers, two plastics

and cork gasket material in fuels containing three methanol concentration levels. The same corrosion and compatibility tests conducted in Task I were used in Task II. The Task II test period is ending at this time; results of the evaluation will be published in the final report of the project.

REFERENCES

1. "Program Planning Document, Highway Vehicle Alternative Fuels Utilization Program (AFUP)," U.S. Department of Energy Report No. DOE/CS-0029, April 1978.
2. "Project Planning Document, Highway Vehicle Alternative Fuels Utilization Program (AFUP)," U.S. Department of Energy Report No. DOE/CS-0093, April 1979.
3. Standard Recommended Practice for "Preparing, Cleaning, and Evaluating Corrosion Test Specimens," ASTM G1-72 (Reapproved 1979).
4. Standard Recommended Practice for "Conducting Plant Corrosion Tests," ASTM G4-68 (Reapproved 1974).
5. Standard Recommended Practice for "Laboratory Immersion Corrosion Testing of Metals," ASTM G31-72 (Reapproved 1979).

6. Standard Recommended Practice for "Flamination and Evaluation of Pitting Corrosion," ASTM G46-76.
7. Test Method, "Antirust Properties of Petroleum Products Pipeline Cargoes," NACE Standard TM-01-72 (1976 Revision).
8. General Motors Corporation, "Unleaded Gasohol," Engineering Standards GM6161-M and GM6162-M, November 1979, Section 3.
9. Standard Test Method for "Rubber Properties in Tension," ASTM D 412-80.
10. Standard Test Method for "Rubber Properties - Effect of Liquids," ASTM D 471-79.
11. Standard Test Method for "Tensile Properties of Plastics," ASTM D 638-80.
12. Standard Test Method for "Rubber Properties - Durometer Hardness," ASTM D 2240-81.

ACKNOWLEDGMENTS

The project is being conducted on DOE Contract No. DEN3-267 with Mr. George M. Prisk, NASA-Lewis, serving as Project Manager. The project is a part of the AFUP being performed by the Stirling Engine and Alternative Fuels Project Office (Energy Directorate, LeRC) for the Office of Vehicle and Engine R&D, Office of Conservation and Renewable Energy at the Department of Energy.

QUESTION AND ANSWER PERIOD

Q: Jerry Panzer, Exxon Research. I have two questions, but let's take them one at a time. How did you decide which alloys and elastomer formulations to select for testing of each of the particular generic groups that you did select?

A: Most of these choices were based on the materials that are used currently and in a couple of cases, such as the fluorocarbons, those that are projected to be used to gain more extensive use in field systems as we know them now.

Q: You mean the auto companies told you which elastomers they use in their cars?

A: No sir.

Q: Then how do you know which ones to use?

A: We compiled as much of this information from our own experience and from whatever other sources are available. We consult with George here on these things and we talk to as many people as we possibly can in the automotive areas.

Q: The second question deals with the fuel formulations. I notice that the ratio of methanol to cosolvent was considerably higher than in the blends which are currently being marketed commercially or are approved by EPA. Are you planning to take a look at those kinds of combinations in any of your future work?

A: We haven't gotten that far yet.

This paper is subject to revision. Statements and opinions advanced in papers or discussions are the author's and are his responsibility, not SAE's; however, the paper has been edited by SAE for uniform styling and format. Discussion will be printed with the paper if it is published in SAE Transactions. For permission to publish this paper in full or in part, contact the SAE Publications Division.

Persons wishing to submit papers to be considered for presentation or publication through SAE should send the manuscript as a 300 word abstract of a proposed manuscript to: Secretary, Engineering Activity Board, SAE.

End of Document